



Material and Component Development for Thermal Energy Storage

Task 58 / ES Annex 33

Abd, Amir ; Aigenbauer, Thomas ; Angerer, Michael ; Bahrami, Majid ; Baldini, Luca; Bauer, Dan ; Bayón, Rocio; Beaupere, Noé; Beving, Max ; Biedenbach, Michael

Total number of authors:
85

Publication date:
2020

Document Version
Publisher's PDF, also known as Version of record

[Link back to DTU Orbit](#)

Citation (APA):

Abd, A., Aigenbauer, T., Angerer, M., Bahrami, M., Baldini, L., Bauer, D., Bayón, R., Beaupere, N., Beving, M., Biedenbach, M., Blanchard, D., Brütting, M., Cabeza, L. F., Cuypers, R., Dagueuet-Frick, X., Dannemand, M., de Lange, R., Gracia, M. D., Diarce, G., ... Zsembinszki, G. (2020). *Material and Component Development for Thermal Energy Storage: Task 58 / ES Annex 33*. IEA.

General rights

Copyright and moral rights for the publications made accessible in the public portal are retained by the authors and/or other copyright owners and it is a condition of accessing publications that users recognise and abide by the legal requirements associated with these rights.

- Users may download and print one copy of any publication from the public portal for the purpose of private study or research.
- You may not further distribute the material or use it for any profit-making activity or commercial gain
- You may freely distribute the URL identifying the publication in the public portal

If you believe that this document breaches copyright please contact us providing details, and we will remove access to the work immediately and investigate your claim.



TASK 58 ANNEX 33

MATERIAL AND COMPONENT DEVELOPMENT FOR THERMAL ENERGY STORAGE

Final Report

May 2020

Submitted for

the 89th ECES ExCo meeting May 2020.

Operating Agent SHC:

Wim van Helden

AEE Intec

Austria

Operating Agent ECES:

Andreas Hauer

ZAE Bayern

Germany



ABOUT THIS REPORT

To **International Energy Agency**
Executive Committee of the Energy Storage technology collaboration programme (ES TCP).

Presented by **Bavarian Center for Applied Energy Research (ZAE Bayern)**

Walther-Meissner-Strasse 6

85748 Garching

Dr. Andreas Hauer (Operating Agent)

andreas.hauer@zae-bayern.de



AUTHORS (ALPHABETICAL ORDER)

Amir Abdi, KTH

Thomas Aigenbauer, ASiC

Michael Angerer, TU Munich

Majid Bahrami, Simon Fraser University

Luca Baldini, EMPA

Dan Bauer, DLR

Rocio Bayón, CIEMAT

Noé Beaupéré, Université d'Artois

Max Beving, Eindhoven University of Technology

Michael Biedenbach, Fraunhofer ISE

Didier Blanchard, DTU

Michael Brütting, ZAE Bayern

Luisa F. Cabeza, University of Lleida

Ruud Cuypers, TNO

Xavier Dagueuet-Frick, SPF

Mark Dannemand, DTU

Rick de Lange, Eindhoven University of Technology

Mónica Delgado Gracia, University of Zaragoza

Gonzalo Diarce, University of the Basque Country

Reda Djebbar, CanmetENERGY

Pim Donkers, TNO

Stefania Doppiu, CIC EnergiGune

Phil Eames, Loughborough University

Jon Elvins, Swansea University

Gerald Englmaier, DTU



Mohammed Farid, University of Auckland

Oliver Fellmann, HSLU

Markus Fink, AIT

Fabian Fischer, ZAE Bayern

Andrea Frazzica, CNR

Benjamin Fumey, EMPA

Simon Furbo, DTU

Paul Gantenbein, SPF

Jaume Gasia, University of Lleida

Georg Gravogl, TU Vienna

Dominic Groulx, Dalhousie University

Stefan Gschwander, Fraunhofer ISE

Saman Gunasekara, KTH

Andrea Gutierrez, DLR

Andreas Hauer, ZAE Bayern

Thomas Haussmann, Fraunhofer ISE

Thomas Herzog, TH Wildau

Stephan Höhle, University of Bayreuth

Gayaney Issayan, University of Applied Sciences Upper Austria

Kevyn Johannes, INSA Lyon

Maike Johnson, DLR

Anastasiia Karabanova, DTU

Henner Kerskes, ITW / University of Stuttgart

Christian Knoll, TU Vienna

Rebekka Köll, AEE INTEC

Weiqiang Kong, DTU

Andreas König-Haagen, University of Bayreuth



Lia Kouchachvili, CanmetENERGY

Frederic Kuznik, INSA Lyon

Daniel Lager, AIT

Eric Laurenz, Fraunhofer ISE

Ana Lazaro, University of Zaragoza

Raffaele Liberatore, ENEA

Viktoria Martin, KTH

Emanuela Mastronardi, Northwestern University

Emanuela Mastronardo, University of Messina

Candida Milone, University of Messina

Danny Mueller, TU Vienna

Gunther Munz, Fraunhofer ISE

Melissa Obermeyer, HSLU

Elena Palomo del Barrio, CIC EnergiGune

Elpida Piperopoulos, University of Messina

Christoph Rathgeber, ZAE Bayern

Rebecca Ravotti, HSLU

Alenka Ristic, NIC

Sylvie Rouge, CEA

Mina Rouhani, Simon Fraser University

Justin Searle, Swansea University

Alexandre Skrylnyk, University of Mons

Anastasia Stamatiou, HSLU

Wim van Helden, AEE INTEC

Annelies Vandersickel, TU Munich

Waldemar Wagner, AEE INTEC

Sara Mae Walsh, Swansea University



Rebecca Weber, University of Stuttgart

Robert Weber, EMPA

Peter Weinberger, TU Vienna

Laurent Zalewski, Université d'Artois

Bernhard Zettl, University of Applied Sciences Upper Austria

Gabriel Zsembinszki, University of Lleida

Contents

About this Report.....	1
Authors	2
List of Abbreviations	10
Key Messages	11
Main Results In a Nutshell.....	12
1 Executive Summary.....	15
1.1 Short Description of Annex 33.....	15
1.1.1 Objectives and Scope.....	15
Objectives	15
Scope.....	15
1.1.2 Organisational structure	16
1.1.3 Workplan.....	17
1.1.4 Start and end of the Annex	18
1.1.5 Experts Meetings	18
1.1.6 Status of Participation.....	19
1.2 Summary of Subtasks	20
1.2.1 Subtask 1 – Energy Relevant Applications for an Application-oriented Development of Improved Storage Materials.....	20
1.2.2 Subtask 2 - Development and Characterization of Improved Materials	26
1.2.1 Subtask 3 - Measuring Procedures and Testing under Application Conditions	32
1.2.2 Subtask 4 - Component Design for Innovative TES Materials	34
Final Report.....	39
1 Objectives, Structure and Approach of the Annex	40
1.1 Objectives	40
1.2 Scope	40
1.3 Structure and Approach of the Annex.....	40
1.4 Meetings and Participating Countries and TCPs	42

2	Subtask 1 – Energy Relevant Applications for an Application-oriented Development of Improved Storage Materials	43
2.1	The Approach of Application-oriented Development of Improved Storage Materials	43
2.2	What are Energy relevant Applications?	44
2.2.1	Relevance by Statistics	44
2.2.2	Relevant Applications	44
2.3	How to Define Operation Conditions	45
2.3.1	Why focus on temperatures?	46
2.4	Definition of Temperatures for PCM and TCM Storage Systems to Describe the Operation Conditions	46
2.4.1	2-Temperature-Approach for PCM	46
2.4.2	4-Temperature-Approach for TCM	47
2.5	Collection of Operation Conditions	47
2.5.1	Building Applications	48
2.5.2	Other Applications	49
2.6	Temperature guideline for testing compact thermal energy storage systems in buildings	50
2.6.1	Introduction	51
2.6.2	Method	52
2.6.3	Results and Discussion	54
2.6.4	Conclusions	60
2.6.5	Acknowledgements	60
2.6.6	Funding	60
2.6.7	References	60
3	Subtask 2 – Development and Characterization of Improved Materials	63
3.1	Subtask 2P: Development and Characterization of Improved PCM	63
3.1.1	Introduction	63
3.1.2	Material development: List of novel developed PCM as well as blends and mixtures	63

3.1.3	Characterization of PCMs: Extended list of material properties for the characterization of novel PCM (D2P2)	65
3.1.4	Database: Measured material data for the maintenance and expansion of the PCM Database	74
3.1.5	Wiki for PCM	75
3.2	Subtask 2T: Development and Characterization of Improved Thermochemical Materials.....	76
3.2.1	Introduction.....	76
3.2.2	Development and identification of the novel chemical reactions and composite materials	76
3.2.3	Definition of the relevant material parameters	78
3.2.4	Characterization of novel reactions and materials by material properties	78
3.2.5	Development of the TCM material databases implemented in Task42/Annex 29	119
4	Subtask 3 - Measuring Procedures and Testing under Application Conditions	125
4.1	Subtask 3P: PCM Testing under Application Conditions.....	125
4.1.1	Introduction.....	125
4.1.2	Properties of PCM in the Lab Environment and under Application Conditions	125
4.1.3	Experimental Devices to Investigate Degradation of PCM	138
4.2	Subtask 3T: TCM measuring procedures and testing under application conditions	169
4.2.1	Introduction.....	169
4.2.2	List and description of available and needed TCM characterization procedures for the identified material and reaction properties (D3T1)	170
4.2.3	Result of a round robin test of a TCM candidate (D3T2)	170
4.2.4	Description of a harmonized measurement procedure for the TCM performance under realistic application conditions.....	181
4.2.5	Acknowledgments	189
4.2.6	References	189
5	Subtask 4 - Component Design for Innovative TES Materials	191
5.1	Subtask 4P: Component Design for PCM	191

5.1.1	Inventory of concepts to improve component performance	191
5.1.2	Definition of the targeted performance characteristic for PCM components ..	213
5.2	Subtask 4T: Component Design for TCM	223
5.2.1	Sorption based long-term thermal energy storage – Process classification and analysis of performance limitations: A review	223
5.2.2	Inventory of sorption heat storage component and system designs currently under investigation by task and annex partners	223
6	Appendices	261
6.1	Subtask 2P: Material data sheets	261
6.2	Subtask 3T	308
6.2.1	Appendix A	308
6.2.2	Appendix B	317
6.2.3	Appendix C	324
6.2.4	Appendix D: Results report of the 3rd Zeolite 13X Round Robin	329
6.2.5	Appendix E: Measurement protocol for the evaluation of specific heat capacity $c_p(T)$ of $\text{SrBr}_2 \cdot n\text{H}_2\text{O}$ and SrBr_2 based on heat flow differential scanning calorimetry	331
6.3	Subtask 4P: Information of the systems	338
6.3.1	System A	338
6.3.2	System B	339
6.3.3	System G	341
6.3.4	System H	342
6.3.5	System I	345
6.3.6	System J	347
6.3.7	System K	350

LIST OF ABBREVIATIONS

APO	Aluminum Phosphate
ASTM	American Society for Testing and Materials
CWK	Chemiewerk Bad Köstritz GmbH
DSC	Differential Scanning Calorimetry
ENG	Expanded Natural Graphite
IEA	International Energy Agency
LTA	Linde Type A
MOF	Metal-organic Framework
PCM	Phase Change Material
PHTS	Plugged Hexagonal Templated Silicate
PXRD	Powder X-Ray Diffraction
SAPO	Silicon-Aluminum Phosphate
T58A33	SHC Task 58 / ES Annex 33
TCM	Thermochemical Material
TCP	Technology Collaboration Programme (of the IEA)
TES	Thermal Energy Storage
XRD	X-Ray Diffraction

KEY MESSAGES

GENERAL

- Collaboration in the IEA Task/Annex between materials experts and application experts leads to improved understanding and therefore accelerates development.
- Standards for measurement and for reporting are prerequisite for constructive discussions and rapidly addressing challenges and advancing TES technologies.

SUBTASK 1: ENERGY RELEVANT APPLICATIONS

- A large number of relevant application exists for compact thermal energy storage.
- Standardized reference conditions can be defined for the building sector. For industrial applications, however, the diversity of processes makes it very difficult!

SUBTASK 2: DEVELOPMENT AND CHARACTERIZATION OF IMPROVED PHASE CHANGE MATERIALS / THERMOCHEMICAL MATERIALS

- A number of innovative and improved materials were developed and continuously are being developed, tested in Subtask 3 and introduced in components in Subtask 4.
- Developed characterization methods are the basis for material evaluation and comparison and as well for the database input.
- The material properties cover not only the technical performance, but also questions like stability and compatibility.

SUBTASK 3: MEASURING PROCEDURES AND TESTING UNDER APPLICATION CONDITIONS FOR PHASE CHANGE MATERIALS / THERMOCHEMICAL MATERIALS

- Only testing under application conditions helps identifying the appropriate material for an actual application.
- The actual storage capacity and material stability have to be tested under realistic conditions and requirements.

SUBTASK 4: COMPONENT DESIGN FOR PHASE CHANGE MATERIALS / THERMOCHEMICAL MATERIALS

- Identification of component parameters is necessary to enable the comparison of compact storage concepts.
- The reachable charging/discharging power is strongly influenced by the component design, where the interaction of the storage material with the component is crucial.

MAIN RESULTS IN A NUTSHELL

The goal of Annex 33 is to support an application-oriented development of innovative and compact thermal energy storage materials: Phase Change Materials (PCM) and Thermochemical Materials (TCM). This includes, first, the characterization of a new material concerning its properties like heat of fusion or heat of reaction, specific heat, thermal conductivity, and others. In a second step, the material has to be tested under reference application conditions. These conditions shall be identified for energy relevant applications in a separate approach. The third step focuses on the interaction between the storage material and the storage component, and mainly with the heat and mass transfer performed in the component or reactor. Thereby, first results towards a reliable power and energy density can be deduced.

Subtask 1: “Energy Relevant Applications for an Application-oriented Development of Improved Storage Materials”:

The energy density of a storage material or its specific storage capacity – energy stored per mass or volume – is not a material property! It is strongly depending on the operation conditions during charging and discharging. Therefore, the testing of novel storage materials has to be performed under operation conditions given by relevant applications. These operation conditions have to be identified.

Energy relevant applications for thermal energy storage systems can be described by their impact on the energy system. The following fields of applications were listed by the participants:

- Industrial batch processes and peak shaving applications
- Heating and cooling for single family households (HVAC systems in the building sector)
- Combined heat and power systems
- District heating systems

The most important parameters for the evaluation of a latent or thermochemical storage processes are the temperatures involved. By defining just these temperatures the achievable storage capacity can be experimentally quantified. An approach using 2/4 temperatures for PCM/TCM was elaborated. The operation temperatures for a number of actual applications were collected and analysed. For building applications, reference conditions seem to be available. For applications like combined heat & power, district heating, and especially industrial applications, the definition of a set of standard operation temperatures is very difficult or even impossible. The diversity of the actual process parameters is too vast.

Subtask 2: “Development and Characterization of Improved Materials”

In total, 20 different Phase Change Materials (PCM) were developed or investigated by the experts. The focus of the survey was on the comparison of

the melting enthalpies, melting temperatures, and the degree of supercooling of the PCM. PCM with melting temperatures between $-20\text{ }^{\circ}\text{C}$ and $+180\text{ }^{\circ}\text{C}$ and melting enthalpies up to 300 kJ/kg on material level were investigated.

Round robin tests on the PCM RT70HC (a paraffin) were performed to develop a procedure for measuring thermal diffusivity via laser flash method. Especially the way of preparing the specimen and the appropriate adjustment of the laser pulse energy turned out to have a significant influence on the measuring accuracy.

In order to establish a common wording of relevant phenomena in the context of PCM, a Wiki has been started. Experts have worked on definitions and explanations of terms such as nucleation temperature, supercooling, specific heat determination via DSC etc. The PCM Wiki is open for everyone to add further entries.

The databases for PCM and Thermochemical Materials (TCM) have been maintained and extended to add further material data, for example viscosity measurements. Material properties for PCM and TCM, partly “novel” materials, have been measured and uploaded to the databases.

The development of improved TCM included sorption materials (micro/mesoporous solids and liquids), chemical reactions (salt hydrates and metal oxides/hydroxides), and combinations of both (zeolites/graphite + salt hydrates/metal oxides). Sorption materials with desorption temperatures between $80\text{ }^{\circ}\text{C}$ and $140\text{ }^{\circ}\text{C}$ and desorption enthalpies up to $2,200\text{ kJ/kg}$ on material level were investigated. Chemical reactions with reaction temperatures up to $800\text{ }^{\circ}\text{C}$ showed reaction enthalpies up to $1,500\text{ kJ/kg}$ on material level.

Subtask 3: “Measuring Procedures and Testing under Application Conditions”

In the context of PCM testing under application conditions, a comparison of material properties of PCM in the lab environment and under application conditions was elaborated. Thereby, most input was collected for the properties degree of supercooling, phase separation, storage capacity, and long-term stability of PCM. A step further was taken in the case of long-term stability of PCM: Information on experimental devices to investigate the long-term stability of PCM were gathered. The experiments include tests on the stability of PCM over thermal cycling, on the stability of PCM with stable supercooling, and on the stability of Phase Change Slurries (PCS).

In the context of TCM testing under application conditions, measurement procedures for mass and enthalpy change with defined conditions for sorption materials and salt hydrates were developed. In addition, a measurement procedure for specific heat capacity measurements of salt hydrates was tested. Round robin tests showed a good agreement with respect to mass change among the participants. Both enthalpy change and specific heat capacity showed larger deviations and, thus, pointed to the necessity to pro-

ceed with standardizing measurement methods including sample preparation and handling. Based on the measured material properties of zeolite 13X, a scale-up procedure from material properties to lab scale was proposed.

Subtask 4: “Component Design for Innovative TES Materials”

To provide an overview on PCM component design, an inventory of heat exchanger concepts was done. Following this, a definition of performance for PCM components in term of capacity and storage density was agreed upon. In order to be able to compare different PCM concepts in terms of power, a review on assessment approaches was carried out. Therefore, power-time curves upon charging and discharging were compared, preliminary performance parameters were defined, and a procedure based on a validated numerical model was proposed.

In the case of TCM, the starting point was a basic description of investigated TCM storage processes and their impact on the component design. In addition, an inventory of actual TCM component designs currently under investigation was elaborated. Thereby, a common graphical representation was used to classify component concepts as open or closed and fixed or transported systems. Further efforts were undertaken to identify a possible TCM performance degradation from lab-scale measurements to pilot installations. A “Do’s and Don’ts” paper in the context of TCM component design is currently in preparation.

1 EXECUTIVE SUMMARY

1.1 SHORT DESCRIPTION OF ANNEX 33

Past IEA SHC and ECES Tasks/Annexes, especially Task42/Annex24 and its successor Task42/Annex29, achieved substantial progress in the understanding of compact thermal storage materials and systems and created a strong basis of collaborating experts from both the field of materials and systems applications from a large number of countries, mainly in Europe and Japan. From these seven years of collaboration, it was concluded that a continuation is needed, especially in the further material development, materials characterisation techniques and component development.

Annex 33 tries to support an application-oriented development of innovative storage materials in three steps. The **first step** is the characterization of the new material concerning its properties like heat of fusion or heat of reaction, specific heat, thermal conductivity, and others.

In a **second step** the material has to be tested under identified reference application conditions. Following the findings of Annex 24 and 29, these conditions include 2 temperatures for PCM (charging and discharging temperature) and 4 temperatures or concentrations for TCM (temperature and reactant concentration at charging and discharging). After this testing, for the first time, a theoretical energy density can be derived because the energy density is not a material property, but a process depending value!

The **third step** focuses on the interaction between the storage material and the storage component, and mainly with the heat and mass transfer performed in the component or reactor. Thereby, first results towards a reliable power and energy density, which is now related to the mass and volume of the component, can be deduced.

1.1.1 OBJECTIVES AND SCOPE

OBJECTIVES

The key objectives of the joint Annex/Task are:

- Mapping and evaluating the TES application opportunities concerning the requirements for the storage material
- Development and characterisation of storage materials to enhance TES performance
- Development of materials characterisation procedures and a methodology for material testing under application conditions
- Development of components for compact thermal energy storage systems

SCOPE

This joint Annex/Task deals with advanced materials for latent and thermochemical energy storage: Phase Change Materials (PCM) and Thermochemical Materials (TCM).

It covers the material development, the characterization, and the testing under application conditions. Finally, it describes the interaction between material and the storage component and the expected storage performance of the innovative materials.

Because seasonal storage of solar heat for solar assisted heating of buildings is the main focus of the IEA-SHC TCP, this will also be a focus area of this task. However, because there are many more relevant applications for TES, and because material research is not and cannot be limited to one application only, this task will include multiple application areas.

1.1.2 ORGANISATIONAL STRUCTURE

The work of the Annex has been divided into 4 Subtasks. Two of the planned subtasks will concentrate on the material itself, its characterization, and the definition of testing procedures. Subtask 1 and 4 deal with the relation between the new material and the storage component and the actual application, respectively.

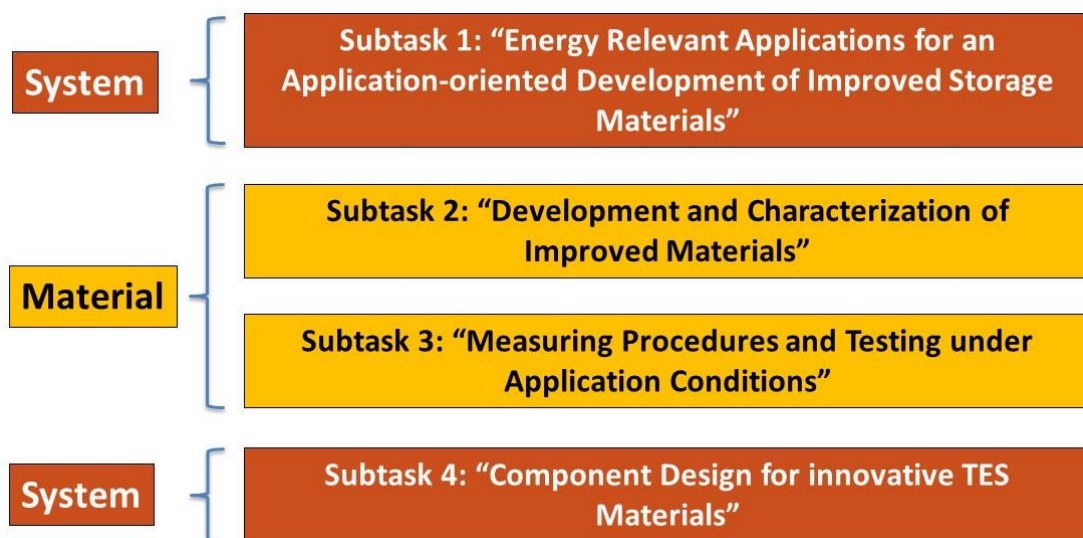


FIGURE 1.1-1: SUBTASK STRUCTURE OF ANNEX 33

There are two reasons for a further breakdown of the materials and components subtasks into a PCM (-P) and a TCM (-T) track. The first is that, although there are a lot of common approaches for the two classes of materials, the basic materials principles differ and need a different approach. The second reason is that, with the relatively high number of experts, it is more effective to break down the work in a larger number of subgroups. However, this holds not for subtask 1, which is valid for both storage technologies. The following subtask division has been applied. Under each subtask (for the PCM and the TCM track), a subtask leader was appointed.

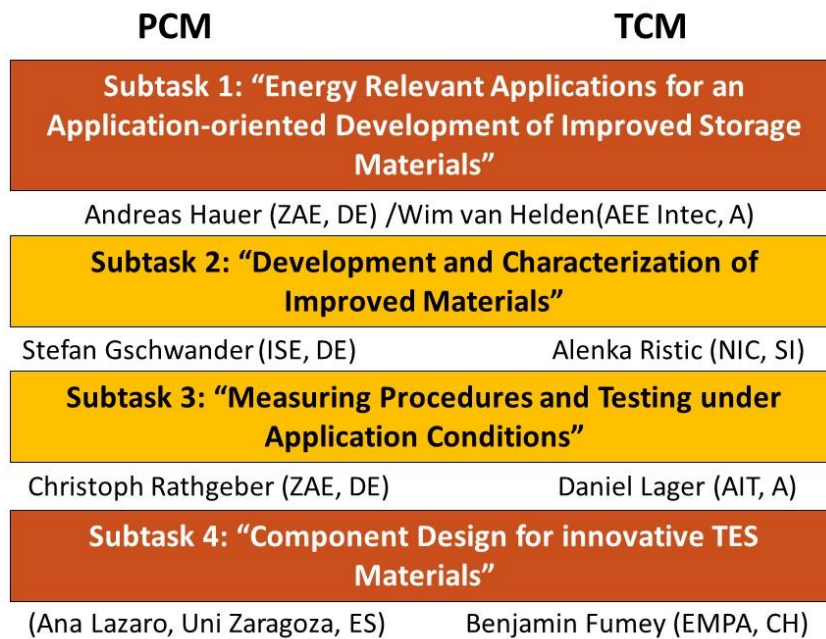
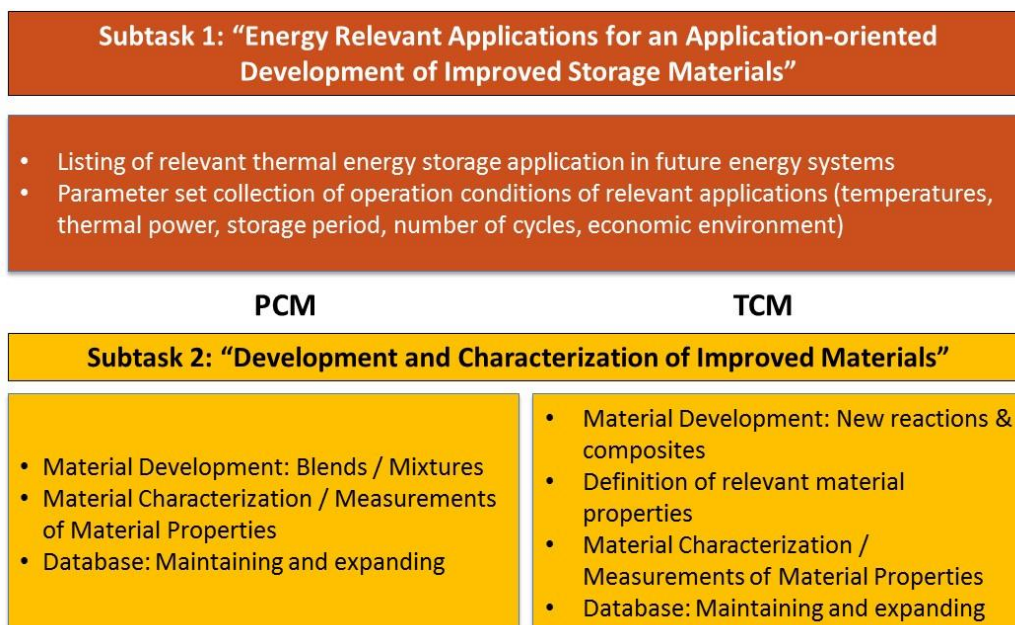


FIGURE 1.1-2: SUBTASK LEADERS OF THE PCM AND THE TCM TRACKS OF ANNEX 33

1.1.3 WORKPLAN

An overview of the activities within the Subtasks is shown below.



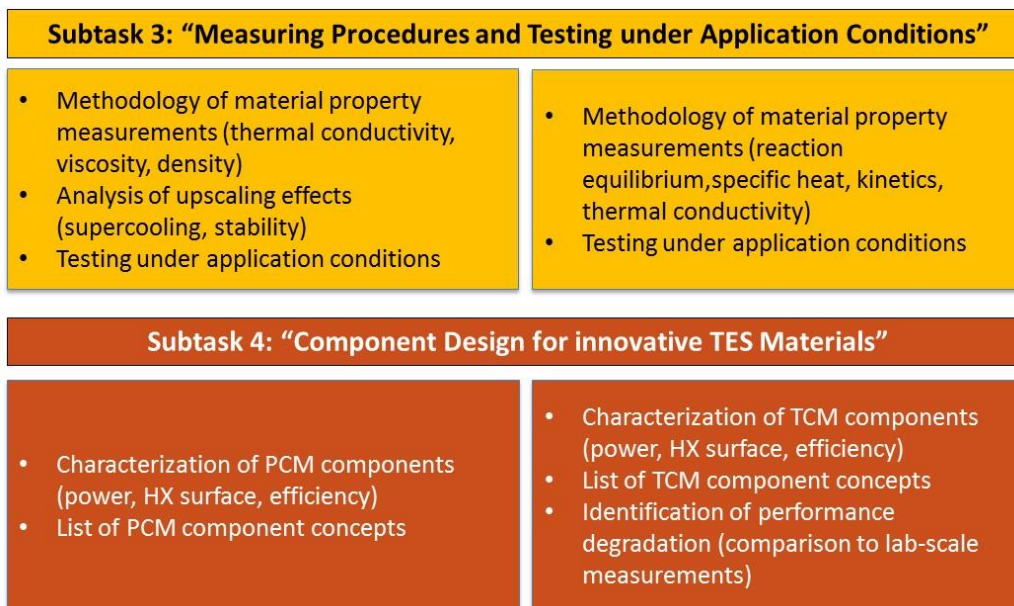


FIGURE 1.1-3: ACTIVITIES WITHIN THE SUBTASKS OF ANNEX 33

1.1.4 START AND END OF THE ANNEX

The activities of the joint Task/Annex started at 1 January 2017 and ended at 31 December 2019.

1.1.5 EXPERTS MEETINGS

The predecessor Task4224 and Task4229 covered a period of 7 years in which 14 Experts Meetings were held. The table below shows an overview of the expert meetings in Annex 33. Six experts meetings were held. The right column indicated the number of participants at a meeting.

Table 1.1-1: Expert meetings

#	Location	Country	Date	Participants
1	Lyon	France	April 5-7, 2017	64
2	Zurich	Switzerland	October 4-6, 2017	46
3	Ljubljana	Slovenia	April 9-11, 2018	45
4	Graz	Austria	October 1-2, 2018	42
5	Ottawa	Canada	May 1-3, 2019	43
6	Messina	Italy	October 9-10, 2019	42

1.1.6 STATUS OF PARTICIPATION

10 institutions from 8 countries participate officially in this Annex.

Table 1.1-2: Participating Countries

Country	Participant
Germany	ZAE Bayern
Germany	Fraunhofer ISE
Belgium	Univ. Mons
France	Univ. Bordeaux
Slovenia	NIC
Spain	Univ. Lleida
Spain	Univ. Zaragoza
Sweden	KTH
Switzerland	EMPA
Turkey	Çukurova Univ.

The list contains only the countries officially participating through the Energy Storage TCP. For example countries like Austria and Italy participated through the Solar Heating and cooling TCP in the beginning.

Overall more than 13 countries participated in the experts meetings and workshops.

1.2 SUMMARY OF SUBTASKS

1.2.1 SUBTASK 1 – ENERGY RELEVANT APPLICATIONS FOR AN APPLICATION-ORIENTED DEVELOPMENT OF IMPROVED STORAGE MATERIALS

THE APPROACH OF APPLICATION-ORIENTED DEVELOPMENT OF IMPROVED STORAGE MATERIALS

The energy density of a storage material or its specific storage capacity – energy stored per mass or volume – is not a material property! It is strongly depending on the operation conditions during charging and discharging. Therefore, it can be described as a process variable. The storage process is depending on the actual storage application. Parameters like the available charging temperature and the usable temperature at the consumer side are determined by the application.

The goal of this subtask is to provide a list of thermal energy storage applications relevant for our future energy system. The storage application sets the technical and economic environment of the storage system and defines the operation conditions. These conditions include available charging and required discharging temperatures, available and required thermal power in- and output, as well as the available reactant concentrations for the process in the case of thermo-chemical energy storage.

The list could also include parameters like the expected number of storage cycles, the predicted lifetime and the required system size. All these parameters can be utilized for integrated system simulations, which finally can give first estimations of performance improvement of the new storage materials.

This cross-cutting subtask was planned as an ongoing discussion forum, where the material designers meet the application engineers and, thus, the gap between these two groups could be bridged.

The actual approach is starting from defining relevant applications. In a next step these applications provide operation conditions. It has to be investigated whether the class of applications provides standard conditions or more individual energy storage solutions. The identified operation conditions are the basis of any application-oriented testing of novel thermal energy storage materials.

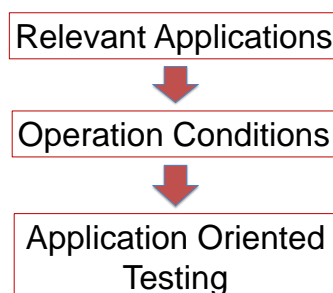


FIGURE 1.2-1: APPROACH OF SUBTASK 1 TOWARDS AN APPLICATION-ORIENTED TESTING

WHAT ARE ENERGY RELEVANT APPLICATIONS?

Energy relevant applications for thermal energy storage systems can be described by their impact on the energy system. This impact can be quantified with respect to the overall CO₂ emissions or to the final energy demand connected to this class of applications.

RELEVANCE BY STATISTICS

Looking at the statistical sectors – industry, private households, trade & commerce, and transport – the CO₂ emissions and final energy demand can be visualized. Figure 1.2-2 shows the different energy forms responsible for these emission in Germany. With focus on thermal energy, like process heat, space heating, domestic hot water (DHW), process cold and AC cold, the sectors industry, private households, trade & commerce seem to be relevant.

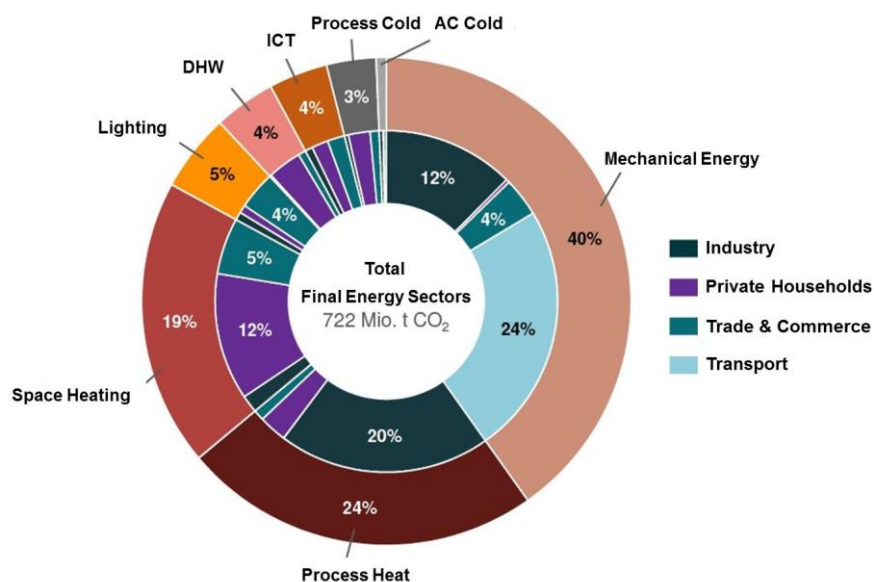


FIGURE 1.2-2: CO₂ EMISSIONS IN GERMANY LINKED TO STATISTICAL SECTORS AND ENERGY DEMAND [M. RASCH, A. REGETT, S. PICHLMAIR, J. CONRAD, S. GREIF, A. GUMINSKI, E. ROUYRRE, C. ORTHOFER AND T. ZIPPERLE, EINE ANWENDUNGSORIENTIERTE EMISSIONSBILANZ – KOSTENEFFIZIENTE UND SEKTORENÜBERGREIFENDE DEKARBONISIERUNG DES ENERGIESYSTEMS, FORSCHUNGSSTELLE FÜR ENERGIEWIRTSCHAFT FFE, BWK, AUSGABE 03/2017]

From the figure it is obvious that thermal energy demand and the connected emissions are with more than 50% the dominant factor for any measures to stop the global warming. This is a strong point for the relevance of thermal energy storage to support the integration of renewables and to increase energy efficiency in general.

RELEVANT APPLICATIONS

The most relevant fields of application for thermal energy storage systems can be defined as:

- Industrial Processes
- Buildings

These two fields of application would stand for 27% (process heat and cold) and 24% (space heating, DHW and AC cold) of the CO₂ emissions in Germany.

In the last phase of the Annex, this list was updated and only the most relevant applications were extracted:

- Industrial batch processes and peak shaving applications
- Heating and cooling for single family households (HVAC systems in the building sector)
- Combined heat and power systems
- District heating systems

In a first attempt, it was tried to collect operation conditions from these applications. And, if possible, to extract reference conditions for material testing.

HOW TO DEFINE OPERATION CONDITIONS

In order to develop a novel material for thermochemical heat storage (TCM) a strong link to the targeted application is crucial. The proposed approach offers an easy method for first experimental testing of new materials under real conditions.

WHY FOCUS ON TEMPERATURES?

The most important parameters for the evaluation of materials within latent or thermochemical storage systems are the temperatures involved. By adjusting just these temperatures, the achievable storage capacity can be experimentally quantified. Any other operation conditions (like the thermal power requirement or the number of cycles) should be neglected at this first step of testing. The presented approach will focus exclusively on the temperatures as the operation conditions.

2-TEMPERATURE-APPROACH FOR PCM

For PCM thermal energy storage systems, 2 temperatures are sufficiently describing the charging and discharging process in any application.

- **Charging Temperature T_{char}** : The necessary charging temperature is given by the melting temperature of the PCM. It has to be above the melting temperature in order to melt the PCM in the charging process. The minimum necessary temperature difference between charging and melting temperature, as fixed value for each material, is given by heat exchanger design.
- **Consumer Temperature T_{cons}** : The necessary discharge temperature is given by the application. Each application has its own fixed usable temperature level. Below this level, heat cannot be used. The consumer temperature should be below the melting temperature in order to utilize the melting enthalpy. The minimum necessary temperature difference between melting temperature and usable temperature level is given by heat exchanger design.

4-TEMPERATURE-APPROACH FOR TCM

For thermochemical energy storage, not only the heat transport in and out of the material, described by the temperatures, but also the mass transfer, given by the concentrations of the reactants, defines the achievable storage capacity. The concentrations however can be translated into available temperatures. These temperatures could be equivalent to partial pressures or dewpoints (in the case of water as the reactant) in open systems. In closed systems, the concentrations are given by the temperature of the condenser and the evaporator. In the following, these temperatures are called “ambient” temperatures, because they determine the actual heat flux in or out of the thermochemical energy storage system. Thus 4 temperatures are necessary to describe the charging and discharging process in any application.

- **Charging Temperature T_{Char}** : The available charging temperature, which is depending on the temperature of the heat source and the quality of the heat exchanger.
- **T_{AmbChar} (only for TCM)**: The ambient condition during charging is given by the dew point or partial pressure or concentration of the reactant for an open system and by the condenser temperature for a closed system.
- **Consumer Temperature T_{Cons}** : The minimum required temperature for the consumer (including the necessary temperature difference for the heat exchanger).
- **$T_{\text{AmbDischar}}$ (only for TCM)**: The ambient condition during discharging is given by the dew point or partial pressure or concentration of the reactant for an open system and by the evaporator temperature for a closed system.

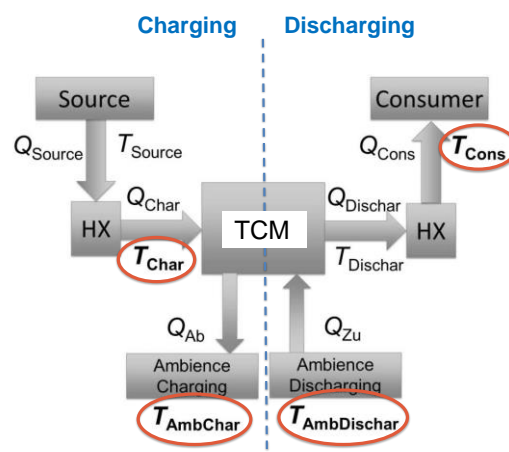


FIGURE 1.2-3: SCHEME OF A TCM SYSTEM AND THE 4 RELEVANT TEMPERATURES DURING CHARGING AND DISCHARGING

COLLECTION OF OPERATION CONDITIONS

The participants were asked to fill in templates for the most relevant applications in order to identify the operation temperatures according to the above-mentioned methodology.

BUILDING APPLICATIONS

Figure 1.2-4 shows the provided charging and consumer temperature for heating and domestic hot water applications. All applications are based on a solar-thermal input. This limits the charging temperatures below or around 100 °C. Exceptions are coming from systems assuming high temperature thermal collectors (e.g. vacuum tubes) or electrical heating systems.

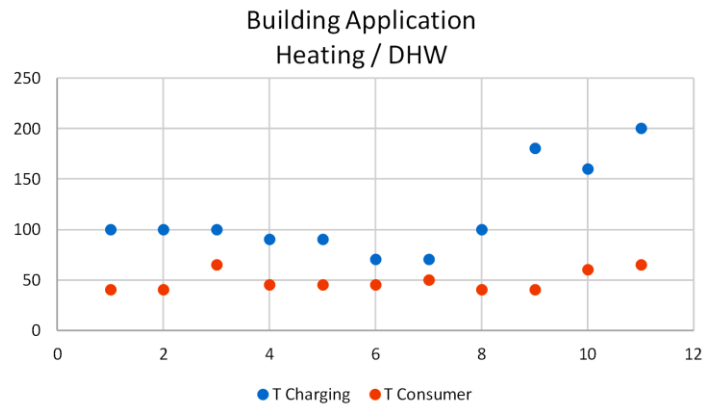


FIGURE 1.2-4: CHARGING AND CONSUMER TEMPERATURE FOR BUILDING APPLICATIONS

For the class of building applications, it seems possible to define reference conditions or at least temperature ranges in which a first material testing could be performed.

OTHER APPLICATIONS

The other relevant applications - combined heat and power, district heat, and process heat – are listed in Table 1.2-1.

TABLE 1.2-1: OPERATION TEMPERATURES OF MOST RELEVANT APPLICATIONS IN OTHER SECTORS ACCORDING TO PARTICIPANTS INPUT

Institution	Application	T Charging	T Amb Char	T Consumer	T Amb Dischar
Combined Heat & Power					
ZAE Bayern	CHP Waste Heat (low-T)/ Short Term TES / Process Heat (Food Industry)	80 °C	20 °C	100-110 °C	20 °C
ZAE Bayern	CHP Waste Heat (combustion gases)/ Short Term TES / Process Heat (Food Industry)	350 °C	20 °C	100-110 °C	21 °C
District Heating					
AEE Intec	Renewable Electricity / Short Term TES / District Heating	> 100 °C	10-20 °C	80 °C	10-20 °C
Process Heat					
Univ. Artois	Solar Wall / / Daily TES / Process Heat (Greenhouse effect)	<80°C		25°C - 35°C	
TUM	Renewable Electricity / Power-to-Process Heat & Power	> 650°C	160°C	475°C	120°C
TUM	Renewable Electricity / Power-to-Process Heat	> 650°C	160°C	192°C	90-100°C

The content of Table 1.2-1 is coming from actual R&D projects of the international participating institutes. It is no representative view on the real situation of relevant application. However, it remains obvious that a certain set of reference temperatures cannot be identified for the listed



applications. Especially in the field of process heat and industrial applications, the diversity of operation conditions is huge. Thus, no reference conditions can be defined at the moment.

1.2.2 SUBTASK 2 - DEVELOPMENT AND CHARACTERIZATION OF IMPROVED MATERIALS

SUBTASK 2P

The work of Subtask 2P “Development and Characterization of Improved PCM” covered 4 topics:

- PCM Material development
- Developing measurement procedures
- Filling the PCM Database
- Developing a Wiki for terms used in the context of PCM

DEVELOPMENT OF NEW PCM

As the material development is done at different institutions, the first objective was to collect information on the PCM which are under development. Questionnaires from the experts were gathered to get an overview on the most relevant properties of these materials and the application which are addressed. Figure 1.2-5 depicts an overview of the investigated and/or developed PCM in terms of melting temperature vs. melting enthalpy. In total, 20 PCM with melting temperatures between -20 °C and +180 °C and melting enthalpies up to 300 kJ/kg on material level were investigated by the participants.

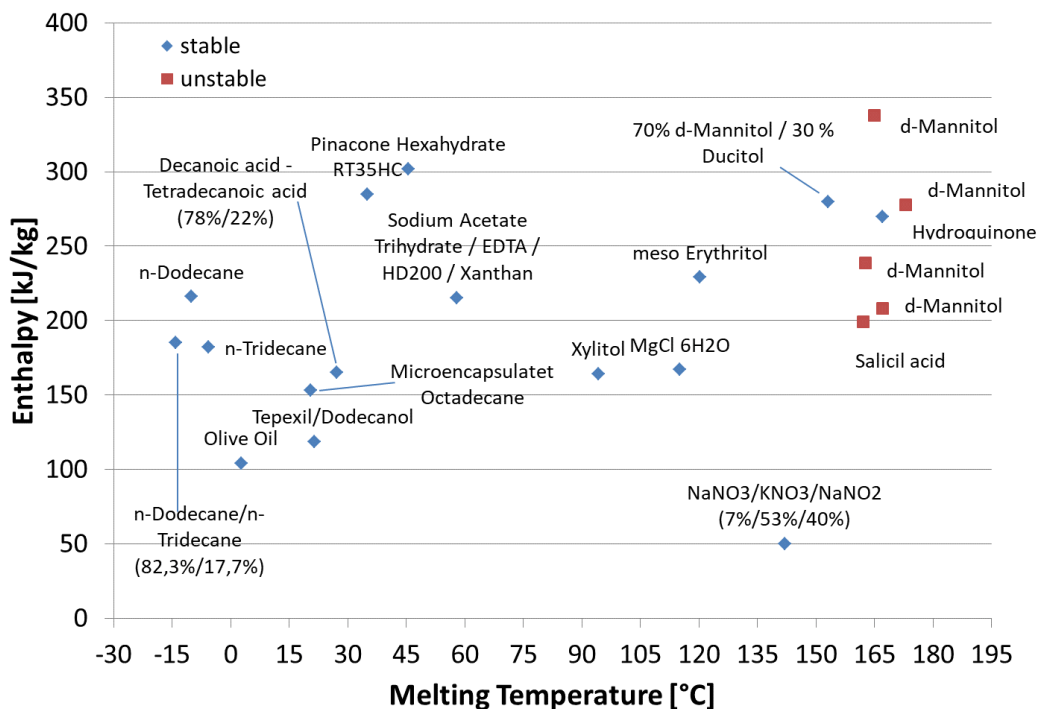


FIGURE 1.2-5: OVERVIEW ON MATERIALS COLLECTED WITH THEIR PHASE CHANGE ENTHALPY AND MELTING TEMPERATURE, RED INDICATES THE UNSTABLE MATERIALS

MEASUREMENT PROCEDURE FOR THERMAL DIFFUSIVITY

An intercomparative test of thermal diffusivity was carried out. The scope of the test was to develop a guideline for determination of thermal diffusivity and conductivity of PCM by means

of flash technique in order to ensure reliable measurement data. The investigated sample material was RT70HC with a melting temperature around 70 °C. Two different cooling rates were used for the sample preparation: slow cooling (2 K/h) or fast cooling (quenching with liquid nitrogen). In the first measurement round, the thermal diffusivity of the solid PCM RT70HC was measured at 40 °C and 50 °C. In the second measurement round, the pulse energy was varied systematically. With rising pulse energy, a trend towards lower thermal diffusivity can be observed for all measurements. In a third measurement round the specimens were prepared by the participating laboratories themselves in order to test the influence of sample preparation. As a consequence, compared to the previous measurement rounds, the standard deviation of the results was increased.

In Figure 1.2-6, the statistical results of the different measurement rounds demonstrate the achievements compared to the results obtained in the previous phase (T42A29). In the case of round 2, with uniform specimen and adjusted pulse energy, a very low standard deviation of less than 3% was observed among the participants.

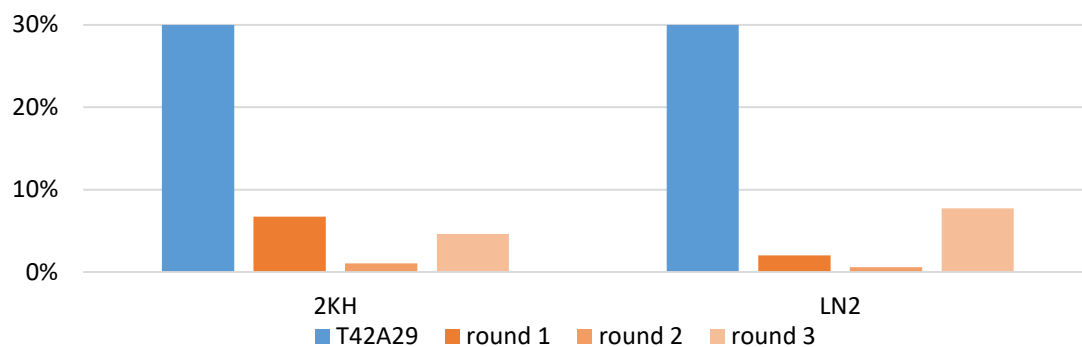


FIGURE 1.2-6: RELATIVE STANDARD DEVIATIONS OF THE MEASUREMENT RESULTS IN THE DIFFERENT MEASUREMENT ROUNDS FOR SPECIMENS WITH DIFFERENT COOLING RATES: 2 K/H (2KH) OR QUENCHING WITH LIQUID NITROGEN (LN2)

MEASUREMENT PROCEDURE FOR VISCOSITY

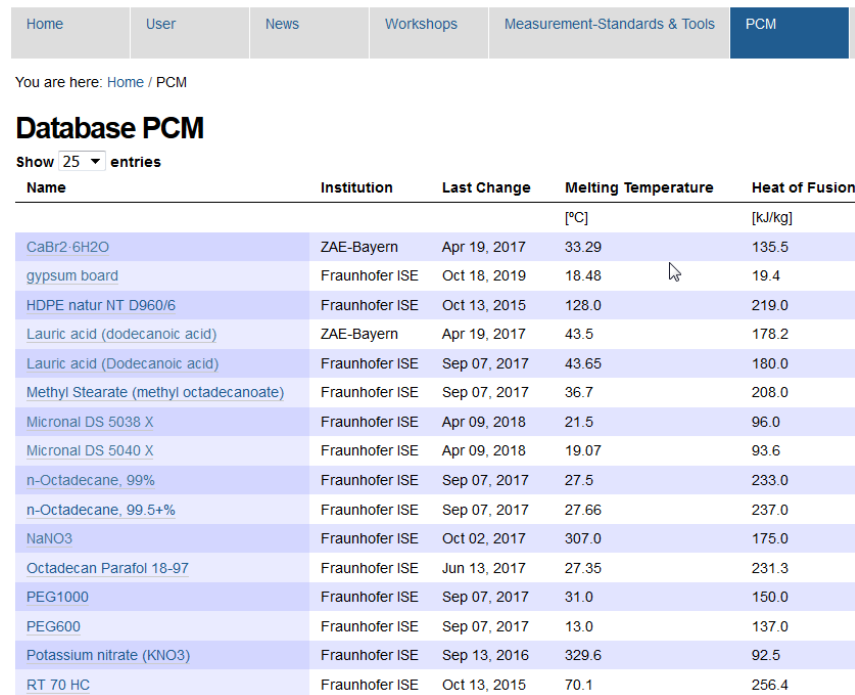
In addition, a measurement procedure for viscosity was developed. Therefore, a workshop on the measurement of viscosity via rotational rheometers was organized. Figure 1.2-7 depicts some impressions from the workshop.



FIGURE 1.2-7: WORKSHOP ON MEASUREMENT OF VISCOSITY VIA ROTATIONAL RHEOMETERS, FROM LEFT TO RIGHT: PRESENTATIONS, THE HIGH TEMPERATURE MEASUREMENT GEOMETRY FILLED WITH MOLTEN NITRATE SALT, FILLING THE GAP FOR THE MEASUREMENT OF RT70HC

PCM DATABASE

New material properties have been feed into the database which was developed during previous tasks and annexes. So far, data of 56 measurements are available in the private section from which 16 datasets are publicly available. Figure 1.2-8 shows on the overview table of public available materials.



Home User News Workshops Measurement-Standards & Tools **PCM**

You are here: Home / PCM

Database PCM

Show 25 entries

Name	Institution	Last Change	Melting Temperature [°C]	Heat of Fusion [kJ/kg]
CaBr ₂ ·6H ₂ O	ZAE-Bayern	Apr 19, 2017	33.29	135.5
gypsum board	Fraunhofer ISE	Oct 18, 2019	18.48	19.4
HDPE natur NT D960/6	Fraunhofer ISE	Oct 13, 2015	128.0	219.0
Lauric acid (dodecanoic acid)	ZAE-Bayern	Apr 19, 2017	43.5	178.2
Lauric acid (Dodecanoic acid)	Fraunhofer ISE	Sep 07, 2017	43.65	180.0
Methyl Stearate (methyl octadecanoate)	Fraunhofer ISE	Sep 07, 2017	36.7	208.0
Micronal DS 5038 X	Fraunhofer ISE	Apr 09, 2018	21.5	96.0
Micronal DS 5040 X	Fraunhofer ISE	Apr 09, 2018	19.07	93.6
n-Octadecane, 99%	Fraunhofer ISE	Sep 07, 2017	27.5	233.0
n-Octadecane, 99.5+%	Fraunhofer ISE	Sep 07, 2017	27.66	237.0
NaNO ₃	Fraunhofer ISE	Oct 02, 2017	307.0	175.0
Octadecan Parafol 18-97	Fraunhofer ISE	Jun 13, 2017	27.35	231.3
PEG1000	Fraunhofer ISE	Sep 07, 2017	31.0	150.0
PEG600	Fraunhofer ISE	Sep 07, 2017	13.0	137.0
Potassium nitrate (KNO ₃)	Fraunhofer ISE	Sep 13, 2016	329.6	92.5
RT 70 HC	Fraunhofer ISE	Oct 13, 2015	70.1	256.4

FIGURE 1.2-8: SCREEN SHOT OF THE PUBLIC AVAILABLE DATASETS (WWW.THERMALMATERIALS.ORG)

PCM Wiki

In order to establish a common wording of relevant phenomena in the context of PCM, a Wiki has been started. Experts have worked on definitions and explanations of terms such as nucleation temperature, supercooling, specific heat determination via DSC etc. The Wiki is open so that everybody can add new terms and definitions or to change/comment on existing ones. Figure 1.2-9 shows a screen shot of the PCM Wiki.

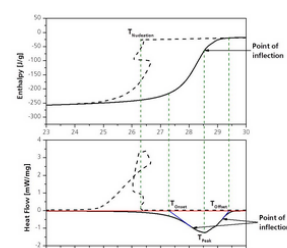
Offset Temperature	Wiki PCM	
Onset Temperature	How to use and edit	
Baseline	To put a new entry to the Wiki go to the Wiki-PCM page and choose "Add new" -> "Page", give the title and go to "Body Text" to write the description. Therefore insert a table with 2 cols and 1 row. Please write text using format "Heading cell" into the left col and put images into the right col. You can also use subheadings to include sub headings in your text.	Please insert images here (tree icon above) (graphs, pictures fotos) use png or jpg format. Best image width is 285 dots. Therefore upload images to the image-folder in Wiki-PCM (see description there).
Melting Temperature	You can publish the new entry by choosing "publish" after you have saved the text (bottom below).	
Nucleation or Crystallization Temperature	Offset Temperature	
Peak Temperature	The extrapolated offset-temperature (according to DIN EN ISO 11357-1:2010-03) is the designed intersection point of the extrapolated baseline and the inflectional tangent at the end of the melting or crystallization peak (see image onset temperature). The baseline and the inflectional tangent are determined from the temperature-dependent heat flow signal.	
Enthalpy	Onset Temperature	
Zero-line	The extrapolated onset-temperature (according to DIN EN ISO 11357-1:2010-03) is the designed intersection point of the extrapolated baseline and the inflectional tangent at the beginning of the melting or crystallization peak. The baseline and the inflectional tangent are determined from the temperature-dependent heat flow signal. In the case of pure and homogeneous materials, the onset-temperature can be indicated as melting temperature. In contrast to peak-temperature, the onset-temperature is less dependent on heating rate and sample mass. Furthermore onset-temperatures are usually used for temperature calibration of a DSC.	
Subcooling		
Supercooling		
T-History		
Nucleation		
DSC		
Specific heat determination (DSC)		

FIGURE 1.2-9: SCREEN SHOT OF THE WIKI FOR PCM (WWW.THERMALMATERIALS.ORG/WIKI-PCM)

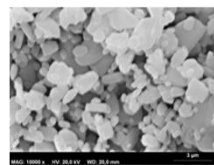
SUBTASK 2T

Subtask 2T "Development and Characterization of Improved TCM" included 4 activities:

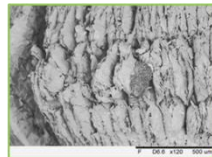
- Develop and identify novel chemical reactions and composite materials
- Define relevant material parameters
- Characterize novel reactions and materials by material properties
- Maintenance and expansion of the material database implemented in Task42/Annex 29

DEVELOPMENT OF NEW TCM MATERIALS AND COMPOSITES

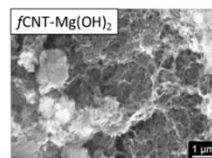
The development of improved TCM included sorption materials (micro/mesoporous solids and liquids), chemical reactions (salt hydrates and metal oxides/hydroxides), and combinations of both (zeolites/graphite + salt hydrates/metal oxides). Figure 1.2-10 shows microscope images different TCM materials developed and/or characterized by participants.



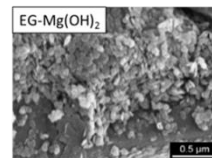
$\text{CaC}_2\text{O}_4 \cdot \text{H}_2\text{O}$
Institute of Applied
Synthetic Chemistry
(TU Wien)
Dr. Peter Weinberger



Vermiculite- CaCl_2
Swansea University
Dr. Jonathon Elvis



Carbon nanotube- $\text{Mg}(\text{OH})_2$



Expanded graphite- $\text{Mg}(\text{OH})_2$
University of Messina –
Engineering Department
Prof. dr. Candida Milone

FIGURE 1.2-10: IMAGES OF TCM MATERIALS DEVELOPED AND INVESTIGATED WITHIN THE GROUP OF EXPERTS

Sorption materials with desorption temperatures between 80 °C and 140 °C and desorption enthalpies up to 2.200 kJ/kg on material level were investigated (Figure 1.2-11).

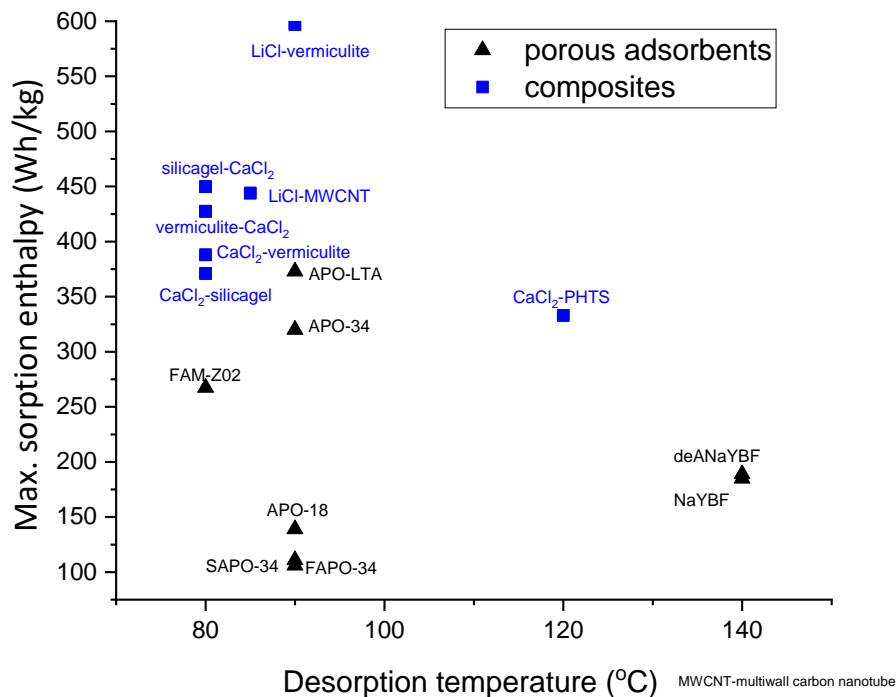


FIGURE 1.2-11: MAX. SORPTION ENTHALPY VERSUS DESORPTION TEMPERATURE OF POROUS SOLIDS AND COMPOSITES (ADSORBATE: WATER)

Chemical reactions with reaction temperatures up to 800 °C showed reaction enthalpies up to 1.500 kJ/kg on material level (Figure 1.2-12).

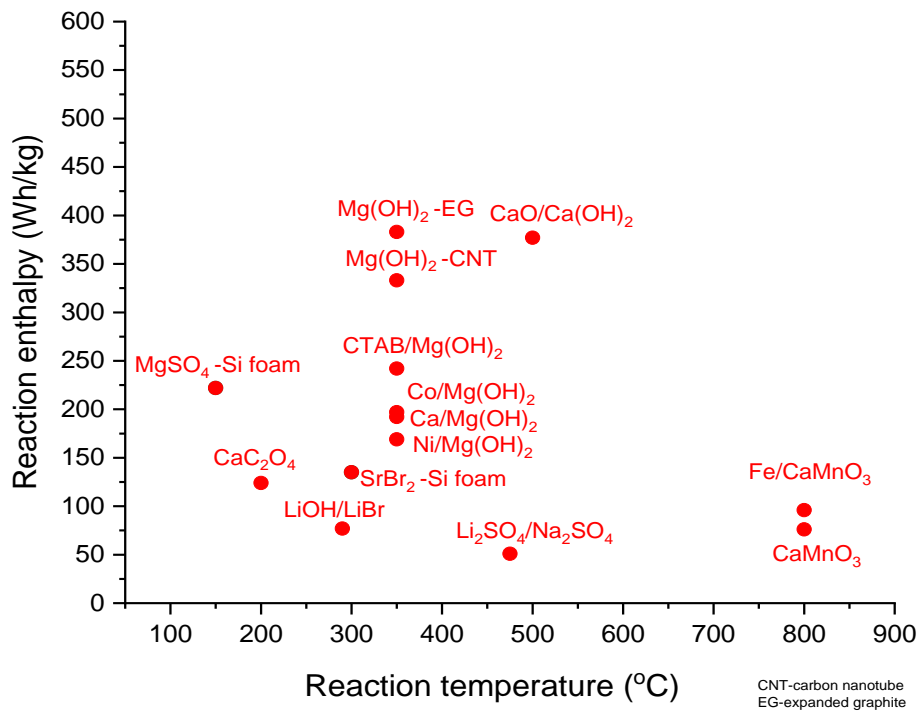


FIGURE 1.2-12: CHEMICAL REACTIONS AND COMPOSITES INVESTIGATED AS TCM: REACTION ENTHALPIES VS. TEMPERATURE

TCM DATABASE

Due to complexity and different relevant materials properties, it was decided to prepare three databases: one on chemical reactions (salt hydrates, oxides, composites), one on adsorption (porous solids and composites), and one on absorption (liquids). A screen shot of the chemical reaction database is shown in Figure 1.2-13.

Basic chemical composition	Name Dopant	Name Stabilizer/Matrix	E/V (kWh/m ³)	T _{eq} @ x mbar (K)	Price (€/kg)	Institute
K ₂ CO ₃ *1.5H ₂ O	-	-	-	-	1	Technical University of Eindhoven
MgCl ₂ *6 H ₂ O	-	-	-	-	-	Technical University of Eindhoven
Na ₂ S*5 H ₂ O	-	-	-	-	-	Technical University of Eindhoven
NaOH / H ₂ O	-	-	-	-	0,30	Empa
Mg(OH) ₂	-	-	194	531	-	University of Messina-Engineering Department
Mg(OH) ₂ + C	-	Expanded graphite	330	531	-	University of Messina-Engineering Department
Mg(OH) ₂ + C	-	Functionalized Carbon Nanotubes	326	531	-	University of Messina-Engineering Department
Na ₂ S.5H ₂ O	-	-	-	-	0,348	TNO

FIGURE 1.2-13: SCREEN SHOT OF THE CHEMICAL REACTION DATABASE (WWW.THERMALMATERIALS.ORG)

1.2.1 SUBTASK 3 - MEASURING PROCEDURES AND TESTING UNDER APPLICATION CONDITIONS

SUBTASK 3P

PCM testing under application conditions can be considered as a link between the measured material properties in the lab and the observed phase change behaviour of the PCM in an actual application (cf. Figure 1.2-14).

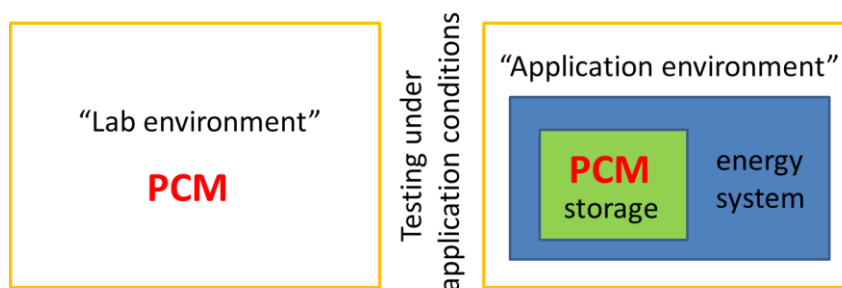


FIGURE 1.2-14: PCM TESTING UNDER APPLICATION CONDITIONS

In this subtask, a comparison of material properties of PCM in the lab environment and under application conditions was elaborated. Thereby, most input was collected for the properties degree of supercooling, phase separation, storage capacity, and long-term stability of PCM.

A step further was taken in the case of long-term stability of PCM: Information on experimental devices that are used by the experts of Task 58 / Annex 33 to investigate the long-term stability of PCM were gathered (some of them are shown in Figure 1.2-15). The experiments include tests on the stability of PCM over thermal cycling, on the stability of PCM with stable supercooling, and on the stability of Phase Change Slurries (PCS).

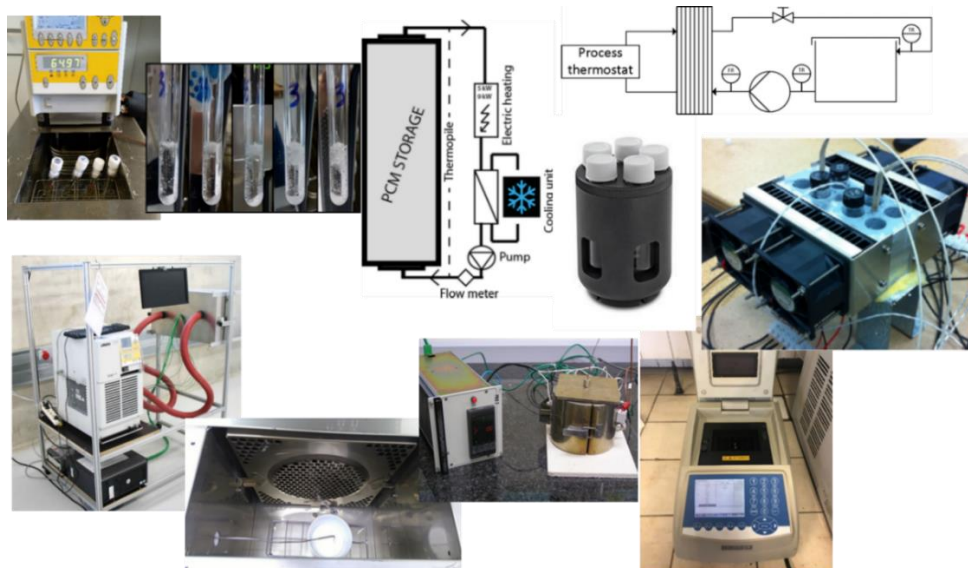


FIGURE 1.2-15: EXPERIMENTAL DEVICES USED BY THE PARTICIPANTS TO INVESTIGATE THE LONG-TERM STABILITY OF PCM

SUBTASK 3T

This Subtask aimed to have reliable thermal analysis methods/protocols and procedures for the characterization of material and reaction properties for sorption and chemical reactions of thermal energy storage (TES) applications.

Therefore, measurement procedures for mass and enthalpy change with defined conditions for sorption materials and salt hydrates were developed. The biggest part of the activities in this subtask was to develop a common sense for enthalpy and mass change measurements of sorption and thermochemical materials as well as a procedure to compare results on lab scale. Different round robin tests on a zeolite and salt hydrate were conducted and evaluated. These results were used to further develop the measurement procedures. In addition, a measurement procedure for specific heat capacity measurements of salt hydrates was tested.

The performed round robin tests showed a good agreement with respect to mass change among the participants. Both enthalpy changes and specific heat capacity showed larger deviations σ :

- Adsorption enthalpy of zeolite 13X: $\sigma(\Delta H_{\max}) \sim 12\%$
- Hydration enthalpy of SrBr \cdot 6H $_2$ O: $\sigma(\Delta H_{\max}) \sim 40\%$
- Specific heat capacity of SrBr \cdot 6H $_2$ O: $\sigma(c_{p,\max}) \sim 23\%$ (Figure 1.2-16)

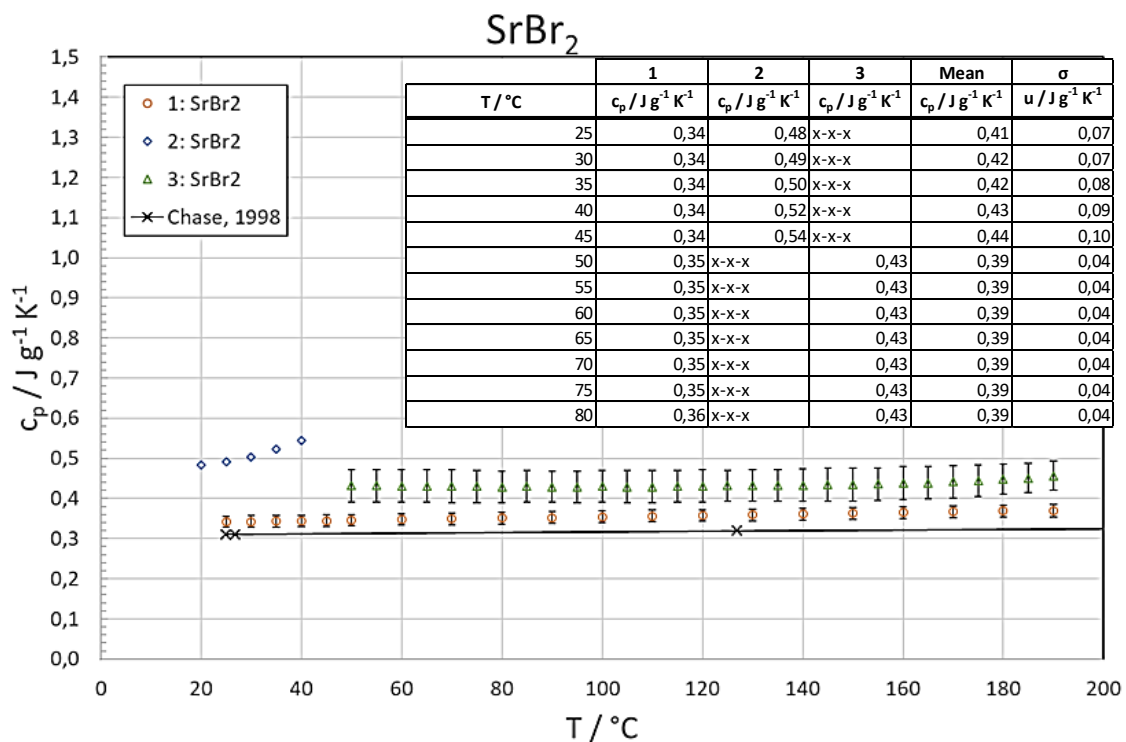


FIGURE 1.2-16: THE ROUND ROBIN TEST OF THE SPECIFIC HEAT CAPACITY OF A SALT HYDRATE SHOWED DEVIATIONS UP TO 23%

The deviations in terms of enthalpy point to the necessity to proceed with developing standardized measurement methods including sample preparation and handling.

1.2.2 SUBTASK 4 - COMPONENT DESIGN FOR INNOVATIVE TES MATERIALS

SUBTASK 4P

Latent heat storage systems using PCM should meet the application requirements in terms of technical and economical parameters. Among the technical parameters, high thermal power is one of the most challenging characteristics. Most of the materials used as PCM have an intrinsically low thermal conductivity, for which component design has to compensate for.

Several finished and ongoing projects have worked on improving the design of PCM components (storage containment, heat exchangers) with the aim to increase the thermal performance. As a first step for a performance comparison between the different solutions, this subtask listed the various concepts, previously or currently studied, for PCM thermal storage in terms of geometries, heat exchange systems and the nature of the PCM used. The following figures, Figure 1.2-17 to Figure 1.2-20, show examples of storage concepts developed by the participants.

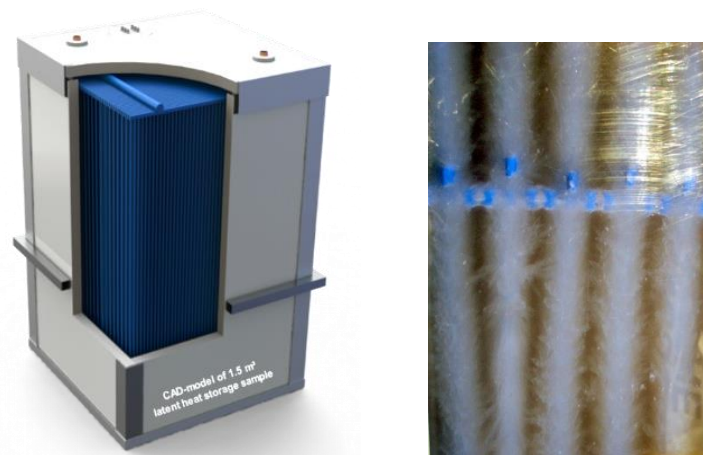


FIGURE 1.2-17: LEFT: CAD MODEL OF A PCM STORAGE WITH CAPILLARY TUBE HEAT EXCHANGER (SOURCE: ZAE BAYERN), RIGHT: PCM CRYSTALLIZING AT CAPILLARY TUBES (SOURCE: ZAE BAYERN)

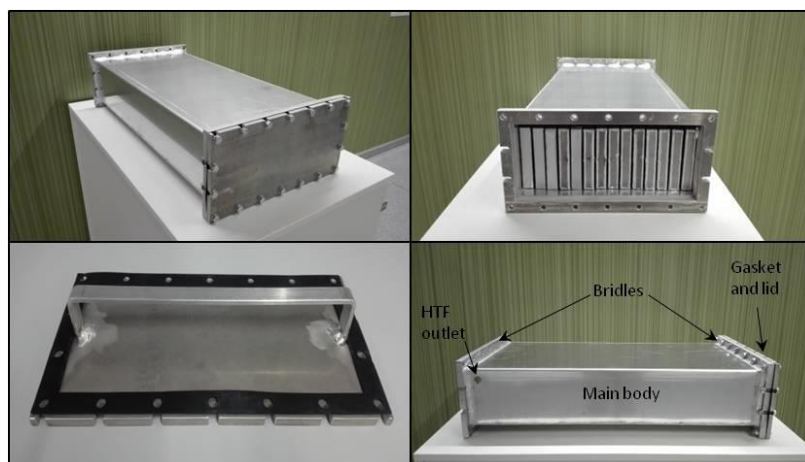


FIGURE 1.2-18: A LABORATORY-SCALE TES SYSTEM WITH MACROENCAPSULATED PCM IN FLAT PLATES PLACED IN PARALLEL (SOURCE: DIARCE ET AL. 2018).

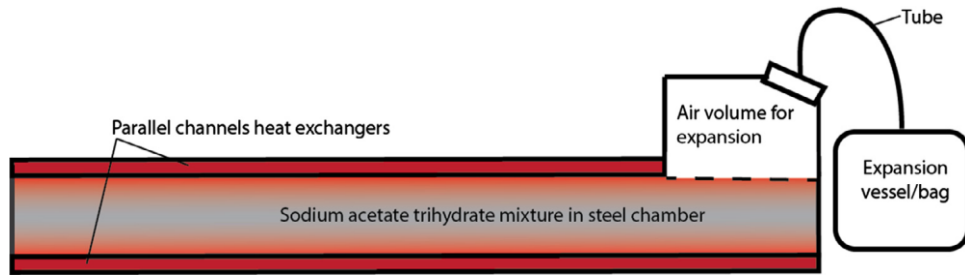


FIGURE 1.2-19: FLAT PLATE STORAGE WITH PCM CHAMBER AND EXTERNAL EXPANSION (SOURCE: DANNEMAND ET AL. 2016).

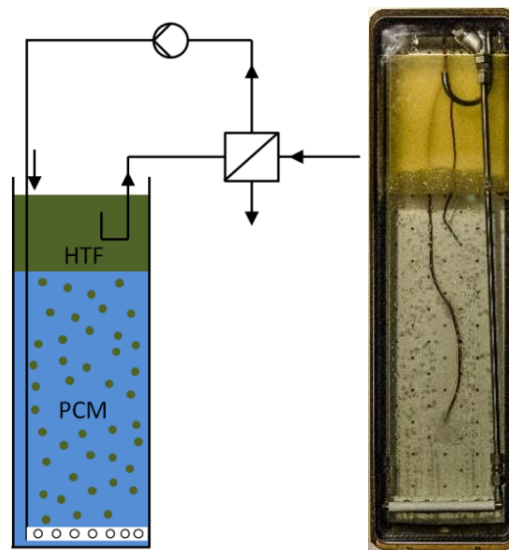


FIGURE 1.2-20: (LEFT) SCHEMATIC REPRESENTATION OF DIRECT CONTACT LATENT HEAT STORAGE PRINCIPLE WHERE THE HTF IS FLOWING DIRECTLY THROUGH THE PCM EXCHANGING HEAT AT THE BUBBLE/PCM INTERFACE AND CAUSING SOLIDIFICATION OR MELTING OF THE STORAGE MATERIAL; (RIGHT) DIRECT CONTACT LATENT HEAT STORAGE TEST-RIG DEVELOPED AT LUCERNE UNIVERSITY OF APPLIED SCIENCES AND ARTS (SOURCE: LUCERNE UNIVERSITY OF APPLIED SCIENCES AND ARTS)

Following this, a definition of performance for PCM components in term of capacity and storage density was agreed upon. In order to be able to compare different PCM concepts in terms of power, a review on assessment approaches was carried out. Therefore, power-time curves upon charging and discharging were compared (cf. Figure 1.2-21), preliminary performance parameters were defined, and a procedure based on a validated numerical model was proposed.

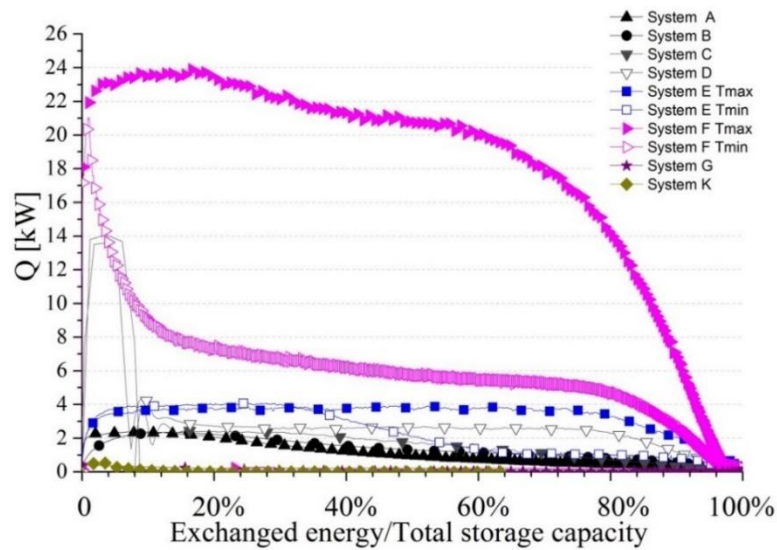


FIGURE 1.2-21: HEAT EXCHANGE RATE OVER STATE OF CHARGE OF THE PCM COMPONENTS STUDIED IN SUBTASK 4P

SUBTASK 4T

In the case of TCM component design, the starting point was a basic description of investigated TCM storage processes and their impact on the component design. In addition, an inventory of actual TCM component designs currently under investigation was elaborated. The following figures, Figure 1.2-22 to Figure 1.2-24, show examples of storage concepts developed by the participants.

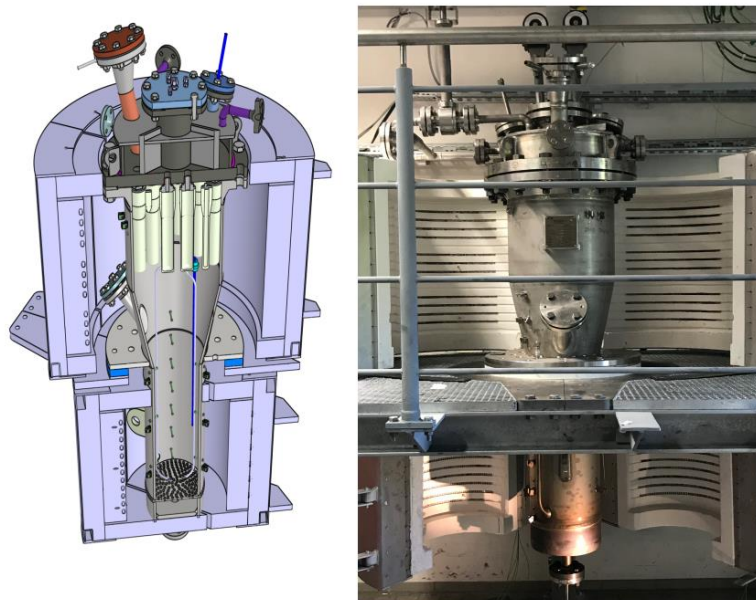


FIGURE 1.2-22: 3D-CAD IMAGE AND PHOTO OF THE FLUIDIZED BED REACTOR FOR HIGH TEMPERATURE HEAT STORAGE USING A REVERSIBLE CHEMICAL GAS-SOLID REACTION USING STEAM AND METAL OXIDES SUCH AS $\text{CaO}/\text{Ca}(\text{OH})_2$ OR $\text{MgO}/\text{Mg}(\text{OH})_2$ (SOURCE: TECHNICAL UNIVERSITY MUNICH)

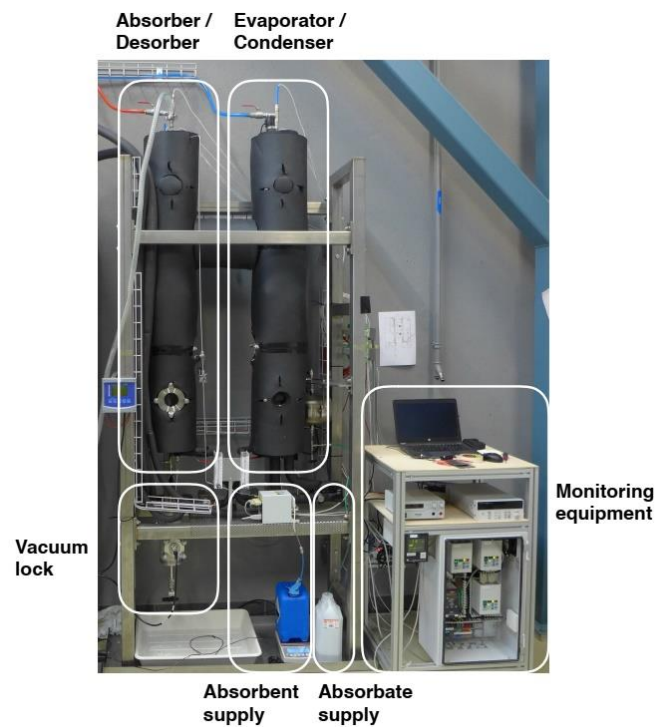


FIGURE 1.2-23: SCHEMATICS AND PICTURE OF EMPA'S NaOH / H₂O LABORATORY LIQUID ABSORPTION SYSTEM (SOURCE: EMPA)

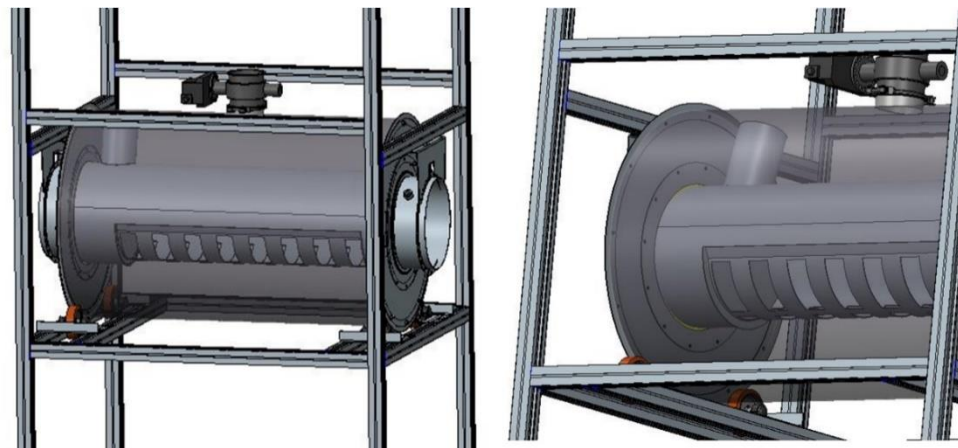


FIGURE 1.2-24: CONSTRUCTION DETAILS OF THE ROTATING CYLINDRICAL ADSORPTION REACTOR USING ZEOLITE-WATER AS SORPTION WORKING PAIR (SOURCE: UNIVERSITY FOR APPLIED SCIENCE UPPER AUSTRIA)

To compare and discuss different TCM component concepts, a common graphical representation was used to classify the concepts as open or closed and fixed or transported systems (Figure 1.2-25).

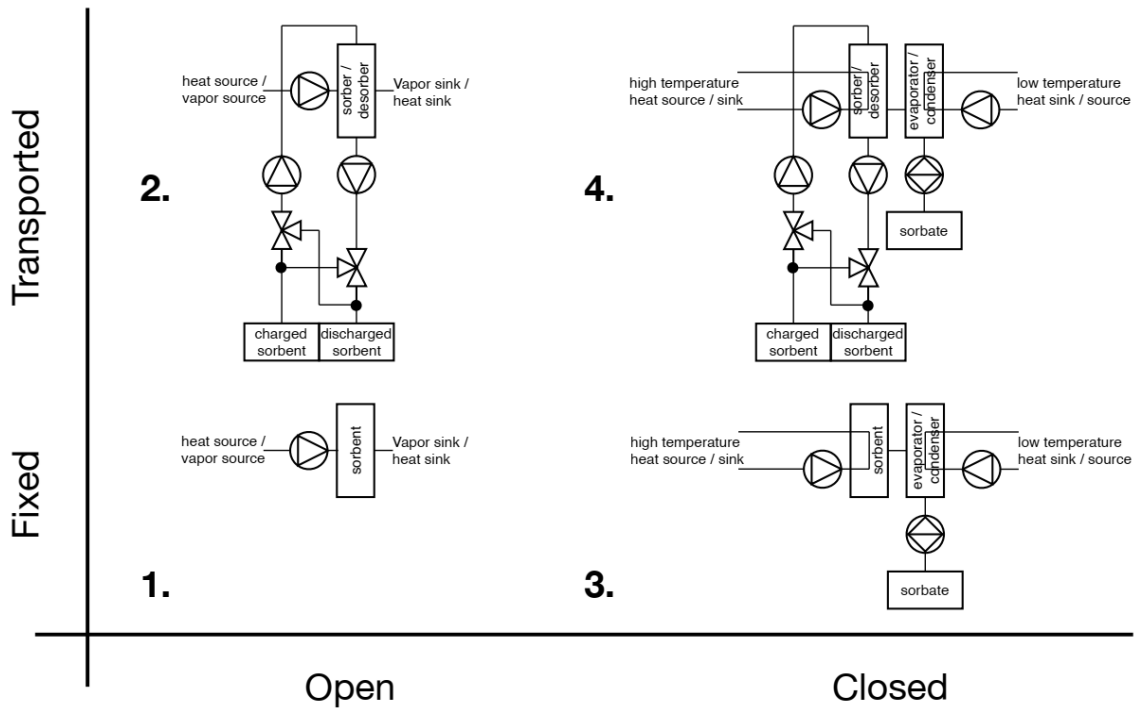


FIGURE 1.2-25: ILLUSTRATION OF THE BASIC SORPTION HEAT STORAGE SYSTEMS.

Further efforts were undertaken to identify a possible TCM performance degradation from lab-scale measurements to pilot installations. A “Do’s and Don’ts” paper in the context of TCM component design is currently in preparation.



SHC | 58
ECES | 33



FINAL REPORT

1 OBJECTIVES, STRUCTURE AND APPROACH OF THE ANNEX

1.1 OBJECTIVES

The overall goal of Annex 33 is to support an application-oriented development of innovative and compact thermal energy storage materials: Phase Change Materials (PCM) and Thermochemical Materials (TCM). This includes the following objectives :

- Mapping and evaluating the TES application opportunities concerning the requirements for the storage material
- Development and characterisation of storage materials to enhance TES performance
- Development of materials characterisation procedures and a methodology for material testing under application conditions
- Development of components for compact thermal energy storage systems

1.2 SCOPE

This joint Annex/Task deals with advanced materials for latent and thermochemical energy storage: Phase Change Materials (PCM) and Thermochemical Materials (TCM).

It covers the material development, the characterization, and the testing under application conditions. Finally, it describes the interaction between material and the storage component and the expected storage performance of the innovative materials.

Because seasonal storage of solar heat for solar assisted heating of buildings is the main focus of the IEA-SHC TCP, this will also be a focus area of this task. However, because there are many more relevant applications for TES, and because material research is not and cannot be limited to one application only, this task will include multiple application areas.

1.3 STRUCTURE AND APPROACH OF THE ANNEX

The work of the Annex has been divided into Subtasks. Two of the planned subtasks concentrate on the material itself, its characterization, and the definition of testing procedures. Subtask 1 and 4 deal with the relation between the new material and the storage component and the actual application, respectively.

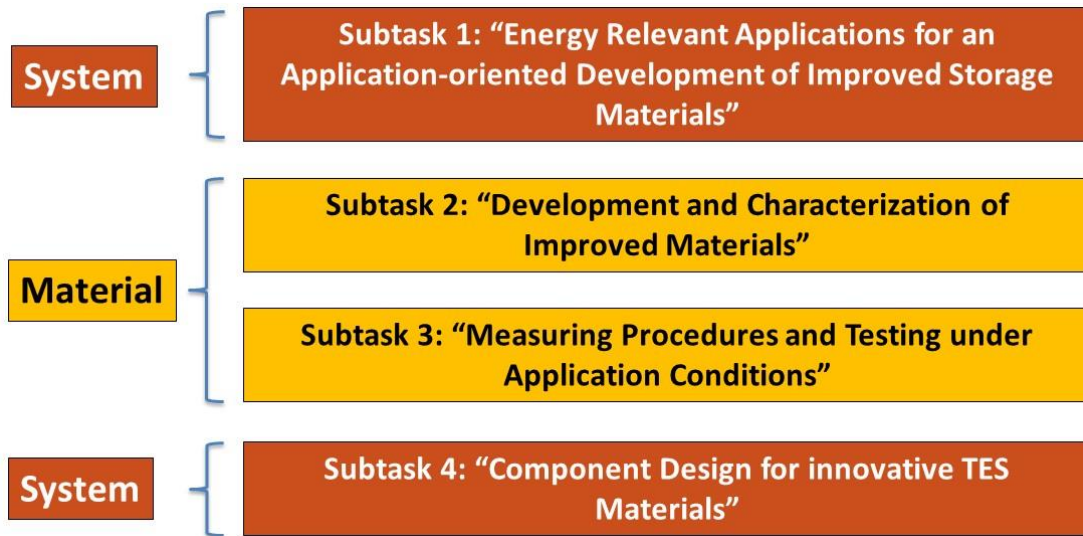


FIGURE 1-1: SUBTASK STRUCTURE OF ANNEX 33

There are two reasons for a further breakdown of the materials and components subtasks into a PCM (-P) and a TCM (-T) track. The first reason is that, although there are a lot of common approaches for the two classes of materials, the basic materials principles differ and need a different approach. The second reason is that, with the relatively high number of experts, it is more effective to break down the work in a larger number of subgroups. However, this holds not for subtask 1 which is valid for both storage technologies. Subtasks were divided as follows:

PCM	TCM
Subtask 1: "Energy Relevant Applications for an Application-oriented Development of Improved Storage Materials"	
Andreas Hauer (ZAE, DE) /Wim van Helden(AEE Intec, A)	
Subtask 2: "Development and Characterization of Improved Materials"	
Stefan Gschwander (ISE, DE)	Alenka Ristic (NIC, SI)
Subtask 3: "Measuring Procedures and Testing under Application Conditions"	
Christoph Rathgeber (ZAE, DE)	Daniel Lager (AIT, A)
Subtask 4: "Component Design for innovative TES Materials"	
(Ana Lazaro, Uni Zaragoza, ES)	Benjamin Fumey (EMPA, CH)

FIGURE 1-2: SUBTASK LEADERS OF THE PCM AND THE TCM TRACKS OF ANNEX 33

Under each subtask (for the PCM and the TCM track), a subtask leader was appointed.

1.4 MEETINGS AND PARTICIPATING COUNTRIES AND TCPs

Six experts meetings and workshops were held. The table below gives an overview of the location and the number of participants of the expert meetings.

#	Location	Country	Date	Participants
1	Lyon	France	April 5-7, 2017	64
2	Zurich	Switzerland	October 4-6, 2017	46
3	Ljubljana	Slovenia	April 9-11, 2018	45
4	Graz	Austria	October 1-2, 2018	42
5	Ottawa	Canada	May 1-3, 2019	43
6	Messina	Italy	October 9-10, 2019	42

Table 1-1: Participating Countries

Country	Participant
Germany	ZAE Bayern
Germany	Fraunhofer ISE
Belgium	Univ. Mons
France	Univ. Bordeaux
Slovenia	NIC
Spain	Univ. Lleida
Spain	Univ. Zaragoza
Sweden	KTH
Switzerland	EMPA
Turkey	Çukurova Univ.

The list contains only the countries officially participating through the Energy Storage TCP. For example countries like Austria and Italy participated through the Solar Heating and cooling TCP in the beginning.

Overall more than 13 countries participated in the experts meetings and workshops.

2 SUBTASK 1 – ENERGY RELEVANT APPLICATIONS FOR AN APPLICATION-ORIENTED DEVELOPMENT OF IMPROVED STORAGE MATERIALS

2.1 THE APPROACH OF APPLICATION-ORIENTED DEVELOPMENT OF IMPROVED STORAGE MATERIALS

The energy density of a storage material or its specific storage capacity – energy stored per mass or volume – is not a material property! It is strongly depending on the operation conditions during charging and discharging. Therefore, it can be described as a process variable. The storage process is depending on the actual storage application. Parameters like the available charging temperature and the usable temperature at the consumer side are determined by the application.

The goal of this subtask is to provide a list of thermal energy storage applications relevant for our future energy system. The storage application sets the technical and economic environment of the storage system and defines the operation conditions. These conditions include available charging and required discharging temperatures, available and required thermal power in- and output, as well as the available reactant concentrations for the process in the case of thermochemical energy storage.

The list could also include parameters like the expected number of storage cycles, the predicted lifetime and the required system size. All these parameters can be utilized for integrated system simulations, which finally can give first estimations of performance improvement of the new storage materials.

This cross-cutting subtask was planned as an ongoing discussion forum, where the material designers meet the application engineers and, thus, the gap between these two groups could be bridged.

The actual approach is starting from defining relevant applications. In a next step these applications provide operation conditions. It has to be investigated, whether the class of applications provides standard conditions or more individual energy storage solutions. The identified operation conditions are the basis of any application-oriented testing of novel thermal energy storage materials.

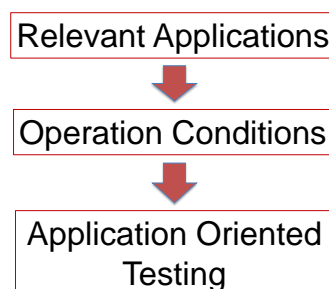


FIGURE 2-1: APPROACH OF SUBTASK 1 TOWARDS AN APPLICATION-ORIENTED TESTING

2.2 WHAT ARE ENERGY RELEVANT APPLICATIONS?

Energy relevant applications for thermal energy storage systems can be described by their impact on the energy system. This impact can be quantified with respect to the overall CO₂ emission or to the final energy demand connected to this class of applications.

2.2.1 RELEVANCE BY STATISTICS

Looking at the statistical sectors – industry, private households, trade & commerce, and transport – the CO₂ emissions and final energy demand can be visualized. Figure 2-2 shows the different energy forms responsible for these emissions in Germany. With focus on thermal energy, like process heat, space heating, domestic hot water (DHW), process cold and AC cold, the sectors industry, private households, trade & commerce seem to be relevant.

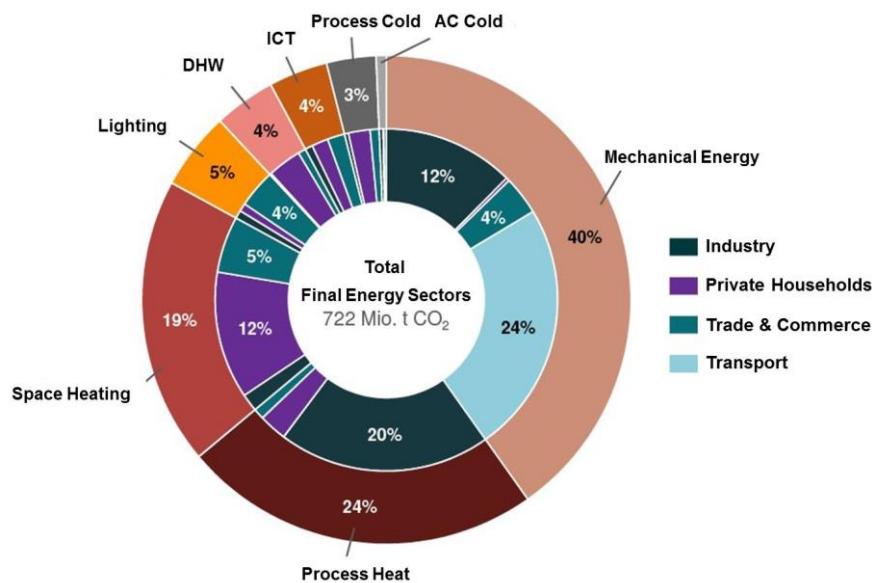


FIGURE 2-2: CO₂ EMISSIONS IN GERMANY LINKED TO STATISTICAL SECTORS AND ENERGY DEMAND [M. RASCH, A. REGETT, S. PICHLMAIR, J. CONRAD, S. GREIF, A. GUMINSKI, E. ROUYRRE, C. ORTHOFER AND T. ZIPPERLE, EINE ANWENDUNGSORIENTIERTE EMISSIONSBILANZ – KOSTENEFFIZIENTE UND SEKTORENÜBERGREIFENDE DEKARBONISIERUNG DES ENERGIESYSTEMS, FORSCHUNGSSTELLE FÜR ENERGIEWIRTSCHAFT FFE, BWK, AUSGABE 03/2017]

From the figure it is obvious that thermal energy demand and the connected emissions are with more than 50% the dominant factor for any measures to stop the global warming. This is a strong point for the relevance of thermal energy storage to support the integration of renewables and to increase energy efficiency in general.

2.2.2 RELEVANT APPLICATIONS

The most relevant fields of application for thermal energy storage systems can be defined as:

- Industrial Processes
- Buildings

These two fields of application would stand for 27% (process heat and cold) and 24% (space heating, DHW and AC cold) of the CO₂ emissions in Germany.

In an earlier phase of this Annex, the following figure (Figure 2-3) was published. It shows the possible energy source for the storage system, it describes the main properties of the storage systems, and finally it gives the final demand at the consumer side. The list is not complete and is based on the actual activities within the Annex.

Source	Storage	Demand
Waste Heat	short term high power	Drying Cooling
Solar Thermal	long term high capacity	Heating DHW
	short term high power	Cold (AC) Dehumidification
Electricity (renewable or „price difference“)	short term high power	Cold (AC) Dehumidification
CSP	short term high temperature	Power Plant (turbine)
CHP	short term high capacity	Heating DHW

FIGURE 2-3: ENERGY STORAGE CONFIGURATIONS BY SOURCE, STORAGE AND DEMAND

In the last phase of the Annex, this list was updated and only the most relevant applications were extracted:

- Industrial batch processes and peak shaving applications
- Heating and cooling for single family households (HVAC systems in the building sector)
- Combined heat and power systems
- District heating systems

In a first attempt, it was tried to collect operation conditions from these applications. And, if possible, to extract reference conditions for material testing.

2.3 HOW TO DEFINE OPERATION CONDITIONS

In order to develop a novel material for thermochemical heat storage (TCM), a strong link to the targeted application is crucial. The proposed approach offers an easy method for first experimental testing of new materials under real conditions.

First step is the material characterization, where parameters like the melting or reaction enthalpy / sorption enthalpy have to be measured. These measurements give a maximum value for the achievable storage capacity. The next step is the material evaluation under reference conditions given by the actual application. Goal of these experimental investigations is a first

quantification of the achievable storage capacity. After this step, it is possible to compare the novel PCM- or TCM-system to sensible heat storage (with hot water for example) systems.

2.3.1 WHY FOCUS ON TEMPERATURES?

The most important parameters for the evaluation of a latent or thermochemical storage system are the temperatures involved. By adjusting just these temperatures, the achievable storage capacity can be experimentally quantified. Any other operation conditions like the thermal power requirement or the number of cycles shall be neglected at this first step of testing under application conditions. The presented approach will focus exclusively on the temperatures as the operation conditions.

2.4 DEFINITION OF TEMPERATURES FOR PCM AND TCM STORAGE SYSTEMS TO DESCRIBE THE OPERATION CONDITIONS

2.4.1 2-TEMPERATURE-APPROACH FOR PCM

For PCM thermal energy storage systems, 2 temperatures are sufficiently describing the charging and discharging process in any application.

- **Charging Temperature T_{Char}** : The necessary charging temperature is given by the melting temperature of the PCM. It has to be above the melting temperature in order to melt the PCM in the charging process. The minimum necessary temperature difference between charging and melting temperature, as fixed value for each material, is given by heat exchanger design.
- **Consumer Temperature T_{Cons}** : The necessary discharge temperature is given by the application. Each application has its own fixed usable temperature level. Below this level heat cannot be used. The consumer temperature should be below the melting temperature in order to utilize the melting enthalpy. The minimum necessary temperature difference between melting temperature and usable temperature level is given by heat exchanger design.

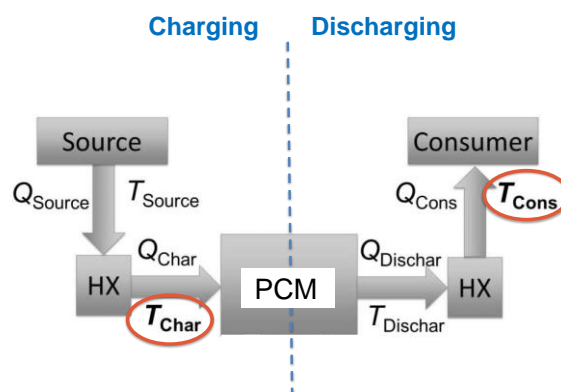


FIGURE 2-4: SCHEME OF A PCM SYSTEM AND THE 2 RELEVANT TEMPERATURES DURING CHARGING AND DISCHARGING

2.4.2 4-TEMPERATURE-APPROACH FOR TCM

For thermochemical energy storage, not only the heat transport in and out of the material, described by the temperatures, but also the mass transfer, given by the concentrations of the reactants, defines the achievable storage capacity. The concentrations however can be translated into available temperatures. These temperatures could be equivalent to partial pressures or dewpoints (in the case of water as the reactant) in open systems. In closed systems, the concentrations are given by the temperature of the condenser and the evaporator. In the following, these temperatures are called “ambient” temperatures because they determine the actual heat flux in or out of the thermochemical energy storage system. Thus, 4 temperatures are necessary to describe the charging and discharging process in any application.

- **Charging Temperature T_{Char}** : The available charging temperature, which is depending on the temperature of the heat source and the quality of the heat exchanger.
- **T_{AmbChar} (only for TCM)**: The ambient condition during charging is given by the dew point or partial pressure or concentration of the reactant for an open system and by the condenser temperature for a closed system.
- **Consumer Temperature T_{Cons}** : The minimum required temperature for the consumer (including the necessary temperature difference for the heat exchanger).
- **$T_{\text{AmbDischar}}$ (only for TCM)**: The ambient condition during discharging is given by the dew point or partial pressure or concentration of the reactant for an open system and by the evaporator temperature for a closed system.

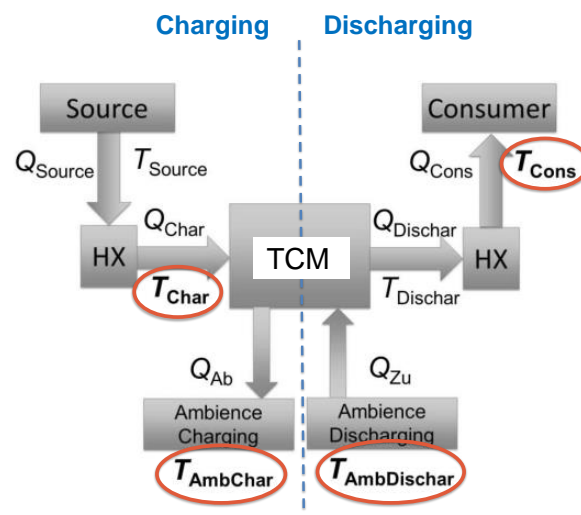


FIGURE 2-5: SCHEME OF A TCM SYSTEM AND THE 4 RELEVANT TEMPERATURES DURING CHARGING AND DISCHARGING

2.5 COLLECTION OF OPERATION CONDITIONS

The participants were asked to fill in a template for the most relevant applications in order to identify the operation temperatures according to the above-mentioned methodology. The results are summarized in Table 2-1.

2.5.1 BUILDING APPLICATIONS

Table 2-1 shows the results for building applications. It is also indicated where the data come from.

TABLE 2-1: OPERATION TEMPERATURES OF MOST RELEVANT APPLICATIONS IN THE BUILDING SECTOR ACCORDING TO PARTICIPANTS INPUT

Institution	Application	T Charging	T Amb Char	T Consumer	T Amb Dischar
Buildings					
ZAE Bayern	Solar Thermal / Seasonal TES / Heating (Low-T)	100 °C	25 °C	40 °C	0 °C
ZAE Bayern	Solar Thermal / Seasonal TES / Heating (Low-T) + UTES	100 °C	25 °C	40 °C	10 °C
ZAE Bayern	Solar Thermal / Seasonal TES / Heating (convent.)/DHW + UTES	100 °C	25 °C	65 °C	11 °C
DTU COMTES de	Solar Thermal/ Seasonal TES/ DHW+SH + combined short and long-term heat storage in "Smart" energy systems	90 °C		<=45 °C	
DTU Building hea	Solar Thermal/ Seasonal TES/ DHW+SH + combined short and long-term heat storage in "Smart" energy systems	90 °C		45 °C	
DTU LOT (Latent	DHW	70 - 90 °C		45-60 °C	
Univ. Artois (Lab	Solar Domestic Water Heating Systems (SDWHS)	<90°C		50°C	
AEE Intec	Solar Thermal /Seasonal TES / Heating	100 °C	10-15 °C	40 °C	10-15 °C
AEE Intec	Solar Thermal (evacuated tube) /Seasonal TES / Heating	180 °C	10-15 °C	40 °C	10-15 °C
ASiC	Solar Thermal /Seasonal TES / Heating(Low-T) + DHW	160°C	15-20°C	60°C	5-10°C
AEE Intec	Electricity/short or mid term storage/DHW & SH	<200 °C	65-15 °C	65 °C	10-15 °C
Uni Zaragoza	Heat Pump+short term TES (heating)	60 °C	20 °C	45 °C	10 °C
Uni Zaragoza	Heat Pump+short term TES (cooling)	5 °C	25 °C	10 °C	28 °C

Figure 2-6 shows the provided charging and consumer temperature for heating and domestic hot water applications. All applications are based on a solar-thermal input. This limits the charging temperatures below or around 100 °C. Exceptions are coming from systems assuming high temperature thermal collectors (e.g. vacuum tubes) or electrical heating systems. The heat pump and cooling applications were not included in the figure.

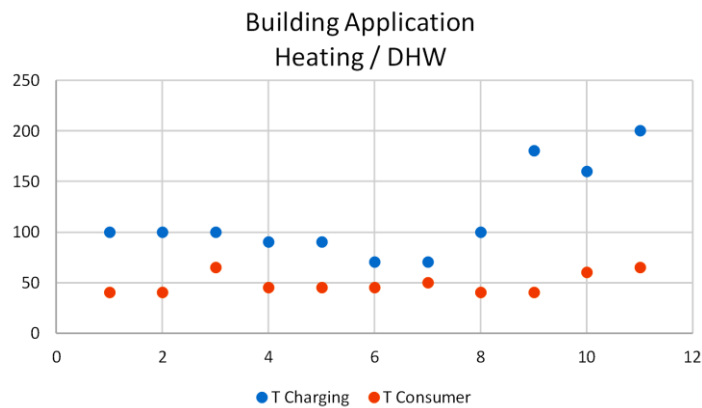


FIGURE 2-6: CHARGING AND CONSUMER TEMPERATURE FOR BUILDING APPLICATIONS

For the class of building applications, it seems possible to define reference conditions or at least temperature ranges in which a first material testing could be performed. Following the template, this could be:

- **Charging Temperature T_{Char}** : 70 – 100 °C
- T_{AmbChar} : 10-25 °C
- **Consumer Temperature T_{Cons}** : 40 – 65 °C
- $T_{\text{AmbDischar}}$: 0 – 15 °C

For a “worst case” testing, the lowest charging temperature combined with the highest ambient temperature during charging and the highest consumer temperature combined with the lowest ambient temperature during discharging should be used. The resulting achievable storage capacity will be remarkably lower compared to a “best case” scenario using the reversed assumptions for the operation temperatures.

A different approach based on existing standards for the building sector is presented later in section 2.6.

2.5.2 OTHER APPLICATIONS

The other relevant applications - combined heat and power, district heat and process heat – are listed in Table 2-2.

TABLE 2-2: OPERATION TEMPERATURES OF MOST RELEVANT APPLICATIONS IN OTHER SECTORS ACCORDING TO PARTICIPANTS INPUT

Institution	Application	T Charging	T Amb Char	T Consumer	T Amb Dischar
	Combined Heat & Power				
ZAE Bayern	CHP Waste Heat (low-T)/ Short Term TES / Process Heat (Food Industry)	80 °C	20 °C	100-110 °C	20 °C
ZAE Bayern	CHP Waste Heat (combustion gases)/ Short Term TES / Process Heat (Food Industry)	350 °C	20 °C	100-110 °C	21 °C
	District Heating				
AEE Intec	Renewable Electricity / Short Term TES / District Heating	> 100 °C	10-20 °C	80 °C	10-20 °C
	Process Heat				
Univ. Artois	Solar Wall / / Daily TES / Process Heat (Greenhouse effect)	<80°C		25°C - 35°C	
TUM	Renewable Electricity / Power-to-Process Heat & Power	> 650°C	160°C	475°C	120°C
TUM	Renewable Electricity / Power-to-Process Heat	> 650°C	160°C	192°C	90-100°C

The content of Table 2-2 is coming from actual R&D project of the international participating institutes. It is no representative view on the real situation of relevant application. However, it remains obvious, that a certain set of reference temperatures cannot be identified for the listed applications. Especially in the field of process heat and industrial applications, the diversity of operation conditions is huge. Thus, no reference conditions can be defined at the moment.

2.6 TEMPERATURE GUIDELINE FOR TESTING COMPACT THERMAL ENERGY STORAGE SYSTEMS IN BUILDINGS

Within the course of the Annex, a guideline concerning the testing of compact thermal energy storage was developed. This guideline focusses on the operation temperatures and develops a detailed procedure for PCM and TCM systems.

Authors: Fumey B.^{1,*}, Baldini L.¹, Lazaro A.², Fischer F.³, Hauer A.³, Englmaier G.⁴, Furbo S.⁴, Zettl B.⁵, Cuypers R.⁶, Köll R.⁷, van Helden W.⁷

1. Empa Swiss Federal Laboratories for Materials Science and Technology, Überlandstrasse 129, 8600 Dübendorf, Switzerland
2. Aragón Institute for Engineering Research (I3A), Thermal Engineering and Energy Systems Group, University of Zaragoza, Spain
3. ZAE Bavarian Center for Applied Energy Research, Walther-Meißner-Str. 6, 85748 Garching, Germany
4. Technical University of Denmark, Department of Civil Engineering, Brovej, Building 118, 2800 Kgs. Lyngby, Denmark
5. University of Applied Sciences Upper Austria, A-4600 Wels, Stelzhamerstr. 26, Austria
6. TNO the Netherlands organization for applied scientific research, Leeghwaterstraat 44, 2628 CA Delft, Netherlands
7. AEE - Institut für Nachhaltige Technologien, Feldgasse 19, 8200 Gleisdorf, Austria

2.6.1 INTRODUCTION

To enable large renewable fraction in building operation, there is a need for a diversity of energy storage ranging from short-term diurnal to inter-seasonal storage. Inter-seasonal storage is challenging due to the low energy turnover and thus high storage price per energy unit [1]. For this reason, a focus is set on thermal, inter-seasonal storage with prospect for low-cost solutions for building space heating and domestic hot water as well as in some cases space cooling. The field of thermal energy storage can be subdivided into sensible, latent and sorption heat storage [2]. Sensible heat storage involves the temperature change of a material with its capacity dependent on the specific heat of the employed material. Latent heat storage extends this process to include a phase change of the storage material, commonly between solid and liquid. In comparison to sensible thermal storage, latent systems are generally characterized by a narrow temperature range around the phase change. Sorption heat storage is an umbrella term referring to processes involving adsorption, liquid absorption and solid absorption such as hydration and hydroxide reaction with large heat release [2]. In sorption heat storage not sensible heat is stored, but the potential to release heat through sorption and reaction [2-9].

Due to the continuous heat loss, sensible heat storage for inter-seasonal storage is only fitting at large scale, where surface to volume ratios are sufficiently small, reducing heat loss. Commercial applications for buildings are found, for example, in the form of large building internal storage tanks [10] or building external pit-based storage vessels [11]. Work is ongoing in the field of latent and sorption heat storage towards compact systems by increased volumetric energy density compared to water. There is a diversity of potential materials studied, and many attempts to design heat storage systems have been made and reported, with research ongoing [12, 13].

Past reviews and research papers on compact inter-seasonal thermal storage have compared reported energy densities indifferent of the operation schemes [9,14-18]. In [19] the erroneous practice in sorption heat storage is pointed to, and the authors proceeded to develop a method to compare the reported performance independent of the applied temperature profile. This method is based on the sorption charging to discharging temperature difference ratio, termed temperature effectiveness. Interestingly, it is noted that in several of the studied examples incomplete operating conditions are provided [20-23]. It is concluded that in order to assess progress in the field of compact thermal energy storage, simple, clearly defined temperature profiles are required in order to enable comparison along the scale of development from material to system as well as across the landscape of diverse materials and systems. In [24] this issue is approached by studying the heat supply and space heating demand in Germany and Sweden, providing a dynamic ambient temperature profile, but limiting the evaluation to space heating for Nearly Zero Energy buildings and closed, fixed bed solid sorption processes. By assuming Nearly Zero Energy buildings, the required floor heating temperatures are taken to be very low, generally not applicable for retrofitting. Heating return temperatures, an important parameter especially for the transported process, are not provided, and wet bulb temperatures for open systems are also missing. For this reason, the challenge to define a simple unified methodology

to identify the potential application of seasonal sorption storage technology is not met, covering only one of four basic processes and only for a particular building type.

In this paper a simple static temperature profile for latent and sorption heat and cold storage for building applications is sought, not limiting to a specific climate, building or process type, and enabling uniform evaluation. The profile covers both heat transport fluid inbound and outbound temperatures and material temperatures. Is applied to well characterized compact thermal storage materials as examples and compared to the respective thermal capacity of water.

2.6.2 METHOD

In order to establish a well-defined temperature profile for testing compact thermal storage materials and systems, a uniform thermal storage system schematic is proposed, shown in Figure 2-7. The schematic indicates heat transport fluid (liquid or gas) return and outbound temperatures for both source and sink as well as material temperature and temperature difference between sorbate and sorbent, specific for the sorption heat storage approach. Temperature difference $\Delta\vartheta^*$ is applicable only for heat transport fluid and sorbent counter flow, in which case the sorbent is cooled below the minimum output temperature [19]. For open sorption heat storage systems, where sorbate is exchanged with the ambient, wet bulb temperatures (WBT) are provided in brackets [19]. For latent heat storage systems solely the building side source and sink are relevant.

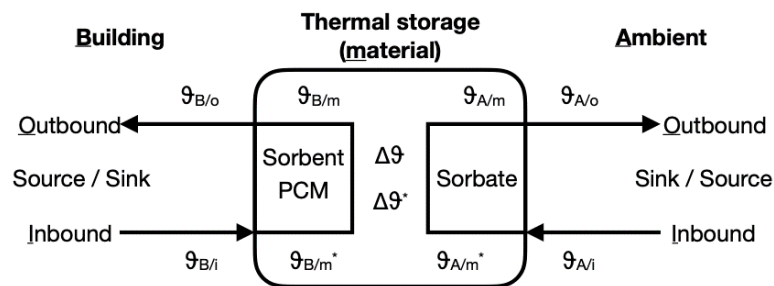


FIGURE 2-7: UNIFORM HEAT STORAGE SCHEMATIC FOR LATENT AND SORPTION SYSTEMS. INDICATED ARE THE HEAT TRANSPORT FLUID TEMPERATURES, INBOUND AND OUTBOUND AS WELL AS THE MATERIAL TEMPERATURE AND THE TEMPERATURE DIFFERENCE BETWEEN SORBATE AND SORBENT IN SORPTION SYSTEMS. THE ORIGINS OF THE SUBSCRIPTS ARE NOTED BY UNDERSCORE IN THE RESPECTIVE LABELS.

On the building level, there are both solar thermal and electric energy sources available. Renewable electricity may be harvested on-site or sourced from the electric grid. This is an approach to energy sector coupling including thermal energy storage. The maximum temperature of a conventional solar thermal system is limited to 95°C according to the EN 12897 standard “Water supply - Specification for indirectly heated unvented (closed) storage water heaters”. Electricity based charging permits more diversity, whereby increased efficiency can be reached by using a heat pump and temperatures beyond that of the thermal system can be achieved by direct resistive heating. For this reason, it is proposed that the maximum storage charging temperature be set to 95°C with the possibility of resistive or perhaps micro-wave [25] or inductive heating

up to 200°C. It is important to note that in the heat exchange process there is difference between return and outbound and between heat transport fluid and heat storage material temperature. The EN 14511 standard follows a 3K temperature spread between the fluid inbound and outbound temperature. This is adopted and also imposed on the temperature difference between fluid to storage material. The respective resulting temperatures are provided in Table 2-3. The temperature difference between outbound fluid and storage material strongly depends on the storage material and especially in sorption systems, on the choice of process [19]. For solid sorbents in open fixed systems, for example, the temperature difference may be substantially larger than 3K.

Sorption cold storage follows the same charging profile as the heat storage and latent cold storage requires a heat pump for heat removal in charging. In this case, flexibility in charging temperature is provided by the cooling machine. For this reason, in Table 2-3 under cold charging temperature, a specific temperature is not provided, but the temperature relations, as discussed, are indicated. A restrictive parameter when considering the cold charging temperature is the HP efficiency (energy efficiency ratio EER).

Table 2-3: Temperature profiles for latent and sorption thermal storage for heating and cooling in buildings.

	Charging		Discharging			
	High temperature	Low temperature	Space Heating	Sorbent space cooling	Latent space cooling	DHW supply
$\vartheta_{B/i}$	95 °C, 200 _R °C	A °C	25 °C	24 °C (17 °C)	24 °C	25 °C
$\vartheta_{B/o}$	92 °C	A °C + 3 K	35 °C	18 °C	18 °C	65 °C
$\vartheta_{B/m}$	89 °C	A °C + 6 K	38 °C	15 °C	15 °C	68 °C
$\vartheta_{B/m}^*$	92 °C	-	28 °C	-	-	28 °C
$\vartheta_{A/i}$	30 °C (24 °C)	-	7 °C (6 °C)	30 °C	-	7 °C
$\vartheta_{A/o}$	35 °C (35 °C)	-	4 °C	35 °C	-	4 °C
$\vartheta_{A/m}$	38 °C	-	1 °C	38 °C	-	1 °C
$\vartheta_{A/m}^*$	-	-	-	33 °C	-	-
$\Delta\vartheta$	51 K	-	37 K	23 K	-	67 K
$\Delta\vartheta^*$	54 K	-	27 K	18 K	-	27 K

There are three discharging conditions found in a building; space heating, space cooling and domestic hot water. To prevent arbitration in the choice of temperature, the proposed temperatures are based on European standards. For space heating and cooling the EN 14511 [26] is used and for domestic hot water the EN 16147 [27] and the CEN/TR 16355 [28] are consulted. There are two means of heat distribution for space heating, air and liquid. For liquid distribution, three temperature levels are provided; low, medium and high. Due to the fact that sorption heat storage systems generally do not reach high output temperatures, it is suggested to follow the

low temperature profile for floor heating, with 35°C outbound and 25°C return temperature. The inbound temperature is an average between 30°C defined for liquids and 20°C given for direct air heating. Room comfort temperature is 22 °C, defined by the standard EN15251 [29].

In space cooling, again liquid and air distribution are considered. Water-based floor cooling has an outbound temperature of 18 °C and 23 °C return. Air cooling has a return temperature of 24 °C with a WBT of 17 °C whereby the outbound temperature is not defined. In order to reduce this to one profile, 18 °C outbound and 24 °C (17 °C) return temperature is proposed.

Domestic hot water is required to reach a temperature of 65 °C, due to issues with legionella growth at lower temperatures as stated by EN 16147 and CEN/TR 16355. It is proposed that the cold water temperature is 25°C, a mean return temperature from a fresh hot water station or bottom temperature of a semi discharged domestic hot water tank.

As illustrated in the uniform heat storage schematics, sorption-based systems require heat source and sink both in charging as well as discharging. In charging, the heat sink can be the ambient air or a ground source heat exchanger. Air heat sink conditions can be taken from the EN 14511 standard for space cooling. These are 30 °C (24 °C) return and 35°C outbound. Outbound WBT is not defined in the standard. It is proposed that saturated condition can be assumed.

In respect to heat source for heating, the EN14511 standard provides high medium and low source temperatures for both ambient air and ground. Since most sorbent systems operate with water vapor, subzero conditions are not applicable. It is suggested to refer to the standard air source setting with return temperature 7 °C (6 °C) and thus outbound temperature 4 °C. All discussed temperatures are listed in Table 2-3.

2.6.3 RESULTS AND DISCUSSION

Having fully defined a proposed set of temperatures to be followed for compact thermal storage evaluation for buildings, these are now applied to well characterized latent and sorption materials as examples and compared to water storage as bench mark. Heat loss in water storage is not taken into consideration. In respect to energy density, best practice is followed, whereby reference is made to the maximum material volume.

The thermal capacity of water for space heating is 0.23 GJ m⁻³ (63.78kWh m⁻³) based on the water density of 0.9619g cm⁻³ at 95 °C and 57 K temperature difference. The respective energy density for DHW is 0.11GJ m⁻³ (30.21kW m⁻³). For cold storage the capacity is 0.06GJ m⁻³ (16.3kWh m⁻³) based on a minimum temperature of 1°C, thus not including the water phase change, and a temperature difference of 14 K. In Table 2-4, the discussed examples are listed.

3.1. Latent thermal storage examples

The minimum phase change temperature for latent heat storage for space heating, is 38 °C since lower temperatures are inadmissible. A material fitting to this application is the Rubitherm RT42

with a phase change between 38 °C and 42 °C. Figure 2-8 shows the respective partial enthalpy diagram in J g^{-1} . Beyond 43 °C this material has a low partial enthalpy, thus charging up to the maximum material temperature of 89 °C has little benefit. Charging is so limited to an input temperature of approximately 49 °C and the complete scope cannot be used. From the partial enthalpy diagram in Figure 2-8, a material specific volumetric energy density of 0.11 GJ m^{-3} (30.4 kWh m^{-3}) is derived, based on the accumulated partial enthalpies of 144 J g^{-1} between 38 °C and 43 °C and the specific density of the PCM in its liquid state of 760 kg m^{-3} [30]. This is 0.48 times the respective water capacity.

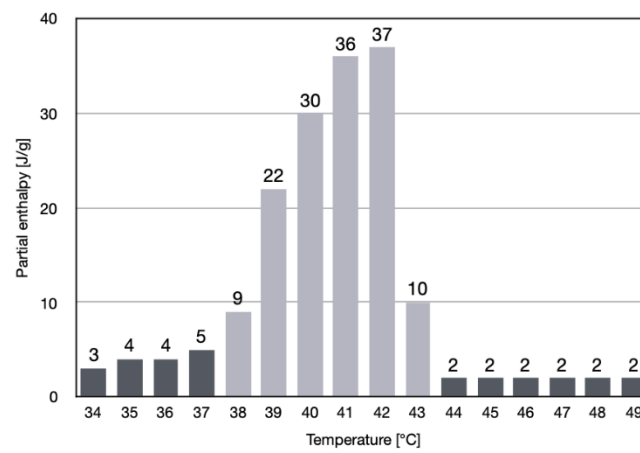


FIGURE 2-8: PARTIAL ENTHALPY VS TEMPERATURE INTERVAL OF RT42. INDICATED IN LIGHT GREY IS THE TEMPERATURE RANGE OF APPLICATION FOR SPACE HEATING [30].

A phase change material incorporating supercooling, a state where the material remain liquid below its solidification temperature, is sodium acetate trihydrate. Supercooling is a method applied for inter-seasonal storage to prevent loss over time. Sodium acetate trihydrate can so be used as both short- and long-term storage. In the short-term application for the floor heating, it has a specific sensible heat capacity of 2.9 J (g K)^{-1} and a liquid density of 1280 kg m^{-3} , resulting in a volumetric sensible heat capacity of 0.19 GJ m^{-3} (52.6 kWh m^{-3}). This is 0.83 times the equivalent water capacity. The phase change enthalpy is 0.32 GJ m^{-3} (88 kWh m^{-3}) in respect to the liquid density when the liquid is initially cooled to 38 °C before solidification is started [31, 32]. Thus, the complete capacity is 0.51 GJ m^{-3} (140.6 kWh m^{-3}) and 2.22 times the capacity of water.

The latent cold storage is charged by electrically powered compression heat pump. The specific charging temperature can thus be, to a certain extent, freely adapted. Important is the maximum material temperature. The Rubitherm RT11 material has a phase change at 9 °C to 12 °C, as shown in Figure 2-9, and is thus fitting to the application. Discharging can be followed up to a material temperature of 15 °C. Under the defined conditions, a volumetric energy density of 0.15 GJ m^{-3} (42.6 kWh m^{-3}) is reached, based on the accumulated partial enthalpies of 199 J g^{-1} and the material specific density in its liquid state of 770 kg m^{-3} [30]. This material is thus 2.61 times better than water, if the water phase change is not engaged.

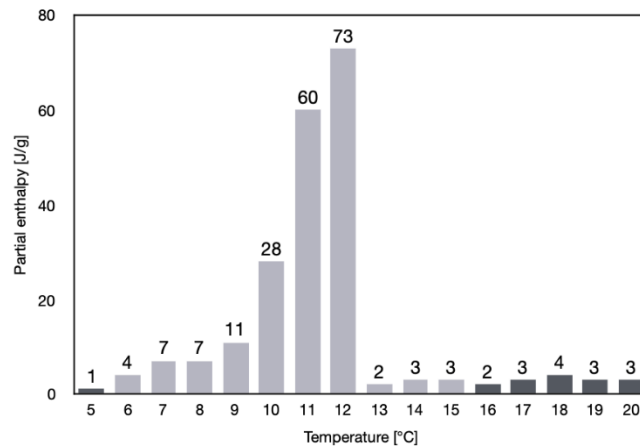


FIGURE 2-9: PARTIAL ENTHALPY VS TEMPERATURE INTERVALS OF RT11. INDICATED IN LIGHT GREY IS THE TEMPERATURE RANGE OF APPLICATION FOR SPACE COOLING [30].

3.2. Sorption thermal storage examples

An aqueous absorbent studied and reported in literature is sodium hydroxide. It is proposed that true counterflow of absorbent and heat transport fluid is possible in as far as the sorbent concentration does not exceed 50 wt%, due to the risk of solidification [33]. This limits the utilization of available charging temperature to 80 °C, also limiting the temperature gain in discharging as illustrated in the operation process in vapor vs. temperature diagram in Figure 2-10 [34]. Under the defined conditions, the maximum sorbent temperature in discharging is 38 °C, and due to the counter flow process, a material temperature of 28 °C can be reached, resulting in a concentration difference from 50 wt% to 42 wt%. The capacity is so 0.63 GJ m⁻³ (176 kWh m⁻³), or 2.74 times the water equivalent.

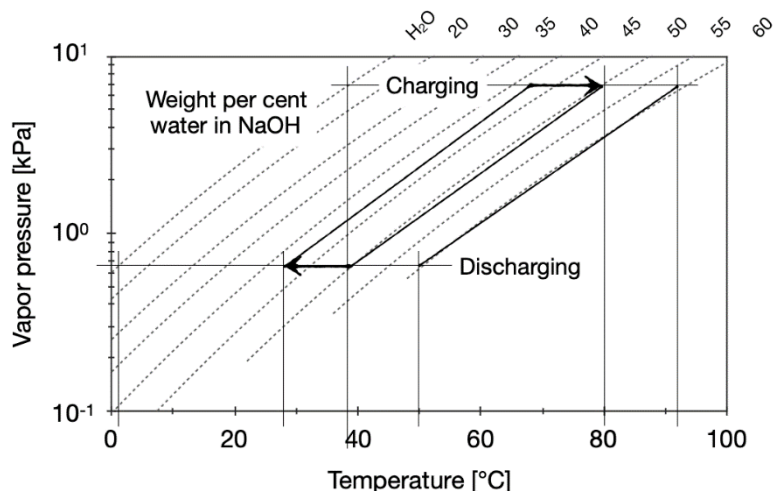


FIGURE 2-10: VAPOR VS. TEMPERATURE DIAGRAM OF NaOH. INDICATED IS THE CHARGING AND DISCHARGING PROCESS BASED ON THE REALISTIC TEMPERATURE PROFILE FOR SH [33, 34].

In the sorption process, charging for heating or cooling is identical. Figure 2-11 shows the cooling process with NaOH, again based on true counterflow. In this case the discharged concentration

is 35 wt% and a storage capacity of 1.08 GJ m^{-3} (300 kWh m^{-3}) is reached. This is 18.4 times the water equivalent for cooling.

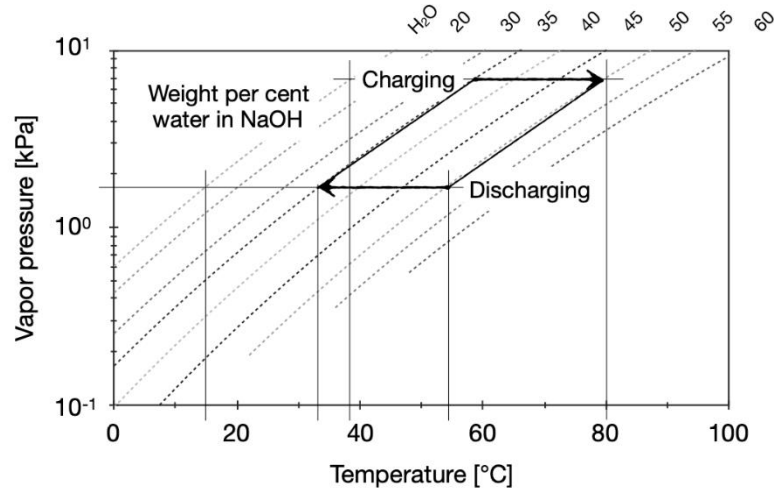


FIGURE 2-11: VAPOR VS. TEMPERATURE DIAGRAM OF NaOH. INDICATED IS THE CHARGING AND DISCHARGING PROCESS BASED ON THE REALISTIC TEMPERATURE PROFILE FOR SC [33, 34].

A solid adsorbent reported in literature is zeolite 13X. Both open and closed processes have been studied, generally operating with fixed beds. In Figure 2-12, the process is illustrated based on the closed approach. A change in water mass fraction from 0.206 to 0.22 can be reached under the defined temperature profile with solar thermal charging. The volumetric energy density is thus $0,032 \text{ GJ m}^{-3}$ (9 kWh m^{-3}). This is 0.14 times the water energy density equivalent. If a transported design with true counterflow is followed the degree of discharge can be increased, as shown in Figure 2-12 by the dashed charge and discharge arrow. In this case the energy density is slightly improved to $0,054 \text{ GJ m}^{-3}$ (15 kWh m^{-3}), or a water equivalent of 0.24.

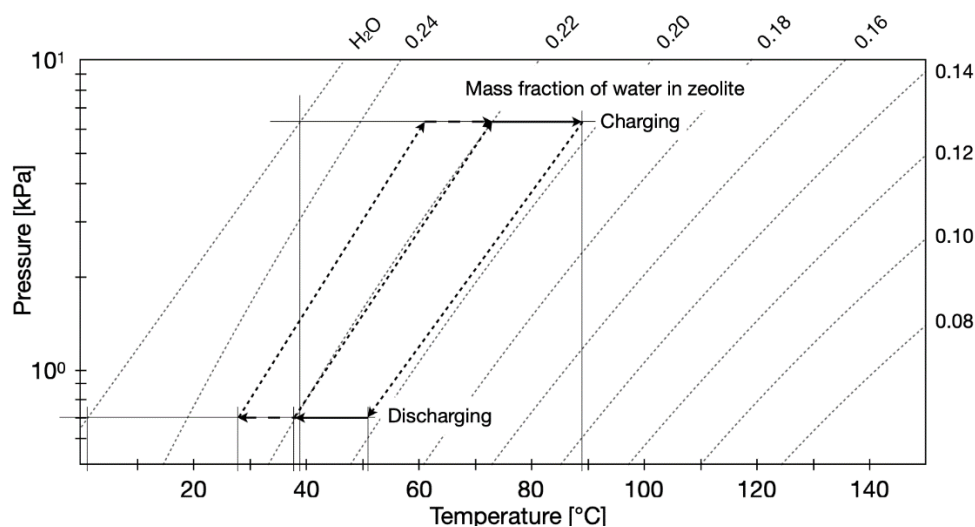


FIGURE 2-12: VAPOR VS. TEMPERATURE DIAGRAM OF ZEOLITE 13X IN A CLOSED PROCESS. INDICATED IS CHARGING AND DISCHARGING PROCESS FOR THE FIXED AND TRANSPORTED PROCESS WITH SOLID AND DASHED ARROWS RESPECTIVELY. ADAPTED FROM [35].

From the previous example it is clear that for zeolite a higher charging temperature is required. Figure 2-13 shows the performance with resistive heating and counter flow. In this case a water mass fraction difference from 0.08 to 0.29 can be reached, resulting in a storage energy density of 0.486 GJ m^{-3} (135 kWh m^{-3}). This is 2.12 times the water-based capacity.

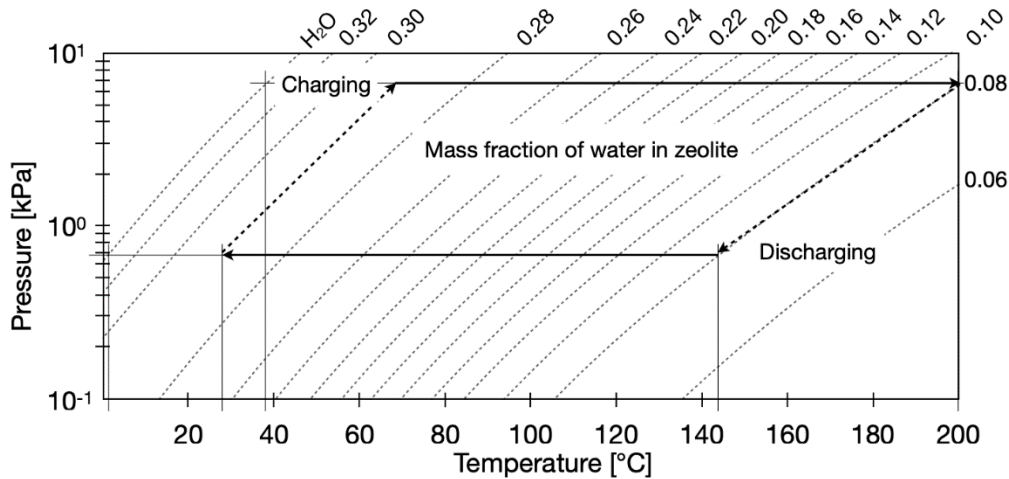


FIGURE 2-13: VAPOR VS. TEMPERATURE DIAGRAM OF ZEOLITE 13XBF IN A CLOSED SYSTEM. INDICATED IS THE CHARGING AND DISCHARGING CYCLE AT REALISTIC TEMPERATURE PROFILES USING ELECTRIC RESISTIVE HEATING FOR CHARGING INSTEAD OF SOLAR THERMAL HEATING [36].

Salt hydrates are a type of solid absorbent, they are characterized by a stepwise uptake and release of absorbate. A salt hydrate studied for sorption heat storage is potassium carbonate (K_2CO_3). Figure 2-14 shows the pressure vs. temperature diagram of this salt at a hydration step from anhydrous to 1.5 water molecules per salt molecule, including the water curve. In this case, the process is drawn as a single line, since hydration and dehydration occur only along the hydration step curve. The energy density reached under the application specific temperatures is 0.96 GJ m^{-3} (361 kWh m^{-3}). This is 4.2 times the water equivalent.

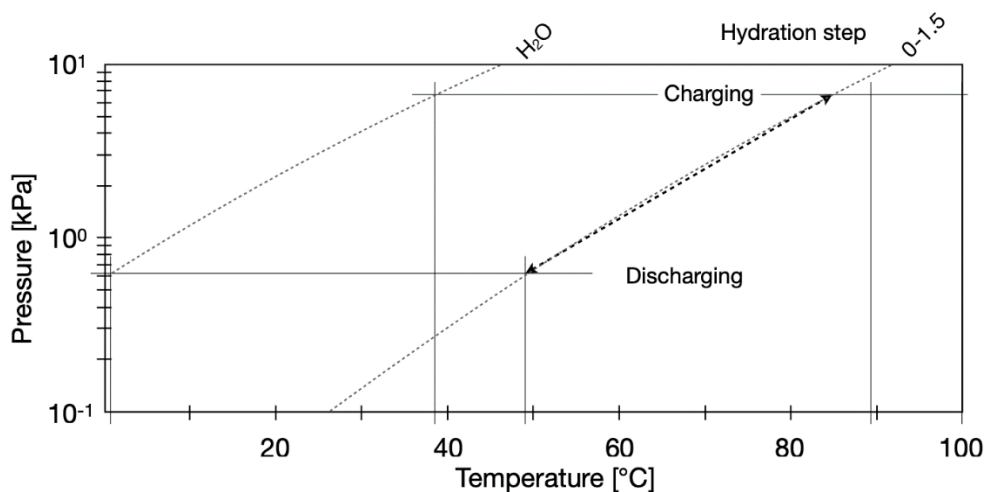


FIGURE 2-14: VAPOR VS. TEMPERATURE DIAGRAM OF POTASSIUM CARBONATE IN A CLOSED PROCESS. INDICATED IS THE CHARGING AND DISCHARGING PROCESS BASED ON THE REALISTIC TEMPERATURE PROFILE [37, 38].

Table 2-4: Comparison of the various materials in respect to water and literature where available.

Material	Type	Application	Energy density	Water equivalent
Water	Sensible	Space heating	0.23 GJ m ⁻³ (63.78 kWh m ⁻³)	1
Water	Sensible	Space cooling	0.06 GJ m ⁻³ (16.3 kWh m ⁻³)	1
Rubitherm 42	Latent	Space heating	0.11 GJ m ⁻³ (30.4 kWh m ⁻³)	0.48
sodium acetate trihydrate	Latent (super-cooled)	Space heating	0.51 GJ m ⁻³ (140.6 kWh m ⁻³)	2.22
Rubitherm 11	Latent	Space cooling	0.15 GJ m ⁻³ (41.6 kWh m ⁻³)	2.55
Sodium hydroxide	Liquid absorption	Space heating	0.63 GJ m ⁻³ (176 kWh m ⁻³)	2.74
Sodium hydroxide	Liquid absorption	Space cooling	1.08 GJ m ⁻³ (300 kWh m ⁻³)	18.4
Zeolite 13X	Adsorption fixed	Space heating	0,032 GJ m ⁻³ (9 kWh m ⁻³)	0.14
Zeolite 13X	Adsorption transported	Space heating	0,054 GJ m ⁻³ (15 kWh m ⁻³)	0.24
Zeolite 13XBF	Absorption electric	Space heating	0.486 GJ m ⁻³ (135 kWh m ⁻³)	2.12
Potassium carbonate	Solid absorption	Space heating	0.96 GJ m ⁻³ (361 kWh m ⁻³)	4.18

The provided examples show the application of the presented realistic temperature profile for thermal storage in buildings. Based on the good characterization of a potential compact thermal energy storage material and this temperature profile, a solid initial evaluation of performance can be reached. Promising materials can then be further evaluated in conjunction with component development based on the fluid specified temperatures provided. At this point, additional loss will be encountered due to mass and heat transport as well as reaction kinetics. This permits an evaluation of performance along the development from material to component design and systems as well as comparing varying potential materials and processes upon a solid basis. Inaccurate comparison as followed by Yu et al. [17] is so prevented, where due to the lack of data available, energy storage capacity is outlined dependent on charging temperature, not taking into account condensing temperature in sorbent charging, nor evaporating temperature as well as inbound and outbound heat transport fluid temperature in discharging.

Based on the definition of the realistic temperature profile, it can be recognized that the preparation of domestic hot water with solar thermally charged sorption heat storage is not practicable. This is due to the fact that the maximum temperature difference between sorbent and sorbate in charging is 54 K, but a temperature difference of 67 K is required to reach 65 °C outbound temperature in discharging. Under heat storage application, where condensing temperature in

charging is greater than evaporating temperature in discharging, this requirement cannot be fulfilled [19]. On the other hand, if electric charging is followed, as in the zeolite 13XBF example, domestic hot water can be produced. The energy density in this case depends on the chosen process, fixed or transported. In the transported approach the energy density is equal to the space heating example, in the fixed process, the energy density is reduced since the discharge temperature increases.

2.6.4 CONCLUSIONS

Work on compact thermal energy storage for buildings is proceeding, and there are many new materials, components and systems developed. For this reason, there is a need for uniform testing conditions in order to enable progress assessment and comparison along the development scale and across the variety of materials, ideas and processes. Such a temperature-based profile is presented in the work, largely derived from existing European heat pump testing standards. This profile is applicable for both latent and sorption heat storage, for space heating, domestic hot water and space cooling. From the temperature profile it is recognized that coverage of domestic hot water cannot be reached by solar thermal charging.

By following this proposed temperature profile, good comparison between materials, components and systems will be made possible and assessment of technology progress will be achieved.

The experts from the IEA SHC Task 58 and ECES Annex 33 encourage colleagues in the field of compact heat storage for buildings to use this proposed profile, if not rigorously, at least as a basis upon which to argue how other temperature regimes are achieved.

2.6.5 ACKNOWLEDGEMENTS

The authors thank the IEA SHC task 58 / ECES annex 33 members for the fruitful discussions in the semi-annual meetings that substantially shaped and supported this work.

2.6.6 FUNDING

This work was supported by: The Swiss Innovation Agency Innosuisse in the frame of the Swiss Competence Centre for Energy Research Heat and Electricity Storage (SCCER HaE), grant Nr. 1155002545, The Swiss Federal Office of Energy SFOE grant Nr. SI/501605-01, The Spanish Government (Energy Program) partially funded project ENE2017-87711-R, The Spanish Government of Aragon grant reference T55-17R, The EU Social Fund (FEDER Program 2014-2020 "Building Europe from Aragon"), The Danish Energy Agency through the EUDP program, The Austrian Ministry BMVIT, Projekt: IEA SHC TES 858138, program call: IEA Ausschreibung 2016, eCall Nummer: 8592411. The Dutch ministry of Economic Affairs, Energy in the Built Environment, Project Nr. 060.37230", The European Commission H2020 funded project CREATE, grant Nr. 680450.

2.6.7 REFERENCES

[1] Rathgeber Ch, Hiebler S, Lävemann E, Dolado P, Lazaro A, Gasia J, de Gracia A, Miró L, Cabeza LF, König-Haagen A, Brüggemann D, Campos-Celador A, Franquet E, Fumey B, Dannemand M, Badenhop T, Diriken J, Nielsen JE, Hauer

- A. IEA SHC task 42/ECES Annex 29 – a simple tool for the economic evaluation of thermal energy storages. *Energy Procedia* 2016;91:197–206.
- [2] Zondag HA. Sorption heat storage. In: Sørensen B, editor. *Solar energy storage*. Netherlands: Academic Press; 2015. p. 135–54.
- [3] Garg HP, Mullick SC, Bhargava AK. *Solar thermal energy storage*. Dordrecht: Reidel Publishing Company; 1985.
- [4] Hauer A. Sorption theory for thermal energy storage. In: Paksoy HÖ., editor. *Thermal energy storage for sustainable energy consumption*. Netherlands: Springer; 2007. p. 393–408.
- [5] Kawasaki H, Watanabe T, Kanzawa A. Proposal of a chemical heat pump with paraldehyde depolymerization for cooling system. *Appl Therm Eng* 1999;19(2):133–43.
- [6] Boman BD, Hoysall DC, Staedter MA, Goyal A, Ponkala MJ, Garimella S. A method for comparison of absorption heat pump working pairs. *Int J Refrig* 2017;77:149–75.
- [7] Aristov YI. Challenging offers of material science for adsorption heat transformation: a review. *Appl Therm Eng* 2013;50(2):1610–8.
- [8] N'Tsoukpoe KE, Liu H, Le Pierrès N, Luo L. A review on long-term sorption solar energy storage. *Renew Sustain Energy Rev* 2009;13(9):2385–96.
- [9] Cabeza LF, Solé A, Barreneche C. Review on sorption materials and technologies for heat pumps and thermal energy storage. *Renew Energy* 2017;110:3–39.
- [10] <http://jenni.ch/products-446.html>, [accessed 02.2020].
- [11] <http://www.saisonalspeicher.de>, [accessed 02.2020].
- [12] <http://task58.iea-shc.org>, [accessed 02.2020].
- [13] <https://iea-eces.org/annexes/material-component-development-thermal-energy-storage/>, [accessed 02.2020].
- [14] Kuznik F, Johannes K, Obrecht Ch, David D. A review on recent developments in physisorption thermal energy storage for building applications. *Renew Sustain Energy Rev* 2018;94:576–86.
- [15] Palomba V, Frazzica A. Recent advancements in sorption technology for solar thermal energy storage applications. *Sol Energy* 2019; 192:69-105
- [16] Solé A, Martorell I, Cabeza LF. State of the art on gas–solid thermochemical energy storage systems and reactors for building applications. *Renew Sustain Energy Rev* 2015; 47:386–98.
- [17] Yu N, Wang RZ, Wang LW. Sorption thermal storage for solar energy. *Prog Energy Combust* 2013; 39:489–514.
- [18] Abedin AH, Rosen MA. A critical review of thermochemical energy storage systems. *Open Renew Energy J* 2011; 4:42–6.
- [19] Fumey B, Weber R, Baldini L. Sorption based long-term thermal energy storage – Process classification and T analysis of performance limitations: A review. *Renewable and Sustainable Energy Reviews* 2019; 111:57–74.
- [20] Tatsidjoudoung P, Le Pierrès N, Heintz J, Lagre D, Luo L, Durier F. Experimental and numerical investigations of a zeolite 13X/water reactor for solar heat storage in buildings. *Energy Convers Manag* 2016;108:488–500.
- [21] Johannes K, Kuznik F, Hubert JL, Durier F, Obrecht C. Design and characterisation of a high powered energy dense zeolite thermal energy storage system for buildings. *Appl Energy* 2015;159:80–6.
- [22] Gaeini M, Javed MR, Ouwerkerk H, Zondag HA, Rindt CCM. Realization of a 4kW thermochemical segmented reactor in household scale for seasonal heat storage. *Energy proced* 2017;135:105–14.
- [23] Zhang YN, Wang RZ, Li TX. Experimental investigation on an open sorption thermal storage system for space heating. *Energy* 2017;141:2421–33.
- [24] Frazzica A, Brancato V, Dawoud B. Unified Methodology to Identify the Potential Application of Seasonal Sorption Storage Technology. *Energies* 2020;13:1037.
- [25] Zettl B, Lachner M. An Advanced Desorption Concept for TES-Materials, Proc. International Conference on Solar Heating and Cooling for Buildings and Industry, SHC 2015, 2-4 Dec 2015, Istanbul
- [26] EN 14511 “Air conditioners, liquid chilling packages and heat pumps with electrically driven compressors for space heating and cooling - Part 2: Test conditions”

- [27] EN 16147 “Heat pumps with electrically driven compressors –Testing, performance rating and requirements for making of domestic hot water units”
- [28] CEN/TR 16355 “Recommendations for prevention of Legionella growth in installations inside buildings conveying water for human consumption”
- [29] EN15251 “Indoor Environmental Criteria”
- [30] www.rubitherm.eu, [accessed 02.2020]
- [31] Englmaier G, Moser C, Furbo S, Dannemand M, Fan J. Design and functionality of a segmented heat-storage prototype utilizing stable supercooling of sodium acetate trihydrate in a solar heating system. *Appl. Energy* 2018;221:522-34.
- [32] Englmaier G, Furbo S, Dannemand M, Fan J, Experimental investigation of a tank-in-tank heat storage unit utilizing stable supercooling of sodium acetate trihydrate. *Appl. Therm. Eng.* 2020;167.
- [33] Fumey B, Weber R, Baldini L. Liquid sorption heat storage – a proof of concept based on lab measurements with a novel spiral fined heat and mass exchanger design. *Appl Energy* 2017;200:215–25.
- [34] Olsson J, Jernqvist Å, Aly G. Thermophysical properties of aqueous NaOHH₂O solutions at high concentrations. *Int. J. Thermophys.* 1997;18:779–93.
- [35] Finck Ch, Li R, Kramer R, Zeiler W. Quantifying demand flexibility of power-to-heat and thermal energy storage in the control of building heating systems, *Appl Energ*, 2018;209:409-25.
- [36] B. Mette, H. Kerskes, H. Drück, und H. Müller-Steinhagen, „Experimental and numerical investigations on the water vapor adsorption isotherms and kinetics of binderless zeolite 13X“, *Int. J. Heat Mass Transf.*,2014;71:555–61.
- [37] Greenspan L. Humidity fixed points of binary saturated aqueous solutions. *J Res Natl Bur Stand Phys Chem* 1977;81(1):89–96.
- [38] Glasser, L. Thermodynamics of Inorganic Hydration and of Humidity Control, with an Extensive Database of Salt Hydrate Pairs. *J. Chem. Eng.* 2014;59:526–30.

3 SUBTASK 2 – DEVELOPMENT AND CHARACTERIZATION OF IMPROVED MATERIALS

3.1 SUBTASK 2P: DEVELOPMENT AND CHARACTERIZATION OF IMPROVED PCM

3.1.1 INTRODUCTION

The work of Subtask 2P is split into 4 topics:

- Material development
- Developing measurement procedures
- Filling the PCM Database
- Developing a Wiki for terms used in the context of PCMs

As the material development is done at different institution the objective of the work was to collect the materials which are under research and development to get an overview on the most relevant properties of these materials and application which are addressed.

In the frame of this subtask investigations on results obtained at different institutions using various measurement methods for different material properties have been conducted. Procedures have been developed, for thermal conductivity and the determination of viscosity.

New material properties have been feed into the database which was developed during previous tasks and annexes.

And finally, a wiki for the terms uses in the context of PCMs have been developed based on a content management web-based tool.

3.1.2 MATERIAL DEVELOPMENT: LIST OF NOVEL DEVELOPED PCM AS WELL AS BLENDS AND MIXTURES

The objective of this work was to collect the PCMs and applications focused on within the participants of the SHC Task 58 and ECES Annex 33 (T58A33). Another target is to determine the challenges of the development process. For the collection of this data a questionnaire was prepared which was send to the T58A33 mailing list. Nine different institutions reported about the development or investigation of 20 different materials and the supposed applications.

PCMs

- Organic (alkanes, fatty acids, sugar alcohols and others)
- Inorganic (salt hydrates, salt)
- Eutectic mixtures (organic, inorganic)

Applications

- Cold storages, precooling of refrigerants
- Passive cooling for buildings and industrial processes
- Heat pump applications
- Mobile heat storage

- Waste heat / process heat / steam generation
- Thermal protection of electronics / battery cooling
- Solar heating / long-term storage

The main work is done on organic PCMs and on mixtures of either organic or inorganic materials. Figure 3-1 is indicating the materials which are under research. The majority of materials are developed for storage temperature below 100 °C. A few materials are under research in the temperature range between 100 und 150 °C. Above 150 °C many institutions doing research on d-Mannitol, which is only once rated as stable as well as a mixture of d-Mannitol and Dulcitol. Another material which is under research on this temperature level is hydroquinone, which is also rated as not stable.

Supercooling of almost all materials is below 10 K except d-Mannitol, pinacone hexahydrate, and sodium acetate trihydrate. The last one was optimized to be used as supercooled storage material.

Almost all contributors tested the stability of materials by thermal cycling except one who kept the temperature above the melting point. The number of cycles has been very different and reaches from 5 up to 5,000 cycles. There is no clear indication for stability e.g. based on a limit for the decrease of enthalpy or change in phase transition temperature.

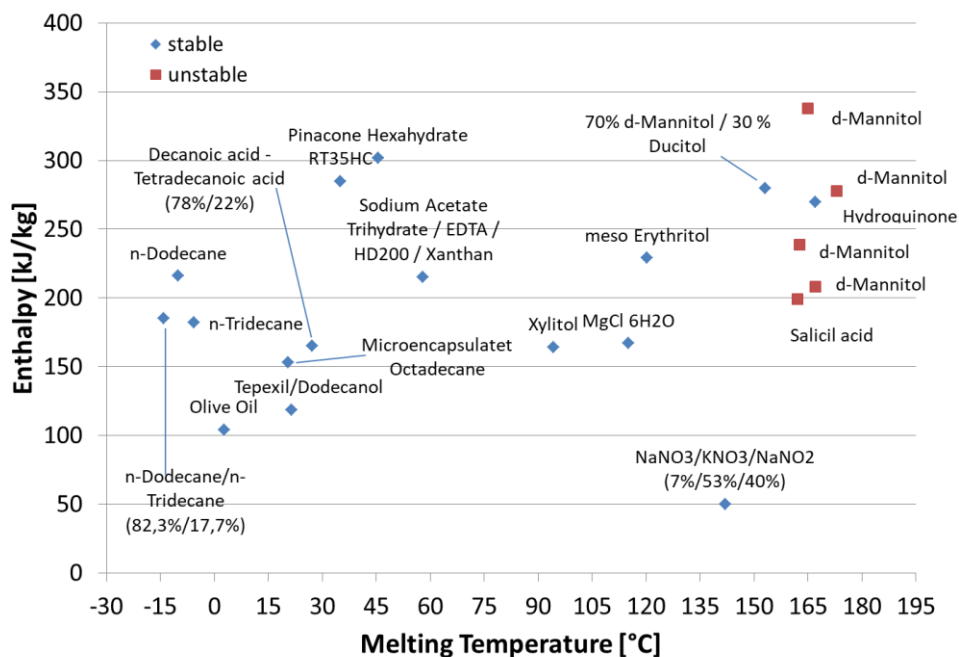


FIGURE 3-1: OVERVIEW ON MATERIALS COLLECTED WITH THEIR PHASE CHANGE ENTHALPY AND MELTING TEMPERATURE, RED INDICATES THE UNSTABLE MATERIALS

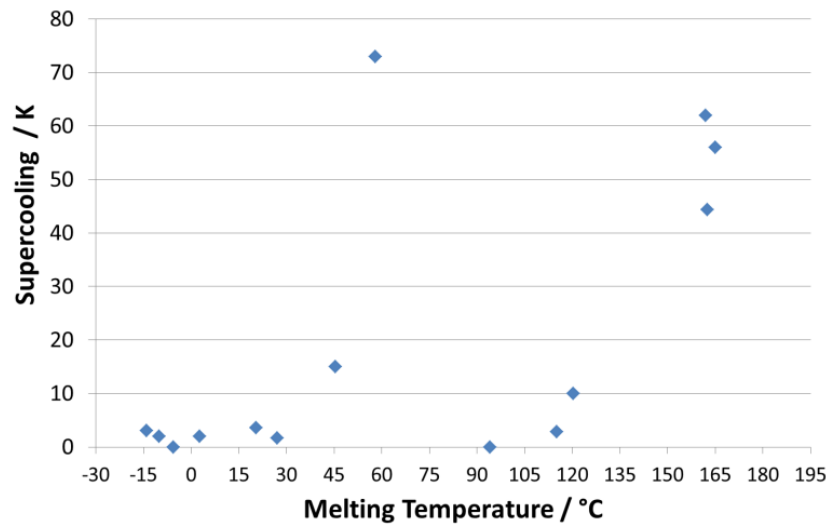


FIGURE 3-2: SUPERCOOLING BEHAVIOUR OF THE MATERIALS

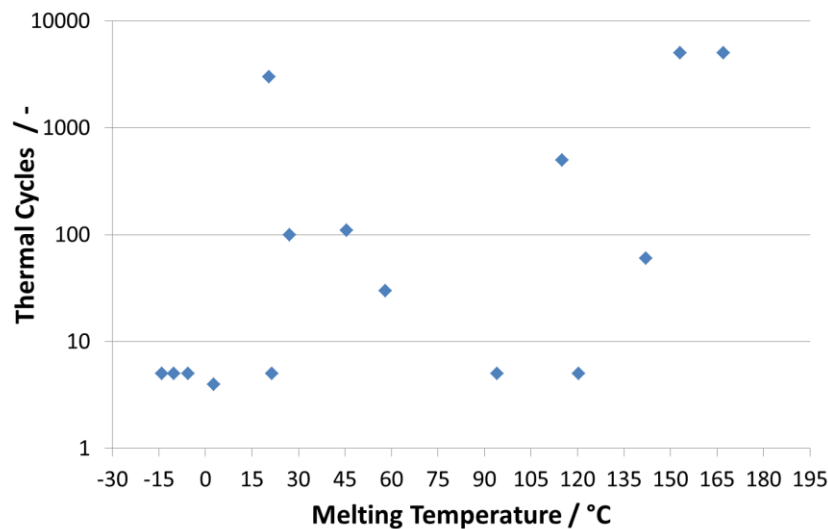


FIGURE 3-3: STABILITY OF MATERIALS, NUMBER OF CYCLES TESTED

3.1.3 CHARACTERIZATION OF PCMs: EXTENDED LIST OF MATERIAL PROPERTIES FOR THE CHARACTERIZATION OF NOVEL PCM (D2P2)

THERMAL CONDUCTIVITY

An intercomparative test of thermal diffusivity was carried out under the guidance of ZAE Bayern. The scope of the test was to develop a guideline for determination of thermal diffusivity and conductivity of PCM by means of flash technique in order to ensure reliable measurement data.

The investigated sample material was RT70HC provided by Rubitherm and was from the same batch used for the DSC intercomparison of IEA SHC Task 42 ECES Annex 29. The melting range of the PCM is around 70 °C.

In the first comparison in Task 42 Annex 29 different measurement methods were used and no procedures for the measurement and specimen preparation were defined. The results showed high deviations in the measurement results between the different laboratories (standard deviation of about $\pm 30\%$). Therefore, it was decided to continue the work in Task 58 Annex 33.

To reduce the number of different measurement methods, it was decided to focus on the flash method, since it is the method available in most laboratories.

In order to avoid deviations caused by the sample preparation, the measured specimens were all prepared by the pilot laboratory. Since the cooling rate of the material has an influence on the crystal structure of the material and again the thermal conductivity, the specimens were prepared with two significantly different cooling rates (slow: 2 K/h; fast: LN₂).

In the first measurement round the thermal diffusivity of the solid PCM RT70HC was measured at 40 °C and 50 °C by five different laboratories with the flash technique. The results showed a lower standard deviation in the measurement results for the different cooling rates and a significant difference in the thermal diffusivity values between the different cooling rates of about 23%.

In the second measurement round the pulse energy was varied systematically. With rising pulse energy, a trend towards lower thermal diffusivity can be observed for all measurements. The values at 0% pulse energy are calculated by linear extrapolation of the measured values. By this procedure the standard deviation of the results is reduced again.

In a third measurement round the specimens were prepared by the participating laboratories in order to test the influence of sample preparation. Compared to the previous measurement rounds, the standard deviation of the results was increased. Figure 3-4 the statistical results of the different measurement rounds are compared and in Figure 3-5 the results of the third measurement round are compared to the results of the previous Task/Annex.

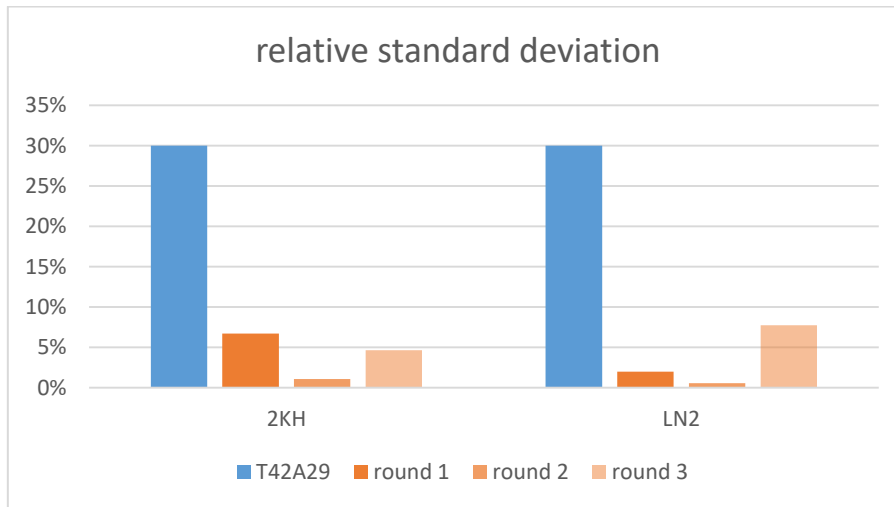


FIGURE 3-4: RELATIVE STANDARD DEVIATIONS OF THE MEASUREMENT RESULTS IN THE DIFFERENT MEASUREMENT ROUNDS FOR SPECIMENS WITH DIFFERENT COOLING RATES.

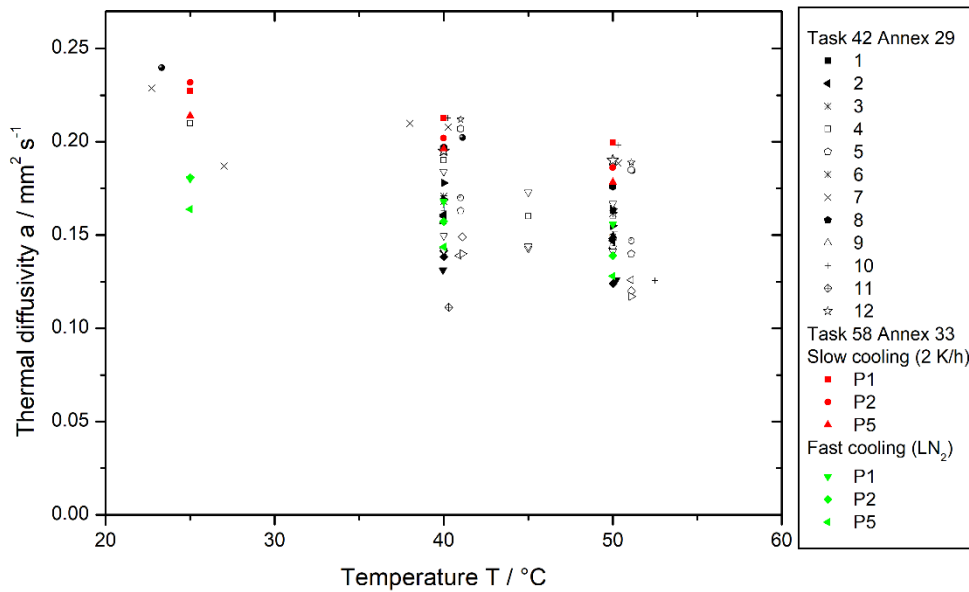


FIGURE 3-5: COMPARISON OF THERMAL DIFFUSIVITY MEASUREMENT RESULTS FROM TASK 42 ANNEX 29 AND TASK 58 ANNEX 33.

VISCOSITY

This work was led by the University of Zaragoza. A comparison of viscosity measurement devices was conducted for which Univ. Zaragoza, Univ. Bayreuth, and Fraunhofer ISE contributed. A publication on this was done in 2018¹. Figure 3-6 and Figure 3-7 depict two results from this publication, which show the comparison of a measurement using a standard oil and of a paraffin.

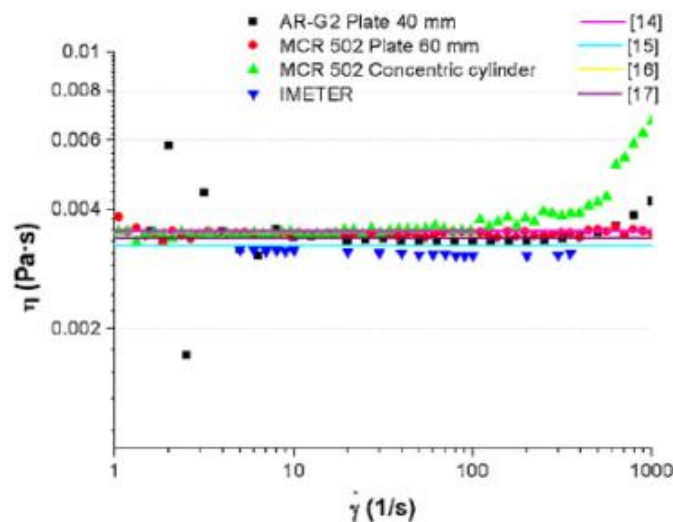


FIGURE 3-6: COMPARISON OF DIFFERENT MEASUREMENT DEVICES FOR VISCOSITY; MEASUREMENT OF A STANDARD OIL

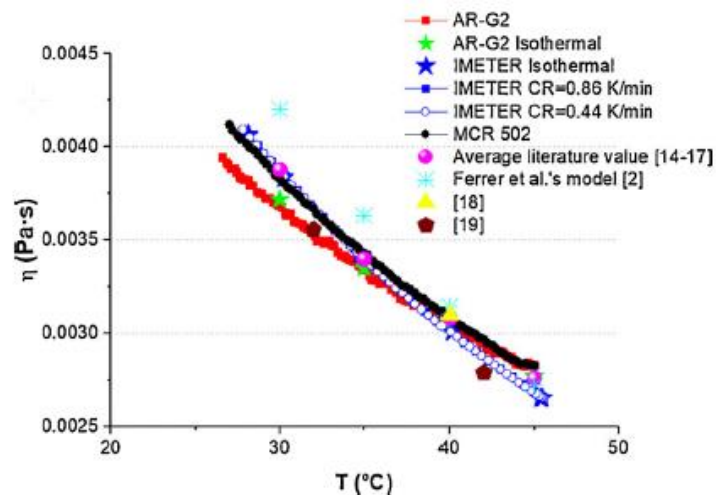


FIGURE 3-7: COMPARISON OF DIFFERENT MEASUREMENT DEVICES FOR VISCOSITY; MEASUREMENT OF A PARAFFIN

At March 7th and 8th 2018, a workshop on viscosity measurement of paraffin and salt nitrates was organised by the University of Zaragoza and hosted by Fraunhofer ISE in Freiburg. For the

¹ Delgado et al., Intercomparative tests on viscosity measurements of phase change materials, *Thermochemica Acta* 668 (2018) 159–168

workshop Rheometers from TA-Instruments, Anton Paar and Thermo-Scientific were available in the lab. Previous to the measurement in the lab presentation were given by:

- Monica Delgado (Uni. Zaragoza) on the measurement procedure for PCMs
- Helena Navarro (Uni. Birmingham) on the measurement of high temperature PCMs
- Stephan Höhle (Uni. Bayreuth) on the IMETER measurement principle
- Mr. Schwab, TA-Instruments, introduction into DHR 2 Rheometer

Figure 3-8 shows some impressions from the workshop and Figure 3-9 shows the viscosity of RT70HC in dependency of temperature.



FIGURE 3-8: WORKSHOP ON MEASUREMENT OF VISCOSITY VIA ROTATIONAL RHEOMETERS, FROM ABOVE CLOCKWISE: PRESENTATIONS, PROGRAMMING A RHEOMETER, THE HIGH TEMPERATURE MEASUREMENT GEOMETRY FILLED WITH MOLTEN NITRATE SALT, FILLING THE GAP FOR THE MEASUREMENT OF RT70HC

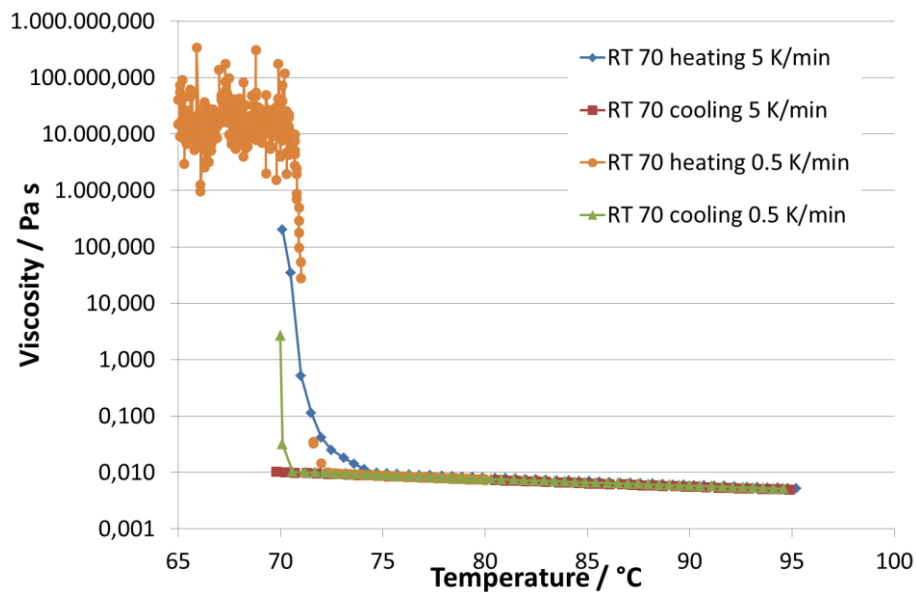


FIGURE 3-9: EXAMPLE: RESULT ON THE MEASUREMENT OF RT70HC, MEASURING FROM LIQUID TO THE PHASE TRANSITION, OSCILLATORY METHOD

SPECIFIC HEAT MEASUREMENTS VIA DSC

COMPARISON OF MEASUREMENTS

A comparison of specific heat capacity measurement via DSC was conducted. Five institutions contributed to this comparison. The measurements were done using different heating rates to determine the influence of low heating rates on the results. The target was to determine the resolution errors that are made using different DSCs and to check whether slow measurement is possible as the procedure to measure the enthalpy is based on slow heating rates. The results show, that for some devices slow heating rates lead to larger deviations (Figure 3-10, Figure 3-11, Figure 3-12), which is also observed in the comparison of the different results (Figure 3-13). The result shows that for a common measurement procedure to determine c_p of PCMs it is not possible to use slow heating rates. Therefore, the measurement according to ASTM 1269 is suggested.

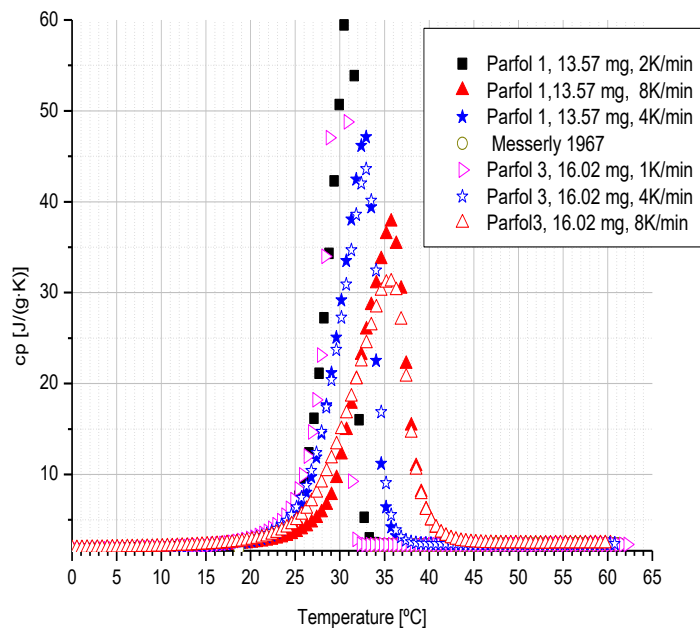


FIGURE 3-10: INFLUENCE OF HEATING RATE ON THE SHAPE OF THE MELTING PEAK (MEASURED BY UNIVERSITY OF ZARAGOZA)

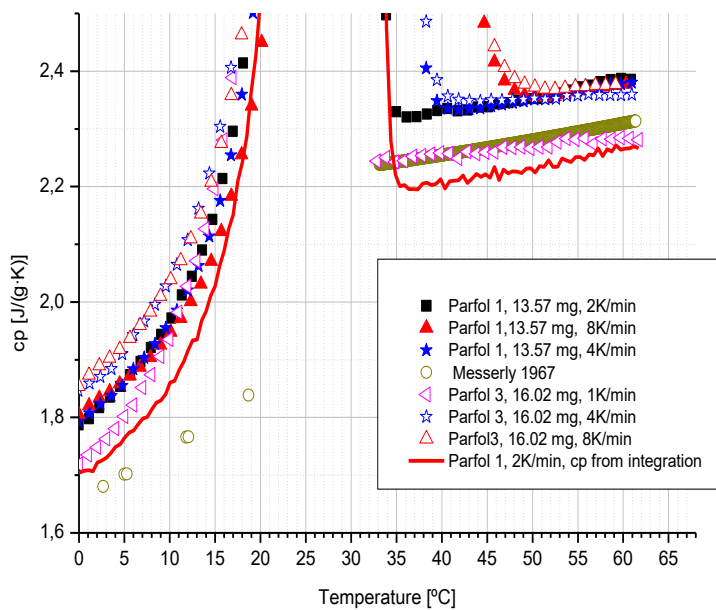


FIGURE 3-11: INFLUENCE OF HEATING RATE ON RESULT, MEASURED BY UNIVERSITY OF ZARAGOZA

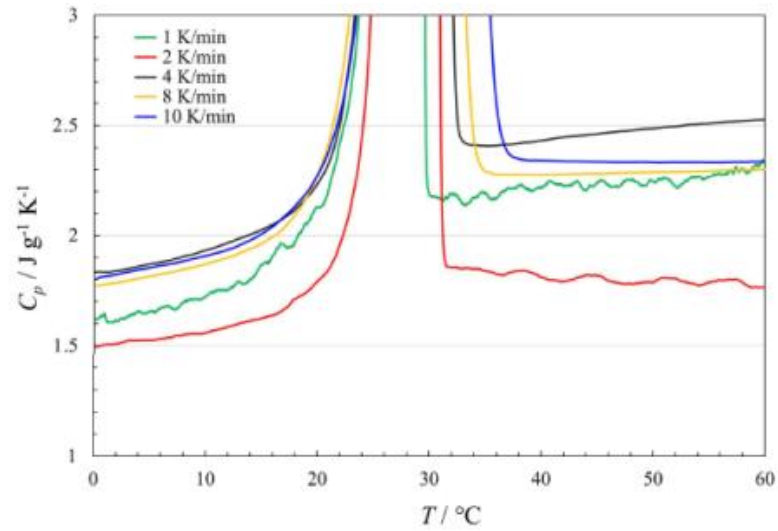


FIGURE 3-12: INFLUENCE OF HEATING RATE ON RESULT, MEASURED BY DALHOUSIE UNIVERSITY

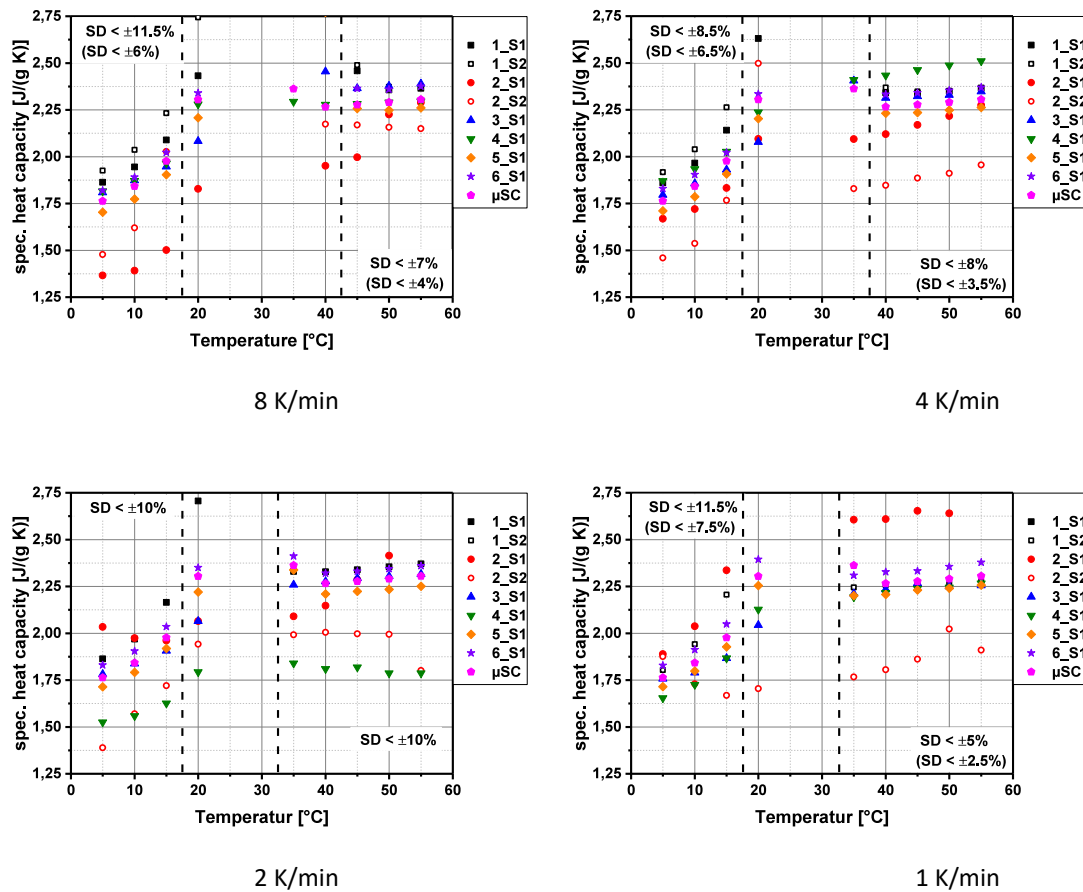


FIGURE 3-13: COMPARISON OF CP-MEASUREMENT CONDUCTED AT DIFFERENT INSTITUTIONS. STANDARD DEVIATION (SD) IN BRACKETS WITHOUT MEASUREMENT OF CONTRIBUTOR 2, DASHED LINES MARK THE TEMPERATURE RANGE IN WHICH THE MATERIAL PARAFOL 18-97 IS MELTING

METHOD SUGGESTION BASED ON ASTM 1269

Short abstract from the ASTM1269 (not complete):

Reference Material—Synthetic sapphire.

1. Purge the DSC apparatus with dry nitrogen (or other inert gas) at a flow rate of 10 to 50 mL per min throughout the experiment.
2. Weigh a clean, empty specimen holder plus lid to a precision of 60.01 mg. Record as the tare weight.
3. Position the empty specimen holder plus lid and a reference specimen holder plus lid (weight-matched, if possible) in the DSC apparatus. NOTE 7—The same reference specimen holder + lid should be used for the sapphire standard run and for the test specimen run.
4. Heat or cool the DSC test chamber to the initial temperature for the experiment at 20 °C/min.
5. Hold the DSC test chamber isothermally at the initial temperature for at least 4 min to establish equilibrium. Record this thermal curve (refer to 12.4).
6. Heat the test specimen from the initial to final temperature at a rate of 20 °C/min. Continue to record the thermal curve. NOTE 8—The precision of this test method is enhanced by this high heating rate. Other heating rates may be used but shall be reported.
7. Record a steady-state isothermal baseline at the upper temperature limit. Refer to 12.4.
 - 7.1. Terminate the thermal curve after this period.
 - 7.2. Cool the DSC test chamber to ambient temperature.
8. Place the sapphire standard into the same specimen holder plus lid used in 13.1.2.
9. Weigh sapphire standard and specimen holder plus lid to a precision of 0.01 mg and record the weight.

Following the additional definitions (12., 13., 14., and 15.) for conditioning, procedure, calculation, and report.

DENSITY MEASUREMENT

A comparison of density measurement was undertaken. The contributors used different technologies for the measurement (oscillating U-tube, Archimedes principle, helium pycnometer). Results are shown in Figure 3-14. The results reveal large deviations between measurement principals and different institutions. During the T58A33 it was decided not to proceed with this task.

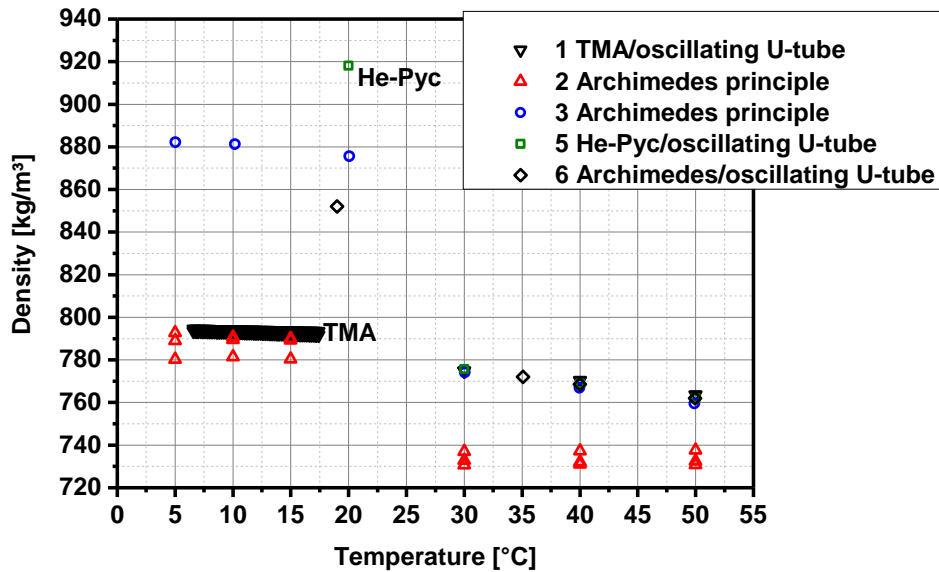


FIGURE 3-14: COMPARISON OF DENSITY MEASUREMENT DONE AT DIFFERENT INSTITUTIONS

3.1.4 DATABASE: MEASURED MATERIAL DATA FOR THE MAINTENANCE AND EXPANSION OF THE PCM DATABASE

The database has a private and a public section. Data of 56 measurements are available in the private section from which 16 datasets are publicly available. The last material uploaded was in October 2019. Figure 3-15 shows on the overview table of public available materials. Figure 3-16 illustrates one example for details available for a PCM.

Home User News Workshops Measurement-Standards & Tools **PCM** Sorption-Materials Wiki PCM

You are here: Home / PCM

Database PCM

Show 25 entries

Search:

Name	Institution	Last Change	Melting Temperature [°C]	Heat of Fusion [kJ/kg]	Density (liquid) [kg/m ³]	Thermal Conductivity (liquid) [W/mK]	Viscosity (liquid) [mPas]
CaBr ₂ ·6H ₂ O	ZAE-Bayern	Apr 19, 2017	33.29	135.5	1956.0		
gypsum board	Fraunhofer ISE	Oct 18, 2019	18.48	19.4			
HDPE natur NT D960/6	Fraunhofer ISE	Oct 13, 2015	128.0	219.0			
Lauric acid (dodecanoic acid)	ZAE-Bayern	Apr 19, 2017	43.5	178.2			
Lauric acid (Dodecanoic acid)	Fraunhofer ISE	Sep 07, 2017	43.65	180.0			
Methyl Stearate (methyl octadecanoate)	Fraunhofer ISE	Sep 07, 2017	36.7	208.0			
Micronal DS 5038 X	Fraunhofer ISE	Apr 09, 2018	21.5	96.0			
Micronal DS 5040 X	Fraunhofer ISE	Apr 09, 2018	19.07	93.6			
n-Octadecane, 99%	Fraunhofer ISE	Sep 07, 2017	27.5	233.0			
n-Octadecane, 99.5+%	Fraunhofer ISE	Sep 07, 2017	27.66	237.0			
NaNO ₃	Fraunhofer ISE	Oct 02, 2017	307.0	175.0			
Octadecan Parafol 18-97	Fraunhofer ISE	Jun 13, 2017	27.35	231.3			
PEG1000	Fraunhofer ISE	Sep 07, 2017	31.0	150.0			
PEG600	Fraunhofer ISE	Sep 07, 2017	13.0	137.0			
Potassium nitrate (KNO ₃)	Fraunhofer ISE	Sep 13, 2016	329.6	92.5			
RT 70 HC	Fraunhofer ISE	Oct 13, 2015	70.1	256.4			

FIGURE 3-15: SCREENSHOT OF THE PUBLIC AVAILABLE DATASETS (WWW.THERMALMATERIALS.ORG)

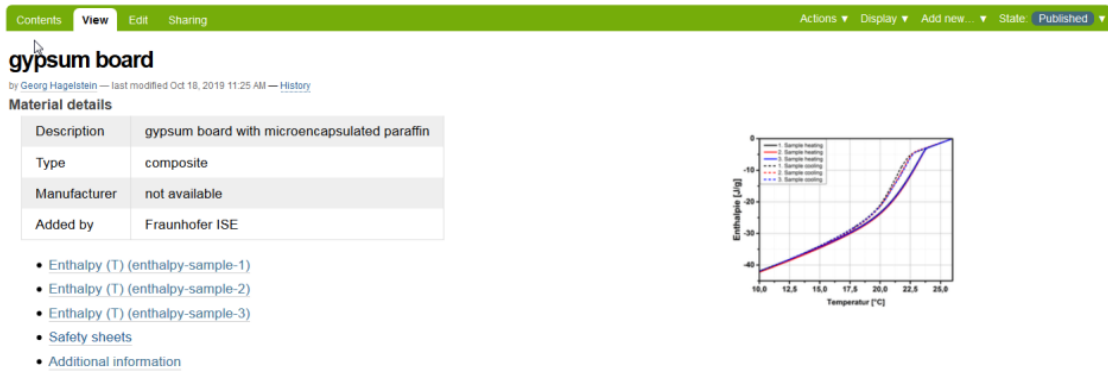


FIGURE 3-16: DETAILS EXAMPLE FOR COMPOUND OF GYPSUM AND PCM

3.1.5 WIKI FOR PCM

A Wiki was developed to document the nomenclature which is used in the field of PCMs. The Wiki is open, so that everybody can add new terms and definitions or to change existing ones. Figure 3-17 shows a screenshot.

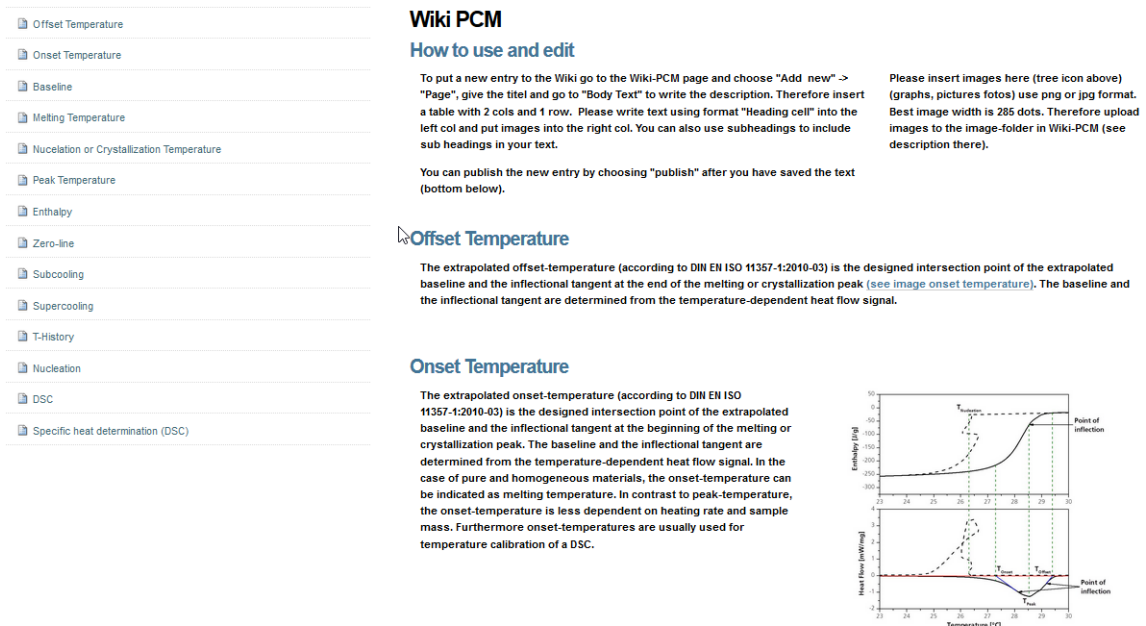


FIGURE 3-17: SCREENSHOT OF THE WIKI FOR PCM (WWW.THERMALMATERIALS.ORG/WIKI-PCM, 30/01/2020)

3.2 SUBTASK 2T: DEVELOPMENT AND CHARACTERIZATION OF IMPROVED THERMO-CHEMICAL MATERIALS

3.2.1 INTRODUCTION

The Subtask 2T focuses on the development of improved TCM materials, which are based on sorption (micro/mesoporous solids and liquids (hydroxides)), chemical reactions (salt hydrates and metal oxides/hydroxides) and combinations of both (zeolites/graphite+salt hydrates/metal). The activities of the Subtask 2T include the listing of new and improved existing materials, determination of material properties, measurement of thermo-physical properties and expanding the database implemented within the previous task.

One of the goals is to determine the differential heat of sorption / reaction of TCM materials, which can be expressed as a characteristic curve in order to derive possible storage performance.

This Working Group 2T includes the following activities:

1. Develop and identify novel chemical reactions and composite materials
2. Define relevant material parameters
3. Characterize novel reactions and materials by material properties
4. Maintenance and expansion of the material database implemented in Task42/Annex 29

In the framework of the Task/Annex 58/33 (IEA, TCPs ES/SHC 2017-2019), significant R&D effort was directed toward the development of new or improved TES materials. TCM used for thermal energy storage are an important class of materials which substantially contribute to the efficient use and conservation of waste heat and solar energy and lead to low carbon society. Comparing to the previous task the number of TCM groups increased significantly. Detailed information on R&D of compact TCM materials is presented in section 3.2.4.

3.2.2 DEVELOPMENT AND IDENTIFICATION OF THE NOVEL CHEMICAL REACTIONS AND COMPOSITE MATERIALS

Development of TCM materials has been devoted to characterization of new and improved TCM materials as powders: chemical reactants and sorption materials and composites as well as liquids. Novel chemical reactions and composite materials were developed and identified. Water and ammonia were used in chemical reactions, while only water was used for sorption materials. Table 3-1 presents different types of TCM materials, based on the following mechanism: adsorption, chemical reactions, absorption and mixture of all three mechanisms, investigated during the last 3 years.

TABLE 3-1: DIFFERENT TCMS DEVELOPED AT THE JOINT TASK/ANNEX 58/33 FROM 2017 TO 2019

Sorption materials	Chemical reactions	Composites	Liquids
MOFs: MIL-160, MIL-101, MIL-125,	CuCl ₂ -H ₂ O, MgCl ₂ -H ₂ O LiCl-H ₂ O, CaCl ₂ -H ₂ O	SAPO-34/Al	LiCl

	LaCl ₂		
Zeolites: 13X binder-free (BF) and with binder, YBF, deaYBF, Y with binder, 4A with binder and BF	SrBr ₂ -H ₂ O MgBr ₂ -H ₂ O	Mg(OH) ₂ -EG (expanded graphite), Mg(OH) ₂ -CNT (carbon nanotube)	LiBr
Aluminophosphates: APO-LTA, APO-34, APO-18, FAPO-34, SAPO-34, FAM-ZO2, APO-5	K ₂ CO ₃ -H ₂ O	MgCl ₂ -silica gel CaCl ₂ -silica gel SrBr ₂ -silica gel	NaOH
Porous SiC foam	MgO- Mg(OH) ₂ CTABr-Mg(OH) ₂ Ca/MgO-Ca/Mg(OH) ₂ , Co/MgO- Co/Mg(OH) ₂ , Ni/MgO- Ni/Mg(OH) ₂ ,	SrBr ₂ -graphite	ZnCl ₂
Silica gel	CaO/Ca(OH) ₂ ,	LiCl-vermiculite, clinoptilolite	
	Fe/CaMnO ₃ , CaMnO ₃ Copper oxides Iron oxides (redox reaction)	HKUST-1, CAU-10, MIL-100, Al-fumarate, SAPO-34-Al ₂ O ₃ foam HKUST-1, CAU-10, MIL-101, UiO-66-ceramic foam HKUST-1, CAU-10-SiC foam CAU-10, MIL-100, Al-fumarate-Al foam	
	Li ₂ SO ₄ /Na ₂ SO ₄	Ca/Mg/LiX-Al ₂ O ₃ foam Ca/Mg/LiX-ceramic cellular foams	
	LiOH/LiBr	CaCl ₂ -PHTS, SG, vermiculite, clinoptilolite	
	NiCl ₂ , CoCl ₂ , FeCl ₃ , CuCl ₂ -NH ₃	SrCl ₂ -ENG-NH ₃	
	MgCl ₂ , SrCl ₂ -NH ₃	MgSO ₄ -silicone foam	
	CoSO ₄ , FeSO ₄ , CuSO ₄ -NH ₃		

	Ba(OH) ₂ -H ₂ O		
	Na ₂ SO ₄ , Na ₂ S		
	Ettringite (Ca ₆ Al ₂ (SO ₄) ₃ (OH) ₁₂ ·26H ₂ O)		
	CuCaYCl ₂ , Ca _x Ti _y Cu ₂ Cl ₂ -NH ₃		
	CaCl ₂ -attapulgit/cellulose		

3.2.3 DEFINITION OF THE RELEVANT MATERIAL PARAMETERS

Relevant material parameters were defined and incorporated into two databases based on chemical reactions and adsorption of gas on solids, respectively. See overviews of the databases in the corresponding section.

3.2.4 CHARACTERIZATION OF NOVEL REACTIONS AND MATERIALS BY MATERIAL PROPERTIES

SORPTION MATERIALS

NATIONAL INSTITUTE OF CHEMISTRY SLOVENIA

DR. ALENKA RISTIĆ

TCM TYPE: COMPOSITE

1. Introduction: New composite water sorbents CaCl₂-PHTS for low-temperature sorption heat storage were prepared. The influence of water sorption on the structural properties of the composites of the plugged hexagonal templated silica (PHTS) with different contents of calcium chloride was studied.

2. Preparation of materials and/or supplier: Novel composites composed of PHTS (plugged hexagonal templated silicate) with hexagonal pore arrangement as the matrix and 4 wt%, 10wt% and 20 wt% of calcium chloride have been developed by incipient wetness impregnation. PHTS was synthesized by modification of the SBA-15 synthesis using long-chain surfactant triblock copolymer Pluronic P123 to prepare the plugged hexagonal templated silica with ordered hexagonal mesopore arrangement with average pore size lower than 6 nm.

3. Results: The structural, texture and adsorption properties of the matrix and the composites were determined and found out that the water sorption capacity of the composite material depends on the pore size of the matrix, the amount of hygroscopic salt in the pores, the matrix synthesis and the preparation of the composite.

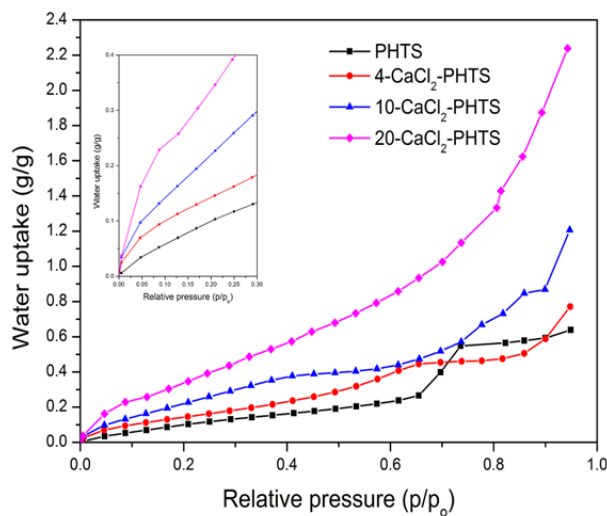
a. Structural properties for porous materials and composites / formula

TABLE 3-2: STRUCTURAL PROPERTIES OF PHTS AND THE PREPARED COMPOSITES.

Sample	S_{BET} (m^2/g)	V_{tot} (cm^3/g)	Average pore size (nm)
PHTS	810	0.705	5.7
4-CaCl ₂ -PHTS	461	0.492	5.6
10-CaCl ₂ -PHTS	322	0.377	5.8
20-CaCl ₂ -PHTS	163	0.189	6.2

S_{BET} , the BET surface area; V_{tot} , total pore volume, mesopore diameters

b. Sorption properties / reaction



WATER UPTAKE CURVES AT 40 °C

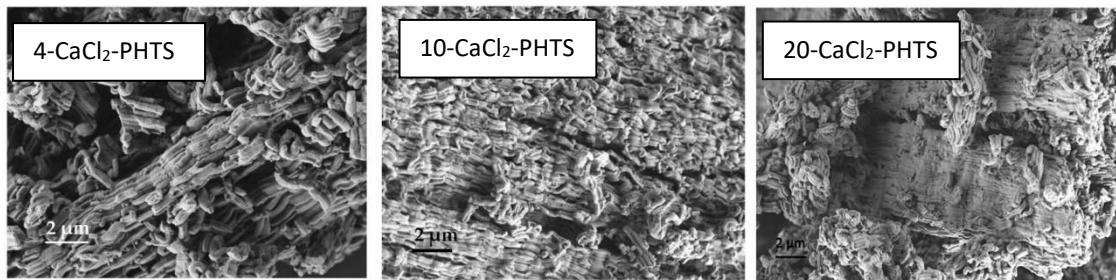
c. Thermochemical properties:

The integral heat of adsorption was calculated for the given boundary conditions: adsorption temperature at 40 °C, desorption temperature at 120 °C and a dew point temperature was set at 10 °C. The integral heat of adsorption Q_{ads} of all composites is listed in Table 3-3.

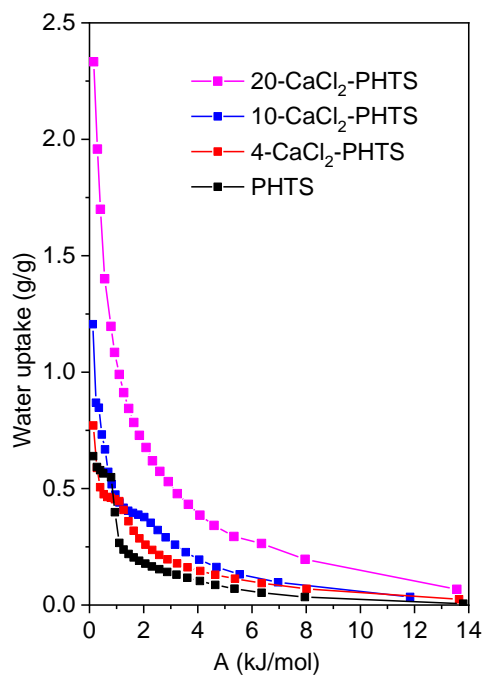
Table 3-3: Water loading lift and the integral heat of adsorption for the composites

Sample	Δw (kg/kg)	Q_{ads} (Wh/kg)	Q_{ads} (kJ/kg)
PHTS	0.073	71	256
4-CaCl ₂ -PHTS	0.100	81	292
10-CaCl ₂ -PHTS	0.142	119	428
20-CaCl ₂ -PHTS	0.239	193	694

d. Picture/image/photograph of the material: Scanning Electron Microscope (SEM) images



e. Graph: Characteristic curve



4. Summary: The increased salt content in the composites impacted the sorption performance of these composites, e.g. higher content of the salt higher energy storage capacity. The storage capacity of these composites can be increased by increasing the desorption temperature and decreasing the adsorption temperature. Water sorption caused structural modifications of the composites, showing the re-dispersion and possible agglomeration of the salt in the pores, which caused some blocking of pores (lower total pore volume and specific surface areas) after hydration and dehydration at 40 °C. On the other hand, repeated sorption/desorption cycles between 40 and 140°C at 56 mbar caused the improvement of structural properties (increase of specific surface area, total pore volume and pore size) of the 10-CaCl₂ and 20-CaCl₂ composites, indicating that highly dispersed salt is still present in the pores. During the cyclic test, there was no leaching of the salt from the PHTS matrix, showing the ability of the PHTS matrix to create a stable nano-environment for confinement of calcium chloride.

5. References

RISTIĆ, Alenka, ZABUKOVEC LOGAR, Natasa. New composite water sorbents CaCl₂-PHTS for low-temperature sorption heat storage: determination of structural properties. *Nanomaterials*, Jan. 2019, vol. 9, iss. 1, p. 1-16

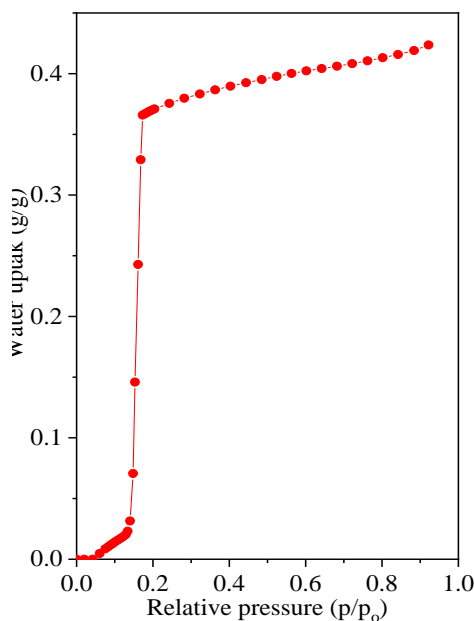
TCM TYPE: SORPTION MATERIAL

1. Introduction: In this study, a porous zeolite-like aluminophosphate adsorbent with LTA (Linde Type A) topology is inspected as an energy storage and heat transformation material. According to sorption and calorimetric tests, the aluminophosphate outperforms all other zeolite-like and metalorganic porous materials tested so far.

2. Preparation of materials and/or supplier: APO-LTA was hydrothermally synthesized from a fluoride medium using Kriptofix 222 (K222) as a structure-directing agent. (Krajnc, 2017) The as-synthesized sample was calcined in air at 600 °C over night.

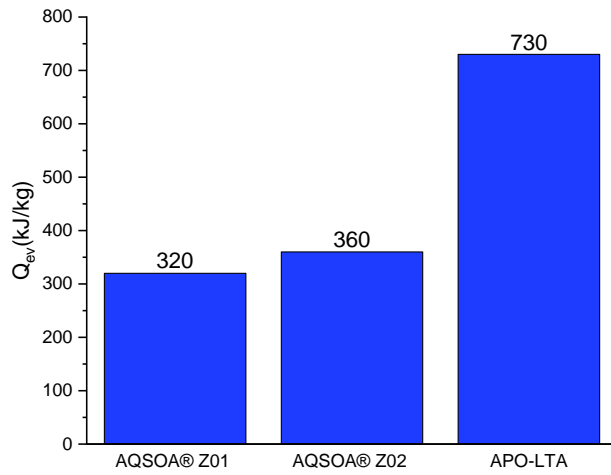
3. Results: Material shows remarkable cycling stability; after 40 cycles of adsorption/desorption its capacity drops by less than 2%. It adsorbs water in an extremely narrow relative-pressure interval ($0.10 < p/p_0 < 0.15$) and exhibits superior water uptake (0.42 g/g) and energy storage capacity (527 kW h/m³). Furthermore, its heat pump performance is very high, allowing efficient cooling in demanding conditions with cooling power up to 350 kWh/m³ even at 30 °C temperature difference between evaporator and environment. Desorption temperature for this material, which is one of crucial parameters in the applications, is lower from desorption temperatures of other tested materials by 10–15 °C. COP and cooling enthalpy for cooling application at boundary conditions: evaporator temperature $T_{ev} = 5$ °C, cooling temperature $T_{con} = 30$ °C and desorption temperature $T_{des} = 65$ °C is determined to be 0.70 and 730 kJ/kg, respectively.

a. Sorption properties / reaction



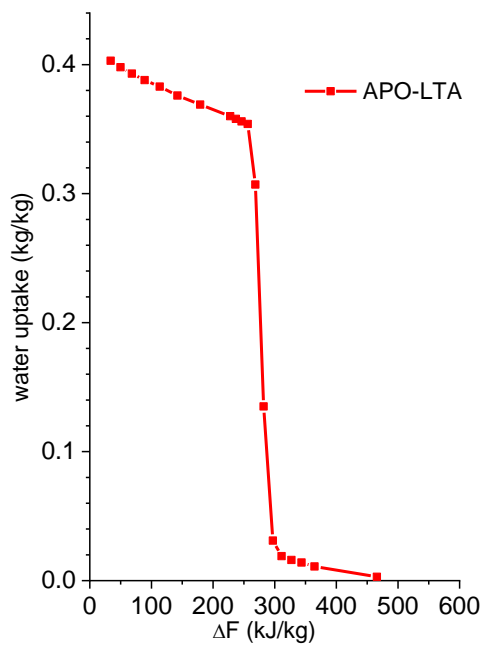
WATER UPTAKE CURVE AT 25 °C

b. Thermochemical properties:

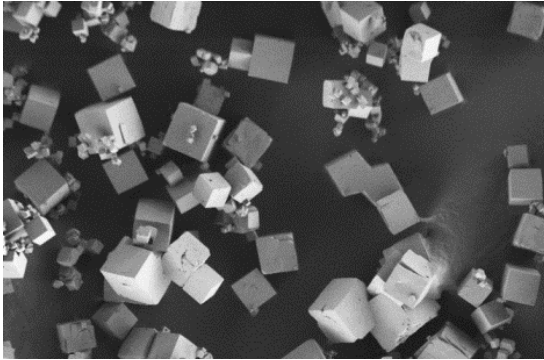


COMPARISON OF THE COOLING ENTHALPY Q_{EV} FOR BOUNDARY CONDITIONS ($T_{EV} = 5\text{ }^{\circ}\text{C}$, $T_{CON} = 30\text{ }^{\circ}\text{C}$, $T_{DES} = 65\text{ }^{\circ}\text{C}$)

c. Graph: Characteristic curve



d. Picture/image/photograph of the material:



SCANNING ELECTRON MICROSCOPE IMAGE

4. Summary: New aluminophosphate adsorbent full fills requirements for the ideal performance in the low-temperature (solar energy) heat transformation applications because it performs in the proper relative pressure range with S-shaped water adsorption isotherm. The charging or regeneration temperature is 65 °C. Comparing the cooling enthalpy of AQSOA® Z01 and Z02 adsorbents for air conditioning with regeneration temperature of 65 °C ($T_{ev} = 5$ °C, $T_{con} = 30$ °C) to APO-LTA, the later achieves two times higher cooling enthalpy.

5. References:

Krajnc, A., Varlec J., Mazaj, M., Ristić, A., Logar, N.Z., Mali, G., Superior Performance of Microporous Aluminophosphate with LTA topology in solar-energy storage and heat reallocation 2017, *Adv. Ener. Mat.*, 7, 201601815-1.

Alenka Ristić, Andraž Kranjc, Nataša Zabukovec Logar, New water adsorbent for adsorption driven chillers, 8th International Conference on Solar Air Conditioning, September 12-13, 2018, Rapperswil, Switzerland.

NATIONAL INSTITUTE OF CHEMISTRY SLOVENIA AND ZAE BAYERN GERMANY

DR. ALENKA RISTIĆ AND DR. FABIAN FISHER

TCM TYPE: SORPTION MATERIAL

1. Introduction: We present the use of the commercial granulated binder-free zeolite NaY as the adsorbent for sorption heat storage and the post-synthesis modification of this zeolite in order to decrease the desorption temperature and preserve energy storage density. We have studied the effect of HCl and H₄EDTA treatments, as well as the impact of sequential ion-exchange acid treatment on the material storage performance.

2. Preparation of materials and/or supplier: Binder-free granulated zeolite NaY (parent sample) was supplied from CWK (Bad Köstritz, Germany). Modified samples were prepared using one-step and two-step procedures:

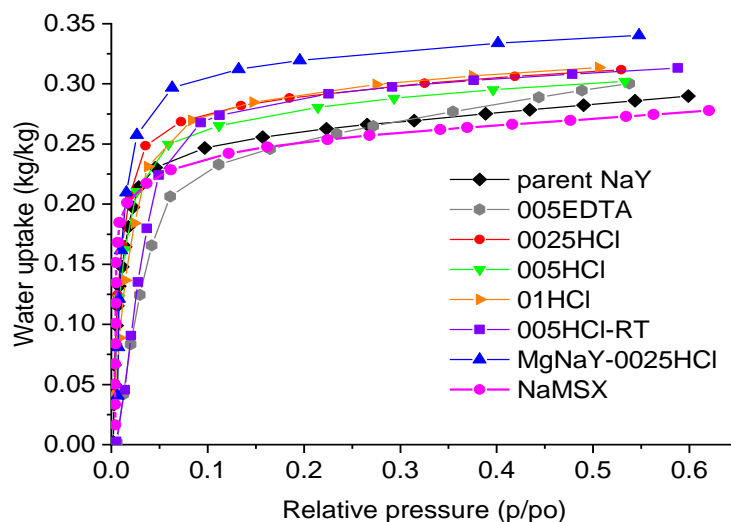
Samples	Treatment	Temperature (°C)	Time (h)
Parent NaY	-	-	-
0025HCl	0.025M HCl	100	1
005HCl	0.05M HCl	100	1
01HCl	0.1M HCl	100	1
005HCl-RT	0.05HCl	RT	120

005EDTA MgNaY-0025HCl	0.05M H ₄ EDTA 1M Mg(NO ₃) ₂ ;0.025M HCl	100 85;100	20 2;1
--------------------------	---	---------------	-----------

3. Results

a. Structural properties for porous materials and composites / formula: Less hydrophilic granulated samples can be prepared by nondestructive post-synthesis modifications using mild HCl treatment and chemical treatment with H₄EDTA, leading to a reduction in desorption temperature ranging from 10 to 30 °C. Mild acid treatment caused the generation of defects, which served as a binding sites for water, thus increasing water uptake for 10%. The H₄EDTA treatment introduced mesoporosity and improved the pore accessibility by removal of Al from the framework. On the other hand, a two-step procedure with sequential Mg-exchanged acid treatment can bring about enhanced water sorption capacity and desorption temperature.

b. Sorption properties / reaction



WATER UPTAKE AT 25 °C OF THE PARENT SAMPLE NaY, THE MODIFIED SAMPLES AND NaMSX.

c. Thermochemical properties:

Water uptake in equilibrium after adsorption (40 °C) $X_{S,ads}$ and after desorption (140 °C) $X_{S,des}$, water loading spread ΔX_s and the integral heat of adsorption in Wh/kg.

Sample	$X_{S,ads}$ (kg/kg)	$X_{S,des}$ (kg/kg)	ΔX_s (kg/kg)	q_{ads} (Wh/kg)
Parent NaY	0.2898	0.0783	0.2115	185.0
0025HCl	0.2931	0.0776	0.2155	187.9
005HCl	0.2775	0.0735	0.2040	177.4
01HCl	0.2833	0.0703	0.2130	185.3
005HCl-RT	0.2836	0.0730	0.2106	183.3

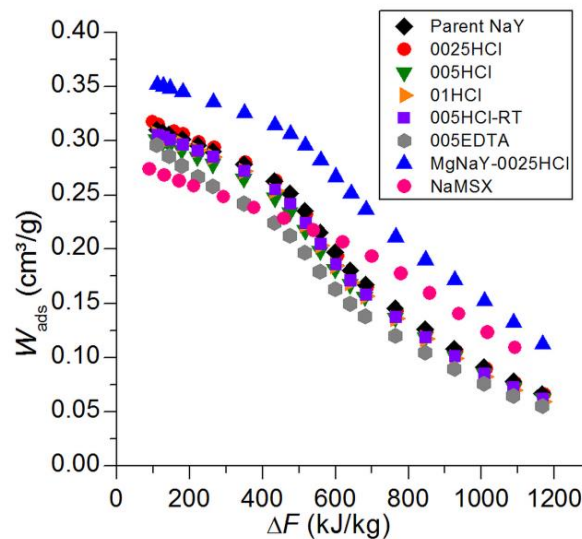
005EDTA	0.2573	0.0653	0.1920	166.1
MgNaY-0025HCl	0.3336	0.1331	0.2005	179.4
NaMSX	0.2501	0.1101	0.1400	127.0

d. Picture/image/photograph of the material:



SEM IMAGE OF BINDER-FREE ZEOLITE NAY

e. Graph: Characteristic curve



THE CHARACTERISTIC CURVES OF THE PARENT NAY, THE MODIFIED SAMPLES AND NAMSX

4. Summary: Commercial granulated binder-free NaY zeolite can be used as the adsorbent in the sorption storage system to recover industrial waste heat at a temperature of 140 °C. The performance of adsorbents in sorption heat storage depended on the type of post-synthesis treatment, for example the H₄DTA treatment improved pore accessibility by removal of Al from the framework, while mild acid treatment caused the generation of defects, which served as the binding sites for water, thus the water uptake was increased. Post-synthesis modifications lead to a reduction in desorption temperature ranging from 10 to 30 °C and to an increase of the evaluated energy storage densities of the parent NaY and the modified samples for up to 40% above the value of the NaX zeolite at a desorption temperature of 140 °C.

5. References

Ristic, A.; Fischer, F.; Hauer, A.; Logar, N. Z., Improved performance of binder-free zeolite Y for low-temperature sorption heat storage. Journal of Materials Chemistry A 2018, 6 (24), 11521-11530.

UNIVERSITY OF APPLIED SCIENCES UPPER AUSTRIA, RESEARCH GROUP ASiC

DR. BERNHARD ZETTL, GAYANEH ISSAYAN

TCM TYPE: ADSORPTION

1. Introduction: Project OFFSOR-Open Sorption Storage Technology for Building Applications: Project aimed to develop and build a laboratory prototype with automatic control for mass and heat transfer for both, adsorption and desorption cycles. The main goal of thermo-physics were to find measures for adsorption-kinetics that are useful for modelling the heat storage reactions in the relevant set of parameters typical for applications.

2. Preparation of materials and/or supplier: The zeolite granules were purchased in granule form, ready to use and no further sample manipulations occurred. Following zeolite molecular sieves were subject to investigation:

- 4A Silkem
- 4A CWK
- 4A BF CWK
- 13X CWK
- 13X BF CWK

3. Results:

a. Structural properties for porous materials and composites / formula & b. Sorption properties / reaction

The utilized zeolites have following properties according to datasheet:

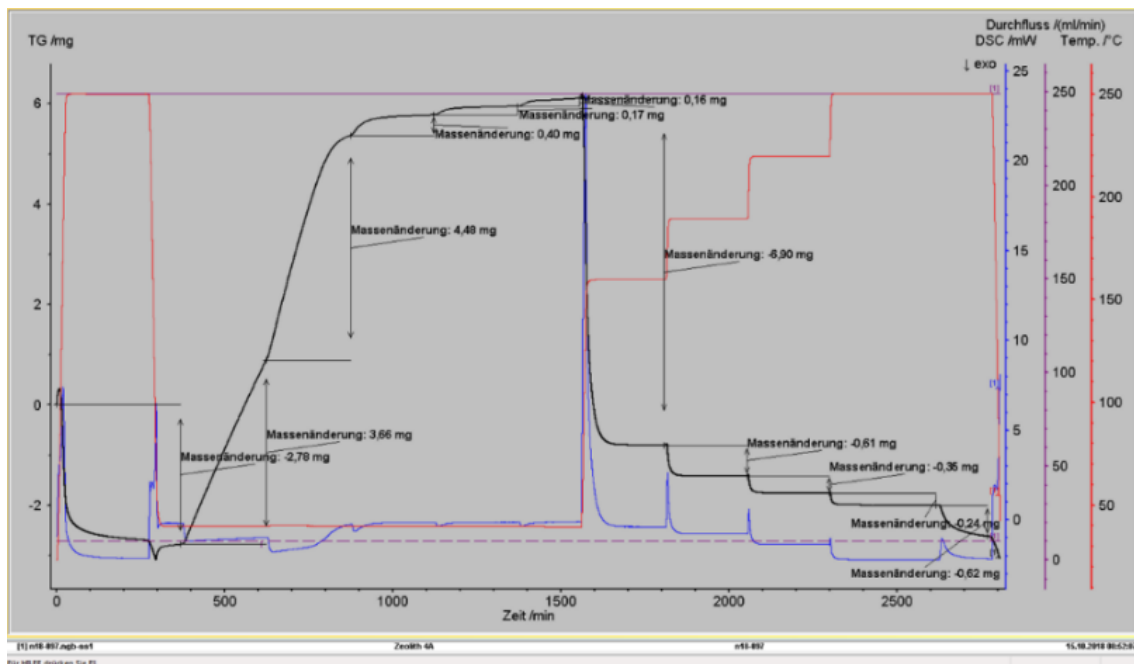
CWK	Type	Pore Size in Å	Granule Size in mm	Adsorption capacity in cm ³ /g (min 55% RH, 20°C)	Formula
4A	LTA	4	1.6-2.5	21.5 H ₂ O	Na ₂ O·Al ₂ O ₃ ·2.0SiO ₂ ·nH ₂ O
4A BF	LTA	4	2.5-5	24 H ₂ O	Na ₂ O·Al ₂ O ₃ ·2.0SiO ₂ ·nH ₂ O
13X	FAU	9	1.2-2	26.5 H ₂ O	Na ₂ O·Al ₂ O ₃ ·mSiO ₂ ·nH ₂ O (m<= 2.35)
13X BF	FAU	9	1.2-2	30 H ₂ O	Na ₂ O·Al ₂ O ₃ ·mSiO ₂ ·nH ₂ O (m<= 2.35)
Silkem					
4A	LTA	-----	2-3.5	-----	Na ₂ O(17-19%), Al ₂ O ₃ (28-30%), SiO ₂ (31-34%), H ₂ O(18-22%)

c. Thermochemical properties

4A Zeolith: Silikem				
Materialtemperatur	Gasfeuchte	Exposition	Programmierte Temperatur	Quelle für T(Segment) _{neu}
250°	0 g/kg	240 min	265	STA-sDSC:n18-094
40°	2 g/kg	240 min	46,5	STA-sDSC:n18-094
40°	4 g/kg	240 min	46,5	STA-sDSC:n18-094
40°	6 g/kg	240 min	46,5	STA-sDSC:n18-094
40°	8 g/kg	240 min	46,5	STA-sDSC:n18-094
40°	10 g/kg	240 min	46,5	STA-sDSC:n18-094
160°	10 g/kg	240 min	170	STA-sDSC:n18-094
190°	10 g/kg	240 min	201,5	STA-sDSC:n18-094
220°	10 g/kg	240 min	233	STA-sDSC:n18-094
250°	10 g/kg	240 min	265	STA-sDSC:n18-094
250° (=Start)	0 g/kg	240 min	265	STA-sDSC:n18-094

FIGURE 3-18 TEMPERATURE AND HUMIDITY PARAMETERS FOR THERMAL ANALYSIS MEASUREMENTS.

The thermal analysis measurements were executed by DSC/TG. The parameters summed up in Figure 3-18 describe realistic year-round conditions for material temperature and air humidity. The cycle starts with fully dried material at 250°C. The adsorption in winter can be controlled by increasing the humidity stepwise, which leads to higher material temperature. Those conditions were taken into account for DSC measurements, whereby the exposition time was also specified in Figure 3-18. The results are depicted in Figure 3-19.



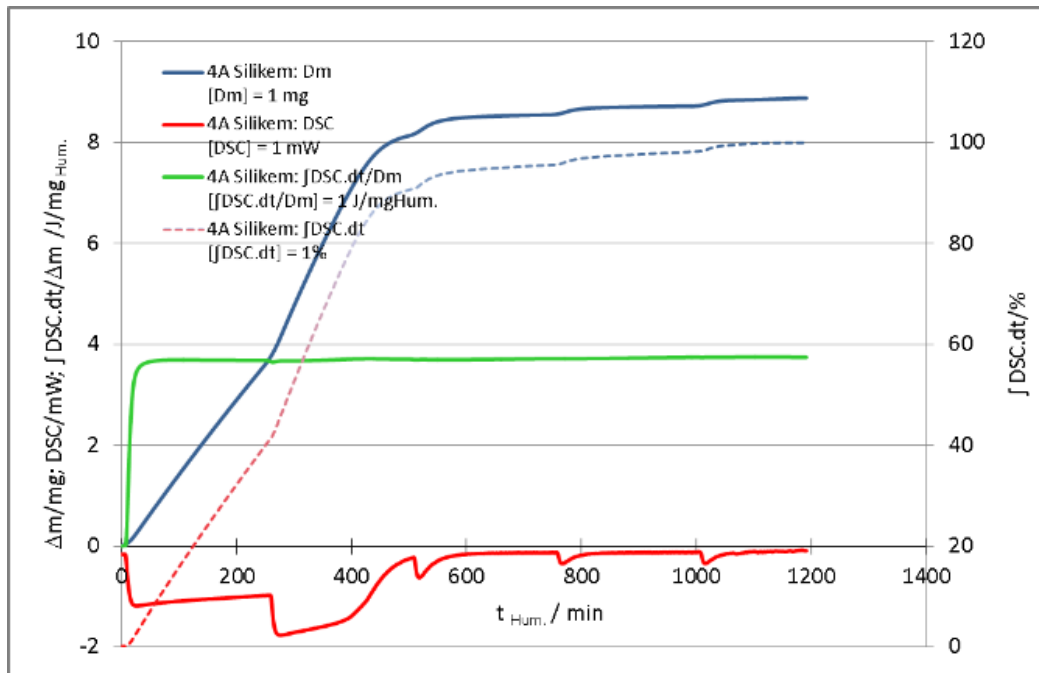


FIGURE 3-19 4A SILIKEM TG/DSC MEASUREMENTS FOR ONE CYCLE OF ADSORPTION AND DESORPTION. MEASUREMENTS BY DR. WOLFGANG HOHENAUER AIT.

d. Picture/image/photograph of the material

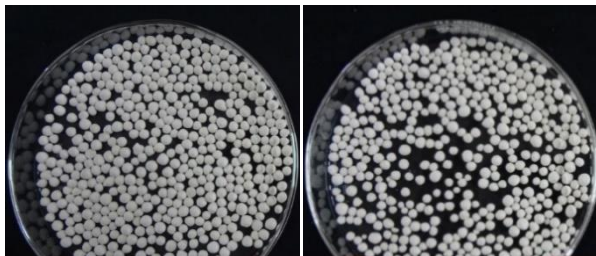


FIGURE 3-20 MATERIAL 4A BF CWK (LEFT) AND 4A SILKEM (RIGHT).

e. Graph: characteristic curve (adsorbed volume w_{ads} as a function of the adsorption potential ΔF (kJ/kg))

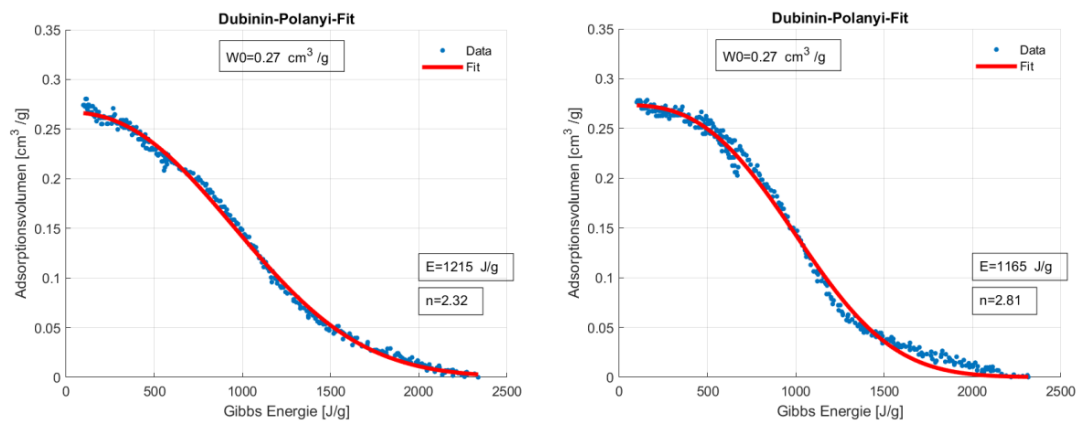


FIGURE 3-21 COMPARISON CHARACTERISTIC CURVE OF ZEOLITE 4A FROM DIFFERENT PRODUCERS: CWK (LEFT) AND SILKEM (RIGHT). BOTH ZEOLITES SHOW THE SAME ADSORPTION SATURATION VOLUME OF 0.27 CM³/G.

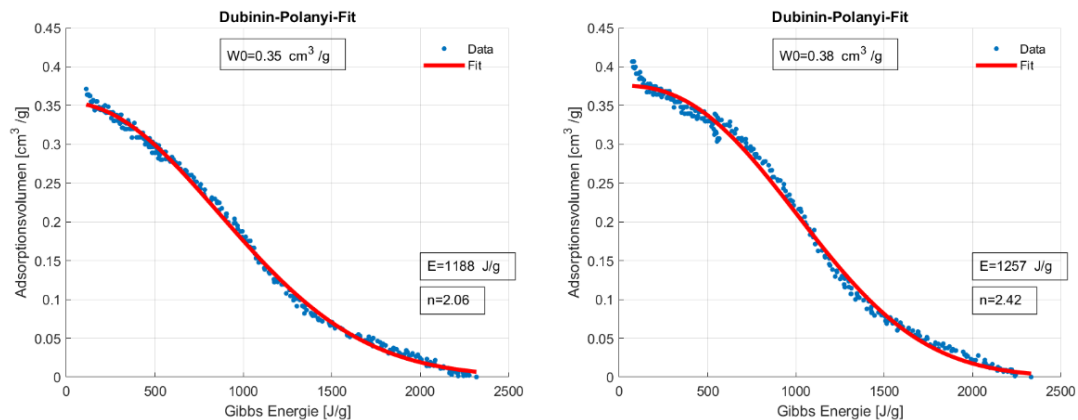


FIGURE 3-22 COMPARISON CHARACTERISTIC CURVE OF 13X ZEOLITES (LEFT) AND 13 BF (RIGHT). BINDER FREE ZEOLITES SHOW HIGHER ADSORPTION SATURATION VOLUME THAN THE ONES WITH BINDER.

4. Summary: A setup was developed to measure the water vapor adsorption/desorption of zeolites, which had to be purchased in bulk for the designed rotating bed open heat storage (Figure 3-23). The selection of appropriate zeolite was supported by the mentioned setup. The measurements results were analysed based on the characteristic curves. The results showed a constant tendency of higher saturation values for adsorption volume. However the comparison of different materials confirmed the legitimacy of measurement method and the setup. The results show that both 4A zeolite samples purchased from different suppliers yielded the same saturation values and the binder free 13X zeolite indicated a better performance regarding the adsorbed volume.



FIGURE 3-23 ROTATING BED OPEN HEAT STORAGE PROTOTYPE DEVELOPED IN PROJECT OFFSOR.

TCM TYPE: CHEMICAL REACTION-ADSORPTION

Project New TCM- Development of Highly Efficient Thermochemical Storage Materials

This project aims to investigate and develop stabilization methods of salts and characterize the relevant parameters for process technologies. Disc granulation is chosen to stabilize the salts in combination of porous materials and binders. The granules will be tested on their adsorption capabilities, tensile strength and cycling abilities.

Clinoptilolite IPUS ($\text{Ca, K, Na, Mg}_6(\text{Si,Al})_{36}\text{O} \cdot 20\text{H}_2\text{O}$) with high concentration of Ca, less K and rare amounts of Mg and Na. Multiple binder and coating materials in experimental phase. Salt hydrates LiCl anhydrate (Leverton), CaCl_2 dihydrate (CIECH Soda Polska) and anhydrate (Carl Roth)

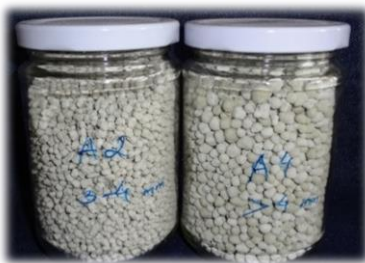


FIGURE 3-24 FIRST GRANULATION STEPS WITH SALTS AND POROUS MATERIALS.

The project is in process and there are no results available yet.

CANMETENERGY OTTAWA, NATURAL RESOURCES CANADA ¹

LABORATORY FOR ALTERNATIVE ENERGY CONVERSION (LAEC), SCHOOL OF MECHATRONIC SYSTEMS

ENGINEERING, SIMON FRASER UNIVERSITY ²

¹DR. LIA KOUCHACHVILI, DR. REDDA DJEBBAR

²PROF. MAJID BAHRAMI, DR. MINA ROUHANI

TCM TYPES: SORPTION MATERIAL, COMPOSITES AND CHEMICAL REACTION

Introduction (objectives): This research aimed at development, characterization, and screening of thermochemical materials to develop high efficient and economically viable thermal energy storage systems.

TCM types:

1- Adsorbent (AQSOA FAM-Z02)

2- Composite sorbents (silica gel+CaCl₂; vermiculite+CaCl₂)

3- Salt hydrates (Na₂S n.H₂O)

Material preparation/ suppliers: AQSOA FAM-Z02 (SAPO-34 Al_{0.56}Si_{0.02}P_{0.42}O₂) Mitsubishi Plastic Inc



- silica gel+CaCl₂; Developed at LAEC

Commercial silica gels (Silicycle Inc., Quebec, Canada) with 4 distinct pore size distributions and 0.2–0.5 mm irregular-shaped grains were wetted with ethanol. Aqueous CaCl₂ solution was added to silica. The mixtures were dried for 24 h in a fume hood. The damp material was baked at 200°C until judged dry by successive weight measurements



- Vermiculite+CaCl₂; MULTISORB Technologies

Vermiculite (50-75%), CaCl₂ (15-50%), High density polyethylene fiber (5 - 15%)



- Na₂S n.H₂O n=0-9; Samples from four different international suppliers



Results – Energy Storage Performance [1,2,3]:

Energy storage density based on dry mass, averaged from the last two cycles:

Sample	Energy storage density (MJ/kg)	Energy storage density (Wh/kg)
AQSOA FAM-Z02	0.963	267.5
silica gel +CaCl ₂	1.619	449.7
Vermiculite +CaCl ₂	1.539	427.5
Na ₂ S·9H ₂ O	3.435	954.1
Na ₂ S·xH ₂ O (commercial-grade)	3.124	867.8

Desorption condition: dry nitrogen with the flow of 20 and 50 ml·min⁻¹, at temperature of 80°C, and heating rate of 1 K·min⁻¹; **Sorption condition:** temperature of 25°C, and water vapor pressure of 12 mbar (i.e., equivalent to 10°C), and cooling rate (after the desorption and before the sorption) of 5 K min⁻¹.

Summary: FAM-Z02 showed the highest discharging rate (k_{dch}) of $7 \times 10^{-4} \text{ s}^{-1}$, using $\frac{(\omega - \omega_0)}{(\omega_\infty - \omega_0)} = 1 - \exp(-k_{dch}t)$. Na₂S n.H₂O provided the highest specific power (SP) and energy storage density (ESD). Among the rest of sorbent candidates, highest discharge SP (0.431 kWkg⁻¹) was for FAM-Z02 and highest charge SP (0.541 kWkg⁻¹) was for vermiculite+CaCl₂. Silica gel+CaCl₂ showed ESD of 1.6 MJkg⁻¹. Due to the low volumetric ESD (low density) of vermiculite+CaCl₂, and potential agglomeration of Na₂S n.H₂O samples, the preliminary results seems to point to the silica gel+CaCl₂ as a best candidate to explore more.

References:

- [1] L. Kouchachvili, R. Djebbar, M. Rouhani, M. Bahrami, (2018) "Characterization of commercial grade sodium sulfide for residential heating applications", ISEC 2018, Graz, Austria.
- [2] M. Rouhani, L. Kouchachvili, R. Djebbar, M. Bahrami, (2019) "Thermochemical energy storage for residential applications", 5th Experts meeting of IEA SHC T58/ECES A33, Ottawa, Canada.

[3] M. Rouhani, (2019) "Sorpton thermal energy storage for sustainable heating and cooling", PhD Thesis, Simon Fraser University.

SWANSEA UNIVERSITY

DR. JONATHON ELVIS

TCM TYPE: COMPOSITE MATERIALS

1. Introduction (objectives): Assessment of energy density, heat evolution (ΔT) and cyclic efficiency of TCM as a function of flow rate (Litres per minute (LPM))

2. Material preparation/ suppliers: Vermiculite//CaCl₂ synthesised using insipient wetness technique; Vermiculite supplied by Dupre, CaCl₂·XH₂O supplied by Sigma Aldrich

3. Results:

a. Structural properties for porous materials and composites / formula

Vermiculite: $(Mg, Fe^{+2}, Fe^{+3})_3[(Al, Si)_4O_{10}](OH)_2 \cdot 4H_2O$ // CaCl₂·XH₂O (X=0,1,2,4,6)

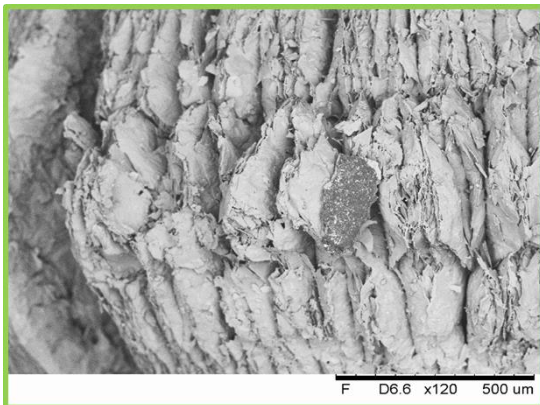
b. Sorption properties / reaction

Typically: CaCl₂·2H₂O → CaCl₂·6H₂O

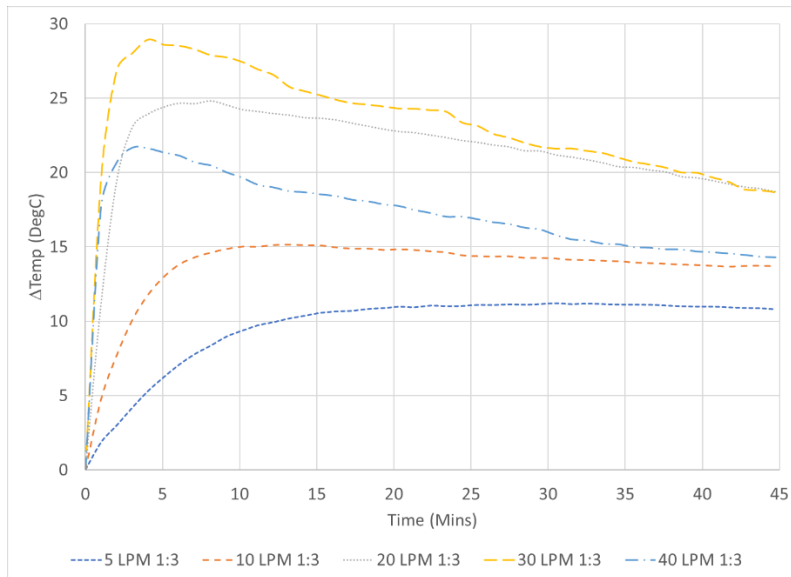
c. Thermochemical properties:

Energy Density: 80 – 250 kWh/m³

d. Picture/image/photograph of the material



e. Graph: Characteristic curve



Summary: Varying the volumetric flow rate has a significant effect upon on both the peak ΔT achieved and the overall energy released during these short-term experiments. In these tests, a lower flow rate produces a small temperature rise but allows a more controlled release of energy over the experimental period. As the flow rate is increased up to 30LPM, the ΔT steadily rises as does the overall energy released. Beyond 30LPM, the temperature rise achieved is again reduced, along with the overall energy released.

CHEMICAL REACTION

TECHNICAL UNIVERSITY OF DENMARK (DTU)¹, KTH ROYAL INSTITUTE OF TECHNOLOGY- SWEDEN²
AND

[IFE- NORWAY³, AMMINEX EMISSION TECHNOLOGY (AET)- DENMARK⁴]

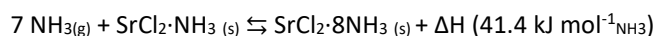
ANASTASIIA KARABANOVA¹, DR. DIDIER BLANCHARD¹

DR. SAMAN NIMALI GUNASEKARA², DR. VIKTORIA MARTIN²

[STEFANO DELEDDA³, PERIZAT BERDIYEVA³, BENOIT CHARLAS⁴]

TCM TYPE: CHEMICAL REACTION (ABSORPTION)

The reversible chemical reaction system $\text{SrCl}_2\text{-NH}_3$ is used, specifically for the absorption/ desorption between $\text{SrCl}_2\text{-NH}_3$ and $\text{SrCl}_2\text{-}8\text{NH}_3$, of which the reaction equation is shown in eq. 1 [1]



EQ. 1

1. Introduction: the aim of the research -Neutrons for Heat Storage (NHS)

The Neutrons for Heat Storage (NHS) project aims to develop a TCS system for low-temperature heat storage (40-80 °C). Here, absorption and desorption between metal halides and NH_3 is used. From the project partners, DTU, Denmark, IFE-Norway (collaborating with Amminex Emission Technology (AET) and KTH-Sweden. DTU and IFE are involved in synthesizing and characterizing new mixed metal halides for energy storage using their reaction with ammonia, thermal

conductivity improvements of these salts by impregnating these into materials with better thermal conductivity, and performing neutron imaging and numerical modelling (in COMSOL) to characterize the behavior of the salts in reactors. KTH is involved in designing a bench-scale TCS system and its reactors (with numerical modelling using Aspen plus and COMSOL), for the chemical reaction system $\text{SrCl}_2\text{-NH}_3$ for simultaneous heat storage and release operation.

2. Preparation of materials and/or supplier:

The (pristine) SrCl_2 was so far provided by AET, and ENG boards are purchased from SGL carbon GmbH [2]. The SrCl_2 -ENG composites preparation by impregnation (and in certain cases by mechanical compression), followed by ammoniation of the composite to obtain $\text{SrCl}_2\cdot 8\text{NH}_3$ -ENG and their characterizations are conducted by DTU. Prior to the composite preparation, the ENG pellet was placed in a vacuum furnace at $120\text{ }^\circ\text{C}$ for 12 h to remove any moisture (to measure the right weight of the pellet before impregnation). Then, the pellet was immersed in ethanol (used as a surfactant) for 2 h, to lower the surface tension between the hydrophobic ENG pellet and the aqueous SrCl_2 solution. 1. Thereafter, the pellet was taken out of ethanol and immersed in an aqueous SrCl_2 solution for 24 h. Afterwards, the pellet was taken out and placed in a ventilated furnace at $90\text{ }^\circ\text{C}$ for 12 h to remove the free water, followed by placing in a vacuum furnace at $200\text{ }^\circ\text{C}$ for 12 h to remove any water left. Finally, this dried disc was pressed into the desired compaction.

3. Results

a) Structural properties for porous materials and composites / formula

In the NHS project, initially DTU and IFE synthesized certain new metal halides (e.g. $\text{Ca}_x\text{Ti}_y\text{Cu}_z\text{Cl}_2$, $\text{Cu}_x\text{Ca}_y\text{Y}_z\text{Cl}_2$, $\text{Sr}_x\text{Ca}_y\text{Cl}_2$, and $\text{Ni}_x\text{Ca}_y\text{Cl}_2$) with successful characterization using Differential scanning calorimetry (DSC) and X-ray Diffraction (XRD). However, these alloys failed to produce stable phases. Therefore, the reaction pair $\text{SrCl}_2\text{-NH}_3$ is then chosen for the project continuation. To improve thermal conductivity of this salt (SrCl_2), by DTU, it is then inserted (embedded) into expanded natural graphite (ENG) boards from SGL carbon GmbH [2], to form the composite. With salt impregnation and ammoniation experiments conducted at DTU, the SrCl_2 -ENG composites were found as can be effectively made to contain 79% w/w% salt in the composite with a bulk density of 615 kg m^{-3} . An example of such prepared composite is shown in Figure 3-25. The volume expansion after full-ammoniation in this composite was found to be negligible (i.e., the porosity of the ENG board was sufficient to accommodate the $\text{SrCl}_2\cdot 8\text{NH}_3$). The thermal properties of this composite is currently under investigation by DTU.

b) Sorption properties/reaction:

Shown in eq. 1.

c) Thermochemical properties:

The specific reaction enthalpy for the conversion between $\text{SrCl}_2\text{-NH}_3$ and $\text{SrCl}_2\cdot 8\text{NH}_3$ is $41.4\text{ kJ mol}_{\text{NH}_3}^{-1}$ and the entropy is $230\text{ J mol}_{\text{NH}_3}^{-1}\text{ K}^{-1}$ [3]. The thermal conductivity of both these amines (pristine) are approximated to be $1.1\text{ W m}^{-1}\text{ K}^{-1}$ [4]. The effective thermal conductivity of

the ENG in the bulk $\text{SrCl}_2 \cdot 8\text{NH}_3$ -ENG composite (which includes the porosity of the sample) for in-plane and through-plane directions are considered (using linear regression of available data [2]) as $26 \text{ W m}^{-1} \text{ K}^{-1}$ and $10.5 \text{ W m}^{-1} \text{ K}^{-1}$ (for the compacted new density of ENG: 172 kg m^{-3}).

d) Picture/image/photograph of the material



FIGURE 3-25. SRCL2 IMPREGNATED INTO ENG

e) Graph: characteristic curve

As this system concerns a chemical reaction involving absorption, the characteristic curve is the equilibrium pressure curve. This is compiled into Figure 3-26 (combined with the phase diagram of NH_3), for absorption-desorption between the monoamine and octaamine of SrCl_2 . The Van't Hoff's equation, as in eq. 2 [1], [3] expresses the equilibrium pressure of this conversion. In this, p_{eq} is the equilibrium pressure (Pa), p_0 is the reference pressure (1 Pa), ΔH and ΔS are the reaction enthalpy (J/mol) and entropy (J/(mol·K)) respectively, R is the ideal gas constant (8.314 J/(mol·K)) and T is the reaction temperature (K).

$$p_{eq} = p_0 \cdot \exp\left(-\frac{\Delta H}{RT} + \frac{\Delta S}{R}\right) \quad \text{EQ. 2}$$

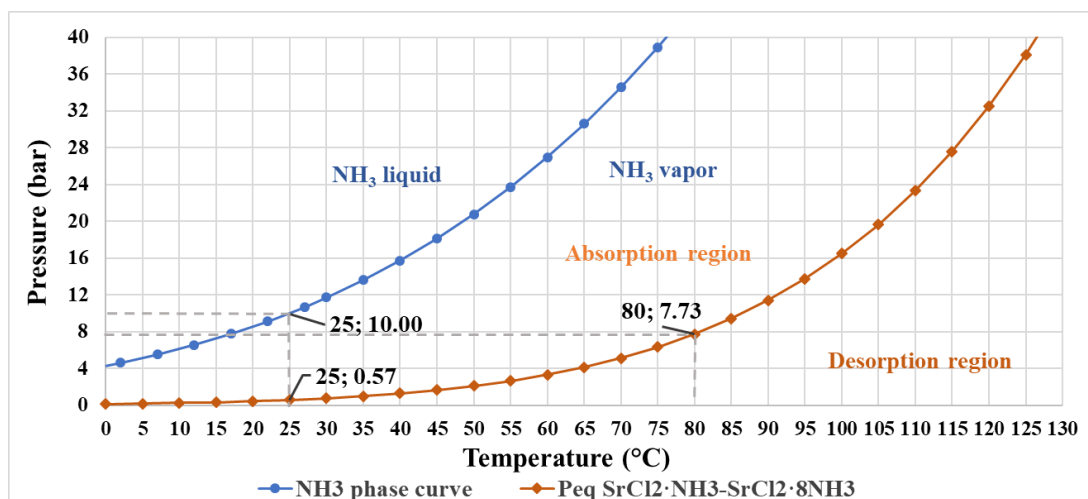


FIGURE 3-26. NH_3 PHASE DIAGRAM (BASED ON DATA FROM [5]) AND $\text{SrCl}_2 \cdot \text{NH}_3$ - $\text{SrCl}_2 \cdot 8\text{NH}_3$ EQUILIBRIUM PRESSURE (P_{eq})-TEMPERATURE (T_{eq}) PLOT (BASED ON THE VAN'T HOFF EQUATION, COMBINING DATA FROM [1] AND [3] INTO [6])

The reaction kinetic parameters were determined experimentally using a Sieverts-type apparatus, which are compared with literature data as in Table 3-4. This detailed method and the most updated results are currently being formulated into a scientific article.

Table 3-4. The comparison of the kinetics parameters from literature and obtained experimentally [8]

Parameter	Absorption		Desorption	
	Literature [7]	Experiment	Literature [7]	Experiment
f(x)	$(1-x)^{2.96}$	$2(1-x)^{3/2}$	$(1-x)^{3.02}$	$4(1-x)^{1/4}$
k_0	0.019	28.1	0.125	$1.8 \cdot 10^8$
E_d	6921	31000	9000	75000
m	1	1	1	0.44

4. Summary

In the NHS project, initially DTU and IFE synthesized certain new metal halides (e.g. $\text{Ca}_x\text{Ti}_y\text{Cu}_z\text{Cl}_2$, $\text{Cu}_x\text{Ca}_y\text{Y}_z\text{Cl}_2$, $\text{Sr}_x\text{Ca}_y\text{Cl}_2$, and $\text{Ni}_x\text{Ca}_y\text{Cl}_2$) with successful characterization using DSC and XRD. However, these alloys failed to produce stable phases. Therefore, the reaction pair $\text{SrCl}_2\text{-NH}_3$ is then chosen for the project continuation. By DTU, the reaction media is made into composites of $\text{SrCl}_2 \cdot 8\text{NH}_3$ in ENG (79:21 SrCl_2 :ENG w/w), for thermal conductivity enhancements. In-addition, DTU has performed kinetic parameters determination of absorption and desorption of the chosen reaction pair ($\text{SrCl}_2 \cdot \text{NH}_3$ and $\text{SrCl}_2 \cdot 8\text{NH}_3$) using a Sieverts-type apparatus. KTH is in the process of designing and constructing a bench-scale TCS system for the same reaction pair with two identical reactors (0.5 kWh storage capacity each). The reactor is of a cylindrical packed-bed type, combined with a heat exchange unit. Some of these results of these various study aspects of the NHS project were already presented and published at several conferences with some more planned to be presented in certain upcoming conferences and into journal manuscripts.

5. Presentations and publications

- 1) Anastasiia Karabanova, Perizat Berdiyeva, Didier Blanchard, Rune E. Johnsen, Stefano Deledda
Comparison between Numerical Simulation and Neutron Radiography of Ammonia Sorption in SrCl_2 for Application in Thermochemical Storage System for Waste Heat Recovery, Eurotherm Seminar n-112: 15-17 May 2019, Spain.
- 2) P. Berdiyeva, A. Karabanova, D. Blanchard, R. E. Johnsen, B.C. Hauback S. Deledda, *Neutron Imaging study of Strontium Chloride Ammine system for Heat Storage*, Workshop on neutron imaging and scattering on engineering materials (Dec. 6.-7, 2018 in Copenhagen)
- 3) Saman Nimali Gunasekara, Michail Laios, Anastasiia Karabanova, Viktoria Martin and Didier Blanchard, 2019. *Design of a bench-scale ammonia- SrCl_2 thermochemical storage system using numerical modelling*. Eurotherm Seminar n-112 (<http://eurotherm.udl.cat/>), Lleida, Spain. 15-17 May 2019.
- 4) Saman N. Gunasekara, Stefano Soprani, Anastasiia Karabanova, Viktoria Martin and Didier Blanchard, 2019. *Numerical Design of a Reactor-Heat Exchanger Combined Unit for Ammonia- SrCl_2 Thermochemical Storage System*. ISES SWC-2019 (<https://www.swc2019.org/home.html>), 4-7 Santiago, Chile.

6. References

- [1] S. Soprani, "MODELING – TES system based on SrCl_2 - NH_3 ," Technical University of Denmark (DTU), Lyngby, 2017.
- [2] SGL Carbon GmbH, "SIGRATHERM L and LN - Graphite lightweight board for thermal management.," SGL Carbon GmbH, 2019. [Online]. Available: <https://www.sglcarbon.com/en/markets-solutions/material/sigratherm-graphite-lightweight-board/>. [Accessed 29 August 2019].

- [3] S. Lysgaard, A. L. Ammitzbøll, R. E. Johnsen, P. Norby, U. J. Quaade and T. Vegge, "Resolving the stability and structure of strontium chloride amines from equilibrium pressures, XRD and DFT," *International Journal of Hydrogen Energy*, vol. 37, pp. 18927-18936, 2012.
- [4] L. Jiang, L. W. Wang, Z. Q. Jin, R. Z. Wang and Y. J. Dai, "Effective thermal conductivity and permeability of compact compound ammoniated salts in the adsorption/desorption process," *International Journal of Thermal Sciences*, vol. 71, pp. 103-110, 2013.
- [5] e. John R. Rumble, "Fluid Properties - Vapor Pressure of Fluids at Low Temperatures," in *CRC Handbook of Chemistry and Physics*, 99 ed., vol. 99th Print Edition (Internet Version 2018), Boca Raton, FL, CRC Press/Taylor & Francis.
- [6] S. N. Gunasekara, M. Laios, A. Karabanova, V. Martin and D. Blanchard, "Design of a bench-scale ammonia-SrCl₂ thermochemical storage system using numerical modelling," in *Eurotherm Seminar n-112- Advances in Thermal Energy Storage*, Lleida, 2019.
- [7] H.-J. Huang, G.-B. Wu, J. Yang, Y.-C. Dai, W.-K. Yuan and H.-B. Lu, "Modeling of gas-solid chemisorption in chemical heat pumps," *Separation and Purification Technology*, vol. 34, p. 191-200, 2004.
- [8] A. Karabanova, P. Berdiyeva, S. Soprani, R. E. Johnsen, S. Deledda and D. Blanchard, "Comparison between Numerical Simulation and Neutron Radiography of Ammonia Ab- and Desorption in SrCl₂ for Application in Thermochemical Storage System for Waste Heat Recovery," in *Eurotherm Seminar nr. 112- Advances in Thermal Energy Storage*, Lleida, 2019.
- [9] A. Erhard, K. Spindler and E. Hahne, "Test and simulation of a solar powered solid sorption cooling machine," *International Journal of Refrigeration*, vol. 21, no. 2, pp. 133-141, 1998.

MATERIALS SCIENCE & ENG. DEPARTMENT NORTHWESTERN UNIVERSITY, EVANSTON, USA
INSTITUTE OF CATALYSIS AND PETROCHEMISTRY, SUPERIOR COUNCIL FOR SCIENTIFIC RESEARCH,
MADRID, SPAIN

DR. EMAUELA MASTRONARDO

TCM TYPE: CHEMICAL REACTION

1. Introduction: In this study Fe-doped CaMnO₃ perovskites have been investigated for high temperature thermochemical heat storage. The working principle of a TCS system based on perovskite consists of the following reaction: $ABO_3 \pm \delta O(s) \rightleftharpoons ABO_3 \pm \delta O - \delta(s) + \delta O_2(g)$ (2)

Where, δO is the initial oxygen non stoichiometry and thus $(3 \pm \delta O)$ stands for the initial oxygen content in the material. The reduction, being endothermic, comprises the heat storage step, whereas the exothermic oxidation releases heat when it is required. The heat that can be stored (chemical heat) is directly proportional to the reduction/re-oxidation enthalpy and extent (δ). CaMnO₃ oxide can be considered a promising candidate since it is able to release oxygen in a wide temperature range (800-1000 °C) at different oxygen partial pressures (p_{O_2}) suitable for Concentrated Solar Power (CSP) plants. However, it undergoes decomposition at $p_{O_2} < 0.008$ atm and at temperature ≥ 1100 °C. In order to overcome this limitation and to extend the operating temperature range, in this study B-site doping with Fe (CaFe_xMn_{1-x}O_{3- δ O}) was used as approach for preventing its decomposition.

The thermodynamic parameters were determined through the van't Hoff approach [1] applied to thermogravimetric profiles obtained at different oxygen partial pressures.

2. Preparation of materials: Fe-doped CaMnO₃ samples (CaMn_{1-x}Fe_xO₃), with a dopant amount (x) of 0.1 were prepared according to a modified Pechini method as reported in literature [2].

Composition	Code	Dopant
CaMnO ₃ -δO	CM	0
CaMn _{0.9} Fe _{0.1} O ₃ -δO	CMF91	0.1

3. Results:

a. Structural properties

The X-Ray Diffraction (XRD) patterns (see Figure 1) perfectly match that of Pnma orthorhombic CaMnO₃ (PDF 04-007-8030). No other phases were detected. Hence, 10 at% Fe is incorporated into the CaMnO₃ structure without the formation of any secondary phase. A shift toward lower 2-theta angles reflects a slight increase in the lattice parameters (and the unit cell volume), in response to the Fe doping. A slight broadening of the peaks similarly reflects the incorporation of the dopant into the structure.

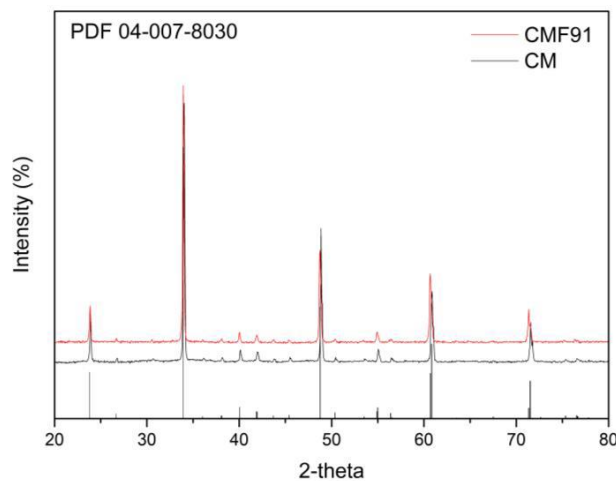


FIGURE 1. XRD PATTERN OF UN-DOPED AND FE-DOPED CAMNO3.

b. Thermochemical properties: Thermogravimetric (TG) analysis in the temperature range 200-1200 °C under a $p_{O_2}=0.008$ atm have been carried on the as prepared samples. From CM profile it can be observed that the sample is not able to fully re-oxidize. XRD analysis of the sample after TGA detected the presence of residual spinel structure (CaMn₂O₄) which most likely prevented the complete re-oxidation of the sample. In case of Fe-doped CaMnO₃, oxygen begins to be released at lower temperature with respect to CM. Moreover, the reduction process is fully reversible for CMF91 sample.

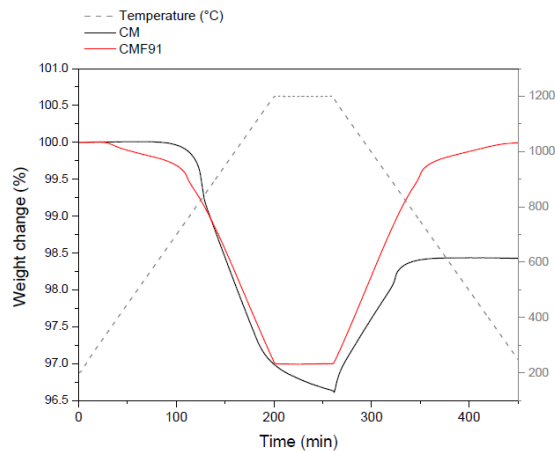


FIGURE 2. TG PROFILES OF CM AND CMF91 UNDER A $p_{O_2}=0.008$ ATM.

c. Picture/image/photograph of the material

Cylindric porous pellets used for TG analysis for the extraction of the thermodynamic data.



FIGURE 3. CILINDRIC POROUS PELLETS USED FOR TG ANALYSIS.

d. Graph: characteristic curve (QM (kJ/kg ABO_3) Vs. Temperature)

The heat storage capacity of the two materials as a function of temperature for $p_{O_2}=0.008$ atm is shown in Figure 4. This analysis reveals that CMF91 has a higher heat storage capacity (344.3 ± 0.6 kJ/kg ABO_3 or 639.0 ± 1.1 MJ/m³) than CM (272.5 ± 1.1 kJ/kg ABO_3 or 315.3 ± 1.3 MJ/m³). In addition, at equal p_{O_2} , CMF91 is also able to store heat up to higher temperature (1200 °C), thus widening the operating temperature range. A small quantity of heat can also be stored between 400-800 °C.

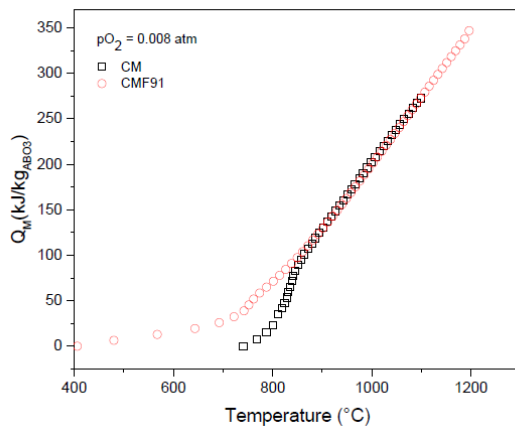


FIGURE 4. HEAT STORAGE CAPACITY OF THE TWO MATERIALS AS A FUNCTION OF TEMPERATURE FOR $p_{O_2}=0.008$ ATM.

4. Summary: In this study, $\text{CaMn}_{0.9}\text{Fe}_{0.1}\text{O}_3$ oxide, formed of earth-abundant, inexpensive, non-toxic elements, has been investigated as a possible heat storage material for concentrated solar power plants. It has been demonstrated that the presence of Fe allows the CaMnO_3 to operate at higher temperature (1200 °C) than the un-doped material, thus increasing the reversible reduction oxidation extent. Indeed, Fe-doping prevented the irreversible decomposition of CaMnO_3 above 1100 °C for $p_{O_2}<0.01$. The heat storage capacity (Q_M) has been estimated to be ~ 344 kJ/kg ABO_3 . Moreover, in case of the Fe-doped CaMnO_3 the oxygen release onset temperature is lowered below 400 °C and the reduction can be carried out up to 1200 °C, thus widening the operating temperature range.

5. References

- [1] Y. Hao, C. K. Yang, and S. M. Haile, Chem. Mater. 26, pp. 6073–6082 (2014).
 [2] D. Sastre, A.J. Carrillo, D.P. Serrano, P. Pizarro, J.M. Coronado, Top. Catal. 60, pp. 1108–1118 (2017).

Acknowledgments: This project has received funding from the European Union’s Horizon 2020 research and innovation programme under the Marie Skłodowska-Curie grant agreement N° 74616. Support of the US Department of Energy, Office of Energy Efficiency and Renewable Energy, Award DE-EE0008089.0000, is also acknowledged.

UNIVERSITY OF MESSINA – ENGINEERING DEPARTMENT

PROF. CANDIDA MILONE

TCM TYPE: CHEMICAL REACTION

1. Introduction: Newly developed hybrid materials made of magnesium hydroxide deposited onto expanded graphite (EG), pristine and functionalized carbon nanotubes (*p*-CNT, *f*-CNT respectively) were proposed as heat storage medium for $\text{MgO}/\text{H}_2\text{O}/\text{Mg}(\text{OH})_2$ chemical heat pumps.

2. Preparation of materials and/or supplier: Samples were synthesized by deposition-precipitation (DP) method.

3. Results

a. Structural properties for porous materials and composites / formula

$\text{Mg}(\text{OH})_2$ supported on expanded graphite/pristine and functionalized CNT

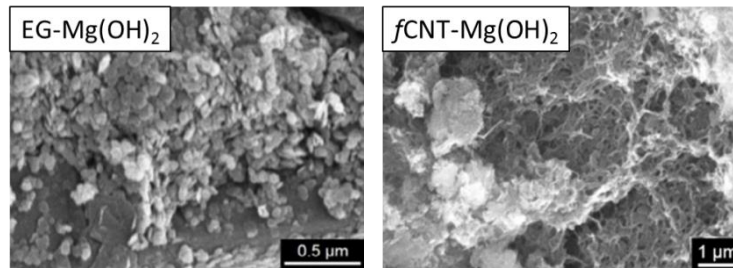
b. Sorption properties / reaction



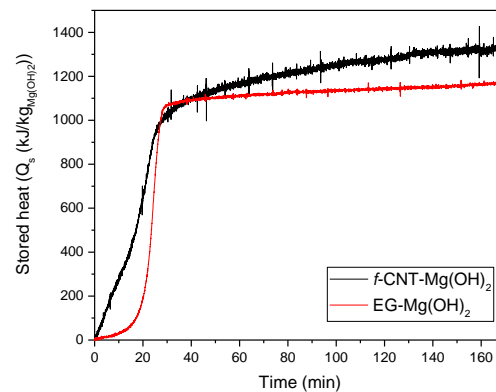
$$\Delta H_0 = \pm 1389 \text{ kJ/kg}_{\text{Mg(OH)}_2}$$

c. **Thermochemical properties:** The performances of the synthesized materials were evaluated by thermogravimetric analysis, which simulates the chemical heat pump cycle.

d. **Picture/image/photograph of the material:** Scanning Electron Microscope (SEM) images



e. **Graph:**



4. Summary: As main results it is found that :i) at given Mg(OH)_2 load DP method allows to enhance the thermochemical performance of hybrid materials; ii) heat storage/output capacities of EG-Mg(OH)_2 ($\text{Mg(OH)}_2 = 50 \text{ wt\%}$) approaches $1200 \text{ kJ/kg}_{\text{Mg(OH)}_2}$; iii) f-CNT-Mg(OH)_2 (30 wt\% Mg(OH)_2) reaches the highest heat storage/output capacities ($\approx 1300 \text{ kJ/kg}_{\text{Mg(OH)}_2}$).

5. References

E. Mastronardo, L. Bonaccorsi, Y. Kato, E. Piperopoulos, M. Lanza, C. Milone. Strategies for the enhancement of heat storage materials performances for $\text{MgO/H}_2\text{O/Mg(OH)}_2$ thermochemical storage system. Applied Thermal Engineering 120 (2017) 626-634. DOI: 10.1016/j.applthermaleng.2017.04.004

E. Mastronardo, Y. Kato, L. Bonaccorsi, E. Piperopoulos, C. Milone. Thermochemical storage of middle temperature wasted heat by functionalized C/Mg(OH)₂ hybrid materials. Energies 10 (2017) 70. DOI: 10.3390/en10010070

Emanuela Mastronardo, Yukitaka Kato, Lucio Bonaccorsi, Elpidia Piperopoulos, Candida Milone. "Thermochemical Storage of Middle Temperature Wasted Heat by Functionalized C/Mg(OH)₂ Hybrid Materials" Energies 10, (2017),70-86 (16 pp)

TCM TYPE: CHEMICAL REACTION

1. Introduction: Pure $\text{Mg}(\text{OH})_2$ (MH) shows a poor durability to several dehydration/hydration reactions, decreasing its reacted fraction to $\sim 50\%$ after only three cycles. The performance implementation of this storage medium is still object of study. Here, it has been investigated how the heat storage capacity of $\text{Mg}(\text{OH})_2$ is influenced by the dispersing agent addition during the synthesis.

2. Preparation of materials and/or supplier: Samples were synthesized by deposition-precipitation (DP) method in the presence of cationic surfactant, cetyl trimethyl ammonium bromide (CTAB) that is used as a dispersing agent for inhibiting the natural tendency of $\text{Mg}(\text{OH})_2$ to aggregate.

3. Results

a. Structural properties for porous materials and composites / formula

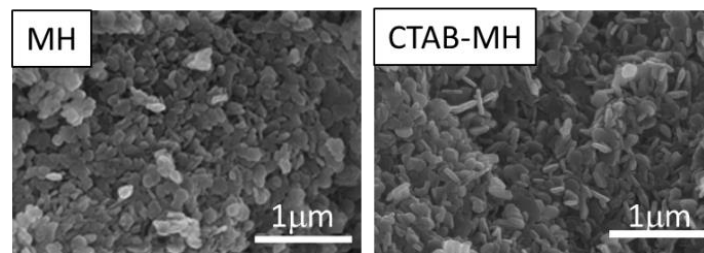
$\text{Mg}(\text{OH})_2$ powder

b. Sorption properties / reaction

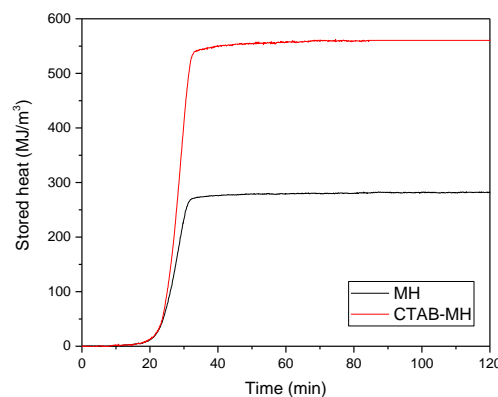


c. Thermochemical properties: The performances of the synthesized materials were evaluated by thermogravimetric analysis, which simulates the chemical heat pump cycle.

d. Picture/image/photograph of the material: Scanning Electron Microscope (SEM) images



e. Graph:



4. Summary: The results obtained show that CTAB addition promotes the formation of well separated $\text{Mg}(\text{OH})_2$ particles. Moreover, CTAB-MH sample exhibits the highest volumetric stored/released heat capacity, $\sim 560 \text{ MJ/m}^3$, almost 2 times higher than that measured over $\text{Mg}(\text{OH})_2$ prepared in absence of CTAB. Cyclic experiments evidence an excellent stability of the

sample up to 13 dehydration/hydration reactions. That means, for technological application, smaller volume at equal stored/released heat.

5. References

Emanuela Mastronardo, Lucio Bonaccorsi, Yukitaka Kato, Elpida Piperopoulos, Maurizio Lanza, Candida Milone. "Strategies for the enhancement of heat storage materials performances for MgO/H₂O/Mg(OH)₂ thermochemical storage system" Applied Thermal Engineering 120, (2017), 626-634.

Elpida Piperopoulos, Emanuela Mastronardo, Marianna Fazio, Maurizio Lanza, Signorino Galvagno, Candida Milone. "Enhancing the volumetric heat storage capacity of Mg(OH)₂ induced by the addition of a cationic surfactant during its synthesis" Applied Energy 215 (2018) 512-522.

TCM TYPE: CHEMICAL REACTION

1. Introduction: Metal (Ca²⁺, Ni²⁺, and Co²⁺) doped Mg(OH)₂ (MH) was investigated to study the doping effect on the thermochemical (TCM) material's behaviour. Metal ions (Me) were inserted in Mg(OH)₂ matrix and the subsequent materials were structurally, morphologically and thermochemically characterized.

2. Preparation of materials and/or supplier: The synthesis was conducted by precipitation method, using 50 mL of a solution containing Mg²⁺ and the metal ion (Ca²⁺ or Ni²⁺ or Co²⁺) in a nominal molar ratio Me/Mg²⁺ of 0.2. This was gradually added to 150 mL of NH₄OH solution, under magnetic stirring. The resulting solution was aged at ambient temperature for 24 h, then it was vacuum filtered; the collected solid was washed with deionized water and dried in a vacuum oven at 50 °C overnight.

3. Results

a. Structural properties for porous materials and composites / formula

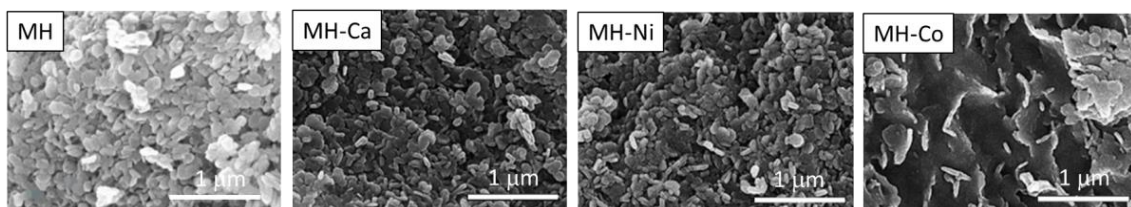
Doped Mg(OH)₂ powder

b. Sorption properties / reaction

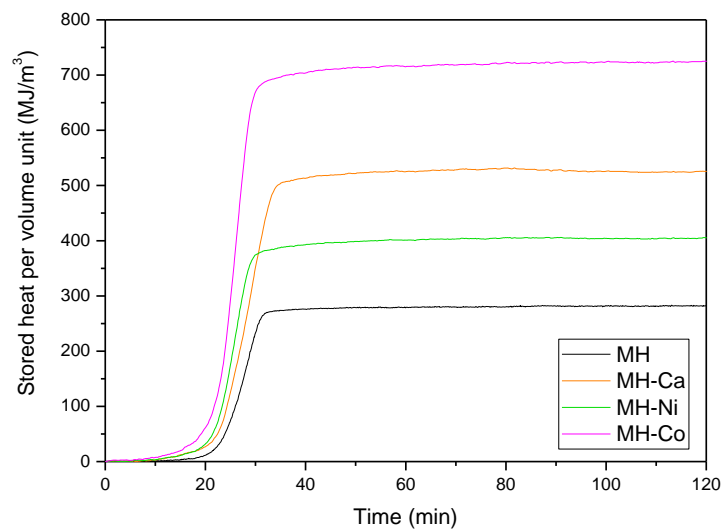


c. Thermochemical properties: The performances of the synthesized materials were evaluated by thermogravimetric analysis, which simulates the chemical heat pump cycle.

d. Picture/image/photograph of the material: Scanning Electron Microscope (SEM) images



e. Graph:



4. Summary: The obtained results show that metal doping strictly influences morphological and structural properties. The apparent density increase effects the volumetric stored/released heat capacity. The highest value is reported for MH-Co sample (725 MJ/m^3), and it is almost three times higher than MH's value.

5. References

Elpida Piperopoulos, Marianna Fazio, Emanuela Mastonardo "Synthesis of Me Doped $\text{Mg}(\text{OH})_2$ Materials for Thermochemical Heat Storage", *Nanomaterials*, 8 (2018) 573-590

CIC ENERGIGUNE SPAIN

STEFANIA DOPPIU

TCM TYPE: CHEMICAL REACTION

1. Introduction: The aim of the investigations is the development of thermal energy storage materials for high temperature applications (above 250°C). This includes the synthesis, the modification, the structural characterization and the TES performance optimization. The materials investigated are based on solid-solid chemical reactions (eutectoids and peritectoids) and solid-liquid chemical reactions (peritectics) in salt-based and metals-based binary mixtures.

2. Preparation of the materials: Solid-solid reactions: The materials were studied as received (testing the performances without modification) and after modification (synthesis of nanostructured materials bay ball milling techniques) to increase the reactivity in the solid state and to Investigate the relationship between microstructure and reactivity. **Solid-liquid reactions:** The materials were studied as received and after addition of nanoparticles and infiltration in porous matrixes (preparation of hybrid materials) to increase the reactivity.

3. Results: Solid-solid reactions: In the system $\text{Li}_2\text{SO}_4/\text{Na}_2\text{SO}_4$ two compositions (a eutectoid reaction and a solid-solid phase transition) have been identified with very promising TES performances (enthalpies between $185 - 190 \text{ kJ/kg}$ and 160 kJ/kg respectively). The DSC (three cycles)

relevant to the two compositions are shown in Figure 1a. **Solid-liquid reactions:** The peritectic composition in the system LiOH/LiBr presents an enthalpy of reaction + melting of 284 kJ/kg. If the sensible contribution is taken into account ($\Delta T = 60^\circ\text{C}$) the total energy is 382 kJ/kg (Enthalpy of reaction and reaction + melting relevant to each point studied in the phase diagram are shown in Figure 1 b).

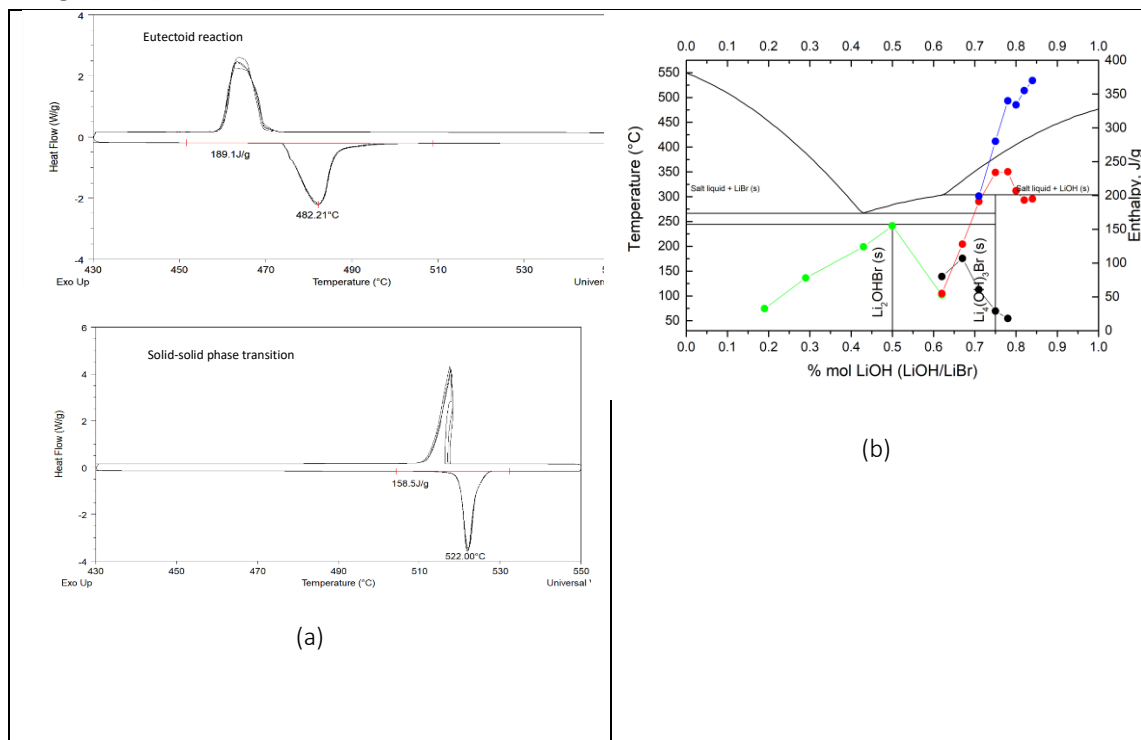


FIGURE 1: A) SOLID-SOLID REACTION AND B) SOLID-LIQUID REACTIONS

4. Summary: The investigation allowed to identify several promising solid-solid and solid liquid chemical reactions and transitions for TES at high temperature. The work is still going on in order to maximize the reactivity of both systems and to clarify some discrepancies obtained from the theoretical studies.

5. References:

- 1) Doppiu, S., Dauvergne, J. L., & Palomo del Barrio, E. (2019). "Solid-State Reactions for the Storage of Thermal Energy". *Nanomaterials*, 9(2), 226.
- 2) Mahroug, I; Doppiu, S.; Palomo Del Barrio, E.; "Peritectic compounds for thermal energy storage: Experimental investigation and optimization", XI Congreso Nacional y II Internacional de Ingeniería Termodinámica, Albacete (2019)

INSTITUTE OF APPLIED SYNTHETIC CHEMISTRY (TU WIEN)

DR. PETER WEINBERGER

TCM TYPE: CHEMICAL REACTION

1. Introduction: The de-respectively rehydration behavior of $\text{CaC}_2\text{O}_4 \cdot x \text{H}_2\text{O}$ was studied via thermal analysis and powder X-ray diffraction (PXRD). Furthermore, Cycle stability of the material was tested by a long-term stress experiment involving 100 charging and discharging cycles.

2. Preparation of materials and/or supplier: Calcium oxalate monohydrate (CAS 5794-28-5) was obtained from Sigma-Aldrich and used as supplied.

3. Results

Material: Calcium oxalate monohydrate

Chemical formula: $\text{CaC}_2\text{O}_4 \cdot \text{H}_2\text{O}$

Reactive gas: H_2O

The hydration behavior of $\text{CaC}_2\text{O}_4 \cdot \text{H}_2\text{O}$ is quite unusual compared to other salt hydrates that are considered as TES material, since, depending on water vapour concentration the hydration reaction can occur well above 100 °C. An increased water vapour concentration shifts the phase stability boundary towards higher temperatures, thus extending the stability regime of the hydrate phase. In absolute values, the peak_{max} temperature for the rehydration reaction is shifted from 157.1 °C for a vapour concentration of 0.4 g $\text{H}_2\text{O h}^{-1}$ ($p(\text{H}_2\text{O})=0.084$ bar) to 199.8 °C for 5 g $\text{H}_2\text{O h}^{-1}$ ($p(\text{H}_2\text{O})=0.53$ bar)(Fig. 1a and b).

Cycle stability of the material was tested by a long-term stress experiment involving 100 charging and discharging cycles where no signs of material fatigue or reactivity loss were found (Fig. 2a and b).

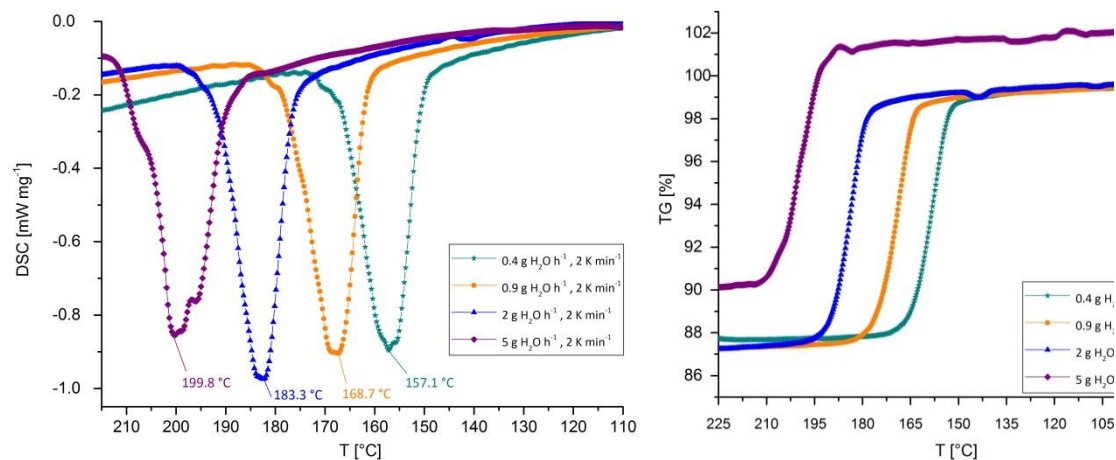


FIG. 1 A: HEAT-FLOW OF THE REHYDRATION REACTION WITH RESPECT TO THE WATER VAPOUR CONCENTRATION; B: MASS-CHANGE DURING THE REHYDRATION REACTION WITH RESPECT TO THE WATER VAPOUR CONCENTRATION. FOR ALL 4 CURVES FULL CONVERSION WAS ACHIEVED. THE SHIFT OF THE 5 G $\text{H}_2\text{O h}^{-1}$ CURVE ABOUT 2 % IS CAUSED BY CONDENSATION ISSUES.

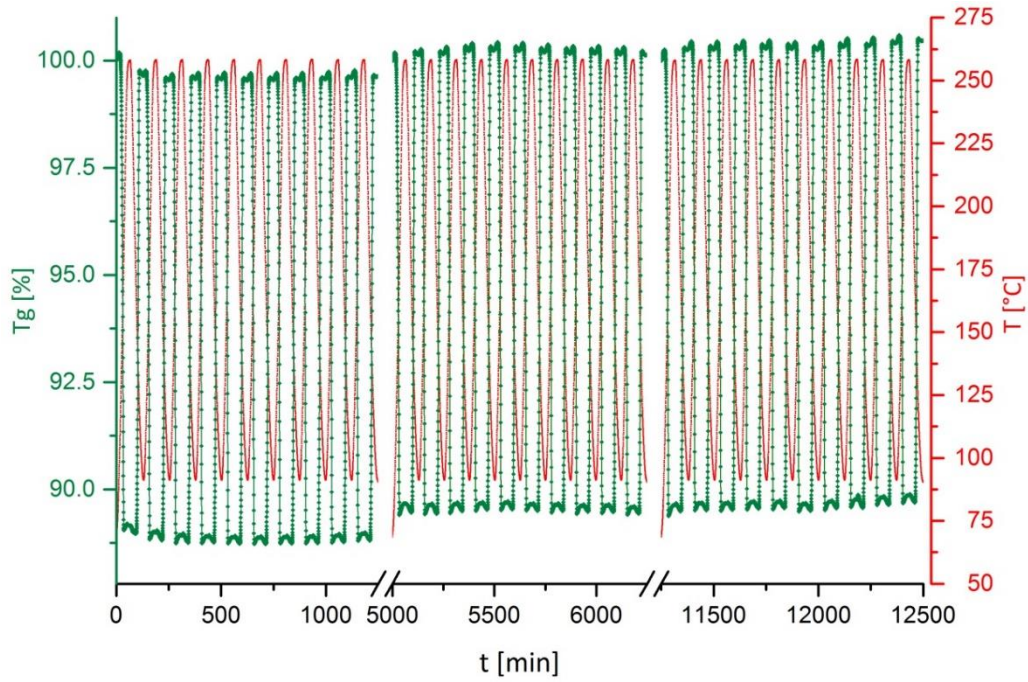


FIG.

FIG 2A TG-CURVE OF CYCLES 1-10, 51-60 AND 91-100 OF THE $\text{CaC}_2\text{O}_4 \cdot \text{H}_2\text{O}$ DEHYDRATION / REHYDRATION REACTION WITH $0.5\text{G H}_2\text{O H}^{-1}$, 5 K MIN^{-1} .

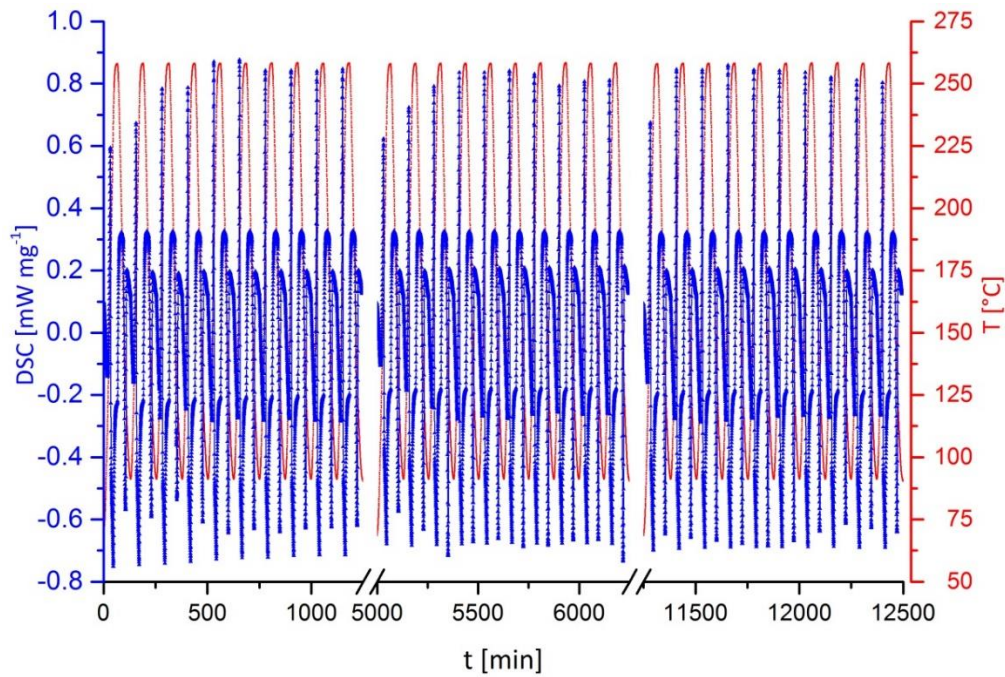


FIG. 2B DSC-CURVE OF CYCLES 1-10, 51-60 AND 91-100 OF THE $\text{CaC}_2\text{O}_4 \cdot \text{H}_2\text{O}$ DEHYDRATION / REHYDRATION REACTION WITH $0.5\text{G H}_2\text{O H}^{-1}$, 5 K MIN^{-1} .

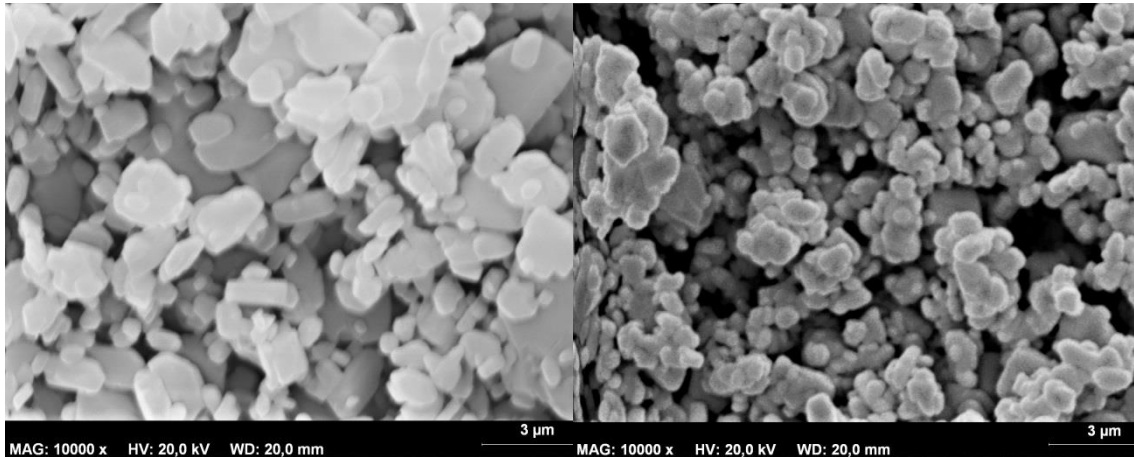


FIG. 3A: $\text{CaC}_2\text{O}_4 \cdot \text{H}_2\text{O}$, STARTING MATERIAL

FIG. 3B: CaC_2O_4 , ANHYDRATE PHASE BEFORE 1ST CYCLE

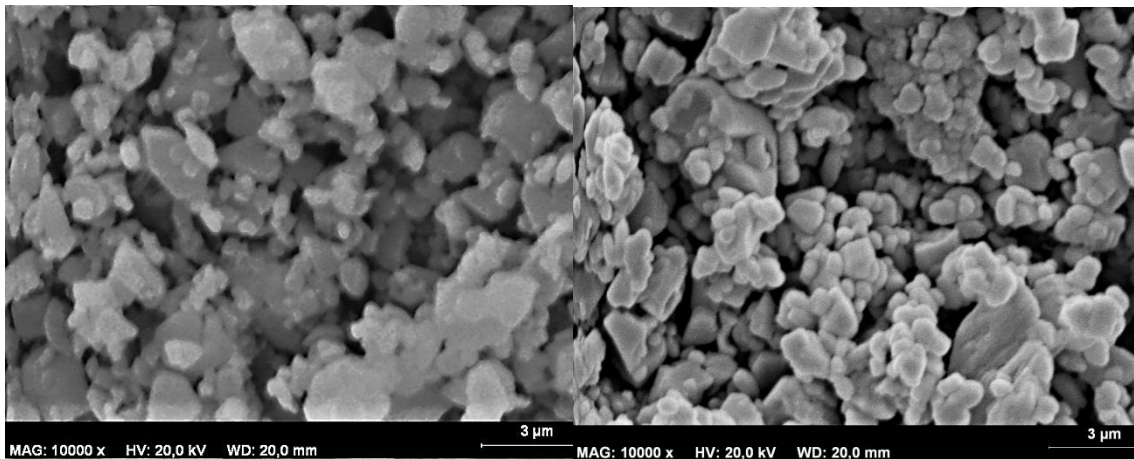


FIG. 3C: $\text{CaC}_2\text{O}_4 \cdot \text{H}_2\text{O}$ AFTER 10 CYCLES

FIG. 3D: $\text{CaC}_2\text{O}_4 \cdot \text{H}_2\text{O}$ AFTER 100 CYCLES

4. Summary: The properties rendering calcium oxalate an attractive material for technical TES application, in addition to cycle stability and the rapid conversion evidenced in the P-XRD, the most interesting property of this system is its broad operational range. Most salt hydrates considered for TES purposes form their hydrate at temperatures below 100 °C. $\text{CaC}_2\text{O}_4 \cdot \text{H}_2\text{O}$ is unusual in this regard, since, depending on water vapour concentration the release of the stored energy can occur well above 100 °C. This would allow for release of the stored heat at temperatures only slightly below the charging temperature. For industrial purposes it is preferable that the temperature difference between charging and discharging reactions be small, leading to a high exergy. An increased water vapour concentration shifts the phase stability boundary towards higher temperatures, thus extending the stability regime of the hydrate phase. These shifts of the peak temperature related to the vapour concentration allow for a potential application as a chemical heat pump, thus having a broad operational possibility at high temperatures. Our results state an operational range between room-temperature and 200 °C. This region may be further extended by higher water vapour concentrations.

5. References

Knoll et al., "Probing cycle stability and reversibility in thermochemical energy storage–CaC₂O₄·H₂O as perfect match?." Applied energy 187 (2017): 1-9.

TCM TYPE: CHEMICAL REACTION

1. Introduction: Calcium doping of magnesium oxide results in significantly increased water dissociation rates, thus enhancing both hydration rate and reaction completeness of hydration compared to pure MgO. A series of mixed magnesium-calcium oxides (Mg_xCa_{1-x}O) with varying Ca contents between 0% and 40% was synthesized and the reaction itself was followed via in situ powder X-ray diffraction (P-XRD).

2. Preparation of materials and/or supplier: Mixtures of the appropriate amounts of MgCl₂·6H₂O and CaCl₂·6H₂O to produce 0.2 mol of the mixed oxide, were dissolved in 75 ml degassed H₂O. Freshly prepared 20 % NaOH solution in degassed H₂O (0.4 mol, 50 ml) were added, resulting in immediate precipitation of a voluminous white precipitate. The Mg_xCa_{1-x}(OH)₂ precipitated was centrifuged and washed three times with 100 ml degassed H₂O until chloride free (verified by silver-nitrate test). The hydroxides were calcined in an electric furnace under static atmosphere for 4 hours at 375 °C, yielding the oxides of the composition Mg_xCa_{1-x}O, where x= 1-0.5 in almost quantitative yields.

3. Results

Material: Calcium doped magnesium oxide - (Mg,Ca)O

Chemical formula: (Mg,Ca)O

Reactive gas: H₂O

All experimentally investigated Ca²⁺-doped oxides show a significantly higher rehydration rate than a commercial MgO sample which was used as reference sample. The fastest reaction rate was found for Mg_{0.9}Ca_{0.1}O for which, after 80 min, the oxide was completely converted to the mixed hydroxide. For larger Ca²⁺ amounts, the final conversion decreased slightly to roughly 80% hydroxide phase.

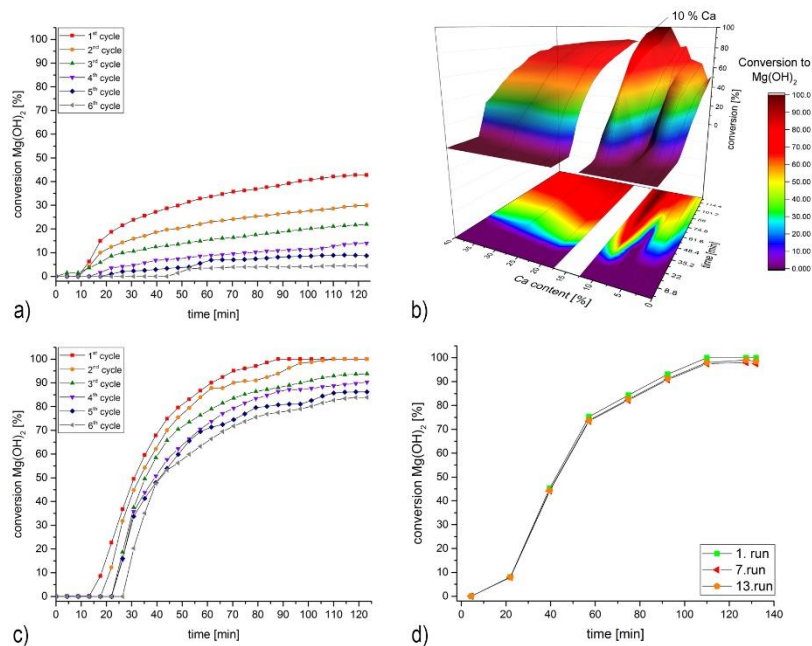


FIG. 4: REHYDRATION RATE AND CYCLE STABILITY OF VARIOUS $Mg_{1-x}Ca_xO$ SAMPLES. A) COMMERCIAL MgO AS REFERENCE. B) COMPARISON OF $Mg_{1-x}Ca_xO$ WITH Ca^{2+} CONTENT BETWEEN 0% AND 40% (THE 3D PLOT COMPARES THE FINAL CONVERSION OF THE DIFFERENT SAMPLES, WHEREAS THE CONTOUR PLOT AT THE BOTTOM DIRECTS THE FOCUS ON THE REACTION RATE/INITIAL DELAY). C) $Mg_{0.9}Ca_{0.1}O$ D) HYDRATION RATE OF $Mg_{0.9}Ca_{0.1}O$ TO $Mg_{0.9}Ca_{0.1}(OH)_2$ FOR TWO CONSECUTIVE CYCLES BEFORE AND AFTER 1ST AND 2ND REGENERATION IN LIQUID WATER

4. Summary: It was demonstrated that doping MgO with Ca^{2+} by calcination of the co-precipitated mixed $Mg_{1-x}Ca_x(OH)_2$ species, the kinetic barrier to the water dissociation step of MgO rehydration could be significantly reduced. The maximum rehydration rate and cycle stability were dramatically increased for MgO doped with 10 % Ca^{2+} , $Mg_{0.9}Ca_{0.1}O$, enabling full conversion to the corresponding hydroxide within 80 minutes. The decrease in rehydration reactivity during the following cycles was attributed to agglomeration of material during the consecutive calcination / rehydration steps, impeding the access to the reactive surface. Rehydration of the less reactive material in liquid water regenerates the initial reactivity due to degradation of the aggregates. DFT calculations demonstrated the effect of the Ca^{2+} doping as both electronic and steric in nature. Expanding the lattice-constants of an MgO (001)-surface towards the values of a corresponding CaO surface results in a more stable water adsorption together with an increased tendency toward water dissociation (size effect), whereas exchange of Mg^{2+} atoms with Ca^{2+} lowers this energy even further (electronic effect).

5. References

Müller et al., "Calcium doping facilitates water dissociation in magnesium oxide." *Advanced Sustainable Systems* 2.1 (2018): 1700096.

TCM TYPE: CHEMICAL REACTION

1. Introduction

The carbonation behavior of PbO was studied via PXRD at a CO₂ pressure of 2-8 bar as well as temperature regime of 25-500 °C.

2. Preparation of materials and/or supplier

PbCO₃ was decomposed in an electric tube furnace at 375 °C for 4 hours under constant argon (0.2 L min⁻¹) flow to obtain a very reactive PbO sample.

3. Results

Material: lead oxide (Fig. 5a)

Chemical formula: PbO

Reactive gas: CO₂

One of the first experiments was an isobaric heating reaction from 25° to 500°C at 8 bar CO₂ with a permanent CO₂ flow passing the reaction chamber. During heating carbonation of PbO phase occurs above 240 °C, forming shannonite, a mixed 1:1 carbonate-oxide phase with a composition of PbCO₃·PbO. Above 340 °C parallel to the shannonite-phase a second carbonate-oxide phase with the composition PbCO₃·2PbO forms. Above 400 °C the shannonite-phase is decomposed, resulting in pure PbCO₃·2PbO phase. During slow cooling to 50 °C under 8 bar CO₂ the composition of the sample remains unchanged.

The carbonation of PbO also results in these intermediates before reaching PbCO₃. As PbCO₃ is not detected during the reaction this suggests that either increased CO₂-pressures or higher temperatures might produce pure PbCO₃. In a second step an isothermal storage cycle, triggered by a change in CO₂ pressure was developed. Treating PbO at 500 °C with 8 bar CO₂ results in rapid conversion of PbO to the mixed carbonate-oxide PbCO₃·2PbO. Once the CO₂ pressure is decreased to 2 bar, the PbCO₃·2PbO phase decomposes, regenerating PbO (Fig 5b).

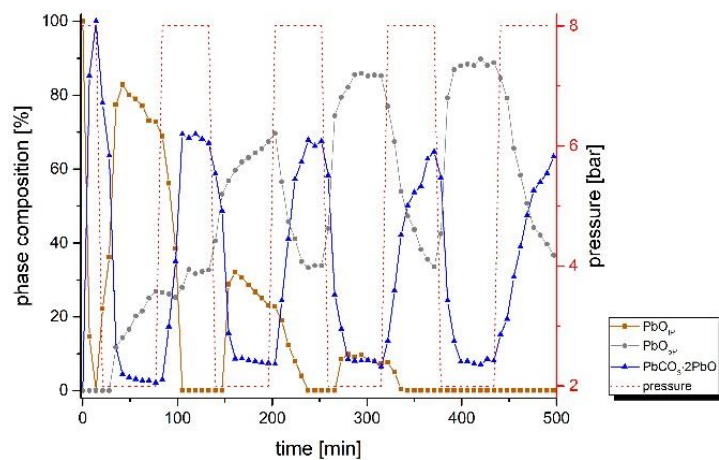


FIG. 5A: RAW MATERIAL (PbO); FIG. 5B: ISOTHERMAL STORAGE CYCLE AT 500 °C BETWEEN PbCO₃·2PbO AND PbO TRIGGERED BY A CHANGE IN CO₂ PRESSURE FROM 8 TO 2 BAR

4. Summary

Carbonatization of metal oxides offers a dual advantage, allowing to capture CO₂ and at the same time store thermal energy by means of a thermochemical storage cycle. For CoO, MnO, PbO and ZnO the reactivity towards CO₂ in the presence / absence of moisture for pressures between 8-50 bar and temperatures between 25-500 °C was investigated.

Isobaric heating of PbO to 500 °C at 8 bar CO₂ results in a mixed carbonate-oxide phase (PbCO₃·PbO) above 240 °C. Above 340 °C PbCO₃·2PbO a second carbonate-oxide phase starts to form. Furthermore, an isothermal storage was developed. By changing the CO₂ pressure from 8 to 2 bar a cycle between the two phases PbCO₃·2PbO and PbO and can be triggered.

5. References

Gravogl et al., "Pressure effects on the carbonation of MeO (Me= Co, Mn, Pb, Zn) for thermochemical energy storage." Applied Energy 252 (2019): 113451.

TECHNICAL UNIVERSITY MÜNCHEN – INSTITUTE FOR ENERGY SYSTEMS

DR. ANNELIES VANDERSICKEL

TCM TYPE: CHEMICAL REACTION

1. Introduction: AIM: Development of cost-effective large scale (MWh/GW) & long term energy storage for high temperature applications (300-700 °C) $\text{CaO} + \text{H}_2\text{O} \leftrightarrow \text{Ca}(\text{OH})_2 + 104 \text{ kJ/mol}$
APPROACH: To exploit the low cost of the material (~ 0.15 €/kg), a separation of storage power (with its associated high cost for heat exchange and reactor design) and storage capacity is strived for. This is achieved using a continuously operated fluidised bed reactor. The key material requirement is therefore: good particle stability & high heat transfer in (kinetics are not limiting)

2. Preparation of materials and/or supplier

- technical grade CaCO₃ ((Kohlensaurer Kalk, 0.09-1.0 mm) by Märker-Gruppe GmbH
- sieved with a tumbler screening machine (TSM1200, Allgaier Process Technology) to 280-450 µm
- calcination in pure nitrogen at 800 °C for 10 min

3. Results:

a. Structural properties for porous materials and composites / formula

- Molecular Weight: CaO = 56,08 g/mol / Ca(OH)₂ = 74,1 g/mol
- Bulk density: CaO = 738 kg/m³ / Ca(OH)₂ = 835,5 kg/m³ - declining over multiple cycles depending on operating conditions
- Specific Heat Capacity (at 25 /400°C): 0,75 / 0,91 kJ/kg K - 1,18 /1,48 kJ/kg K [2]

b. Sorption properties / reaction

- Reaction enthalpy @ 100°C:
 $\text{CaO}(s) + \text{H}_2\text{O}(\text{liquid resp. gas}) \rightarrow \text{Ca}(\text{OH})_2(s) + (\Delta H_R \cong -67 \text{ resp. } -108 \text{ kJ/mol})$

c. Thermochemical properties

Reaction enthalpy @ 500°C (steam/gas): 100,5 kJ/mol

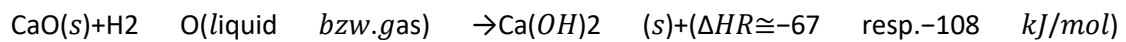
	in kJ/mol	in %
Reaction enthalpy ΔHR	100,46	100,00
Evaporation enthalpy	40,67	40,48
Chemically stored energy	59,79	59,52

d. Picture/image/photograph of the material:



Source [1]

→ Reaction enthalpy @ 100°C:



Reaction enthalpy @ 500°C (steam/gas): 100,5 kJ/mol

	in kJ/mol	in %
Reaction enthalpy ΔHR	100,46	100,00
Evaporation enthalpy	40,67	40,48
Chemically stored energy	59,79	59,52

Source: [1]

4. Summary: Very fast kinetics in pure steam atmosphere over a wide range of H₂O pressure (1.5 till 3 bar).

5. References

[1] Moritz Becker, Thermochemische Energiespeicherung Mit Calcium-Oxid Und -Hydroxid: Entwicklung Eines Reaktorkonzeptes, Dissertation, Technical University Munich, Institute for Energy Systems (submitted)

[2] CHASE, Malcolm: *NIST-JANAF Thermochemical Tables, 4th Edition* : American Institute of Physics, 1998 (NIST-JANAF Thermochemical Tables, 4th Edition)

[3] M. Angerer, M. Becker, S. Härzschel, K. Kröper, S. Gleis, A. Vandersickel, H. Spliethoff, Design of a MW-scale thermo-chemical energy storage reactor, *Energy Reports* **4** (2018) 507-519.

THE NETHERLANDS ORGANIZATION FOR APPLIED SCIENTIFIC RESEARCH TNO – DEPARTMENT OF SUSTAINABLE PROCESS & ENERGY SYSTEMS (SPES)

DR. RUUD CUYPERS

TCM TYPE: CHEMICAL REACTION

1. Introduction:

Newly developed salt hydrate materials made of sodium sulphide (Na_2S) with different percentages of enhancing additives are used as heat storage medium for closed-sorption (vacuum) compact heat batteries for dwellings (heating, domestic hot water), for charging up to 80°C , and discharging up to 65°C .

2. Preparation of materials and/or supplier:

Samples were synthesized by mixing/melting and co-crystallization of pure materials to form scales/powder. Materials are separated into different sieve fractions. Pellets can be prepared should this be desired.

3. Results

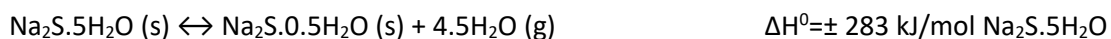
Materials are used in several different analyses to investigate pT-diagrams and sorption behavior, kinetics, outgassing behavior, cycling behavior, all as single-layers and as packed-beds. In addition, materials are tested in a mock-up heat battery under relevant testing conditions to investigate power and heat storage capacity.

a. Structural properties for porous materials and composites / formula

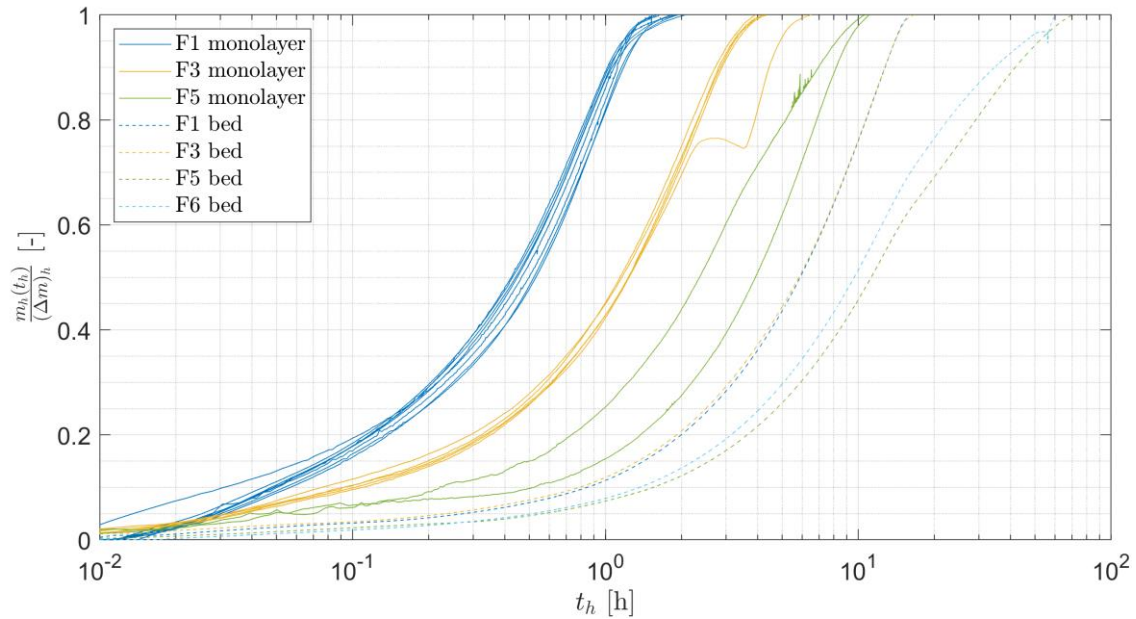
Materials are present as scales and/or as pellets, with typical dimensions of 1-6mm length and 1-2mm thickness, depending on the sieve fractions used.

b. Sorption properties / reaction

Materials can exist as anhydrate, hemihydrate, dihydrate, pentahydrate and nonahydrate. The utilized reactions proceed from hemihydrate to pentahydrate and vice versa and goes as follows:



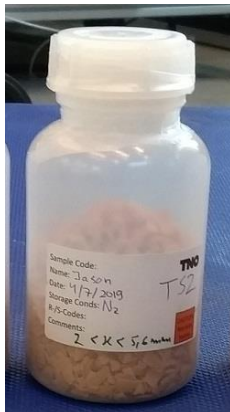
Below, a typical result for multiple hydration / dehydration cycles of single layers (solid lines) and packed bed (dashed lines) of several sieve fractions of materials is given with mass fraction reacted as a function of time in hours (logarithmic).



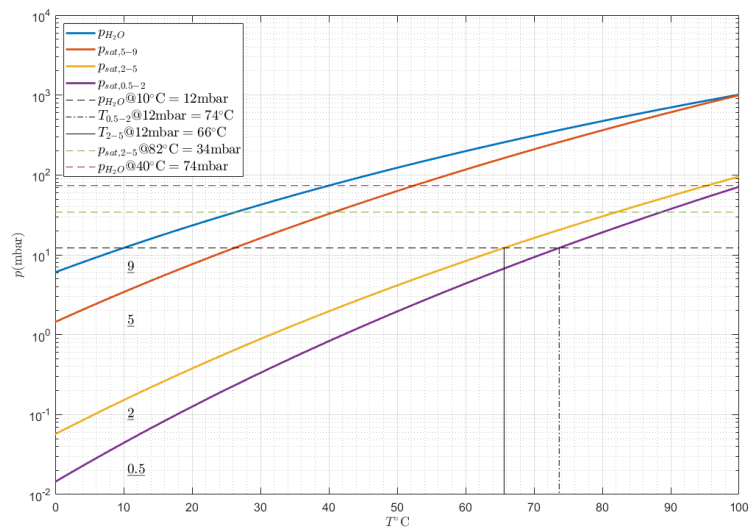
c. Thermochemical properties:

The performances of the synthesized materials were evaluated by thermogravimetric analysis, which simulates the use in the closed-sorption heat battery. A storage density of 1.5 GJ/m³ (based on pentahydrate density of 1580 kg/m³ and co-storage of 0.76 m³ water per m³ pentahydrate) was calculated (validation in a heat battery still to be done).

d. Picture/image/photograph of the material:



e. Graph:



4. Summary: As main results it is found that i) materials can be cycled between charged and discharged state without noticeable deterioration as a function of the number of cycles; ii) monolayers of smaller particles charge and discharge much faster than those of larger particles; iii) heat and mass transfer inside these particles is described, but still under further investigation.

5. Reference

“Preparation & characterization of sodium sulfide hydrates for application in thermochemical storage systems”, M. Roelands, R. Cuyppers, K. Kruit, H. Oversloot, A.J. de Jong, H. van 't Spijker, W. Duvalois, L. van Vliet, C. Hoegaerts, Energy Procedia, 2015, 70, 257 – 266.

OVERVIEW OF TCM MATERIALS: ENERGY STORAGE CAPACITY OR REACTION ENTHALPY VERSUS DESORPTION OR REACTION TEMPERATURE

Some of data for sorption couples and chemical reactions are selected and summarized in Figures 1 and 2, respectively, to give an overview of relations between energy storage capacities (reaction enthalpies) and desorption (reaction) temperatures. The data listed in Figure 1 are based on experiment results (4T approach), while Figure 2 contains theoretical calculations. The data were provided by: University Messina and CNR-ITAE Messina Italy, National Institute of Chemistry Slovenia, CanmetEnergy Ottawa and Simon Fraser University, Canada, CIC Energigune Spain, TU Wien Austria, Materials Science & Eng. Department Northwestern University, USA and Institute of Catalysis and Petrochemistry, Madrid, Spain.

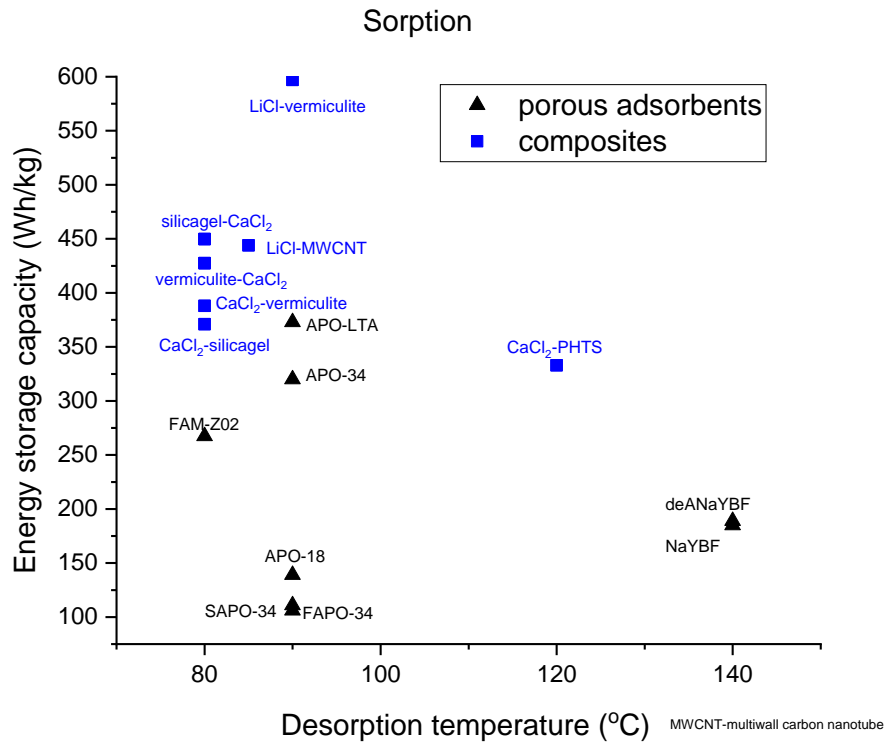


FIGURE 1: ENERGY STORAGE CAPACITY VERSUS A DESORPTION TEMPERATURE OF POROUS SOLIDS AND COMPOSITES (ADSORBATE WATER) INVESTIGATED BETWEEN 2017-2019 FOR SORPTION HEAT STORAGE

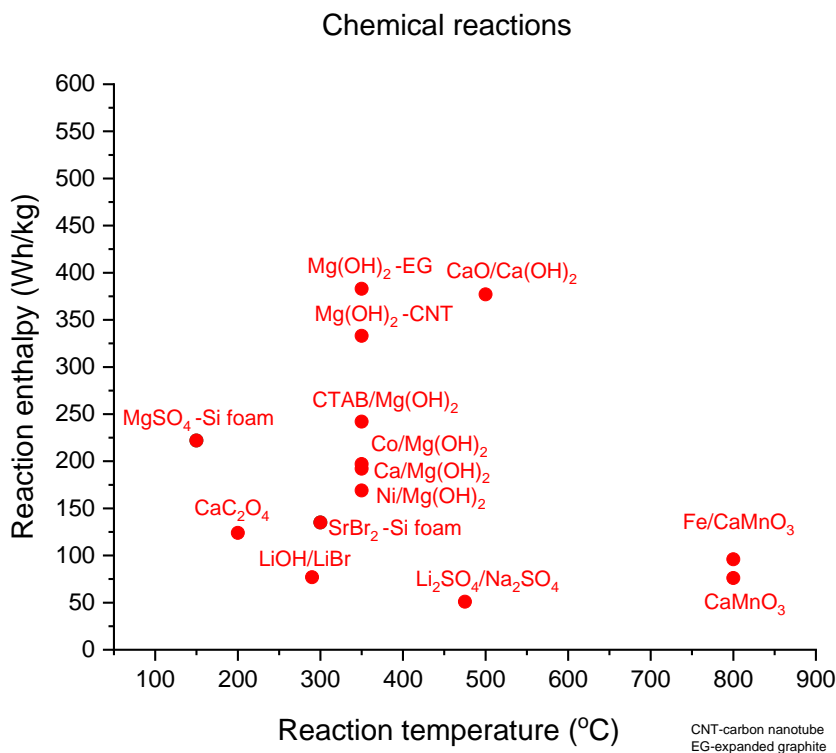


FIGURE 2: REACTION ENTHALPIES OF OXIDES AND COMPOSITES VERSUS REACTION TEMPERATURE FOR DIFFERENT TCMS

3.2.5 DEVELOPMENT OF THE TCM MATERIAL DATABASES IMPLEMENTED IN TASK42/ANNEX 29

Due to complexity and different relevant materials' properties it was decided to prepare three databases: one on chemical reactions (salt hydrates, oxides, composites), one on adsorption (porous solids and composites) and one on absorption (liquids). Materials parameters were determined for the first two databases (see section a in b) and are similar, while the third one is completely different and much more complex. As such it cannot be incorporated in the present frame for chemical reactions and sorption materials.

MATERIAL PARAMETERS FOR THE CHEMICAL REACTION DATABASE USING $K_2CO_3 \cdot 1.5 H_2O$ AS AN EXAMPLE

Overview TCM DATABASE task 58

X mbar vapor pressure

will be used to calculate the T_{eq} in table below

Basic chemical composition	Name Dopant	Name Stabilizer/Matrix	E/V (kWh/m ³)	T_{eq} @ x mbar (K)	Price (€/kg)	Institute
$K_2CO_3 \cdot 1.5H_2O$	-	-	-	-	1	Technical University of Eindhoven
$MgCl_2 \cdot 6H_2O$	-	-	-	-	-	Technical University of Eindhoven
$Na_2S \cdot 5H_2O$	-	-	-	-	-	Technical University of Eindhoven
$NaOH / H_2O$	-	-	-	-	0,30	Empa
$Mg(OH)_2$	-	-	194	531	-	University of Messina - Engineering Department
$Mg(OH)_2 + C$	-	Expanded graphite	330	531	-	University of Messina - Engineering Department
$Mg(OH)_2 + C$	-	Functionalized Carbon Nanotubes	326	531	-	University of Messina - Engineering Department
$Na_2S \cdot 5H_2O$	-	-	-	-	0,348	TNO

Calculated based on $T = \Delta H / (R(-\ln(P/P_0) + \Delta S/R))$

$R = 8.3145$; ΔS and ΔH are given on slide 3; P_0 is 1 and P

Basic chemical composition : $K_2CO_3 \cdot 1.5H_2O$

Starting Materials properties Reaction data Testing conditions and performance Cyclability and effect on the material Additional information	Starting Materials properties	Basic chemical Composition	Main component which contribute to the studied equilibrium reaction	$K_2CO_3 \cdot 1.5H_2O$
		wt.% active phase		100
		Name Dopant	Material which is affecting the reaction, but not the main chemical used in the sample, i.e. Ca in MgO ₂	nvt
		wt.% dopant		nvt
		Name Stabilizer/Matrix	Material which is 'inactive' in the reaction, i.e. ethylcellulose around salt hydrates or silicagel as matrix encapsulation	nvt
		wt.% stabilizer/Matrix		nvt
		Commercial	Y/N	Y
		Cas-number		6381-79-9
		Supplier		SigmaAldrich
		Preparation method	Link to description	
		Mean particle size of active phase (mm)		
		Primary crystallite size (µm)		
		Main Crystallographic phases (XRD)		$K_2CO_3 / K_2CO_3 \cdot 1.5H_2O$
Surface Area (m ² /g) (BET method)				

[Back to TCM overview](#)

Basic chemical composition : $K_2CO_3 \cdot 1.5H_2O$

Starting Materials properties Reaction data Testing conditions and performance Cyclability and effect on the material Additional information	Reaction data	<i>Number of transitions</i>		1
		Equilibrium reaction ($aA+bB \leftrightarrow cC+heat$)	Type of reaction	hydration
		Name A		K_2CO_3
		state of A	Gas/Liquid/Solid	Solid
		a		1
		Molar Mass A	g/mol	138
		Melting point A	K	?
		Specific density A	kg/m ³	
		Specific heat capacity A	J/(g.K)	
		Deliquescence point a (at 25 °C)	Mbar	
		Name B		H ₂ O
		state of B	Gas/Liquid/Solid	Gas
		b		1,5
Molar Mass B	g/mol	18,02		
Specific density B	kg/m ³			
Melting point B	K	nvt		
Specific heat capacity B	J/(g.K)			
Deliquescence point B (at 25 °C)	Mbar			
Name C		$K_2CO_3 \cdot 1.5H_2O$		
State of C	Gas/Liquid/Solid			
c		1		
Molar Mass c	g/mol	165		
Specific density C	kg/m ³			
Melting point c	K	?		
Specific heat capacity C	J/(g.K)			
Deliquescence point c (at 25 °C)	mbar			
ΔS° (standard entropy of the equilibrium reaction)	J/(mol.K)	151		
ΔH° (standard enthalpy of the equilibrium reaction)	kJ/mol	62.5		
$T_{eq} = \Delta H^\circ / \Delta S^\circ$	K			
pT diagram	link to referene			
Theoretical energy density	kJ/kg			
Deliquescence line	Link to reference			

[Back to TCM overview](#)

Basic chemical composition : $K_2CO_3 \cdot 1.5H_2O$

Starting Materials properties	Material properties under testing conditions	Apparent (bulk) heat conductivity (charged state; A)	(W/(m·K))	
		Specific heat conductivity single grain (charged state; A)	(W/(m·K))	
Reaction data	Material properties under testing conditions	Apparent (bulk) heat conductivity (discharged state; C)	(W/(m·K))	
		Specific heat conductivity single grain (discharged state; C)	(W/(m·K))	
Testing conditions and performance	Material properties under testing conditions	Reference		
		Instrument used for testing (i.e. TGA, lab-scale reactor...)		TGA
Cyclability and effect on the material	Material properties under testing conditions	Test cell volume (m ³)		60
		Starting temperature (K)		75
Additional Information	Material properties under testing conditions	Final temperature (K)		0.5
		heating rate (K/min)		air
Back to TCM overview	Material properties under testing conditions	Type of gas		500
		Total flow rate (ml/min)		--
Back to TCM overview	Material properties under testing conditions	Total flow speed at reactor/sample (m/s)		1000
		Total pressure (mbar)		0
Back to TCM overview	Material properties under testing conditions	Mass flow solid phase (g/s)		0.00919
		Residence time in reactor of solid material (s)		0.00522
Back to TCM overview	Material properties under testing conditions	partial pressure reactive gas (mbar)		7.5
		Time (min)		33.3
Back to TCM overview	Material properties under testing conditions	Initial sample mass (g)		0.00522
		Method of determination mass variation		TGA
Back to TCM overview	Material properties under testing conditions	Mass variation (g)		0.001399
		Starting temperature (K)		39
Back to TCM overview	Material properties under testing conditions	Final temperature (K)		25
		heating rate (K/min)		-0.5
Back to TCM overview	Material properties under testing conditions	Type of gas		air, N ₂
		Total flow rate (ml/min)		500
Back to TCM overview	Material properties under testing conditions	Total pressure (mbar)		1000
		Total flow speed at reactor/sample (m/s)		--
Back to TCM overview	Material properties under testing conditions	Mass flow solid phase (g/s)		0
		Residence time in reactor of solid material (s)		0.005
Back to TCM overview	Material properties under testing conditions	partial pressure reactive gas (mbar)		7.5
		Time (min)		53.3
Back to TCM overview	Material properties under testing conditions	Initial sample mass (g)		0.00522
		Method of determination mass variation		TGA
Back to TCM overview	Material properties under testing conditions	Mass variation (g)		0.001399
		Charging power (W/g) - peak		W/g
Back to TCM overview	Material properties under testing conditions	Mean charging power (W/g) - based on complete charging period		W/g
		Discharging power (W/g)		W/g
Back to TCM overview	Material properties under testing conditions	Mean discharging power (W/g) - based on complete discharging period		W/g
		Experimental Charging efficiency		kWh/Kg
Back to TCM overview	Material properties under testing conditions	Experimental Released efficiency		kWh/Kg
		Experimental Storage Energy Density		(kWh/m ³)
Back to TCM overview	Material properties under testing conditions	Experimental Released Energy Density		(kWh/m ³)
		Diagram of the experiment		(picture)
Back to TCM overview	Material properties under testing conditions	Reference of kinetic study of described reaction		

Basic chemical composition : $K_2CO_3 \cdot 1.5H_2O$

Starting Materials properties Reaction data Testing conditions and performance Cyclability and effect on the material Additional Information	Cyclability and effect on the material	Number of cycles studied	%	9
		Storage Efficiency at n cycle ($\eta = \text{Storage Energy Density at n cycle} / \text{Storage Energy Density at 1st cycle}$)	nm	1
		Mean particle size of grains (nm) after n th cycle	um	
		Mean primary crystallite size (um) after n th cycle		
		Picture of the particles (before/during/after experiment)		
		Diagram of the experiment		
		Reference to experiment	N	
		Crushing strength Starting material	N	
		Crushing strength after n th	%	

[Back to TCM overview](#)

Basic chemical composition : $K_2CO_3 \cdot 1.5H_2O$

Starting Materials properties Reaction data Testing conditions and performance Cyclability and effect on the material Additional Information	Additional Information	Price (euro/kg; euro/MJ)	(euro/kg)	1
			Supplier	nvt
			(euro/MJ)	
			Link to MSDS data	
			Link to corrosion data	
			General references about this material/reaction/....	G. P. Thiel and J. H. Lienhard, Desalination, vol. 346, pp. 64–69, Aug 2014
			References	

[Back to TCM overview](#)

MATERIAL PARAMETERS FOR THE SORPTION MATERIALS DATABASE

Materials properties Testing conditions and performance Cyclability and effect on the material Additional Information	Materials properties	Adsorbent material		Zeolite 13X	Text
		Supplier		Chemiewerk Bad Köstritz, Germany	Text
		Sample conditions	Powder, granulated, extruded...	granulated beads, binder-free, diameter: 1.6–2.5 mm	Text
		Synthesis route		REFERENCE reported in the reference section	Text
		Adsorbate		Water	Text
		Gas carrier	If any	Air	Text
		Adsorbent density	bulk, crystallographic, fixed bed	680 kg/m ³ - bulk	Integer + text
		Density source	from "measurements", "literature" or the material "supplier"	REFERENCE reported in the reference section	Text
		Density Measurement Temperature		25°C	Integer

Starting Materials properties Testing conditions and performance Cyclability and effect on the material Additional Information	Testing conditions and performance	Desorption conditions	Temperature applied for desorption stage (°C)	479°C	Integer
			Pressure of the adsorbate applied during desorption – Absolute or partial (mbar)	<0,2 mbar	Floating
			Pressure in the sorption reactor during the desorption desorption – Absolute or partial (mbar)	Ambient pressure	Text
		Adsorption conditions	Temperature for the adsorption (equilibrium) (°C)	30 °C	Integer
			Partial pressure of the adsorbate during adsorption	5 mbar	Floating
			Pressure in the sorption reactor during the adsorption – Absolute or partial (mbar)	Ambient pressure	Text
		Sample dry mass (g)		5g	Floating
		Measurement method	Instrument used for testing (i.e. Self-built setup or apparatus)	REFERENCE reported in the reference section	Text
		Saturated Adsorbate Uptake	(g/g or g/cm ³)		Floating
		Adsorption isotherm	Complete isotherms: literature reference, data set of measurements, figures		Image / text / floating
		Heat of adsorption	(kWh/m ³ or Wh/kg)		Floating
		Specific heat of "dry" material	(kJ/kg K)		Floating

Starting Materials properties Testing conditions and performance Cyclability and effect on the material Additional Information	Cyclability and effect on the material	Amount of degradation	%	10%	Floating
		Number of cycles		25	Integer
		Testing conditions	Partial ad-desorption Complete ad-desorption		Text

Starting Materials properties Testing conditions and performance Cyclability and effect on the material Additional Information	Additional Information	Price	(euro/kg)	1	Floating
		Supplier		nvt	Text
		Safety	Link to MSDS data		Text
		Corrosion	Link to corrosion data		Text
		References	General references about this material/reaction/....	G. P. Thiel and J. H. Lienhard, Desalination, vol. 346, pp. 54–69, Aug. 2014	Text
		Comments			Text

4 SUBTASK 3 - MEASURING PROCEDURES AND TESTING UNDER APPLICATION CONDITIONS

4.1 SUBTASK 3P: PCM TESTING UNDER APPLICATION CONDITIONS

4.1.1 INTRODUCTION

...

4.1.2 PROPERTIES OF PCM IN THE LAB ENVIRONMENT AND UNDER APPLICATION CONDITIONS

BACKGROUND

Deliverable 1 of Subtask 3P is an inventory of properties of Phase Change Materials (PCM) that change comparing experiments in the lab environment with tests under application conditions. Examples where no change is observed are also included. The inventory is reported in the following sections containing a short description of the property and a table summarizing the relevant information. The considered properties are: degree of supercooling, phase separation, storage capacity, long-term stability, crystal structure, stability of phase change emulsions, and thermal conductivity.

The structure of the tables is as follows: The first column indicates the observation from the comparison between experiments in the lab environment with tests under application conditions. Columns 2 and 3 specify for which experimental conditions and which PCM (class) the changes of properties have been observed. Column 4 contains corresponding references and column 5 comments. In column 4, either publications or the institutions providing input are indicated. The following abbreviations, listed in alphabetical order, were used for these institutions.

DLR: German Aerospace Center, Germany

DTU: Technical University of Denmark, Denmark

HSLU: Institute of Mechanical Engineering and Energy Technology IME / CC Thermal Energy Storage, Lucerne University of Applied Sciences and Arts, Switzerland

ISE: Fraunhofer Institute for Solar Energy Systems ISE, Germany

LAMTE: Laboratory of Applied Multiphase Thermal Engineering, Dalhousie University, Canada

LTTT: Lehrstuhl für Technische Thermodynamik und Transportprozesse, University of Bayreuth, Germany

TUE: Technical University of Eindhoven, The Netherlands

UPV/EHU: University of the Basque Country, Spain

ZAE: Bavarian Center for Applied Energy Research (ZAE Bayern), Germany

INVENTORY TABLES

DEGREE OF SUPERCOOLING

As stated in the PCM Wiki [1], “Supercooling during the liquid-solid phase change is the phenomenon when a material’s crystallization initiation occurs at a temperature below its freezing temperature. That is, the nucleation starts at a temperature below the real freezing point of the material. Thus, a material that tends to supercool should be cooled considerably below its expected freezing point to initiate freezing. Once its nucleation initiates, the material temperature rises to its real freezing point, and then continues freezing at that temperature.”

The degree of supercooling depends on the applied measurement conditions: Sample size, purity, cooling conditions, level of heating above the melting point, design of PCM container and heat exchanger, and additives. Besides the experimental conditions, the degree of supercooling also depends on the material class under investigation. Usually, salt hydrates, water, and sugar alcohols exhibit a higher degree of supercooling compared with organic PCM like paraffins, fatty acids, and fatty alcohols. [2][3] Table 4-1 contains the observations related to the degree of supercooling when comparing experiments in the lab environment with tests under application conditions.

Table 4-1: Degree of supercooling

#	OBSERVATION	EXPERIMENTAL CONDITIONS	MATERIAL (CLASS)	REF.	COMMENTS
1.1	Nucleation temperature: DSC: -11 °C 10 L: 4-8 °C 500 L: 5.1-7.8 °C	DSC device 10 L container 500 L storage	TBAB40 + water	HSLU	500 L storage: sometimes different degree of supercooling in different sensors
1.2	Nucleation temperature: DSC: ~-10 °C, T-History and storage: 25 – 27 °C	DSC, T-History, 1 and 1.5 m ³ storage	CaCl ₂ ·6H ₂ O	ZAE [4]	Varied test conditions: purity, sample size, cooling rate
1.3	Degree of supercooling: DSC: 32 K 12 L: 6 – 18 K	DSC device 12 L container	Erythritol	ISE	Supercooling depends on previous temperature level during melting process
1.4	Freezing point: 20 L setup: 49 °C “Easymax”: -10 °C	20 L container; “Easymax 102” cycling device	35% Alum amon hydrate slurries	HSLU	

		and synthesis station			
1.5	Heat sodium acetate trihydrate (SAT) to temperatures +20 K above its melting point resulted in supercooling of 40 K	closed steel tanks, prototype heat storage units with SAT mixtures	SAT with additives, extra water, thickening agents	DTU [5][6][7][8]	In a closed PCM tank, the expansion of SAT has to be considered, local pressure changes and tank deformations may cause nucleation starting at crack in a similar way as the metal disc in the hand warmers.
1.6	Minimum crystallization temperatures of supercooled SAT composites: * SAT and SAT +9% water: -24 °C; * SAT +5% CMC and SAT +3% liquid polymer -18 °C; * All SAT composites in contact with rusty steel: -15 °C	Supercooled SAT composite samples (60 g) were cooled down in a freezer	SAT with additives, extra water, thickening agents, liquid polymers	DTU [9]	Varied test conditions: purity, supercooling duration.
1.7	DSC: - Erythritol: 60 K - Xylitol: > 90 K - MgCl ₂ ·6H ₂ O: 30 K 3-Layer-Calorimeter: - Erythritol: 47 K - Xylitol: > 90 K - MgCl ₂ ·6H ₂ O: < 3 K Macro-capsule: - MgCl ₂ ·6H ₂ O: < 3 K	3 different setups: DSC (sample size 10 mg), 3-Layer-Calorimeter (100 g), macro-capsules (281 g)	Technical grade sugar alcohols (Erythritol, Xylitol) and salt hydrate (MgCl ₂ ·6H ₂ O)	LTTT [10][11]	Degree of supercooling depends on applied sample volume. The sample mass of 100 g in the 3-Layer-Calorimeter is in the magnitude of PCM mass of the later on applied macro-capsules.

1.8	Highly increased supercooling in small volumes	Micro/nano scale	All material classes, also paraffins	ISE	
1.9	Sample size, maximum holding temperature and holding time affect significantly the nucleation process of Glauber's salt nucleated with borax. Glauber's salt nucleated with borax: DSC measurements will render a value of the supercooling reduction well below the actual values for large samples [20].	DSC (10 mg) vs 25 ml flasks Several cooling rates and maximum holding temperatures	Glauber's salt ($\text{Na}_2\text{SO}_4 \cdot 10\text{H}_2\text{O}$) with additives (borax)	UPV/EHU [12]	Within the ranges of the work referred, the cooling rate seems not to play an important role.
1.10	No supercooling at large scale, slight supercooling (1-2 K) in DSC	DSC to multi liter scale	Dodecanoic acid	LAMTE [13][14][15]	At large scale, no supercooling (maximum temperature of the PCM during testing never exceeds 80 °C, less than 40 K above melting temperature) In [13] and [14]: solidification plateau at the expected melting temperature.

PHASE SEPARATION

In the case of PCM consisting of more than one component, a separation of different phases might occur during repeated melting and crystallization cycles. If phase separation occurs, a part of the material does not contribute to the melting and crystallization enthalpy any longer, thereby usually reducing the storage capacity of a latent heat storage system. [16] Phase separation depends on the applied test measurement conditions, such as sample size, purity, thermal cycling conditions, heat exchanger design, additives, and container dimensions. Table 4-2 contains observations related to phase separation when comparing experiments in the lab environment with tests under application conditions.

Table 4-2: Phase separation

#	OBSERVATION	EXPERIMENTAL CONDITIONS	MATERIAL (CLASS)	REF.	COMMENTS
2.1	100 ml no separation, 10 L separation	Varying sample container volumes	Salt hydrates or Mixtures of materials with significantly different densities	TUE, ZAE	More related to height of storage rather than volume
2.4	Containments with a large height are worse	Encapsulated PCM	Different material classes	ISE	Example: FlateICE manufacturer recommends to lay the containers
2.2	No difference in separation observed for different sample sizes (during the phase change trough the melting range between solid and liquid state)	Sample sizes from 20 mg to 156 kg	Non eutectic salt mixture of 30 wt.% KNO ₃ and 70 wt.% NaNO ₃	DLR [17]	
2.3	In PCM storage with SAT and extra water phase separation occurs over time/repeated cycles when the PCM is not actively mixed. Thickening agents can effectively reduce phase separation also in tall storages. There is also high potential for using various polymers for reduction of phase separation.	200 g to 200 kg	SAT with additives; extra water, thickening agents (CMC or Xanthan rubber), EDTA, liquid polymers	DTU [6] [18] [19] [20] [21]	Results from prototype storage unit testing have been compared to experiments with smaller sample sizes. Also EDTA and similar additives with chelating effect can be used for avoiding phase separation.

STORAGE CAPACITY

“In applications, the maximum storage capacity (MSC) of a PCM is a crucial value. It corresponds to the enthalpy difference between minimum and maximum operating temperature and thus, besides the latent heat in the temperature interval under consideration also contains sensible heat.” [22] The storage capacity (SC) observed in experiments under application-oriented conditions depends on, amongst others, the sample purity and the cooling conditions. In the case of PCM mixtures, a possible deviation from the correct concentration also affects the storage

capacity. Table 4-3 contains observations related to storage capacity when comparing experiments in the lab environment with tests under application conditions.

Table 4-3: Storage capacity (SC)

#	OBSERVATION	EXPERIMENTAL CONDITIONS	MATERIAL (CLASS)	REF.	COMMENTS
3.1	Decreased SC due to a deviation from the correct concentration	DSC; 1 to 1.5 m ³ storage	Salt hydrates	ZAE [22]	“In large latent heat storages with the used PCM being a salt hydrate, it is difficult to assure the stoichiometrically correct hydrate concentration of the salt hydrate and to verify the concentration.” [22]
3.2	Change in SC due to impurities	DSC; 1 to 1.5 m ³ storage		ZAE	Impurities can act as “inert” material and thus decrease SC. Impurities can affect crystallinity.
3.3	SC (melting enthalpy) of technical grade PCM agrees with results from analytical grade samples.		Technical grade sugar alcohols (Erythritol, Xylitol) and salt hydrate (MgCl ₂ ·6H ₂ O)	LTTT [10]	Comparison of technical grade PCM with values from literature
3.4	SC of polymers is affected by cooling conditions	DSC with varying cooling rate and different minimum temperatures reached upon cooling	Polymers	ZAE	Crystallinity of polymers depends on cooling conditions → different phase change temperature ranges due to different phase fraction of amorphous and crystalline (or different crystals) solid material
3.5	Polymorphism affects SC as different melting points and enthalpies can be obtained in succeeding thermal cycles	DSC	Sugar alcohol (Erythritol)	LTTT [10]	Repeated melting and crystallisation cycles with same heating and cooling rate

3.6	Reduction of melting enthalpy due to decreased purity of fatty acids		Fatty acids: Stearic Acid (SA) and Palmitic Acid (PA)	UPV/EHU [23]	“Industrial grade SA and PA rendered melting enthalpies 24 and 20% lower than the ones for the analytical purity compounds. A noticeable decrease was also noticed for the melting temperatures, being also the melting interval for the industrial compounds significantly wider than the analytical one.”[23]
3.7	Maximum storage capacity, i.e. enthalpy difference in temperature range of 15 K (25-40 °C): Pure: 164 J/g Technical: 134 J/g	DSC, 2 K/min heating and cooling rate	CaBr ₂ ·6H ₂ O Pure: crystals grown from solution Technical: prepared from aqueous CaBr ₂ solution	ZAE [24]	The purity of the used basic raw material to prepare the salt hydrate has an influence on the maximum storage capacity.
3.8	No difference in storage capacity	DSC measurements and tests at experimental scale	Dodecanoic acid	LAMTE [14] [25][26]	For the work that was done with dodecanoic acid, the authors have not seen any difference between thermal storage as determined from DSC data, and then measured through the charging or discharging at the experimental scale. Papers [14][25][26] show the theoretical prediction (from measured DSC properties) matching the experimental prediction within the error measurements

The storage capacity is also affected by changes of the phase change temperature range.

The phase change temperature range is the temperature range in which the phase change occurs. In the case of an ideal PCM – being described by the model of a perfect single crystal of infinite expansion – a single melting temperature (or melting point) is obtained: Since all atoms are fixed at their lattice locations and thus have the same binding energy, all atoms undergo a phase transition at the same temperature. However, most PCM show a widened phase transition range, since the crystal has a finite expansion and slightly different binding energies can be assigned to the individual crystal components (ions, molecules, etc.) due to impurities, crystal defects, grain boundaries, and surface effects. The real crystal then has a melting temperature

range, which extends to lower temperatures compared to the perfect, infinitely extended crystal. The upper limit of the melting range of the real crystal corresponds to the melting point of the ideal crystal. During experiments, the measured phase change temperature range can be broadened depending on the experimental conditions, such as purity of the sample and applied heating / cooling rates. For example, a decreased purity of the sample lowers the melting temperature. Increased heating and cooling rates lead to an increased temperature gradient within the sample and, thus, to an apparently broadened phase change temperature range.

LONG-TERM STABILITY

In this report, stability refers to the stability of the PCM itself subjected to different static and/or dynamic conditions (temperature, contact to atmosphere, and contact to container/heat exchanger). Stating that a PCM is stable means that the relevant properties of the PCM remain constant within specific limits (which are to be identified) over the desired period of time. Long-term stability depends on the applied test and measurement conditions, such as the interaction with the environment or the storage component materials, the stability of additives, and the temperature the PCM is subjected to. In the case of organic PCM, the thermal stability and stability in contact with oxygen is crucial. In the case of salt hydrates and PCM mixtures, long-term stability is affected by a decreased thermal cycling stability due to phase separation processes. Table 4-4 contains observations related to long-term stability when comparing experiments in the lab environment with tests under application conditions.

Table 4-4: Long-term stability

#	OBSERVATION	EXPERIMENTAL CONDITIONS	MATERIAL (CLASS)	REF.	COMMENTS
4.1	NaNO ₃ thermally stable at 350 °C	Isothermal long-duration test, batch furnace, mass losses at specific times with an analytical balance $T_{\max} = 350 \text{ °C}$, $T = 2600 \text{ h} = 108 \text{ d}$	NaNO ₃ , ($T_m = 305 \text{ °C}$), from BASF, purity of min. 99%	DLR [27]	small amount of nitrite formed (equilibrium reaction)
4.2	Phase change temperature detected at the same temperature level as in laboratory experiments ($T_m = 305 \text{ °C}$)	Long-term test in a lab-scale module $T_{\max} = \text{above } 350 \text{ °C}$, typical cycle temperature: 280 – 330 °C, 200 cycles	NaNO ₃ ($T_m = 305 \text{ °C}$) Amount of PCM: 320 kg	DLR [28]	
4.3	Thickening agents such as CMC and Xanthan rubber may degrade		SAT with thickening agents	DTU [29]	The colour of a SAT mixture with CMC or Xanthan will change

	over time at high temperatures.				when exposed to high temperatures over a period. The thickening effect may or may not remain.
4.4	No change in onset melting temperature or latent heat of fusion over 3000 to 4000 cycles	Setup built and used to run thermal cycling is presented in [30]	Paraffins and other organic PCM	LAMTE [26] [30] [31]	Study on a dozen PCM (half paraffin, half other organics): no change in melting temperature onset or latent heat of fusion over 3000 to 4000 cycles
4.5	500 cycles in DSC between 55 and 155 °C: → 1 % decrease of melting enthalpy (below the accuracy of the DSC device) → Small change of melting temperature (0,3 K) 30 cycles with macro-capsules (between 95 and 135 °C): → No decrease of the stored energy observed.	DSC with sealed crucibles; macro-capsules in lab-scale storage unit	Salt hydrate (MgCl ₂ ·6H ₂ O)	LTTT [10] [11]	

CRYSTAL STRUCTURE

“The crystal structure itself is obtained by associating with each lattice point an identical assembly of asymmetric units. The asymmetric units might be as small as an atom of neon or as large as a virus.”[32] In the context of solid-liquid PCM, a change in the crystal structure of a PCM can affect many properties, such as the melting temperature and enthalpy of the PCM.

Especially in the case of organic materials, the crystal structure that is obtained during experiments depends on the applied test conditions. The cooling program and the sample size under investigation are two test conditions influencing the crystal structure.

Table 4-5 contains observations related to crystal structure when comparing experiments in the lab environment with tests under application conditions.

Table 4-5: Crystal structure

#	OBSERVATION	EXPERIMENTAL CONDITIONS	MATERIAL (CLASS)	REF.	COMMENTS
5.1	Formation of different polymorphic crystal structures depending on the applied cooling conditions	DSC and storage tank	Sugar alcohols, e.g. D-mannitol	[33]	“The experiments performed by DSC have shown that the D-mannitol presents polymorphic structural changes and, therefore, its thermal properties are not always the same. Depending on the polymorphic phase obtained, D-mannitol has different melting temperature. This behaviour was corroborated in a storage tank, where it may be seen that the cooling rate of the D-mannitol is a key parameter in the formation of the different polymorphic phases.” [33]
5.2	Formation of different crystals		TBAB	HSLU	It is not sure if this is affected by the storage volume
5.3	Formation of different polymorphic crystal structures depending on the applied cooling conditions		Sugar alcohols, e.g. erythritol, xylitol, sorbitol and their eutectic mixtures	EHU [34]	“Under the cooling conditions employed for the preparation of the samples (quench cooling down to room temperature), erythritol crystallized forming the metastable polymorph: form II. When the samples were subsequently heated from room temperature, form II transformed to form I. Xylitol revealed no formation signs of the metastable structure” [35]
5.4	“During a DSC thermal cycling of the eutectic mixture, the metastable Form II of erythritol crystallized 6 times	DSC	Organic eutectic mixtures (erythritol and urea)	EHU [35]	Note that these two observations also influence the storage capacity and phase change temperature range.

out of 85 cycles. On those cycles, the mixture crystallized at 71 °C instead of 82 °C. Besides, the enthalpy of the mixture displayed a value of 190–195 J/g instead of the shown value on the remaining cycles: 240 J/g.” [35]

STABILITY OF PHASE CHANGE EMULSIONS

Phase change emulsions are fluids containing PCM and a carrier fluid. A phase change emulsion is stable if the emulsified PCM droplets do not agglomerate. Among others, the stability of a phase change emulsion depends on the investigated sample and particle size.

Table 4-6 contains observations related to stability of phase change emulsions when comparing experiments in the lab environment with tests under application conditions.

Table 4-6: Stability of phase change emulsions

#	OBSERVATION	MATERIAL (CLASS)	REF.
6.1	Solidification of some PC dispersions has been observed in small scale (50-100 ml), but not in large scale (10 kg)	Paraffin-in-water emulsions	HSLU
6.2	Separation and shear stability depend on particle sizes: <1 µm: stable, >1 µm unstable	Paraffin-in-water emulsions	ISE

THERMAL CONDUCTIVITY

Thermal conductivity is a material property that determines the heat flow through a material on the basis of thermal conduction. In the PCM context, the thermal conductivity of the PCM affects the thermal power during charging and discharging of the latent heat storage. The measured thermal conductivity depends on the applied test conditions, such as purity of the sample, heating and cooling rates, and the existence of voids in the solid sample.

Table 4-7 contains observations related to thermal conductivity when comparing experiments in the lab environment with tests under application conditions.

Table 4-7: Thermal conductivity

#	OBSERVATION	MATERIAL (CLASS)	REF.	COMMENTS
---	-------------	------------------	------	----------

7.1	Voids within the sample can reduce the measured thermal conductivity	All material classes	ZAE	Internal voids in the solid phase or gas bubbles in the liquid phase
7.2	Different cooling rates can lead to different crystal structures with different thermal conductivities.	All material classes	ZAE	High cooling rates in small lab scale samples, but low cooling rates in application size.

REFERENCES

- [1] Definition of Supercooling, Wiki PCM <https://thermalmaterials.org/wiki-pcm/supercooling>
- [2] Rathgeber, C., Schmit, H., Miró, L., Cabeza, L. F., Gutierrez, A., Ushak, S. N., & Hiebler, S. (2018). Enthalpy-temperature plots to compare calorimetric measurements of phase change materials at different sample scales. *Journal of Energy Storage*, 15, 32-38.
- [3] Rathgeber, C., Miró, L., Cabeza, L. F., & Hiebler, S. (2014). Measurement of enthalpy curves of phase change materials via DSC and T-History: When are both methods needed to estimate the behaviour of the bulk material in applications?. *Thermochimica Acta*, 596, 79-88.
- [4] Schmit, H., Pfeffer, W., Rathgeber, C., & Hiebler, S. (2016). Calorimetric investigation of the concentration dependent enthalpy change around semicongruent melting CaCl₂·6H₂O. *Thermochimica acta*, 635, 26-33.
- [5] Dannemand, M., Schultz, J. M., Johansen, J. B., & Furbo, S. (2015). Long term thermal energy storage with stable supercooled sodium acetate trihydrate. *Applied Thermal Engineering*, 91, 671-678.
- [6] Dannemand, M., Dragsted, J., Fan, J., Johansen, J. B., Kong, W., & Furbo, S. (2016). Experimental investigations on prototype heat storage units utilizing stable supercooling of sodium acetate trihydrate mixtures. *Applied Energy*, 169, 72-80.
- [7] Rogerson, M. A., & Cardoso, S. S. (2003). Solidification in heat packs: III. Metallic trigger. *AIChE journal*, 49(2), 522-529.
- [8] Englmair, G., Moser, C., Furbo, S., Dannemand, M. & Fan, J. (2018). Design and functionality of a segmented heat-storage prototype utilizing stable supercooling of sodium acetate trihydrate in a solar heating system. *Applied Energy*, 221, 522-534.
- [9] Englmair, G., Jiang, Y., Dannemand, M., Moser, C., Schranzhofer, H., Furbo, S. & Fan, J. (2018). Crystallization by local cooling of supercooled sodium acetate trihydrate composites for long-term heat storage. *Energy and Buildings*, 180, 159-171.
- [10] Höhle, S., König-Haagen, A., & Brüggemann, D. (2017). Thermophysical characterization of MgCl₂·6H₂O, xylitol and erythritol as phase change materials (PCM) for latent heat thermal energy storage (LHTES). *Materials*, 10(4), 444.
- [11] Brüggemann, D., König-Haagen, A., Kasibhatla, R. R., Höhle, S., Glatzel, U. et al. (2017). Entwicklung makroverkapselter Latentwärmespeicher für den straßengebundenen Transport von Abwärme (MALATrans): Laufzeit: 01.07.2013 bis 31.12.2016 (Abschlussbericht). Bayreuth.
- [12] García-Romero, A., Diarce, G., Ibarretxe, J., Urresti, A., & Sala, J. M. (2012). Influence of the experimental conditions on the subcooling of Glauber's salt when used as PCM. *Solar Energy Materials and Solar Cells*, 102, 189-195.
- [13] Liu, C., & Groulx, D. (2014). Experimental study of the phase change heat transfer inside a horizontal cylindrical latent heat energy storage system. *International Journal of Thermal Sciences*, 82, 100-110.
- [14] Murray, R. E., & Groulx, D. (2014). Experimental study of the phase change and energy characteristics inside a cylindrical latent heat energy storage system: Part 1 consecutive charging and discharging. *Renewable Energy*, 62, 571-581.
- [15] Desgrosseilliers, L., Whitman, C. A., Groulx, D., & White, M. A. (2013). Dodecanoic acid as a promising phase-change material for thermal energy storage. *Applied Thermal Engineering*, 53(1), 37-41.

- [16] Rathgeber, C., Grisval, A., Schmit, H., Hoock, P., & Hiebler, S. (2018). Concentration dependent melting enthalpy, crystallization velocity, and thermal cycling stability of pinacone hexahydrate. *Thermochimica Acta*, 670, 142-147.
- [17] Martin, C., Bauer, T., & Müller-Steinhagen, H. (2013). An experimental study of a non-eutectic mixture of KNO₃ and NaNO₃ with a melting range for thermal energy storage. *Applied Thermal Engineering*, 56(1-2), 159-166.
- [18] Kong, W., Dannemand, M., Johansen, J. B., Fan, J., Dragsted, J., Englmaier, G., & Furbo, S. (2016). Experimental investigations on heat content of supercooled sodium acetate trihydrate by a simple heat loss method. *Solar Energy*, 139, 249-257.
- [19] Dannemand, M., Johansen, J. B., Kong, W., & Furbo, S. (2016). Experimental investigations on cylindrical latent heat storage units with sodium acetate trihydrate composites utilizing supercooling. *Applied Energy*, 177, 591-601.
- [20] Englmaier, G., Furbo, S., Dannemand, M., & Fan, J. (2020). Experimental investigation of a tank-in-tank heat storage unit utilizing stable supercooling of sodium acetate trihydrate. *Applied Thermal Engineering*, 167.
- [21] Kong, W., Dannemand, M., Berg, J. B., Fan, J., Englmaier, G., Dragsted, J., & Furbo, S. (2019). Experimental investigations on phase separation for different heights of sodium acetate water mixtures under different conditions. *Applied Thermal Engineering*, 148, 796-805.
- [22] Schmit, H., Pöllinger, S., Pfeffer, W., & Hiebler, S. (2015). Calorimetric and theoretical determination of the concentration dependent enthalpy change around CaBr₂·6H₂O. *Thermochimica Acta*, 609, 20-30.
- [23] Diarce, G., Campos-Celador, Á., Gómez, S., García-Romero, A., Sala, J. M. (2014). Evaluation of the thermal and economical performance of a modular TES system for domestic applications: comparison between paraffinic and fatty acid based pcms. *Eurosun 2014, Aix-les Bains*.
- [24] Rudaleviciene, D. (2017). *Untersuchung technischer Latentwärmespeichermaterialien*. Master Thesis. Universität Tübingen, ZAE Bayern.
- [25] Kabbara, M., Groulx, D., & Joseph, A. (2016). Experimental investigations of a latent heat energy storage unit using finned tubes. *Applied Thermal Engineering*, 101, 601-611.
- [26] Kabbara, M., Groulx, D., & Joseph, A. (2018). A parametric experimental investigation of the heat transfer in a coil-in-tank latent heat energy storage system. *International Journal of Thermal Sciences*, 130, 395-405.
- [27] Bauer, T., Laing, D., & Tamme, R. (2012). Characterization of sodium nitrate as phase change material. *International Journal of Thermophysics*, 33(1), 91-104.
- [28] Laing, D., Bauer, T., Breidenbach, N., Hachmann, B., & Johnson, M. (2013). Development of high temperature phase-change-material storages. *Applied Energy*, 109, 497-504.
- [29] Dannemand, M., Johansen, J. B., & Furbo, S. (2016). Solidification behavior and thermal conductivity of bulk sodium acetate trihydrate composites with thickening agents and graphite. *Solar Energy Materials and Solar Cells*, 145, 287-295.
- [30] Kahwaji, S., Johnson, M. B., Kheirabadi, A. C., Groulx, D., & White, M. A. (2018). A comprehensive study of properties of paraffin phase change materials for solar thermal energy storage and thermal management applications. *Energy*, 162, 1169-1182.
- [31] Kahwaji, S., Johnson, M. B., Kheirabadi, A. C., Groulx, D., & White, M. A. (2016). Stable, low-cost phase change material for building applications: the eutectic mixture of decanoic acid and tetradecanoic acid. *Applied Energy*, 168, 457-464.
- [32] Atkins, P. W. (1990). *Physical Chemistry*, 4th Edition, Oxford University Press, Oxford.
- [33] Gil, A., Barreneche, C., Moreno, P., Solé, C., Fernández, A. I., & Cabeza, L. F. (2013). Thermal behaviour of d-mannitol when used as PCM: Comparison of results obtained by DSC and in a thermal energy storage unit at pilot plant scale. *Applied Energy*, 111, 1107-1113.
- [34] Diarce, G., Gandarias, I., Campos-Celador, A., García-Romero, A., & Griesser, U. J. (2015). Eutectic mixtures of sugar alcohols for thermal energy storage in the 50–90 C temperature range. *Solar Energy Materials and Solar Cells*, 134, 215-226.
- [35] Jesus, A. L., Nunes, S. C., Silva, M. R., Beja, A. M., & Redinha, J. S. (2010). Erythritol: Crystal growth from the melt. *International journal of pharmaceutics*, 388(1-2), 129-135.

- [36] Diarce, G., Quant, L., Campos-Celador, Á., Sala, J. M., & García-Romero, A. (2016). Determination of the phase diagram and main thermophysical properties of the erythritol–urea eutectic mixture for its use as a phase change material. *Solar Energy Materials and Solar Cells*, 157, 894-906.

4.1.3 EXPERIMENTAL DEVICES TO INVESTIGATE DEGRADATION OF PCM

This report was written by Christoph Rathgeber ^a. The content was provided from Rocío Bayón ^b, Luisa F. Cabeza ^c, Gabriel Zsembinszki ^c, Gerald Englmaier ^d, Mark Dannemand ^d, Gonzalo Diarce ^e, Oliver Fellmann ^f, Rebecca Ravotti ^f, Stefan Gschwander ^g, Thomas Hausmann ^g, Dominic Groulx ^h, Stephan Höhle ⁱ, Andreas König-Haagen ⁱ, Laurent Zalewski ^j, Noé Beaupéré ^j.

Affiliations of contributors:

^a Bavarian Center for Applied Energy Research (ZAE Bayern), Walther-Meißner-Str. 6, 85748 Garching, Germany

^b Thermal Storage and Solar Fuels Unit, CIEMAT-PSA, Av. Complutense 40, 28040 Madrid, Spain

^c GREiA Research Group, Universitat de Lleida, Pere de Cabrera s/n, 25001, Lleida, Spain

^d Technical University of Denmark, Department of Civil Engineering, Brovej, Building 118, 2800 Kgs. Lyngby, Denmark

^e University of the Basque Country (UPV/ EHU), Rafael Moreno Pitxitxi 2, 48012 Bilbao, Spain

^f Lucerne University of Applied Sciences and Arts, Technikumstrasse 21, 6048 Horw, Switzerland

^g Fraunhofer Institute for Solar Energy Systems, Heidenhofstr. 2, 79110 Freiburg, Germany

^h Lab of Applied Multiphase Thermal Engineering, Dalhousie University, 5269 Morris St., B3H 4R2 Halifax, Canada

ⁱ Chair of Engineering Thermodynamics and Transport Processes (LTTT), Center of Energy Technology (ZET), University of Bayreuth, Universitätsstraße 30, 95447 Bayreuth, Germany

^j LGCgE, Artois University, Technoparc Futura, 62400 Béthune, France

BACKGROUND



Deliverable 2 of Subtask 3P is a collection of questionnaires regarding experimental devices that are used by the experts of Task 58 / Annex 33 to investigate the degradation of Phase Change Materials (PCM). Three types of experiments are considered: Tests on degradation of PCM over thermal cycling (type I), tests on degradation of PCM with stable supercooling (type II), and tests on degradation of phase change slurries (type III).


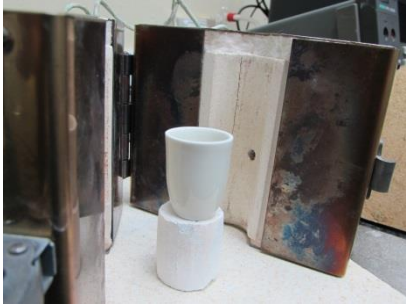
As the content of this deliverable is intended to be published as a peer-reviewed paper, the questionnaires are presented without further discussion in this document.

QUESTIONNAIRES



TYPE I: TESTS ON DEGRADATION OF PCM OVER THERMAL CYCLING

In the case of solid-liquid PCM, heat is stored and released under repeated melting and solidification processes, also referred to as thermal cycles. In order to assess the suitability of a PCM for a thermal storage application, testing its thermal properties (e. g. melting temperature and melting enthalpy) under repeated thermal cycling taking service conditions into account is crucial.

Testing device: "CIEMAT AGH"	
Contact: Rocío Bayón	
<p>Description</p> <p><i>Thermal cycling oven under air atmosphere, controlled heating & cooling rate, sample temperature monitoring, various samples at the same time with different sizes</i></p>	
Picture / scheme	
Set-up outside	Oven inside
	
Min. Temperature [°C] <i>Room temperature</i>	Max. Temperature [°C] <i>350 °C</i>
Typical heating rate [K/min] <i>1-20</i>	Typical cooling rate [K/min] <i>1-20</i>
<p>Typical temperature profile</p> <p><i>Cycles at two temperature levels with transition via linear ramps. ΔT above-below melting temperature depending on the specific application.</i></p> <p><i>Tests at constant temperature (ΔT) above melting point.</i></p>	
Typical number of cycles per day [1/d] <i>1 cycle/day</i>	Max. sample volume [ml] <i>60 - 100</i>
PCM in contact with <i>air</i>	Sample container material <i>Glass beaker, glass tube, ceramic crucible</i>
<p>Measured data</p> <p><i>Temperature-time curve for the sample and oven</i></p>	

<p>Stability checked via...</p> <p><i>Comparison of temperature-time curves of different cycles</i></p> <p><i>DSC measurements after a certain number of cycles or time</i></p> <p><i>Sample mass monitoring after certain number of cycles or time</i></p>	
<p>References (articles, presentations, etc.)</p> <p>R. Bayón, M. Biencinto, E. Rojas, N. Uranga. STUDY OF HYBRID DRY COOLING SYSTEMS FOR STE PLANTS BASED ON LATENT STORAGE. To be presented at ISEC conference in Graz, October 2018.</p> <p>M.M. Rodríguez-García, E. Rojas, R. Bayón, Test campaign and performance evaluation of a spiral latent storage module with Hitec® as PCM, Solar Heating and Cooling Conference 2017, Abu Dhabi, November 2017. Accepted for AIP Conference proceedings</p>	
<p>Comments</p> <p>These tests should be performed under conditions as close as possible to service conditions. They should be considered only as preliminary stability test <u>without any long-term behavior extrapolation.</u></p>	
<p>Testing device: "CIEMAT HDR"</p>	
<p>Contact: Rocío Bayón</p>	
<p>Description</p> <p><i>Thermal cycling oven under air atmosphere, controlled heating and natural cooling, sample temperature monitoring, only one sample</i></p>	
<p>Picture / scheme</p> <div style="display: flex; justify-content: space-around;"> <div style="text-align: center;"> <p>Set-up outside</p>  </div> <div style="text-align: center;"> <p>Oven inside</p>  </div> </div>	
<p>Min. Temperature [°C]</p> <p><i>Room temperature</i></p>	<p>Max. Temperature [°C]</p> <p><i>500 °C</i></p>
<p>Typical heating rate [K/min]</p> <p><i>1-20</i></p>	<p>Typical cooling rate [K/min]</p> <p><i>natural</i></p>
<p>Typical temperature profile</p> <p><i>Cycles at two temperature levels with transition via linear ramps. ΔT above-below melting temperature depending on the specific application.</i></p> <p><i>Tests at constant temperature (ΔT) above melting point.</i></p>	

Typical number of cycles per day [1/d] <i>1 cycle/day</i>	Max. sample volume [ml] <i>10</i>
PCM in contact with <i>air</i>	Sample container material <i>ceramic crucible</i>
Measured data <i>Temperature-time curve for the sample</i>	
Stability checked via... <i>Comparison of temperature-time curves of different cycles</i> <i>DSC measurements after a certain number of cycles or time</i> <i>Sample mass monitoring after certain number of cycles or time</i>	
References (articles, presentations, etc.) R. Bayón, M. Biencinto, E. Rojas, N. Uranga. STUDY OF HYBRID DRY COOLING SYSTEMS FOR STE PLANTS BASED ON LATENT STORAGE. To be presented at ISEC conference in Graz, October 2018. M.M. Rodríguez-García, E. Rojas, R. Bayón, Test campaign and performance evaluation of a spiral latent storage module with Hitec® as PCM, Solar Heating and Cooling Conference 2017, Abu Dhabi, November 2017. Accepted for AIP Conference proceedings	
Comments These tests should be performed under conditions as close as possible to service conditions. They should be considered only as preliminary stability test <u>without any long-term behavior extrapolation.</u>	

Testing device: "CIEMAT SUBMA"	
Contact: Rocío Bayón	
Description <i>Thermal cycling device inside a furnace, controlled heating and natural cooling, sample temperature monitoring, only one sample, different atmospheres are possible.</i>	
Picture / scheme	
Set-up outside +furnace	Set-up inside
	
Min. Temperature [°C]	Max. Temperature [°C]

Room temperature	500 °C
Typical heating rate [K/min] 1-20	Typical cooling rate [K/min] natural
<p>Typical temperature profile</p> <p><i>Cycles at two temperature levels with transition via linear ramps. ΔT above-below melting temperature depending on the specific application.</i></p> <p><i>Tests at constant temperature (ΔT) above melting point.</i></p>	
Typical number of cycles per day [1/d] 1 cycle/day	Max. sample volume [ml] 60
PCM in contact with <i>Air, N₂, Ar or other</i>	Sample container material <i>ceramic crucible</i>
<p>Measured data</p> <p>Temperature-time curve for the sample</p>	
<p>Stability checked via...</p> <p><i>Comparison of temperature-time curves of different cycles</i></p> <p><i>DSC measurements after a certain number of cycles or time</i></p> <p><i>Sample mass monitoring after certain number of cycles or time</i></p>	
<p>References (articles, presentations, etc.)</p> <p>M.M. Rodríguez-García, R. Bayón, E. Rojas, Stability of D-mannitol upon melting/freezing cycles under controlled inert atmosphere, Energy Procedia 91 (2016) 218–225. https://doi.org/10.1016/j.egypro.2016.06.207.</p>	
<p>Comments</p> <p>These tests should be performed under conditions as close as possible to service conditions. They should be considered only as preliminary stability test <u>without any long-term behavior extrapolation.</u></p>	

Testing device “EHU”
Contact: Gonzalo Diarce
<p>Description</p> <p><i>We use an own-made arrangement comprised by a thermostatic bath and airtight tubes. The samples are inserted inside the tubes and these are immersed into the thermostatic bath, which uses a silicone oil as a heat transfer fluid. The tubes are made by glass and include a nylon screwed cap with an O-ring sealing that ensures tightness. They can handle pressures up to 10 bar. The usual sample size is around 5 g, although tubes with variable dimensions can be employed. The arrangement and configuration is flexible and it is adapted to the PCM under study and the kind of degradation expected. The temperature program usually comprises consecutive heating and cooling cycles if physical phase segregation is expected. When the material under study might undergo thermal decomposition, then the program</i></p>

normally consists of submitting different samples to a constant temperature. The samples are extracted after different periods of time and analyzed. The analysis depends on the type of behaviour expected. Several complementary techniques are used. Variations on the thermal behaviour (storage capacity, melting temperatures and others) are evaluated by DSC. Visual control is kept by periodic imaging. Additional information is obtained by X-Ray diffraction, FTIR, liquid chromatography and others.

Picture / scheme



Min. Temperature [°C] -45 °C	Max. Temperature [°C] 200 °C
Typical heating rate [K/min] <i>Depending on the feature under analysis</i>	Typical cooling rate [K/min] <i>Depending on the feature under analysis</i>
Typical temperature profile <i>Depending on the feature under analysis. Thermal cycles or constant temperatures can be employed.</i>	
Typical number of cycles per day [1/d] <i>Variable</i>	Max. sample size [g] 5
PCM in contact with... <i>Air (normally). Other gases (N2, Ar, etc.) can be introduced by the use of a controlled atmosphere chamber</i>	Sample container material <i>Normally glass. Metallic containers have been also used</i>
Measured data	

Temperatures of the thermostatic bath. The inside temperature of the samples could be also controlled by introducing a thermocouple inside a “sacrificed” sample.

Stability checked via...

DSC, optically, X-Ray Diffraction, FTIR.

Testing device “HSLU”

Contact: Oliver Fellmann, Rebecca Ravotti

Description

Easymax 102; cycling device and synthesis station; two heating chambers with various adapters allowing the measurement with one to five vessels (1x100ml, 3x25ml, 5x8ml) per chamber; magnetic or mechanical stirring. However, the Easymax 102 only contains one temperature sensor per chamber. Therefore, an external logging device to record the temperature of the other vessels is used.

Different heating and cooling rates can be applied, either using a fixed rate or by controlled heating so that a ΔT between measured inside temperature and the temperature of the jacket is not exceeded. If more than one vessel per chamber is applied, only heating by rate is possible.

Picture / scheme

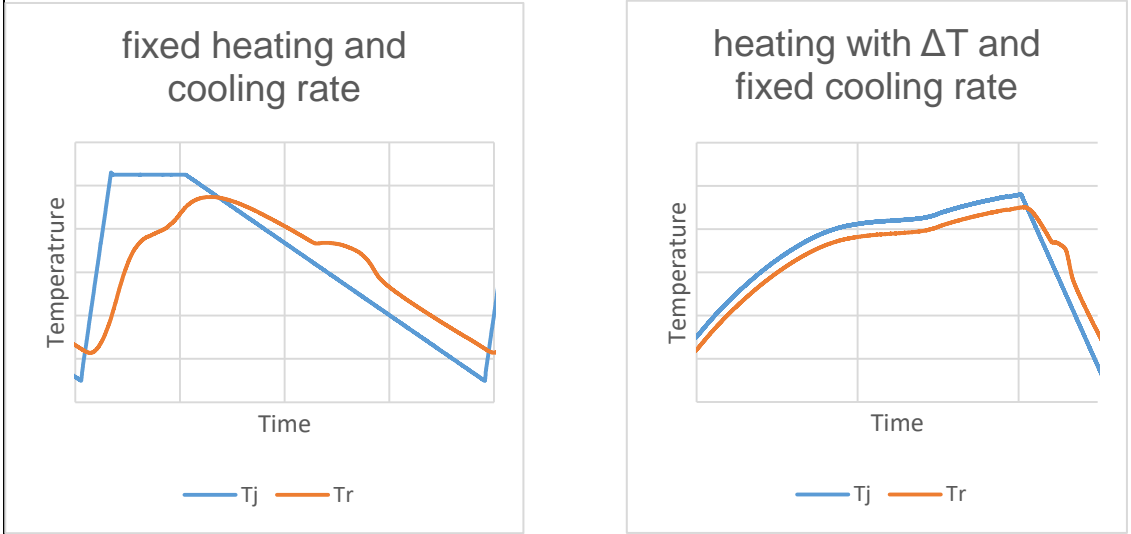




Min. Temperature [°C] -40	Max. Temperature [°C] 180
------------------------------	------------------------------

Typical heating rate [K/min] 10	Typical cooling rate [K/min] 0.5
------------------------------------	-------------------------------------

Typical temperature profile



Temperature

Typical number of cycles per day [1/d] 10	Sample volume [ml] 1x100 ml, 3x25 ml, 5x8 ml
--	---

PCM in contact with... air	Sample container material glass
-------------------------------	------------------------------------

Measured data
Temperature, reaction enthalpy, heat transfer coefficient, specific heat

Stability checked via...
Optical appearance of PCM; comparison of temperature-time curves of different cycles; DSC measurements after a certain number of cycles

Testing device "LAMTE"

Contact: Dominic Groulx

Description

PCM Thermal Cycler; simultaneous cycling of 8 samples within a similar range of phase transition temperature.

Uses two cartridge heaters embedded in an aluminum block as heat sources, and four thermoelectric coolers for cooling of the system.

Picture / scheme

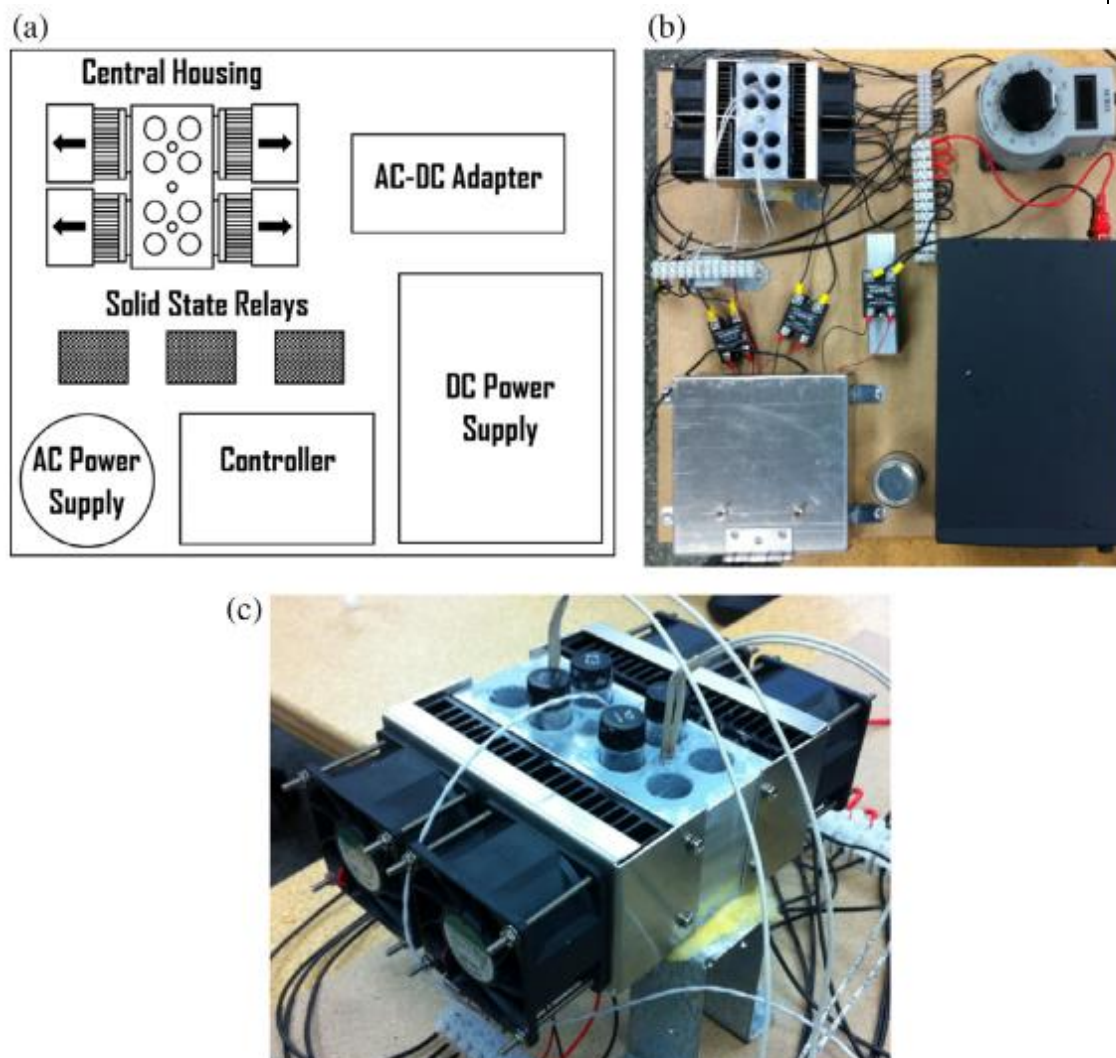


Fig. a) Schematic diagram showing the various components of the thermal cycler general assembly, b) photograph of the actual experimental setup, and c) photograph of the housing unit with the heating and cooling elements and vials containing PCMs [1].

Min. Temperature [°C] -5	Max. Temperature [°C] 125
Typical heating rate [K/min] 13	Typical cooling rate [K/min] 7
<p>Typical temperature profile</p>	
Typical number of cycles per day [1/d] <i>Up to 140 cycle per day (1,000 cycle a week).</i>	Sample volume [ml] 3 - 6
PCM in contact with... <i>Aluminum, with thermal grease between Aluminum and the PCM vial to reduce thermal resistance to conduction.</i>	Sample container material <i>Dram vial with a 15-425 threaded PTFE/Silicone liner cap</i>
<p>Measured data <i>T(t) saved on an SD card during the cycling and can be inspected at the end of the process.</i></p>	
<p>Stability checked via... <i>DSC testing looking at the latent heat of transition and the onset of melting temperature of the cycled PCM (compared to the original pre-cycled PCM), with cycled PCM tested after every 500 or 1000 cycles.</i></p>	
<p>References (articles, presentations, etc.)</p> <p>[1] KAHWAJI, S., JOHNSON, M.B., KHEIRABADI, A.C., GROULX, D., WHITE, M.A. (2016) <i>Stable, low-cost phase change material for building applications: The eutectic mixture of decanoic acid and tetradecanoic acid</i>, Applied Energy, v.168, p.457-464.</p> <p>Modeling of the system for design:</p>	

[2] C. KHEIRABADI, A., GROULX, D. *Design of an Automated Thermal Cycler for Long-term Phase Change Material Phase Transition Stability Studies*. in *COMSOL Conference 2014*. 2014. Boston, MA (USA).

Paper published with results from the setup [1], and:

[3] KAHWAJI, S., JOHNSON, M.B., KHEIRABADI, A.C., GROULX, D., WHITE, M.A. (2017) *Fatty acids and related phase change materials for reliable thermal energy storage at moderate temperatures*, *Solar Energy Materials and Solar Cells*, v.167, p.109-120.

[4] KAHWAJI, S., JOHNSON, M.B., KHEIRABADI, A.C., GROULX, D., WHITE, M.A. (2018) *A comprehensive study of properties of paraffin phase change materials for solar thermal energy storage and thermal management applications*, *Energy*, v.162, p.1169-1182.

Comments

A complete report about design, construction, equipment needed, etc., was also written and presented to the industrial partner (Intel). This report can be shared with interested groups.

Testing device "LTTT"

Contact: Stephan Höhle, Andreas König-Haagen

Description

Thermal cycling device with 4-channel PT100 data logger (expandable)

Picture / scheme



Min. Temperature [°C]

0 °C (water)

-20 °C (oil)

Max. Temperature [°C]

90 °C (water)

180 °C (oil)

Typical heating rate [K/min]

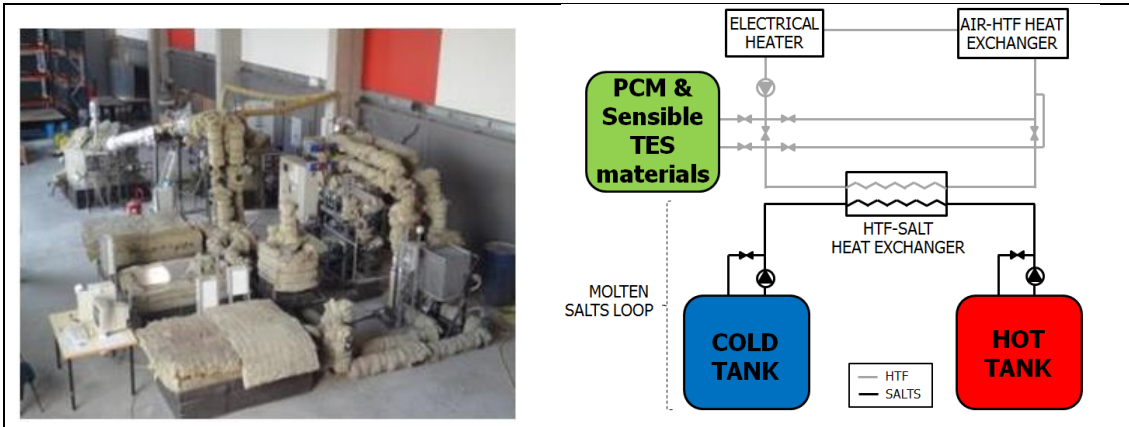
Typical cooling rate [K/min]

<i>variable</i>	<i>variable</i>
<p>Typical temperature profile</p> <p><i>One temperature level above and one below phase-change temperature. Rapid change between the temperature levels.</i></p>	
<p>Typical number of cycles per day [1/d]</p> <p><i>variable</i></p>	<p>Max. sample volume [ml]</p> <p><i>~ 10 ... ~ 100 (depending on chosen container)</i></p>
<p>PCM in contact with...</p> <p><i>air</i></p>	<p>Sample container material</p> <p><i>glass, plastics, metals</i></p>
<p>Measured data</p> <p><i>T(t)</i></p>	
<p>Stability checked via...</p> <p><i>temperature-time curves of different cycles; DSC measurements after defined cycles</i></p>	

<p>Testing device "UDL-GREiA I"</p>	
<p>Contact: Luisa F. Cabeza, Gabriel Zsembinski</p>	
<p>Description</p> <p><i>GeneQ BIOER TC-18/H(b) thermal cycler allows to perform thermal cycles from room temperature up to 100 °C using samples of PCM and other materials, to determine the stability of the samples over time. It simulates the melting and solidification cycles of real applications. The thermal cycler allows to place 18 samples at the same time in 0.5 ml eppendorfs. The eppendorf must not be filled completely because only the lower part will be subjected to heating and cooling cycles. It is recommended to fill 2/3 parts of the eppendorf.</i></p>	
<p>Picture / scheme</p>	

Min. Temperature [°C] 4	Max. Temperature [°C] 99.9
Typical heating rate [K/min] 50	Typical cooling rate [K/min] 50
Typical temperature profile <i>Many different temperature profiles can be experimented depending on the aim of the study.</i>	
Typical number of cycles per day [1/d] 100	Max. sample volume [ml] 18×0.5
PCM in contact with... <i>Eppendorf, which is in contact with the metallic part of the device</i>	Sample container material <i>Polypropylene</i>
Stability checked via... <i>DSC, TGA analysis, FT-IR</i>	
References (articles, presentations, etc.) <i>Navarro, L, Solé, A, Martín, M, Barreneche, C, Olivieri, L, Tenorio, JA, Cabeza, LF. Benchmarking of useful phase change materials for a building application. Energy and Buildings 2019;182:45-50.</i>	

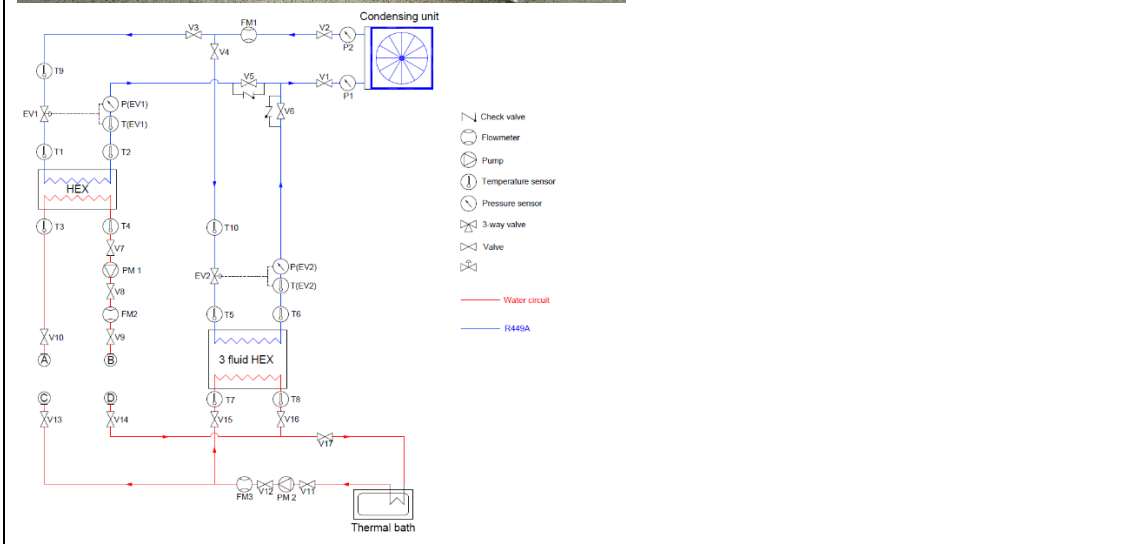
Testing device “UDL-GREiA II”
Contact: Luisa F. Cabeza, Gabriel Zsembinski
<p>Description</p> <p><i>The University of Lleida pilot plant was built to accurately test different thermal energy storage (TES) systems working with latent or sensible heat storage materials. This facility is composed by an electrical boiler of 24 kWe to heat up the heat transfer fluid (HTF) acting as energy source during the charging process, different storage tanks containing phase change material (PCM), and an air heat exchanger of 20 kWe to cool down the HTF acting as energy consumption. All the piping that connects the different devices of the pilot plant are insulated using rock wool and the bottom of the storage tanks are insulated with foamglass and refractory cement to minimize the heat losses to the surroundings. Two different HTF were tested in the pilot plant facility: the synthetic oil Therminol VP-1 and the silicone fluid Syltherm 800.</i></p> <p><i>A data acquisition system consisting of all the temperature, pressure and flow rate sensors as well as the different dataloggers and a personal computer, was integrated in the facility to measure and register the HTF flows, HTF pressures, and HTF and PCM temperatures in the boiler and storage tank, respectively.</i></p>
Picture / scheme



Min. Temperature [°C] 20	Max. Temperature [°C] 400
Typical heating rate [K/min] 1.0	Typical cooling rate [K/min] Not available.
Typical temperature profile <i>Many different temperature profiles can be experimented depending on the aim of the study.</i>	
Typical number of cycles per day [1/d] 1	Max. sample volume [ml] 154,000
PCM in contact with... <i>Stainless steel 316L</i>	Sample container material <i>Stainless steel 316L</i>
Measured data <i>Temperature, pressure, flow rate</i>	
Stability checked via... <i>DSC, TGA analysis, FT-IR</i>	
<p>References (articles, presentations, etc.)</p> <ul style="list-style-type: none"> • Oró, E, Gil, A, Miró, L, Peiró, G, Álvarez, S, Cabeza, LF. <i>Thermal energy Storage Implementation Using Phase Change Materials for Solar Cooling and Refrigeration Applications. Energy Procedia 2012;30:947-56.</i> • Gil, A, Oró, E, Castell, A, Cabeza LF. <i>Experimental analysis of the effectiveness of a high temperature thermal storage tank for solar cooling applications. Appl Therm Eng 2013;54: 521-27.</i> • Gil, A, Oró, E, Miró, L, Peiró, G, Ruiz, A, Salmerón, JM, Cabeza LF. <i>Experimental analysis of hydroquinone used as phase change material (PCM) to be applied in solar cooling refrigeration. Int J Refrig 2014;39:95-103.</i> • Peiró G, Gasia J, Miró L, Cabeza LF. <i>Experimental evaluation at pilot plant scale of multiple PCMs (cascaded) vs. single PCM configuration for thermal energy storage. Renew Energy 2015;83:729-36.</i> • Prieto C, Miró L, Peiró G, Oró E, Gil A, Cabeza LF. <i>Temperature distribution and heat losses in molten salts tanks for CSP plants. Sol Energy 2016;135:518-26.</i> 	

- Peiró G, Gasia J, Miró L, Prieto C, Cabeza LF. *Experimental analysis of charging and discharging processes, with parallel and counter flow arrangements, in a molten salts high temperature pilot plant scale setup.* *Appl Energy* 2016;178:394–403.
- Gasia J, de Gracia A, Peiró G, Arena S, Cau G, Cabeza LF. *Use of partial load operating conditions for latent thermal energy storage management.* *Appl Energy* 2018;216:234–42.
- Peiró G, Prieto C, Gasia J, Jové A, Miró L, Cabeza LF. *Two-tank molten salts thermal energy storage system for solar power plants at pilot plant scale: lessons learnt and recommendations for its design, start-up and operation.* *Renew Energy* 2018;121:236–48.
- Gil, A, Peiró, G, Oró, E, Cabeza LF. *Experimental analysis of the effective thermal conductivity enhancement of PCM using finned tubes in high temperature bulk tanks.* *Appl Therm Eng* 2018;142: 736-44.
- Gasia J, de Gracia A, Zsembinszki G, Cabeza LF. *Influence of the storage period between charge and discharge in a latent heat thermal energy storage system working under partial load operating conditions.* *Appl Energy* 2019;235:1389–99.

Testing device “UDL-GREiA III”
Contact: Luisa F. Cabeza, Gabriel Zsembinszki
<p>Description</p> <p><i>This experimental set-up of the GREiA lab at the University of Lleida was built to test the behaviour of different types of heat exchangers and thermal energy storage tanks, which are usually innovative components of different European projects. Both charging and discharging of the thermal energy storage modules can be performed, by means of two separate circuits: one cooling circuit connected to a variable capacity condensing unit, and one heating circuit connected to a thermal bath. There is the possibility to connect the heating bath to a water storage tank to increase the thermal inertia and provide a more stable water temperature to the heat exchangers.</i></p>
Picture / scheme



Min. Temperature [°C] -10	Max. Temperature [°C] 80
Typical heating rate [K/min] 0.5	Typical cooling rate [K/min] 1.0
Typical temperature profile <i>Many different temperature profiles can be experimented depending on the aim of the study.</i>	
Typical number of cycles per day [1/d] 2	Max. sample volume [ml] 8,000
PCM in contact with... <i>Aluminium, stainless steel</i>	Sample container material <i>Aluminium, stainless steel</i>
Measured data <i>Temperature, pressure, flow rate</i>	

Stability checked via...
DSC, TGA analysis, FT-IR

Testing device "ZAE"

Contact: Christoph Rathgeber

Description

Thermal cycling device; simultaneous measurement of 3 samples with similar melting temperatures

Picture / scheme



Min. Temperature [°C] -30	Max. Temperature [°C] 220
Typical heating rate [K/min] 1	Typical cooling rate [K/min] 1
Typical temperature profile <i>two temperature levels for melting and freezing, e.g. 50 °C and 20 °C; transition via linear ramps, typically 1 h</i>	
Typical number of cycles per day [1/d] 2	Max. sample volume [ml] 60
PCM in contact with... <i>air</i>	Sample container material <i>glass, stainless steel</i>
Measured data	

$T(t)$
Stability checked via... <i>photographs during cycling; comparison of temperature-time curves of different cycles; DSC measurements after a certain number of cycles</i>
References (articles, presentations, etc.) Rathgeber, C., Grisval, A., Schmit, H., Hooek, P., & Hiebler, S. (2018). Concentration dependent melting enthalpy, crystallization velocity, and thermal cycling stability of pinacone hexahydrate. <i>Thermochimica acta</i> , 670, 142-147.

Testing device "ISE Peltier"	
Contact: Stefan Gschwander, Thomas Haussmann	
<p>Description: <i>Multiple Peltier Test Rig</i></p> <p><i>Flexible Peltier test rig for cycling in the temperature range -30°C to 200°C. Up to 16 Peltier modules with a max heating and cooling power of 30W each and a surface of 65x65mm can be flexible combined in x and z direction. Each Peltier module has two Peltier elements. One on the bottom and one on top. The upper Peltier elements are single point fixed to compensate non parallel surfaces. The contact pressure of the upper Peltier element can be controlled by pressurized air.</i></p> <p><i>Up to eight individual temperature controllers are used to control the temperature of samples. Peltier elements can be individually attached to each controller. Temperature profiles are composed of basic segments. Basic segments are: sudden temperature change, ramp or isotherms. Heating and cooling rate can be defined individually. Sample crucibles are designed as needed. Solid samples like construction materials can be tested without additional crucible. In line stability check is not foreseen. External Check with DSC, optical inspection or others is necessary.</i></p>	
Picture / scheme	
<i>Peltier Test rig</i>	
Min. Temperature [°C]	Max. Temperature [°C]
-30	200

Typical heating rate [K/min] <i>adjustable, depending on setup</i>	Typical cooling rate [K/min] <i>Adjustable, depending on setup</i>
Typical temperature profile <i>Programmable Profiles: temperature jump, Ramp, Isotherm</i> <i>Typical Program: switching between temperature limits above and below melting range</i>	
Typical number of cycles per day [1/d] <i>Up to 24</i>	Max. sample volume [ml] <i>Not defined, typical 10-100ml</i>
PCM in contact with... <i>Crucible material or containment</i>	Sample container material <i>Raw materials: typical stainless steel, chosen as necessary</i>
Measured data <ul style="list-style-type: none"> - <i>Temperatures of the PCM (middle or surface)</i> - <i>Temperature of Peltier surface</i> 	
Stability checked via... <ul style="list-style-type: none"> - <i>External stability check, e.g. with DSC</i> 	

Testing device “ISE macro capsules”	
Contact: Stefan Gschwander, Thomas Haussmann	
<p>Description <i>Macro Capsule Cycling Test Rig</i></p> <p><i>The test facility consists of an open bath in which the encapsulated PCM samples are located in and circulated with tap water as a heat transfer fluid. The flow rate can be adjusted manually by means of a pump with a downstream restriction. The bath temperature can be controlled by a thermostat, which supplies heat to the test circuit by a heat exchanger. Temperature sensors at the flow and return line of the bath as well as a volume flow sensor allow thermal balancing of the heat stored in the PCM macro-capsules.</i></p>	
<p>Picture / scheme</p>	
Min. Temperature [°C] -10	Max. Temperature [°C] 80
Typical heating rate [K/min] <i>~1 K/min (depends on PCM and macro capsule)</i>	Typical cooling rate [K/min] <i>~1 K/min (depends on PCM and macro capsule)</i>

<p>Typical temperature profile</p> <p><i>Temperature steps are set, which are repeated cyclically. The set temperatures depend on the PCM used and are usually set 5 K below and above the melting temperature of the PCM.</i></p>	
<p>Typical number of cycles per day [1/d]</p> <p><i>10 (depends on PCM and macro capsule)</i></p>	<p>Max. sample volume [ml]</p> <p><i>22 L bath volume</i></p>
<p>PCM in contact with...</p> <p><i>Macro capsule material (metal, polymer)</i></p>	<p>Sample container material</p> <p><i>Polystyrene</i></p>
<p>Measured data</p> <ul style="list-style-type: none"> - <i>Temperature at feed and return line of the bath</i> - <i>Volumetric flow sensor</i> 	
<p>Stability checked via...</p> <ul style="list-style-type: none"> - <i>Repeating optical inspection of the macro capsules (reflected light microscope)</i> - <i>Gravimetric analysis</i> - <i>DSC analysis of the encapsulated PCM</i> 	
<p>References</p> <p><i>BIEDENBACH, M., KLÜNDER, F., GSCHWANDER, S. (2018). Investigations on the stability of metallic cans for PCM macro-encapsulation. International Institute of Refrigeration (IIR). https://doi.org/10.18462/iir.pcm.2018.0053</i></p>	

<p>Testing device “LGCgE / Fluxmetric bench”</p>
<p>Contact: Laurent Zalewski, Noé Beaupéré</p>
<p>Description</p> <p><i>The Fluxmetric bench (Figure 1) is a thermal cycling device used to impose temperature ramps on both larger sides of a parallelepipedal Polymethyl methacrylate (PMMA) sample containing PCM (Figure 2). Temperature ramps are applied thanks to exchanger plates each of which is connected to a refrigerated/heating circulators controlled by a computer, example of temperature ramps are presented in Figure 3. The four smaller faces of the sample are insulated so as to minimize lateral heat losses (Figure 2). In its current configuration, the container is filled with 270 ml of PCM. This configuration allows to limit convective flow when the PCM is in liquid state. A heat flux meter incorporating a T-type thermocouple is placed on each side of the PMMA sample in order to calculate the energy balance at each heat cycle and to identify the melting and solidification temperatures. Between each temperature ramp, an isothermal step is imposed to return to an equilibrium (isothermal state and heat flux = 0) (Figure 4). For each fusion, the latent heat is estimated by subtracting the sensible energy stored (stored by PMMA and PCM) from the total stored energy measured by heat flux meters.</i></p> <p><i>For example, multiple heating and cooling ramps (Figure 3) have been imposed on Sodium Acetate Trihydrate (SAT / CH₃COONa.3H₂O) to study its ageing by following the variation in the amount of latent heat involved in each melting phase change. On the other hand, at each cooling ramp, the temperature of the stochastic solidification (or degree of supercooling) can be identified. The decrease in the amount of latent heat is related to the ageing of the PCM (Figure 5a). For each cooling ramp by observing the</i></p>

peak of heat flux at the moment of crystallization, the degree of supercooling can be estimated (Figure 5b). The curves below are coming from BEAUPERE's PhD work on SAT [1].



Figure 4-1: Fluxmetric bench



Figure 4-2: PMMA sample containing PCM with the lateral heat flux meters before installation in the insulation

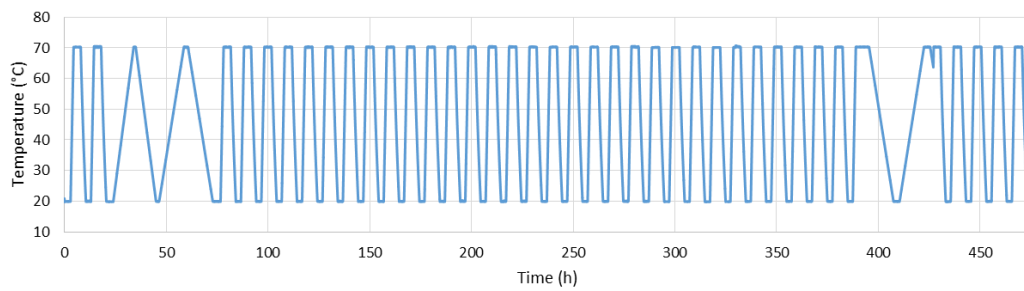


Figure 4-3: Feasible series of temperature ramps imposed on the sample

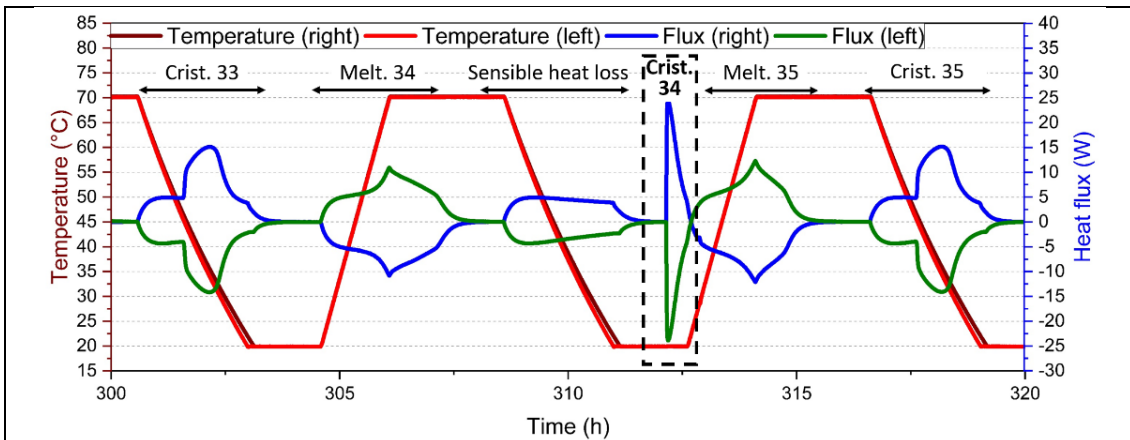


Figure 4-4: Ramps of temperature and heat fluxes measurements

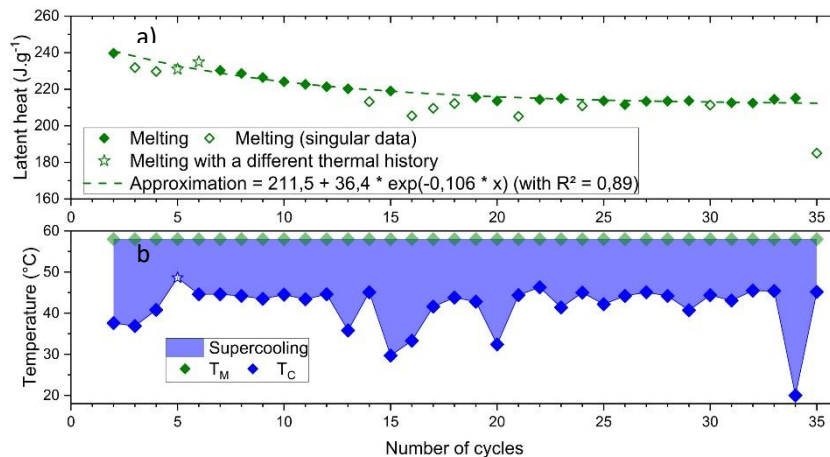


Figure 4-5: Evolution of latent heat and the solidification temperature vs number of cycles

References



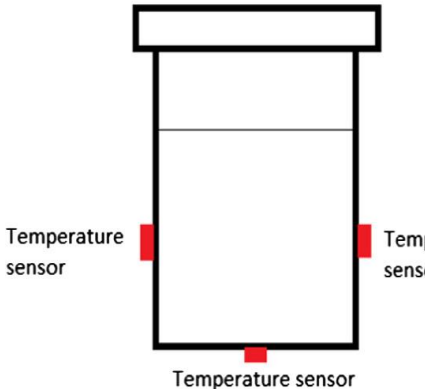
[1] BEAUPERE Noé, Pilotage de la libération de chaleur et étude du vieillissement de matériaux à changement de phase, PhD, Université d'Artois/CEA Grenoble, 11/2019.

TYPE II: TESTS ON DEGRADATION OF PCM WITH STABLE SUPERCOOLING

A concept for medium and long-term thermal energy storage is to utilize the ability of certain PCM to be stored as a liquid in the supercooled state. As investigated by Englmaier et al. ² and

² Englmaier, G., Jiang, Y., Dannemand, M., Moser, C., Schranzhofer, H., Furbo, S. & Fan, J. (2018). Crystallization by local cooling of supercooled sodium acetate trihydrate composites for long-term heat storage. Energy and Buildings, 180, 159-171.

Desgrosseilliers³, application of sodium acetate trihydrate (SAT) in closed containers permits the use of its sensible heat capacity after melting while preserving its heat of fusion at room temperature in a state of stable supercooling. The result is a thermal energy storage capacity that can be used on-demand by controlled initialization of crystallization. To investigate the stability of PCM with stable supercooling, dedicated test procedures are required. In addition to temperature-time profiles of regular thermal cycling tests, both degree and duration of supercooling are parameters of interest.

Testing device “DTU heat loss method”	
Contact: Gerald Englmaier, Mark Dannemand	
Description <i>T-history method: Testing of the heat content of (supercooled) PCM material in large sample size (200 g).</i>	
Picture / scheme	
	
(a)	(b)
	
(c)	
Fig. : (a) Glass jar with lid, (b) the well-insulated box, (c) locations of temperature sensors.	
Min. Temperature [°C] 20	Max. Temperature [°C] 90
Typical heating rate [K/min] 1 (forced convection in oven)	Typical cooling rate [K/min] natural cooling
Typical temperature profile	
<ul style="list-style-type: none"> a) Heat-up in oven (20°C to 90°C) b) Cool-down to ambient temperature (about 20°C) → when supercooling applied c) Controlled crystallization in insulated chamber → when supercooling applied 	

³ Desgrosseilliers, L. (2016). Design and evaluation of a modular, supercooling phase change heat storage device for indoor heating, Dalhousie University.

d) Measurement of cool-down temperature curve (figure below)

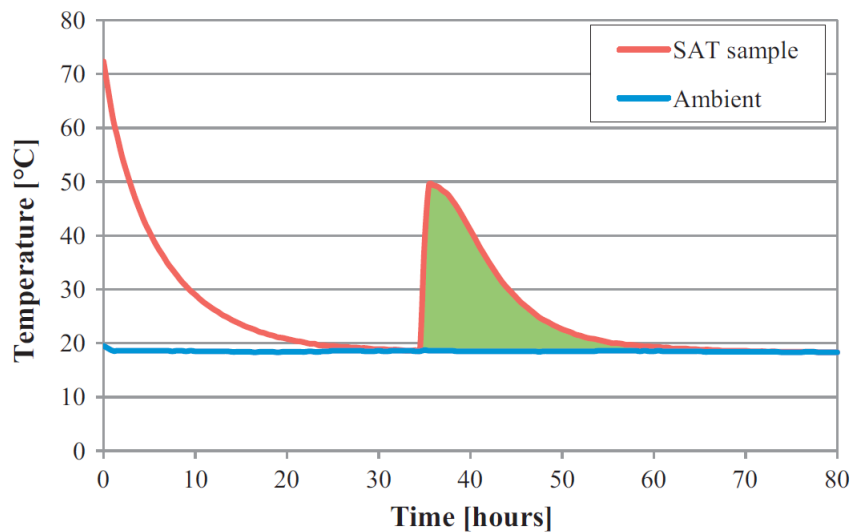


FIG.: AN EXAMPLE OF COOLING PROCESS OF PCM.

Typical number of cycles per day [1/d]

0.25 with supercooling

0.5 without supercooling

Max. sample size [g]

200

PCM in contact with...

Glass and air

Sample container material

Glass jar (metal lid)

Measured data

Temperature profile during material solidification; Ambient temperature.

Stability checked via...

Comparison of samples:

- *Heat content via comparison of sample material with known properties (e.g. water, oil).*

Cyclic stability via comparison of samples with different heat storage cycles applied or with different material composition (screening for stabilizing additives).

References (articles, presentations, etc.)

W. Kong, M. Dannemand, J.B. Johansen, J. Fan, J. Dragsted, G. Englmair, S. Furbo, Experimental investigations on heat content of supercooled sodium acetate trihydrate by a simple heat loss method, Sol. Energy 139 (2016) 249–257.

Comments

Applied temperatures (heat-up, ambient temperature) should be in accordance to aimed application conditions.

Testing device “DTU full scale”

Contact: Gerald Englmaier, Mark Dannemand

Description

Full scale heat storage prototype testing. Cyclic PCM stability in contact to PCM container material.

Picture / scheme

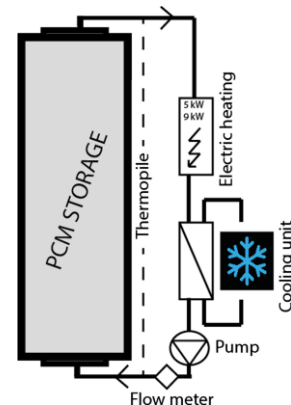


FIG.: PCM HEAT STORAGE TEST FACILITY AT DTU BYG (LEFT); SCHEMATIC OF CHARGE AND DISCHARGE LOOP (RIGHT).

Min. Temperature [°C]

20

Max. Temperature [°C]

90

Typical heating rate [K/min]

1 (depending on the storage prototype)

Typical cooling rate [K/min]

0.5 (depending on the storage prototype)

Typical temperature profile

- e) Charge (20°C to 90°C)
- f) Cool-down to ambient temperature (about 20°C) → when supercooling applied
- g) Controlled crystallization → when supercooling applied
- h) Discharge to ambient temperature (about 20°C)

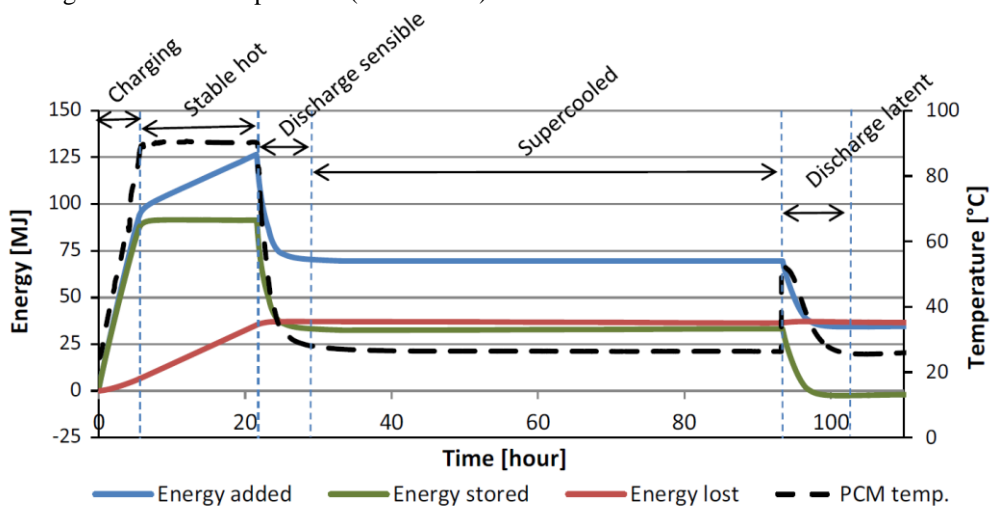


FIG.: TEMPERATURE PROFILE OF A TEST CYCLE WITH SUPERCOOLING OF PCM.

Typical number of cycles per day [1/d]

0.2 with supercooling

Max. sample volume [ml]

100,000 – 200,000

<i>0.4 without supercooling</i>	
PCM in contact with... <i>PCM container material(s)</i>	Sample container material <i>Typically metal or polymers</i>
<p>Measured data</p> <ul style="list-style-type: none"> • <i>Heat transfer fluid: temperatures (flow, return), volume flow rate, temperature difference (in-out).</i> • <i>Ambient temperature</i> • <i>Heat storage surface temperature</i> 	
<p>Stability checked via...</p> <p><i>Comparison of the heat store's energy content in repeated storage cycle.</i></p> <p><i>Heat losses must be experimentally determined for each heat storage prototype.</i></p>	
<p>References (articles, presentations, etc.)</p> <p><i>M. Dannemand, J. Dragsted, J. Fan, J.B. Johansen, W. Kong, S. Furbo, Experimental investigations on prototype heat storage units utilizing stable supercooling of sodium acetate trihydrate mixtures, Appl. Energy 169 (2016) 72–80.</i></p> <p><i>M. Dannemand, J.B. Johansen, W. Kong, S. Furbo, Experimental investigations on cylindrical latent heat storage units with sodium acetate trihydrate composites utilizing supercooling, Appl. Energy 177 (2016) 591–601.</i></p>	
<p>Comments</p> <p><i>The same testing device (setup) can be used for testing performance characteristics of PCM heat stores.</i></p>	

Testing device “DTU multiple storage”
Contact: Gerald Englmaier, Mark Dannemand
<p>Description</p> <p><i>Multiple (10) identical heat storage units (water storage with sodium acetate trihydrate as PCM) subject to repeated heating and cooling cycles with various temperature levels. Focus is on effect of temperature levels and duration of charge on the supercooling stability and spontaneous solidification.</i></p>
Picture / scheme

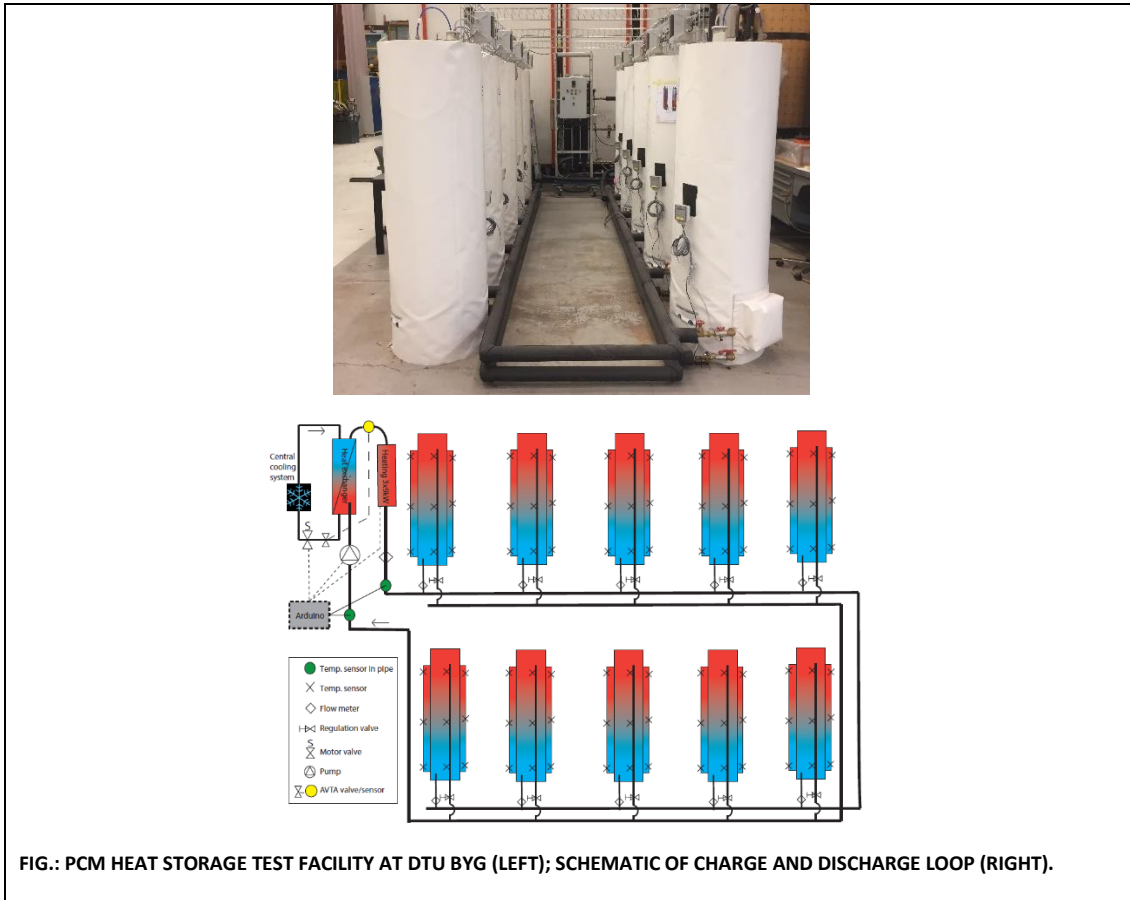


FIG.: PCM HEAT STORAGE TEST FACILITY AT DTU BYG (LEFT); SCHEMATIC OF CHARGE AND DISCHARGE LOOP (RIGHT).

Min. Temperature [°C] 8	Max. Temperature [°C] 93
Typical heating rate [K/min] 0.15	Typical cooling rate [K/min] 3 - 4
<p>Typical temperature profile</p> <ul style="list-style-type: none"> i) Charge in periods 8 to 16 hours 10°C to 90°C j) Discharge to 10-30°C k) 72 hours observation period, looking for spontaneous crystallization of the supercooled PCM l) Intentional initialization of solidification and discharge (10-30°C) 	

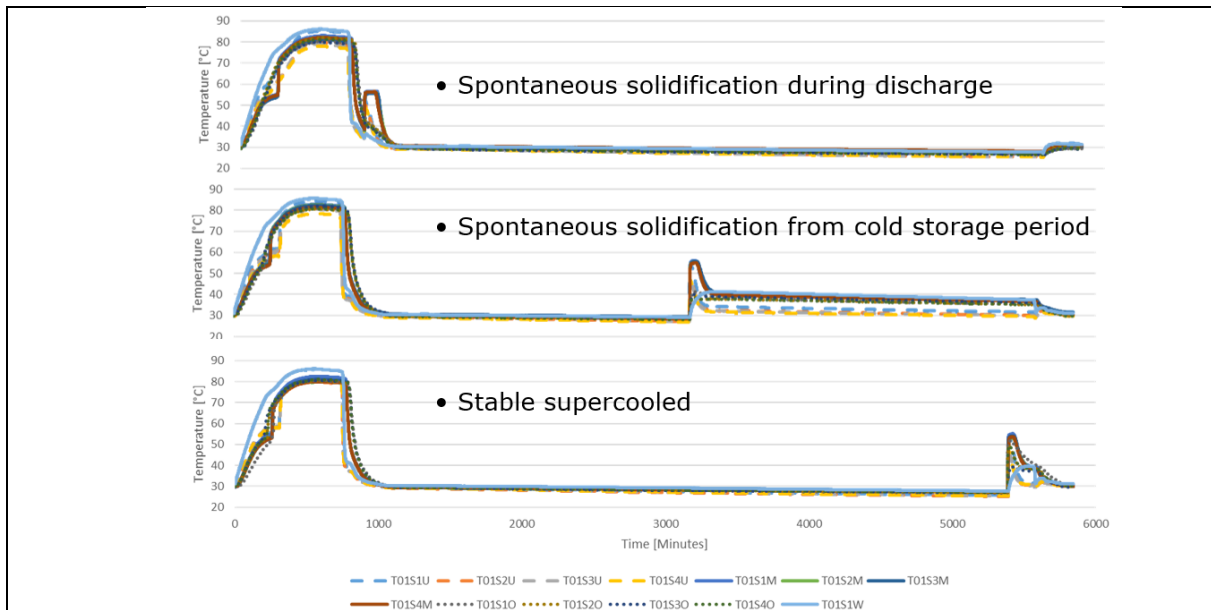


FIG.: TEMPERATURE PROFILES OF TEST CYCLES WITH SUPERCOOLING OF PCM.

Typical number of cycles per day [1/d] <i>0.25</i>	Max. sample volume [ml] <i>10 * 30,000</i>
PCM in contact with... <i>PCM container / air</i>	Sample container material <i>Stainless steel</i>
Measured data <ul style="list-style-type: none"> • Heat transfer fluid: temperatures (flow, return), volume flow rate, temperature difference (in-out). • Ambient temperature • Heat storage surface temperature 	
Stability checked via... <i>Observation of temperature development in test cycle</i>	
References (articles, presentations, etc.) Dannemand, M., & Furbo, S. (2018). Supercooling stability of sodium acetate trihydrate composites in multiple heat storage units. Refrigeration Science and Technology, 2018-, 227–231. https://doi.org/10.18462/iir.pcm.2018.0031 Dannemand, M., Schultz, J. M., Johansen, J. B., & Furbo, S. (2015). Long term thermal energy storage with stable supercooled sodium acetate trihydrate. Applied Thermal Engineering, 91, 671–678. https://doi.org/10.1016/j.applthermaleng.2015.08.055	

TYPE III: TESTS ON DEGRADATION OF PHASE CHANGE SLURRIES (PCS)

Phase change slurries (PCS) are fluids containing PCM and a carrier fluid. A PCS is stable if the emulsified or encapsulated PCM droplets do not degrade during operation, e.g. due to an agglomeration of droplets or a PCM leakage in the case of capsules. Among others, the stability of PCS depends on the investigated sample and particle size and the applied flow rate. Performance validation of PCS is carried out with self-built experimental devices that provide application-oriented charging and discharging conditions.

Testing device "ISE PCS"

Contact: Stefan Gschwander, Thomas Haussmann

Description

Phase Change Slurry (PCS) Cycling Test Rig

In principle, the test setup consists of two heat exchangers which are connected in a test circuit (called secondary circuit). The heat exchangers each have a heating and a cooling thermostat, which act as heat source and heat sink (here called primary circuit). In the primary circuit it is possible to determine the transferred heat flux (and heat amount) using a volume flow sensor (MID) and temperature sensors at the flow and return flow of the two heat exchangers in the primary circuit. In the secondary circuit, the PCS to be tested is conveyed using a centrifugal pump. The PCS is heated or cooled to an adjustable target temperature (and thus the PCM contained is melted or crystallized). The volume flow in the secondary circuit can be monitored using a volume flow meter (MID). The cooling heat exchanger is additionally equipped with pressure sensors at the flow and return flow which determine the pressure loss of the slurry via the heat exchanger. This pressure difference can also be used to determine the degradation of the slurry, since in a degraded PCS the dispersed PCM is present as a free phase in the slurry and successively blocks the cooling/heat exchanger.

Picture / scheme



Min. Temperature [°C] -10	Max. Temperature [°C] 80
Typical heating rate [K/min] ~140 K/min @ 200L/h	Typical cooling rate [K/min] ~100 K/min @ 200L/h
<p>Typical temperature profile</p> <p>Constant temperature at the output of the heating and cooling heat exchanger in the secondary circuit. Temperature level depends on the melting point of the PCM in the PCS.</p>	
Typical number of cycles per day [1/d] ~1,300 @ 200 L/h	Max. sample volume [ml] 3,500
<p>PCM in contact with...</p> <p>Slurry test setup: PCM only in contact with water (continuous phase)</p>	<p>Sample container material</p> <p>Heat exchangers: stainless steel</p> <p>Piping: stainless steel</p> <p>Pump: ceramic impeller</p>
<p>Measured data</p> <ul style="list-style-type: none"> - Temperatures at the flow and return flow of the heating and cooling heat exchanger in the primary and secondary circuits - Volume flows in both primary circuits and in the secondary circuit - Pressure loss in the secondary circuit of the cooling heat exchanger 	
<p>Stability checked via...</p> <ul style="list-style-type: none"> - Pressure loss of the cooling heat exchanger (live) - Regular sampling of samples (~50 mL) which are analysed by particle size analysis, DSC and viscosity. 	
<p>References (articles, presentations, etc.)</p> <p>Niedermaier, S., Biedenbach, M., Gschwander, S. (2016). Characterisation and Enhancement of Phase Change Slurries. <i>Energy Procedia</i>, 99, 64–71. https://doi.org/10.1016/j.egypro.2016.10.098</p>	

ACKNOWLEDGEMENTS

This work has been carried out within the framework of IEA ECES Annex 33 / SHC Task 58 “Material and Component Development for Compact Thermal Energy Storage”, a joint working group of the “Energy Storage” (ES) and the “Solar Heating and Cooling” (SHC) Technology Collaboration Programmes of the International Energy Agency (IEA).

The work of ZAE Bayern is part of the project properPCM and was supported by the German Federal Ministry of Economic Affairs and Energy under the project code 03ET1342A.

The work of CIEMAT is part of two projects has been supported by Comunidad de Madrid and European Structural Funds through ACES2030 Project (S2018/EM-4319) and by European Union's Horizon H2020 Research and Innovation Programme through SFERA III Project (GA No 823802).

The work of DTU was supported by HM Heizkörper GmbH and the Danish Energy Agency through the EUDP program.

The work of EHU is part of the project Sweet-TES (RTI2018-099557-B-C22), funded by the Spanish Ministry of Science, Innovation and Universities.

The work of GREiA was partially funded by the Ministerio de Ciencia, Innovación y Universidades de España (RTI2018-093849-B-C31). This work was partially funded by the Ministerio de Ciencia, Innovación y Universidades - Agencia Estatal de Investigación (AEI) (RED2018-102431-T). The authors would like to thank the Catalan Government for the quality accreditation given to their research group (GREiA 2017 SGR 1537). GREiA is certified agent TECNIO in the category of technology developers from the Government of Catalonia. This work is partially supported by ICREA under the ICREA Academia programme.

The work of HSLU was partially funded by the Swiss Competence Centre for Energy Research on Heat and Electricity (SCCER HaE). The authors would like to thank the SCCER HaE as well as METTLER TOLEDO AG. for the support given.

The work of LTTT is part of the project MALATrans and was funded by the German Federal Ministry for Economic Affairs and Energy (BMWi) under the project code 03ESP227B.

4.2 SUBTASK 3T: TCM MEASURING PROCEDURES AND TESTING UNDER APPLICATION CONDITIONS

4.2.1 INTRODUCTION

AIMS AND OBJECTIVES

This Subtask aims to have reliable thermal analysis methods/protocols and procedures for the characterization of material and reaction properties for sorption and chemical reactions of thermal energy storage (TES) applications. One goal is an inventory of already standardized measurement procedures for TCM as well as of needed characterization procedures.

One challenge in the development of thermochemical storage systems is the difference between tests on micro scale and on laboratory scale, as has been found in many instances in practice. In order to have reliable tools for optimisation of storage materials for a given TES application, both the dependencies of the final storage performance on the actual material properties must be investigated and testing under operation conditions given by the application should be performed

The main objectives of Subtask 3T are therefore:

- Establishing common procedures for measuring material properties (starting with reaction equilibrium and including all material properties in the end)
- Testing of novel TCM under application conditions

One of the first tasks was to collect the already used methods/protocols especially for caloric information like enthalpy changes. A list with relevant literature existing of new publications, standards, etc. was established during the activities which is still a living document.

The biggest part of all activities in this subtask was to develop a common sense for enthalpy and mass change measurements of sorption and thermochemical materials as well as a procedure to compare results on lab scale. Different round robin tests on a zeolite and salt storage material were conducted and evaluated. These results were used to further develop the measurement procedures.

DELIVERABLES

According to the objectives and the defined work plan, following deliverables were defined:

- D3T1: List and description of available and needed TCM characterization procedures for the identified material and reaction properties
- D3T2: Result of a round robin test of a TCM candidate (e.g. Zeolite 13X)
- D3T3: Description of a harmonized measurement procedure for the TCM performance under realistic application conditions

The next sections summarize the outputs for each deliverable.

4.2.2 LIST AND DESCRIPTION OF AVAILABLE AND NEEDED TCM CHARACTERIZATION PROCEDURES FOR THE IDENTIFIED MATERIAL AND REACTION PROPERTIES (D3T1)

A list with relevant literature existing of new publications, standards, etc. was established during the activities which is still a living document. A file server was set up so that all participants can upload their literature or references.

Table 4-8: Extract from the reference list created

Nr	Title	Type	Year	Author
1	Thermal Properties of Materials for Thermo-chemical Storage of Solar Heat	Report	2005	Ch. Bales et al
2	Thermophysical analysis of sorption materials for thermal energy storage	Poster	2015	D. Lager
3	Round Robin Test on Enthalpies of Redox Materials for Thermochemical Heat Storage	Paper	2016	J. González-Ag
4	High-Temperature Energy Storage: Kinetic Investigations of the CuO/Cu ₂ O Reaction Cycle	Paper	2017	M. Deutsch et
5	Experimental approaches to analyse thermophysical properties of thermochemical heat storage materials	Present	2017	D. Lager
6	Thermochemical heat storage – from reaction storage density to system storage density	Paper	2016	A.J. de Jong et
7	Preparation & characterization of sodium sulfide hydrates for application in thermochemical storage systems	Paper	2015	M. Roelands e
8	A review on properties of salt hydrates for thermochemical storage	Paper	2014	F. Trausel et a

The file server is still available for all contributors and the list can still be updated with new relevant literature references regarding characterization techniques for TCMs.

The most important outcome is, that there is no standardized procedure the evaluate caloric and mass information (enthalpy and mass change) on sorption and salt hydrate candidates at application conditions. This new developed procedures and defined application conditions for sorption materials and chemical reactions are documented in D3T2.

4.2.3 RESULT OF A ROUND ROBIN TEST OF A TCM CANDIDATE (D3T2)

INTRODUCTION

Materials' testing and characterisation procedures for the SrBr₂*nH₂O and the Zeolite 13X as well as the measurement results from the participating laboratories is summarised in this report.

SALT HYDRATE ROUND ROBIN TESTS

The material samples for SrBr₂*nH₂O used by all the participating laboratories was provided by INSA-Lyon.

PRELIMINARY TEST METHOD FOR THE 2ND ROUND ROBIN (SRBR₂*NH₂O)

The proposed measuring procedure is given in Appendix A. The testing equipment by the participating laboratories as well as some of the testing conditions are summarized in Table 4-9.

TABLE 4-9. PARTICIPANTS' LABORATORY EQUIPMENT AND SPECIFIC VARIABLES

Participants	Instruments	crucible	Cooling method/cooling rate	Initial sample mass [mg]	Carrier gas	Period of measurement [hours]
CanmetENERGY	STA Netzsch	Al ₂ O ₃	Air (3K/min)	27.16	N ₂	33

CETHIL-INSA	Sensys Evo TG-DSC Setaram	SiO ₂	N ₂ (1K/min)	4.3	He	63

The measured sample mass obtained by the two participating laboratories for all measurement points 1 to 8 is summarised in Table 4-10.

Table 4-10. Sample mass (absolute) for all measurement points 1 to 6.

Point #	Symbol	Sample Mass [mg]	
		CanmetENERGY	CETHIL-INSA
P 1	$m_{dry/P1}$	26.07	3.016
P 2	$m_{Ads2'/P2}$	34.00	4.216
P 3	$m_{Des1/P3}$	25.84	3.194
P 4	$m_{Ads1/P4}$	33.72	4.223
P 5	$m_{Des2/P5}$	21.60	3.203
P 6	$m_{Ads2/P6}$	31.02	4.221
P7	$m_{dry/P7}$	19.79	3.014
P8	$m_{Hyd4/P8}$	26.52	4.217

The measured water uptake during hydration: Hyd₁, Hyd₂, Hyd₃ and Hyd₄ achieved by the different laboratories is summarised in Table 4-11.

Table 4-11. Water uptake between Hyd₁, Hyd₂, Hyd₃ and Hyd₄

Description	Symbol	Water uptake [g/g]		Standard Deviation	Water uptake [mol H ₂ O/mol SrBr ₂]		Standard Deviation
		Canmet ENERGY	CETHIL-INSA		Canmet ENERGY	CETHIL-INSA	

Uptake after Hyd1 related to dry mass $m_{dry/P1}$	ΔX_1	0.30	0.398	14%	4.564	5.472	9%
Uptake after Hyd2 related to mass Deh1 $m_{Deh1/P3}$	ΔX_2	0.30	0.322	3.5%			
Uptake after Hyd3 related to mass Deh2 $m_{Deh2/P5}$	$\Delta X_1'$	0.43	0.319	14.8%			
Uptake after Hyd4 related to dry mass $m_{dry/P7}$	$\Delta X_2'$	0.34	0.399	7.9%	4.676	5.484	8%

The measured hydration heat during the four-hydration steps Hyd₁, Hyd₂, Hyd₃ and Hyd₄ is summarized in Table 4-12.

Table 4-12. Measured hydration heat

Description	Symbol	CETHIL-INSA		CanmetENERGY		Standard Deviation
		Hydration time [min]	Heat [J/g]	Hydration time [min]	Heat [J/g]	
Hydration Heat during Hyd1	H_{Hyd1}	$t_{Hyd1/P2} = 540$	838.06	$t_{Hyd1/P2} = 240$	486	26.6%
Hydration Heat during Hyd2	H_{Hyd2}	$t_{Hyd2/P4} = 420$	727.85	$t_{Hyd2/P4} = 240$	490.6	19.5%
Hydration Heat during Hyd3	H_{Hyd3}	$t_{Hyd3/P6} = 355$	730.90	$t_{Hyd3/P6} = 240$	690.5	2.8%
Hydration Heat during Hyd4	H_{Hyd4}	$t_{Hyd4/P8} = 520$	844.69	$t_{Hyd4/P8} = 240$	433.75	32%

It was agreed by the participants to not pursue the preliminary test method for the 2nd round robin for the SrBr₂ any further.

FINAL TEST METHOD FOR THE 2ND ROUND ROBIN (SrBr₂*nH₂O)

The proposed final test method for the 2nd Round Robin is given in Appendix B.

The testing equipment by the participating five laboratories as well as some of the testing conditions are summarized in Table 4-13.

Table 4-13. Participants' Specific Variables

Participants	Instruments	crucible	Cooling method/cooling rate	Pre-treatment time at 120oC, hr	Pre-treatment time at 180oC, hr	Period of measurement
TNO	Setaram TG/DSC	Al	N ₂ (2K/min)	24	12	4 days
TUe	Mettler Toledo TGA/DSC 3+	Al	(1K/min)	6	3	
CanmetENERGY	STA Netzsch	Al ₂ O ₃	Air (3K/min)	10	3	32 hours
CETHIL-INSA	Sensys Evo TG-DSC Setaram	SiO ₂	N ₂ (1K/min)	6	8	96 hours
Fraunhofer ISE	Setaram SET-SYS EVOLUTION	Pt		40	10	~ 7 days

The measured test sample mass by the different laboratories for points 1 to 6 is summarised in Table 4-14.

Table 4-14. Sample mass (absolute) for all measurement points 1 to 6.

Point #	Symbol	Sample [mg]					Mass
		TNO	TUe	CanmetENERGY	CETHIL-INSA	Fraunhofer ISE	
P 1	$m_{dry/P1}$	20.88	4.556	4.60	2.516	15.171	

P 2	$m_{\text{Ads2}'/P2}$	21.05	4.587	4.85	2.515	15.672
P 3	$m_{\text{Des1}/P3}$	20.97	4.588	4.85	2.511	15.673
P 4	$m_{\text{Ads1}/P4}$	27.70	5.995	6.36	3.285	20.44
P 5	$m_{\text{Des2}/P5}$	19.60	4.294	4.51	2.333	14.707
P 6	$m_{\text{Ads2}/P6}$	21.02	4.585	4.80	2.496	15.666

The measured water uptake during Des₁/Ads₁ and Des₂/Ads₂ is summarised in Table 4-15 and Table 4-16. The standard deviation of the measured water uptake by the different participating laboratories is within 4% confirming the reliability of the test procedure used.

Table 4-15. Water uptake between Des₁ / Ads₁ and Des₂ / Ads₂

Description	Symbol	Sample Mass [g/g]					Standard Deviation
		TNO	TUe	Canmet ENERGY	CETHIL- INSA	Fraunhofer ISE	
Uptake between Des ₁ / Ads ₁ related to dry mass	ΔX_1	0.322	0.3088	0.328	0.308	0.314	2.4%
Uptake between Des ₂ / Ads ₂ related to dry mass	ΔX_2	0.068	0.0643	0.0630	0.065	0.063	2.8%
Uptake between Des ₁ / Ads ₁ related to mass Des ₂	$\Delta X_1'$	0.343	0.3277	0.335	0.332	0.324	1.95%
Uptake between Des ₂ / Ads ₂ related to mass Des ₂	$\Delta X_2'$	0.072	0.0678	0.064	0.07	0.065	4.4%

Table 4-16. Water uptake between Des₂ / Ads₂ relative to dry mass at P₅

Participants	Mass at P ₅	Uptake between Des ₂ / Ads ₂ related to mass Des ₂ (P ₅)

	[mg]	[mole]	[g/g]	[mole H ₂ O/ mole SrBr ₂]
TNO	19.6	0.0000792	0.072	0.9959596
TUe	4.294	0.0000173544	0.068	0.93348085
CanmetENERGY	4.51	0.0000182	0.064	0.88461538
CETHIL-INSA	2.333	0.000009429	0.069	0.96086542
Fraunhofer ISE	14.707	0.00005944	0.0652	0.89670256
Standard Deviation			4.4%	4.38%

The measured heat of salt hydration during the four hydration steps Hyd₁, Hyd₂, Hyd₃ and Hyd₄ is summarized in Table 4-17.

Table 4-17. Heat of salt hydration between Des₁ / Ads₁ and Des₂ / Ads₂. Unit is J/g.

Description	Symbol	Heat of adsorption					Standard Deviation
		TNO	TUe	Canmet ENERGY	CETHIL-INSA	Fraunhofer ISE	
Heat of Adsorption (material specific) Des ₁ / Ads ₁	H_{Ads1}	970	883	830	690.0	713	18%
Heat of Adsorption (material specific) Des ₂ / Ads ₂	H_{Ads2}	256	184	177.2	43.0	172	41%
Heat of Adsorption (adsorbate specific) Des ₁ / Ads ₁	H'_{Ads1}	3000	2858	2530	2240.3	3060	11%
Heat of Adsorption (adsorbate specific) Des ₂ / Ads ₂	H'_{Ads2}	3765	2875	2812.7	661.5	2810	39.7%

Results of the heat of hydration shows a considerable gap between the reported values from the different laboratories. Further refinement of the test method is required.

EVALUATION OF THE SPECIFIC HEAT CAPACITY $C_p(T)$ OF $SrBr_2 \cdot 6H_2O$, $SrBr_2 \cdot 1H_2O$ AND $SrBr_2$ BASED ON HEAT FLOW DIFFERENTIAL SCANNING CALORIMETRY (HF-DSC)

The objective of this round robin test was the evaluation of the specific heat capacity of $\text{SrBr}_2 \cdot 6\text{H}_2\text{O}$, $\text{SrBr}_2 \cdot 1\text{H}_2\text{O}$ and SrBr_2 based on heat flow Differential Scanning Calorimetry (hf-DSC). This task was split in two subtasks:

- Definition of a measurement protocol based for DSC measurements
- Evaluation of the measured data

The definition of the measurement protocol was developed within the participants, the resulting procedure can be found in the section: "Measurement protocol for the evaluation of specific heat capacity $c_p(T)$ of $\text{SrBr}_2 \cdot n\text{H}_2\text{O}$ and SrBr_2 based on heat flow differential scanning calorimetry".

3 Institutes were joining the first run:

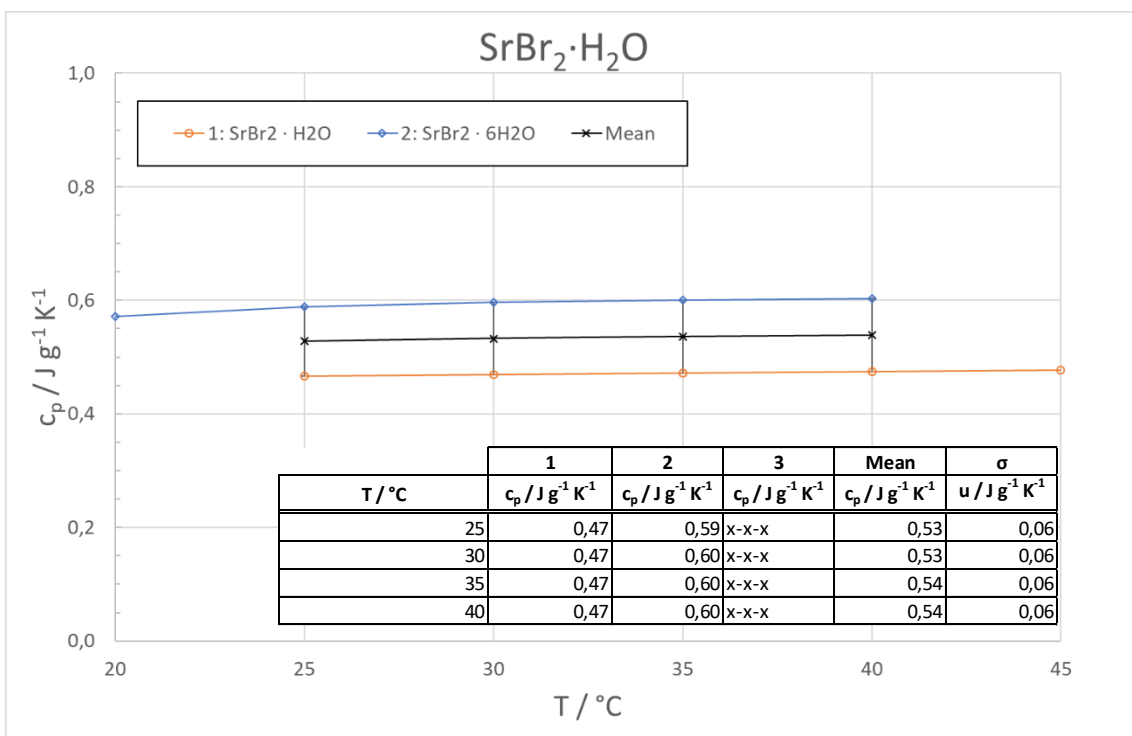
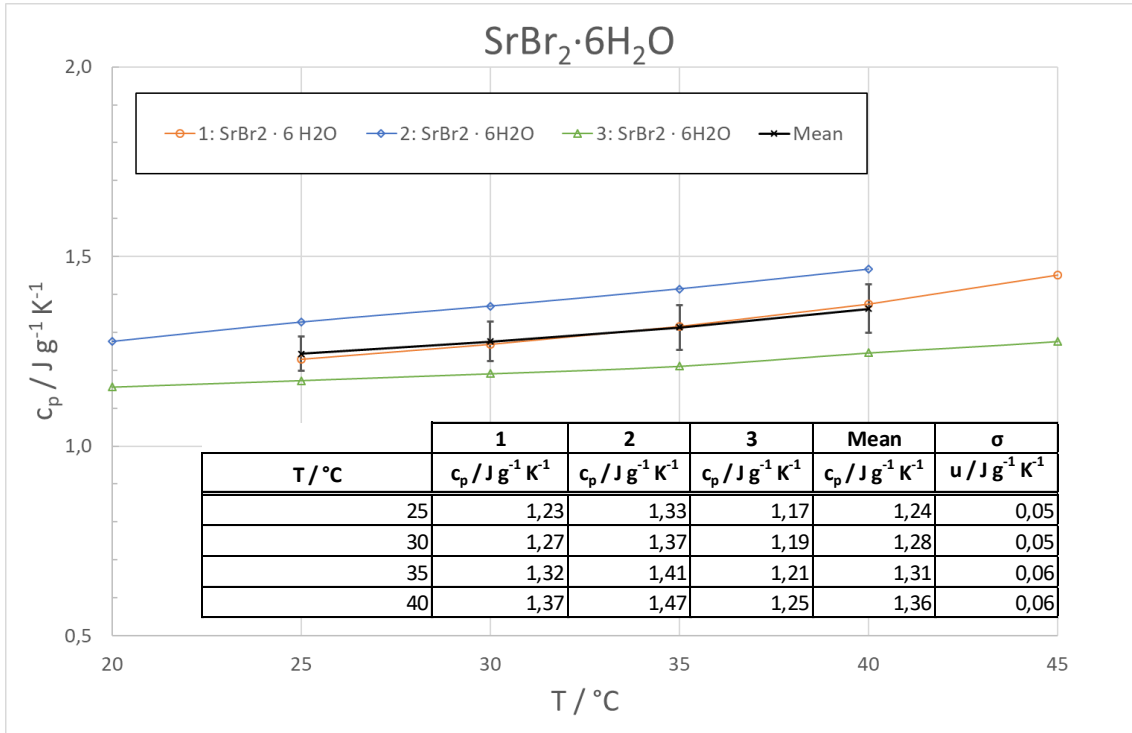
- National Resources Canada NRC - Innovation and Energy Technology – CanmetENERGY
- Fraunhofer - Institute for Solar Energy Systems - ISE
- Austrian Institute of Technology AIT – Center for Energy – Sustainable Thermal Energy Systems

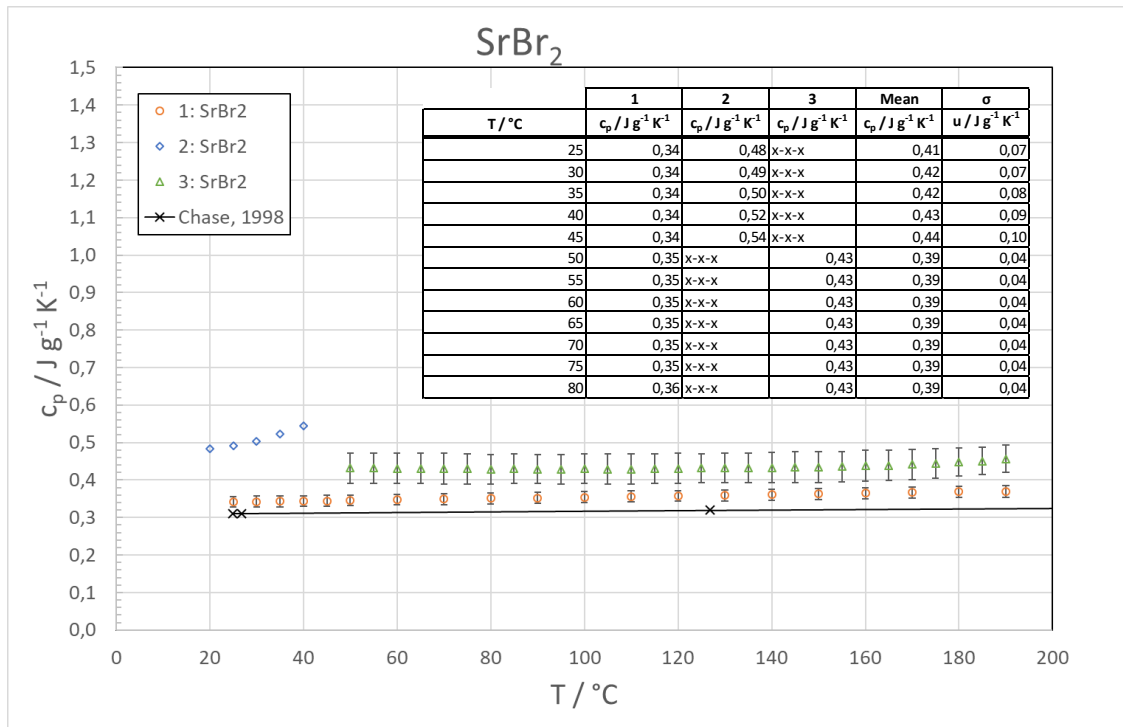
In the following tables and figures the results of the three participating institutes are represented. The shown numbers represent the institute and are assigned randomly.

Used devices and operating conditions

	1	2	3
System	DSC	NETZSCH STA	NETZSCH DSC 204 F1
Crucible		Al; d = 5 mm; h = 2mm	Al; 40 μ l
Gas		N2 40 ml/min	N2 40 ml/min
Reference		Sapphire m = 21.55mg	Sapphire m = 21.10mg
Heating Rate	10 K/min	10 K/min	10 K/min
Tmin	25	20	0
Tmax	190	40	190

Specific heat capacity results of $\text{SrBr}_2 \cdot 6\text{H}_2\text{O}$:





Because this round robin was in a first round executed at the end of the overall project, there are still open questions about the reasons of the displayed deviations. A possible explanation lies in the different ways of sample preparation.

This would be a starting point for further activities in a follow-up project to further improve the measurement procedure in a second round.

THE ZEOLITE 13X ROUND ROBIN TESTS

1ST AND 2ND ZEOLITE 13X ROUND ROBIN

The results of the first round robin showed large deviations between the measured water uptake and enthalpy based on already defined measurement protocols which were not clearly defined. Especially the procedure for the detection of the dry mass was not clearly defined.

The second round robin described already a more detailed measurement procedure for the TCM performance under realistic application conditions. Following table shows the discussed boundary conditions for the measurement:

Point #	Label	Sample Temperature [°C]	Vapor pressure [mbar]	Corresp. Dew point [°C]
P 1	Pretreatment / Dry mass	350	< 1 e-3	< -150
P 2	Adsorption 2'	55	8.7	5
P 3	Desorption 1	130	56.3	35
P 4	Adsorption 1	35	17.1	15
P 5	Desorption 2	180	17.1	15
P 6	Adsorption 2	55	8.7	5

Improvements compared to 1st Round Robin:

- Clear defined measurement procedure and sent around as a document
- Developed a results report sheet and sent around as a document
- Temperatures close to realistic applications
- A second reference point was included for those who can't detect the dry sample mass (due to apparatus limitations)

The results showed still deviations in water uptake and heat of adsorption. The lessons learned from this round robin was, that

- the definition of a reference mass in addition to dry mass shows a positive effect, however not the most important point
- The definition of a measurement procedure helped all participants
- There is still potential for improvement regarding:
 - Heat of adsorption should be measured from desorption point to adsorption point and not vice versa
 - Calculating vs. measuring the heat of adsorption must be discussed

These results lead to a new procedure for the third round robin with:

- A simplified measurement procedure (only one water vapor pressure for the whole procedure)
- Measurement of the heat of adsorption from a desorption point to an adsorption point and not vice versa
- Same scenarios and temperatures for the salt and the zeolite round robin
- Scenarios should fit the application conditions for domestic

3RD ZEOLITE 13X ROUND ROBIN

The proposed measuring procedure for the 3rd zeolite 13X round robin is given in Appendix C. The material samples, NaMSX zeolite is a 13X type zeolite with binder, used by all the participating laboratories was provided by ZAE Bayern.

The reported sample mass at the different test points (P₁-P₆) measured by the participating laboratories is summarized in Table 4-18.

Table 4-18. Sample mass (absolute) for all measurement points 1 to 6

Point #	Symbol	Sample Temperature [°C]	Sample Mass [mg]	
			ZAE	CanmetENERGY
P 1	$m_{dry/P1}$	350	197.6035	32.01
P 2	$m_{Ads2'/P2}$	65	240.316	38.82
P 3	$m_{Des1/P3}$	95	232.638	37.54
P 4	$m_{Ads1/P4}$	35	247.431	40.065
P 5	$m_{Des2/P5}$	180	209.7705	33.85
P 6	$m_{Ads2/P6}$	65	240.501	38.875

The water uptake measured by the laboratories during Des₁ / Ads₁ and Des₂ / Ads₂ is summarized in Table 4-19. The standard deviation of the measured water uptake by the different participating laboratories is within 3% confirming the reliability of the test procedure used.

Table 4-19. Water mass uptake between Des₁ / Ads₁ and Des₂ / Ads₂

Description	Symbol	Uptake [g/g]		Standard Deviation
		ZAE	CanmetENERGY	
Uptake between Des ₁ / Ads ₁ related to dry mass	ΔX_1	0.0749	0.0789	2.6%
Uptake between Des ₂ / Ads ₂ related to dry mass	ΔX_2	0.1555	0.157	0.5%
Uptake between Des ₁ / Ads ₁ related to mass Des ₂	$\Delta X_1'$	0.07055	0.0746	2.8%
Uptake between Des ₂ / Ads ₂ related to mass Des ₂	$\Delta X_2'$	0.14645	0.14845	0.7%

The measured heat of absorption between Des₁ / Ads₁ and Des₂ / Ads₂ by the participating laboratories is summarized in Table 4-20. These reported results from only two participating laboratories cannot be conclusive. Additional participation is required.

Table 4-20. Heat of adsorption between Des₁ / Ads₁ and Des₂ / Ads₂. Unit is J/g.

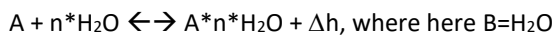
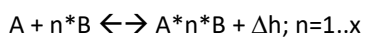
Description	Symbol	Heat [J/g zeolite]		Standard deviation
		ZAE	CanmetENERGY	

Heat of Adsorption (material specific) Des1 / Ads1	H_{Ads1}	230.1	295.5	12.45%
Heat of Adsorption (material specific) Des2 / Ads2	H_{Ads2}	530.85	549.35	1.7%
		[J/g water]		
Heat of Adsorption (adsorbate specific) Des1 / Ads1	H'_{Ads1}	3073.5	3745.92	9.9%
Heat of Adsorption (adsorbate specific) Des2 / Ads2	H'_{Ads2}	3413.4	3499.12	1.24%

4.2.4 DESCRIPTION OF A HARMONIZED MEASUREMENT PROCEDURE FOR THE TCM PERFORMANCE UNDER REALISTIC APPLICATION CONDITIONS

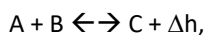
The contributors to this Task 58 Annex 33 focus on laboratory scale thermo-chemical energy storages (TES) where phase transitions and thermo-chemical reactions contain the energy potential.

In an adsorption or absorption storage, the following exothermic (discharging) and endothermic (charging) reactions of components A plus B are taking place:



where A can be a zeolite, silica gel (adsorption) or base or salt solution (absorption) and in most of the applications B is water (H₂O) or water vapour, respectively.

For a thermo-chemical storage, the simplest reaction equation is given by:



where the reaction of A plus B ends in a new component C plus the heat Δh .

For the assigned application, the thermo-physical properties of the materials have to be known. The materials quality and possible impurities will influence the power and energy performance of the TES unit through the physical parameters.

Thermal energy storage components are designed to foster the task of keeping and delivering thermal energy in the power and capacity range needed for application. If the storage material selection or development is done, then the question is how to transfer the material thermo-physical properties to a storage component with an optimal operation function. This means, depending on the concept, to design a heat and mass transfer unit and thus a power unit and a materials container (tank) unit, the capacity unit. The storage component itself is a part of a storage system containing several additional technical parts. In this deliverable, the focus is on adsorption-based storage concepts, which means the sorbent is a solid and the sorbate is a gas (vapour, e.g. water vapour), but could also be a liquid.

Therefore, the material properties determined for example in a TGA- DSC measurement have to be transferred to a heat and mass exchanger lab scale component – on multi-particle level of several hundred grams - to determine the heat transfer coefficient and the mass transfer coefficient in a combined experiment. This experiment has to be designed to optimally use/convert the advantageous properties of the storage material to an energy output. To do so, a heat and mass transfer experimental concept similar to the aimed large scale (power and capacity described in T4D1 of the task) unit has to be defined as part of the storage component development process. Out of this development process, a small-scale experimental setup can be built and a simulation model could be defined. In this experimental setup, the temperature level of the heat sources and heat sinks have to reach the measurement temperatures of the TGA-DSC apparatus. For future scaling reasons, ideally the experimental power of this unit is in the range of several hundred Watts up to 1 kW. Using the experimental results, the simulation model (if there is any) will be validated within the measured parameter range and scaling correlations are resulting (dimensionless correlations). If the fundamental heat and mass exchange properties – the collective phenomena – do not change, a scaling to a higher power of several kW is possible. This means that the task of transfer (to transfer the process) into the aimed application is possible – which in other simple words means – the development of “engineering relations” for the design and scaling of the storage component is possible.

In the following sections a “harmonized measurement procedure” - Description of a harmonized measurement procedure for the TCM performance under realistic application conditions – is presented.

PROCEDURE

The experimental work performed in the thermal energy storage projects contributing to the IEA Task 58 ECES Annex 33 has the target of transferring the know-how to the application areas. These areas can be the building sector for heating and cooling, process industry, transportation or any other technology where thermal energy storages are technically feasible, economically profitable and are contributing to sustainability. This aim implies the challenge of **scaling up** the small or medium **lab scale experiments to higher power and capacity**.

At the current level of effort and as unwritten agreement, the IEA work groups pursue a “**harmonised measurement procedure**” for the “lab storage performance assessment”. **This procedure and the measurements performed based in it is linked to the second deliverable relating the temperature scenarios.**

THERMAL ENERGY STORAGE TYPE – “CLASSIFICATION”

A variety of thermo-chemical storage laboratory designs are on the research level. Based on the solid sorbent and sorbate flow and treatment processes, a “classification” in “**types of thermal energy storage**” is proposed⁴. This “classification” comprises 4 adsorption storages:

open: A) *fixed sorbent bed air and sorbate flow reactor*
B) *continuous moving sorbent bed air and sorbate flow reactor*
C) *mixed sorbent batch air and sorbate flow reactor*

closed: D) *fixed sorbent bed sorbate flow reactor*

In this “classification”, *absorption* is not considered because the *sorbent is liquid*. And a *zeolite molecular sieve* is rather not a reactant of a chemical reaction and therefore *chemical reactions* are at this stage of document not included here. But the author has to decide whether the fundamental exothermic process is a *physi-sorption* or a *chemi-sorption*.

CONSERVATION LAWS AND TRANSFER FUNCTIONS

In the field of thermal energy storage R&D and technology, the power (W) and the capacity (Wh) of the storage units are the key “dimensions” or “figures”. Like in all other process technology areas, the conservation laws of **mass, momentum and energy** are the base frame for a comprehensive and complete assessment of the relevant storage versions. And with the boundary conditions of the (laboratory) system comprising of heat sources, heat sinks (their power and temperature level) and the storage unit, the knowledge of the steady state or part load operation is required. In other words, “the transfer functions of power and temperature have to be known”. Furthermore, the knowledge of the start-up and switching off behaviour in function of time is required. The list below is a summary (presume: *conservation of geometry*):

- *mass (sorbent, sorbate, fluid, container)*
- *momentum (sorbent, sorbate, fluid)*
- *power and energy / enthalpy*
- *steady state behaviour in function of power and temperature*
- *part load behaviour*
- *start-up /switching off behaviour*

MEASUREMENT PARAMETERS AND ANALYSIS

For the analysis of the laboratory storage unit it is obvious that the physical parameters have to be measured in an appropriate precision as well as in time and geometrical resolution. The measurement data uncertainty estimation gives a hint for sensor precision and, if necessary, an

⁴ Main criteria are: operation condition, temperature level and heat transport, residence time, “phase arrangement” (gravimetric separation), mass flow in heterogeneous systems and external reactions.

idea of improvement. In case a simulation model (CFD) will be developed or is available, a validation will be possible. A validated model will allow the reduction of the experimental effort.

As a requirement of this deliverable a round-robin TGA-DSC measurement campaign with Zeolite 13X (SrBr₂) was done and described in the second deliverable (Lia Kouchachvili, Reda Djebbar, 2019). The amount of 13X (SrBr₂) material is in the g (gram) range and thus the sorbate (water) uptake lays in the sub-gram range. The TGA-DSC measurements serves quasi as one of the «Single Particle» experiments.

With the assumption of the available thermo-physical properties of the storage material – the sorbent-sorbate combination - as well as of the container material (storage material, heat transfer fluid etc.), the following list contains the parameters to be or may be measured and deduced thereof:

- *mass m (kg) & mass flow dm/dt (kg/s, kg/h) (sorbent, sorbate, heat transfer fluids)*
- *volume flow rate (m^3/s , m^3/h) (sorbent, sorbate, heat transfer fluids)*
- *temperature T (°C; K) (sorbent, sorbate, heat transfer fluids)*
- *time t , time step Δt / time resolution (s)*
- *pressure p (mbar, Pa) (sorbent, sorbate, heat transfer fluids)*
- *enthalpy h (J/kg) & enthalpy flow dh/dt (J/kg*s)*
- *input and output power (W) & input and output energy (J)*
- *auxiliary power (W) & energy (J)*

MEASUREMENT TEMPERATURES - SCENARIOS

In the application of a sorption (ad- and ab-) thermal energy storage, the boundary conditions are of the heat sinks and sources are required for the power (W) and the temperature level (°C, K). As there is a broad variety of TES types, it is challenging to restrict to a common heat sources and sinks parameter range in this Task 58 Annex 33 working group.

But to keep the temperatures in the TGA-DSC measurements (Round Robin Test – Zeolite 13X) and following the **4 temperatures approach the desorption (des) – adsorption (ads) process steps** - for the 13X sorbent material should be done at 2 scenarios:

- Scenario 1: **95 °C (des) / 10 °C condensation & 35 °C (ads) / 10 °C evaporation.**
- Scenario 2: **180 °C (des) / 10 °C condensation & 65 °C (ads) / 10 °C evaporation.**
- Scenario 2b: **130 °C (des) / 10 °C condensation & 35 °C (ads) / 10 °C evaporation** (if scenario 2 not useful).

Nevertheless, air-conditioning (room heating and/or cooling and hot tap water) is mentioned in all contributions as one of the application areas. Within this application area, the remaining common parameter - the **dependent parameter** (variable) - is the “output” **temperature T** (and power) level of the storage:

- Application **temperature range T = 35 °C (heating) to 65 °C (ads +5 K to reach 60 °C DHW)**.

All other **independent parameters** (variables like air humidity – open storage – and/or water vapour pressure – closed storage) have to be chosen and adjusted to reach the above-mentioned temperature range.

EXPERIMENTAL

In the Kick Off meeting from Lyon it was agreed to use as sorbent material the zeolite molecular sieve KÖSTROLITH® NaMSXK with a particle size of 1.6 to 2.5 mm (supplied by Fabian Fischer of ZAE Bayern). Further information about the sorbent materials is given in Table 4-21. Water will be used as sorbate because of the excellent thermodynamic properties. Figure 4-6 and Figure 4-7 are showing the vapour pressure curves of water and the combination of water and zeolite (from literature).

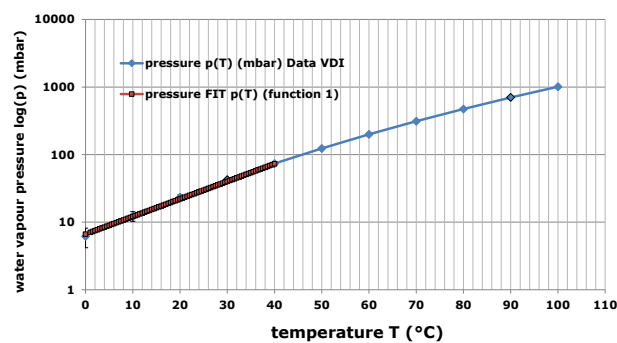


FIGURE 4-6 WATER VAPOUR PRESSURE P CURVE IN FUNCTION OF TEMPERATURE T. VDI DATA AND A FIT FUNCTION IN THE RANGE OF T=0°C TO 40°C.

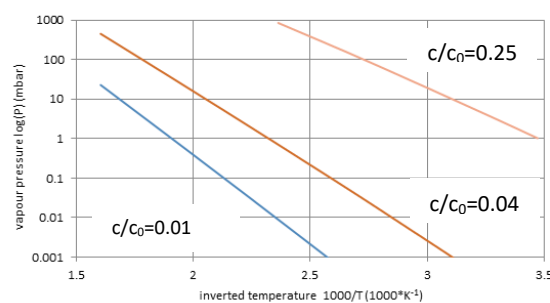


FIGURE 4-7 VAN-T HOFF OR VAPOUR PRESSURE P CURVES (1/T - LOG(P) DIAGRAM) OF A SORBENT IN FUNCTION OF TEMPERATURE AND LOAD c/c_0 . ADOPTED FROM LITERATURE. I WOULD LIKE TO HAVE THIS CURVES FOR ZEOLITE MOLECULAR SIEVE KÖSTROLITH® NAMSXK (1.2 – 2.5 MM).

SORBENT AND SORBATE

Table 4-21. Specifications for the used sorbent: zeolite molecular sieve KÖSTROLITH® NaMSXK (1.2 – 2.5 mm), chemical formula $\text{Na}_2\text{O} \cdot \text{Al}_2\text{O}_3 \cdot m \text{SiO}_2 \cdot n \text{H}_2\text{O}$

	Method	NaMSXK (1.2 – 2.0 mm)	NaMSXK (1.6 – 2.5 mm)
Beads Size Range (nominal, mm) (approx. mesh size)		1.2 – 2.0 10 x 16	1.6 – 2.5 8 x 12
Bulk Density (compacted, g/l)	CWKM-118	680 - 725	680 - 725
Attrition (% wt.)	CWKM-122	max. 0.2	max. 0.2
Crush Strength (N/bead)	CWKM-108	min. 10	min. 25
Moisture Content (as delivered, % wt.)	CWKM-408	max. 1.0	max. 1.0
Water Adsorption Capacity* (55 % rel. hum., 20 °C, % wt.)	CWKM-403	min. 26.5	min. 26.5
CO ₂ Adsorption Capacity* at 2.4 mbar CO ₂ pressure (cm ³ (STP) / g)	CWKM-409	min. 24.0	min. 24.0

LAB SCALE STORAGE UNIT

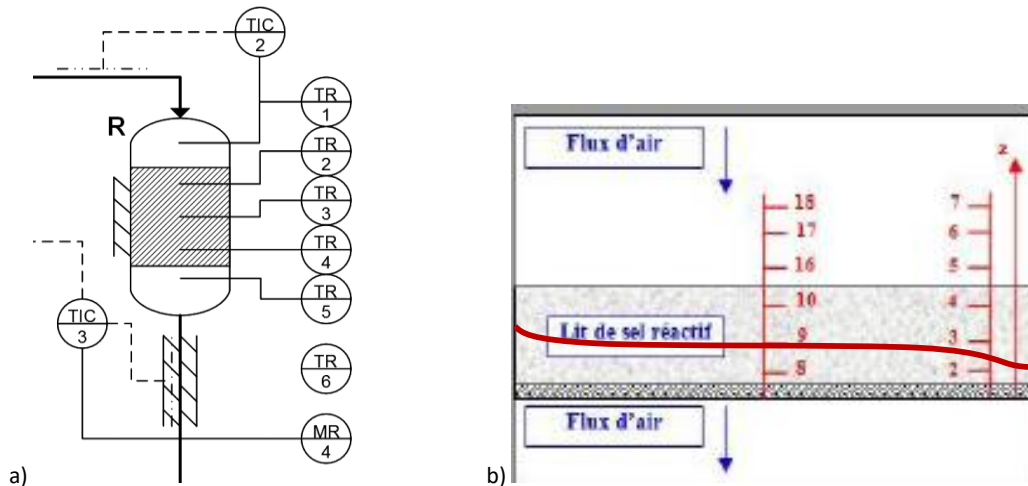


FIGURE 4-8 EXAMPLES OF STORAGE COMPONENT TYPE/CLASS A, “FIXED SORBENT BED AIR AND SORBATE FLOW REACTOR”. ADOPTED FROM THOMAS NONNEN ET AL., 2016. R=REACTOR, TIC=TEMPERATURE INDICATOR/CONTROLLER, TR=THERMOCOUPLE / TEMPERATURE SENSOR, MR=MOISTURE SENSOR. B) TEMPERATURE PROFILE FROM F. MARIAS, 2014. THE NUMBERS 2 TO 18 INDICATE TEMPERATURE SENSOR POSITIONS.

Table 4-22. Range of the independent parameters in the experiment to reach (measure) the dependent variable temperature T: most of you already have done this section

Geometry: maybe you already have done this section
Material: Container material thermo-physical properties
Geometry: particle size see Table 4-21 (distribution)
Mass: Sorbent mass or mass range: m_{\min} to m_{\max} , Sorbate mass range: m_{\min} to m_{\max}
Etc.

RESULTS

DATA, FIGURES, TABLES AND DIAGRAMS

Measurement results are figures, graphs, tables and if fit functions were use eventually equations. The analysis and interpretation of the results follows. An example (Steffen Beckert, Sylvie Rougé) is shown in Figure 4-9. The heat transfer zone (temperature) and their time dependent development in function of position can be seen in Figure 4-10.

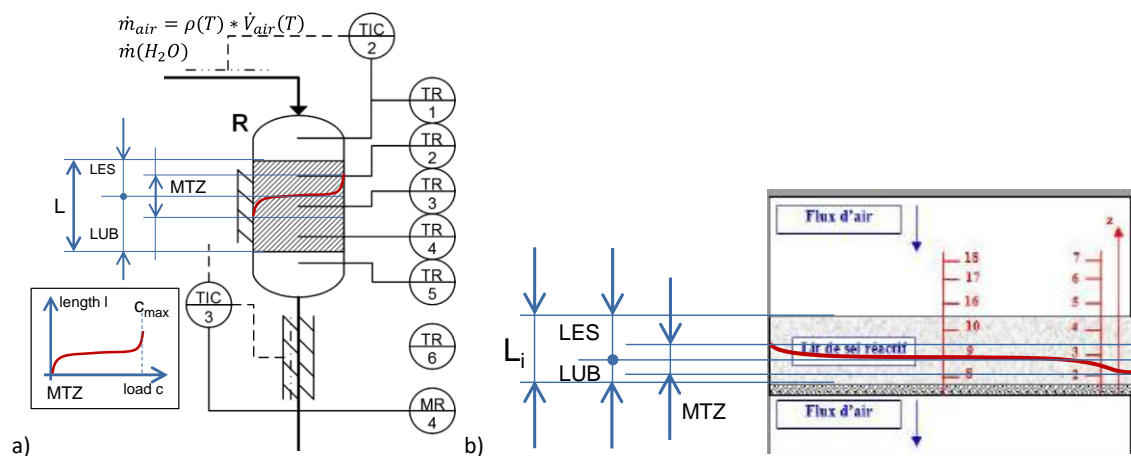


FIGURE 4-9 MEASURED MASS TRANSFER ZONE: EXAMPLES OF STORAGE COMPONENT TYPE/CLASS A) “FIXED SORBENT BED AIR AND SORBATE FLOW REACTOR”. A) LEFT, ADOPTED FROM THOMAS NONNEN ET AL, 2016. R=REACTOR, TIC=TEMPERATURE INDICATOR/CONTROLLER, TR=THERMOCOUPLE / TEMPERATURE SENSOR, MR=MOISTURE SENSOR. L=LENGTH OF THE FIXED SORBENT BED, LES= LENGTH OF EQUILIBRIUM PART, MTZ=MASS TRANSFER ZONE, LUB=LENGTH OF UNUSED BED. INSERT: MTZ GRAPH WITH MAXIMUM LOAD c_{MAX} AND ARBITRARY UNITS. B) RIGHT, ADOPTED FROM F. MARIAS, 2015.

Possible presentation of measurement results of an open system are the outlet air conditions in a **psychrometric chart or Mollier Diagram**. Or, like in Figure 4-10, the temperature $T(t, z)$ in function of time t and position z in the solid sorbent bed.

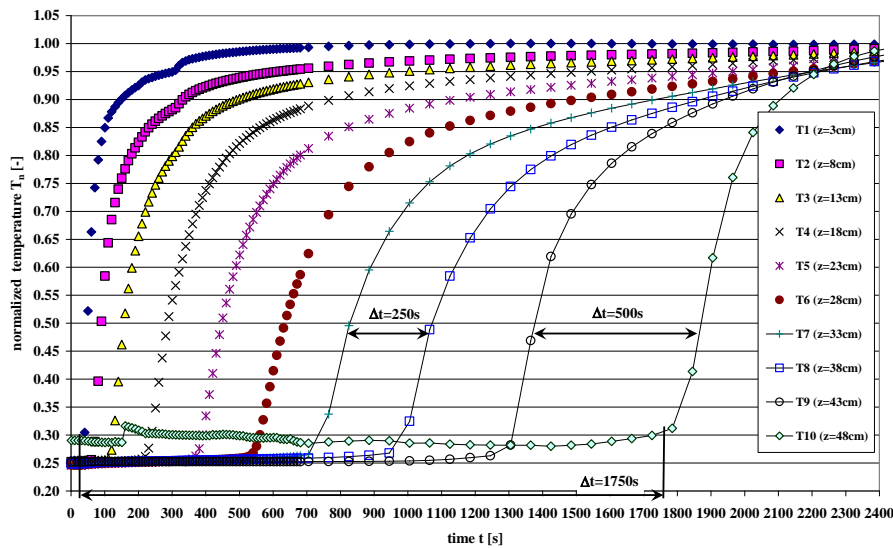


FIGURE 4-10 EVOLUTION OF THE SORBENT BED TEMPERATURES T1 TO T10 (NORMALISED) IN FUNCTION OF TIME T AND POSITION Z DURING THE WATER VAPOUR ADSORPTION PROCESS. ADOPTED FROM OWN MEASUREMENTS.

UNCERTAINTY ESTIMATION

Contributors: Please do an uncertainty estimation of your experimental results. Follow for example NIST Technical Note 1297 or JCGM 100:2008 (Barry N. Taylor and Chris E. Kuyatt, 1994, Joint Committee for Guides in Metrology, 2008) or ISO 21748:2017 (Guidance for the use of repeatability, reproducibility and trueness estimates in measurement uncertainty evaluation, 2017) or appropriate methods.

DISCUSSION AND ASSESSMENT

Contributor – laboratory experiment: Each experiment of a contributor and the results are discussed by you. In this way, the comparison with other experiments (which may have totally different geometric dimensions etc.) can/could be easier done.

One of the more obvious performance indicators is the maximal temperature lift achievable during the discharging process. This temperature difference is measured between the temperature level at which the heat can be delivered and the low temperature heat source. By increasing this temperature difference, the delivered output power usually decreases until reaching the equilibrium point (null output power).

Depending on the boundary condition, the discharging power ($Q_{discharging}$) can be used to calculate the discharging efficiency ($\eta_{discharging}$) according to following equation:

$$\eta_{discharging} = \frac{Q_{discharging}}{Q_{thermochemical}}$$

with $Q_{thermochemical}$ based on the sorbent status

In the same way, a charging efficiency ($\eta_{charging}$) can be defined:

$$\eta_{charging} = \frac{Q_{charging}}{Q_{thermochemical}}$$

Allowing determining the system global efficiency (η_{global}):

$$\eta_{global} = \frac{Q_{discharging}}{Q_{charging}} = \eta_{discharging} \cdot \eta_{charging}$$

This efficiency calculated on a lab scale prototype should stay unchanged for a demonstrator using the same technology and is a major output to get an assessment of the storage density (kWh/m^3) – the storage energy per used volume. In fact, the aim for high energy density storages is the reduction of the foot-print or just the reduction of the volume.

CONSIDERATIONS ABOUT SCALING-UP

The system characterisation is described in Deliverable D4T1 (Benjamin Fumey et al.). Nevertheless, scaling from lab scale processes to the system (of real application, one or two orders higher, or more) is a challenge. In this task, inputs from the measurements done on the lab scale prototype (like dimensionless numbers) may be used for the modelling. In fact, generally, the measurement results are analysed in dimensionless presentation like $T(t)/T_{max}$, $p(t)/p_{max}$, etc. Furthermore, in heat and mass transfer process scaling, the dimensionless numbers (heat transfer) like $Nu = Nu(Re, Pr)$ and (mass transfer) $Sh = Sh(Sc, Pr)$ play an important role.

4.2.5 ACKNOWLEDGMENTS

This research in the section "Description of a harmonized measurement procedure for the TCM performance under realistic application conditions" was supported by the Swiss Federal Office of Energy in the frame of the ABSTOREX project, by the Commission of Technology and Innovation in the frame of SCCER Heat and Electricity Storage as well as by the University of Applied Sciences of Rapperswil.

4.2.6 REFERENCES

ISO 21748:2017(en). Guidance for the use of repeatability, reproducibility and trueness estimates in measurement uncertainty evaluation.

Barry N. Taylor and Chris E. Kuyatt, Guidelines for Evaluation and Expressing the Uncertainty of NIST Measurement Results. NIST National Institute of Standards and Technology, United States Department of Commerce, NIST Technical Note 1297 Edition 1994.

Foivos Marias, 2015. Analyse, Conception et expérimentation de procédés de stockage thermique résidentiel de longue durée par réaction thermochimique à pression atmosphérique. Thermique [physics.class-ph]. Université Grenoble Alpes, 2015.

Foivos Marias, Pierre Neveu, Gwennyn Tanguy, Philippe Papillon, 2014.

JCGM 100:2008, 2008. Joint Committee for Guides in Metrology (JCGM/WG 1). Evaluation of measurement data – Guide to the expression of uncertainty in measurement; 2008.

Lia Kouchachvili, Reda Djebbar, Summary of the Round Robin Tests for SRBr2 and 13X, 2019.

Thermodynamic analysis and experimental study of solid/gas reactor operating in open mode. Energy 66 (2014) 757-765.

Thomas Nonnen et al. 2016. A Thermochemical Long-Term Heat Storage System Based on a Salt/Zeolite Composite. Chem. Eng. Technol. 2016, 39, No. 12, 2427-2434.

5 SUBTASK 4 - COMPONENT DESIGN FOR INNOVATIVE TES MATERIALS

5.1 SUBTASK 4P: COMPONENT DESIGN FOR PCM

5.1.1 INVENTORY OF CONCEPTS TO IMPROVE COMPONENT PERFORMANCE

INTRODUCTION

Thermal energy storage (TES) systems using Phase Change Materials (PCMs) should meet the application requirements in terms of technical and economical parameters. Among the technical parameters, high thermal power is one of the most challenging characteristics for a PCM thermal storage. Most of the materials currently used as PCM have intrinsically low thermal conductivity; therefore, the component design has to compensate for it.

Several finished and ongoing projects have worked on improving the design of PCM components (storage containment, heat exchangers) with the aim to increase the thermal performance. As a first step for a performance comparison between the different solutions, this report aims to list the various concepts, previously or currently studied, for PCM thermal storage in terms of geometries, heat exchange systems and the nature of the PCM used.

LIST OF CONCEPTS

Latent heat storage (LHS) systems can be classified according to different criteria (active/passive operation, macro/micro encapsulated, working heat transfer fluid (HTF), etc.). In this report, concepts will be presented based on the geometry of the heat exchanger. Those latent heat storage systems can be considered as heat exchangers where one fluid is the PCM and the other is the heat transfer fluid (HTF). It is noteworthy that in some systems, the PCM slurry is used as the HTF.

The list of concepts agreed to within the working group is as follows:

- 1 Compact flat plate heat exchanger (no circulation of PCM)
- 2 Tanks with internal heat exchanger (PCM bulk, no circulation of PCM in the tanks):
 - 2.1 Shell-and-tubes (PCM in shell)
 - 2.2 Shell-and-tubes (PCM in shell) with finned heat exchanger
- 3 Tanks with internal macro-encapsulated PCM heat exchanger:
 - 3.1 PCM in flat plates
 - 3.2 PCM in spheres
 - 3.3 PCM in short cylinders
 - 3.4 Shell-and-tubes (PCM in tubes)
- 4 Compact flat plate heat exchanger (PCM emulsion/slurry circulating)

- 5 Tanks with internal heat exchanger (PCM emulsion/slurry in the tank, HTF circulating in the internal coil)
- 6 Tanks with external heat exchanger (PCM emulsion/slurry as HTF in the internal coil)
- 7 Direct contact PCM-HTF
- 8 Tank-in-tank
- 9 PCM for building components
- 9.1 Micro PCM composite for wall
- 9.2 Macro PCM for solar wall
- 10 Active PCM systems
- 10.1 Mechanical removal of PCM layer
- 10.2 Moving bed of PCM over heat transfer area

Table 5-1 shows a matrix of the list of concepts and the institutions developing each concept.

Table 5-1. Matrix of the list of concepts and the institutions developing each concept.

Institution/concept	1	2.1	2.2	3.1	3.2	3.3	3.4	4	5	6	7	8	9	10.1	10.2
ASiC			X			X									
Çukurova University															
Dalhousie University	X	X	X	X											
DLR	X	X				X								X	X
DTU			X	X							X	X			
University of Basque Country, EHU				X											
Fraunhofer ISE	X	X		X	X	X	X			X			X		
Hochschule Luzern			X					X			X		X		
ITCAS					X	X									
KTH Royal Institute of Technology	?	X	X	X	X	X	X				X				
Rubitherm			X	X		X									
TU-Graz							X								
Universität Bayreuth						X									

University of Zaragoza				X	X					X					X		
Vaillant		X						X									
ZAE Bayern		X	X	X	X	X	X	X			X				X		
University of Lleida,	X	X	X	X													
Université d'Artois, LGCgE															X	X	

DESCRIPTION OF CONCEPTS

COMPACT FLAT PLATE HEAT EXCHANGER (NO CIRCULATION OF PCM)

Compact flat plate heat exchangers (HX), also called plate-and-frame heat exchangers, have become increasingly popular device for traditional fluid-to-fluid heat exchange. This is due to their high level of compactness and higher heat transfer rates from one fluid to the other. The geometric arrangement is simple: numerous plates are put together, leaving a small spacing between each, in a way that the fluids run counterflow successively along the length of the plates as illustrated in Figure 5-1.



FIGURE 5-1: SCHEMATIC OF A TRADITIONAL FLUID-TO-FLUID COMPACT FLAT PLATE HEAT EXCHANGER (IMAGE PRESENTING THE NORTHERN LIGHTS SOLAR SOLUTION PLATE HEAT EXCHANGER TAKEN FROM WWW.SOLARTUBS.COM).

PCM compact flat plate heat exchangers could be constructed directly by filling one of the fluid channels of a traditional/commercial flat plate heat exchanger with the selected PCM. By ensuring the PCM remains in the heat exchanger by blocking the inlet and outlet for that original fluid stream, and circulating a heat transfer fluid (HTF) in the remaining fluid section of the heat exchanger, a thermal storage system can quickly be obtained; as shown in Figure 5-2 with the typical small distances between plates, it is expected that high heat transfer rates in and out of the PCM would be expected. However, by the very design of a compact flat plate heat exchanger, 50% or less of the available volume will be used, leading to a low overall storage density per total volume of the system.

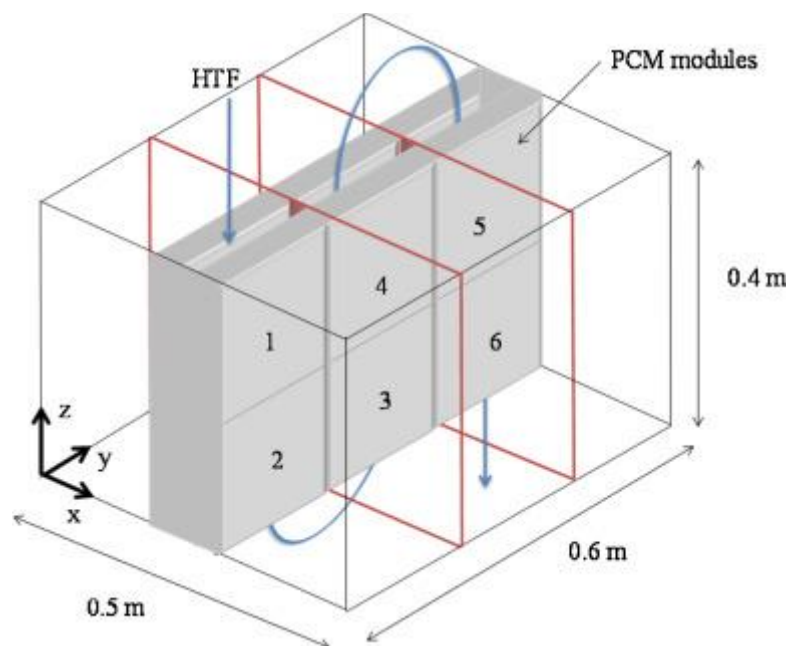


FIGURE 5-2: SCHEMATIC OF ONE HEAT TRANSFER FLUID LAYER AND TWO PCM LAYERS IN A COMPACT FLAT PLATE PCM HEAT EXCHANGER [PRIETO *ET AL.* 2016]

Medrano *et al.* (2009) tested a commercial plate and frame HX while evaluating commercially available HX for use with PCMs (Figure 5-3). This specific study found such a system to offer extremely normalized thermal power.

It appears no other references could be easily found for work using an actual compact flat plate heat exchanger with PCM. Numerous systems use encapsulated PCM in flat plates, and then incorporate the plates in a fluid stream. Such a geometry falls within the tanks with internal macro encapsulated PCM heat exchanger section.



FIGURE 5-3: COMMERCIALY AVAILABLE PLATE AND FRAME HX EVALUATED BY MEDRANO ET AL. (2009).

TANKS WITH INTERNAL HEAT EXCHANGER (PCM BULK, NO CIRCULATION OF PCM IN THE TANKS) SHELL-AND-TUBES (PCM IN SHELL)

In this concept, the PCM is stored in a container of cylindrical or rectangular shape. The heat exchanger is immersed into the bulk PCM. The heat transfer fluid circulates through metal tubes or plastic capillary tubes. The arrangement could be from one to several passes of the heat transfer fluid through the shell to increase the heat transfer surface, as seen in Figure 5-4.

Due to the continuous PCM volume, supercooling is likely reduced, and the concentration of the PCM can be checked and, if necessary, adjusted after the storage installation. In addition, a state-of-charge measurement based on the determination of the volume change is possible, and the heat exchanger can easily be tested in terms of leakproofness. To ensure long-term cycling stability, appropriate measures to prevent phase separation of the PCM, for those PCM at risk, have to be taken into account.

Figure 5-5 presents various examples of shell-and-tube geometries.

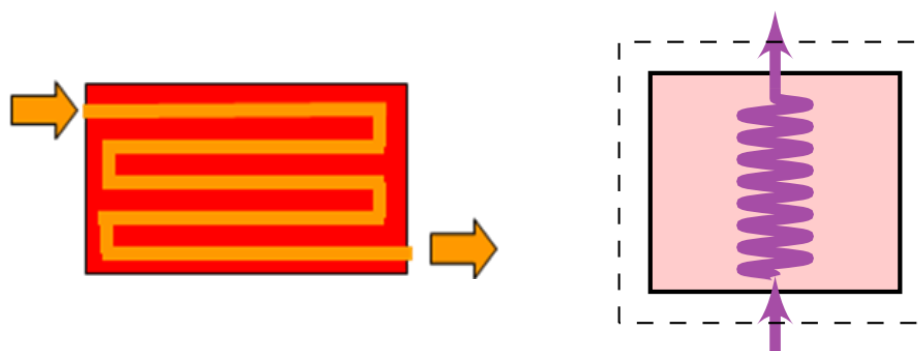
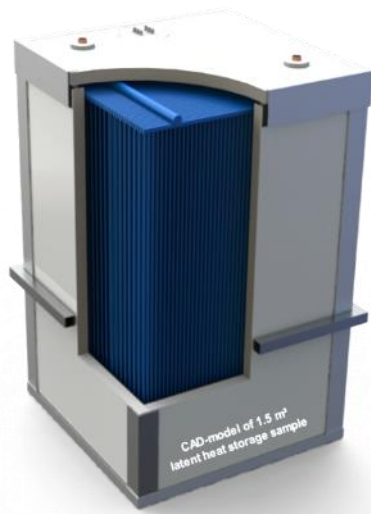


FIGURE 5-4: SCHEMATIC DRAWINGS OF THE CONCEPT "TANKS WITH INTERNAL HEAT EXCHANGER": RECTANGULAR HEAT EXCHANGER (LEFT) AND CYLINDRICAL HEAT EXCHANGER (RIGHT) (SOURCE: ZAE BAYERN)



CAD MODEL OF A PCM STORAGE WITH CAPILLARY TUBE HEAT EXCHANGER (SOURCE: ZAE BAYERN)

PCM CRYSTALLIZING AT CAPILLARY TUBES (SOURCE: ZAE BAYERN)

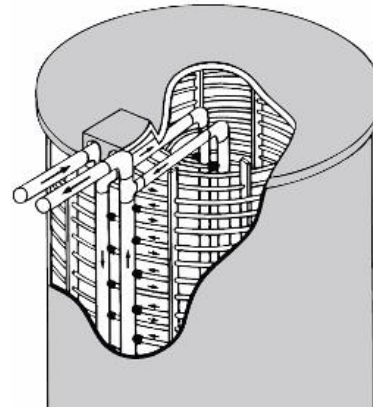


Shell-and-tube heat exchanger embedded in a PCM/graphite heat storage compound (SIGRA λ)

(SOURCE: SGL TECHNOLOGIES, MEHLING AND CABEZA 2008)



CROSS SECTION OF CALMAC'S ICEBANK® COLD STORAGE SYSTEM (SOURCE: CALMAC, MEHLING AND CABEZA 2008)



FLOW DIRECTIONS OF THE CALMAC STORAGE (SOURCE: CALMAC, MEHLING AND CABEZA 2008)

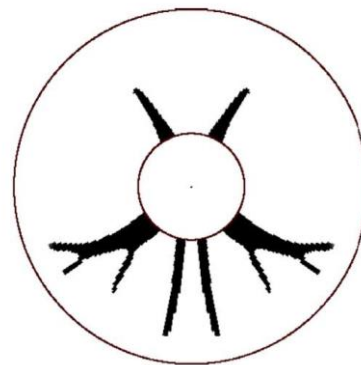
FIGURE 5-5: EXAMPLES OF GEOMETRIES OF THE CONCEPT "TANKS WITH INTERNAL HEAT EXCHANGER"

SHELL-AND-TUBES (PCM IN SHELL) WITH FINNED HEAT EXCHANGER

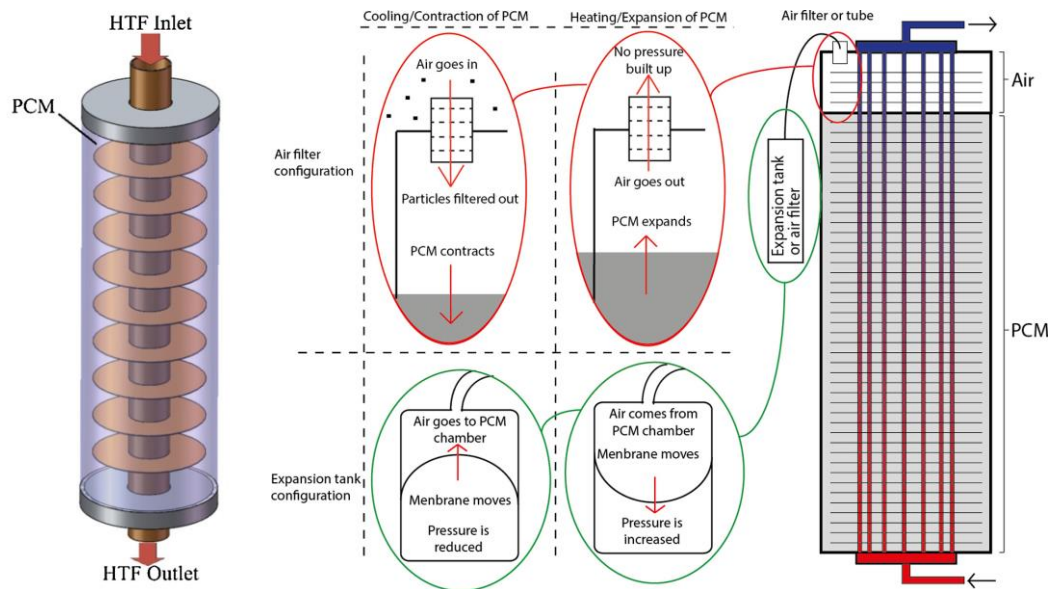
The shell-and-tube concept has been further developed by adding fins to the heat exchange surfaces (tube) of the heat exchanger. Dozens and dozens of research paper, exploring the effect of those fins on the overall heat transfer and behaviour of the PCM have been published. Fins can be vertical (Herbinger *et al.*, 2019), horizontal (Dannemand *et al.*, 2016), annular (Yang *et al.*, 2017), branching (Skaalum and Groulx, 2020) or based on more complex biomimicry (Pizzolato *et al.*, 2017); some examples are presented in Figure 5-6.



Vertical finned tubes (source: Herbinger *et al.* 2019)



Optimized fins for melting (source: Pizzolato *et al.* 2017)



Annular fins (source: Yang *et al.* 2017)

Horizontal fins in a shell-and-tube cylindrical storage system (source: Dannemand *et al.* 2016)

FIGURE 5-6: EXAMPLES OF SHELL-AND-TUBE HX WITH FINNED TUBE.

Details of such a design can be obtained by looking at the horizontal fin system (bottom right of Figure 5-6) in more detail. The cylinder is filled with approximately 90% of the storage mediums, leaving an air gap in the top of the cylinder to accommodate the expansion/contraction of the PCM during heating and cooling. An air filter can be installed either directly on the top of the tank or at the end of a tube connected to the PCM chamber. This allows the PCM to expand/contract without pressure build-up in the PCM chamber while limiting the possibility of airborne particles to enter and disturb the stability of the supercooling of the PCM.

During heating when the PCM expands, some of the air in the top of the PCM chamber is pushed out through the air filter, keeping ambient pressure in the PCM chamber. During cooling and contraction of the PCM, air is sucked into the chamber through the air filter while particles in the air are filtered out, still keeping ambient pressure inside the PCM chamber.

Alternatively, the top of the PCM chamber can be connected to an external expansion tank without pre-pressure via a tube, hence having a closed PCM chamber where the PCM could expand with reduced pressure build-up. Vapour could possibly escape from the unit when the air filter is installed, whereas this is avoided with the expansion tank installed.

TANKS WITH INTERNAL MACRO ENCAPSULATED PCM HEAT EXCHANGER



Spheres, Cristopia



Plates, Rubitherm GmbH



Cylinders, SCALORIC GmbH



Ribbed spheres, PureTemp



Disks, Axiotherm GmbH



Pouches, Climator

FIGURE 5-7: EXAMPLES OF COMMERCIAL MACROCAPSULE GEOMETRIES FOR PCM WITH THE CORRESPONDING PRODUCER

Figure 5-7 shows some examples of commercial macro capsules for PCM. It includes representative geometries and is not meant as an exhaustive list of all commercially available products. It should be noted that many variations of these geometries exist, in different dimensions and various polymeric and metallic encapsulation materials. The compatible PCM also vary strongly. Different classes of PCM have been incorporated in macro capsules, either in a pure form or including additives (*e.g.* thickening agents, nucleation agents etc.)

PCM IN FLAT PLATES

In this concept, the PCM is enclosed within rectangular plates. These containers can present different aspect ratios and they might be arranged vertically or horizontally. The HTF flows around the outer part of the plates, so an external shell is needed to encompass both the PCM plates and the HTF.

The main advantages of this configuration are:

- High surface to volume ratio (high charging and discharging rate)
- Optimal integration in reduced spaces with squared shapes (*e.g.*: ducts, buildings)

- High modularity, due to the use of single plates as storage units, which can be easily arranged in different configurations that respond to the specific requirements of each case.

As an example, the system developed in Diarce *et al.* (2018) is presented. In that design, the PCM is contained within tight hollow plates made of aluminum, which are placed vertically. The in-parallel arrangement of the plates, with narrow channels between the plates, forms the channels where the HTF flows through. A compact stack of several in-parallel plate-channels form the basic stack of the latent heat thermal energy storage (LHTES) system (see Figure 5-8). Several stacks can be placed in-series and/or in-parallel as well. Therefore, there is no need to use larger plates when large storage volume is required, neither to provide a large number of plates in-series: several compact stacks can be placed in-parallel, piled up or any combination of both. In this way, specific designs can be provided for a defined application, adapted to the space availability.

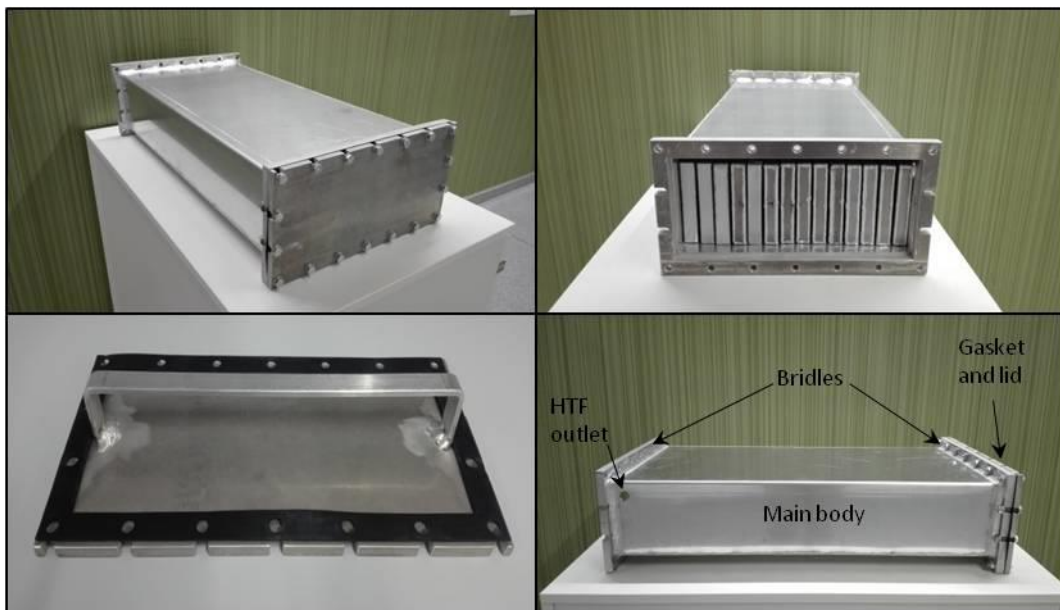


FIGURE 5-8: EXAMPLE OF THE CONCEPT 3.1: A LABORATORY-SCALE TES SYSTEM FORMED BY PCM MACROENCAPSULATED IN FLAT PLATES PLACED IN PARALLEL (SOURCE: DIARCE *ET AL.* 2018).

This geometry also finds advantages when working with PCM that have a tendency to segregate, as seen in the work of Dannemand *et al.* (2016). Flat rectangular chambers for the PCM with small internal height of 50 mm) are used, as seen in Figure 5-9. The small height is to reduce the risk of phase separation. At one end of the heat storage, an extension in the height of the PCM chamber is located to allow for expansion of the PCM with the help of an inflatable plastic bag or expansion vessel. The density change between the cold solid and the warm liquid salt can cause pressure changes and deformations of the tank. Small cracks on the inside of the PCM chamber can in combination with pressure changes and deformations disturb supercooling of PCM. The inner surfaces of the PCM chamber are designed and manufactured to be simple and

smooth without cracks or gaps. This is to avoid spontaneous nucleation caused by possible movement of cracks. The heat storage has separate heat exchangers at the top and bottom of the PCM chamber. The small height also enables the PCM to be heated to a relatively uniform temperature.

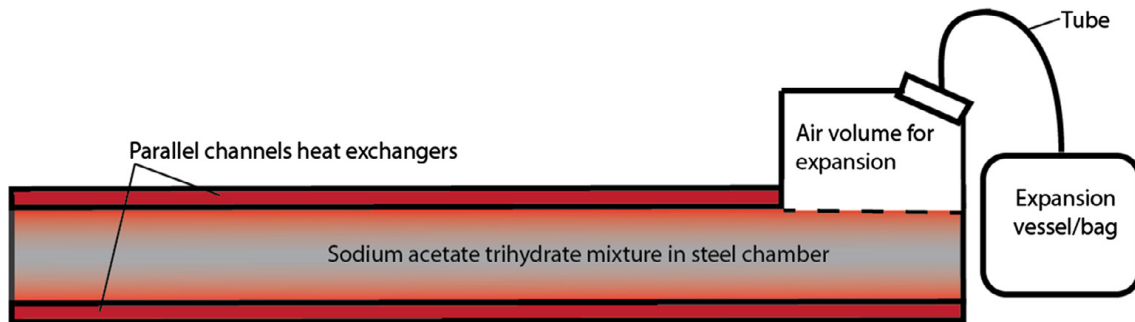


FIGURE 5-9: FLAT PLATE STORAGE WITH PCM CHAMBER, INTEGRATED AND EXTERNAL EXPANSION (SOURCE: DANNEMAND ET AL. 2016).

PCM IN SPHERES

This concept consists of a tank filled with spherical capsules where the PCM is placed. The heat transfer fluid flows through the tank, around the capsules. The tank can be vertical, horizontal or rectangular (concrete). Normally the volumetric fraction of PCM is up to 50% of the total volume of the tank. This concept was first developed for ice-storage. Nowadays, there are different storage tank geometries and PCM commercially available. Figure 5-10 shows one of these commercial products. The spheres are designed so that the volume expansion during the phase change is absorbed. There are different diameters from 10 to 15 cm.

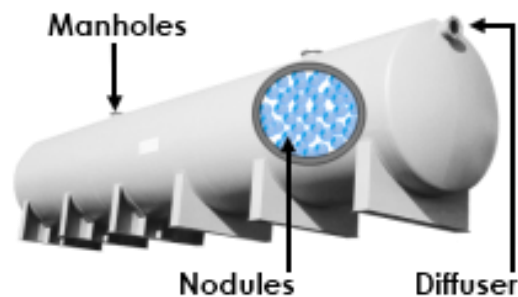


FIGURE 5-10: EXAMPLE OF HORIZONTAL TANK FILLED WITH SPHERICAL CONTAINER OF PCM. [SOURCE: [HTTP://WWW.CRISTOPIA.COM](http://www.cristopia.com), VISITED 20/09/2018}

PCM IN SHORT CYLINDERS

In PCM storage units with the PCM encapsulated in cylinders, also shown as a commercially available product in Fig. 7, the goal is to increase the surface area for heat exchange between the HTF and the PCM. One way to do this is to incorporate the PCM in cylinders that are then

immersed in the HTF, which flows around the tubes, as discussed in Tamme *et al.* (2008) and Buschle *et al.* (2006). A bundle of such cylinders is shown in Figure 5-11.



FIGURE 5-11: BUNDLE OF CYLINDERS CONTAINING PCM FOR HIGH TEMPERATURE APPLICATIONS (SOURCE: BUSCHLE *ET AL.* 2006).

This concept was studied by H hlelein *et al.* (2018) for lower temperatures of up to 150  C. The project results reveal that the charging and discharging power is high compared to other approaches [Br uggemann *et al.*, 2016]. However, the manufacturing of the capsules is a challenging task and leads to high overall costs. A promising alternative is the use of capsules available as mass products – *e.g.* food cans. First results indicate that costs of less than 1   per dm³ of encapsulated PCM are reachable [H hlelein *et al.*, 2018].

SHELL-TUBES (PCM IN TUBES)

Conventional shell-and-tube heat exchangers can be used as latent heat storage where the PCM is placed inside the tubes and the heat transfer fluid flows in the shell. In this concept, the conduction heat transfer resistance is limited to the diameter of the tubes. The number of cylindrical tubes and flow of the heat transfer fluid can be designed in a wide range of different configurations.

COMPACT FLAT PLATE HEAT EXCHANGER (PCM EMULSION/SLURRY CIRCULATING)

This concept is based on flat heat exchanger, but the PCM is in the form of a slurry. Therefore, the PCM is also pumped and flows through the heat exchanger. Conventional heat transfer fluids flow on the primary side and PCM slurries on the secondary side [Streicher *et al.*, 2006].

Despite this geometry offering a high heat transfer area and high compactness, when working with PCM slurries, it is critical to assess possible phenomena of channel clogging as well as the pressure drop. Figure 5-12 shows examples found in literature reporting this phenomenon.

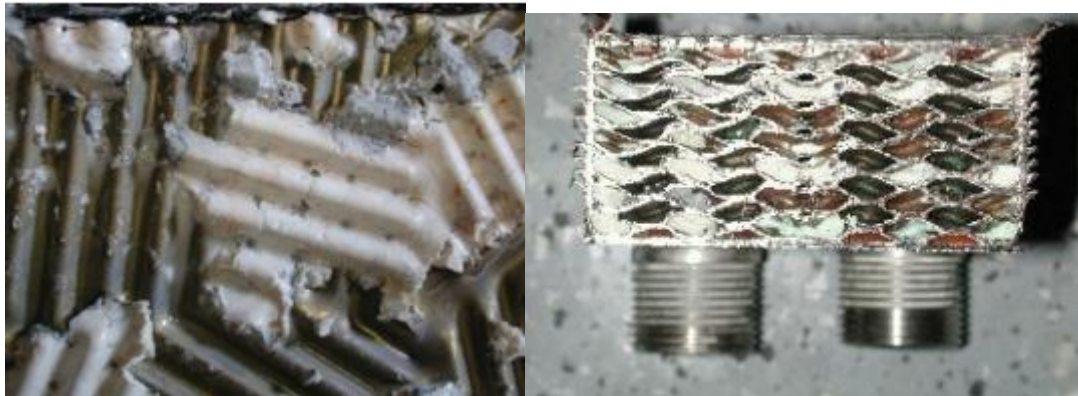


FIGURE 5-12: CLOGGING OF THE PLATE HEAT EXCHANGER CHANNELS AFTER FLOWING FOR THREE WEEKS WITH A PCM SLURRY WITH A MICROCAPSULE SIZE OF 20 MM (SOURCE: GSCHWANDER AND SCHOSSIG 2006).

TANKS WITH INTERNAL HEAT EXCHANGER (PCM EMULSION/SLURRY IN THE TANK, HTF CIRCULATING IN THE INTERNAL COIL)

In this concept, a PCM slurry is placed in a tank and a HTF is circulated through the tank. Recent studies have experimentally studied tanks containing PCM slurries as thermal storage material, where water flowed as HTF through a spiral type internal heat exchanger [Heinz and Streicher, 2006; Diaconu *et al.*, 2010; Huang *et al.*, 2011; Delgado *et al.*, 2017], through an external plate heat exchanger [Voerbeck *et al.*, 2013; Kappels *et al.*, 2014], or through a tube-bundle heat exchanger [Allouche *et al.*, 2015]. Figure 5-13 shows an example of this concept with a spiral internal coil.

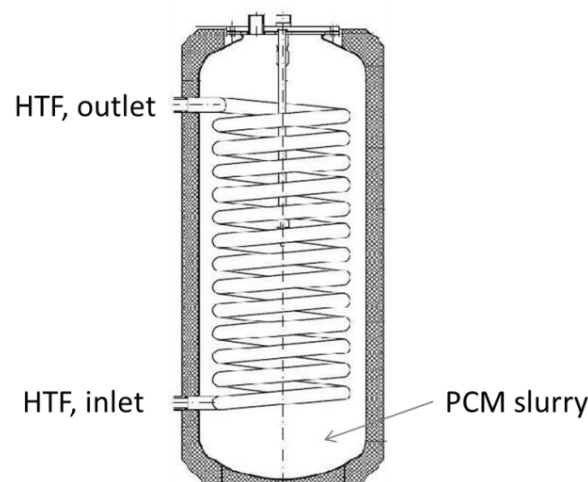


FIGURE 5-13: EXAMPLE OF CONCEPT 5, PCM SLURRY CONTAINED IN A TANK WITH HTF CIRCULATING IN AN INTERNAL COIL (SOURCE: DELGADO *ET AL.* 2015).

TANKS WITH EXTERNAL HEAT EXCHANGER (PCM EMULSION/SLURRY AS HTF IN THE INTERNAL COIL)
An alternative to the internal heat exchanger is to use an external heat exchanger. So the functionality of storage and heat transfer is separated which allows the dimensioning of the storage

capacity and thermal power independently. As storage a simple tank can be used, usually flat plate type heat exchangers are used. Pumps in the primary and secondary cycle allow a good control of the heat transfer with high power due to forced convection (Figure 5-14 and Figure 5-15).

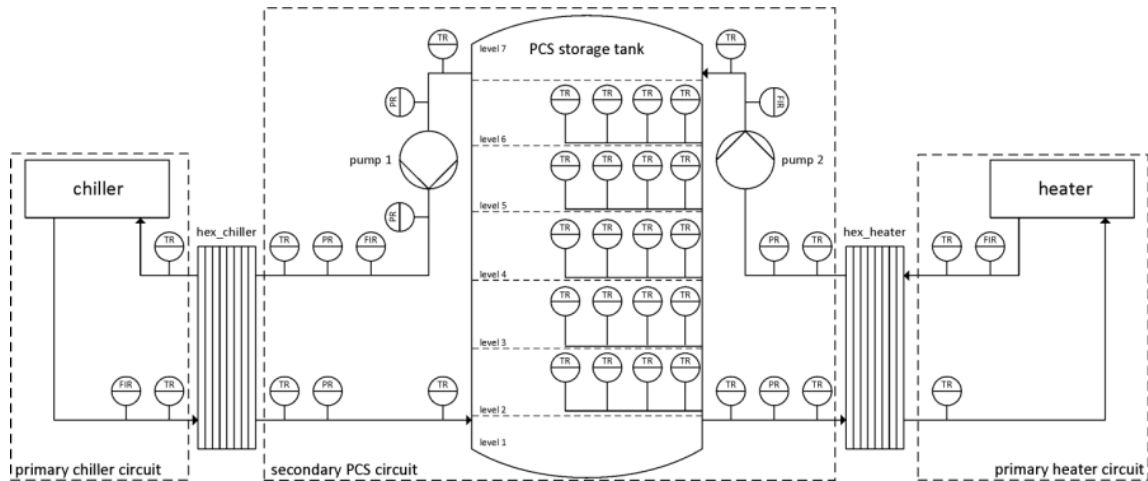


FIGURE 5-14: SCHEMATIC DRAWING OF A STORAGE TEST FACILITY WITH TWO EXTERNAL HEAT EXCHANGERS (FRAUNHOFER ISE).



FIGURE 5-15: 5 M³ PCS STORAGE WITH EXTERNAL HEAT EXCHANGER, INSTALLATION AT RUD. OTTO MEYER TECHNIK LTD. & CO. KG (© ROM TECHNIK).

DIRECT CONTACT PCM-HTF

Direct contact latent heat storage is based on a direct flow of the heat transfer fluid (HTF) through the PCM. In cases where the HTF has a lower density than the PCM, the HTF is pumped

at the bottom of the storage to form bubbles (see Figure 5-16). The bubbles flow upwards and simultaneously release or absorb heat causing the melting or solidification of the PCM. If the HTF has a higher density than the PCM, the HTF is pumped at the top of the storage tank and is collected at the bottom. One main advantage of this type of storage is its ability to generate large heat exchange surface area at the interface of the HTF bubbles and the PCM which can result in high thermal power without needing an additional complex heat exchanger structure.

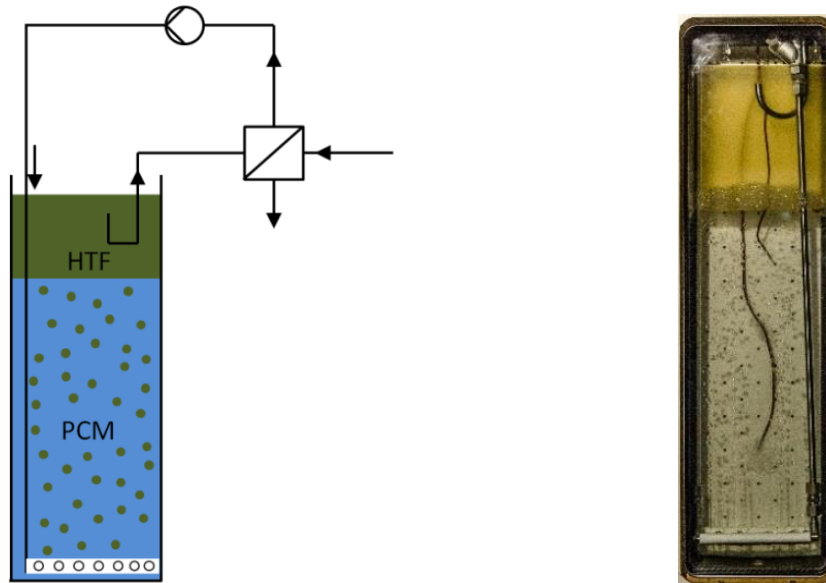


FIGURE 5-16: (LEFT) SCHEMATIC REPRESENTATION OF DIRECT CONTACT LATENT HEAT STORAGE PRINCIPLE WHERE THE HTF IS FLOWING DIRECTLY THROUGH THE PCM EXCHANGING HEAT AT THE BUBBLE/PCM INTERFACE AND CAUSING SOLIDIFICATION OR MELTING OF THE STORAGE MATERIAL; (RIGHT) DIRECT CONTACT LATENT HEAT STORAGE TEST-RIG DEVELOPED AT LUCERNE UNIVERSITY OF APPLIED SCIENCES AND ARTS (HSLU)

TANK-IN-TANK

To realize heat exchange via the outer surface of a macro-encapsulated PCM volume, a tank-in-tank heat storage can be utilized. The inner tank contains the PCM, centered in an outer tank. In between, the heat transfer fluid is circulated. An expansion volume in the inner tank is necessary to address density changes of the PCM. This volume can be connected to ambience or to a membrane expansion vessel to avoid built-up of static pressure.

Large differences in tank volumes result in a large volume of HTF, which is in direct contact to the heat exchange surface. In this way, hybrid latent-sensible heat storage can be realized. As shown in Figure 5-17, an internal heat exchanger (e.g. spiral heat exchanger) can be used to increase the heat transfer to/from the PCM volume. HTF circulation in the internal heat exchanger or in between the tanks can be applied separately or in parallel. Two separate HTF lines offer the opportunity for combined storage of heat for domestic hot water and space heating applications in households.

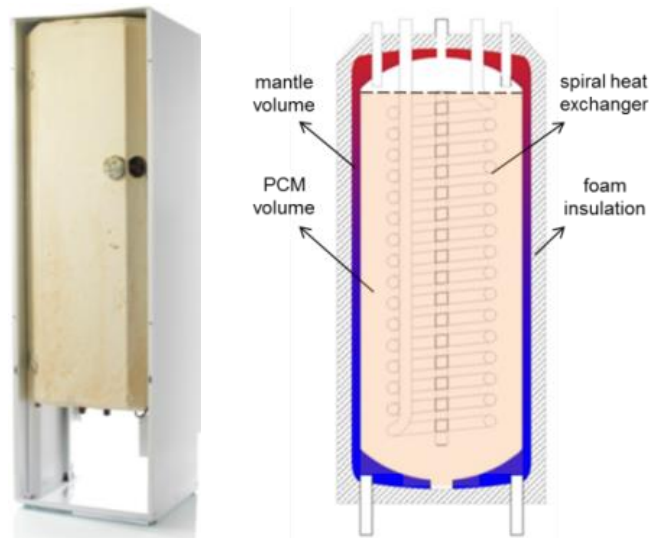


FIGURE 5-17: LEFT: PHOTOGRAPHY OF A CYLINDRICAL TANK IN TANK HEAT STORAGE; RIGHT: SCHEMATIC DRAWING (INTERSECTION) (DTU).

PCM FOR BUILDING COMPONENTS

MICRO PCM COMPOSITE FOR WALL

Microencapsulation prevents PCMs from leakage when molten which contribute to greatly expand the PCM integration possibilities in construction materials such as cement, lime, concrete, mortar, artificial marble, sealants, paints, textiles, and other coatings. Microencapsulation contributes to improve heat transfer by increasing the heat exchange surface between the PCM and the construction material. Melting temperatures are chosen to increase thermal mass of the construction material in a temperature range between 21 and 26 °C. The material is basically used to prevent overheating inside buildings. Therefore, the PCM composite is placed on inside walls and ceilings [Schossig *et al.*, 2005].

Figure 5-18 shows the principle of a lightweight construction with a PCM gypsum plaster placed on the inside of a wall, as well as a SEM image of a gypsum plaster with microencapsulated PCM. Figure 5-19 depicts the room temperatures of two similar test rooms, one equipped with PCM plaster and the other as reference without PCM.

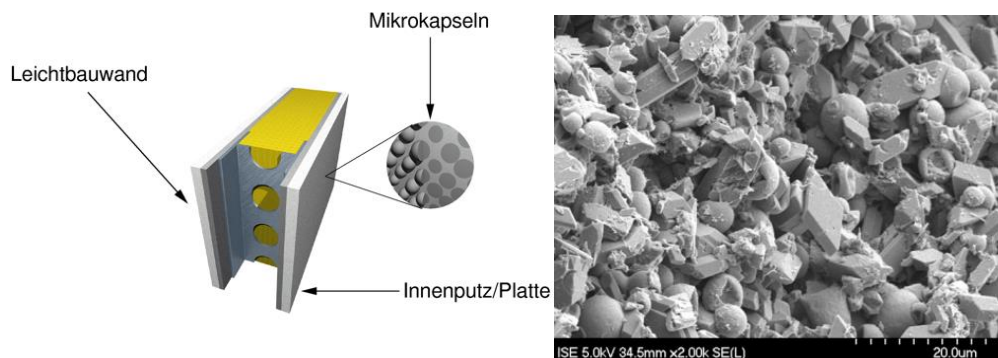


FIGURE 5-18: LEFT: SCHEMATIC DRAWING OF A LIGHTWEIGHT WALL WITH MICROENCAPSULATED PCM INSIDE THE GYPSUM PLASTER OF THE INNER WALL. RIGHT: SEM IMAGE OF GYPSUM PLASTER WITH MICROENCAPSULATED PCM (FRAUNHOFER ISE).

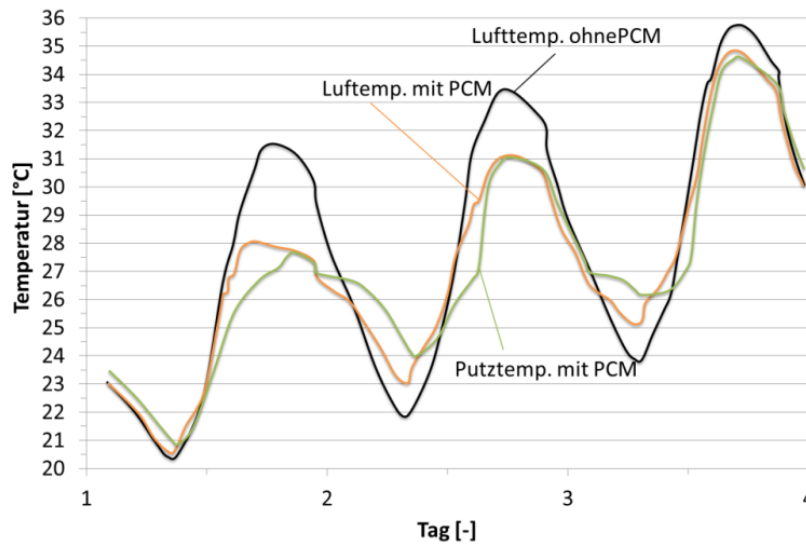


FIGURE 5-19: MEASURED ROOM AIR (BLACK LINE WITHOUT PCM, ORANGE WITH PCM) AND WALL TEMPERATURE (GREEN LINE) OF TWO TEST ROOM EQUIPPED WITHOUT AND WITH MICRO-PCM-GYPSUM-PLASTER (FRAUNHOFER ISE).

Micro-encapsulated PCM integrated in building materials can modify the thermal and mechanical characteristics of the original material. The Laboratoire de Génie Civil et GéoEnvironnement (LGCgE) with the Laboratoire de Thermique Énergétique et Procédé (LaTEP) have worked on the characterisation of thermal properties of these composite materials [Joulin *et al.*, 2014; Zalewski *et al.*, 2019]. They are composed of cement mortar including micro-encapsulated PCM (BASF Micronal 5001DX). The storage properties of this composite material integrating 19% PCM by mass have been highlighted compared to those of a conventional mortar (Figure 5-20).

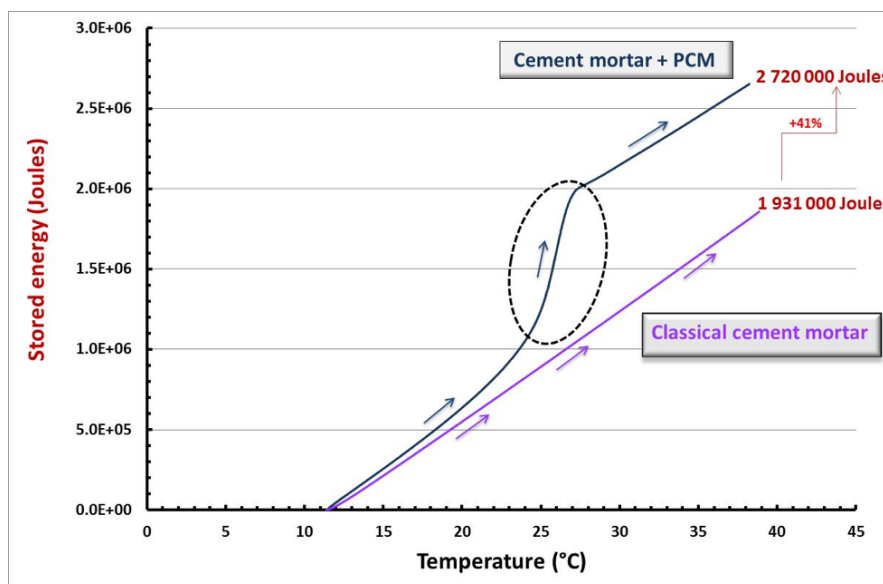


FIGURE 5-20: AMOUNT OF HEAT STORED BY BOTH MATERIALS (FOR 1 M² OF WALL; THICKNESS OF 40 MM) (SOURCE: UNIVERSITÉ D'ARTOIS, LGCGE)

MACRO PCM FOR SOLAR WALL

The use of solar walls makes sense in view of the desire to reduce energy costs in buildings. One of the obstacles to their development is related to implementation constraints. The heavy material storage wall is one of these constraints. To reduce them and facilitate the installation of solar walls, the idea is to prefabricate them in a factory. For transport and ease of installation, the heavy material is replaced by a lighter storage wall made of macro PCM (Figure 5-21 to Figure 5-24).



FIGURE 5-21: MACROENCAPSULATION OF HYDRATED SALTS IN POLYOLEFIN BRICK; CRISTOPIA $T_{MELTING}: 27^{\circ}\text{C}$



FIGURE 5-22: MACROENCAPSULATION OF ORGANIC PCM DERIVED FROM RENEWABLE AND BIO-BASED; CRODATHERM™ 53 ; $T_{MELTING}: 53^{\circ}\text{C}$



FIGURE 5-23: STORAGE OF SOLAR WALL (SOURCE: UNIVERSITÉ D'ARTOIS, LGCGE)



FIGURE 5-24: COMPOSITE SOLAR WALL (SOURCE: FAVIER *ET AL.*, 2016)

The ultimate objective is the best possible use of energy for the current or improved comfort requirements and environmental benefits [Stutz *et al.*, 2017; Favier *et al.*, 2016; Leang *et al.*, 2017; Zalewski *et al.*, 2012]. The building will have a higher social acceptability. Beyond energy aspect, the higher efficiency buildings allow to overcome energy precarity.

ACTIVE PCM SYSTEMS

In active PCM systems, the solidified PCM is moved away from the heat transfer surface by some means, thereby allowing for a constant power during discharging. This also enables separating the design components of power and capacity.

MECHANICAL REMOVAL OF PCM LAYER

In concepts in which the PCM layer that solidifies during discharging is mechanically removed, this layer is scraped off in some way. Research has been done on these methods for high temperature applications by Zipf *et al.* (2103), Nepustil *et al.* (2016) and Bauer *et al.* (2017). In the screw heat exchanger design discussed in Zipf *et al.* (2018) and shown in Figure 5-25, the screw is turned in the PCM and an HTF flows through the screw. PCM solidifies on the screw and is mechanically removed from it.

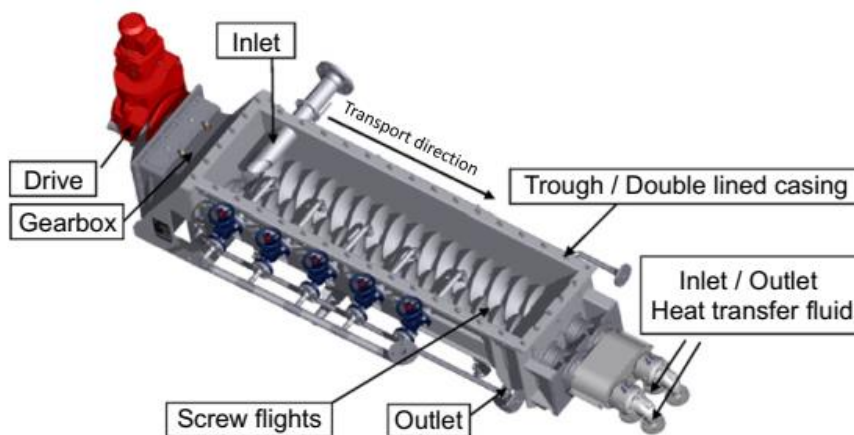


FIGURE 5-25: SCREW HEAT EXCHANGER FOR THE MECHANICAL REMOVAL OF PCM, ALLOWING FOR A SEPARATION OF POWER AND CAPACITY (SOURCE: ZIPF *ET AL.* 2013).

In the system developed by Nepustil *et al.* (2016), a flat plate PCM storage concept is further developed to have a mechanical scraper pass across the heat transfer surface in the PCM volume repeatedly, thereby removing the solidified layer of PCM on this surface and maintaining a constant power level during discharging (Figure 5-26).

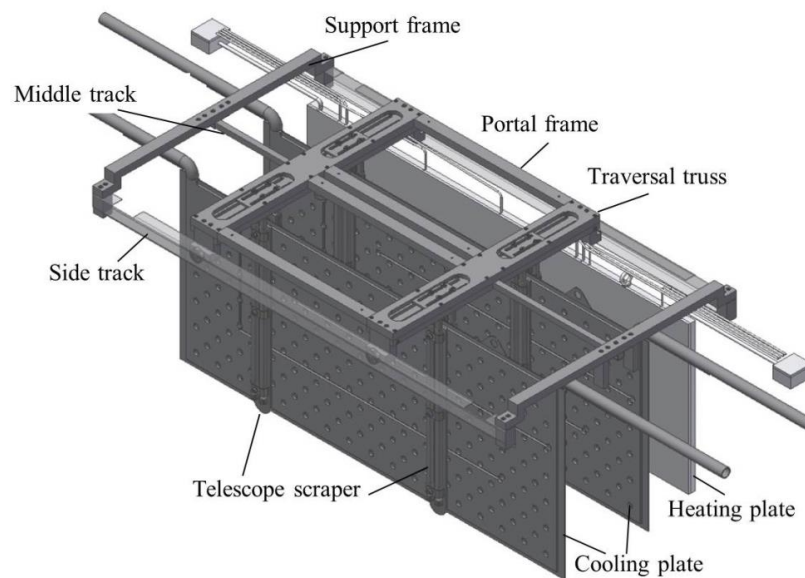


FIGURE 5-26: FLAT PLATE PCM STORAGE WITH MECHANICAL SCRAPER (SOURCE: NEPUŠTIL *ET AL.* 2016).

In the rotating drum concept of Bauer *et al.* (2017), HTF flows through a rotating cylinder or drum, which is (partially) immersed in PCM (Figure 5-27). The PCM solidifies on the rotating drum (shown in the schematic in red) and is scraped off by a scraper (shown in yellow-green). This allows for repeated use of the same heat transfer surface area, and a separation of power and capacity.

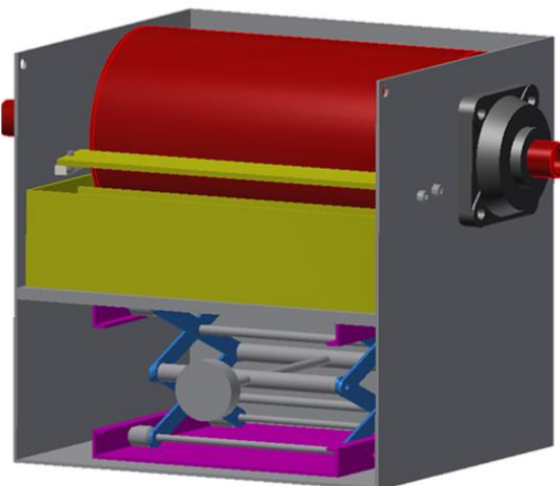


FIGURE 5-27: SCHEMATIC OF ROTATING DRUM PCM CONCEPT (SOURCE: BAUER *ET AL.* 2017).

MOVING BED OF PCM OVER HEAT TRANSFER AREA

In a second area of active PCM concepts, the PCM is moved away from the heat transfer surface through movement of a bed of PCM, as discussed by Pointner and Steinmann (2016). In this concept, shown in Figure 5-28, PCM is in open capsules or containers, which are pulled or pushed

across a heat transfer tube and surface area. Through control of the movement speed, the rate of heat transfer can be matched to the flow of the HTF in the tubes to maintain the constant and required power of the integration goal. Through further development of this concept with heat transfer structures integrated into the PCM containers, more adaptability of the power level is possible.

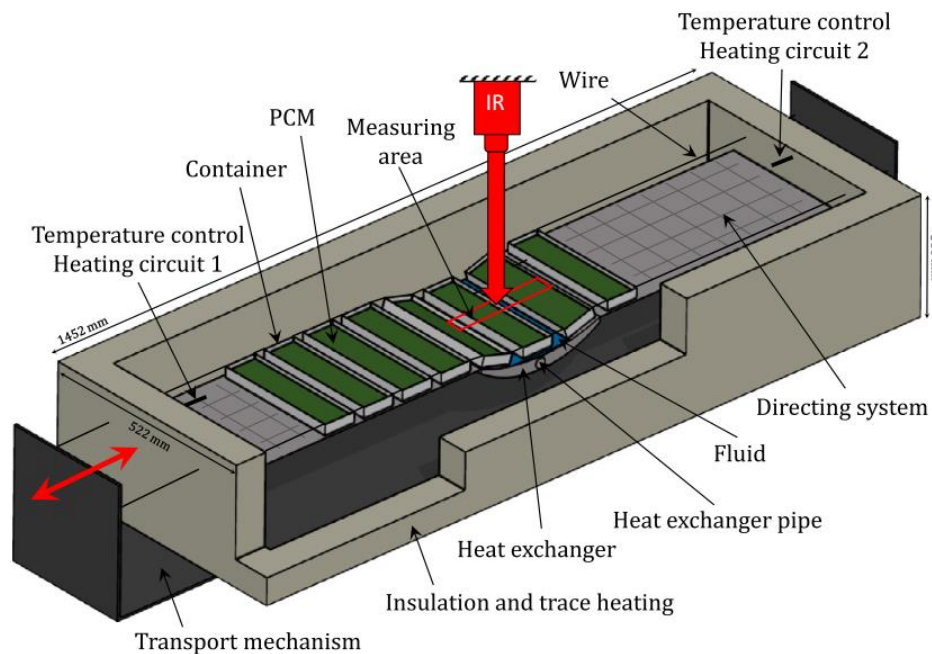


FIGURE 5-28: SCHEMATIC OF MOVING BED PCM STORAGE CONCEPT SOURCE: POINTNER AND STEINMANN 2016).

REFERENCES

- Allouche, Y., Varga, S., Bouden, C., Oliveira, A. C. (2015) Experimental determination of the heat transfer and cold storage characteristics of a microencapsulated phase change material in a horizontal tank. *Energy Conversion and Management*, 94, 275-285.
- Bauer, D., Jockenhöfer, H., Johnson, M., Seitz, M. (2017) Rotating Drum Latent Heat Thermal Energy Storage for CSP. *SolarPACES*, Santiago de Chile, Chile.
- Brüggemann, D., König-Haagen, A., Kasibhatla, R. R., Höhlein, S., Glatzel, U., Völkl, R., Agarkov, N. (2017) *Entwicklung makroverkapselter Latentwärmespeicher für den Transport von Abwärme (MALATrans): Abschlussbericht: Laufzeit: 01.07. 2013 bis 31.12. 2016*. Universität Bayreuth, Lehrstuhl für Technische Thermodynamik und Transportprozesse (LTTT).
- Buschle, J., Steinmann, W.-D., Tamme, R. (2006) Latent heat storage for process heat applications. *Ecstock Conference* New Jersey, USA.
- Dannemand, M., Dragsted, J., Fan, J., Johansen, J. B., Kong, W., Furbo, S. (2016) Experimental investigations on prototype heat storage units utilizing stable supercooling of sodium acetate trihydrate mixtures. *Applied Energy*, 169, 72-80.
- Dannemand, M., Johansen, J. B., Kong, W., Furbo, S. (2016) Experimental investigations on cylindrical latent heat storage units with sodium acetate trihydrate composites utilizing supercooling. *Applied Energy*, 177, 591-601.

- Delgado, M., Lazaro, A., Mazo, J., Peñalosa, C., Dolado, P., Zalba, B. (2015) Experimental analysis of a low cost phase change material emulsion for its use as thermal storage system *Energy Conversion and Management*, 106, 201-212.
- Delgado, M., Lazaro, A., Mazo, J., Penalosa, C., Marin, J. M., Zalba, B. (2017) Experimental analysis of a coiled stirred tank containing a low cost PCM emulsion as a thermal energy storage system. *Energy*, 138, 590-601.
- Diaconu, B. M., Varga, S., Oliveira, A. C. (2010) Experimental study of natural convection heat transfer in a microencapsulated phase change material slurry. *Energy*, 35, (6), 2688-2693.
- Diarce, G., Campos-Celador, A., Sala, J. M., Garcia-Romero, A. (2018) A novel correlation for the direct determination of the discharging time of plate-based latent heat thermal energy storage systems. *Applied Thermal Engineering*, 129, 521-534.
- Favier, P., Zalewski, L., Lassue, S., Anwar, S. (2016) Designing an Automatic Control System for the Improved Functioning of a Solar Wall with Phase Change Material (PCM). *Open Journal of Energy Efficiency* 05, 19–29.
- Gschwander, S., Schossig, P. (2006) Phase Change Slurries as heat transfer and storage fluids for cooling applications. *Ecostock Conference*, New Jersey, USA.
- Heinz, A., Streicher, W. (2006) Application of phase change materials and PCM-slurries for thermal energy storage. *Ecostock Conference*, New Jersey, USA, 2006.
- Herbinger, F., Patil, A., Groulx, D. (2019) Characterization of Different Geometrical Variations of a Vertical Finned Tube-and-Shell Heat Exchanger. *Eurotherm Seminar #112 Advances in Thermal Energy Storage*, 10 p.
- Huang, M. J., Eames, P. C., McCormack, S., Griffiths, P., Hewitt, N. J. (2011) Microencapsulated phase change slurries for thermal energy storage in a residential solar energy system. *Renewable Energy*, 36, (11), 2932-2939.
- Höhlein, S., König-Haagen, A., Brüggemann, D. (2018) Macro-Encapsulation of Inorganic Phase-Change Materials (PCM) in Metal Capsules. *Materials* 11.9, 1752.
- Joulin, A., Zalewski, L., Lassue, S., Naji, H. (2014) Experimental investigation of thermal characteristics of a mortar with or without a micro-encapsulated phase change material. *Applied Thermal Engineering* 66, 171–180.
- Kappels, T., Kohnen, T., Hanu, G. L., Pollerberg, C. (2014) Design and retrofitting of a cold storage replacing water with phase change slurries. *Eurotherm Seminar #99. Advances in Thermal Energy Storage*, Lleida (Spain).
- Leang, E., Tittlein, P., Zalewski, L., Lassue, S. (2017) Numerical study of a composite Trombe solar wall integrating microencapsulated PCM. *Energy Procedia, CISBAT 2017 International Conference Future Buildings & Districts – Energy Efficiency from Nano to Urban Scale* 122, 1009–1014.
- Medrano, M., Yilmaz, M. O., Nogues, M., Martorell, I., Roca, J., Cabeza, L. F. (2009) Experimental evaluation of commercial heat exchangers for use as PCM thermal storage systems. *Applied Energy*, 86, (10), 2047-2055.
- Mehling, H., Cabeza, L. F. (2008) *Heat and cold storage with PCM*. Berlin: Springer.
- Nepustil, U., Laing-Nepustil, D., Lodemann, D., Sivabalan, R., Hausmann, V. (2016) High Temperature Latent Heat Storage with Direct Electrical Charging - Second Generation Design. *10th International Renewable Energy Storage Conference*, 99, 314-320.
- Pizzolato, A., Sharma, A., Maute, K., Sciacovelli, A., Verda, V. (2017) Design of effective fins for fast PCM melting and solidification in shell-and-tube latent heat thermal energy storage through topology optimization, *Applied Energy*, 208, 210-227.
- Pointner, H., Steinmann, W. D. (2016) Experimental demonstration of an active latent heat storage concept. *Applied Energy*, 168, 661-671.
- Prieto, M.M., Gonzalez, B., Granado, E. (2016) Thermal performance of a heating system working with a PCM plate heat exchanger and comparison with a water tank. *Energy and Buildings*, 122, 89-97.
- Schossig P., Henning H. -M., Gschwander S., Hausmann T. (2005) Micro-encapsulated phase-change materials integrated into construction materials. *Solar Energy Materials and Solar Cells*, 89, 297-306.

- Skaalum, J., Groulx, D. (2020) Heat transfer comparison between branching and non-branching fins in a latent heat energy storage system. *International Journal of Thermal Sciences*, 152, 106331.
- Streicher, W., Heinz, A., Puschnig, P., Schranzhofer, H., Eisl, G., Heimrath, R., et al. (2006) Fortschrittliche Wärmespeicher zur Erhöhung von solarem Deckungsgrad und Kesselnutzungsgrad sowie Emissionsverringern durch verringertes Takten. Proj IEA-SHC Task 2006. 32.
- Stutz, B., Le Pierres, N., Kuznik, F., Johannes, K., Palomo Del Barrio, E., Bédécarrats, J.-P., Gibout, S., Marty, P., Zalewski, L., Soto, J., Mazet, N., Olives, R., Bezia, J.-J., Minh, D.P. (2017) Storage of thermal solar energy. *Comptes Rendus Physique, Demain l'énergie* 18, 401–414.
- Tamme, R., Bauer, T., Buschle, J., Laing, D., Muller-Steinhagen, H., Steinmann, W. D. (2008) Latent heat storage above 120 degrees C for applications in the industrial process heat sector and solar power generation. *International Journal of Energy Research*, 32, (3), 264-271.
- Vorbeck, L., Gschwander, S., Thiel, P., Luedemann, B., Schossig, P. (2013) Pilot application of phase change slurry in a 5 m³ storage. *Applied Energy*, 109, 538-543.
- Yang, X., Lu, Z., Bai, Q., Zhang, Q., Jin, L., Yan, J. (2017) Thermal performance of a shell-and-tube latent heat thermal energy storage unit: Role of annular fins. *Applied Energy*, 202, 558-570.
- Zalewski, L., Franquet, E., Gibout, S., Tittlein, P., Defer, D. (2019) Efficient Characterization of Macroscopic Composite Cement Mortars with Various Contents of Phase Change Material. *Applied Sciences* 9, 1104.
- Zalewski, L., Joulin, A., Lassue, S., Dutil, Y., Rousse, D. (2012) Experimental study of small-scale solar wall integrating phase change material. *Solar Energy* 86, 208–219.
- Zipf, V., Willert, D., Neuhauser, A. (2018) "Chapter 5 - Dynamic Concept at Fraunhofer" Editor(s): Cabeza, Tay, *High Temperature Thermal Storage Systems Using Phase Change Materials*, Academic Press, Pages 109-128.
- Zipf, V., Neuhauser, A., Willert, D., Nitz, P., Gschwander, S., Platzer, W. (2013) High temperature latent heat storage with a screw heat exchanger: Design of prototype. *Applied Energy*, 109, 462-469.

5.1.2 DEFINITION OF THE TARGETED PERFORMANCE CHARACTERISTIC FOR PCM COMPONENTS

NOMENCLATURE

NTU number of transfer units

LMTD logarithmic average of the temperature difference

HTF Heat transfer fluid

CFD computational fluid dynamics

PCM Phase Change Material

ϵ : efficiency

m: mass [kg]

cp: specific heat [kJ/(kg·K)]

h: enthalpy [kJ/kg]

\dot{Q} : Heat exchange rate [kW]

\dot{m} : mass flow [kg/s]

Subscripts

In: located at the inlet of the heat transfer fluid into the PCM component

Out: located at the outlet of the heat transfer fluid from the PCM component

INTRODUCTION

In literature there are examples of studies aiming to compare different geometries and to assess the technical performance of PCM heat exchangers. These works highlight the difficulties encountered due to the lack of a standard to show the performance parameters of latent heat storages (Zondag et al, (2018), Delgado (2015), Pinnau (2009) and Brüggemann et al. (2017)). Therefore, the comparison of different system configurations and the assessment of the improvement achieved are based on the re-calculation or estimation from the data showed by the authors.

The heat exchanger performance of latent heat storage shows a transient nature because various key properties, such as temperature, PCM effective heat capacity, density and viscosity are not constant over the charging and discharging processes. Therefore, as it is deeply justified in Groulx (2018), conventional heat exchanger analysis (ϵ -NTU, LMTD) is not directly suitable for the performance assessment.

Unlike steady state heat exchanger analysis, transient heat exchanger analysis is very complex. The main conclusions obtained from the literature review for evaluation of performance of heat exchanger under unsteady-state condition are as follows:

- There are many solutions available in literature to the transient heat exchanger problem. However, each solution is valid over a limited range of independent parameters.
- Analytic solution, CFD and experimental characterization are the approaches most commonly adopted
- In those cases, non-steady state conditions are due to a change in the temperature at the inlet or a variation of the HTF mass flow over time.

The transient heat transfer effectiveness $\epsilon(t)$ is presented in literature (Gao et al., Amagour et al. and Ma et al.) as a performance parameter for the transient response of heat exchangers. Some examples of ϵ -NTU approach applied to PCM heat exchangers are found in literature. Ismail et al. (1999) present a performance study based on dimensionless numbers for PCM heat exchangers. In this study, the efficiency is defined based on an ideal heat exchange during charging assuming the PCM temperature at the higher temperature over the melting temperature range. Numerical results show the proposed parameters: solidified mass fraction, NTU and effectiveness over dimensionless time for different Biot numbers and dimensionless ratio. Belusko et al. (2012) applied this methodology to the flat plate geometry. In these works, authors highlight the difficulty to define the temperature for the ϵ -NTU methodology in PCM heat exchangers. Ma et al. (2018) proposed dimensionless design parameters of a one-tank thermocline heat storage system based on the effectiveness-number of transfer units method.

Previous works have dealt with this issue focused on PCM heat exchangers. As a result, several technical parameter definitions can be found in Rojas et al. (2011) and Romani et al. (2018). However, the overall comparison in terms of power and capacity aimed in this working group (to compare different concepts, neither depending on the operating conditions nor the size of the system) is not completed in those approaches.

As a conclusion of the literature review it can be stated that a unified procedure that allows a proper comparison of the response curves of PCM components would be useful, but it has not been developed up to date.

OBJECTIVES

This report pursues to present a set of parameters to describe the performance behaviour of PCM components and to enable the performance comparison.

In the framework of the working group 4P the PCM component consist of the arrangement of the heat exchanger and other the auxiliary component (e.g. valves, pumps or fans) which are strictly needed to run the heat exchange process between the PCM and the heat transfer fluid.

The different geometries were described in section 5.1.1.

PARAMETER DISCUSSION

A selection of suitable parameters for the assessment of PCM components for TES systems was first performed. The technical parameters are defined in two categorical groups: capacity and power.

CAPACITY

The capacity parameters were selected based on a performed literature review and they are shown in Table 5-2. The parameter descriptions and required calculation steps found in literature were discussed and completed when considered necessary. Following the obtained procedure, a capacity assessment of different TES laboratory-scale prototypes previously realised by the authors in their respective institutions was performed and shown in Table 5-3.

TABLE 5-2: CAPACITY PERFORMANCE PARAMETERS PROPOSAL FOR PCM THERMAL ENERGY STORAGE SYSTEMS.

	Parameter	Definition/calculation	Units	Additional information	Reference
Capacity	Energy storage capacity of the system	$ESC_{sys}=ESC_{mat}+ESC_{comp}$	kJ or MJ	Temperature range [Tmax,Tmin] $ESC_{mat}=m_{mat}\cdot\Delta h_{mat}$ $ESC_{comp}=m_{comp}\cdot\Delta h_{comp}$ Δh : Enthalpy variation within the temperature range	[Romani et al. 2018]

	Energy storage density	ESD: ESC_{sys}/V ESD _{without ins} : $ESC_{sys}/V_{without ins}$	kJ/m^3 or MJ/m^3	V: Total volume of the heat exchanger, considering insulation and vessel (m^3) $V_{without ins}$: Total volume of the heat exchanger and vessel, but not considering insulation (m^3)	
--	------------------------	--	------------------------------------	---	--

POWER OVER TIME

The first approach to characterize the power performance was assessed by comparison of the heat exchange rate over time. This approach is simple and straightforward, because the PCM component is assumed to work using a heat transfer fluid (HTF) with no phase change. Therefore, it only requires the inlet and outlet temperatures and mass flow rate data to achieve an initial estimation. The heat transfer rate is then calculated as shown in equation 1:

$$\dot{Q}(t) = \dot{m}_{HTF} \cdot c_{p,HTF} \cdot (T_{HTF,in}(t) - T_{HTF,out}(t)) \text{ eq. 1}$$

Usually the HTF mass flow is kept constant during the testing. Temperature of the HTF at the inlet of the PCM component often is constant. However, the heat exchange rate and the outlet temperature vary over time.

Table 5-3 presents the systems studied in this working group and more detailed information on the systems is provided in the appendices.

Table 5-3: Capacity and configuration characteristics of the PCM components studied in the working group.

	System A	System B	System C	System D	System E	System F	System G	System H	System I	System J	System K
<i>Institution</i>	EHU-UPV	U. Bay-reuth	Unizar	Unizar	Unizar	ZAE	KTH	DTU	DTU	DTU	LAMTE
<i>HTF mass flow (kg/min)</i>	2.4	2.5	6.65	6.5	1.68	(3 m ³ /h) 50		5	10	7	9
<i>HTF fluid</i>	water	thermal oil	water	water	air	water	water	water	water	water	water
<i>Storage capacity (MJ)</i>	2.95	8.5	5.3	6.9	24.4	288	282	Total: 108 MJ [1] Short-term: 61 MJ [1] Long-term: 47 MJ [1]	Total: 98 MJ [1] Short-term: 56 MJ [1] Long-term: 42 MJ [1]	Total: 50 MJ [1] Short-term: 26 MJ [1] Long-term: 24 MJ [1]	2.8 MJ
<i>Storage density (MJ/m³)</i>	78	32.6	113.9	139	44	288 (without insulation)	201	100	248	167	204
<i>Concept</i>	PCM in flat plates (3.3.1)	PCM in cylinders (3.3)	Tank+Internal coil (3.5)	System C+stirrer (3.5)	PCM in flat plates (3.3.1)	Capillary tubes (3.2.1)		PCM in flat plates (3.3.1)	Tank in tank(8)	Tank with internal H.X. (2.2)	Shell-and-tube (PCM in shell, fins on tubes) (2.1)

Figure 5-29 shows the heat exchange rate (Power) over time of the PCM components presented in Table 5-3. The results are dependent on the system size, HTF temperature and operating conditions. Systems working with water as HTF show noticeable greater values of power in the first period of the discharging process. The greater values are caused by the flowing out of the initial volume of water at the initial temperature of the PCM. Then the heat transfer rate, evaluated by the temperature difference between inlet and outlet of the PCM component, does not correspond to a heat transfer between PCM and water. These values can be corrected by the estimation of the thermal energy stored as HTF at the PCM initial temperature.

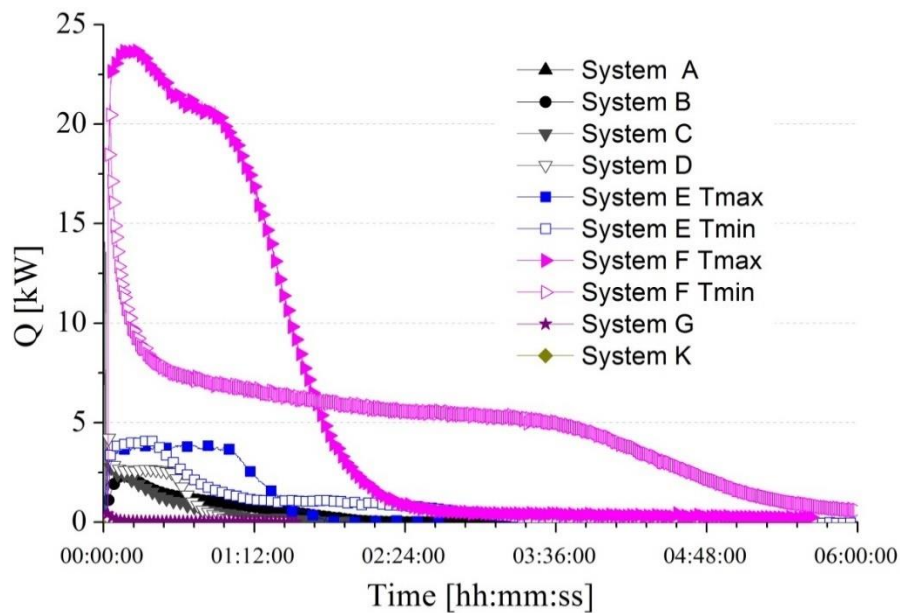


FIGURE 5-29: HEAT EXCHANGE RATE OVER TIME OF THE PCM COMPONENTS STUDIED IN THE WORKING GROUP.

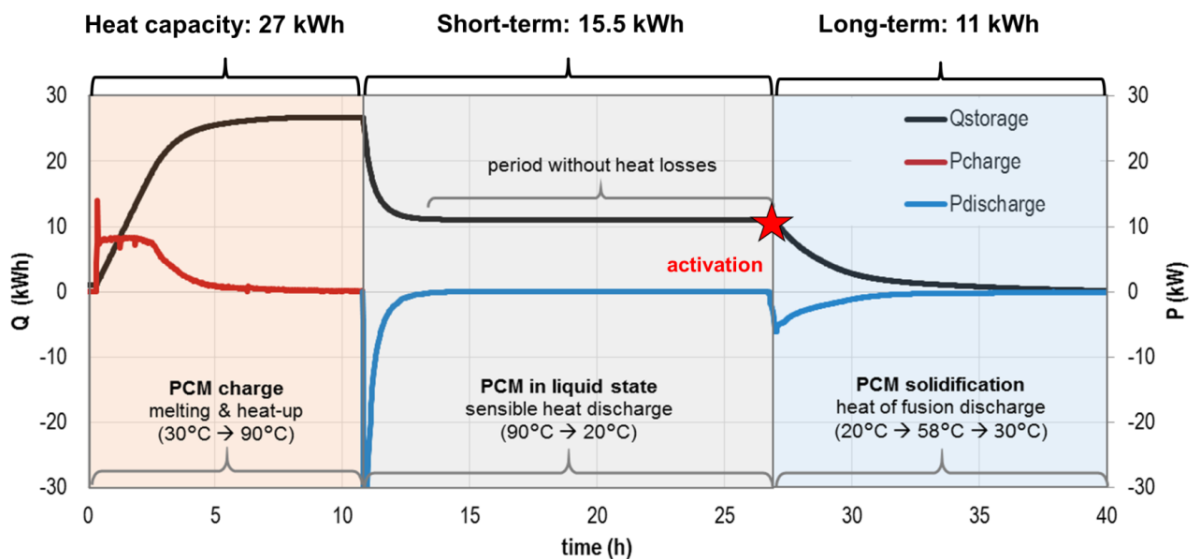


FIGURE 5-30: ENERGY STORED AND HEAT TRANSFER RATE OVER TIME OF A PCM COMPONENT USING A SUPERCOOLED PCM.

POWER OVER STATE OF CHARGE

In order to find a more comparable parameter with minimum influence of the size and the temperature range of operation, the heat exchange rate (Power) is represented over the state of charge. The state of charge estimation is based on the ratio between the energy exchanged until the moment t and the total storage capacity. Total storage capacity is estimated by integration of the heat transfer rate over time. The comparison is sensible to the criteria adopted to select the end of integration.

As shown in Figure 5-31 and Figure 5-32, the dependency on operation conditions has a high influence on the power curves. To extract some conclusion on the power performance of the systems more information is needed.

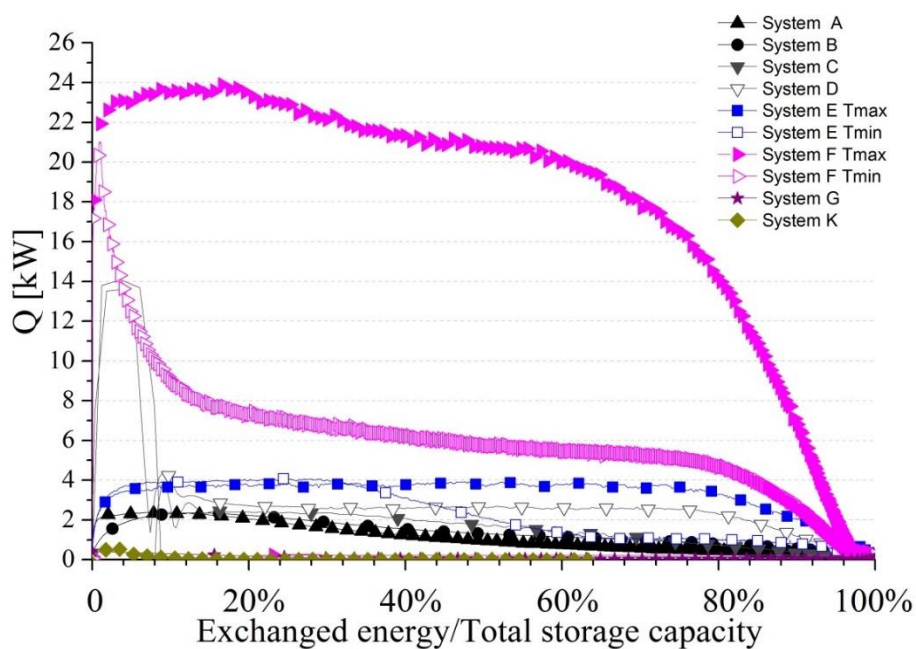


FIGURE 5-31: HEAT EXCHANGE RATE OVER STATE OF CHARGE OF THE PCM COMPONENTS STUDIED IN THE WORKING GROUP.

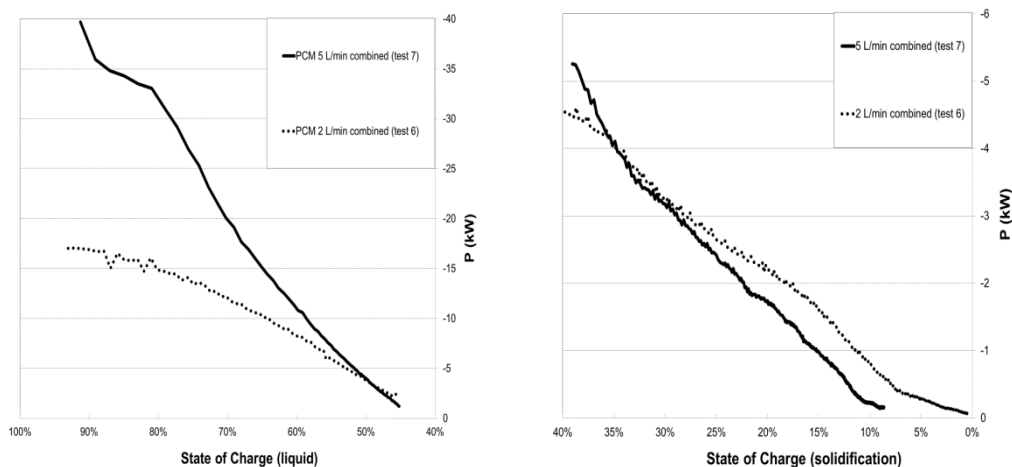


FIGURE 5-32: HEAT EXCHANGE RATE OVER STATE OF CHARGE OF A PCM COMPONENT USING A SUPERCOOLED PCM.

OVERALL HEAT TRANSFER COEFFICIENT (U·A)

The overall heat transfer coefficient (U·A) can be determined over the energy stored and used as parameter for comparison. The estimation of U·A coefficient relies on the estimation of the average temperature difference between the HTF and the PCM (equations 2-6).

$$\dot{Q}(t) = \dot{m}_{\text{HTF}} \cdot c_{\text{HTF}} \cdot (T_{\text{HTF,in}} - T_{\text{HTF,out}}(t)) \quad (\text{eq. 2})$$

$$\dot{Q}(t) = UA \cdot \overline{\Delta T_m} \quad (\text{eq. 3})$$

$$\overline{\Delta T_m} = \frac{\Delta T_2 - \Delta T_1}{\ln\left(\frac{\Delta T_2}{\Delta T_1}\right)} \quad (\text{eq. 4})$$

$$\Delta T_1 = T_{\text{HTF,in}} - \overline{T}_{\text{ref},1} \quad (\text{eq. 5})$$

$$\Delta T_2 = T_{\text{HTF,out}}(t) - \overline{T}_{\text{ref},2} \quad (\text{eq. 6})$$

As explained before, the transient nature of the PCM melting or solidification processes implies non-linear variations of the PCM temperature over time and over the volume of PCM. In order to have a more comparable parameter the mean of UA over energy stored instead of over time is proposed (eq. 7).

$$UA_{\text{mean}} = \frac{\int UA \cdot dQ}{Q} \quad (\text{eq. 7})$$

Lazaro et al. (2019) investigated the most adequate definition of reference temperatures T_{ref} . In this study, six different alternatives were defined and studied as reference temperatures. The study was accomplished using a numerical model validated against experimental measurements for flat plate geometry. The HTF studied were water and air. The results showed that using the maximum temperature of the storage when a discharging process is analyzed, $T_{\text{max}}(t)$, as reference temperature the UA_{mean} value is less dependent on the operating conditions and storage size. If the information on temperature distribution inside the system is not available, the initial temperature of the storage system would be the best alternative to $T_{\text{max}}(t)$.

NORMALIZED POWER IN RELATION TO THE VOLUME AND TEMPERATURE DIFFERENCES (\dot{Q}_{norm})

Lazaro et al. (2019) proposed the use of a normed \dot{Q}_{norm} parameter [W/(m³·K)] (eq. 8). The proposed parameter is a normalized power in relation to the volume (power compactness) and temperature differences (operation temperatures).

$$\dot{Q}_{\text{norm}} = \frac{\dot{Q}_{\text{mean}}}{V \cdot \Delta T} \quad (\text{eq. 8})$$

Where V is the volume of the storage [m³], \dot{Q}_{mean} [W] is the mean of the exchanged power using an exchanged energy basis and ΔT [K] is the temperature difference evaluated in equation 9 with $T_{\text{h,mean}}$ [K] evaluated in equation 10. In these equations, H_{PCM} and H_{HTF} are the corresponding enthalpies [J] as a function of temperature of the PCM and the heat transfer fluid in the storage unit.

$$\Delta T = \frac{\text{abs}(T_{\text{h,mean}} - T_{\text{initial}}) \cdot \text{abs}(H_{\text{PCM,in}} - H_{\text{PCM,initial}}) + \text{abs}(T_{\text{in}} - T_{\text{initial}}) \cdot \text{abs}(H_{\text{HTF,in}} - H_{\text{HTF,initial}})}{\text{abs}(H_{\text{PCM,in}} - H_{\text{PCM,initial}}) + \text{abs}(H_{\text{HTF,in}} - H_{\text{HTF,initial}})} \quad (\text{eq. 9})$$

$$T_{h,mean} = \frac{\int_{T_{initial}}^{T_{in}} H_{PCM}(T) - H_{PCM_{initial}} dT}{H_{PCM_{in}} - H_{PCM_{initial}}} \quad (\text{eq. 10})$$

PROCEDURE PROPOSED

Attending to the discussion on the definition of performance parameter presented in section 3, the following procedure is proposed.

Capacity:

- Energy storage capacity of the system

$$ESC_{sys} = ESC_{mat} + ESC_{comp}$$

$$ESC_{mat} = m_{mat} \cdot \Delta h_{mat}$$

$$ESC_{comp} = m_{comp} \cdot \Delta h_{comp}$$

Where the enthalpy variation (Δh) of all the components and materials of the storage system are determined over the operation temperatures (Temperature range $[T_{max}, T_{min}]$).

- Energy storage density.

Two parameters are used to describe the storage density:

$$ESD = ESC_{sys} / V$$

$$ESD_{without\ ins} = ESC_{sys} / V_{without\ ins}$$

Where V is the total volume of the heat exchanger, considering insulation and vessel (m^3) and $V_{without\ ins}$ is the total volume of the heat exchanger and vessel, but not considering insulation (m^3)

Power:

- UA_{mean} values (eq. 7) based on the stored energy and estimated using the maximum temperature T_{max} as reference temperature for the logarithmic mean temperature difference are proposed to compare PCM components during discharging processes. If registered temperatures do not allow to identify the maximum temperature, then initial temperature can be used for the UA estimation. For those system using water as HTF, the thermal capacity of the water volume at the beginning of the measurement should be subtracted from power curves. The end of integration of power curves over time is determined at the moment when the exchanged energy is 90% of the total storage capacity.

- \dot{Q}_{norm} parameter [$\text{W}/(\text{m}^3 \cdot \text{K})$] estimated according to equations 8-10.

REFERENCES

- Amagour, M. E. H., Rachek, A., Bennajah, M. & Touhami, M. E. (2018) Experimental investigation and comparative performance analysis of a compact finned-tube heat exchanger uniformly filled with a phase change material for thermal energy storage. *Energy Conversion and Management* 165:137-151.
- Belusko, M., Halawa, E. & Bruno, F. (2012) Characterising PCM thermal storage systems using the effectiveness-NTU approach. *International Journal of Heat and Mass Transfer* 55(13-14):3359-3365.
- Brüggemann, D., König-Haagen A., Kasibhatla R. R., Höhle S., Glatzel U., Völkl R., and Agarkov N. (2017) Entwicklung makroverkapselter Latentwärmespeicher für den Transport von Abwärme (MALATrans): Abschlussbericht: Laufzeit: 01.07. 2013 bis 31.12. 2016. Universität Bayreuth, Lehrstuhl für Technische Thermodynamik und Transportprozesse (LTTT)
- Delgado, M., Lazaro, A., Mazo, J., Penalosa, C., Dolado, P. & Zalba, B. (2015) Experimental analysis of a low cost phase change material emulsion for its use as thermal storage system. *Energy Conversion and Management* 106:201-212.
- Gao, T. Y., Geer, J. & Sammakia, B. (2015) Development and verification of compact transient heat exchanger models using transient effectiveness methodologies. *International Journal of Heat and Mass Transfer* 87:265-278.
- Groulx, D. (2018) The rate problem in solid-liquid phase change heat transfer: efforts and questions toward heat exchanger design rules In Proceedings of Proceedings of the 16th International Heat Transfer Conference IHTC-16.
- Ismail, K. A. R. & Goncalves, M. M. (1999) Thermal performance of a pcm storage unit. *Energy Conversion and Management* 40(2):115-138.
- Lazaro, A., Delgado, M., König-Haagen, M. A., Höhle, S. and Diarce, G. (2019) Technical performance assessment of phase change material components, presented, International Conference on Solar Heating and Cooling for Buildings and Industry, SHC 2019, Santiago de Chile, Chile.
- Ma, Z., Li, M.-J., Yang, W.-W. & He, Y.-L. (2018) General performance evaluation charts and effectiveness correlations for the design of thermocline heat storage system. *Chemical Engineering Science* 185:105-115.
- Pinnau S. (2009) Strömungs- und kältetechnische Optimierung von Latentkältespeichern, Abschlussbericht, Universität Dresden
- Rojas, E., Bayon, R., Adinberg, R., Valenzuela, L., Laing, D., Py, X., Bauer, T. & Fabrizi, F. (2011) Definition of standardised procedures for testing thermal storage prototypes for concentrating solar thermal plants. WP 15 report, SFERA project available on line at http://sfera.sollab.eu/index.php?page=downloads_jra_reports (17/07/2019).
- Romani, J., Gasia, J. & Cabeza, L. F. (2018) Definitions of technical parameters for thermal energy storage (TES). Available on line from International Energy Agency, ECES, Annex 30: Thermal Energy Storage for cost effective energy management & CO2 mitigation. <https://www.eces-a30.org/> (17/07/2019).
- Zondag, H. A., De Boer, R., Smeding, S. F. & Van Der Kamp, J. (2018) Performance analysis of industrial PCM heat storage lab prototype. *Journal of Energy Storage* 18:402-413.



5.2 SUBTASK 4T: COMPONENT DESIGN FOR TCM

5.2.1 SORPTION BASED LONG-TERM THERMAL ENERGY STORAGE – PROCESS CLASSIFICATION AND ANALYSIS OF PERFORMANCE LIMITATIONS: A REVIEW

Abstract: In sorption heat storage, one of the sources of discrepancy between theoretical material-based energy storage potential and resulting system performance is the choice of process type. In this paper, in order to understand this performance deviation, a sorption heat storage process categorisation is proposed. This is followed by a review of reported sorption systems categorised according to the proposed process classification. An analysis of the reported systems is then undertaken, focusing on the ratio of resulting temperature gain in sorption (ad- or absorption), compared to required temperature lift in desorption. This measure is termed temperature effectiveness and enables a form of system performance evaluation in the broad landscape of sorption thermal energy storage demonstrators. It is argued that other performance parameters such as volumetric energy storage density and volumetric charge and discharge power density are not adequate for comparison due to the highly varying testing conditions applied. From the system evaluation, it is seen that best temperature effectiveness is generally found in a closed, transported process with the ability of single sorbent pass and true counter flow heat exchange.

Reference: Fumey, B., Weber, R., & Baldini, L. (2019). Sorption based long-term thermal energy storage–Process classification and analysis of performance limitations: A review. *Renewable and Sustainable Energy Reviews*, 111, 57-74.

5.2.2 INVENTORY OF SORPTION HEAT STORAGE COMPONENT AND SYSTEM DESIGNS CURRENTLY UNDER INVESTIGATION BY TASK AND ANNEX PARTNERS

INTRODUCTION

This document features a collection of 2+ page descriptions of the sorption based heat storage systems currently investigated by the IEA SHC Task 58 and ECES Annex 33 partner institutes. In this report, sorption includes solid adsorption and liquid as well as solid absorption, involving hydration and hydroxide reaction.

Based on the various sorbent materials, solid or liquid, their specific reactivity as well as chemical and mechanical stability, four basic system designs, open versus closed [Bales 2005] and fixed versus transported [Sørensen et al. 2015] are followed. The former refers to contact to the ambient air and the later refers to the sorbent material handling. Figure 5-33 illustrates the basic system variations.

Choice of design is largely based on choice of sorbent material. Sorbents that react with CO₂, are hazardous or easily airborne are studied in closed systems [N'Tsoukpoe et al. 2013], and non-hazard-

ous mainly solid materials are considered for open system [Kerskes et al. 2011]. Fixed sorbent systems are applied for solid sorbents [Zondag et al., 2013] and transported sorbent systems are used for liquids [Weber and Dorer, 2008]. Even so, as this document shows, variations are found.

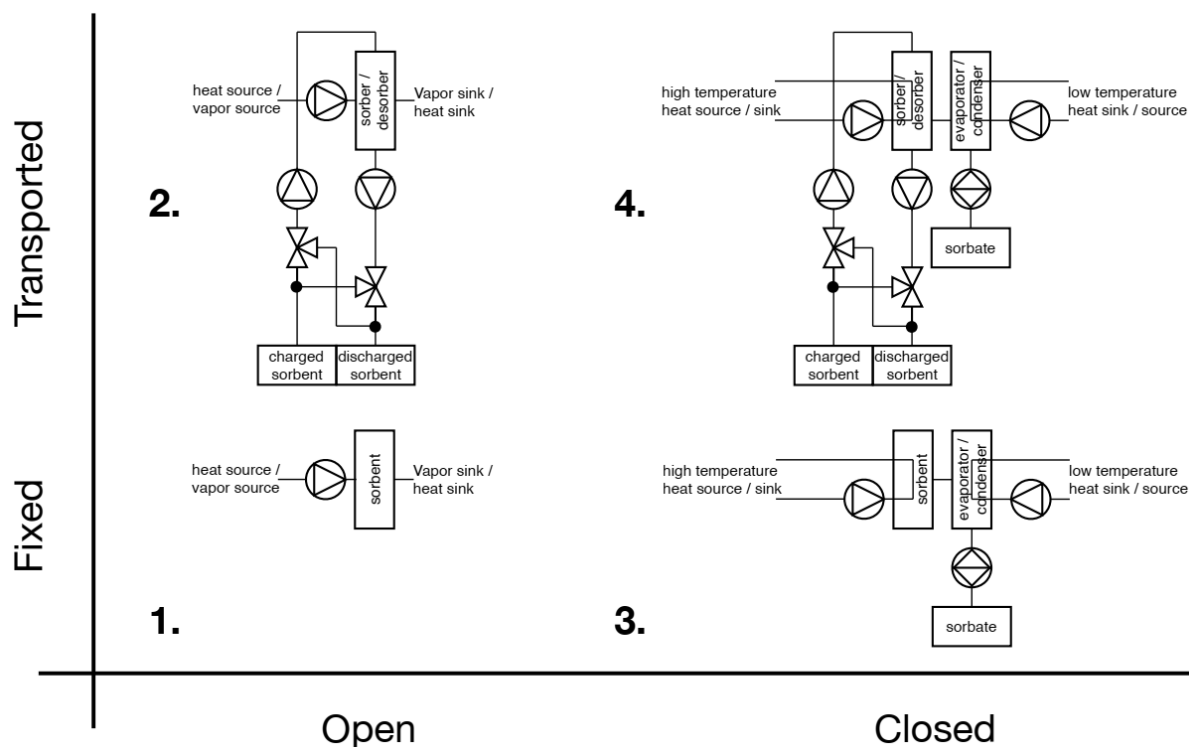


FIGURE 5-33: ILLUSTRATION OF THE BASIC SORPTION HEAT STORAGE SYSTEMS.

The following inventory of sorption heat storage systems is divided into the four basic system approaches. The described systems include a short overview followed by a uniform system schematics for simplicity of system comparison, a list of major components, a discussion of benefits and challenges and further examples in literature. The uniform system schematics is a unique approach followed in this documentation, in an attempt to enable a simple system overview.

References

Bales, C., 2005. Thermal Properties of Materials for Thermo-chemical Storage of Solar Heat, A Report of IEA Solar Heating and Cooling programme – Task 32.

Sørensen et al. 2015, Bent Sørensen, "Solar Energy Storage", Academic Press, June 2015, ISBN: 9780124095496

N'Tsoukpoe K.E., Le Pierrès N., Luo L., "Experimentation of a LiBr-H₂O absorption process for long-term solar thermal storage: prototype design and first results", Energy 2013.

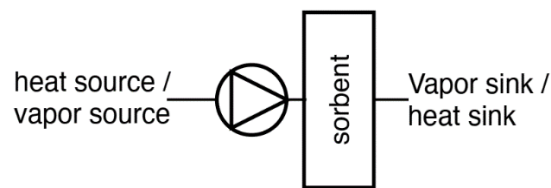
Kerskes, H., Mette, B., Bertsch, F., Asenbeck, S., Drück, H., 2011. Development of a ThermoChemical Energy Storage for Solar Thermal Applications. In: ISES Solar World Congress 2011.

Zondag H., Kikkert B., Smeding S., de Boer R., Bakker M., Prototype thermochemical heat storage with open reactor system, Applied Energy, Volume 109, 2013, Pages 360-365.

Weber R., Dorer V. Long-term heat storage with NaOH. Vacuum 2008;82(7):708–16.

OPEN-FIXED SYSTEMS

The open and fixed bed process is the simplest approach followed. Sorbents with a high affinity to water are used and in general, air is used for both sorbate (water vapor) transport and heat transport, as illustrated. A variation can be air-based vapor transport and water-based heat transport. Main challenges encountered are, high pressure drop through the adsorbent material and low temperature gain due to high flow of inert gas and mean adsorbent temperature.



THERMOCHEMICAL ENERGY STORAGE FOR DOMESTIC APPLICATIONS

TECHNICAL UNIVERSITY OF EINDHOVEN – NETHERLAND, MAX BEVING

Process description: Open sorption process represents a general class of solid/gas thermochemical energy storage, heat transforming and heat upgrading processes. It can be implemented for numerous reversible solid/gas exothermic and endothermic interactions, including adsorption principle, chemical sorption by salt hydrates and chemical reactions. The solid component is called sorbent and is usually placed in a specially designed vessel, the so-called reactor. The gaseous component is called working fluid and is a mixture of inert and reactant gases. The inlet and outlet reactor boundaries are openly connected to the surrounding environment, whereby the working fluid circulates as shown on Figure 5-34, enabling heat supply/evacuation and mass transfer (in terms of reactant gas molecules) to the solid sorbent.

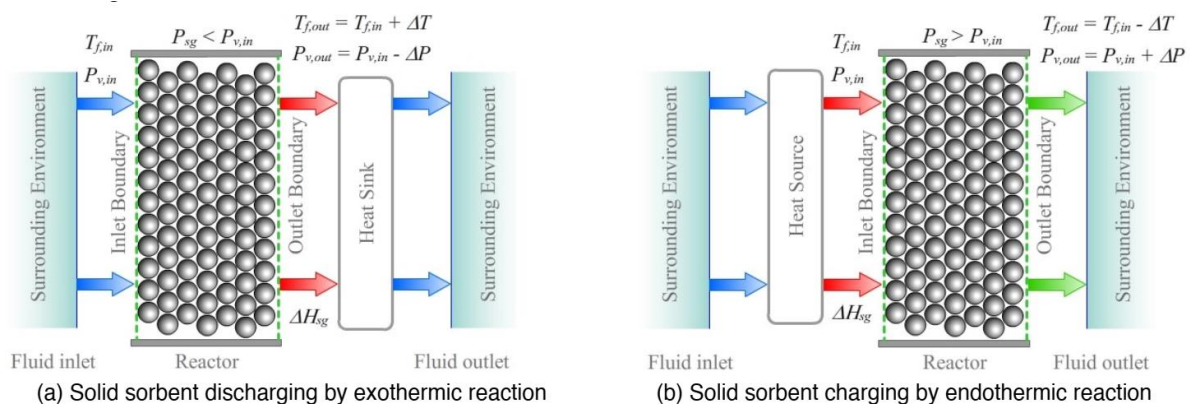


FIGURE 5-34: OPEN SORPTION PROCESS OPERATING PRINCIPLE.

The process is driven by operating conditions defined by fluid temperature $T_{f,in}$ and partial pressure of reactant gas $P_{v,in}$ at the reactor inlet. When $P_{sg} < P_{v,in}$, where P_{sg} is solid/gas equilibrium pressure, the molecules of reactant gas are being captured by porous solid sorbent that provokes the heat release (exothermic reaction). The reaction heat ΔH_{sg} is evacuated from the reactor by the inert gas, whose outlet temperature rises $T_{f,out} = T_{f,in} + \Delta T$. On the contrary, when $P_{sg} > P_{v,in}$, the molecules of reactant gas are being released from porous solid and carried away with inert gas, that corresponds to the endothermic reaction, and the reaction heat ΔH_{sg} must be supplied to the reactor from the heat source.

In thermochemical energy storage applications, the exothermic reaction is used to supply the released heat to the heat sink at the required temperature level $T_{f,out}$ and is called energy discharging operation (see Figure 5-34a), while the regeneration of the solid sorbent follows by the endothermic reaction and is called energy charging operation (see Figure 5-34b).

Schematics: The open sorption reactor investigated at the Eindhoven University of Technology operates under atmospheric pressure and uses moist air as working fluid. The thermochemical material used for energy storage in this reactor, is 250 liter Zeolite 13X. The goal of this setup is to investigate the possibility of using energy harvested by solar thermal collectors (currently simulated by electric heaters) to dry the zeolite during summer and extract the stored heat from the zeolite during winter. This energy can be used for floor heating or domestic hot tap water production. The schematic of the setup is shown in Figure 5-35 and the uniform schematics is shown in Figure 5-36.

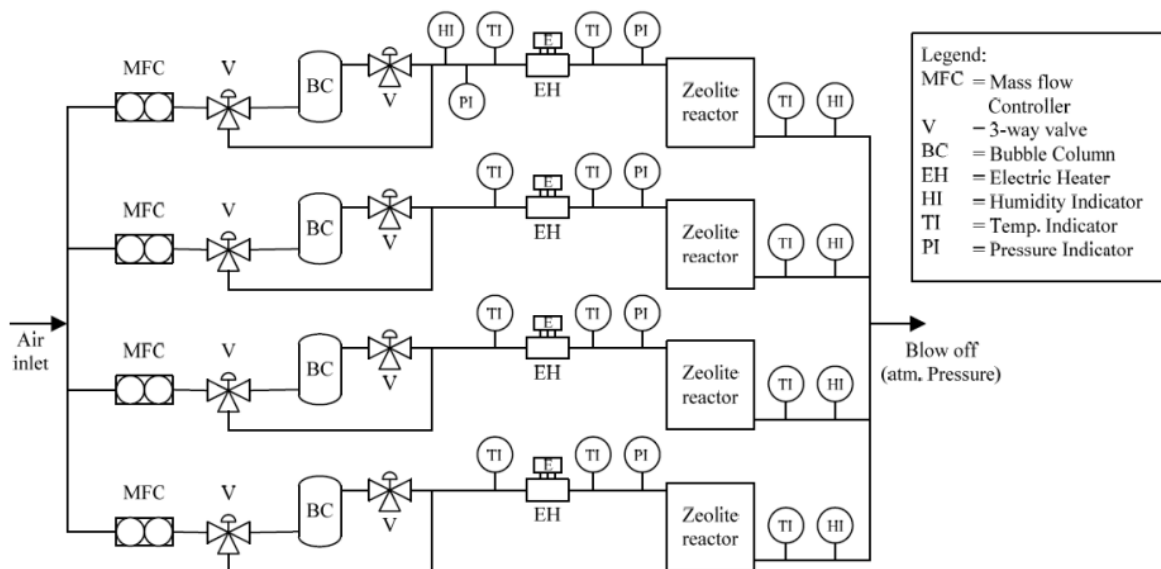


FIGURE 5-35: SCHEMATIC OF THE ZEOLITE PILOT REACTOR.

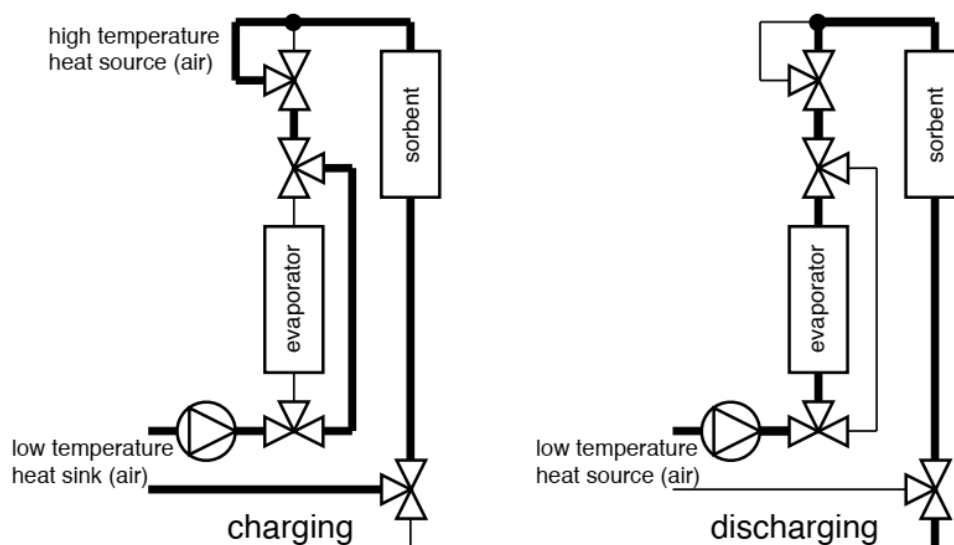


FIGURE 5-36: UNIFORM SCHEMATICS OF THE EINDHOVEN UNIVERSITY OF TECHNOLOGY OPEN FIXED SYSTEM, SHOWING THE CHARGING AND DISCHARGING PROCESS.

The air fed to the setup comes from a pressurized grid. Mass flow controllers are installed to control the air mass flow rates. After the mass flow controllers, 3-way valves have been installed. Using these valves, the air can be fed to the bubble columns for hydration, or the bubble columns can be bypassed for dehydration. After the bubble columns another 3-way valve is placed to blow off the air flow until the temperature after humidification is constant. The water level in the bubble columns can be controlled to reach the desired air humidity. The air passes through electric heaters simulating the solar thermal system. The zeolite bed is charged at a maximum temperature of 180°C. After the heaters, the air passes through the reactors and is then blown off to the outdoor environment. Temperature and pressure sensors track the air temperature and pressure drop respectively.

Major components: Major components are the reactor vessels filled with zeolite, bubble columns (BC) to moisturize the air, electric heaters (EH) to simulate solar thermal panels supplying air of 180°C. The components allow an air mass flux of maximum 50g/s.

Benefits and challenges: The system is designed to be modular and in parallel. The modularity of the system makes it easy to scale up the thermal capacity. A parallel configuration reduces the pressure drop over the components. Currently, a temperature step from 10°C to 30°C is obtained, and a challenge is to improve the outlet temperature from 30°C to at least 65°C for hot tap water production. Implementation of hot tap water production is scheduled in the near future.

Possible working pairs: Currently, zeolite/H₂O is used in the reactors because of its stability. This setup is suitable for nontoxic, non-corrosive thermochemical materials, for example some salt-hydrate/H₂O materials (assuming they remain stable even after multiple charging or discharging cycles).

Example in literature

Hauer A. Thermal energy storage with zeolite for heating and cooling applications. In: 2nd International heat powered cycles conference - cool heat power generation systems, Paris. p. 343–8. Working pair Zeolite 13X / H₂O, amount: 7000kg, Open System, year 1997.

Bales C, Gantenbein P, Jaenig D, Kerskes H, Summer K, van Essen VM, et al. Laboratory tests of chemical reactions and prototype sorption storage units. Borlange;

de Boer R, Vanhoudt D, Claessens B, De Ridder F, Reynders G, Cuypers R, et al. Energy-hub for residential and commercial districts and transport - D3.2 report on a combination of thermal storage techniques and components. Working pair Zeolite 13X / H₂O, amount: 150kg, Open System, year 2014.

Krönauer A, Lävemann E, Hauer A. Mobile sorption heat storage in industrial waste heat recovery. In: 9th Int renew energy storage conf IRES 2015, vol. 73. Elsevier B.V.; 2015. p. 1–8. Working pair: Zeolite 13X / H₂O, amount 14000kg, Open System, year 2015.

MOBILE ADSORPTION STORAGE FOR INDUSTRIAL WASTE HEAT RECOVERY

ZAE BAYERN - GERMANY, FABIAN FISCHER, ANDREAS KRÖNAUER, EBERHARD LÄVEMANN, ANDREAS HAUER

Process description: ZAE has investigated within the public funded demonstration project “MobS II” the feasibility to transport heat on a truck from a waste incineration plant to an industrial drying process [Lävemann et al.]. The mobile heat storage is based on an open adsorption process. 14 tons of zeolite 13X were used as adsorbent. An energy storage capacity of 2.3 MWh was experimentally determined.

Schematics: In Figure 5-37 the charging process of the mobile storage is sketched and Figure 5-38 shows the respective uniform schematics. Heat from a turbine of the waste incineration plant is used to increase the temperature of the ambient air to about 130 °C. For this purpose, a steam/air heat exchanger was installed. The hot air removes the water from the zeolite. For increasing the efficiency, a heat recovery system with a cross flow air/air heat exchanger was integrated which preheats the air to the steam/air heat exchanger.

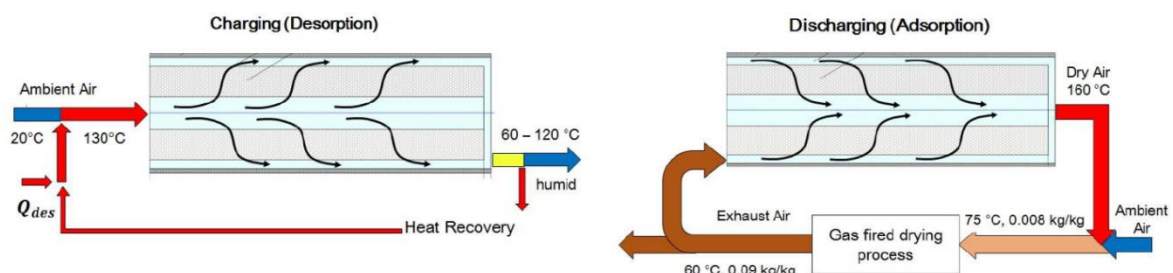


FIGURE 5-37: LEFT: SCHEMATICS OF THE CHARGING PROCESS, RIGHT: SCHEMATICS OF THE DISCHARGING PROCESS [KRÖNAUER ET AL.].

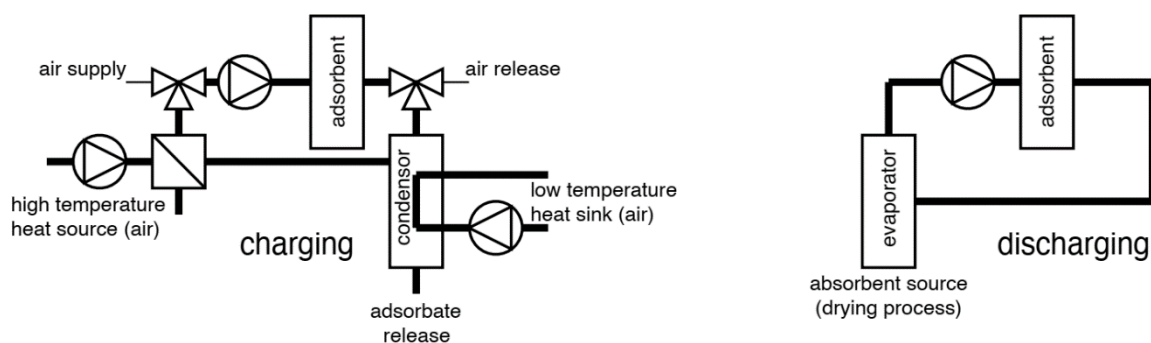


FIGURE 5-38: UNIFORM SCHEMATICS OF THE ZAE HEAT TRANSPORT SYSTEM, SHOWING THE CHARGING AND DISCHARGING PROCESS.

The discharging process is shown in Figure 5-38 right. The direction of the air flow through the storage was changed to reduce the heat losses during charging and discharging. The aim of the mobile storage is to reduce the amount of gas which is needed for the drying process. Humid air from the drying process enters the storage and the heat of adsorption is released. The hot and dry air flow at the outlet of the storage is used to preheat the ambient air for the gas burner of the drying process.

Major components: The storage system consists of three major components: the mobile storage, the charging station at the waste incineration plant and the discharging station at the drying process. The charging and discharging station need to be individually adapted to each waste heat source and to each consumer, while the storage design does not need not be modified.

Benefits and challenges: The feasibility of the project to transport heat by means of a mobile adsorption storage could be proven. Thus, the mobile storage can be used to deliver e.g. waste heat to another location, where the heat can be used and substituted for fossil fuels. The heat production costs of the mobile storage, which were calculated for an optimized scenario, are with a value of about 67 €/MWh still above the gas prices for industry in Germany (approx. 40 €/MWh). This means that the storage is currently not economically viable.

Possible working pairs: Since the open adsorption process is connected to the ambient, the process is limited to water as adsorbate. As adsorbent, hydrophobic solid sorbents which can be shaped as beads are in principle appropriate. In economics terms, only adsorbents which are already produced and commercially available are relevant. For this reason, a zeolite 13X was used.

Examples in literature: To our knowledge, the mobile storage of ZAE is the only realized mobile adsorption system so far. Mobile heat storage based on PCM have been investigated since more than 20 years and are commercially available [<http://www.ktg-agrar.de>]. The economic efficiency of a mobile PCM storage was investigated by Deckert et al.

References

Lävemann, Eberhard, et al. "Mobile Sorptionspeicher zur industriellen Abwärmenutzung, Grundlagen und Demonstrationsanlage - MobS II" (2015) Final Report Funded by German Federal Ministry of Economics and Technology [grant number 0327383B].

Krönauer, Andreas, et al. "Mobile sorption heat storage in industrial waste heat recovery." Energy Procedia 73 (2015): 272-280. <http://www.ktg-agrar.de/geschaeftsfelder/energieproduktion-biogas/latherm.html> (30.04.2018) Deckert, Marco, et al. "Economic efficiency of mobile latent heat storages." Energy Procedia 46 (2014): 171-177.

OPEN SORPTION PROCESS WITH FIXED BED STORE FOR SEASONAL HEAT STORAGE APPLICATIONS IN BUILDINGS

ITW UNIVERSITY STUTTGART - GERMANY, REBECCA WEBER, HENNER KERSKES

Process description: Open sorption processes are open to the atmosphere and therefore in general operated under atmospheric pressure. Open sorption systems can be subdivided into fixed bed or transported material systems. In the case of a fixed bed store, heat has to be supplied to the fixed bed of storage material to charge the store. This can either be realized by heat exchangers inside the fixed bed or by heated air, flowing through the store. For the discharging process, the adsorptive, which is water in many cases, has to be supplied to the fixed bed of storage material. The adsorptive is usually transported by a carrier fluid, like ambient air. A basic principle of the ad- and desorption process is depicted in Figure 5-39.

The temperature lift is mainly dependent on the water vapor content of the air stream (partial pressure). The output power is dependent on the water vapor content and the mass flow of the air stream. The energy density depends on the difference of the adsorbed and desorbed state of the storage material. This results from the available temperature and the water vapor content of the air during the ad- and desorption process.

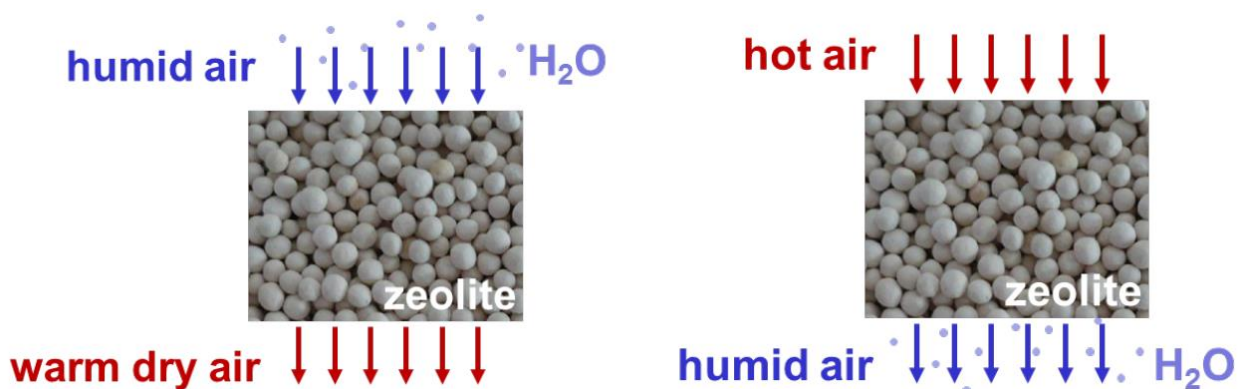


FIGURE 5-39: PRINCIPLE OF AN OPEN SORPTION PROCESS, LEFT: ABSORPTION, RIGHT: DESORPTION.

Schematics: An open sorption system for seasonal energy storage for the purpose of solar thermal space heating, developed at ITW within the project SolSpaces, is depicted in Figure 5-40 and shown in the uniform schematics in Figure 5-41. The systems main components are a fixed bed sorption store, a vacuum tube air collector and an air/air heat exchanger.

In the discharging mode of the store (adsorption) water vapor is supplied to the store via an air stream. The water vapor is adsorbed by the adsorption material, releasing heat of adsorption.

For the application of solar thermal space heating, the water vapor is supplied by the extract air from the building. The containing water vapor is adsorbed and heat of adsorption is released, heating up the air stream. This heat is transferred to the fresh air in the air/air heat exchanger. The heated fresh air then serves for space heating via the ventilation system of the building. During the heating period, the building is preferentially heated with hot air from the solar air collector through the ventilation system. Only if solar radiation is not sufficient to satisfy the demand for heat, the sorption store is discharged.

In the charging mode (desorption) high temperature heat is supplied to the store by heated air. The desorbed water is removed from the store with the air stream.

For the application of solar thermal space heating, the heat is supplied by the vacuum tube air collector on the roof of the building. Energy is recovered in the air/air heat exchanger while the fresh air is preheated. Charging mainly takes place in summer, when a plenty of solar radiation is available.

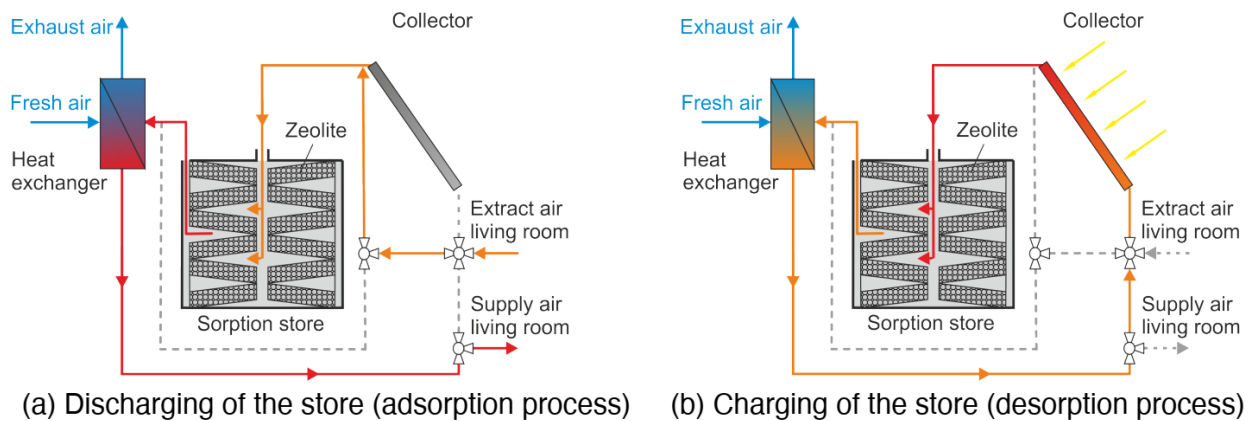


FIGURE 5-40: SCHEMATICS OF AN OPEN SORPTION PROCESS WITH FIXED BED STORE DEVELOPED FOR SEASONAL ENERGY STORAGE FOR SPACES HEATING PURPOSES (ITW, SOLSPACES PROJECT)

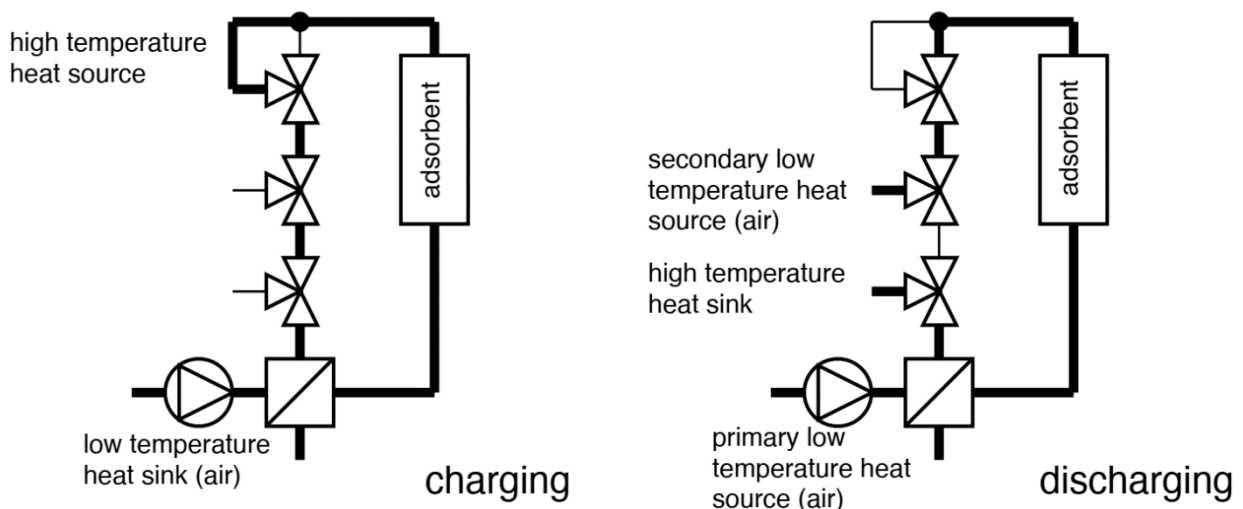


FIGURE 5-41: UNIFORM SCHEMATICS OF THE ITW SOLSPACES PROJECT SYSTEM, SHOWN THE CHARGING AND DISCHARGING PROCESS.

Major components: The major components of the open adsorption system for solar thermal space heating are the sorption store, the solar collector (vacuum tube air collector) and the air/air heat exchanger. Furthermore, there are valves, air ducts and two fans (one in the fresh air stream, one in the exhaust air stream). Fans can be placed on the cold sides of the heat exchanger, so no high temperature equipment is needed.

Benefits and challenges: Equipment requirements are reduced for open sorption processes, compared to closed adsorption systems, as vacuum tightness is difficult to handle. Open systems are well suited for the implementation in the ventilation system of a building for spaces heating purposes, especially when an air collector is used as heat source. Supplying heat for desorption is challenging, as the thermal conductivity is usually low for solid sorption materials. Furthermore, the output power is rather low for solid sorption materials and the thermal response of a large volume of storage material is slow, so there is no immediate availability of heat when space heating demand arises. Moreover, the pressure drop inside a large fixed bed store is high, requiring a high fan power. The characteristic of the newly developed sorption store within the SolSpaces project is the subdivision into smaller segments instead of having one large volume of sorption material. This segmentation offers several advantages concerning the above-named challenges: a high desorption temperature within a limited period of time (limited by solar radiation hours per day), a fast thermal response and a low pressure drop. Finally, an excellent heat recovery in the air/air heat exchanger is essential for an efficient operation of the system.

Possible working pairs

- Hygroscopic adsorbent materials (e.g. zeolite, silica gel, AIPO, SAPO, MOF,...) / H₂O
- Composite materials (e.g. salt impregnated zeolite, ...) / H₂O
- Salt hydrates / H₂O

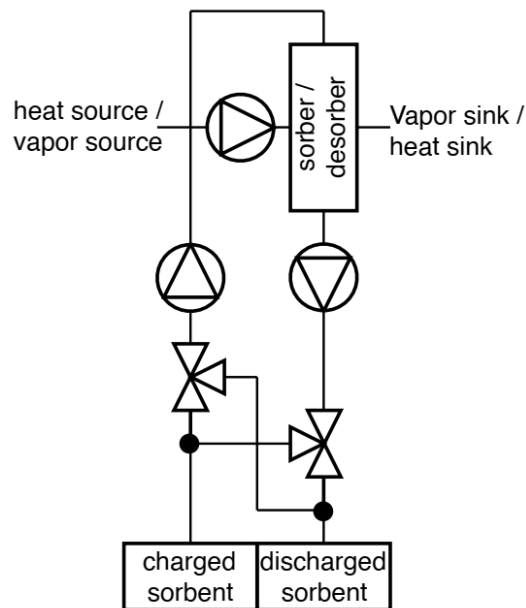
Examples in literature: The German Institute for Thermodynamics and Thermal Engineering (ITW) is working on open adsorption heat storage, with fixed bed systems for seasonal heat storage applications in buildings (SolSpaces) [Weber et al. 2016a], [Weber et al. 2016b] as well as with transported material systems (EnErChem) [Nonnen et al. 2016].

References

- Rebecca Weber, Sebastian Asenbeck, Henner Kerskes, Harald Drück, SolSpaces – Testing and performance analysis of a segmented sorption store for solar thermal space heating, *Energy Procedia* 91 (2016a) 250–258
- Rebecca Weber, Sebastian Asenbeck, Henner Kerskes, Ralf Jaudas. SolSpaces – Entwicklung und Erprobung einer autarken solaren Wärmeversorgung für energieeffiziente Kompaktgebäude, Abschlussbericht, 2016b
- Thomas Nonnen, Steffen Beckert, Kristin Gleichmann, Alfons Brandt, Baldur Unger, Henner Kerskes, Barbara Mette, Sebastian Bonk, Thomas Badenhop, Frank Salg, Roger Gläser. A Thermochemical Long-Term Heat Storage System Based on a Salt/Zeolite Composite. *Chemical Engineering Technology* (2016) 39, No. 12, 2427–2434

OPEN-TRANSPORTED SYSTEMS

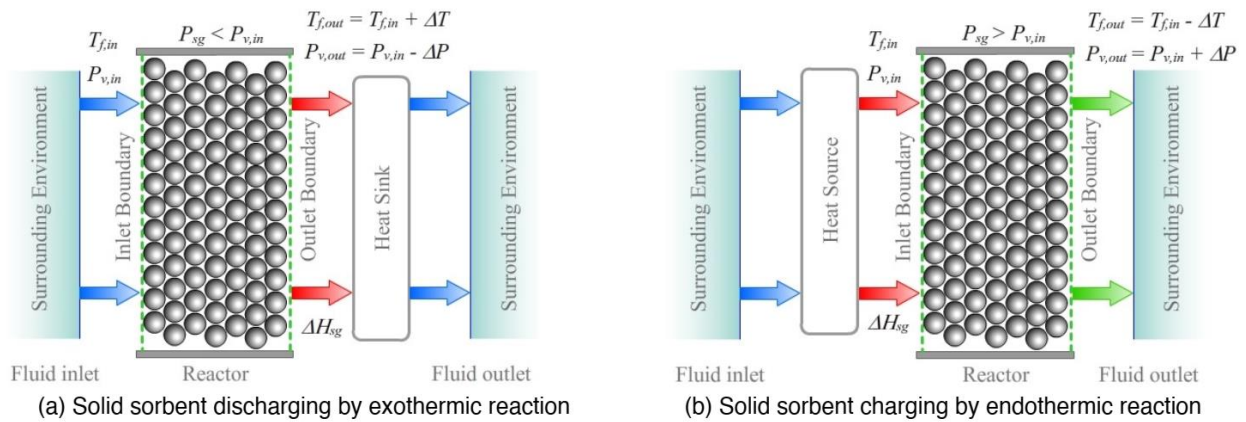
In the open and transported process, the sorbent material is transported from storage containments to the sorber / desorber compartment, and back. The benefit of this approach is the reduced active material, both in sorption and desorption. This reduces the pressure drop in operation and potentially improves temperature gain. In the transported process variations of cross or counter flow are possible, enabling better charging and discharging performance. The challenge is found in the transporting of solid sorbents.



OPEN SORPTION PROCESS FOR THERMOCHEMICAL ENERGY STORAGE FOR RESIDENTIAL HVAC APPLICATIONS

UNIVERSITY OF MONS - BELGIUM, ALEXANDRE SKRYLNYK, EMILIE COURBON, NICOLAS HEYMANS, MARC FRÈRE, JACQUES BOUGARD

Process description: Open sorption process represents a general class of solid/gas thermochemical energy storage, heat transforming and heat upgrading processes. It can be implemented for numerous reversible solid/gas exothermic and endothermic interactions, including adsorption principle, chemical sorption by salt hydrates and chemical reactions. The solid component is called sorbent and is usually placed in a specially designed vessel, the so-called reactor. The gaseous component is called working fluid and is a mixture of inert and reactant gases. The inlet and outlet reactor boundaries are openly connected to the surrounding environment, whereby the working fluid circulates as shown on the following figure enabling heat supply/evacuation and mass transfer (in terms of reactant gas molecules) to the solid sorbent.



The process is driven by operating conditions defined by fluid temperature $T_{f,in}$ and partial pressure of reactant gas $P_{v,in}$ at the reactor inlet. When $P_{sg} < P_{v,in}$, where P_{sg} is solid/gas equilibrium pressure, the molecules of reactant gas are being captured by porous solid sorbent that provokes the heat release (exothermic reaction). The reaction heat ΔH_{sg} is evacuated from the reactor by the inert gas, whose outlet temperature rises $T_{f,out} = T_{f,in} + \Delta T$. On the contrary, when $P_{sg} > P_{v,in}$, the molecules of reactant gas are being released from porous solid and carried away with inert gas, that corresponds to the endothermic reaction, and the reaction heat ΔH_{sg} must be supplied to the reactor from the heat source.

In thermochemical energy storage applications, the exothermic reaction is used to supply the released heat to the heat sink at the required temperature level $T_{f,out}$ and is called energy discharging operation (see figure (a)), while the regeneration of the solid sorbent follows by the endothermic reaction and is called energy charging operation (see figure (b)).

Schematics: The open sorption process investigated at the Research Institute for Energy (University of Mons, Belgium) within SOTHERCO and STOCC projects operates under normal atmospheric pressure and uses moist air as a working fluid. The investigated process is used for a seasonal solar energy storage in building heating and domestic hot water preparation applications as shown in Figure 5-42 and in Figure 5-43 in the unified schematics.

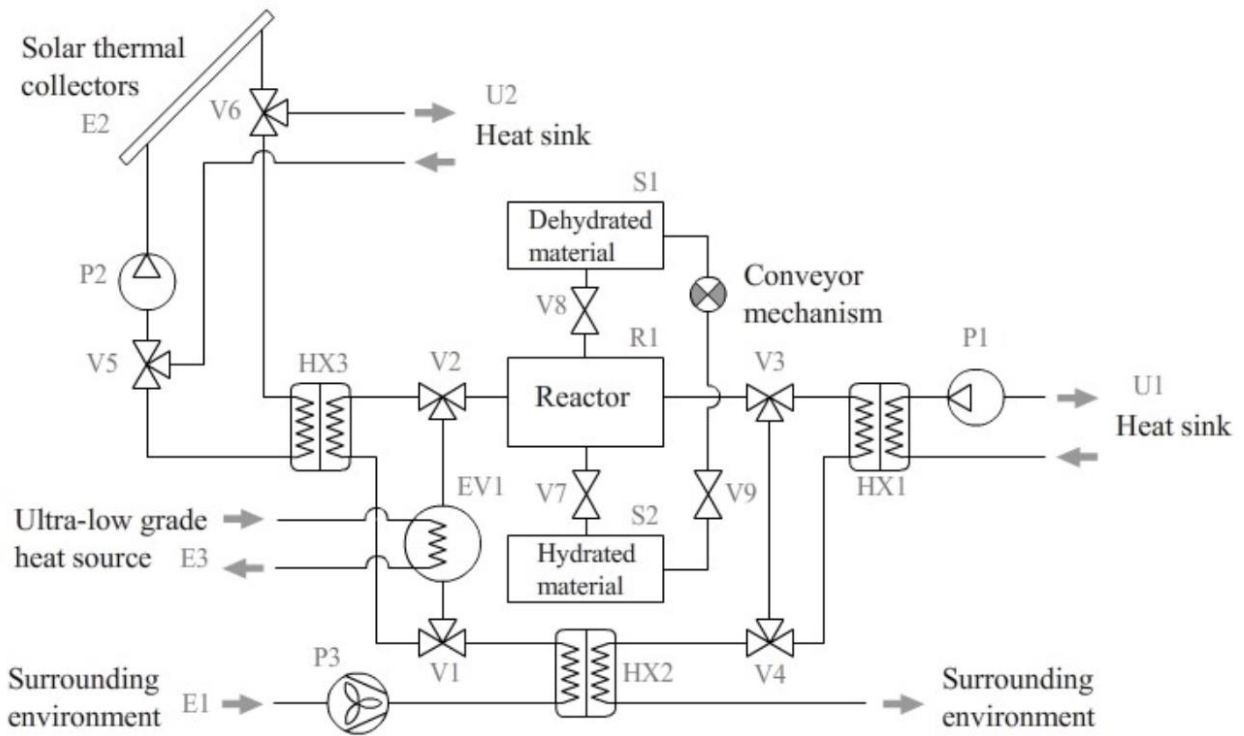


FIGURE 5-42: SCHEMATICS OF AN OPEN SORPTION PROCESS DEVELOPED FOR SEASONAL ENERGY STORAGE.

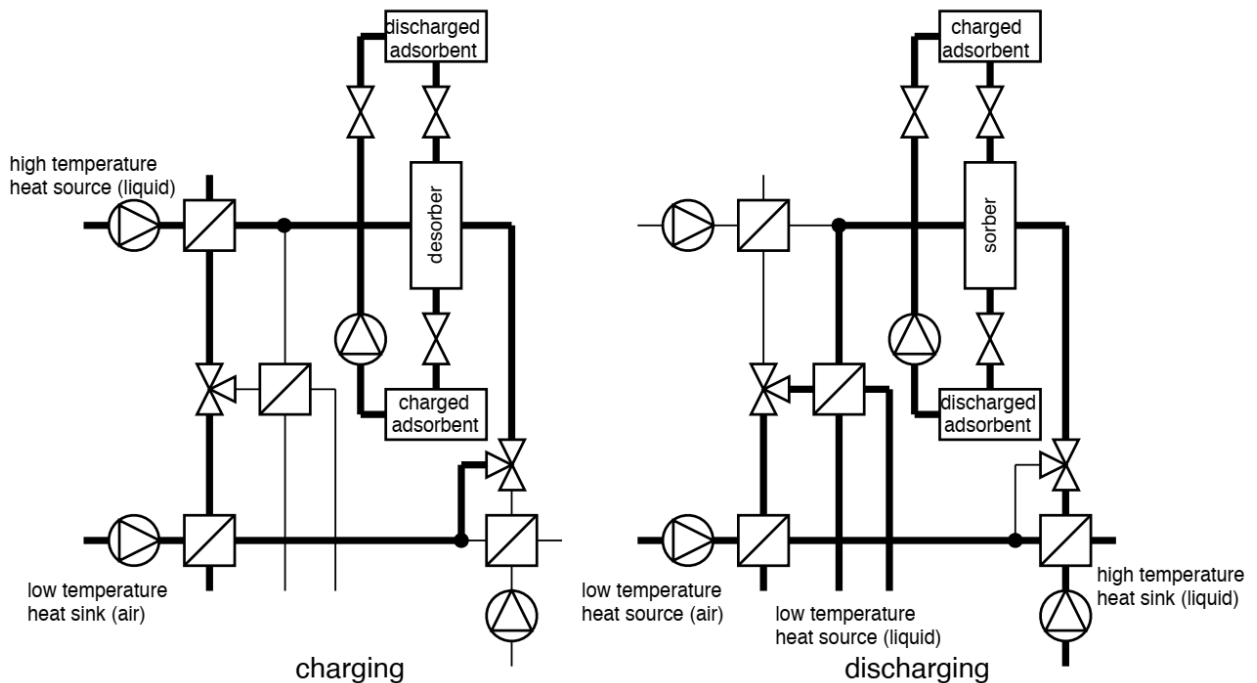


FIGURE 5-43: UNIFORM SCHEMATICS OF THE SOTHERCO AND STOCC PROJECT SYSTEM.

This process can be implemented for a fixed packed-bed or moving/fluidized bed reactor. The fixed packed-bed reactor stores at the same time all solid material (in either hydrated or dehydrated state)

in R1. In case of implementation of the moving/fluidized reactor, the dehydrated and hydrated material is stored in the storage vessels S1 and S2, separately from the reactor R1, and transported by a special conveyor mechanism (see Figure 5-42).

During the energy charging operation, the solar thermal collectors E2 provide the higher-grade heat (>80 °C) that is sufficient to dehydrate the material. The air is taken from the surrounding environment at the inlet E1 and blown through the air loop of heat exchangers HX2, HX3, reactor R1. The evaporator EV1 and the heat exchanger HX1 stay by-passed by the valves V1, V2, V3 and V4. The conveyor mechanism moves first the hydrated material from the storage vessel S2 to S1, and then to the reactor R1. Then the dehydrated material is removed from the reactor R1 to the appropriate storage vessel. The excess of solar energy can be supplied to the user at the system output U2.

During the energy discharging operation, the moist air is taken from the surrounding environment E1 and supplied to the reactor R1 passing through the heat exchanger HX2 and evaporator EV1. The ultra-low grade heat source E3 (<20 °C) must be connected to the evaporator EV1, which allows the stable operating condition to be achieved. The dehydrated material is transported from the storage vessel S1 to the reactor R1. The hot air from the reactor outlet is directed to the heat exchanger HX1, where the reaction heat is supplied to the user U1. The solar thermal collectors E2 are used to supply a hot water to the user U2.

Major components: Major components are reactor unit R1, material storage vessels S1 and S2, evaporator EV1, solar thermal collectors E2, air-to-air heat exchanger HX2, air-to-water heat exchangers HX1 and HX3, hydraulic pumps P1 and P2, fan unit P3. In case of fixed packed-bed reactor, no storage vessels S1 and S2 are needed. In case of moving/fluidized bed reactor, the material conveyor mechanism must be designed. The dehydrated material must be kept away from outside humidity in a tight storage vessel. The compatibility of materials must be studied for the sake of corrosion issues induced by the contact of hydrated material with the storage vessels S1, S2 and the reactor unit R1.

Benefits and challenges: Open sorption process is relatively easy to implement for residential applications using standard HVAC commercial components. It is possible to implement district heating process by using industrial waste heat or supplying the heat from CHP plant as a heat source E2 (see Figure 5-42). No special heat exchanger between solid sorbent and flowing gas is needed to be integrated to the reactor unit R1, that increases the system overall efficiency, output thermal power and energy density (in terms of reactor unit R1 and storage vessels S1, S2) in comparison with a solid-to-liquid heat exchanger coated with material. The process uses the moist air, which is a free and ecological energy source. For the fixed packed-bed reactor, the main challenge is to ensure the homogeneous sorption by optimizing the hydrodynamics of fluid/porous medium interaction. For the moving-bed/fluidized reactor, the main challenge consists in the design of reactor unit R1, material storage vessels S1, S2, as well as material conveyor mechanism. Thermal losses and low efficiency of heat exchangers can degrade the performances of the open sorption process by 36% - 70%. The use of outside moist air is related to the unpredictable variation of air humidity, thus the sufficient energy must be provided at E3 input (see Figure 5-42).

Possible working pairs

- Hygroscopic materials based on adsorption principle (e.g. selective water sorbents and molecular sieves such as silica gel, zeolites, MOF, AIPO, SAPO etc.) / H₂O.
- Salt hydrates (e.g. SrBr₂, MgCl₂, CaCl₂, MgSO₄ etc.) / H₂O.
- Composite materials, the so-called salt-in-matrix materials (e.g. selective water sorbent, molecular sieve, carbonaceous support + salt hydrate) / H₂O.

Examples in literature: Michel et al. investigated open thermochemical process based on SrBr₂/H₂O for seasonal energy storage purposes. The process operates with moist air. The reactor design is a fixed multiple packed-bed configuration. Marias et al. developed thermochemical open sorption process for seasonal storage of solar energy using SrBr₂/H₂O. The proposed storage process uses outside moist air and is designed as a fixed packed-bed configuration. Liu et al. simulated numerically a composite mesoporous thermochemical energy storage process. The open sorption process uses moist air flowing through the energy storage unit made from the mesoporous Wakkanai siliceous shale impregnated with CaCl₂. Skrylnyk et al. analyzed numerically energy performances of different open sorption thermochemical energy storage systems considering moving-bed reactor design. The proposed configurations are used for building heating application.

References

- B. Michel, N. Mazet and P. Neveu, "Experimental investigation of an innovative thermochemical process operating with a hydrate salt and moist air for thermal storage of solar energy: Global performance", *Applied Energy*, vol. 129, pp. 177-186, 2014.
- G. Tanguy, F. Marias, P. Neveu and P. Papillon, "Thermodynamic analysis and experimental study of solid/gas reactor operating in open mode", *Energy*, vol. 66, pp. 757-765, 2014.
- H. Liu and K. Nagano, "Numerical simulation of an open sorption thermal energy storage system using composite sorbents built into a honeycomb structure", *International Journal of Heat and Mass Transfer*, vol. 78, pp. 648-661, 2014.
- O. Skrylnyk, M. Henry, E. Courbon, N. Heymans, M. Frère, G. Tanguy, P. Papillon, J. Bougard, M. Beekmans and G. Descy, "Evaluation of the performance criteria of combined thermochemical energy storage systems for building applications", in *EuroSun 2014 International Conference On Solar Energy And Buildings*, Aix-les-Bains, France, 2014.

AN OPEN SORPTION HEAT STORAGE APPLICATION FOR BUILDING APPLICATION -OFFSORE UNIVERSITY FOR APPLIED SCIENCE UPPER AUSTRIA – AUSTRIA, BERNHARD ZETTL

Short description: The main goal of the project OFFSORE is to build a laboratory prototype (thermal power downsized by factor three compared to real application) with automatic control for mass and heat transfer for both, adsorption and desorption part. Molecular sieves (zeolites) are used actually and composite material (salt impregnated structures) are planned for demonstration as storage material. The goal of modelling and numerical simulation work package is to develop a sufficiently simplified strategy for controlling the storage procedure on several levels: 1. operation control of ad-, and de-sorption under certain conditions, 2. control of daily cycles dominated by solar radiation and user profiles, 3. strategic use of stored energy (seasonal forecast and year-around control).

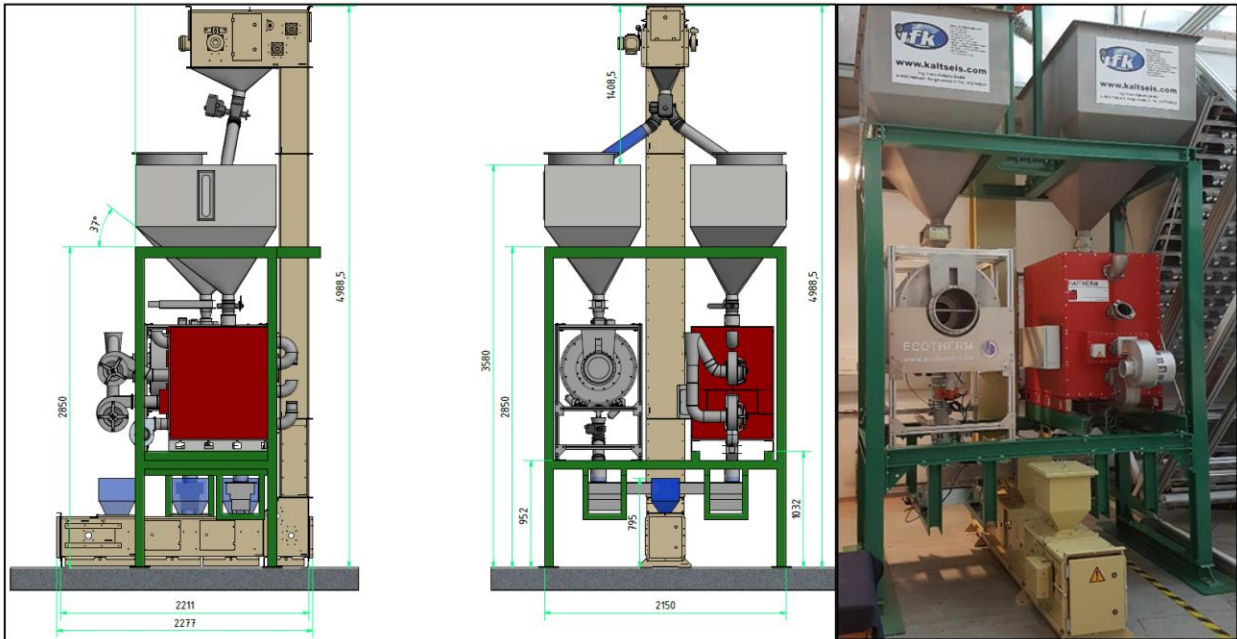


FIGURE 5-44: CONCEPT OF THE PROTOTYPE WITH DIMENSIONS (LEFT), AS BUILT IN THE LABORATORY (RIGHT).



FIGURE 5-45: SOLAR THERMAL HOT AIR INSTALLATION ON TOP OF THE UNIVERSITY-BUILDING (RIGHT), WITH DETAILS OF THE TUBE IN TUBE AIR CHANNEL (LOWER LEFT) AND MANIFOLD CONSTRUCTION (UPPER LEFT).

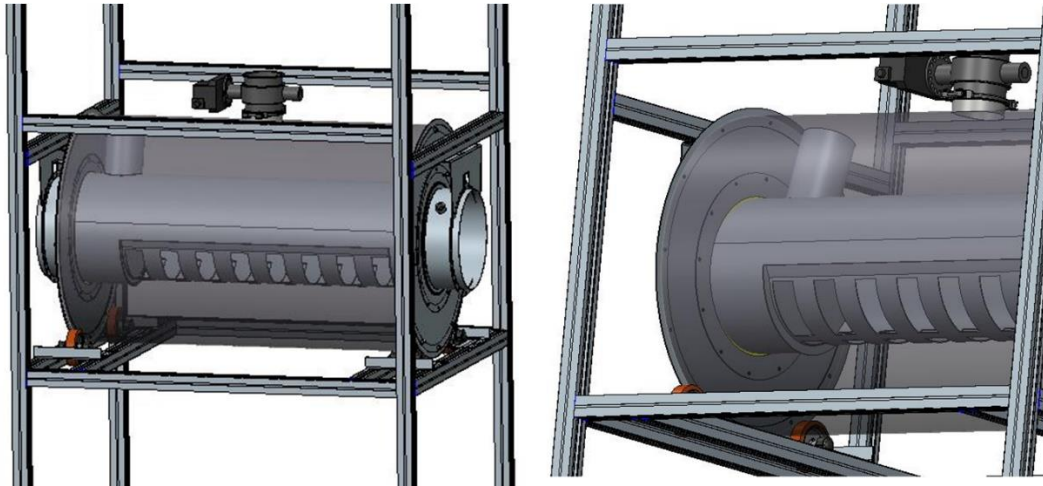


FIGURE 5-46: CONSTRUCTION DETAILS OF THE ROTATING CYLINDRICAL ADSORPTION REACTOR

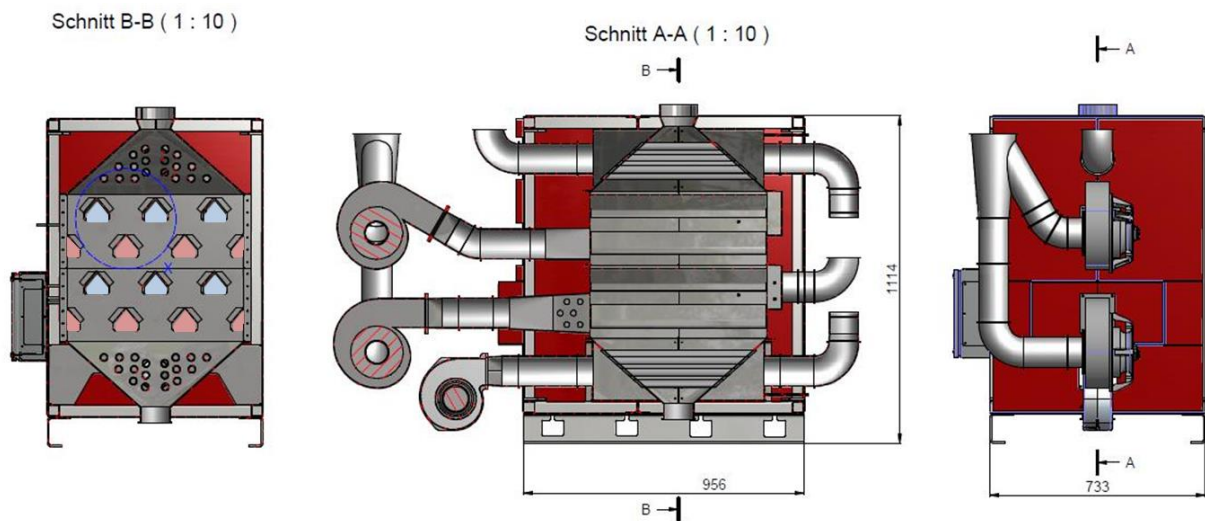


FIGURE 5-47: CONSTRUCTION DETAILS OF THE DESORPTION FURNACE FROM DIFFERENT POINTS OF VIEW

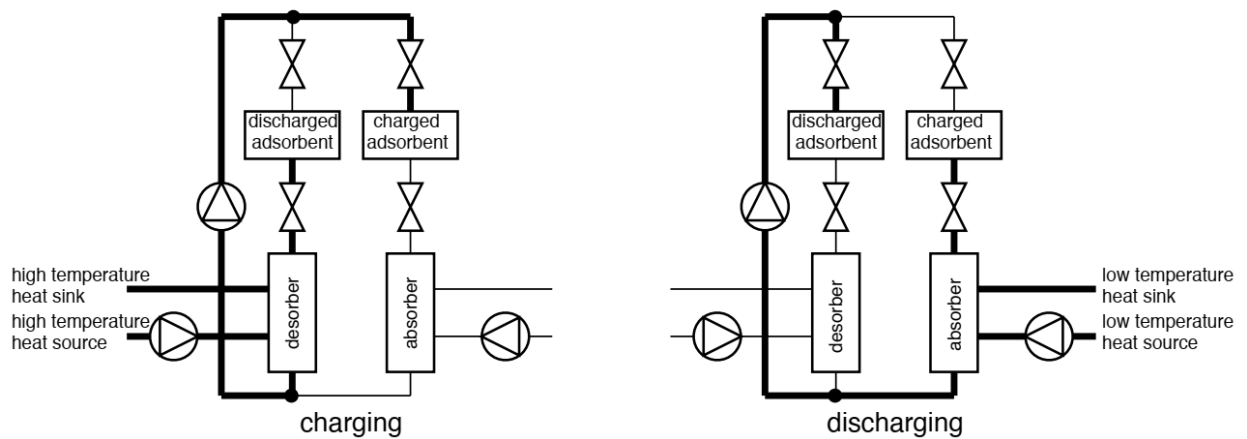


FIGURE 5-48: UNIFORM SCHEMATICS OF THE OFFSHORE STORAGE SYSTEM FROM THE UNIVERSITY OF APPLIED SCIENCE, UPPER AUSTRIA.

Major storage components: The main components of the Prototype are shown in Figure 5-44 and illustrated in the uniform schematic in Figure 5-48. The prototype construction consist of rigid steel frame (green), two containers for dry and humid material (on top), a desorption reactor (furnace, in red), a cylindrical adsorption reactor (rotating heat drum, left of furnace), and a conveyor used to lift the material from bottom to top (brown). In addition, we realized a solar thermal installation at the top of the University building (Figure 5-45). The aim of the hot air solar installation was to get experimental data for operation mode, like the maximal reachable summer temperatures and thermal power (for desorption), the temperature gains during winter used to humidify process air (for adsorption), and to demonstrate the achievable cost per unit of the (relative simple) hot air-collector technology.

Details of the rotating adsorption drum (without storage material) are shown in Figure 5-46. The function principle works as follows: an external ventilator blows process air into the right opening of the central (inner) cylinder. The inner cylinder is fixed, while the outer (together with the material) is rotating. The process air is entering the material bed via the openings at the bottom of the inner cylinder (supported by mesh-material), and flowing through the moving grain bed to the top. Then the air is leaving the material bed at the upper part of the volume where an air channel is formed since only about 80% (approx. 150 liter) of the inner volume is filled. The upper air channel is connected to the left opening of the cylinder by a (chimney like) tube, enabling the air to leave the reactor.

The reactor is filled and emptied by an installed valve (electrical connection via brush contacts) and slowly driven (1 turn per minute) by an AC motor. While passing the grain bed the humidity of the incoming air is transferred to the storage material. This process generates adsorption heat, and the process temperature mainly depends on the air water content and temperature of the incoming air, while the air mass flow determines thermal power. For the aim of warm water generation an internal heat exchanger realised as double wall construction of the inner cylinder can be used, while building heating power would be extracted by an air/air heat exchanger.

The reactor is designed to release a certain thermal power (determined by air mass flow) an energy determined by the amount of material inside the drum. Once the material is discharged (typically after 6...8h) it has to be replaced by new one; the discharged material is transferred to the respective container by the conveyor and new material is fill into the drum from beyond.

Details of the function of the desorption furnace are shown in Figure 5-47. The middle schematic illustrates the passage of the four different air flows through the furnace: the most upper one is connected to the lowest one via a hose. The lowest is used to cool down the hot material at the bottom before it leaves the furnace. The air is guided to the top where it preheats the incoming material (both with tube registers- see Figure 5-47, left schematic). Both of the middle air channels guide the air into the material bed where heating and dehumidification takes place. The air channels (indicated as light red and blue in Figure 5-47, left schematic) are connected with the hot front end (red) or with

the cool back end (blue). The air is forced from the hot end into the red channels, then into the grain bed, through the grain bed towards the blue channels, and then out again. This principle is known from much bigger drying application in agricultural production (for drying crop or corn, for example).

The thermal power for desorption should be supplied from the solar thermal hot air installation and eventually supported by an electrical heater (integrated in the lower heater channel). The furnace and blowers are designed for temperatures of 200°C, thermal power is about 6 kW that should be sufficient to dehydrate approx. 20 kg/h of storage material. A shutter at the bottom opens every few seconds and controls the material mass flow.

Benefits and challenges

Benefits of the system concept:

- Separation of functional units (desorption, adsorption, transportation and storage)
- Optimal thermos-physical design for both, adsorption and desorption
- Separation of power and energy specification

Challenges:

- Wear and dust formation
- Elaborative conveyor installation
- Limited adsorption temperature (compared to fixed bed)
- Higher adsorption requirement (compared to closed sorption) Possible working pairs
- Zeolites beads, composite (salt based) materials
- Requirement on mechanical strength and abrasion resistance

References

Zettl B. et. al (2014), "Development of a revolving drum reactor for open-sorption heat storage processes", in Applied Thermal Engineering 70 (2014) 42-49

Zettl B. and Lachner M. (2015), "An Advanced Desorption Concept for TES-Materials", in Proceedings of SHC 2015, International Conference on Solar Heating and Cooling for Buildings and Industry, Istanbul

Engel, G. et. al (2017), "Simulation of a seasonal, solar-driven sorption storage heating system", in Journal of Energy Storage, vol. 13, pp. 40-47

Krese, G. et. al (2018), "Thermochemical seasonal solar energy storage for heating and cooling of buildings" in Energy and Buildings, vol. 164, pp. 239-253

HIGH TEMPERATURE FLUIDIZED BED REACTOR FOR INDUSTRIAL WASTE HEAT RECOVERY, POWER PLANT FLEXIBILISATION AND POWER-TO-PROCESS HEAT
TECHNICAL UNIVERSITY OF MUNICH - GERMANY DR.-ING. ANNELIES VANDER-SICKEL

Short description At the Institute of Energy Systems at the Technical University Munich a fluidized bed reactor is being developed for high temperature heat storage using a reversible chemical gas-solid reaction using steam and metal oxides such as $\text{CaO}/\text{Ca(OH)}_2$ or $\text{MgO}/\text{Mg(OH)}_2$. Currently, an electrically heated pilot fluidized bed reactor is constructed as shown in the picture in Figure 5-49 and illustrated in the uniform schematics in Figure 5-50. Upscaling to MW scale is ongoing. The fluidized bed storage design allows for a separation of storage power and capacity. Charging and discharging take place in a fluidized bed reactor with an embedded heat exchanger. During charging, the metal hydroxide decomposes in steam and oxide inside the fluidized bed reactor. The oxide is then transferred to and stored in a separate silo, the steam can be used immediately e.g. as process steam. During discharging, the oxide is transported back to the fluidized bed reactor and recombined with steam to produce high temperature heat. The latter steam can be taken either from the process steam lines or generated using waste or low temperature heat (ca. 120°C when operated at 1 bar). During both charging and discharging, the reactor operates with a pure steam atmosphere. This allows direct use or high temperature recovery of the condensation heat contained in the fluidization and reaction steam (released during charging – for CaO ca. 40% of the energy added during charging). The pressure level inside the fluidized bed reactor controls the equilibrium reaction temperature and hence the charging and discharging temperature levels. An increase of the reactor operating pressure therefore allows generating a temperature lift between charging and discharging. Schematics The “open” chemical reaction process consists of three major components, the heat converter in this case the fluidised bed reactor, connection pumps and valves and solid storage silos. The fluidised bed reactor is operated with pure steam. This steam is released from the chemical reaction and hence the fluidised bed reactor during charging, and supplied externally during discharging.

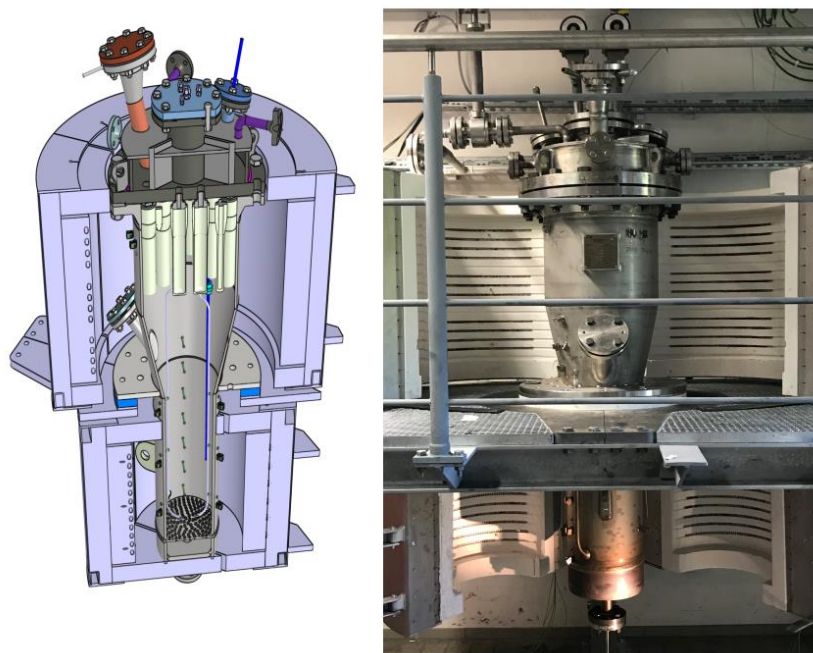


FIGURE 5-49: PHOTO (PRIOR TO INSTALLATION OF MEASUREMENT EQUIPMENT) AND 3D-CAD IMAGE OF THE KWSCALE PILOT REACTOR AT THE TUM.

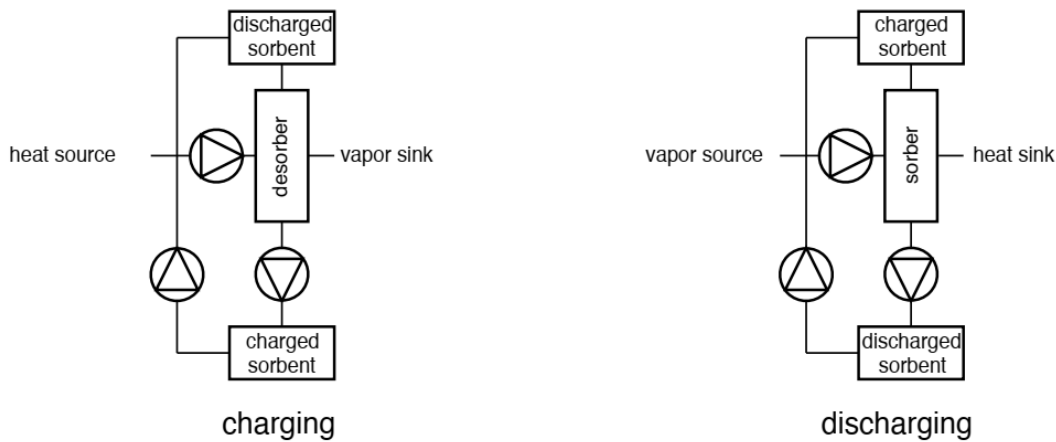


FIGURE 5-50: UNIFORM SCHEMATICS OF THE TUM HEAT STORAGE SYSTEM, SHOWN IN THE CHARGING AS WELL AS THE DISCHARGING PROCESS.

The pilot reactor is electrically heated by the ovens surrounding the reactor vessel. The latter is 3 m high, has a volume of 120 liter with a reaction zone of 30 liter. It can operate at pressures from 1 bis 6 bar and temperatures up to 700 °C. Steam for fluidization (and reaction) is supplied through the bottom plate and extracted at the top. Sintered metal filters avoid particle entrainment out of the reactor. In house designed gas locks allow particle addition and extraction during operation, simulating a continuous operation of the reactor with up to 5 kg/h.

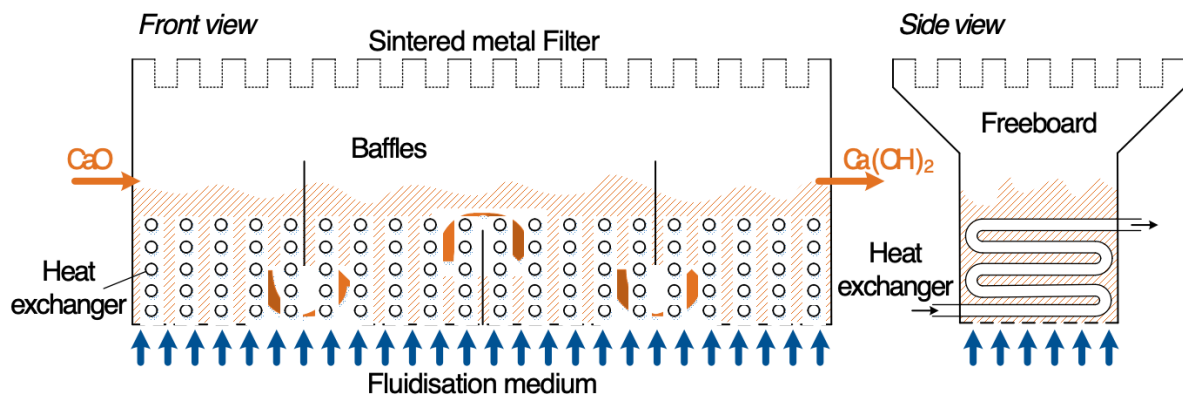


FIGURE 5-51: ILLUSTRATION OF A MW SCALE CONTINUOUS STATIONARY FLUIDIZED BED REACTOR. THE FLUIDIZED BED REACTOR IS CHARGED WITH HIGH TEMPERATURE HEAT (300-700°C) USING EMBEDDED HEAT EXCHANGERS AND FLUIDIZED WITH STEAM (FLUIDIZATION + REACTION STEAM). DURING DISCHARGING, HIGH PRESSURE STEAM CAN BE GENERATED IN THE HEAT EXCHANGER TUBES, LOW PRESSURE STEAM IS USED FOR FLUIDIZATION.

Major components Major components are the heat and mass exchanger, being the fluidized bed reactor, the storage vessels and the connecting valves and conveyers for the solid particles. As charging and discharging do not take place simultaneously, in principle the same reactor could be used for both charging and discharging. However, depending on the process integration and the desired reactor operating temperatures and hence pressures, heat transfer coefficients might differ between charging and discharging requiring a separate design for both. To avoid further reaction of the storage material in the silos, special gas locks are required to feed and extract the material from the

fluidized bed reactor and exchange the steam atmosphere for e.g. dry air or an inert N₂ atmosphere.

Benefits and challenges

Benefits:

- The fluidized bed design allows separation of storage power and capacity & hence long-term storage at little additional cost for the storage capacity
- The special bottom design allows to fluidize CaO/Ca(OH)₂, which is a very cheap material ~0.15 €/kWh with high reaction enthalpy (104 kJ/mol)
- The high temperature level in combination with the operation in pure steam, allow efficient integration into power plants and process heating
- Due to the direct use of the steam, no additional storage for water is required.

Challenges:

- Particle Break-up during reaction and fluidization
- Heat Transfer coefficients to the tube bundles for fine fluidized powers not available
- Impact of tube bundle design on fluidization not clear yet, currently under investigation
- Efficient use of the reaction steam is required to achieve high storage efficiencies

Possible working pairs

- CaO / H₂O
- MgO / H₂O
- and more

References

Michael Angerer, Moritz Becker, Stefan Härzschel, Konstantin Kröper, Stephan Gleis, Annelies Vandersickel, Hartmut Spliethoff, Design of a MW-scale thermo-chemical energy storage reactor, Energy Reports, Volume 4, November 2018, Pages 507-519 Continuous CaO reactor being developed at CEA: S. Rougé, Y. A. Criado, O. Soriano, J.C. Abanades,

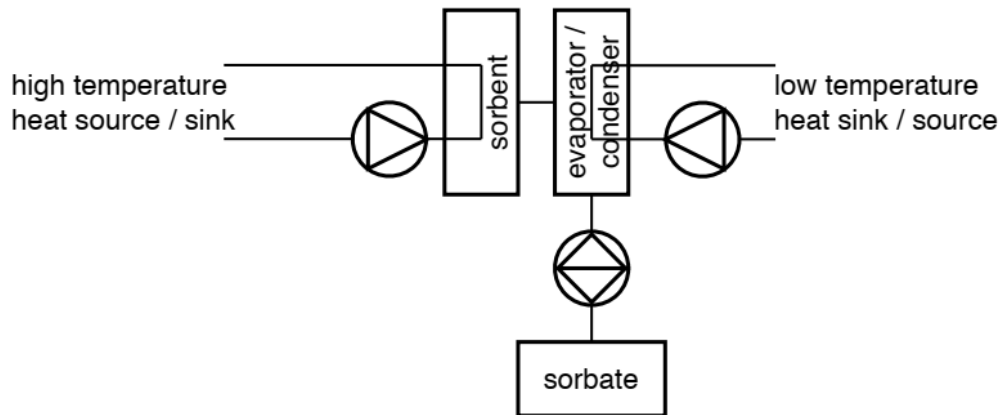
Continuous CaO/Ca(OH)₂ Fluidized Bed Reactor for Energy Storage: First Experimental Results and Reactor Model Validation, Ind. Eng. Chem. Res. 56 (2017) 844–852

Similar reaction system using a moving bed reactor instead of a fluidised bed reactor is being developed at DLR: M. Schmidt, M. Linder, Power generation based on the Ca(OH)₂ / CaO thermochemical storage system – Experimental investigation of discharge operation modes in lab scale and corresponding conceptual process design, Applied Energy 203 (2017) 594–607.

CLOSED-FIXED SYSTEMS

In the closed and fixed bed system, matter is not exchanged with the ambient, but only heat. Due to the stationary sorbent containment, similar issues as with the open fixed process in respect to heat

transport are encountered. Nevertheless, mass transport is not critical, since only sorbate vapor is present in the closed chamber.



CLOSED SOLID SORPTION PROCESS FOR THERMOCHEMICAL ENERGY STORAGE FOR RESIDENTIAL APPLICATIONS AEE INTEC – AUSTRIA, REBEKKA KÖLL, WIM VAN HELDEN

Process description: The solid-adsorption process is based on the adsorption of particles in gaseous phase on the inner surface of porous solid material. The fully reversible and exothermic reaction is used to store surplus of heat e.g. solar thermal energy, waste heat, etc. and store it over a longer period. A closed sorption storage system is working under vacuum. This has the advantage that the evaporation temperature which needs to be provided to start the adsorption can be very low (5 - 20 °C), because of the low evaporation temperature of water in vacuum. The driving force of the vapour flow in the closed system is the pressure difference between the storage modules and the evaporator/condenser. The conventional sorption storage system is extended by a so-called sorption collector to increase the performance of the system by applying the charge boost mode. For the charge boost mode two desorbed tanks on different temperature level and hence different pressure level are used to further dry the hot tank. Schematics The schematic design and the working principle of the charging and discharging process is shown in Figure 5-52 and illustrated in the uniform schematic in Figure 5-53.

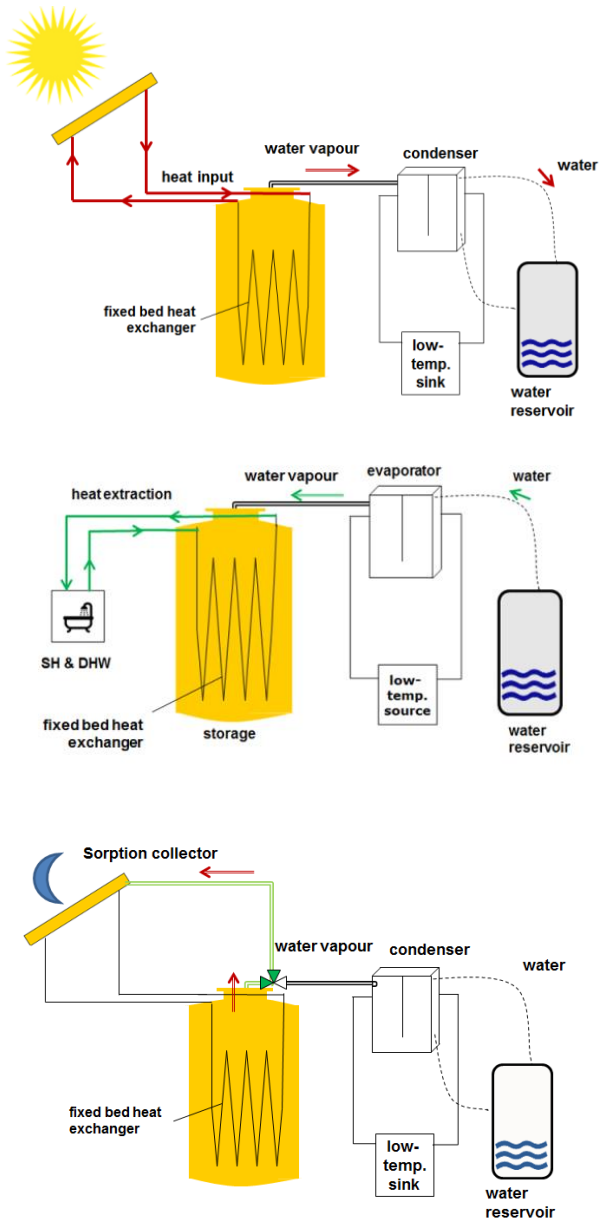


FIGURE 5-52: SCHEME OF MAIN COMPONENTS OF A CLOSED SORPTION STORAGE SYSTEM. THE FIRST FIGURE ON THE LEFT SIDE SHOWS THE CHARGING (DESORPTION) PROCESS OF THE MAIN STORAGE AND THE SORPTION COLLECTOR, THE SECOND FIGURE ON THE RIGHT SIDE SHOWS THE DISCHARGING (ADSORPTION) PROCESS AND THE THIRD FIGURE SHOWS THE CHARGE BOOST PROCESS DURING NIGHT.

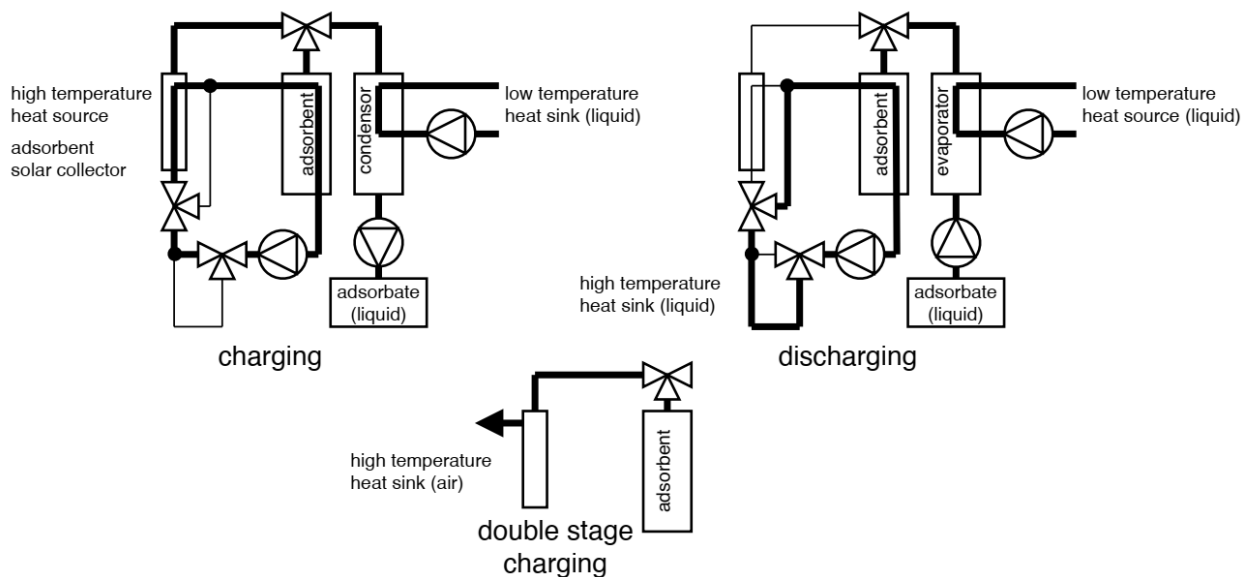


FIGURE 5-53: UNIFORM SCHEMATICS OF THE AEEINTEC DOUBLE STAGE CHARGING HEAT STORAGE SYSTEM.

To charge/desorb the storage heat from the high temperature heat source (sorption collector) is transferred via the fluid system over the fixed bed heat exchanger to the sorption material. The material heats up and water vapor is released. At the same time the sorption material in the sorption collector is heated up and the released water vapor from the main storage and the collector and flows to the condenser due to the pressure difference. The low temperature heat sink takes up the released heat of condensation and the condensed water is flowing back to the water reservoir, where the water can be stored separately from the sorption material.

The charge boost process is applied during night to further increase the energy density of the main storage. Since the collector material cools down during night because of the high radiation losses, also the pressure drops rapidly. The pressure difference between the hot main storage and cold sorption collector is used to transfer vapor from the main storage to the collector and further dry the main storage. On the next sunny day, the desorption of the collector starts again and the process can be repeated and the water concentration lowered step by step.

The discharging process is started by pumping up the process water to the evaporator, where it is evaporated due to the supply of heat at low temperature from the low temperature heat source. Due to the low pressure of the dry and cold material, the generated vapor flows to the storage. As soon as the vapor gets in contact with the material, the adsorption is started and heat is released. The produced heat at high temperature is extracted via the fixed bed heat exchanger and is transferred to the heat distribution system.

Main components: The main components necessary for the storage process are the (1) main storage and the (2) sorption collector, both filled with the solid sorption material, the (3) evaporator/condenser heat exchanger for evaporating the water for adsorption (discharging) and condensing the water vapor during desorption (charging) and (4) a water reservoir, where the condensed process water can be stored separately. Due to the low heat conductivity of the sorption material, which can

be in form of powder, grains, beads, etc. with different diameters, a fixed bed heat exchanger is used to improve the heat transfer within the fixed bed. In addition, a heat source, in this case solar thermal collectors and a buffer storage for short term storage, are implemented.

Benefits and challenges: In general, the technology has the advantage of a high energy density (about 3 times higher than water and there is still potential for increase) and loss-free storing. The closed sorption process has the advantage that due to the low evaporation temperature in vacuum, for the evaporation heat source in winter a low temperature (5-10 °C) is sufficient. This can be provided by ground/air source or like in COMTES via indirect solar energy stored in the buffer. Compared to an open system it has the advantage that the performance of the system is independent of the humidity in the air, higher energy densities can be achieved by better exploitation of the adsorption capacity of the material. Due to the closed system even (slightly) hazardous materials can be used and dust formation is no issue. Challenges for the technology are on the one hand the system compactness. The energy density based on the material is higher, but due to the complexity of the system the other system components like water reservoir or evaporator/condenser also require space. In addition, a significant reduction of the investment costs is necessary to introduce the storage system on the market. The aim is to reduce the costs and the amount of used sorption material as well as to reduce the costs of the system components.

Possible working pairs

- Hygroscopic materials e.g. selective water sorbents and molecular sieves such as silica gel, zeolites, MOF, AIPO, SAPO etc. combined with H₂O, Methanol, Ethanol
- Salt hydrates (e.g. SrBr₂, MgCl₂, CaCl₂, MgSO₄, Na₂S, K₂CO₃) / H₂O.
- Composite materials, the so-called salt-in-matrix materials (e.g. selective water sorbent, molecular sieve, carbonaceous support + salt hydrate) / H₂O.

Examples in literature

Köll et al., experimental results of a real-scale demonstration system based on the material pair zeolite 13XBF and water vapor

Mette et al., investigation of the thermodynamic behavior of zeolite 13XBF

Jänchen and Stach, investigation of adsorption properties of different modified porous sorbents for application in thermo-chemical storages

Wagner et al., Prototype of closed sorption storage system with the working pair silica-gel and water vapor

Cuyppers et al., Experimental investigation of a demonstration system based on the salt hydrate Na₂S

References

R. Köll, W. van Helden, G. Engel, W. Wagner, B. Dang, J. Jänchen, H. Kerskes, T. Badenhop and T. Herzog, "Experimental Investigation of a realistic scale seasonal solar sorption storage system for buildings," Solar Energy, no. 155, pp. 388-397, 2017.

B. Mette, H. Kerskes, H. Drück and H. Müller-Steinhagen, "Experimental and numerical investigations on the water vapor adsorption isotherms and kinetics of binderless zeolite 13X," International Journal of Heat and Mass Transfer, no. 71, pp. 555-561, 2014.

J. Jänchen and H. Stach, "Adsorption properties of porous materials for solar thermal energy storage and heat pump application," Energy Procedia, vol. SHC 2012, no. 30, pp. 289-293, 2012.

W. Wagner, D. Jähnig, C. Isaksson and R. Hausner, "Modularer Energiespeicher nach dem Sorptionsprinzip mit hoher Energiespeicherdichte (MODESTORE)," Final Report, Gleisdorf, 2006.

R. Cuypers, L. van Vliet, P. Bodis, B. Starosielec, M. Bujalski, H. de Beijer, M. Vos, G. Földner, J. Wapler, A. de Gracia, L. Cabeza and C. Hoegaerts, "Successful field test demonstration of seasonal solar thermochemical storage," Gleisdorf Solar, 2016.

CLOSED SOLID-SORPTION PROCESS FOR THERMOCHEMICAL ENERGY STORAGE IN RESIDENTIAL APPLICATIONS TNO – NETHERLANDS – MERITS, RUUD CUYPERS

Short description: The MERITS closed-sorption system is based on solid sorbents (salt hydrate of choice is sodium sulphide), whereby both storage and heat and mass exchanger are under water vapor pressure atmosphere and all other gasses, often referred to as non-condensing gasses, are removed. Typically, our system is under sub atmospheric pressures ranging from 10-40 mbar (water as sorbate, roughly between 10 and 30 °C). Due to the solid state of the salt hydrate, it is fixed in a pacified heat and mass exchanger as shown in Figure 5-54 and in the uniform schematics in Figure 5-55. The sorbate water is cycled back and forth between the salt and the storage vessel, where it is kept as a liquid during storage. This way, the storage energy capacity is dictated from sorbate volume and reaction enthalpy. Upon discharging, heat is released from the storage by evaporation of sorbate by a low temperature heat source and sorption into the salt. In this process heat of condensation (=evaporation enthalpy) and heat of reaction (= reaction enthalpy) are simultaneously released. In the reverse reaction, heat is stored by evaporation of the sorbate from the sorbent by excess heat at a given temperature, and condensing the evaporated sorbate against a condenser at $T < T_{sat}$. The closed sorption heat storage operates thus as an absorption heat pump with intermediate storage. The temperature lift between evaporator and sorber heat exchanger is dependent on the nature of the sorbent and its hydration state change. It follows that the output temperature of the storage system is dependent on the evaporator temperature and the sorbent reactions. Energy density follows from this on knowing the density of the used solid sorption material.

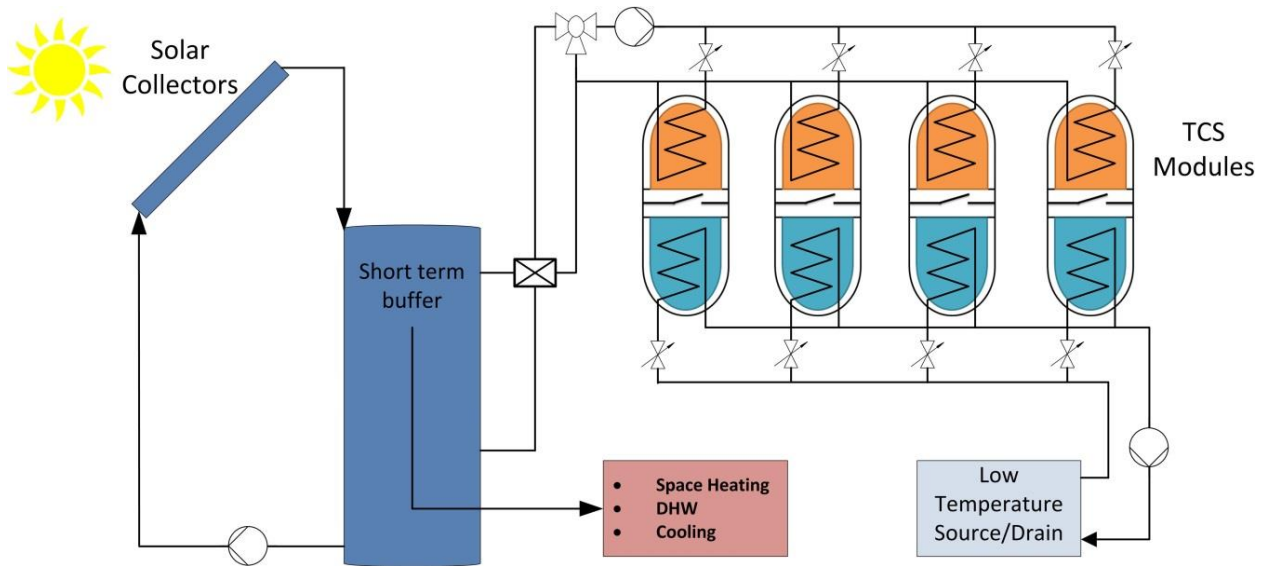


FIGURE 5-54: ILLUSTRATION OF THE MERITS SEASONAL STORAGE SYSTEM, INCLUDING HOT WATER SHORT TERM STORAGE.

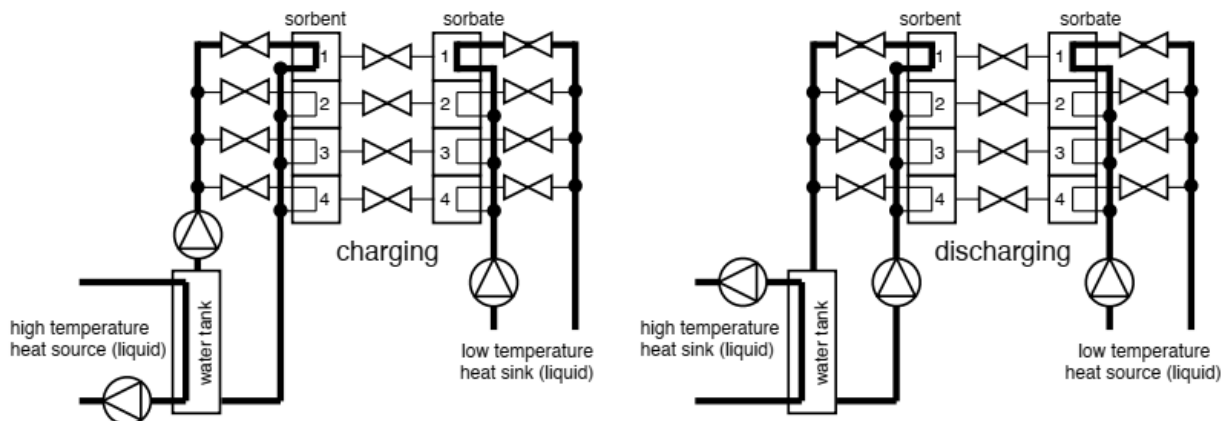


FIGURE 5-55: UNIFORM SCHEMATICS OF THE MERITS HEAT STORAGE SYSTEM, SHOWN IN THE CHARGING AS WELL AS THE DISCHARGING PROCESS.

The close sorption process consists of heat source (solar collectors, via short term storage buffer), heat storage (thermochemical storage modules) and sink (space heating, Domestic hot water application). For evaporation / condensation a low-temperature source / drain is connected to the TCS modules. A vacuum is kept inside these modules. In summer, water is evaporated from the TCS material and condenses in the water storage area. The valve is closed to enable heat storage. In winter, the valve is opened and the low-temperature source evaporates the water for sorption into the thermochemical material.

Major storage components: Long-term storage is the main component in the system, further comprising solar collectors, short term buffer and low-temperature source and drain. Major components in the long-term storage modules are the heat and mass exchanger for sorption (top of module), the storage valve (middle of module) and heat and mass exchanger for evaporation/condensation (bottom of module), in addition to connecting parts, valves and pumps. Heat exchanger materials are

often pacified copper, aluminum, or likewise. For pumps and valves common products are available. Criteria to be met are material compatibility depending on the heat transfer fluid and sufficiently gas tight sealing. Storage vessels are generally built from stainless steel. Resulting from the sub atmospheric pressure in the vessels, increased material thickness is required.

Benefits and challenges: Closed solid-sorption heat storage benefits from theoretically high thermal energy storage density and loss-free storage. Challenges in this system approach are found in material- and system-optimization and sealing. Enabling a high system energy storage density from inherently high material storage density is difficult, for getting high thermal conductivity of active material and good mass transport through the fixed bed are counter acting. Leakage of air into the system rapidly reduces the sorption process, leading to a reduction of temperature increase and energy density. Due to the dependency of the temperature increase on the hydration state of the sorbent, preferably a material with a single pT-line is used. A high slope means a high energy density. The closed absorption heat storage is highly sensitive to operating temperatures. In general, if water is used as sorbate, evaporation temperatures below 0°C are not favorable.

Possible working pairs

- Na₂S, K₂CO₃, CaCl₂
- Furthermore, same as mentioned in other solid sorption options

Examples in literature: TNO (The Netherlands) are working on solid sorption heat storage systems based on Na₂S, K₂CO₃ and CaCl₂. for seasonal and shorter-term heat storage applications in buildings and industry [refs].

References

“Thermochemical heat storage – from reaction storage density to system storage density”, A.J. de Jong, L. van Vliet, C. Hoegaerts, M. Roelands, R. Cuypers, Energy Procedia, 2016, 91, 128-137.

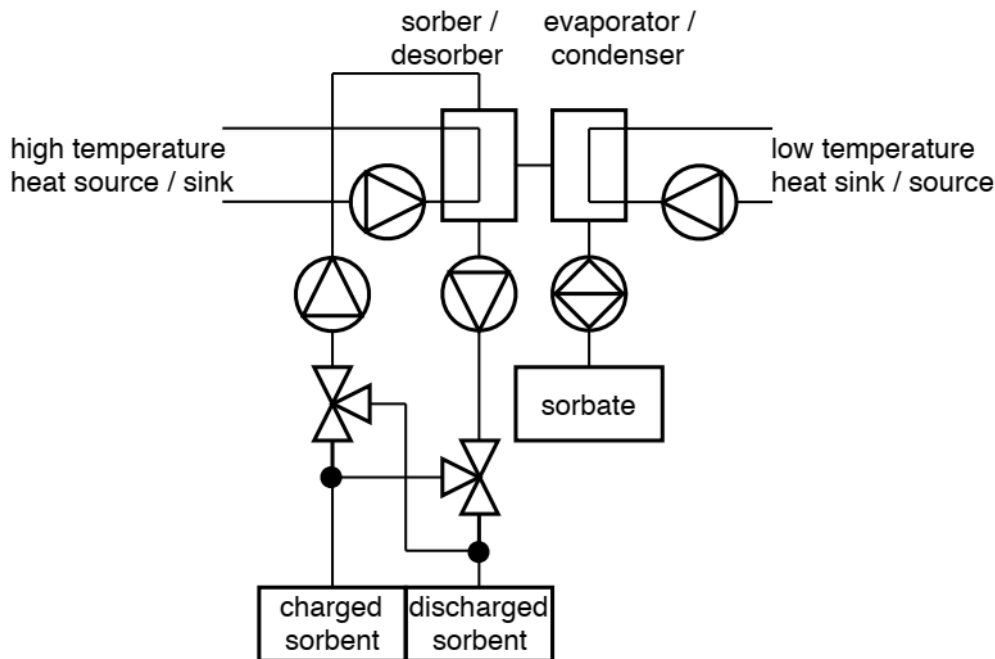
“Preparation & characterization of sodium sulfide hydrates for application in thermochemical storage systems”, M. Roelands, R. Cuypers, K. Kruit, H. Oversloot, A.J. de Jong, H. van ‘t Spijker, W. Duvalois, L. van Vliet, C. Hoegaerts, Energy Procedia, 2015, 70, 257 – 266.

“Thermochemical heat storage (TCS) - system design issues”, A.J. de Jong, C. Finck, H. Oversloot, H. van ‘t Spijker, R. Cuypers, Energy Procedia, 2014, 48, 309 – 319.

“A review on properties of salt hydrates for thermochemical storage”, F. Trausel, A.J. de Jong, R. Cuypers, Energy Procedia, 2014, 48, 447 – 452.

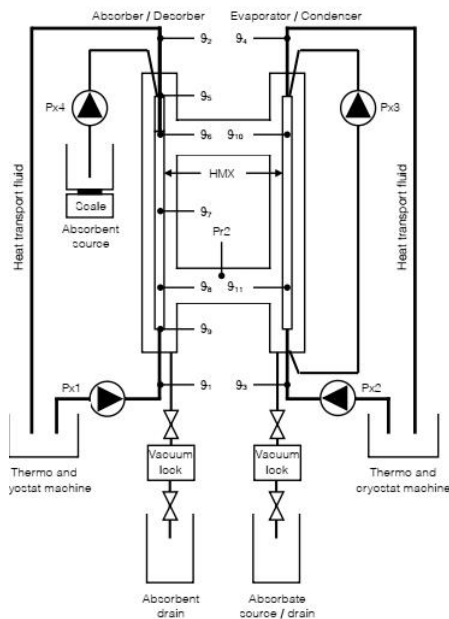
CLOSED-TRANSPORTED SYSTEMS

Closed and transported systems store both sorbent and sorbate in separate vessels and have a heat and mass exchanger (conversion) unit. In this way power and energy capacity are separated. These systems are frequently used for liquid sorbents, due to the simplicity of transporting liquids.



CLOSED LIQUID ABSORPTION HEAT STORAGE, EMPA – SWITZERLAND, BENJAMIN FUMEY

Short description: Closed absorption systems are based on liquid absorbents, whereby both storage and heat and mass exchanger are under vapor pressure atmosphere, all other gasses, often referred to as non-condensing gasses are removed. Thus, in general the system is under sub atmospheric pressure. Due to the liquid state of the absorbent and the absorbate, storage vessels and heat and mass exchanger units can be separated, leading to separation of power from energy capacity. In absorption heat storage heat is stored by separation of absorbate from absorbent working fluid. Heat is released by evaporation of absorbate by low temperature heat source and absorption there of on the absorbent. In this process both heat of condensation and heat of solution are released. In general heat of condensation is the greater part. The closed absorption heat storage operates thus as an absorption heat pump with intermediate absorbent and absorbate storage. The temperature lift between evaporator and absorber is dependent on the absorbent and its concentration. It follows that the output temperature of the storage system is dependent on the evaporator temperature and the absorbent working pair concentration. Working pair energy density on the other hand is dependent on the absorbate difference between charged and discharged absorbent working pair. This is limited to the temperature difference between the evaporator and the minimum absorber temperature.



Component	Description
Px1	Absorber / desorber heat transfer fluid pump
Px2	Evaporator / condenser heat transfer fluid pump
Px3	Absorbate circulation pump
Px4	Absorbent solution supply pump
θ ₁	Temperature of heat transfer fluid to absorber / desorber
θ ₂	Temperature of heat transfer fluid from absorber / desorber
θ ₃	Temperature of heat transfer fluid to evaporator / condenser
θ ₄	Temperature of heat transfer fluid from evaporator / condenser
θ ₅	Temperature of absorbent solution entering heat and mass exchanger
θ ₆	Temperature of absorbent solution after preheating section
θ ₇	Temperature of absorbent solution on heat and mass exchanger
θ ₈	Temperature of absorbent solution on heat and mass exchanger
θ ₉	Temperature of absorbent solution after heat and mass exchanger
θ ₁₀	Temperature of absorbate on heat and mass exchanger
θ ₁₁	Temperature of absorbate on heat and mass exchanger
Pr2	Pressure in heat and mass exchanger chamber

Vacuum lock



Monitoring equipment

Absorbent supply Absorbate supply

FIGURE 5-56: SCHEMATICS AND PICTURE OF EMPA'S NaOH / H₂O LABORATORY LIQUID ABSORPTION SYSTEM.

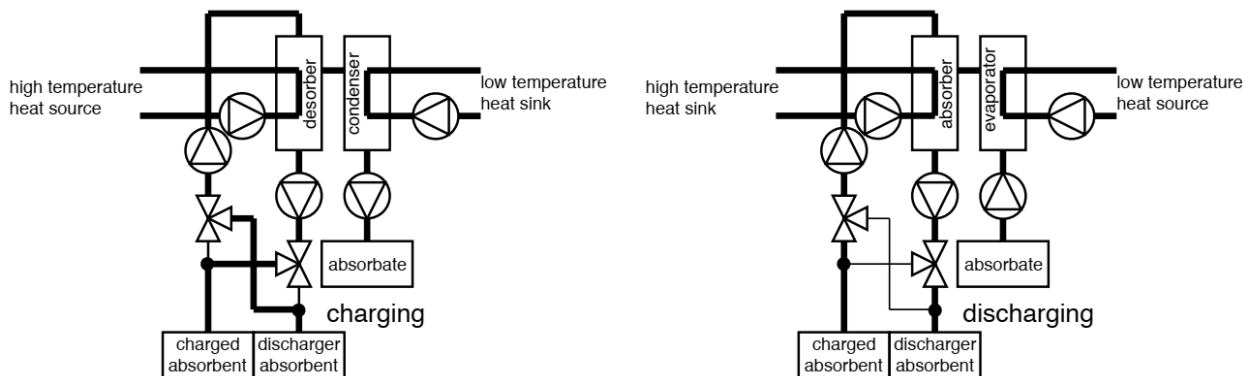


FIGURE 5-57: UNIFORM SCHEMATICS OF SYSTEM.

The close absorption process consists of three major components, heat converter, connection pumps and valves and storage tanks, as shown in Figure 5-56 and in the uniform schematics in Figure 5-57. The complete system is kept air tight. High temperature heat is supplied to the heat and mass exchanger in the schematics from the left and released on the right side in the charging process. In the

discharging process, heat at low temperature is sourced from the right and released at elevated temperature on the left.

Major components: Major components are the heat and mass exchanger, connecting parts and storage vessels. The heat and mass exchanger often consists of an absorber and desorber and a condenser and evaporator unit. Combination of the two operations respectively is possible due to the non-continuous process involved in the storage application, compared to continuous absorption and desorption process found in other absorption systems such as solar chillers. Nevertheless, there is indication that optimized heat and mass exchangers may not permit this combination. For pumps and valves common products are available. Criteria to be met are material compatibility depending on the absorbent and sufficient gas tight sealing. For this reason, often magnetic drive gear pumps are employed. Storage vessels are in general built of mild steel or stainless steel depending on the absorbent involved. Resulting from the sub atmospheric pressure in the vessels, increased material thickness is required. Tank in tank systems are generally required in order to reach safe storage.

Benefits and challenges: Closed absorption heat storage benefits from separation of power and capacity. This enables flexible design and easy application specific optimization. Exclusion of non-condensing masses enables evaporation from low temperature source and reaching higher vapor pressure than open systems at equivalent source temperature as well as reducing resistance to absorption in the gas phase. Challenges in this system approach are found in system sealing. Leakage of air into the system rapidly reduces the absorption process, leading to a reduction of temperature increase and energy density. Due to the dependency of the temperature increase on the absorbent concentration, a single pass process is required. Recirculation leads to reduction of absorbent in the working pair and in turn reduction of temperature lift. Energy density of the working pair is dependent on the absorbate mass difference between charged and discharged absorbent working fluid. High difference leads to increased energy density. The closed absorption heat storage is highly sensitive to operating temperatures. In general, if water is used as absorbate, temperatures below 0°C are not favorable.

Possible working pairs

- LiBr / H₂O
- LiCl / H₂O
- NaOH / H₂O

Example in literature: The Swiss research institute Empa is working on absorption heat storage systems based on the working pair NaOH / H₂O for seasonal heat storage applications in buildings [Fumey et al. 2017]. The University of Savoie in France is working on heat storage for buildings based on LiBr / H₂O [N'Tsoukpoe et al. 2013]. Tsinghua University in China has performed tests with the working pair LiBr / H₂O [Zhang et al. 2014]. The University of Minnesota, USA has worked on liquid calcium chloride [Quinnell et al. 2011] and the University of Dalarna Sweden has worked on liquid LiCl / H₂O solutions [Bales et al. 2006].

References

Fumey B., Weber R., Baldini L., Liquid sorption heat storage – A proof of concept based on lab measurements with a novel spiral fined heat and mass exchanger design, *Applied Energy*, Volume 200, 2017, Pages 215-225,

N'Tsoukpoe K.E., Le Pierrès N., Luo L., “Experimentation of a LiBr-H₂O absorption process for long-term solar thermal storage: prototype design and first results”, *Energy* 2013.

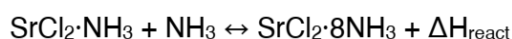
Zhang X., Li M., Shi W., Wang B., Li X., “Experimental investigation on charging and discharging performance of absorption thermal energy storage system”, *Energy Conversion and Management*, 85, 425–434, 2014.

Quinnell, Josh & H. Davidson, Jane & Burch, Jay. (2011). Liquid Calcium Chloride Solar Storage: Concept and Analysis. *Journal of Solar Energy Engineering*. 133. 10.1115/ ES2010-90181.

Bales, C., 2006. Solar cooling and storage with the thermo-chemical accumulator. In: *Eurosun 2006*.

NEUTRONS FOR HEAT STORAGE (NHS) PROJECT: AMMONIA-SRCL₂ ABSORPTION DESORPTION THERMAL ENERGY STORAGE SYSTEM DESIGN DTU - DENMARK / KTH - SWEDEN DIDIER BLANCHARD (DTU), SAMAN NIMALI GUNASEKARA (KTH), STEFANO DELEDDA (IFE), VIKTORIA MARTIN (KTH), AGATA BIALY (AMMINEX), BENOIT CHARLAS (AMMINEX), ANASTASIIA KARABANOVA (DTU) AND PERIZAT BERDIYEVA (IFE).

Short description: The Neutrons for Heat Storage (NHS) project aims to develop a thermochemical heat storage system for low-temperature heat storage (40-80 °C). Here, reversible chemical reactions (absorption and desorption) between metal halides and ammonia are chosen to be used. The project is a Nordic collaboration between DTU and Amminex-Denmark; IFE-Norway; and KTH Sweden. In the project so far, the reversible absorption-desorption of ammonia (NH₃) in SrCl₂ has been considered. The project leader DTU has developed a bench-scale TCM-based storage system for this NH₃-SrCl₂ reaction. In this reaction, the specific reversible conversion between SrCl₂·NH₃ and SrCl₂·8NH₃ is considered (as shown in the below equation), with a reaction enthalpy (ΔH_{react}) of 41.4 kJ/mol NH₃ [1].



In-addition, DTU and the project partners IFE and Amminex will synthesize and characterize new mixed metal halides salts of improved properties. The composition of these mixed halides result from a theoretical screening study performed over more than ten thousand possible multiple cations-halides combination using density functional theory and a genetic algorithm. The project partner KTH will develop an improved bench-scale system, either for the same SrCl₂-NH₃ reaction, or for a successful new mixed metal halide candidate (to react with ammonia) synthesized by the project partners. The project includes Neutron Imaging (diffraction, radiography and tomography) to characterize the micro and micro structural changes of the halides salt during the ammonia absorption-desorption cycling. The information gathered with the neutron imaging will help to rationally design the bench scale system [Soprani 2016]. A schematic of the NH₃-SrCl₂ TCS set-up constructed at DTU-Denmark is shown in Figure 5-58.

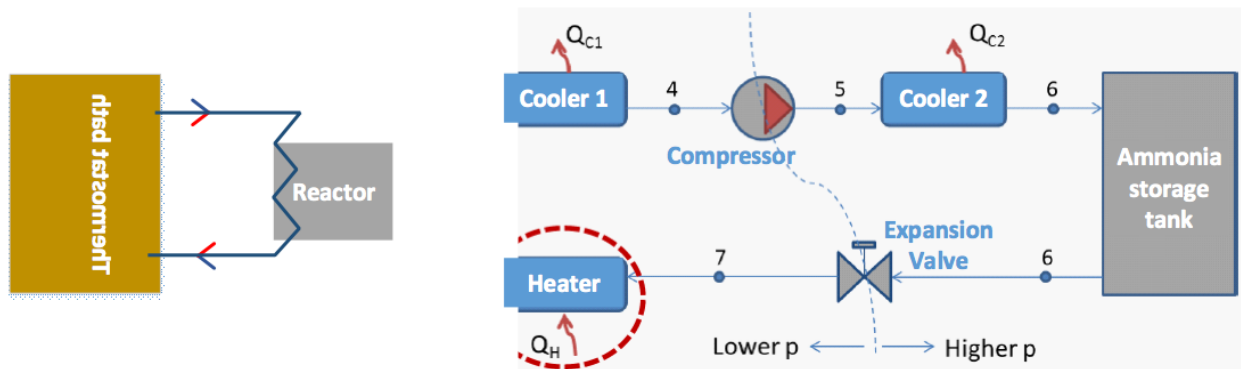


FIGURE 5-58: THE NH₃-SRCL₂ TCS SYSTEM CONSTRUCTED AT DTU, DENMARK, AS A FIRST STEP OF THE NHS PROJECT (MODIFIED BASED ON SOPRANI 2016)

Major Components: This set-up consists of the following major components: an absorption/desorption reactor integrated with a heat exchanger, a thermostat bath (i.e., the heat/cold supply), two passive coolers, a passive heater, an expansion valve, a compressor, and an ammonia storage tank (maintained at ~10 bar and room temperature) [Soprani 2016]. In the NH₃-SrCl₂ TCS set-up constructed at DTU, the reactor is the heat or cold storage unit, respectively at the end of absorption and desorption. The thermostat bath acts respectively as the external cooling and heating source, during absorption and desorption. The two coolers and the heater are heat exchangers exposed to ambient air. During absorption, SrCl₂·NH₃ in the reactor is exposed to gaseous ammonia to form its octa-ammine (SrCl₂·8NH₃). During desorption (i.e., the reverse reaction), the ammoniated metal halide: SrCl₂·8NH₃ converts back into the monoamine, SrCl₂·NH₃ and ammonia gas is released. During absorption which is exothermic, the produced heat is absorbed by the cold thermostat heat transfer fluid (silicon oil) running through the heat exchanger. Thus, the thermostat bath acts as the heat sink. During desorption, which is endothermic, the hot thermostat bath heats the reactor bed, thus making the thermostat bath the heat source [Soprani 2016]. The expansion valve operates only during the absorption cycle, and expands liquid ammonia into vapor, during the absorption cycle. The compressor operates only during the desorption cycle, liquifying the desorbed gaseous ammonia at 10 bars, and room temperature. The heater between the expansion valve and the reactor heats the expanded gaseous ammonia back to room temperature, to enhance the absorption process while avoiding risks of frost formation in the pipes. Cooler 1 cools down the hot ammonia gas released from the reactor during desorption to room temperature. Cooler 2 cools the liquid ammonia that is heated up during the gas-to-liquid compression process, also back to room temperature. This liquid ammonia is then stored in the ammonia storage tank maintained at ~10 bar and room temperature [Soprani 2016].

Benefits and Challenges: The benefits of this type of a TES include, among others, their ability to: provide respectively up to ~25 times and ~5 times larger thermal storage densities as compared to sensible and latent heat storages; store heat/cold with simpler requirements on insulations (as compared to sensible or latent heat storage); and offer a wide operating temperature range that can be changed based on the operating pressure variations. The challenges include: the stricter requirements on the working pair on avoiding contact with ambient air, high-pressure vessels and piping design, and handling and storage of ammonia as a highly toxic gas.

Possible Working Pairs

- $\text{MgCl}_2\text{-NH}_3$ (Mofidi and Udell, 2017)
- $\text{MnCl}_2\text{-NH}_3$ (Li et al., 2010, Bao et al., 2012, Jiang et al., 2016a, 2016b, Zhu et al., 2016, and Li et al., 2016)
- NaBr-NH_3 (Li et al., 2016)
- $\text{BaCl}_2\text{-NH}_3$ (Li et al., 2010)
- $\text{NH}_4\text{Cl-NH}_3$ (Bao et al., 2012)
- $\text{CaCl}_2\text{-NH}_3$ (Jiang et al., 2016a, 2016b, and Zhu et al., 2016)

Examples in Literature:

Examples of NH_3 -metal halide TCS systems from literature are:

- Al-Zareer, Dincer and Rosen, 2017: A TCS system using $\text{SrCl}_2\text{-NH}_3$ has been investigated using experimental and numerical modelling on heat transfer and thermodynamic analyses. Here, solid metal halide powder is circulated within the system, unlike many other similar studies.
- Mofidi and Udell, 2017: A TCS system employing $\text{MgCl}_2\text{-NH}_3$ was studied with heat and mass transfer analyses experimentally and with numerical modelling, to assess the system as a thermochemical battery
- Li et al., 2010: The TCS systems: using $\text{BaCl}_2\text{-NH}_3$ as the low-temperature system, and $\text{MnCl}_2\text{-NH}_3$ as the high-temperature system (with the metal halides embedded in expanded graphite) were experimentally studied as refrigeration cycles.
- Bao et al., 2012: The TCS systems $\text{MnCl}_2\text{-NH}_3$ and $\text{NH}_4\text{Cl-NH}_3$ were experimentally studied, respectively considered as the high-temperature and low-temperature systems, for cold storage and long-distance refrigeration.
- Jiang et al., 2016a, 2016b, and Zhu et al., 2016: The TCS systems $\text{MnCl}_2\text{-NH}_3$ and $\text{CaCl}_2\text{-NH}_3$ were studied experimentally, respectively considered as the high-temperature and low-temperature systems, for power, heat and refrigeration cogeneration.
- Li et al., 2016: An experimental study of a TCS system employing $\text{MnCl}_2\text{-NH}_3$ also compared with a theoretical assessment of another working pair: NaBr-NH_3

References

- S. Soprani, "MODELING – TES system based on $\text{SrCl}_2 - \text{NH}_3$," Roskilde, 2016.
- S. A. H. Mofidi and K. S. Udell, "Study of Heat and Mass Transfer in $\text{MgCl}_2 / \text{NH}_3$ Thermochemical Batteries," J. Energy Resour. Technol., vol. 139, no. 3, p. 032005, 2017.
- T. X. Li, R. Z. Wang, J. K. Kiplagat, and H. Chen, "Experimental study and comparison of thermochemical resorption refrigeration cycle and adsorption refrigeration cycle," Chem. Eng. Sci., vol. 65, no. 14, pp. 4222–4230, 2010.
- H. S. Bao, R. Z. Wang, R. G. Oliveira, and T. X. Li, "Resorption system for cold storage and longdistance refrigeration," Appl. Energy, vol. 93, pp. 479–487, 2012.

L. Jiang, F. Q. Zhu, L. W. Wang, C. Z. Liu, and R. Z. Wang, "Experimental investigation on a $\text{MnCl}_2\text{-CaCl}_2\text{-NH}_3$ thermal energy storage system," *Renew. Energy*, vol. 91, pp. 130–136, 2016.

L. Jiang, L. W. Wang, C. Z. Liu, and R. Z. Wang, "Experimental study on a resorption system for power and refrigeration cogeneration," *Energy*, vol. 97, pp. 182–190, 2016.

F. Q. Zhu, L. Jiang, L. W. Wang, and R. Z. Wang, "Experimental investigation on a $\text{MnCl}_2\text{-CaCl}_2\text{-NH}_3$ resorption system for heat and refrigeration cogeneration," *Appl. Energy*, vol. 181, pp. 29–37, 2016.

T. X. Li, J. X. Xu, T. Yan, and R. Z. Wang, "Development of sorption thermal battery for low-grade waste heat recovery and combined cold and heat energy storage," *Energy*, vol. 107, pp. 347–359, 2016.

M. Al-Zareer, I. Dincer, and M. A. Rosen, "Heat Transfer and Thermodynamic Analyses of a Novel Solid-Gas Thermochemical Strontium Chloride-Ammonia Thermal Energy Storage System," *J. Heat Transfer*, vol. 140, no. February, pp. 1–17, 2017.

CLOSED ABSORPTION AND DESORPTION PROCESSES FOR THERMO-CHEMICAL ENERGY STORAGE FOR RESIDENTIAL APPLICATIONS, SPF - SWITZERLAND PAUL GANTENBEIN

Process description: The absorption process is based on the absorption of sorbate vapour in the liquid sorbent. This reversible and exothermic reaction is used to store solar thermal energy, waste heat, etc. for a long(er) period. A closed sorption storage system is working under sub-atmospheric pressure conditions. The noncondensing gases (i.e. air) have to be excluded for a good heat and mass transfer – which means, the system has to be vacuum tight. Under these conditions, the boiling temperature and thus the evaporation temperature of a liquid correlates with the temperature level of the low temperature heat source. In this system type – a thermally driven heat pump – the evaporation temperature should be in the range of $T = 5\text{ }^\circ\text{C} - 20\text{ }^\circ\text{C}$. The driving force of the vapor flow in the closed system is the pressure difference $\Delta p_{\text{discharging}}$ between the heat and mass transfer units and $\Delta p_{\text{charging}}$, where $\Delta p_{\text{discharging}} = p_E - p_A$ and $\Delta p_{\text{charging}} = p_D - p_C$, A=absorber, C=condenser, D=desorber and E=evaporator. Figure 5-59 shows the schematic design and the working principle of the charging and discharging processes of the absorption storage system with sodium lye as an example for the sorbent and water vapor as the sorbate and Figure 5-60 shows the respective uniform schematics.

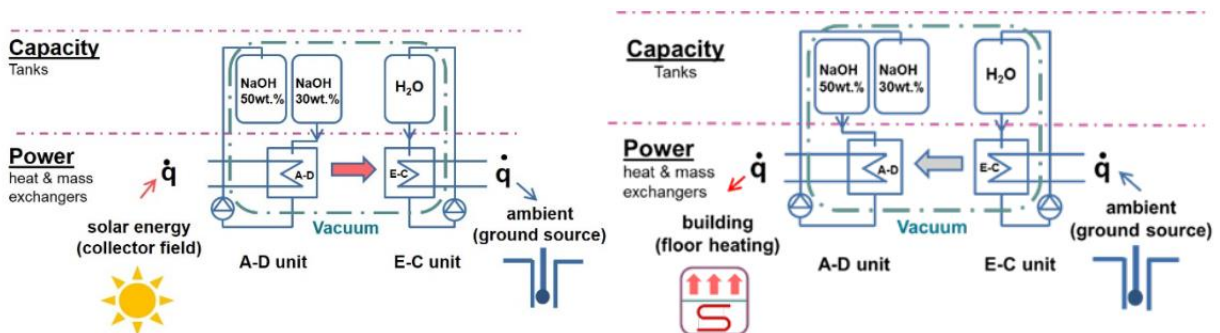


FIGURE 5-59: SCHEMATIC OF A CLOSED ABSORPTION STORAGE SYSTEM. THE SKETCH ON THE LEFT SIDE SHOWS THE CHARGING (DESORPTION) PROCESS, WHEREAS THE SKETCH ON THE RIGHT SIDE SHOWS THE DISCHARGING – THE ABSORPTION – PROCESS.

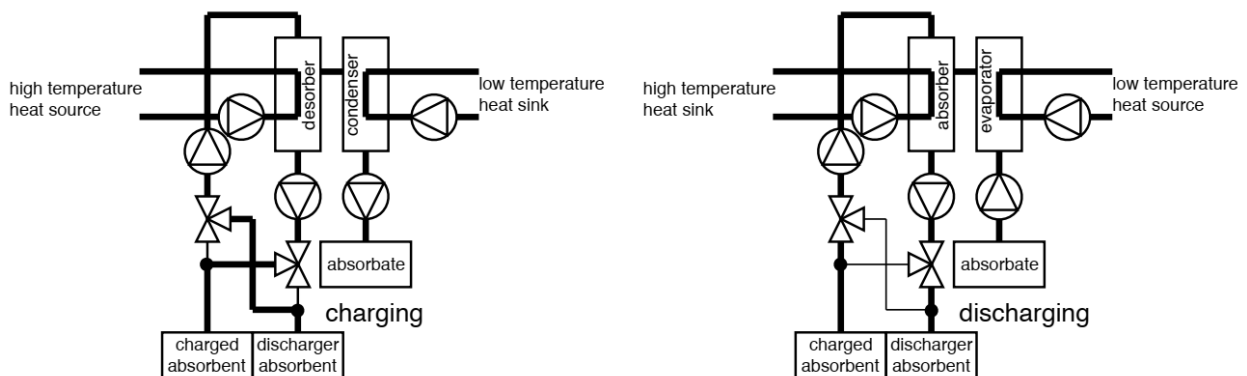


FIGURE 5-60: UNIFORM SCHEMATICS OF SYSTEM.

To charge, thus to evaporate water from the lye solution, the heat from the high temperature heat source is transferred via the fluid pumping system and the desorber heat and mass exchanger to the sorbent lye. The liquid lye is heated up and a part of the water will be evaporated. The pressure in the desorber is increasing and due to the lower pressure in the condenser, the vapour flows to the condenser. The low temperature heat sink transfers the released heat of condensation and the condensed (liquid) water is pumped to the water tank. Both water and the concentrated lye can be stored separately in tanks until the discharging starts. The discharging process is started by pumping the water - i.e. the sorbate - to the evaporator, where it changes the phase to vapor due to the supply of heat from the low temperature heat source. Due to the lower pressure of the concentrated and cold lye (sorbent), the vapor flows to the absorber unit. The water vapor is absorbed by the lye and the heat of absorption is released – the reaction is exothermic. The released heat at higher temperature is transferred via the absorber heat and mass exchanger and transported to the heat distribution system – to the user.

Main components: The main components from an absorption/desorption storage system are the “power unit” and the “capacity unit”. The heat and mass transfer units for evaporation & absorption as well as desorption & condensation are heat and mass exchangers of any type and structure. They form the “power units” of the storage system. The storage tanks for the sorbent and the sorbate form the “capacity units”. A sub-system with dosing pumps for the sorbent and sorbate, and the piping between the power and capacity units are needed. Moreover, a high temperature heat source (in this case solar thermal collectors), a low heat temperature source, e.g. a bore hole and a mid-temperature heat sink (building) are necessary to drive the system. The system has to be equipped with sensors and a controller.

Benefits and challenges: In general, the absorption technology has the advantage of a high energy density (estimated 4 times higher than liquid water depending on the concentration lift Δc of the lye). The potential of storing energy is heat loss-free in case of no running processes. The closed absorption process has the advantage of a low evaporation (boiling) temperature in the sub-atmospheric pressure range. For discharging, a low temperature of $T=5\text{ }^{\circ}\text{C}$ - $10\text{ }^{\circ}\text{C}$ is sufficient in winter time for the evaporation heat source. The heat of evaporation (Δh_v) can be provided by a ground/air source or

indirect, like in the EU COMTES project, using the buffer tanks where the solar energy was stored. Due to their liquid state, the sorbent and the sorbate can be pumped from the storage tanks to the reaction zone and back i.e. the power unit (kW) and the capacity units (kWh) are separated – similar to oil or gas burner and the oil or gas tanks. Compared to an open system, the advantages are: the performance of the system is independent of the humidity in the air and higher energy densities can be achieved by better exploitation of the absorption capacity of the lye. As the system is closed, (slightly) hazardous materials can be used because no mass transfer is occurring to the outside of the system. One challenge for this technology is to reach the system compactness based on the theoretical energy density. The energy density based on the sorbent-sorbate combination is high, but due to the complexity of the system, the other system components require additional room. Moreover, the experiences made in the COMTES project showed that the wetting of the heat and mass exchanger surfaces and the residence time of the lye in the vapor have to be increased. In addition and beside of the technological challenges, our experience from former projects showed that a significant reduction of the investment costs is still necessary to get the storage system into market.

Possible working pairs: General: hygroscopic liquids e.g. lye, salt solutions, ionic liquids combined with H₂O. Specific: sodium lye NaOH-H₂O and water vapour; LiBr-H₂O and water vapour; LiCl-H₂O and water vapour.

Examples in literature

Daguenet-Frick X. et al.: Development of a numerical model for the reaction zone design of an aqueous sodium hydroxide seasonal thermal energy storage.

Daguenet-Frick X. et al.: Seasonal thermal energy storage with aqueous sodium hydroxide - experimental assessments of the heat and mass exchanger unit.

Dudita M. et al.: Closed Sorption Seasonal Thermal Energy Storage with Aqueous Sodium Hydroxide.

References

Daguenet-Frick, X., Gantenbein, P., Frank, E., Fumey, B., Weber, R., 2015a. Development of a numerical model for the reaction zone design of an aqueous sodium hydroxide seasonal thermal energy storage. Sol. Energy, ISES Solar World Congress 2013 (SWC2013) Special Issue 121, 17–30. doi:10.1016/j.solener.2015.06.009.

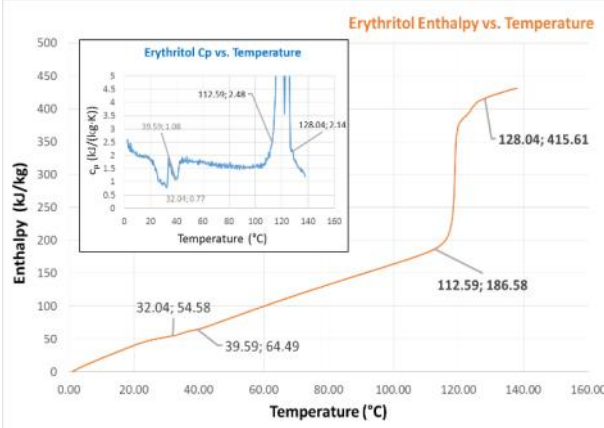
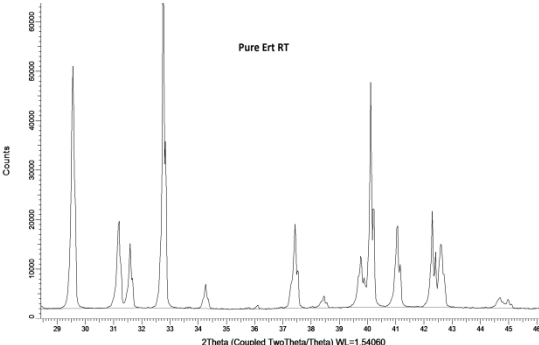
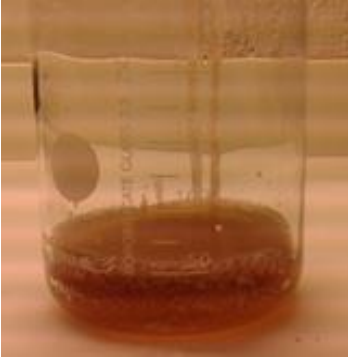
Daguenet-Frick, X., Gantenbein, P., Frank, E., Fumey, B., Weber, R., Goonesekera, K., 2015b. Seasonal thermal energy storage with aqueous sodium hydroxide - experimental assessments of the heat and mass exchanger unit. Presented at the International Conference on Solar Heating and Cooling for Buildings and Industry, Istanbul, Turkey.

Dudita, M., Daguenet-Frick, X., Gantenbein, P., 2018. Closed Sorption Seasonal Thermal Energy Storage with Aqueous Sodium Hydroxide, in: Visa, I., Duta, A. (Eds.), Nearly Zero Energy Communities: Proceedings of the Conference for Sustainable Energy (CSE) 2017. Springer International Publishing, Cham, pp. 239–246. doi:10.1007/978-3-319-63215-5_18.

6 APPENDICES

6.1 SUBTASK 2P: MATERIAL DATA SHEETS

First Name Saman Nimali	Family Name Gunasekara
Institution KTH Royal Institute of Technology	
Address	
Street Brinellvägen 68	
Zip-Code 100 44	City Stockholm
Country Sweden	
email saman.gunasekara@energy.kth.se	Telephone +46 73652 3339
Material Data/Information	Date: 05.12.2017
Material Designation Meso-Erythritol (99% purity), thermo-physical characterizations using the T-History, TPS and XRD methods	
PCM (single component (U)/ composite (Cm) or, a blend: binary (B)/ ternary (T)..., eutectic (E)/ solid solution (Ss)/ compound (C)) 1. meso-erythritol (U)	Composite material(s)
Data for the component/ composite/ blend	
Melting Temperature [°C] 112.6-128.0	Minimum Temperature [°C] 0 (min. of the measurement range)
Storage Capacity [kJ/kg] 229±64	Maximum Temperature [°C] 138 (max. of the measurement range)
Density [kg/l]	Cycle Stability (how many thermal cycles tested, if possible reduction in kJ/kg·h)

<p>Unevaluated</p>	<p>~5 cycles, and the given results exclude the very first melting. The melting enthalpy found here seem at least 19-25 % lower than the literature values, possibly due to the cycled behavior analyzed here.</p>
<p>Supercooling [K] ~10 K</p>	<p>Material compatibility Not yet tested systematically. Nevertheless, it appears to be compatible with metals, but cracks glass (especially at higher temperatures or during solidification respectively).</p>
<p>Technology readiness levels (TRL) Unevaluated</p>	<p>Additional Parameter Thermal conductivity: 0.32 W/m K (liquid at 125 °C), and 0.59 W/m K (solid at 20 °C)</p>
<p>If possible, please insert DSC-curve or other characteristic graph</p> 	<p>Please insert an image/photo</p> <p>Erythritol X-Ray Diffraction (XRD) characteristics at room temperature</p>  <p>Thermally activated change in Erythritol [Gunasekara et al., 2016]:</p> 
<p>Target Applications (up to 4 most relevant)</p> <ol style="list-style-type: none"> 1. district heating 2. mobile heat storage 	





Comments

The main reason for the low melting enthalpy is possibly the thermally activated change (browning and thickening of material at the end of the T-history cycles, conducted within air). However, the literature data for the melting enthalpy of erythritol are also very disparate, within a very wide range: 281–370 kJ/kg, most often presented without specifying the number of cycles these values represent, and if specified, mostly representing only the first melting.

The reuse of this given photograph of the browned erythritol may require permission from the publisher of Gunasekara et al., 2016 (Elsevier).

First Name	Saman Nimali	Family Name	Gunasekara
Institution	KTH Royal Institute of Technology		
Address			
Street	Brinellvägen 68		
Zip-Code	100 44	City	Stockholm
Country	Sweden		
email	saman.gunasekara@energy.kth.se	Telephone	+46 73652 3339
Material Data/Information	Date: 21.12.2017		
Material Designation			
Xylitol (99% purity), thermo-physical characterizations using the T-History, TPS and XRD methods			
PCM (single component (U)/ composite (Cm) or, a blend: binary (B)/ ternary (T)..., eutectic (E)/ solid solution (Ss)/ compound (C))	Composite material(s)		
1. xylitol (U)			
Data for the component/ composite/ blend			
Melting Temperature [°C]	Minimum Temperature [°C]		

90.6–97.7	0 (min. of the measurement range)
Storage Capacity [kJ/kg] 164±46	Maximum Temperature [°C] 138 (max. of the measurement range)
Density [kg/l] Unevaluated	Cycle Stability (how many thermal cycles tested, if possible reduction in kJ/kg·h) ~5 cycles, and the given results exclude the very first melting. This given melting enthalpy is for the 2 nd melting, because, afterwards the melting enthalpy was extremely subtle, due to heavy influence of glass transition. This enthalpy seems at least 19-25 % lower than the literature values, possibly due to the cycled behavior analyzed here.
Supercooling [K] Very large (as it becomes glassy)	Material compatibility Not yet tested systematically. Nevertheless, it appears to be compatible with metals, but cracks glass (especially at higher temperatures or during solidification respectively).
Technology readiness levels (TRL) Unevaluated	Additional Parameter Thermal conductivity: 0.41-0.43 W/m K (liquid at 110 °C), and 0.37 W/m K (solid at 20 °C)
If possible, please insert DSC-curve or other characteristic graph	Please insert an image/photo
	<p>Xylitol X-Ray Diffraction (XRD) characteristics at room temperature</p>
	Thermally activated change in xylitol (browned thickened material) [Gunasekara et al., 2016]:

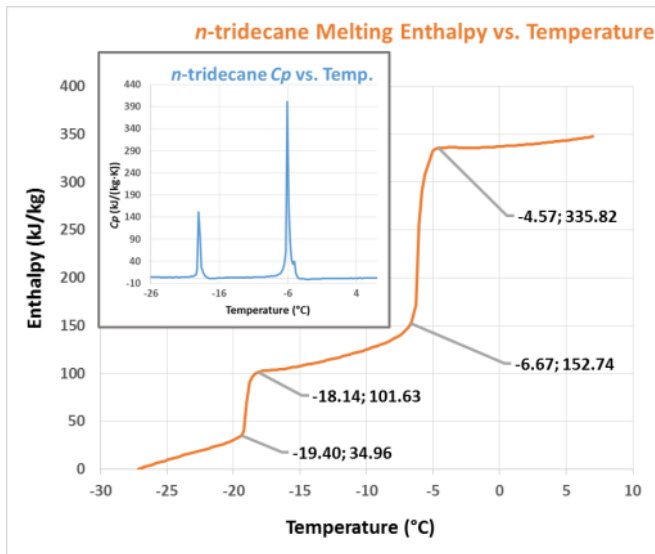
	 <p>Glassy nature of xylitol (the spatula is stuck within the extremely thick glassy liquid) [Gunasekara et al., 2016]:</p> 
<p>Target Applications (up to 4 most relevant)</p> <ol style="list-style-type: none"> 1. district heating 2. mobile heat storage 	
<p>Comments</p> <p>The main reasons for the low melting enthalpy are possibly the heavy influence of glass transition as well as thermally activated change (browning and thickening of material at the end of the T-history cycles, conducted within air). Another reason is that xylitol, before its stable melting, indicated a minor change at a lower temperature (see figures at left-side). The literature data for the melting enthalpy of xylitol are also disparate, within a wide range: 219-280 kJ/kg, most often presented without specifying the number of cycles these values represent, and if specified, mostly representing only the first melting.</p> <p>The reuse of this given photographs of the browned xylitol and glassy xylitol may require permission from the publisher of Gunasekara et al., 2016 (Elsevier).</p>	

<p>First Name Saman Nimali</p>	<p>Name</p>	<p>Family Name Gunasekara</p>
<p>Institution KTH Royal Institute of Technology</p>		
<p>Address</p>		

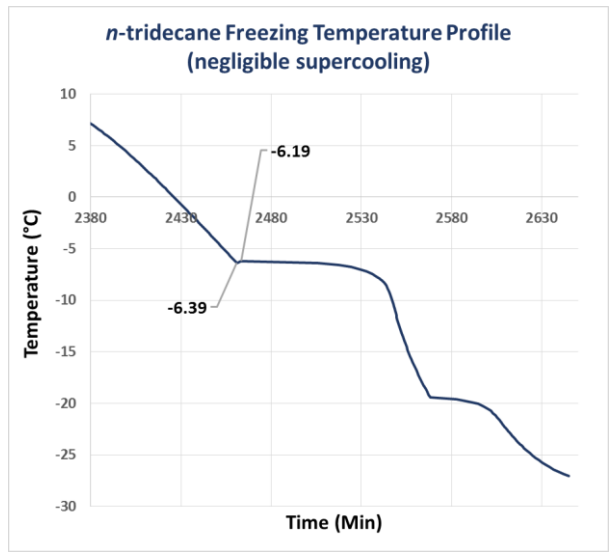
Street	
Brinellvägen 68	
Zip-Code	City
100 44	Stockholm
Country	
Sweden	
email	Telephone
saman.gunasekara@energy.kth.se	+46 73652 3339
Material Data/Information	Date: 05.12.2017
Material Designation	
<i>n</i> -tridecane (99%+ pure), thermal characterizations using T-History method	
PCM (single component (U)/ composite (Cm) or, a blend: binary (B)/ ternary (T)..., eutectic (E)/ solid solution (Ss)/ compound (C))	Composite material(s)
1. <i>n</i> -tridecane CH ₃ (CH ₂) ₁₁ CH ₃ (U)	
Data for the component/ composite/ blend	
Melting Temperature [°C]	Minimum Temperature [°C]
-6.7 to -4.5 (average over 2 nd to 4 th melting cycles)	-28 (min. of the measurement range)
Storage Capacity [kJ/kg]	Maximum Temperature [°C]
182±18 (average over 2 nd to 4 th melting cycles)	8 (max. of the measurement range)
Density [kg/l]	Cycle Stability (how many thermal cycles tested, if possible reduction in kJ/kg·h)
Unevaluated	5 cycles, while the given results exclude the very first melting. The results agree well with the literature values.
Supercooling [K]	Material compatibility
Negligible	Not yet tested systematically. Nevertheless, it appears to be compatible with metals and glass but incompatible with plastics.
Technology readiness levels (TRL)	Additional Parameter
Unevaluated	

Also undergoes a polymorphic phase change, between $-19.4\text{ }^{\circ}\text{C}$ and $-18.2\text{ }^{\circ}\text{C}$ (in heating) and $-19.5\text{ }^{\circ}\text{C}$ and $-20.3\text{ }^{\circ}\text{C}$ (in cooling) with the respective enthalpy changes $66 \pm 7\text{ kJ/kg}$ and $46 \pm 5\text{ kJ/kg}$.

If possible, please insert DSC-curve or other characteristic graph



Please insert an image/photo



Target Applications (up to 4 most relevant)

1. pre-cooling of refrigerants
2. cold storage below $0\text{ }^{\circ}\text{C}$
3. solid-solid PCM applications for cooling (considering the polymorphic phase)

Comments

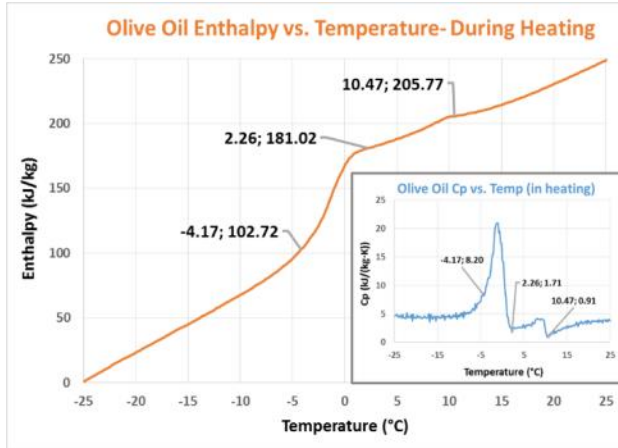
The results shown are for the 3rd melting (and freezing) cycle (in the T-history evaluation). Nonetheless, for all the evaluated cycles the sample displayed very consistent behaviors during both melting and freezing. This material (n-tridecane) also undergoes a polymorphic phase change (detailed under 'Additional Parameters').

First Saman Nimali	Name	Family Name Gunasekara
Institution KTH Royal Institute of Technology		
Address		
Street		

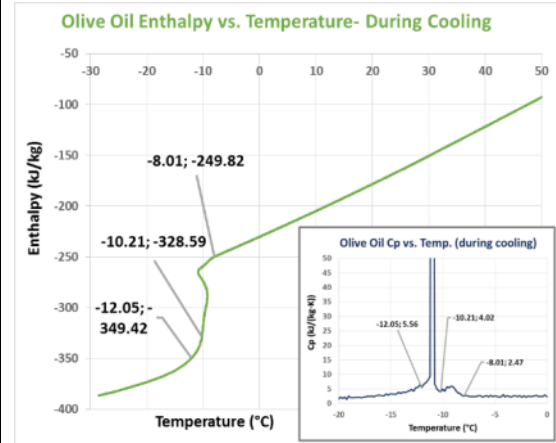
Brinellvägen 68	
Zip-Code 100 44	City Stockholm
Country Sweden	
email saman.gunasekara@energy.kth.se	Telephone +46 73652 3339
Material Data/Information	Date: 04.01.2018
Material Designation Olive Oil (virgin oil, commercial grade, unknown purity), thermal characterizations using T-History method	
PCM (single component (U)/ composite (Cm) or, a blend: binary (B)/ ternary (T)..., eutectic (E)/ solid solution (Ss)/ compound (C)) 1. Olive oil (multicomponent blend)	Composite material(s)
Data for the component/ composite/ blend	
Melting Temperature [°C] -4.5 to 10.3 (average over 2 nd to 4 th melting cycles, of 2 identical samples)	Minimum Temperature [°C] -30 (min. of the measurement range)
Storage Capacity [kJ/kg] 104±10 (average over 2 nd to 4 th melting cycles, of 2 identical samples)	Maximum Temperature [°C] 80 (max. of the measurement range)
Density [kg/l] Unevaluated	Cycle Stability (how many thermal cycles tested, if possible reduction in kJ/kg·h) 4 cycles, while the given results exclude the very first melting. The results agree well with the available literature values.
Supercooling [K] Minor (~2 K)	Material compatibility Not yet tested systematically. Nevertheless, it appears to be compatible generally with metals, glass and plastics.
Technology readiness levels (TRL) Unevaluated	Additional Parameter

Hysteresis is rather considerable (3.5 -22 °C), primarily due to its wide melting temperature range.

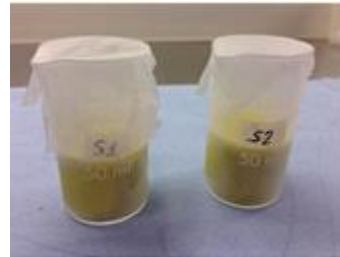
If possible, please insert DSC-curve or other characteristic graph



Please insert an image/photo



Frozen Olive oil samples (from a simple freezing pre-test):



Target Applications (up to 4 most relevant)

1. pre-cooling (within -4.5 to 10.3 °C) in chilling applications

Comments

The results shown are for the 3rd melting (and freezing) cycle (in the T-history evaluation), for one of the 2 tested identical samples. For all the evaluated cycles the samples anyways displayed very consistent behaviors respectively during melting and freezing.

The samples displayed a secondary phase change peak (which is a possible solid-solid phase change) consecutively before the melting c_p peak or, after the freezing c_p peak, respectively. This secondary peak was however smaller during cooling, as compared to that observed during heating.

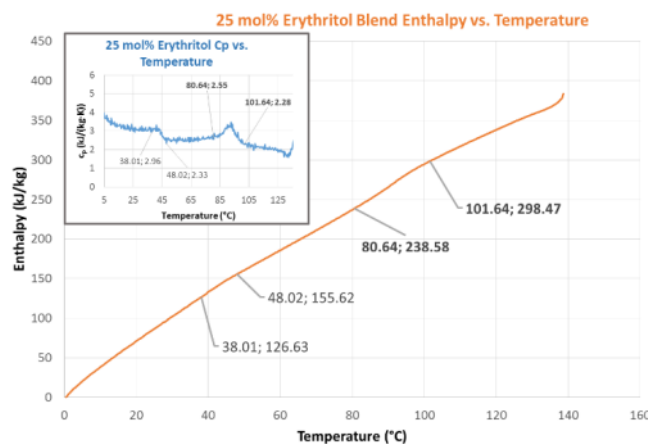
This secondary peak could be an indication of a near-eutectic composition in this multicomponent blend, or could be a polymorphic phase incurred due to the major triglyceride component in olive oil: triolein. The study

indicates that: olive oil is not recommendable as a PCM as it is, however, compositional refinements could yield an attractive renewable PCM out of it.

First Name Saman Nimali	Family Name Gunasekara
Institution KTH Royal Institute of Technology	
Address	
Street Brinellvägen 68	
Zip-Code 100 44	City Stockholm
Country Sweden	
email saman.gunasekara@energy.kth.se	Telephone +46 73652 3339
Material Data/Information	Date: 21.12.2017
Material Designation 25-30 mol% Erythritol in Xylitol, thermal characterizations using the T-History and TPS methods	
PCM (single component (U)/ composite (Cm) or, a blend: binary (B)/ ternary (T)..., eutectic (E)/ solid solution (Ss)/ compound (C)) 1. Erythritol-Xylitol (BE), @ 25-30 mol% Erythritol	Composite material(s)
Data for the component/ composite/ blend (shown for 25 and 30 mol% Erythritol respectively)	
Melting Temperature [°C] 80.6–101.6 and 80.0–91.1	Minimum Temperature [°C] 0 (min. of the measurement range)
Storage Capacity [kJ/kg]	Maximum Temperature [°C]

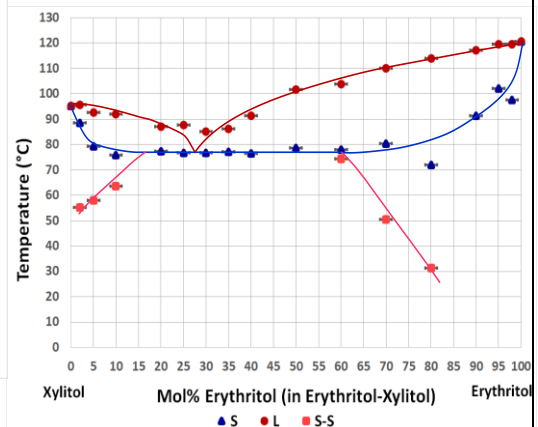
59.5±17 and 45±13 (Total including melting as well as glassy and intermediate changes: 172±48 and 200±56)	138 (max. of the measurement range)
Density [kg/l] Unevaluated	Cycle Stability (how many thermal cycles tested, if possible reduction in kJ/kg·h) ~5 cycles, and the given results exclude the very first melting. This given melting enthalpy is for the 2 nd melting, because, afterwards the melting enthalpy was extremely subtle, due to heavy influence of glass transition. This enthalpy seems at least 19-25 % lower than the literature values, possibly due to the cycled behavior analyzed here.
Supercooling [K] Very large (as it becomes glassy)	Material compatibility Not yet tested systematically. Nevertheless, it appears to be compatible with metals, but cracks glass (especially at higher temperatures or during solidification respectively).
Technology readiness levels (TRL) Unevaluated	Additional Parameter: for 25 mol% erythritol Thermal conductivity: 0.40 W/m K (liquid at 110 °C), and 0.39 W/m K (solid at 20 °C)

If possible, please insert DSC-curve or other characteristic graph



Please insert an image/photo

Erythritol-Xylitol Binary Phase Diagram [Gunasekara et al., 2018]



Target Applications (up to 4 most relevant)

1. district heating
2. mobile heat storage

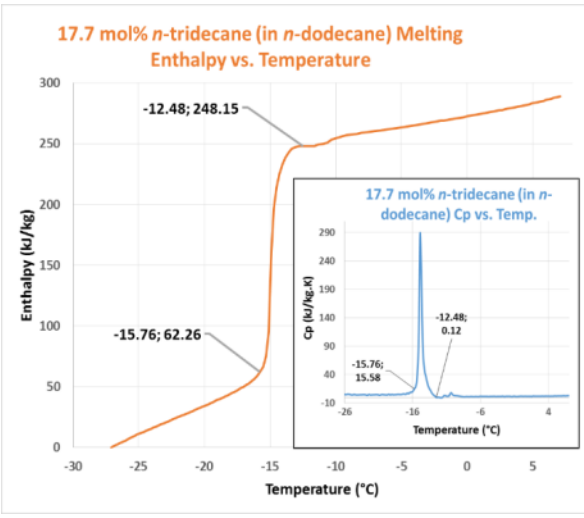
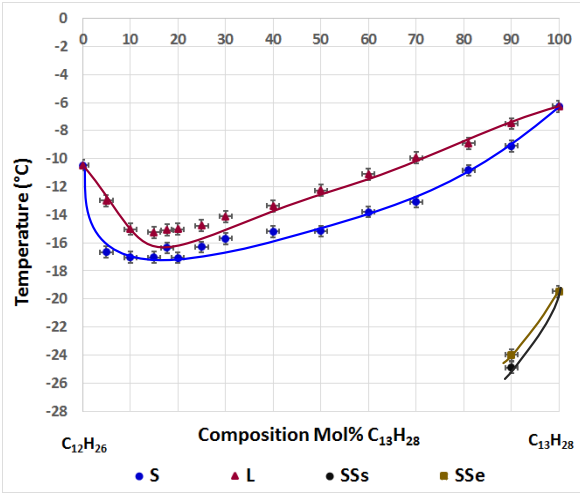


Comments

The eutectic was also heavily affected by glass transition, thus resulting in a very low melting enthalpy. Furthermore, after the 2nd melting (which is what's shown here) the phase change was almost completely overcome by glass transition. This composition also underwent thermally activated change (browning and thickening of material at the end of the T-history cycles, conducted within air), which is another possible reason for lowered melting enthalpy. The literature data for the melting enthalpy of this eutectic blend is larger, however cannot be compared directly as those studies do not specify what cycle it represented.

The reuse of this given phase diagram may require permission from the publisher (Elsevier).

First Name Saman Nimali	Name	Family Name Gunasekara
Institution KTH Royal Institute of Technology		
Address		
Street Brinellvägen 68		
Zip-Code 100 44	City Stockholm	
Country Sweden		
email saman.gunasekara@energy.kth.se	Telephone +46 73652 3339	
Material Data/Information		Date: 05.12.2017
Material Designation <i>n</i> -dodecane- <i>n</i> -tridecane binary system (made from <i>n</i> -dodecane and <i>n</i> -tridecane (i.e., CH ₃ (CH ₂) ₁₁ CH ₃ and CH ₃ (CH ₂) ₁₁ CH ₃) of 99% and 99%+ purity), thermal characterizations using T-History method		
PCM (single component (U)/ composite (Cm) or, a blend: binary (B)/ ternary (T)-, eutectic (E)/ solid solution (Ss)/ compound (C)) 1. <i>n</i> -dodecane- <i>n</i> -tridecane (B, possibly congruent melting Ss), @ ~17.7 <i>n</i> -tridecane		Composite material(s)

Data for the component/ composite/ blend	
Melting Temperature [°C] -15.7 °C to -12.4 °C (average over 2 nd to 4 th melting cycles)	Minimum Temperature [°C] -28 (min. of the measurement range)
Storage Capacity [kJ/kg] 185±19 (average over 2 nd to 4 th melting cycles)	Maximum Temperature [°C] 8 (max. of the measurement range)
Density [kg/l] Unevaluated	Cycle Stability (how many thermal cycles tested, if possible reduction in kJ/kg·h) 5 cycles, while the given results exclude the very first melting. The results agree well with the literature values.
Supercooling [K] Negligible	Material compatibility Not yet tested systematically. Nevertheless, it appears to be compatible with metals and glass but incompatible with plastics.
Technology readiness levels (TRL) Unevaluated	Additional Parameter Hysteresis of this blend is also minor, of around 1-3 °C.
If possible, please insert DSC-curve or other characteristic graph	Please insert an image/photo
	<p><i>n</i>-dodecane-<i>n</i>-tridecane Binary Phase Diagram [Gunasekara et al., 2017]</p> 
Target Applications (up to 4 most relevant) <ol style="list-style-type: none"> pre-cooling of refrigerants cold storage below 0 °C 	



3. solid-solid PCM applications for cooling (considering the polymorphic phase)

Comments

The results shown are for the 3rd melting (and freezing) cycle (in the T-history evaluation). Nonetheless, for all the evaluated cycles the blend displayed very consistent behaviors during both melting and freezing. This system appears to form a congruent minimum melting solid solution at around 17.7 mol% *n*-tridecane composition. That therefore appears to be ideal as a PCM for freezing applications. However, as the phase diagram here was presented only based on thermal characterizations, physicochemical characterizations and cycling stability tests are necessary future steps to confirm its PCM-suitability.

The reuse of the phase diagram given may require permission from the publisher (Elsevier).

First Name Saman Nimali	Name	Family Name Gunasekara
Institution KTH Royal Institute of Technology		
Address		
Street Brinellvägen 68		
Zip-Code 100 44	City Stockholm	
Country Sweden		
email saman.gunasekara@energy.kth.se	Telephone +46 73652 3339	
Material Data/Information		Date: 05.12.2017
Material Designation <i>n</i> -dodecane (99% pure), thermal characterizations using T-History method		

PCM (single component (U)/ composite (Cm) or, a blend: binary (B)/ ternary (T)..., eutectic (E)/ solid solution (Ss)/ compound (C))		Composite material(s)
1. <i>n</i> -dodecane CH ₃ (CH ₂) ₁₀ CH ₃ (U)		
Data for the component/ composite/ blend		
Melting Temperature [°C]	Minimum Temperature [°C]	
-11.4 to -8.8 (average over 2 nd to 4 th melting cycles)	-28 (min. of the measurement range)	
Storage Capacity [kJ/kg]	Maximum Temperature [°C]	
216±22 (average over 2 nd to 4 th melting cycles)	8 (max. of the measurement range)	
Density [kg/l]	Cycle Stability (how many thermal cycles tested, if possible reduction in kJ/kg·h)	
Unevaluated	5 cycles, while the given results exclude the very first melting. The results agree well with the literature values.	
Supercooling [K]	Material compatibility	
Minor (~2 K)	Not yet tested systematically. Nevertheless, it appears to be compatible with metals and glass but incompatible with plastics.	
Technology readiness levels (TRL)	Additional Parameter	
Unevaluated	--	
If possible, please insert DSC-curve or other characteristic graph		Please insert an image/photo



Target Applications (up to 4 most relevant)

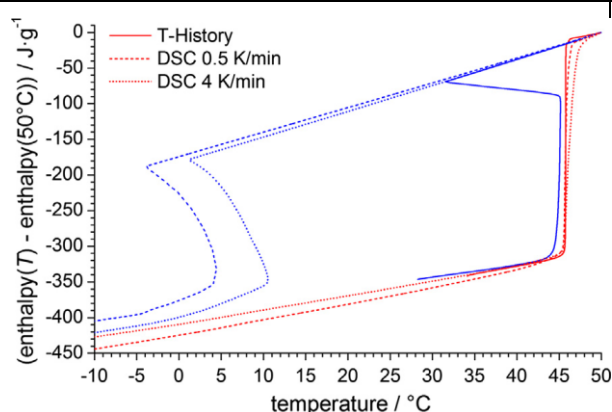
1. pre-cooling of refrigerants
2. cold storage below 0 °C

Comments

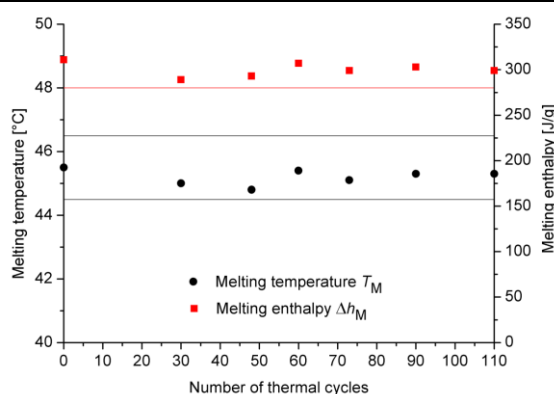
The results shown are for the 3rd melting (and freezing) cycle (in the T-history evaluation). Nonetheless, for all the evaluated cycles the sample displayed very consistent behaviors during both melting and freezing.

First Name Christoph		Family Name Rathgeber
Institution ZAE Bayern		
Address		
Street Walther-Meissner-Str. 6		
Zip-Code 85748	City Garching	
Country Germany		
email christoph.rathgeber@zae-bayern.de		Telephone +49 89 329 442 88
Material Data/Information		Date: 20.03.2018
Material Designation Pinacone hexahydrate		
PCM 1. Pinacone hexahydrate		Compound material(s)
Data for the compound or PCM if no compound		

Melting Temperature [°C] 45.5 °C (onset) [1]	Minimum Temperature [°C] not available
Heat of fusion [kJ/kg] 302 ± 15 [1]	Maximum Temperature [°C] Not tested yet
Density [kg/l] 0.97 (in liquid state) [1]	Cycle Stability (how many thermal cycles tested, if possible reduction in kJ/kg-h) Stable after 110 thermal cycles between 20 and 60 °C (according to PCM RAL stability criteria) [2]
Supercooling [K] ~40 K (DSC), ~15 K (T-History), ~10-15 K (thermal cycling device, 60 ml sample) [1, 2]	Material compatibility Not tested yet
Technology readiness levels (TRL)	Additional Parameter(s)



Source: [1]



Source: [2]

Target Applications (up to 4 most relevant)

1. Intermediate storage for heat pumps in space heating systems
2. Thermal protection of electronics / battery systems

Comments

The main obstacle for an application of pinacone hexahydrate are its costs: 300 €/kg for 99% purity. The costs of technical grade pinacone are unknown. [2]

References

[1] Rathgeber, C., Schmit, H., Hennemann, P., & Hiebler, S. (2014). Investigation of pinacone hexahydrate as phase change material for thermal energy storage around 45 C. *Applied Energy*, 136, 7-13.

[2] Grisval, A. (2017). Investigation on organic hydrates as phase change materials (PCM). Master's Thesis, Technical University Munich.

First Name		Name		Family Name	
Stephan				Höhlein	
Institution					
Chair of Engineering Thermodynamics and Transport Processes (LTTT), University of Bayreuth					
Address					
Street					
Universitätsstraße 30					
Zip-Code		City			
95447		Bayreuth			
Country					
Germany					
email			Telephone		
Stephan.Hoehlein@uni-bayreuth.de			+49 921 55 7520		
Material Data/Information			Date: 12.01.2018		
Material Designation					
Magnesiumchloride Hexahydrate, MgCl ₂ 6H ₂ O					
PCM			Compound material(s)		
1. Magnesiumchloride Hexahydrate					
Data for the compound or PCM if no compound					
Melting Temperature [°C]		Minimum Temperature [°C]			
115,1 (onset) [1]					

Storage Capacity [kJ/kg] 166,9 [1]	Maximum Temperature [°C]
Density [kg/l] 1,5955 (20 °C) [1] 1,4557 (120 °C) [1]	Cycle Stability (how many thermal cycles tested, if possible reduction in kJ/kg·h) 500 cycles at DSC-scale, ~ 1 % reduction in melting enthalpy [1]
Supercooling [K] 30 (sample size ~10 mg) [1] 2,8 (sample size ~100 g) [1]	Material compatibility Anodized aluminium [2]
Technology readiness levels (TRL)	Addition Parameter
<p>Enthalpy and heat capacity of MgCl₂·6H₂O [1]</p>	<p>Crystallization of MgCl₂·6H₂O within an aluminium capsule</p>
Target Applications (up to 4 most relevant)	
<ol style="list-style-type: none"> 1. Waste heat 2. Process heat 3. Mobile storage systems 	
Comments	
<p>[1] S. Höhle, A. König-Haagen, and D. Brüggemann, "Thermophysical Characterization of MgCl₂·6H₂O, Xylitol and Erythritol as Phase Change Materials (PCM) for Latent Heat Thermal Energy Storage (LHTES)," Materials (Basel). vol. 10, no. 4, p. 444, Apr. 2017.</p>	

[2] D. Brüggemann, A. König-Haagen, R. R. Kasibhatla, S. Höhlelein, U. Glatzel, R. Völkl, and N. Agarkov, "Entwicklung makroverkapselter Latentwärmespeicher für den straßengebundenen Transport von Abwärme (MALATrans): Laufzeit: 01.07.2013 bis 31.12.2016 (Abschlussbericht)," Bayreuth, 2017.

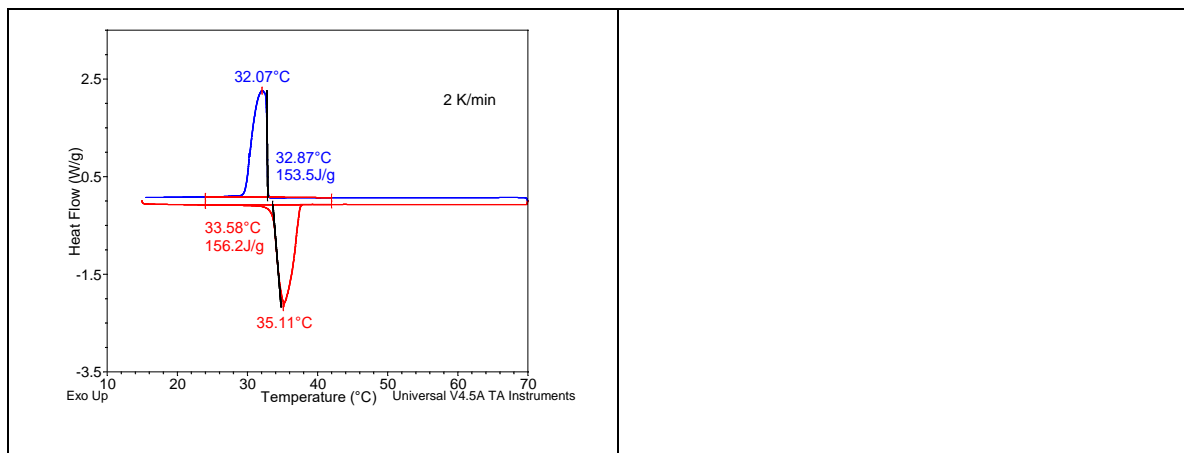
First Name	Mohammed	Family Name	Farid
Institution	University of Auckland		
Address			
Street	University of Auckland, Department of Chemical and Materials Engineering, Grafton 4-6 Park Ave, Auckland, New Zealand		
Zip-Code	City Auckland		
Country	New Zealand		
email	m.farid@auckland.ac.nz	Telephone	+6421812678
Material Data/Information		Date: 19/05/2018	
Material Designation			
PCM (Composite material(s)		
1. Any PCM	1. metal coated microencapsulated PCM		
Data for PCM or composite			
Melting Temperature [°C]	Minimum Temperature [°C]		
Storage Capacity [kJ/kg]	Maximum Temperature [°C]		
Density [kg/l]	Cycle Stability (how many thermal cycles tested, if possible reduction in kJ/kg·h)		

Supercooling [K]	Material compatibility
Technology readiness levels (TRL)	Additional Parameter
Please insert an image/p	
<p>Metal Coated PCM Microcapsules (surface activation by dopamine followed by silver coating)</p> <p>SEM photos and EDX patterns of (a) RT21 microcapsules and (b) RT21-PDA/Ag (Al Shannaq and Farid (2016))</p> <p>If possible, please insert DSC-curve or other characteristic graph that shows the temperature dependency</p>	<p>Thermal Conductivity Enhancement</p> <p>Measured apparent thermal conductivity versus mean diameter of the PCM microcapsules at different silver nitrate concentration used in the coating process (Al Shannaq and Farid (2016))</p>
<p>Target Applications (up to 4 most relevant)</p> <p>1. Cooling of electronic devices using slurry of microencapsulated PCM</p>	

First Name	Samer	
Family Name	Kahwaji	
Institution	Dalhousie University – Department of Chemistry- Group of Prof. Mary Anne White	
Address		
Street	6274 Coburg road	
Zip-Code	City	
B3H 4R2	Halifax	
Country	Canada	



email sam@dal.ca		Telephone 1-902-494-6538	
Material Data/Information		Date: May 22, 2018	
Material Designation Eutectic mixture of fatty acids, new melting point (see Ref. [1])			
PCM 1. Dodecanoic acid (98% pure), 68 mass % 2. Tetradecanoic acid (98% pure), 32 mass %		Composite material(s)	
Data for PCM or composite			
Melting Temperature [°C] 33.6 ±1.5 °C (onset)		Minimum Temperature [°C] 0	
Storage Capacity [kJ/kg] 160 ± 16 kJ/kg		Maximum Temperature [°C] 70	
Density [kg/l] 0.865 (liquid phase)		Cycle Stability (how many thermal cycles tested, if possible reduction in kJ/kg·h) Mixture not cycled. Individual fatty acids tested for 3000 cycles with no significant loss in enthalpy (see Ref. [2])	
Supercooling [K] 0.7 (onset points)		Material compatibility Compatible with stainless steel and aluminum (see Ref. [2])	
Technology readiness levels (TRL)		Additional Parameter Heat capacity (C_p) of solid = 1.95 J/g K (at 10 °C), C_p of liquid = 2.21 J/g K (at 50 °C).	
If possible, please insert DSC-curve or other characteristic graph that shows the temperature dependency		Please insert an image/photo	



Target Applications (up to 4 most relevant)

1. Passive cooling of electronics and batteries.
2. Thermal energy storage in solar thermal collectors.

Comments

Individual fatty acid PCMs with melting temperature around 34 °C are not available, so this mixture makes this temperature accessible. The specified melting temperature and storage capacity are determined from averages of multiple samples and measurements at 2 K/min and 10 K/min, respectively.

References

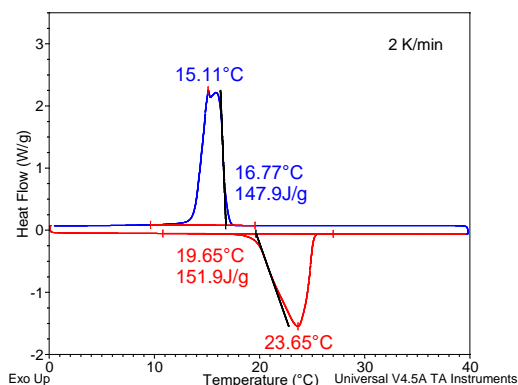
- [1] S. Kahwaji, M.A. White, *Thermochim. Acta.* 660 (2018) 94–100.
- [2] S. Kahwaji, M.B. Johnson, A.C. Kheirabadi, D. Groulx, M.A. White, *Sol. Energy Mater. Sol. Cells.* 167 (2017) 109–120.

First Name Samer	Name	Family Name Kahwaji
Institution Dalhousie University – Department of Chemistry- Group of Prof. Mary Anne White		
Address		
Street 6274 Coburg road		
Zip-Code	City	

B3H 4R2	Halifax	
Country Canada		
email sam@dal.ca	Telephone 1-902-494-6538	
Material Data/Information		Date: May 22, 2018
Material Designation Eutectic mixture of fatty acids, new melting point (see Ref. [1])		
PCM 1. Decanoic acid (99% pure), 78 mass % 2. Tetradecanoic acid (98% pure), 22 mass %	Composite material(s)	
Data for PCM or composite		
Melting Temperature [°C] 20.5±1.5 °C (onset)	Minimum Temperature [°C] 0	
Storage Capacity [kJ/kg] 153 ± 15 kJ/kg	Maximum Temperature [°C] 70	
Density [kg/l] 0.874 (liquid phase)	Cycle Stability (how many thermal cycles tested, if possible reduction in kJ/kg-h) 3000 cycles, no significant loss in enthalpy	
Supercooling [K] 3.6 (onset points)	Material compatibility Compatible with stainless steel and aluminum (see Ref. [2])	
Technology readiness levels (TRL)	Additional Parameter See Ref. [1] for heat capacity, thermal conductivity and thermal diffusivity.	

If possible, please insert DSC-curve or other characteristic graph that shows the temperature dependency

Please insert an image/photo



Target Applications (up to 4 most relevant)

1. Passive cooling of buildings / integration in building materials.
2. Thermal energy storage in solar thermal collectors.

Comments

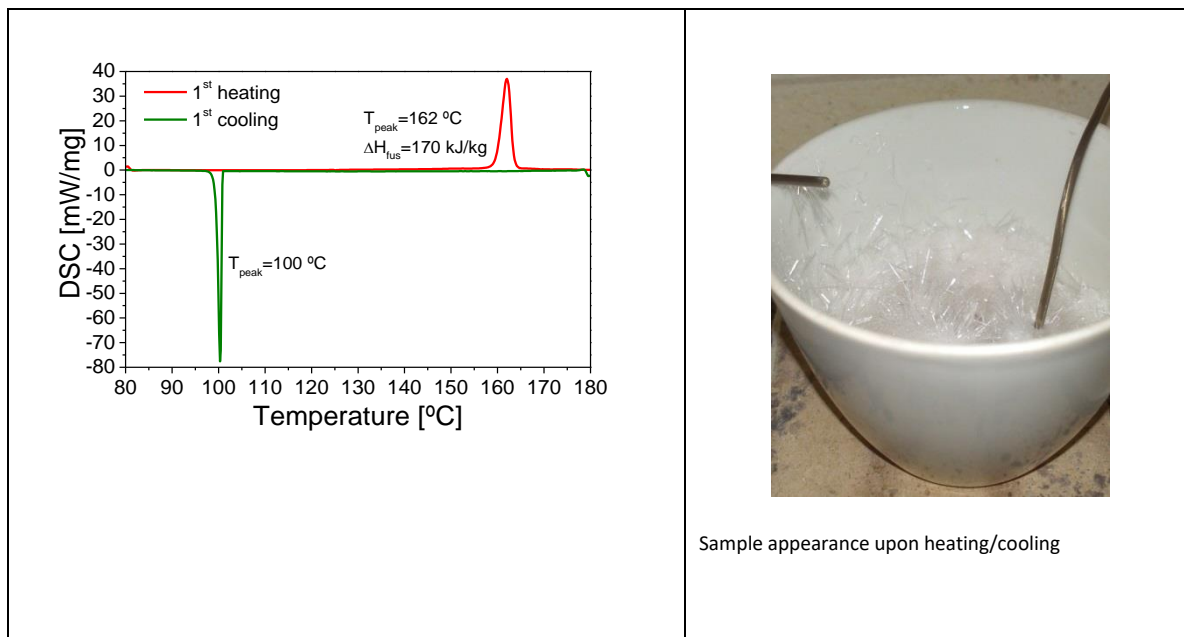
Individual fatty acid PCMs with melting temperature around 20 °C are not available, so this mixture makes this temperature accessible. Purity of mixed fatty acids may affect the exact composition and melting point of the eutectic. The specified melting temperature and storage capacity are determined from averages of multiple samples and measurements.

References

- [1] S. Kahwaji, M.B. Johnson, A.C. Kheirabadi, D. Groulx, M.A. White, Appl. Energy. 168 (2016) 457–464.
- [2] S. Kahwaji, M.B. Johnson, A.C. Kheirabadi, D. Groulx, M.A. White, Sol. Energy Mater. Sol. Cells. 167 (2017) 109–120.
- [3] S. Kahwaji, M.A. White, Thermochim. Acta. 660 (2018) 94–100.

First Rocío	Name	Family Name Bayón
Institution CIEMAT-PSA		
Address		
Street		

Av. Complutense 40	
Zip-Code 28040	City Madrid
Country Spain	
email rocio.bayon@ciemat.es	Telephone +34913466048
Material Data/Information	Date:
Material Designation Salicylic acid	
PCM (s) 1. Salicylic acid	Composite material(s)
Data for PCM or composite	
Melting Temperature [°C] 162 °C	Minimum Temperature [°C] -
Storage Capacity [kJ/kg] 199 kJ/kg	Maximum Temperature [°C] -
Density [kg/l]	Cycle Stability (how many thermal cycles tested, if possible reduction in kJ/kg·h) -
Supercooling [K] In DSC: 70 K	Material compatibility -
Technology readiness levels (TRL) -	Additional Parameter



Target Applications (up to 4 most relevant)

1. Not suitable as storage medium

Comments

- Strong supercooling
- White vapors evolve from sample upon melting
- White needles deposit back on sample surface after cooling

References

- R. Bayón, E. Rojas, Characterization of organic PCMs for medium temperature storage, in: A Méndez-Vilas (Ed.), Materials and Technologies for Energy Efficiency, Brown Walker Press, Boca Ratón, Florida (US), 2015, pp: 157–161.

First Rocío	Name	Family Name Bayón
Institution CIEMAT-PSA		
Address		
Street Av. Complutense 40		

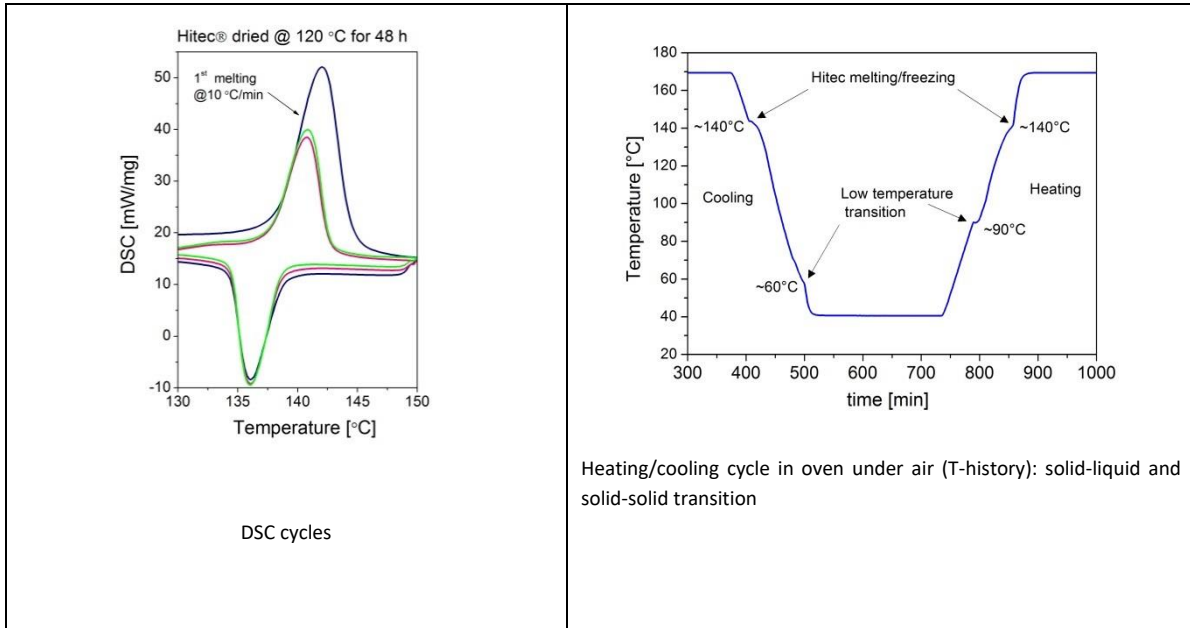


Zip-Code 28040	City Madrid
Country Spain	
email rocio.bayon@ciemat.es	Telephone +34913466048
Material Data/Information	Date:
Material Designation RT35HC from Rubitherm®	
PCM (s) 1. commercial organic mixture	Composite material(s)
Data for PCM or composite	
Melting Temperature [°C] 35 °C	Minimum Temperature [°C] 70 °C (given by manufacturer)
Storage Capacity [kJ/kg] 240 kJ/kg (manufacturer) 285 kJ/kg (measured in DSC)	Maximum Temperature [°C] -
Density [kg/l]	Cycle Stability (how many thermal cycles tested, if possible reduction in kJ/kg·h) -
Supercooling [K] -	Material compatibility -
Technology readiness levels (TRL) 10 (commercial material)	Additional Parameter

<p>RT35HC (organic) a)</p> <p>$T_{\text{melt}} = 34\text{ °C}$</p> <p>$T_{\text{freez}} = 34\text{ °C}$</p> <p>$\Delta H_{\text{melt}} = 285\text{ kJ/kg}$</p> <p>2nd cycle @ 10°C/min</p>	<p>a) RT35HC</p> <p>Temperature [°C]</p> <p>Relative time (h)</p> <p>heating/cooling rate 0,5°C/min Sample size ~4 g</p> <p>2nd cycle 10th cycle 26th cycle</p>
<p>Daily heating/cooling cycles in oven under air (T-history)</p>	
<p>Target Applications (up to 4 most relevant)</p>	
<ol style="list-style-type: none"> 1. Refrigeration 2. Dry cooling 	
<p>Comments</p>	
<ul style="list-style-type: none"> • No supercooling is observed • Sample behavior remains constant after 26 daily heating/cooling cycles • Melting/freezing plateau is observed in T-history curve even when temperature interval is $T_{\text{melt}} \pm 2\text{ °C}$. 	
<p>References</p>	
<ul style="list-style-type: none"> • R. Bayón, M. Biencinto, E. Rojas, N. Uranga. STUDY OF HYBRID DRY COOLING SYSTEMS FOR STE PLANTS BASED ON LATENT STORAGE. To be presented at ISEC conference in Graz, October 2018. 	

<p>First Name Rocío</p>	<p>Name</p>	<p>Family Name Bayón</p>
<p>Institution CIEMAT-PSA</p>		
<p>Address</p>		
<p>Street Av. Complutense 40</p>		
<p>Zip-Code 28040</p>	<p>City Madrid</p>	
<p>Country</p>		

Spain	
email rocio.bayon@ciemat.es	Telephone +34913466048
Material Data/Information	Date:
Material Designation HITEC® commercial eutectic mixture	
PCM (s) 1. NaNO ₃ :7 % w 2. KNO ₃ :53 % w 3. NaNO ₂ :40 % w	Composite material(s)
Data for PCM or composite	
Melting Temperature [°C] 142 °C	Minimum Temperature [°C]
Storage Capacity [kJ/kg] 83 kJ/kg (literature) 50 kJ/kg (measured in DSC)	Maximum Temperature [°C] 535 °C
Density [kg/l]	Cycle Stability (how many thermal cycles tested, if possible reduction in kJ/kg·h) -
Supercooling [K] -	Material compatibility -
Technology readiness levels (TRL) 10 (commercial material)	Additional Parameter



Target Applications (up to 4 most relevant)

1. Medium temperature storage although storage capacity is not very high

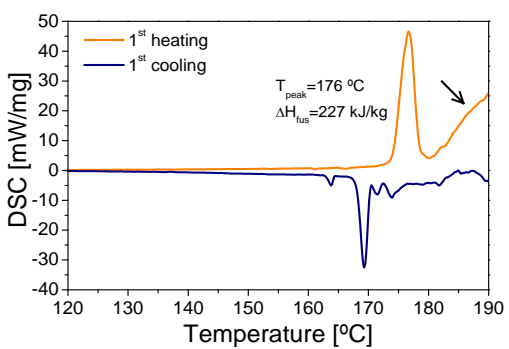

Comments

- Chemical stability after 50-60 daily cycles under air, N₂ and Ar
- No increase in nitrate percentage is observed

References

- M.M. Rodríguez-García, E. Rojas, R. Bayón, Test campaign and performance evaluation of a spiral latent storage module with Hitec® as PCM, Solar Heating and Cooling Conference 2017, Abu Dhabi, November 2017. Accepted for AIP Conference proceedings

Questionnaire Phase Change Materials ECES Annex 33 / SHC Task 58

First Name Rocío		Family Name Bayón	
Institution CIEMAT-PSA			
Address			
Street Av. Complutense 40			
Zip-Code 28040	City Madrid		
Country Spain			
email rocio.bayon@ciemat.es		Telephone +34913466048	
Material Data/Information		Date:	
Material Designation Hidroquinone			
PCM (s) 1. Hidroquinone		Composite material(s) 1.	
Data for PCM or composite			
Melting Temperature [°C] 173 °C		Minimum Temperature [°C] -	
Storage Capacity [kJ/kg] 192-278 kJ/kg		Maximum Temperature [°C] -	
Density [kg/l]		Cycle Stability (how many thermal cycles tested, if possible reduction in kJ/kg·h) -	
Supercooling [K] -		Material compatibility -	
Technology readiness levels (TRL) -		Additional Parameter	
 <p>DSC scan showing degradation upon melting</p>		 <p>Hydroquinone sample appearance upon heating/cooling</p>	
Target Applications (up to 4 most relevant) 1. Not suitable as storage medium			
Comments			
<ul style="list-style-type: none"> • White vapors evolve from sample upon melting • White needles deposit back on sample surface after cooling • Bulk sample browning 			
References			
<ul style="list-style-type: none"> • R. Bayón, E. Rojas, Characterization of organic PCMs for medium temperature storage, in: A Méndez-Vilas (Ed.), Materials and Technologies for Energy Efficiency, Brown Walker Press, Boca Ratón, Florida (US), 2015, pp: 157–161. 			

First Name Rocío		Family Name Bayón
Institution CIEMAT-PSA		
Address		
Street Av. Complutense 40		
Zip-Code 28040	City Madrid	
Country Spain		
email rocio.bayon@ciemat.es		Telephone +34913466048
Material Data/Information		Date:
Material Designation D-mannitol		
PCM (s) 1. D-mannitol		Composite material(s)
Data for PCM or composite		
Melting Temperature [°C] 165 °C	Minimum Temperature [°C] -	
Storage Capacity [kJ/kg] 246-338 kJ/kg	Maximum Temperature [°C] -	
Density [kg/l]	Cycle Stability (how many thermal cycles tested, if possible reduction in kJ/kg·h) -	
Supercooling [K] In DSC: ~56 K	Material compatibility -	

In T-history: ~30 K	
Technology readiness levels (TRL) -	Additional Parameter

<p>DSC scan variation after stability tests</p>	<p>D-mannitol after 166 h melted under air @180 °C</p>
---	--

Target Applications (up to 4 most relevant)

1. Not suitable as storage medium

Comments

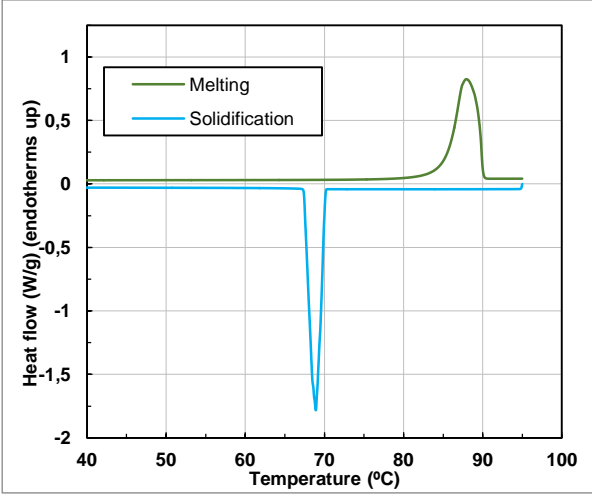
- This material degrades very quickly even under inert atmosphere (N₂, Ar)
- It undergoes caramelization even under O₂-free atmosphere.

References

- R. Bayón, E. Rojas, Feasibility study of D-mannitol as phase change material for thermal storage, AIMS Energy 5 (3) (2017) 404–424. <https://doi.org/10.3934/energy.2017.3.404>.
- M.M. Rodríguez-García, R. Bayón, E. Rojas, Stability of D-mannitol upon melting/freezing cycles under controlled inert atmosphere, Energy Procedia 91 (2016) 218–225. <https://doi.org/10.1016/j.egypro.2016.06.207>.
- R. Bayón, E. Rojas, Characterization of organic PCMs for medium temperature storage, in: A Méndez-Vilas (Ed.), Materials and Technologies for Energy Efficiency, Brown Walker Press, Boca Ratón, Florida (US), 2015, pp: 157–161.

First Name Gonzalo	Name	Family Name Diarce
Institution		

University of the Basque Country (UPV/ EHU)	
Address	
Street <i>Rafael Moreno Pitxitxi 2</i>	
Zip-Code <i>48012</i>	City <i>Bilbao</i>
Country Spain	
email gonzalo.diarce@ehu.es	Telephone <i>+34946014952</i>
Material Data/Information	Date:
Material Designation Eutectic mixture of Urea and Sodium Nitrate; phase diagram, thermal properties, crystallization behaviour, degradation, influence of water uptake	
PCM (1. Urea (71 % w/w) – NaNO ₃ (29 % w/w) (eutectic mixture)	Composite material(s)
Data for PCM or composite	
Melting Temperature [°C] 85 °C (onset)	Minimum Temperature [°C] n.a.
Storage Capacity [kJ/kg] 250 kJ/kg (60 to 95 °C) 172 kJ/kg (melting latent heat)	Maximum Temperature [°C] n.a.
Density [kg/l] 1.48 solid / 1.42 liquid	Cycle Stability (how many thermal cycles tested, if possible reduction in kJ/kg·h) - DSC: Crucibles closed in air. 200 cycles. Reduction of 1.2 % of the original melting enthalpy. - Thermal stability of larger samples is currently under study. The results suggest that there is a significant reduction on the enthalpy in these larger samples, caused by a phase segregation phenomenon that is coupled to the thermal degradation of the sample (formation of ammonia due to the urea decomposition).

<p>Supercooling [K]</p> <p>DSC: around 20 °C</p> <p>Larger samples: 3-5 °C</p>	<p>Material compatibility</p> <p>Not checked. It may be corrosive in contact with some construction materials</p>
<p>Technology readiness levels (TRL)</p> <p>2/3</p>	<p>Additional Parameter</p> <p>none</p>
<p>If possible, please insert DSC-curve or other characteristic graph that shows the temperature dependency</p>  <p>DSC results (heat flow vs. temperature) for the eutectic composition (71.25 % (w/w) urea)</p>	<p>Please insert an image/photo</p>
<p>Target Applications (up to 4 most relevant)</p> <ol style="list-style-type: none"> 1. TES systems for Heating and DHW 2. TES systems for low to medium temperature industrial residual heat 	
<p>Comments</p> <p>We are currently focused on the thermal degradation of the material. However, it is a complex procedure, because Urea undergoes thermal decomposition above its melting point. This effect is kinetic and depends on the time that the PCM stays above the melting temperature. Thus, accelerated thermal cycling studies are not useful to study it. Besides, the mixture tends to segregate when it crystallizes. This is dependent on the sample size and shape, but the effect cannot be decoupled from the thermal decomposition. Other variables such as the gas surrounding the mixture and the moisture content can have also a significant effect. All these factors together become the degradation study really complex.</p>	
<p>References</p>	

G. Diarce, E. Corro-Martínez, L. Quant, Á. Campos-Celador, A. García-Romero. The sodium nitrate–urea binary mixture as a phase change material for medium temperature thermal energy storage. Part I: Determination of the phase diagram and main thermal properties *Solar Energy Materials and Solar Cells*, 2016; 157, 1065 - 1075

G. Diarce, E. Corro-Martínez, Á. Campos-Celador, A. García-Romero, J.M. Sala. The sodium nitrate–urea eutectic binary mixture as a phase change material for medium temperature thermal energy storage. Part II: Accelerated thermal cycling test and water uptake behavior of the material *Solar Energy Materials and Solar Cells*, 2016; 157, 1076 - 1083

First Name Gonzalo		Family Name Diarce
Institution University of the Basque Country (UPV/ EHU)		
Address		
Street <i>Rafael Moreno Pitxitxi 2</i>		
Zip-Code 48012	City <i>Bilbao</i>	
Country Spain		
email gonzalo.diarce@ehu.es		Telephone +34946014952
Material Data/Information		Date:
Material Designation Eutectic mixtures of sugar alcohols; phase diagram, thermal properties, crystallization behaviour, degradation		
PCM 1. Erythritol (21 % w/w) - Xylitol (79 % w/w) (eutectic mixture)	Composite material(s)	
Data for PCM or composite		

Melting Temperature [°C] 82 °C (onset)	Minimum Temperature [°C] n.a.
Storage Capacity [kJ/kg] 250 kJ/kg (latent melting heat)	Maximum Temperature [°C] n.a.
Density [kg/l] n.a.	Cycle Stability (how many thermal cycles tested, if possible reduction in kJ/kg·h) n.a
Supercooling [K] Significant, combined with a slow crystallization rate	Material compatibility Compatible with common construction materials
Technology readiness levels (TRL) 2/3	Additional Parameter none
If possible, please insert DSC-curve or other characteristic graph that shows the temperature dependency 	Please insert an image/photo
DSC thermograms obtained for the erythritol-xylitol system	
Target Applications (up to 4 most relevant) 1. TES systems for Heating and DHW 2. TES systems for low to medium temperature industrial residual heat	

Comments

So far, the studies have been focused on the thermal and crystallization behaviour. We have plans to investigate in the near future the thermal degradation of the mixture, as well as its potential application within a storage device that includes a crystallization triggering system.

References

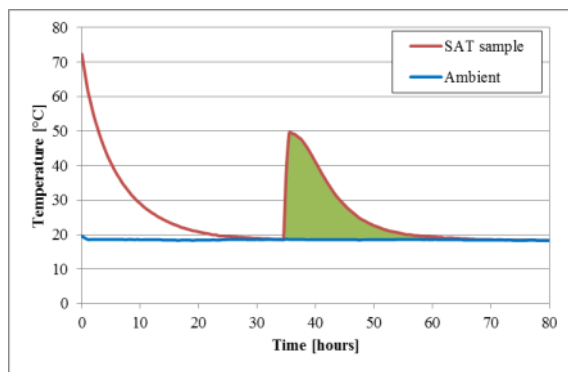
G. Diarce, I. Gandarias, A. Campos-Celador, A. García-Romero, J.M. Sala Eutectic mixtures of sugar alcohols for thermal energy storage in the 50-90 °C temperature range *Solar Energy Materials and Solar Cells*, 2015; 134, 215 - 226

First Name	Gerald	Family Name	Englmair
Institution	Technical University of Denmark		
Address			
Street	Nordvej Building 119		
Zip-Code	2800	City	Kgs. Lyngby
Country	Denmark		
email	gereng@byg.dtu.dk	Telephone	
Material Data/Information	Date:		
Material Designation			
PCM	Sodium Acetate Trihydrate (SAT)		
	Composite material(s). Examples listed. SAT with different weight contents of water, thickening agents, polymer materials can be found in [1] 1. SAT with 1% (wt %) CMC (Carboxymethyl Cellulose)		

	<ol style="list-style-type: none"> 2. SAT with 1% (wt %) water + 1% (wt %) EDTA (Disodium Ethylenediaminetetraacetic acid) 3. SAT with 2% (wt %) EDTA 4. SAT with 4% (wt %) water 5. SAT with 2% (wt %) HD 200 (Polymer material) 6. SAT with 0.5% (wt %) Xanthan Gum
<p>Data for PCM or composite</p>	
<p>Melting Temperature [°C]</p> <p>58</p>	<p>Minimum Temperature [°C]</p> <p>-15 °C (crystallization of liquid SAT) [3]</p>
<p>Storage Capacity [kJ/kg] [1]</p> <ol style="list-style-type: none"> 1. 211 2. 216 3. 215 4. 194 5. 216 6. 214 	<p>Maximum Temperature [°C]</p> <p>~100 °C for SAT composition except: 80 °C for compositions containing CMC (assuming atmospheric pressure conditions).</p>
<p>Density [kg/l]</p> <p>Depending on the state (liquid, solid, liquid supercooled), see reference [2] and diagram below</p> <p>Fig. 4. Density of solid and liquid SAT including SAT with extra water in supercooled state.</p>	<p>Cycle Stability (how many thermal cycles tested, if possible reduction in kJ/kg·h)</p> <p>Stable with above mentioned compositions. Cyclic stability was proven in large containers (heat storage prototypes) up to ~30 cycles.</p> <p>Long-term investigations are ongoing.</p>
<p>Supercooling [K]</p> <p>Down to -15 °C with 73 K degree of supercooling [3]</p>	<p>Material compatibility</p>
<p>Technology readiness levels (TRL)</p> <p>6-7 [4]</p>	<p>Additional Parameter</p> <p>Thermal conductivity</p> <ol style="list-style-type: none"> 1. SAT with 1% CMC 0.57-0.65 W/mK 2. SAT with 0.5 % Xanthan Gum 0.5-0.65 W/mK <p>For more composites, reference [5]</p>

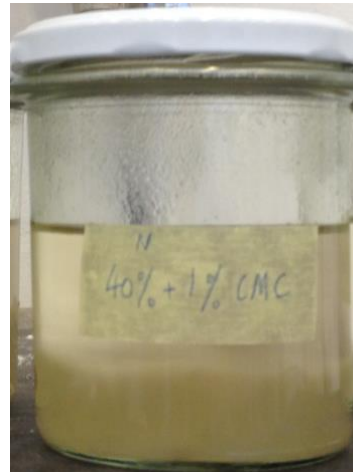
If possible, please insert DSC-curve or other characteristic graph that shows the temperature dependency

Use heat loss method to measure the heat content [1]



Please insert an image/photo

Bulk sample below: SAT with 1% (wt. %) CMC



Target Applications (up to 4 most relevant)

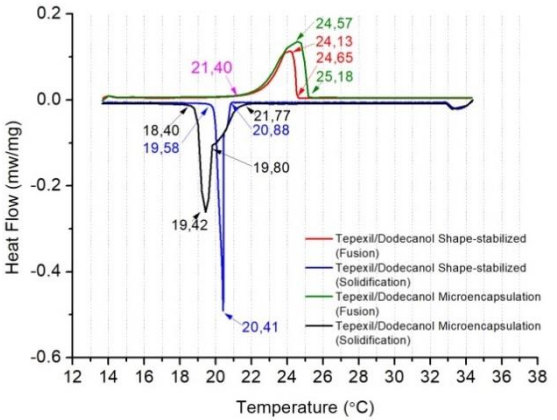

1. Solar thermal heating system for DHW & SH
2. Domestic heating systems with heat pumps
3. Smart grid (increased demand flexibility of buildings)
4. Overall: stable supercooling for combined short – long term heat storage below 100 °C

References

- [1] W. Kong *et al.*, "Experimental investigations on heat content of supercooled sodium acetate trihydrate by a simple heat loss method," *Sol. Energy*, vol. 139, pp. 249–257, 2016.
- [2] M. Dannemand *et al.*, "Porosity and density measurements of sodium acetate trihydrate for thermal energy storage," *Appl. Therm. Eng.*, vol. 131, pp. 707–714, 2018.
- [3] G. Englmair *et al.*, "Crystallization by local cooling of supercooled sodium acetate trihydrate composites for long-term heat storage," *Energy Build.*, vol. 180, pp. 159–171, 2018.
- [4] G. Englmair, C. Moser, S. Furbo, M. Dannemand, and J. Fan, "Design and functionality of a segmented heat-storage prototype utilizing stable supercooling of sodium acetate trihydrate in a solar heating system," *Appl. Energy*, vol. 221, no. April, pp. 522–534, 2018.
- [5] M. Dannemand, J. B. Johansen, and S. Furbo, "Solidification behavior and thermal conductivity of bulk sodium acetate trihydrate composites with thickening agents and graphite," *Sol. Energy Mater. Sol. Cells*, vol. 145, pp. 287–295, Feb. 2016.



First Name JUAN DE DIOS		Family Name CRUZ ELVIRA
Institution INSTITUTO TECNOLOGICO DE OAXACA		
Address		
Street Calz. Tecnológico Esq. Ing. Victor Bravo Ahuja No. 125,Oaxaca de Juarez,Oax.		
Zip-Code 68030	City OAXACA	
Country MEXICO		
email juko_reto@hotmail.com		Telephone +5219512353381
Material Data/Information		Date:
Material Designation Composite Tepexil /Dodecanol		
PCM (1.Dodecanol	Composite material(s) 1.Tepexil	
Data for PCM or composite		
Melting Temperature [°C] 24.5	Minimum Temperature [°C] 21.4	
Storage Capacity [kJ/kg] 118.35	Maximum Temperature [°C] 25.1	
Density [kg/l] 1045	Cycle Stability (how many thermal cycles tested, if possible reduction in kJ/kg·h) 5	
Supercooling [K]	Material compatibility	

Technology readiness levels (TRL)	Additional Parameter TGA (125°C stability)
<p>If possible, please insert DSC-curve or other characteristic graph that shows the temperature dependency</p> 	<p>Please insert an image/photo</p> 
<p>Target Applications (up to 4 most relevant)</p> <ol style="list-style-type: none"> 1. building applications 2. construction materials 	
<p>Comments</p> <p>This work aims to evaluate the thermal properties and performance of a composite material dodecanol/tepexil for thermal comfort in housing.</p>	

First Thomas	Name Family Name Aigenbauer
Institution FH OÖ Forschungs & Entwicklungs GmbH	
Address	
Street Ringstraße 43a	
Zip-Code	City

4600	Wels	
Country Austria		
email Thomas.aigenbauer@fh-wels.at	Telephone +43 50804 46919	
Material Data/Information	Date: 19.09.2019	
Material Designation D-Mannitol 97+% (Alfa Aesar) and Dulcitol 97% (Alfa Aesar)		
PCM (1. D-Mannitol (70 %) 2. Dulcitol (30%)	Composite material(s)	
Data for PCM or composite		
Melting Temperature [°C] 153	Minimum Temperature [°C]	
Storage Capacity [kJ/kg] 280	Maximum Temperature [°C]	
Density [kg/l] 1,505	Cycle Stability (how many thermal cycles tested, if possible reduction in kJ/kg·h) 5000; no separation detected;	
Supercooling [K]	Material compatibility Good with copper and aluminium	
Technology readiness levels (TRL) 5	Additional Parameter	

<p>If possible, please insert DSC-curve or other characteristic graph that shows the temperature dependency</p>	<p>Please insert an image/photo</p>
<p>Target Applications (up to 4 most relevant)</p> <ol style="list-style-type: none"> 1. passive cooling for coating applications 2. mid-temperature industry processes 	

<p>First Name Thomas</p>	<p>Name Family Name Eigenbauer</p>
<p>Institution FH OÖ Forschungs & Entwicklungs GmbH</p>	
<p>Address</p>	
<p>Street Ringstraße 43a</p>	
<p>Zip-Code 4600</p>	<p>City Wels</p>
<p>Country Austria</p>	
<p>email Thomas.aigenbauer@fh-wels.at</p>	<p>Telephone +43 50804 46919</p>
<p>Material Data/Information</p>	<p>Date: 19.09.2019</p>

Material Designation	
D-Mannitol 97+% (Alfa Aesar)	
PCM	Composite material(s)
1. D-Mannitol	
Data for PCM or composite	
Melting Temperature [°C]	Minimum Temperature [°C]
167	
Storage Capacity [kJ/kg]	Maximum Temperature [°C]
270	
Density [kg/l]	Cycle Stability (how many thermal cycles tested, if possible reduction in kJ/kg·h)
1,52	5000; after 456h at 180°C → 208,2 kJ/kg (in copper tube)
Supercooling [K]	Material compatibility
	Good with copper and aluminium
Technology readiness levels (TRL)	Additional Parameter
5	
<p>If possible, please insert DSC-curve or other characteristic graph that shows the temperature dependency</p>	<p>Please insert an image/photo</p>



Target Applications (up to 4 most relevant)

1. passive cooling for coating applications
2. mid-temperature industry processes



6.2 SUBTASK 3T

6.2.1 APPENDIX A

(September 9th, 2018)

IEA Task 58 / Annex 33 Subtask 3T

Measurement Procedure for the 2nd Salt Hydrate Round Robin ($\text{SrBr}_2 \cdot n\text{H}_2\text{O}$)

GOAL OF THIS DOCUMENT

By applying and following this procedure, reproducible and comparable measurement results of hydration/dehydration potential, enthalpy of hydration /dehydration as well as the characterization of the cyclic stability for salt hydrate thermochemical materials (TCM) will be produced, to predict the material performance under particular boundary conditions of an application.

PROCEDURE FOR SALT HYDRATE MATERIALS (E.G. SRBR_2)

The applied methods include gravimetric analyzers with vapor or humidity conditioning, optional with calorimetric extension (TG, TG-DSC, STA). The procedure consists of a pretreatment of the sample, and several hydration- and dehydration points, while all of them have to reach equilibrium state.

DEFINITION OF THE SCENARIOS

Three (3) scenarios of salt hydration shall be applied in order to characterize the hydration potential of the salt, which are derived from boundary conditions in typical applications, and are in good agreement with the temperatures for domestic heating and cooling sent in a document (Temperatures_Buildings) by Benjamin Fumey. The conditions are given in Table 6-1.

PRETREATMENT / DRY MASS DETECTION

A standardized pretreatment is necessary for comparable salt hydration calculations, as the dry mass will serve as one of the reference masses. There is no known existing unified test method at this time for salt hydrate pretreatment. The following proposed sample pretreatment for the present 2nd round robin shall be as follows.

- The optimal sample pretreatment temperature T_{max} should be selected considering and well below the melting point of the considered salt hydrate. For the case of SrBr_2 , the proposed $T_{\text{max}}=200^\circ\text{C}$ is well below the melting temperature of SrBr_2 , which is about 657°C as per the Handbook of Inorganic Compounds
- The sample shall be heated starting from laboratory ambient conditions to T_{max} with a heating rate of $1\text{K}/\text{min}$ followed by an isothermal drying step for another 1 hour (see Figure 1). The total pretreatment time shall be about 3 hours.

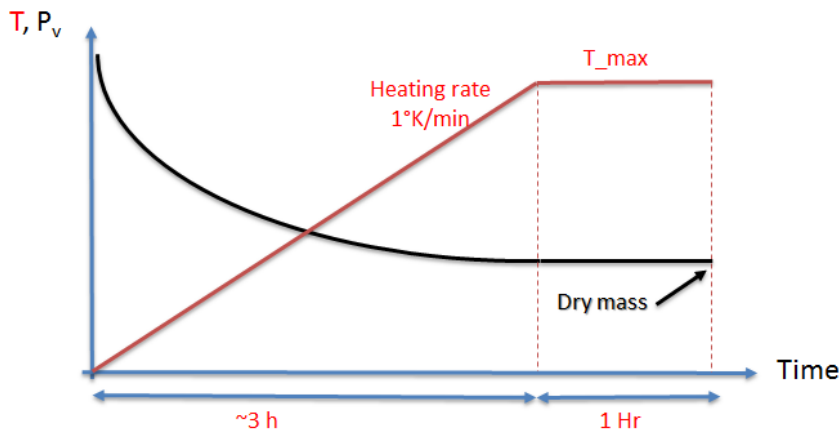


FIGURE 6-1: PROPOSED PRETREATMENT PROCEDURE

Comments to Round-Robin participants of IEA/Annex 58/33: For the case that the measurement setup is not capable of supplying complete dry air during the pretreatment as well as during the dehydration experiments, please indicate this together with the measurement results.

MEASUREMENT OF EQUILIBRIUM POINTS

In the following steps, three hydration and two dehydration equilibrium points along with two pretreatment steps are defined in order to characterize the hydration/dehydration properties and cyclic stability of salt hydrate. The three dew points representative of typical winter ambient water evaporation source conditions include 5, 7 and 10 °C corresponding to water vapor pressures of 8.7, 10 and 12.3 mbar and sample temperatures of 25, 95 and 200 °C (see Table 6-1 and Figure 2). Hydration transition steps are represented in green arrows on Figure 2. Dehydration transitions are represented in blue arrows and the two pretreatment transitions are represented by black arrows. These points are motivated by applications addressed with salt hydrate TCM's, and take care of the chosen reference sample for the round robin test (SrBr₂).

TABLE 6-1: TEMPERATURES AND VAPOR PRESSURE/DEW POINT TEST POINTS

Point #	Label	Sample Temperature [°C]	Vapor Pressure [mbar]	Corresp. Dew point [°C]
P1	Pretreatment / Dry Mass 1	200	< 1 e-3	-150
P2	Hydration 1	25	8.7	5
P3	Dehydration 1	95	< 1 e-3	-150
P4	Hydration 2	25	10	7
P5	Dehydration 2	95	< 1 e-3	-150
P6	Hydration 3	25	12.3	10
P7	Pretreatment / Dry Mass 2	200	< 1 e-3	-150

P8	Cycling test / Hydration 4	25	8.7	5
----	----------------------------	----	-----	---

For all heating dehydration and pretreatment transitions, a heating rate of 1K/min is defined. For all cooling phases to bring the sample hydration reference temperature $T_{Hyd_Ref}=25^{\circ}\text{C}$. Possible cooling rates are dependent on available laboratory equipment and shall be defined and reported. The procedure is defined step-by-step as follows:

1. Initial Pretreatment (P 1):

Reference mass detection; please choose temperature as 200°C , and water vapor pressure $< 1 \text{ e-}3 \text{ mbar}$, heating rate as 1 K/min. When reaching T_{max} , keep constant temperature and lowest water vapor pressure possible for at least 1 Hour.

The mass detected during at the end of this initial and first pretreatment is the initial denoted as mass $m_{in/P1}$ and serving as one of the reference masses for salt hydration potential calculations.

Comparing $m_{dry/P1}$ to the initial sample at the start of the testing m_{start} shall confirm whether the salt has reached the anhydrous state of the salt.

2. Hydration 1 (P 2);

Sample Temperature of 25°C corresponding to the Test hydration Reference mass T_{Hyd_Ref} , dew point of 5°C corresponding to 8.7 mbar ; this hydration point serves as the most stringent test for characterizing the hydration suitability of the salt; the mass detected is labelled as $m_{Hyd1/P2}$ and will be used for reproducibility of the salt cycling suitability check.

The time to reach equilibrium $t_{Hyd1/P2}$ shall be reported

3. Dehydration 1 (P 3);

Sample Temperature of 95°C corresponding to the Test dehydration temperature T_{Dehd_Ref} and water vapor pressure $< 1 \text{ e-}3 \text{ mbar}$, heating rate as 1 K/min, constant temperature and pressure level for at least 1 Hour; the mass detected is labelled as $m_{Deh1/P3}$

The mass detected in reaching this first dehydration cycle will be compared and used as one of the reference masses for salt hydration calculations.

The time to reach equilibrium $t_{Deh1/P3}$ shall be reported

4. Hydration 2 (P 4);

Sample Temperature of 25°C , dew point of 7°C corresponding to 10 mbar ; this hydration point serves as an intermediary winter ambient condition test for the hydration suitability of the salt; the mass detected is labelled as $m_{Hyd2/P4}$ and will be used for reproducibility of the salt cycling suitability check.

The time to reach equilibrium $t_{Hyd2/P4}$ shall be reported

5. Dehydration 2 (P 5);

Sample Temperature of 95°C and water vapor pressure $< 1 \text{ e-}3 \text{ mbar}$, heating rate as 1 K/min, constant temperature and pressure level for at least 1 Hour; the mass detected is labelled as $m_{Deh2/P5}$;

The mass detected in reaching this first dehydration cycle will be compared and used as one of the reference masses for salt hydration calculations.

The time to reach equilibrium $t_{Deh2/P5}$ shall be reported

6. Hydration 3 (P 6);

Sample Temperature of 25 °C, dew point of 10°C corresponding to 12.3 mbar ; this hydration point serves as a maximum winter ambient condition test for the hydration suitability of the salt; the mass detected is labelled as $m_{Hyd3/P6}$ and will be used for reproducibility of the salt cycling suitability check.

The time to reach equilibrium $t_{Hyd3/P6}$ shall be reported

7. 2nd Pretreatment (P 7):

In order to confirm the cyclic suitability of the salt and confirm whether the salt retains its original properties, the first dehydration/hydration cycle shall repeated exactly as was executed at the start of the testing.

After completion of Hydration 3 phase, the salt 2nd pretreatment should be performed similar to P1. Please choose temperature as 200 °C, and water vapor pressure < 1 e-3 mbar, heating rate as 1 K/min, constant temperature and vapor pressure level for at least 1 Hour.

The mass detected during this 2nd pretreatment is the second mass $m_{2/P7}$ serving as one of the reference masses for salt hydration potential calculations.

Comparing $m_{dry/P7}$ to the initial sample at the start of the testing m_{start} shall confirm whether the salt has reached the anhydrous state and shall be compared to $m_{dry/P1}$ for assessing the salt cycling suitability

8. Hydration 4 (P 8);

Sample Temperature of 25 °C, dew point of 5°C corresponding to 8.7 mbar ; this hydration point will be compared to P2; the mass detected is labelled as $m_{Hyd4/P8}$ and will be used for assessing the salt cycling suitability.

The time to reach equilibrium $t_{Hyd4/P8}$ shall be reported

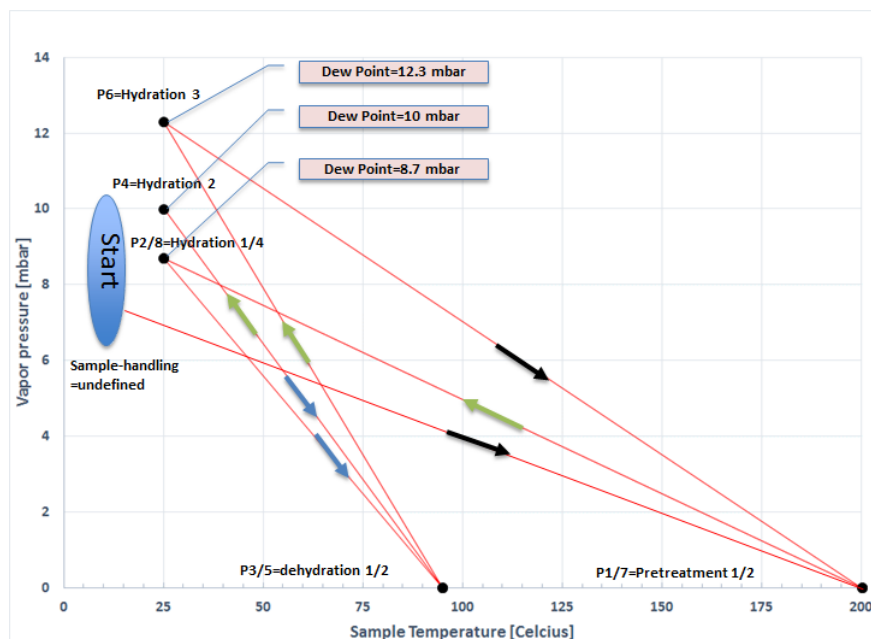


FIGURE 6-2: SCHEME OF THE MEASUREMENT PROCEDURE AS PLOTTED IN THE GRID OF SAMPLE TEMPERATURE AND VAPOR PRESSURE.

DEFINITION OF EQUILIBRIUM STATE

Depending on the measurement setup, salt hydration/dehydration in the segment and kinetics, the time for reaching equilibrium varies severely from several hours to more than a day. An appropriate equilibrium is reached, when there is only balance-related noise left, without any significant tendency of the signal.

A guideline for estimating equilibrium is in progress.

MEASURING THE HEAT (OF HYDRATION/DEHYDRATION)

For this Round Robin, there will be one option, and the consistency of results and applied method for the future will be discussed in the next Task/Annex meeting.

1. Direct measurement with STA / TG-DSC:

According to the procedure, the heat release during hydration can be measured for all of P2, P4, P6 and P8. The heat gain during dehydration can be measured for both P3 and P5. The sensible heat of the adsorption material has to be subtracted (see chapter Heat of Adsorption). This can be done either by performing and subtracting a blank measurement under inert gas atmosphere, or by post-processing of the data (when T-dependent $c_{p, SrBr_2}$ values are available).

2. Calculation from the SrBr₂ characteristic curve:

The heat of adsorption can be calculated by models like.....

If you report values for the heat, please indicate if they are measured or calculated by applying a model and which model was used.

DELIVERY OF RESULTS (VALUES, FORMAT, UNITS)

For comparing the results and for detecting the reasons for deviations, please follow the instructions for delivery of the data in the following. It is proposed to repeat the measurements to ensure repeatable results. Please use the Results Report Sheet which will be sent out with the procedure and use a separate sheet for each measurement run. Please state the uncertainty of each measured value. For the analysis of the results it would also be interesting to indicate the uncertainties of the used apparatus. For this purpose, an additional table is included in the Result Report Sheet. Please choose the fields in the table which are relevant for your apparatus. If the pretreatment of your sample is conducted externally, you can indicate the uncertainty of the external balance in the field "Dry mass determination".

In the following, you find further information for doing the data analysis:

- Sample mass (absolute) for all measurement points 1-8, (please subtract sample holder/crucible), Units [mg]
- Hydration mass uptake of the salt are measured during P2, P4, P6 and P8 equilibrium points, and are compared to the mass of dehydrated salt detected during the preceding dehydrated points (P1, P3, P5 and P7) and dehydration steps 1 and 2, Units [g/g dry mass]

$$\Delta m_1 = \frac{m_{Hyd1/P2} - m_{dry/P1}}{m_{dry/P1}}$$

$$\Delta m_2 = \frac{m_{Hyd2/P4} - m_{Deh1/P3}}{m_{Deh1/P3}}$$

$$\Delta m_3 = \frac{m_{Hyd3/P6} - m_{Deh2/P5}}{m_{Deh2/P5}}$$

$$\Delta m_4 = \frac{m_{Hyd4/P8} - m_{dry/P7}}{m_{dry/P7}}$$

- Hydration heat release of the four-hydration test processes Hyd1, Hyd2, Hyd3 and Hyd4. Unit is J/g of dehydrated mass of salt at the start of the hydration phase; Units [J/g_{salt, dehydrated}]

Calculation according to

$$H_{Hyd1} = \frac{\int_{Hyd1_i}^{Hyd1_f} \dot{Q} dt}{m_{dry/P1}}$$

$$H_{Hyd2} = \frac{\int_{Hyd2_i}^{Hyd2_f} \dot{Q} dt}{m_{Deh1/P3}}$$

$$H_{Hyd3} = \frac{\int_{Hyd3_i}^{Hyd3_f} \dot{Q} dt}{m_{deh5/P1}}$$

$$H_{Hyd4} = \frac{\int_{Hyd4_i}^{Hyd4_f} \dot{Q} dt}{m_{dry/P7}}$$

(Please note: \dot{Q} as exothermal is negative; i and f relate to the start and finish of the hydration process)

- Dehydration heat gain of the two-hydration test processes Deh1, Deh2. Unit is J/g of dehydrated mass of salt measured at the end of the dehydration p; Units [J/g_{salt, dehydrated}]

Calculation according to:



$$H_{Deh1} = \frac{\int_{Deh1_i}^{Deh1_f} \dot{Q}' dt}{m_{Deh1/P3}}$$

$$H_{Deh2} = \frac{\int_{Deh2_i}^{Deh2_f} \dot{Q}' dt}{m_{Deh2/P5}}$$

(Please note: \dot{Q} as endothermal is positive)

- Cyclic behavior of the salt is measured in terms of the reproducibility of dehydrated mass during the two dehydration processes Deh1 and Deh2 when considering the reference application dehydration temperature, T_{Deh_Ref} , which in this case is assumed 95°C. It is also measured in terms of the reproducibility of dry mass during the two pretreatment processes Dry1 and Dry2 when considering $T_{max} = 200^\circ C$, Units [g/g]

$$\Delta m_1' = \frac{m_{Deh2/P5} - m_{Deh1/P3}}{m_{Deh1/P3}}$$

$$\Delta m_2' = \frac{m_{dry/P7} - m_{dry/P1}}{m_{dry/P1}}$$

Cyclic behavior of the salt is also measured by comparing the heat hydration heat release after the pretreatment up to $T_{max} = 200^\circ C$ of the salt sample H_{Hyd1} and H_{Hyd2}

Good luck with the measurements!

Questions / comments / improvement of the procedure, please send an email to

Reda.Djebbar@Canada.ca

When you have performed the measurements and processed the data, please send it to the same email address (using the Results Report Sheet).

References:

- Dale L. Perry, Handbook of Inorganic Compounds, Second Edition

Results report of the Salt Hydrate (SrBr₂ · nH₂O) 2nd Round Robin

Lab:	
Operator:	
Measurement Apparatus:	
Measurement Mode:	<input type="checkbox"/> static (pure water vapor atmosphere)
	<input type="checkbox"/> dynamic (pure water vapor atmosphere)



	<input type="checkbox"/> dynamic with carrier gas:
Pretreatment:	<input type="checkbox"/> Vacuum with final pressure:
	<input type="checkbox"/> other:
Heat of Adsorption	<input type="checkbox"/> measured
	<input type="checkbox"/> calculated, applying model:
Period of Measurement:	

Uncertainty of apparatus (datasheet values). Please choose the fields, which are relevant for your apparatus.

Temperature [°C]	Pressure [mbar]	Relative Humidity [%]	Saturation Temperature [°C]	Balance [mg]	Dry Mass Determination (external) [mg]

1. Sample mass (absolute) for all measurement points 1 to 8. Please also report here the mass of the salt sample at the very start of the testing m_{start} in [mg] Unit is mg.

Point #	Symbol	Sample Temperature [°C]	Vapor Pressure [mbar]	Equilibrium time [min]	Sample Mass [mg]	Uncertainty [mg]
P0	m_{start}	NA	NA	NA		
P 1	$m_{dry/P1}$	200	< 1 e-3	As per Section b		
P 2	$m_{Hyd1/P2}$	25	8.7			
P 3	$m_{Deh1/P3}$	95	< 1 e-3			
P 4	$m_{Hyd2/P4}$	25	10			
P 5	$m_{Deh2/P5}$	95	< 1 e-3			
P 6	$m_{Hyd3/P4}$	25	12.3			
P7	$m_{dry/P7}$	200	< 1 e-3	As per Section b		

P8	$m_{Hyd4/P8}$	25	8.7			
----	---------------	----	-----	--	--	--

2. Hydration mass gain during Hyd1, Hyd2, Hyd3 and Hyd4 equilibrium . Unit is g/g dry mass.

Description	Symbol	Uptake [g/g]	Uncertainty [g/g]
Uptake after Hyd1 related to dry mass $m_{dry/P1}$	Δm_1		
Uptake after Hyd2 related to mass Deh1 $m_{Deh1/P3}$	Δm_2		
Uptake after Hyd3 related to mass Deh2 $m_{Deh2/P5}$	Δm_3		
Uptake after Hyd4 related to dry mass $m_{dry/P7}$	Δm_4		

3. Dehydrated and Dry mass change after the dehydration and the pretreatment cycles. Unit is g/g.

Description	Symbol	Uptake [g/g]	Uncertainty [g/g]
Dehydrated mass change between Deh1 and Deh2	$\Delta m_1'$		
Dry mass change between Dry1 and Dry2	$\Delta m_2'$		

4. Hydration Heat of the four-hydration test processes Hyd1, Hyd2, Hyd3 and Hyd4. Unit is J/g of dehydrated mass of salt at the start of the hydration phase.

Description	Symbol	Hydration time [min]	Heat [J/g]	Uncertainty [J/g]
Hydration Heat during Hyd1	H_{Hyd1}	$t_{Hyd1/P2} =$		
Hydration Heat during Hyd2	H_{Hyd2}	$t_{Hyd2/P4} =$		
Hydration Heat during Hyd3	H_{Hyd3}	$t_{Hyd3/P6} =$		
Hydration Heat during Hyd4	H_{Hyd4}	$t_{Hyd4/P8} =$		

5. Dehydration Heat of the two-hydration test processes Deh1, Deh2. Unit is J/g of dehydrated mass of salt measured at the end of the dehydration cycle.

Description	Symbol	Dehydration time [min]	Heat [J/g]	Uncertainty [J/g]
Dehydration Heat during Deh1	H_{Deh1}	$t_{Deh1/P3}$		
Dehydration Heat during Deh2	H_{Deh2}	$t_{Deh2/P5}$		

6.2.2 APPENDIX B

(January 14th, 2019)

Measurement Procedure for Water Uptake Evaluation of TCMs

IEA Task 58 / Annex 33 Subtask Final Round Robin Procedure for SrBr₂

GOAL OF THIS DOCUMENT:

By applying and following this procedure, reproducible and comparable measurement results of water vapor uptake for thermochemical materials (TCM) will be produced, to predict the material performance under particular boundary conditions of an application.

PROCEDURE FOR SALT HYDRATES (E.G. SRBR₂)

The applied methods include gravimetric analyzers with vapor or humidity conditioning, optional with calorimetric extension (TG, TG-DSC, STA) [1]. The procedure consists of a pretreatment of the sample, and several hyd- and dehydration points, while all of them have to reach equilibrium state.

DEFINITION OF THE SCENARIOS

As performed in the first round robin, two scenarios will be applied, which are derived from boundary conditions in typical applications, and are in good agreement with the temperatures for domestic heating and cooling sent in a document (Temperatures Buildings) by Benjamin Fumey. The conditions are given in Table 6-2.

PRETREATMENT / DRY MASS DETECTION

A standardized pretreatment is necessary for comparable uptake calculations, as the dry mass will serve as one of the reference masses. Please follow the following procedure presented below:

(It must be performed under 1 mbar corresponding of 3.2 % R.H.)

The optimal sample pretreatment temperature T_{max} of 120°C was selected

The sample is heated starting from ambient conditions with a heating rate of 1K/min followed by an isothermal drying step for another ~6 hours ?

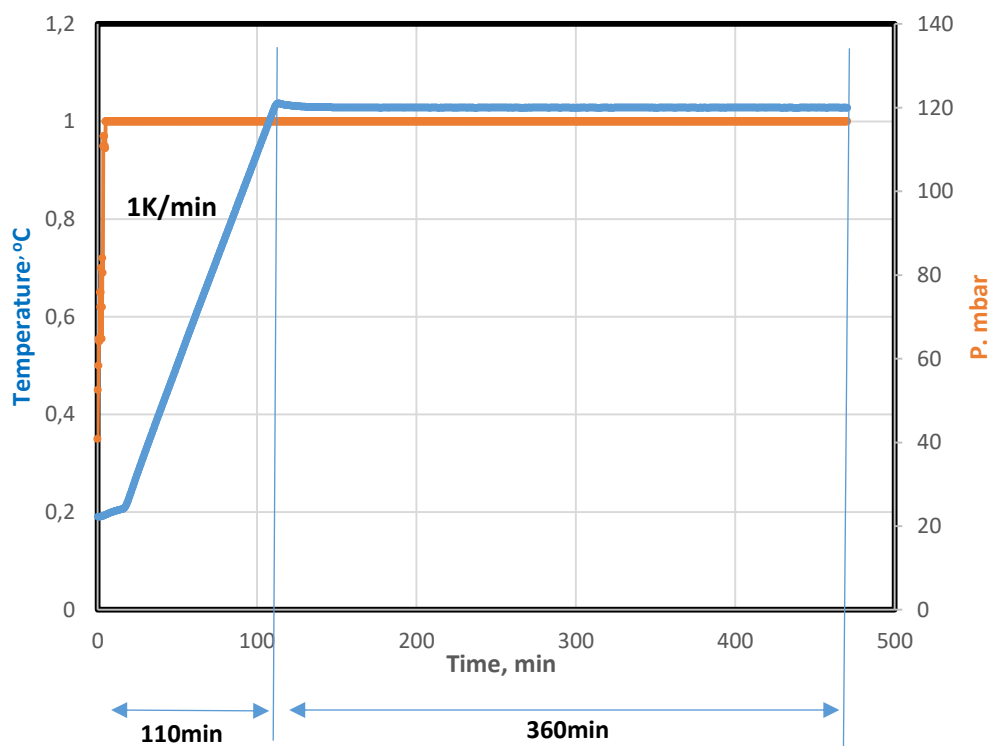


FIGURE 6-3: PROPOSED PRETREATMENT PROCEDURE

MEASUREMENT OF EQUILIBRIUM POINTS

In the following steps, two hydration and dehydration points are carried out, all with a dew point of 10 °C, which corresponds to water vapor pressure of 12.3 mbar, and sample temperatures of 35, 65, 95 and 180 °C (see Table 6-2 and Figure 2). These points are motivated by applications addressed with TCM's, and take care of the chosen reference sample for the round robin test (SrBr₂).

For all heating phases, a heating rate of 1K/min is defined.

TABLE 6-2: TEMPERATURES AND VAPOR PRESSURE/DEW POINT, ACCORDING TO SCENARIO 1 (DEH1, HYD1) AND 2 (DEH2, HYD2)

Point #	Label	Sample Temperature [°C]	Vapor pressure [mbar]	Corresp. Dew point [°C]
P 1	Pretreatment / Dry mass	120	1	-20.1
P 2	Hydration 1	65	12.3	10
P 3	Dehydration 1	95	12.3	10
P 4	Hydration 2	35	12.3	10
P 5	Dehydration2	180	12.3	10

P 6	Hydration 3	65	12.3	10
-----	-------------	----	------	----

The procedure is defined step-by-step:

9. Pretreatment (P 1):

Dry mass detection; please choose temperature as 120 °C, and pressure level 1 mbar, heating rate as 1 K/min, constant temperature and pressure level for at least 6 h.

The mass detected during pretreatment is the dry mass $m_{dry/P1}$ serving as one of the reference masses for uptake calculations.

10. Hydration 1 (P 2);

Sample Temperature of 65 °C, dew point of 10 °C corresponding to 12.3 mbar; this hydration point serves as intermediate step, so that the following dehydration can be approached in dehydration direction, and the two following pairs can measure the heat in hydration mode; the mass detected is labelled as $m_{hyd1/P2}$ and can be used for reproducibility check

11. Dehydration 1 (P 3);

Sample Temperature of 95 °C (heating rate 1K/min), dew point of 10 °C corresponding to 12.3 mbar; the mass detected is labelled as $m_{Deh1/P3}$

12. Hydration 1 (P 4);

Sample Temperature of 35 °C, dew point of 10 °C corresponding to 12.3 mbar; the mass detected is labelled as $m_{hyd2/P4}$

13. Dehydration 2 (P 5);

Sample Temperature of 180 °C (heating rate 1K/min), dew point of 10 °C corresponding to 12.3 mbar; the mass detected is labelled as $m_{Deh2/P5}$;

In addition to the dry mass detected during pretreatment, the mass detected at Dehydration 2 $m_{Deh2/P5}$ will serve as a second reference mass for uptake calculations.

14. Hydration 2 (P 6);

Sample Temperature of 65 °C, dew point of 10 °C corresponding to 12.3 mbar; the mass detected is labelled as $m_{hyd3/P6}$

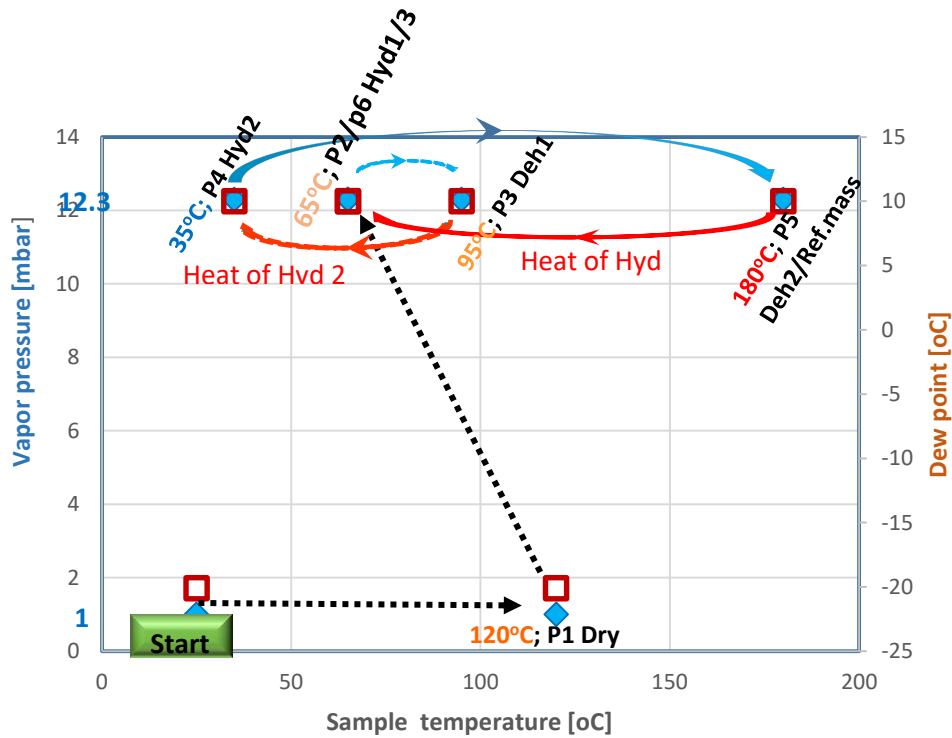
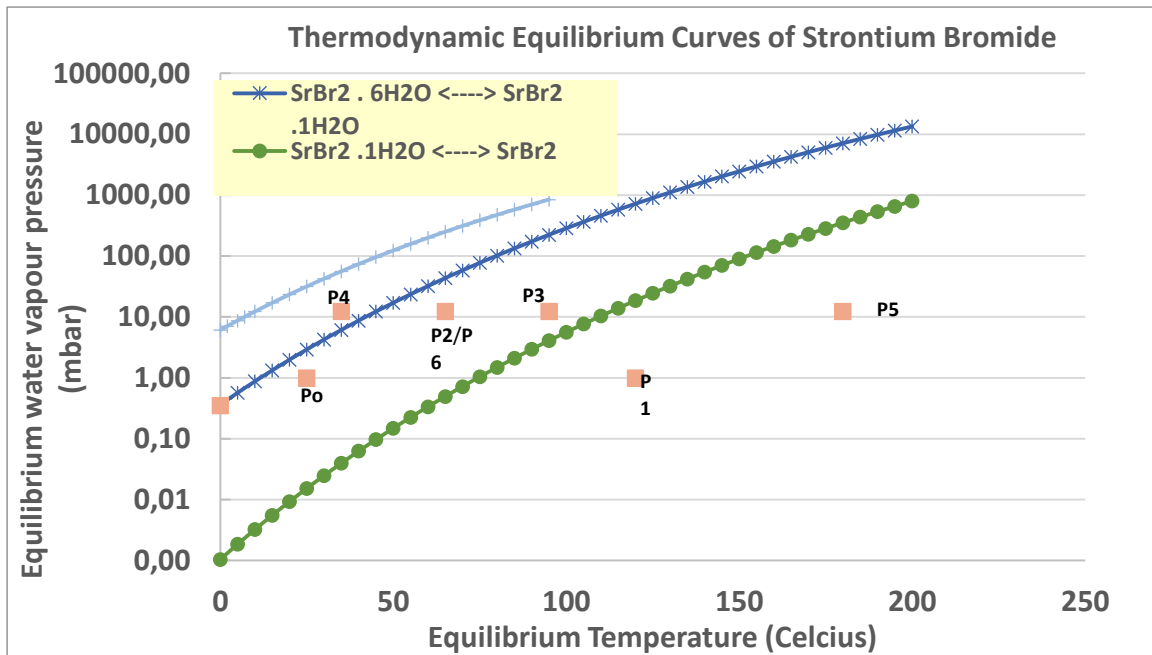


FIGURE 6-4: SCHEME OF THE MEASUREMENT PROCEDURE AS PLOTTED IN THE GRID OF SAMPLE TEMPERATURE AND VAPOR PRESSURE/DEW POINT; THE RED ARROWS INDICATE THE TRANSITIONS WITH MEASUREMENT OF THE HEAT SIGNAL FOR THE HEAT OF HYDRATION DETECTION.



DEFINITION OF EQUILIBRIUM STATE

Depending on the measurement setup, water uptake in the segment and kinetics, the time for reaching equilibrium varies severely from several hours to more than a day. An appropriate equilibrium is reached, when there is only balance-related noise left, without any significant tendency of the signal.

In a supplementary document a guideline for estimating equilibrium, or needed time to reach respectively, is delivered in advance of the Task meeting, to be discussed there.

MEASURING THE HEAT (OF ADSORPTION)

For the first iteration of the Round Robin, there will be two options, and the consistency of results and applied method for the future will be discussed in the Task/Annex meeting in Ljubljana.

Direct measurement with STA / TG-DSC:

According to the procedure so far, the heat (during adsorption) can be measured between Des1 and Ads1, and between Des2 and Ads2. The sensible heat of the adsorption material has to be subtracted (see chapter Heat of Adsorption). This can be done either by performing and subtracting a blank measurement under inert gas atmosphere, or by post-processing of the data (when T-dependent $c_{p, 13X}$ values are available).

Calculation from 13X characteristic curve:

The heat of adsorption can be calculated by models like Clausius-Clapeyron or Dubinin Potential Theory.

If you report values for the heat, please indicate if they are measured, or calculated by applying a model, and which model was used.

DELIVERY OF RESULTS (VALUES, FORMAT, UNITS)

For comparing the results, and to detect the reasons for deviations may appear, please follow the instructions for delivery of the data in the following. Please use the Results Report document, which will be sent out with the procedure.

- Sample mass (absolute) for all measurement points 1-6, (please subtract sample holder/crucible), Units [mg]
- Uptake between Ads1 / Des1 and Ads2 / Des2, related to dry mass detected in pretreatment (P1), Units [g/g]

$$\Delta X_1 = \frac{m_{Ads1/P4} - m_{Des1/P3}}{m_{dry/P1}}$$

$$\Delta X_2 = \frac{m_{Ads2/P6} - m_{Des2/P5}}{m_{dry/P1}}$$

- Uptake between Ads1 / Des1 and Ads2 / Des2, related to reference mass detected in Des2 (P5), Units [g/g]

$$\Delta X_{1'} = \frac{m_{Ads1/P4} - m_{Des1/P3}}{m_{Des2/P5}}$$

$$\Delta X_2 = \frac{m_{Ads2/P6} - m_{Des2/P5}}{m_{Des2/P5}}$$

- Heat of Adsorption (material) detected between Des1 and Ads1, as well as between Des2 and Ads2;
Units [J/g_{Sorbent, dry}]
Calculation according to

$$H_{Ads1} = \frac{\int_{Des1}^{Ads1} \dot{Q} dt - \int_{T_{Des1}}^{T_{Ads1}} c_{p, 13X} dT}{m_{dry/P1}}$$

$$H_{Ads2} = \frac{\int_{Des2}^{Ads2} \dot{Q} dt - \int_{T_{Des2}}^{T_{Ads2}} c_{p, 13X} dT}{m_{dry/P1}}$$

(Please note: \dot{Q} as exothermal is negative)

- Heat of Adsorption (adsorbate) detected between Des1 and Ads1, as well as between Des2 and Ads2;
Units [J/g_{Adsorbate / water}]
Calculation according to

$$H'_{Ads1} = \frac{\int_{Des1}^{Ads1} \dot{Q} dt - \int_{T_{Des1}}^{T_{Ads1}} c_{p, 13X} dT}{m_{dry/P1} * \Delta X_1} = \frac{\int_{Des1}^{Ads1} \dot{Q} dt - \int_{T_{Des1}}^{T_{Ads1}} c_{p, 13X} dT}{m_{Ads1/P4} - m_{Des1/P3}}$$

$$H'_{Ads2} = \frac{\int_{Des2}^{Ads2} \dot{Q} dt - \int_{T_{Des2}}^{T_{Ads2}} c_{p, 13X} dT}{m_{dry/P1} * \Delta X_2} = \frac{\int_{Des2}^{Ads2} \dot{Q} dt - \int_{T_{Des2}}^{T_{Ads2}} c_{p, 13X} dT}{m_{Ads2/P6} - m_{Des2/P5}}$$

with ΔX_1 and ΔX_2 as defined above

If you report values for the heat, please indicate if they are measured, or calculated by applying a model, and which model was used.

Good luck with the measurements!

Questions / comments / improvement of the procedure, please send an e-mail to

Markus.Fink@ait.ac.at

If you have performed the measurements and processed the data, please send it to the same mail address (using the Results_report sheet).

Results report of the Final SrBr₂ Round Robin



Lab:	
Operator:	
Measurement Apparatus:	
Measurement Mode:	<input type="checkbox"/> static (pure water vapor atmosphere)
	<input type="checkbox"/> dynamic (pure water vapor atmosphere)
	<input type="checkbox"/> dynamic with carrier gas:
Pretreatment:	<input type="checkbox"/> Vacuum with final pressure:
	<input type="checkbox"/> other: dynamic with N ₂
Heat of Adsorption	<input type="checkbox"/> measured
	<input type="checkbox"/> calculated, applying model:
Period of Measurement:	

Uncertainty of apparatus (datasheet values). Please choose the fields which are relevant for your apparatus.

Temperature [°C]	Pressure [mbar]	Relative Humidity [%]	Saturation Temperature [°C]	Balance [mg]	Dry Mass Determination (external) [mg]
0.1					

1. Sample mass (absolute) for all measurement points 1 to 6. Unit is mg.

Point #	Symbol	Sample Temperature [°C]	Vapor Pressure [mbar]	Sample Mass [mg]	Uncertainty [mg]
P 1	$m_{\text{dry}/P1}$	120	1		
P 2	$m_{\text{Ads2}'/P2}$	65	12.3		
P 3	$m_{\text{Des1}/P3}$	95	12.3		
P 4	$m_{\text{Ads1}/P4}$	35	12.3		
P 5	$m_{\text{Des2}/P5}$	180	12.3		

P 6	$m_{Ads2/P6}$	65	12.3		
-----	---------------	----	------	--	--

2. Uptake between Des1 / Ads1 and Des2 / Ads2. Unit is g/g.

Description	Symbol	Uptake [g/g]	Uncertainty [g/g]
Uptake between Des1 / Ads1 related to dry mass	ΔX_1		
Uptake between Des2 / Ads2 related to dry mass	ΔX_2		
Uptake between Des1 / Ads1 related to mass Des2	$\Delta X_1'$		
Uptake between Des2 / Ads2 related to mass Des2	$\Delta X_2'$		

3. Heat of Adsorption between Des1 / Ads1 and Des2 / Ads2. Unit is J/g.

Description	Symbol	Heat [J/g]	Uncertainty [J/g]
Heat of Adsorption (material specific) Des1 / Ads1	H_{Ads1}		
Heat of Adsorption (material specific) Des2 / Ads2	H_{Ads2}		
Heat of Adsorption (adsorbate specific) Des1 / Ads1	H'_{Ads1}		
Heat of Adsorption (adsorbate specific) Des2 / Ads2	H'_{Ads2}		

6.2.3 APPENDIX C

Measurement Procedure for the 3rd Zeolite 13X Round Robin

IEA Task 58 / Annex 33 Subtask 3T

GOAL OF THIS DOCUMENT

By applying and following this procedure, reproducible and comparable measurement results of adsorbate uptake for thermochemical materials (TCM) will be produced, to predict the material performance under particular boundary conditions of an application.

PROCEDURE FOR POROUS MATERIALS (E.G. ZEOLITE)

The applied methods include gravimetric analyzers with vapor or humidity conditioning, optional with calorimetric extension (TG, TG-DSC, STA) [1]. The procedure consists of a pretreatment of the sample, and several ad- and desorption points, while all of them have to reach equilibrium state.

DEFINITION OF THE SCENARIOS

As performed in the previous round robin, two scenarios will be applied, which are derived from boundary conditions in typical applications, and are in good agreement with the temperatures for domestic heating and cooling sent in a document (Temperatures_Buildings) by Benjamin Fumey. The conditions are given Table 6-3.

PRETREATMENT / DRY MASS DETECTION

A standardized pretreatment is necessary for comparable uptake calculations, as the dry mass will serve as one of the reference masses. Please follow the procedure according to reference [2]. It must be performed under continuous evacuation (vacuum level: $< 1e-3$ mbar).

The optimal sample pretreatment temperature T_{max} should be selected according to the following classification.

- Strongly hydrophilic zeolites (4A, 13X): pre-treatment $T = 350^{\circ}\text{C}$.

The sample is heated starting from ambient conditions with a heating rate of $1\text{K}/\text{min}$ followed by an isothermal drying step for another 8 hours (Figure 1).

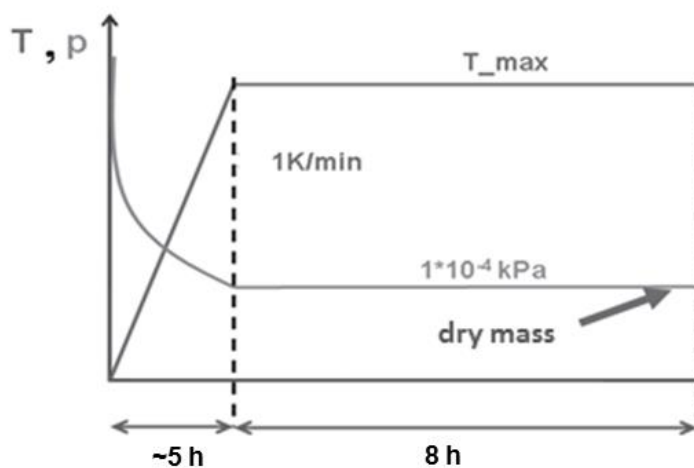


FIGURE 6-5: PROPOSED PRETREATMENT PROCEDURE

Comment to Round-Robin participants of IEA/Annex 58/33: For the case that the measurement setup is not capable of applying vacuum, please indicate this together with the measurement results. To overcome deviations caused by differing partial pressures during pretreatment, an additional reference point will be introduced (see chapter Desorption 2 (P5)).

MEASUREMENT OF EQUILIBRIUM POINTS

In the following steps, two ad- and desorption points are carried out, all with a dew point of 10°C , which corresponds to water vapor pressure of 12.3 mbar, and sample temperatures of 35 , 65 , 95 and 180°C (see Table 6-3 and Figure 2). These points are motivated by applications addressed with TCM's, and take care of the chosen reference sample for the round robin test (13X).

For all heating phases, a heating rate of 1K/min is defined.

TABLE 6-3: TEMPERATURES AND VAPOR PRESSURE/DEW POINT, ACCORDING TO SCENARIO 1 (DES1, ADS1) AND 2 (DES2, ADS2)

Point #	Label	Sample Temperature [°C]	Vapor pressure [mbar]	Corresp. Dew point [°C]
P 1	Pretreatment / Dry mass	350	< 1 e-3	< -150
P 2	Adsorption 2'	65	12.3	10
P 3	Desorption 1	95	12.3	10
P 4	Adsorption 1	35	12.3	10
P 5	Desorption 2	180	12.3	10
P 6	Adsorption 2	65	12.3	10

The procedure is defined step-by-step:

15. Pretreatment (P 1):

Dry mass detection; please choose temperature as 350 °C, and vacuum level < 1e-3 mbar, heating rate as 1 K/min, constant temperature and pressure level for at least 8 h.

The mass detected during pretreatment is the dry mass $m_{dry/P1}$ serving as one of the reference masses for uptake calculations.

16. Adsorption 2' (P 2);

Sample Temperature of 65 °C, dew point of 10 °C corresponding to 12.3 mbar; this adsorption point serves as intermediate step, so that the following desorption can be approached in desorption direction, and the two following pairs can measure the heat in adsorption mode; the mass detected is labelled as $m_{Ads2'/P2}$ and can be used for reproducibility check.

17. Desorption 1 (P 3);

Sample Temperature of 95 °C (heating rate 1K/min), dew point of 10 °C corresponding to 12.3 mbar; the mass detected is labelled as $m_{Des1/P3}$;

18. Adsorption 1 (P 4);

Sample Temperature of 35 °C, dew point of 10 °C corresponding to 12.3 mbar; the mass detected is labelled as $m_{Ads1/P4}$;

19. Desorption 2 (P 5);

Sample Temperature of 180 °C (heating rate 1K/min), dew point of 10 °C corresponding to 12.3 mbar; the mass detected is labelled as $m_{Des2/P5}$;

In addition to the dry mass detected during pretreatment, the mass detected at Desorption 2 $m_{Des2/P5}$ will serve as a second reference mass for uptake calculations.

20. Adsorption 2 (P 6);
Sample Temperature of 65 °C, dew point of 10 °C corresponding to 12.3 mbar; the mass detected is labelled as $m_{Ads2/P6}$;

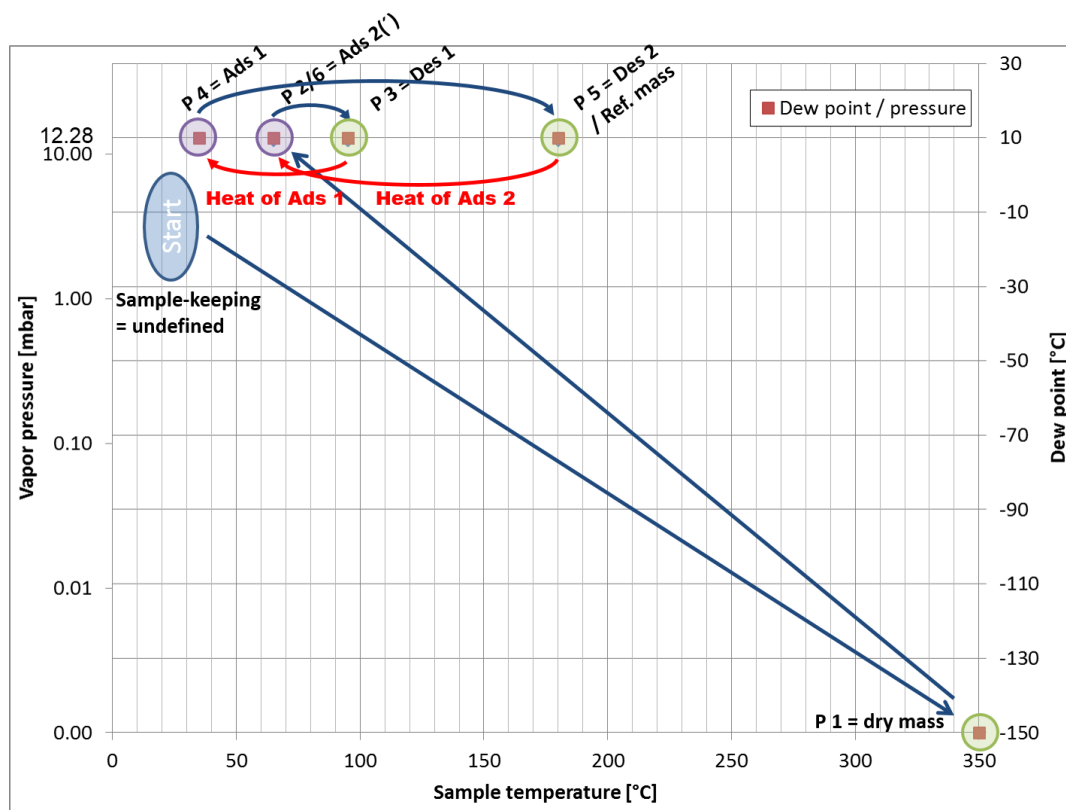


FIGURE 6-6: SCHEME OF THE MEASUREMENT PROCEDURE AS PLOTTED IN THE GRID OF SAMPLE TEMPERATURE AND VAPOR PRESSURE/DEW POINT; THE RED ARROWS INDICATE THE TRANSITIONS WITH MEASUREMENT OF THE HEAT SIGNAL FOR THE HEAT OF ADSORPTION DETECTION.

DEFINITION OF EQUILIBRIUM STATE

Depending on the measurement setup, water uptake in the segment and kinetics, the time for reaching equilibrium varies severely from several hours to more than a day. An appropriate equilibrium is reached, when there is only balance-related noise left, without any significant tendency of the signal.

A guideline for estimating equilibrium is in progress.

MEASURING THE HEAT (OF ADSORPTION)

For this Round Robin, there will be two options, and the consistency of results and applied method for the future will be discussed in the next Task/Annex meeting.

1. Direct measurement with STA / TG-DSC:

According to the procedure so far, the heat (during adsorption) can be measured between Des1 and Ads1, and between Des2 and Ads2. The sensible heat of the adsorption material has to be subtracted (see chapter Heat

of Adsorption). This can be done either by performing and subtracting a blank measurement under inert gas atmosphere, or by post-processing of the data (when T-dependent $c_{p, 13X}$ values are available).

2. Calculation from 13X characteristic curve:

The heat of adsorption can be calculated by models like Clausius-Clapeyron or Dubinin Potential Theory.

If you report values for the heat, please indicate if they are measured or calculated by applying a model and which model was used.

DELIVERY OF RESULTS (VALUES, FORMAT, UNITS)

For comparing the results and for detecting the reasons for deviations, please follow the instructions for delivery of the data in the following. It is proposed to repeat the measurements to ensure repeatable results. Please use the Results Report Sheet which will be sent out with the procedure and use a separate sheet for each measurement run. Please state the uncertainty of each measured value. For the analyzation of the results it would also be interesting to indicate the uncertainties of the used apparatus. For this purpose, an additional table is included in the Result Report Sheet. Please choose the fields in the table which are relevant for your apparatus. If the pretreatment of your sample is conducted externally, you can indicate the uncertainty of the external balance in the field "Dry mass determination".

In the following, you find further information for doing the data analysis:

- Sample mass (absolute) for all measurement points 1-6, (please subtract sample holder/crucible), Units [mg]
- Uptake between Ads1 / Des1 and Ads2 / Des2, related to dry mass detected in pretreatment (P1), Units [g/g]

$$\Delta X_1 = \frac{m_{Ads1/P4} - m_{Des1/P3}}{m_{dry/P1}}$$

$$\Delta X_2 = \frac{m_{Ads2/P6} - m_{Des2/P5}}{m_{dry/P1}}$$

- Uptake between Ads1 / Des1 and Ads2 / Des2, related to reference mass detected in Des2 (P5), Units [g/g]

$$\Delta X_{1'} = \frac{m_{Ads1/P4} - m_{Des1/P3}}{m_{Des2/P5}}$$

$$\Delta X_{2'} = \frac{m_{Ads2/P6} - m_{Des2/P5}}{m_{Des2/P5}}$$

- Heat of Adsorption (material) detected between Des1 and Ads1, as well as between Des2 and Ads2; Units [J/g_{Sorbent, dry}]
Calculation according to

$$H_{Ads1} = \frac{\int_{Des1}^{Ads1} \dot{Q} dt - \int_{T_{Des1}}^{T_{Ads1}} c_{p\ 13X} dT}{m_{dry/P1}}$$

$$H_{Ads2} = \frac{\int_{Des2}^{Ads2} \dot{Q} dt - \int_{T_{Des2}}^{T_{Ads2}} c_{p\ 13X} dT}{m_{dry/P1}}$$

(Please note: \dot{Q} as exothermal is negative)

- Heat of Adsorption (adsorbate) detected between Des1 and Ads1, as well as between Des2 and Ads2;
Units [J/g_{Adsorbate / water}]
Calculation according to

$$H'_{Ads1} = \frac{\int_{Des1}^{Ads1} \dot{Q} dt - \int_{T_{Des1}}^{T_{Ads1}} c_{p\ 13X} dT}{m_{dry/P1} * \Delta X_1} = \frac{\int_{Des1}^{Ads1} \dot{Q} dt - \int_{T_{Des1}}^{T_{Ads1}} c_{p\ 13X} dT}{m_{Ads1/P4} - m_{Des1/P3}}$$

$$H'_{Ads2} = \frac{\int_{Des2}^{Ads2} \dot{Q} dt - \int_{T_{Des2}}^{T_{Ads2}} c_{p\ 13X} dT}{m_{dry/P1} * \Delta X_2} = \frac{\int_{Des2}^{Ads2} \dot{Q} dt - \int_{T_{Des2}}^{T_{Ads2}} c_{p\ 13X} dT}{m_{Ads2/P6} - m_{Des2/P5}}$$

with ΔX_1 and ΔX_2 as defined above

Good luck with the measurements!

Questions / comments / improvement of the procedure, please send an email to

fabian.fischer@zae-bayern.de

When you have performed the measurements and processed the data, please send it to the same email address (using the Results Report Sheet).

LITERATURE

- Henninger SK, Schmidt FP, Henning H-M. Water adsorption characteristics of novel materials for heat transformation applications. Applied Thermal Engineering 2010; 30 (13): 1692–1702
- Henninger SK, Freni A, Schnabel L et al. Unified water adsorption measurements procedure for sorption materials. In: Proceedings ISHPC 2011: 513–522

6.2.4 APPENDIX D: RESULTS REPORT OF THE 3RD ZEOLITE 13X ROUND ROBIN

Lab:	
Operator:	
Measurement Apparatus:	
Measurement Mode:	<input type="checkbox"/> static (pure water vapor atmosphere)



	<input type="checkbox"/> dynamic (pure water vapor atmosphere)
	<input type="checkbox"/> dynamic with carrier gas:
Pretreatment:	<input type="checkbox"/> Vacuum with final pressure:
	<input type="checkbox"/> other:
Heat of Adsorption	<input type="checkbox"/> measured
	<input type="checkbox"/> calculated, applying model:
Period of Measurement:	

Uncertainty of apparatus (datasheet values). Please choose the fields which are relevant for your apparatus.

Temperature [°C]	Pressure [mbar]	Relative Humidity [%]	Saturation Temperature [°C]	Balance [mg]	Dry Mass Determination (external) [mg]

1. Sample mass (absolute) for all measurement points 1 to 6. Unit is mg.

Point #	Symbol	Sample Temperature [°C]	Vapor Pressure [mbar]	Sample Mass [mg]	Uncertainty [mg]
P 1	$m_{dry/P1}$	350	< 1 e-3		
P 2	$m_{Ads2'/P2}$	65	12.3		
P 3	$m_{Des1/P3}$	95	12.3		
P 4	$m_{Ads1/P4}$	35	12.3		
P 5	$m_{Des2/P5}$	180	12.3		
P 6	$m_{Ads2/P6}$	65	12.3		

2. Uptake between Des1 / Ads1 and Des2 / Ads2. Unit is g/g.

Description	Symbol	Uptake [g/g]	Uncertainty [g/g]

Uptake between Des1 / Ads1 related to dry mass	ΔX_1		
Uptake between Des2 / Ads2 related to dry mass	ΔX_2		
Uptake between Des1 / Ads1 related to mass Des2	$\Delta X_1'$		
Uptake between Des2 / Ads2 related to mass Des2	$\Delta X_2'$		

3. Heat of Adsorption between Des1 / Ads1 and Des2 / Ads2. Unit is J/g.

Description	Symbol	Heat [J/g]	Uncertainty [J/g]
Heat of Adsorption (material specific) Des1 / Ads1	H_{Ads1}		
Heat of Adsorption (material specific) Des2 / Ads2	H_{Ads2}		
Heat of Adsorption (adsorbate specific) Des1 / Ads1	H'_{Ads1}		
Heat of Adsorption (adsorbate specific) Des2 / Ads2	H'_{Ads2}		

6.2.5 APPENDIX E: MEASUREMENT PROTOCOL FOR THE EVALUATION OF SPECIFIC HEAT CAPACITY $c_p(T)$ OF $SrBr_2 \cdot nH_2O$ AND $SrBr_2$ BASED ON HEAT FLOW DIFFERENTIAL SCANNING CALORIMETRY

$SrBr_2 \cdot 6H_2O$ is a promising thermochemical energy storage material which was already analysed in the IEA TASK 55 / ECES Annex 33 to determine the phase change and reaction enthalpies based on calorimetric and thermogravimetric measurements. Nevertheless, also the sensible heat or specific heat capacity $c_p(T)$ of the salt hydrates $SrBr_2 \cdot nH_2O$ and the pure $SrBr_2$ salt is needed to describe the enthalpy change for further applications. This document describes a measurement procedure based on a heat flow Differential Scanning Calorimeter (hf-DSC) to evaluate these material properties. The general information in this document are from the dissertation "Evaluation of thermophysical properties for thermal energy storage materials - determining factors, prospects and limitations" [1]. For more detailed information the reader is referred to this document.

DIFFERENTIAL SCANNING CALORIMETRY - DSC

MEASUREMENT PRINCIPLE

According [2] the following definition applies for DSC: "Differential Scanning Calorimetry means the measurement of the change of the difference in the heat flow rate to the sample and to a reference sample while they are subjected to a controlled temperature program". There are two different basic types of DSC, the heat flux and the power compensated DSC. In this work, the heat flux DSC with disk type sensor is described, which was also used for the further experiments. If the reader is interested on other calorimetry instrumentations please refer to [2,3].

CALIBRATION

In case of DSC calibration, this would mean that measurement standards or certified reference materials are needed for the measured quantities temperature T , heat Q and heat flow Φ . In the standard document [4] several points are listed, which are influencing the calibration result. Some of these points are:

- heating and cooling rates
- type and size of the used crucibles
- position of the sample in the sample crucible
- mass and size of the sample
- thermal contact between crucible and sensor

TEMPERATURE CALIBRATION

Temperature calibration in the heating segment of a DSC is done by melting calibration substances in a crucible on the sample side of the DSC sensor. As recommended by [2] at least 3 fixed points of the calibration materials defined in the International Temperature Scale of 1990 (ITS-90) [5] should be used to calibrate temperature in the desired temperature range.

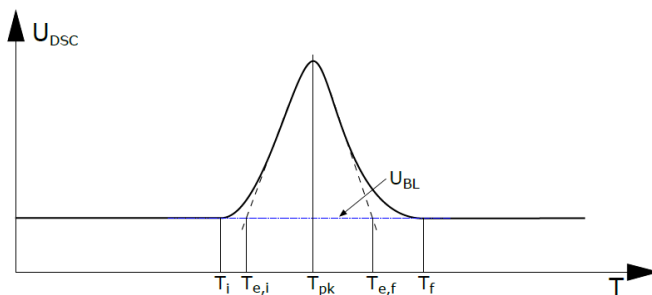


FIGURE 6-7: DSC VOLTAGE U_{DSC} VERSUS T DURING A TRANSITION WITH THE CHARACTERISTIC TEMPERATURES

Since a DSC experiment is no static method, a phase transition measurement results in a peak as shown in Figure 6-7. The shape of the measured peak is changing with different system setup, measurement or sample parameters. For temperature calibrations, the extrapolated initial temperature $T_{e,i}$ is used to compare the measured temperature to the fixed temperature point of the calibration standard.

HEAT FLOW CALIBRATION

A heat flow calibration identifies the relation between the measured voltage U_{DSC} and the true heat flow Φ by measuring a reference material with known specific heat capacity $c_p(T)$ as shown in the following equation.

$$S_{DSC}(T) = \frac{U_{Ref}(T) - U_0(T)}{m_{Ref} c_{p,Ref}(T) \beta}$$

To do a heat flow calibration at least two measurement runs are necessary:

1. a zero-line measurement U_0 with empty crucibles to eliminate system related influences (e.g. asymmetric sensor, different crucible masses)
2. a standard reference measurement with a known $c_p(T)$ in the temperature range of interest

In case of the heat flow calibration, the sensitivity $S_{DSC}(T)$ is valid for the measured temperature range in the temperature resolution of $c_p(T)$ of the standard reference material.

SPECIFIC HEAT CAPACITY MEASUREMENTS

According to [6,7] $c_p(T)$ is the amount of heat required to raise the temperature of a substance by 1 K at constant pressure without a first-order phase transition. To evaluate $c_p(T)$ from an already calibrated and zero-line corrected heat flow Φ of a DSC, the mass m and the heating rate β are needed as shown in the following

$$c_p(T) = \frac{C_p(T)}{m} = \frac{\phi(T)}{m \beta}$$

equation

As described by [2], $c_p(T)$ is only valid in the absence of transitions or reactions (peaks) and it describes the amount of heat needed, to raise the temperature of a substance. According to the German Institute for Standardization (DIN) 51007 standard [6], at least three measurement runs are needed to evaluate $c_p(T)$ of a substance:

- a zero-line measurement with empty crucibles,
- a standard reference measurement (e.g. α -Al₂O₃ Sapphire standard)
- and a sample measurement.

The temperature program starts with an isothermal segment followed by a dynamic heating segment and ends again with an isothermal segment at the maximum temperature as shown in Figure 6-8. The recommended heating rate is $\beta = 10 \text{ K min}^{-1}$.

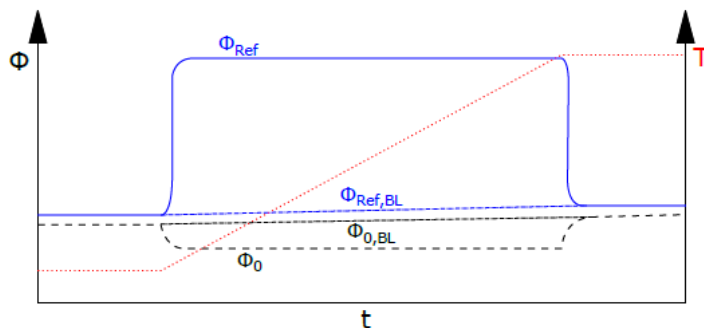


FIGURE 6-8: DSC SIGNALS FOR Φ_{REF} AND Φ_0 TO EVALUATE THE CALIBRATION FACTOR $K(T)$ FOR $C_p(T)$ MEASUREMENTS

A dimensionless calibration factor $K(T)$, as shown in the following equations is used to calibrate the heat flow and to subtract a baseline construction between the isothermal segments of $\Phi_0(T)$ and $\Phi_{\text{Ref}}(T)$. This baseline construction allows a correction if there is an offset of the heat flow Φ between the isothermal segments.

$$K(T) = \frac{C_{p,\text{Ref}}(T) \beta}{[\phi_{\text{Ref}}(T) - \phi_{\text{Ref,BL}}(T)] - [\phi_0(T) - \phi_{0,\text{BL}}(T)]}$$

$$c_{p,S}(T) = \frac{K(T) [\phi_S(T) - \phi_0(T)]}{\beta m_S}$$

In the standard DIN European Standard (EN) International Organization for Standardization (ISO) 11357-4 [7] another procedure for the evaluation of $c_p(T)$ is mentioned as shown in the following equations. As described before, again three measurements are needed to evaluate $c_{p,s}(T)$.

$$c_{p,S}(T) = c_{p,Ref}(T) \frac{m_{Ref}}{m_S} \frac{\phi_S(T) - \phi_0(T)}{\phi_{Ref}(T) - \phi_0(T)}$$

$$c_{p,S}(T) = c_{p,Ref}(T) \frac{m_{Ref}}{m_S} \frac{U_S(T) - U_0(T)}{U_{Ref}(T) - U_0(T)}$$

The main difference between these two standards is that in DIN EN ISO 11357-4 no additional baseline construction between the isothermal segments is needed. Additionally, a starting temperature 30 K below the first evaluated $c_{p,s}(T)$ is recommended. This is due to the time needed to reach a constant heating rate starting from an isothermal segment.

MEASUREMENT PROCEDURE

TEMPERATURES:

Thermogravimetric results of the $\text{SrBr}_2 \cdot 6\text{H}_2\text{O}$ at dry nitrogen gas flow have shown, that dehydration and mass loss already occur at temperatures $T > 25^\circ\text{C}$. Furthermore, the reaction shows a strong dependency on the heating rate as shown in Figure 6-9.

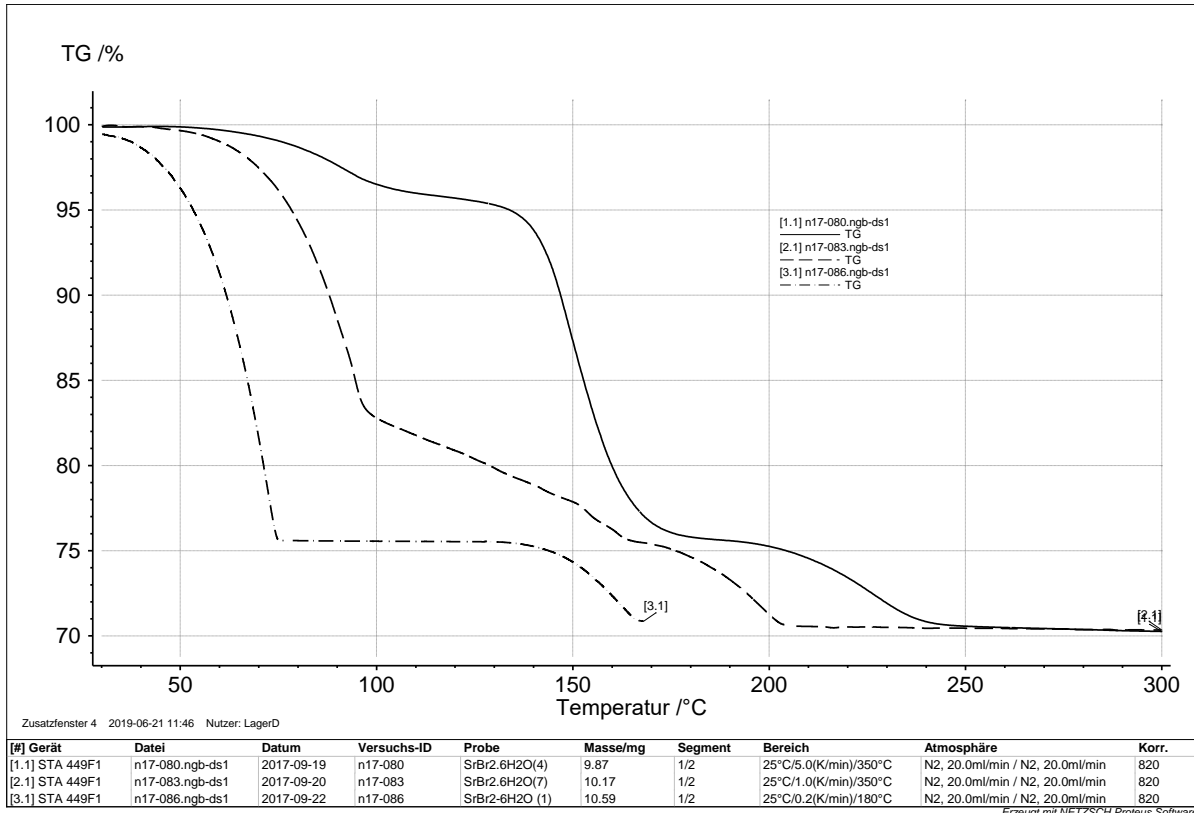


FIGURE 6-9: THERMOGRAVIMETRIC RESULTS AT B = 0.2, 1 AND 5 K MIN⁻¹ OF $\text{SRBR}_2 \cdot 6\text{H}_2\text{O}$ UP TO T = 300 °C

Based on the DSC measurements with a dry N₂ gas flow following temperature boundaries were defined:

- For the evaluation of $c_p(T)$ at $T = 25\text{ °C}$ of SrBr₂·6H₂O it is necessary to start the experiments at least at -5 °C as recommended by ISO 11357-4. Furthermore, at dry N₂ gas flow SrBr₂·6H₂O dehydration starts already at $T = 25\text{ °C}$ that would not allow to evaluate $c_p(T)$ beyond this temperature.
- To evaluate the specific heat capacity of the first product (apparently the SrBr₂·1H₂O) in a bigger temperature interval, the max. temperature is limited with $T \approx 125\text{ °C}$ due to the next dehydration step to the pure SrBr₂ salt at dry N₂ gas flow conditions.
- Due to that, a minimum temperature range of $T = -5\text{ to }200\text{ °C}$ is needed to measure at least one measurement point for SrBr₂·6H₂O and several for SrBr₂·1H₂O and the pure SrBr₂.

Due to the dehydration reaction depending on the actual gas conditions it is recommended to prepare the sample in the wished hydrated form (SrBr₂·6H₂O; SrBr₂·1H₂O and SrBr₂) and hermetically seal them in the used crucible system before the DSC measurement runs.

CALIBRATION

- Calibrate the temperature according the section “Temperature calibration”. Possible calibration substances are:
 - Hg; H₂O; Ga; In; Sn; Zn

SPECIFIC HEAT CAPACITY MEASUREMENTS

Due to the simplicity of the ISO 11357-4 in comparison to the DIN 51007 (no baseline construction, no heat flow calibration needed), the following procedure is based on this standard.

SAMPLES AND CRUCIBLES

- The crucibles for all measurements should not differ more than $\Delta m = 0,1\text{ mg}$
- Due to the high thermal conductivity, aluminium crucibles are recommended
- Prepare the wished hydrated form of the salt sample by applying a suitable method, e.g.
 - **Expose & wait:** Expose the sample in the open crucible to controlled conditions (temperature and vapour pressure) where the wished hydration level is the stable form and wait for equilibrium to settle. This can be done e.g. in a TG or a desiccator. Caution, for some hydration reactions, like SrBr₂·H₂O → SrBr₂·6H₂O, this might take very long time (weeks). Larger distance (in terms of pressure and/or temperature) to the equilibrium lines usually speeds up the process. It is also possible that the reaction speed depends on the direction, e.g. reaching SrBr₂·6H₂O by dehydrating oversaturated SrBr₂·6H₂O (mixture of sat. solution and SrBr₂·6H₂O) might be faster than by hydrating SrBr₂·H₂O.
 - **Dry, fill up & cure:** Determine the sample anhydrous mass by heating the open crucible under controlled humidity (e.g. 180 °C, 10 mbar) for several hours while controlling the weight (TG/heating station). From the anhydrous mass calculate the amount of SrBr₂ and from there the mass of the wished hydrate (target mass). Add DI water into the crucible until reaching the target mass e.g. using a micro pipette. Caution: Some of the required water will be taken

from humid ambient air by spontaneous hydration/deliquescence; only fill up to target mass. Eventually (after sealing) the wished hydrate will form as the most stable phase. This curing process can be slow and might be faster at higher temperatures. Complete curing has occurred of c_p -measurement results are reproducible over several cycles.

- Seal the crucible hermetically quickly right after preparing the sample to the required hydration level/stoichiometry and check by weighing afterwards. Avoid hydration/dehydration from ambient while sealing as much as possible.
- As reference material, use an α - Al_2O_3 (synthetic sapphire) with a purity degree of 99,9 % or higher
- Choose the sample mass according your crucible volume and specific heat of your reference ($C_{p,Ref} \approx C_{p,S}$)
- Check the mass before and after the measurement run, discard measurements if mass changes significantly

TEMPERATURE PROGRAM

- The temperature program is depending on the used DSC furnace and cooling system. The minimum temperature can be chosen according the DSC system possibilities. The first evaluated c_p value should be 30 °C higher than the starting temperature.
- The heating rate β is depending on the sensitivity of the DSC sensor. A recommended $\beta = 10 \text{ K min}^{-1}$.
- The minimum temperature T_{min} can be chosen depending on your cooling possibilities.
- The maximum temperatures are defined with:
 - o 100 °C for $\text{SrBr}_2 \cdot 6\text{H}_2\text{O}$
 - o 200 °C for $\text{SrBr}_2 \cdot 1\text{H}_2\text{O}$
 - o 200 °C for SrBr_2
- Run the program subsequent for several (e.g. four) times and compare c_p by cycle and phase (heating/cooling) to check sample stability/complete sample preparation

GAS CONDITIONS

A dynamic, dry inert gas flow is recommended (e.g. 20 ml/min N_2) to fulfil reproducible gas conditions over all measurements.

REPRODUCIBILITY AND UNCERTAINTY EVALUATION

Several measurements are needed to evaluate an uncertainty of the $c_p(T)$ evaluation. Please refer to the "Guide to the Expression of Uncertainty in Measurement (GUM)" to express your uncertainty of the $c_p(T)$ results. The document is free available at https://www.bipm.org/utis/common/documents/jcgm/JCGM_100_2008_E.pdf.

RESULTS

Material: (e.g. $\text{SrBr}_2 \cdot 6\text{H}_2\text{O}$, $\text{SrBr}_2 \cdot 1\text{H}_2\text{O}$ or SrBr_2)

DSC System: Manufacturer, Model and Type (e.g. NETZSCH, DSC 404C, hf-DSC)

Crucible: material, shape, dimensions, lid (e.g. Al, cylindric, $d = 6 \text{ mm}$; $h = 2 \text{ mm}$; cold welded)

Gas conditions: (e.g. N_2 ; 50 ml/min)

Calibration substances: Type and mass (e.g. Sapphire, $m = 60 \text{ mg}$)

Number and mass of samples before and after measurement: (e.g. 3 Samples, $m_1 = 10,2 \text{ mg}$, $m_2 = 10,3 \text{ mg}$, $m_3 = 10,1 \text{ mg}$)

Temperature program: (e.g. $T_{start} = 25\text{ °C}$; $T_{end} = 300\text{ °C}$; $\beta = 10\text{ K/min}$)

Please use following table as representation of your $c_p(T)$ evaluation:

$T / \text{°C}$	$c_p(T) / \text{J g}^{-1} \text{K}^{-1}$	$u_{c_p(T)} / \text{J g}^{-1} \text{K}^{-1}$
25		
30		
35		
...		

A temperature step of 5 °C is sufficient for the result table. Please use the unit $\text{J g}^{-1} \text{K}^{-1}$ for the evaluated mean of the specific heat data $c_p(T)$ out of at least three measurements. The uncertainty $u_{c_p(T)}$ can be expressed as defined in the GUM.

SYMBOLS AND SUBSCRIPTS

Sym- bol	Description	Unit	Subscript	Description
T	Temperature	°C	e	Extrapolated
c_p	Spec. heat capacity at constant pressure	$\text{J g}^{-1} \text{K}^{-1}$	i	Initial
U	Voltage	V	f	Final
C_p	Heat capacity at constant pressure	J K^{-1}	DSC	Differential Scanning Calorimetry
Φ	Heat flow rate	W	Ref	Reference
u_{c_p}	Uncertainty of c_p	$\text{J g}^{-1} \text{K}^{-1}$	S	Sample
m	mass	kg	0	Zero-line
β	Heating rate	K s^{-1}	BL	Baseline
S	Sensitivity	V W^{-1}		

REFERENCES

- [1] Lager D. Evaluation of thermophysical properties for thermal energy storage materials - determining factors, prospects and limitations. Dissertation. Wien; 2017.
- [2] Höhne GWH, Hemminger WF, Flammersheim H-J. Differential Scanning Calorimetry. Berlin, Heidelberg: Springer Berlin Heidelberg; 2003.

- [3] Sarge SM, Höhne GWH, Hemminger W. Calorimetry: Fundamentals, instrumentation and applications. Weinheim, Germany: Wiley-VCH Verlag; 2014.
- [4] International Organization for Standardization. Plastics -- Differential scanning calorimetry (DSC) -- Part 1: General principles;83.080.01; 2016; Available from: <https://www.iso.org/standard/70024.html>.
- [5] Blanke W (ed.). Die internationale Temperaturskala von 1990: (ITS-90). Braunschweig: Physikal.-Techn. Bundesanst; 1989.
- [6] DIN 51007:2019-04, Thermische Analyse_(TA)_- Differenz-Thermoanalyse_(DTA) und Dynamische Differenzkalorimetrie_(DSC)_- Allgemeine Grundlagen. Berlin: Beuth Verlag GmbH. doi:10.31030/3025544.
- [7] International Organization for Standardization. Plastics – Differential scanning calorimetry (DSC) – Part 4: Determination of specific heat capacity (ISO 11357-4:2014);;83.080.01; 2014; Available from: <https://www.iso.org/standard/65087.html>.

6.3 SUBTASK 4P: INFORMATION OF THE SYSTEMS

6.3.1 SYSTEM A

Institution:

Name of your institution: University of the Basque Country UPV/EHU

Name of contributors from your institution: Gonzalo Diarce

Evaluation of the existing PCM components based on the defined parameters

		Concept number in D4P1	Concept improved
	Parameter	3.1	
Capacity	Energy storage capacity of the system (ESC)	2.95 MJ (50 to 65 °C)	
	Energy Storage Density (ESCD)	78 MJ/m ³	
Losses	Storage efficiency of the TES system (η)	data not available (we don't measure the auxiliary energy consumption of pumps)	
	Time of storage (from the end of the charging to the beginning of	data not available	

	the discharging)		
Reference		Not published yet	

*Provide a description of the improvement (for example fins at PCM side, stirrer...)

Power vs time data

Please provide the power vs time data of your component, two columns as additional file (txt, xls or opj files).

In this file provide the following information:

Describe the basic principles of your power estimation. (Example: Mass flow and inlet/outlet temperature measurements of the heat transfer fluid by using....)

Monitoring recommendations defined in the ANSI/ASHRAE standard 94.1-2002 are followed

Mass flow measurement of the heat transfer fluid (water) is performed by a flowmeter (Key instruments – model FR4L69BVBN: range 1-10 L/min).

T-type thermocouples are placed in the water inlet and outlet for temperature measurement. Data are registered by a data acquisition system every 2 s.

Phase Change temperature range:

The PCM used is RT60 from Rubitherm. Phase change range around 60 °C.

(A complete characterization of the PCM can be found in: G. Diarce, Á. Campos-Celador, J.M. Sala, A. García-Romero, A novel correlation for the direct determination of the discharging time of plate-based latent heat thermal energy storage systems *Applied Thermal Engineering*, 2018; 129, 521 - 534)

Operating conditions: constant mass flow, constant inlet temperature or others.

Constant mass flow is used: 2.4 L/min for the case involved

Constant inlet temperature is used: 65 °C on charging/ 50 °C on discharging

Any additional information you consider relevant for the comparison.

6.3.2 SYSTEM B

Institution:

Name of your institution: University of Bayreuth

Name of contributors from your institution: Stephan Höhlelein and Andreas König-Haagen

Evaluation of the existing PCM components based on the defined parameters

		Concept number in D4P1	Concept improved
	Parameter	3.3	Different diameters were tested
Capacity	Energy storage capacity of the system (ESC)	5 – 8.5 MJ for a delta T of 10 – 40 K	
	Energy Storage Density (ESCD)	30.0 kWh/m ³ for 40 mm capsules 32.6 kWh/m ³ for 60 mm capsules (Only the melting enthalpy)	
Losses	Storage efficiency of the TES system (η)	About 60–80 %, depending on the boundary conditions. (It's that high as it is a rather small storage unit)	
	Time of storage (from the end of the charging to the beginning of the discharging)	The discharging started directly after the charging.	
Reference		D. Brüggemann, Universität Bayreuth, Lehrstuhl für Technische Thermodynamik und Transportprozesse, Universität Bayreuth, Lehrstuhl für Metallische Werkstoffe, A. König-Haagen, R. R. Kasibatla, S. Höhlelein, U. Glatzel,	

	R. Völkl, N. Agarkov: Entwicklung makroverkapselter Latentwärmespeicher für den Transport von Abwärme (MALATrans), 2017	
--	---	--

6.3.3 SYSTEM G

Institution:

Name of your institution: KTH-Royal Institute of Technology

Name of contributors from your institution: Amir Abdi

Evaluation of the existing PCM components based on the defined parameters

		Concept number in D4P1	Concept improved
	Parameter	1	data not available
Capacity	Energy storage capacity of the system (ESC)	282 (kJ)	data not available
	Energy Storage Density (ESCD)	201 (MJ/ m ³)	data not available
Losses	Storage efficiency of the TES system (η)	data not available	data not available
	Time of storage (from the end of the charging to the beginning of the discharging)	data not available	data not available

Reference		
------------------	--	--

Power vs time data

The power vs time data of my component is provided in a separate file.
Below, additional information is provided:

- The power is estimated by measuring the flow rate and the inlet/outlet temperatures of the heat transfer fluid (water).
- Phase Change temperature range: the PCM used in the experiment is Eicosane with phase change temperature of 35-37°C.
- Operating conditions: constant mass flow and constant inlet temperature
- The inlet temperature of HTF is 60°C and the initial temperature of PCM has been 15°C.
- The heat exchanger volume is 0.0014m³

6.3.4 SYSTEM H

Institution:

Name of your institution: Technical University of Denmark

Name of contributors from your institution: Gerald Englmaier, Simon Furbo, Mark Dannemand, Gang Wang

Evaluation of the existing PCM components based on the defined parameters

		Concept number in D4P1	Concept improved*
	Parameter	3.1 (PCM in flat plates) A single flat plate with 10 cm foam insulation	Stack of 14 plates with a common insulation
Capacity	Energy storage capacity of the system (ESC)	Total: 108 MJ [1] Short-term: 61 MJ [1] Long-term: 47 MJ [1]	Values of left column x 14
	Energy Storage Density (ESCD)	Total: 100 MJ/m ³ [1]	Total: 202 MJ/m ³ [3]
Losses	Storage efficiency of the TES system (η)	Maximum (daily heat storage cycles, charge and discharge in the temperature range 50–90 °C): 0.8–1	See left column

	Time of storage (from the end of the charging to the beginning of the discharging)	Minimum (long-term heat over months without utilization of sensible heat capacity): 0.42 [2]	
Reference		<p>[1] M. Dannemand, J. Dragsted, J. Fan, J.B. Johansen, W. Kong, S. Furbo, Experimental investigations on prototype heat storage units utilizing stable supercooling of sodium acetate trihydrate mixtures, Appl. Energy. 169 (2016) 72–80. doi:10.1016/j.apenergy.2016.02.038.</p> <p>[2] G. Englmaier, C. Moser, S. Furbo, M. Dannemand, J. Fan, Design and functionality of a segmented heat-storage prototype utilizing stable supercooling of sodium acetate trihydrate in a solar heating system, Appl. Energy. 221 (2018) 522–534.</p>	<p>[3] G. Englmaier, W. Kong, J. B. Berg, S. Furbo, and J. Fan, “Demonstration of a solar combi-system utilizing stable supercooling of sodium acetate trihydrate for heat storage”, submitted to Applied Thermal Engineering.</p>

Power vs. time data

- Test conditions:

Set max. charging power: 6–9 kW;

Set max. charging temperature: 90 °C;

Mass flow charge: ~5 L/min;

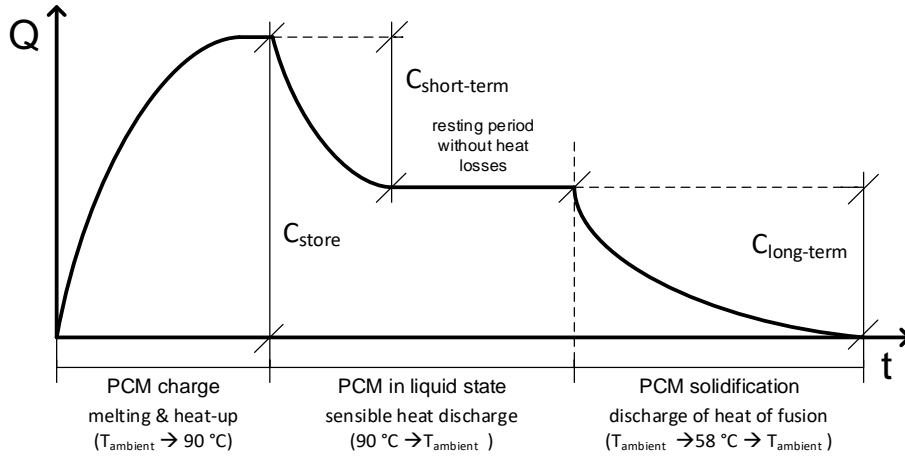
Mass flow discharge: ~5 L/min with PCM in liquid state; 2.13 L/min during solidification.

Constant inlet temperature during discharge: 22.5 °C

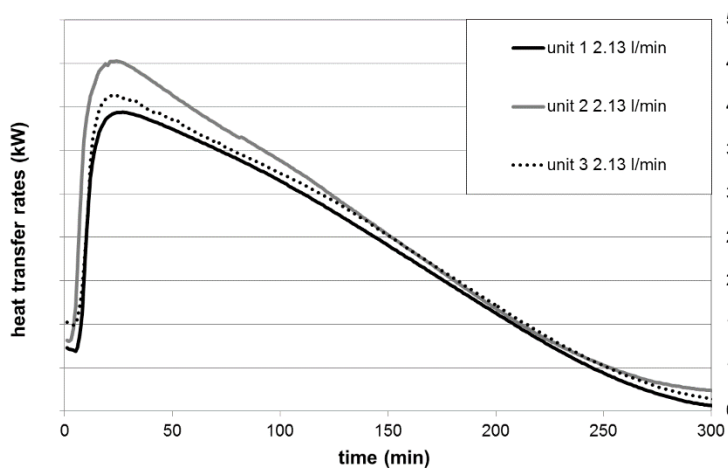
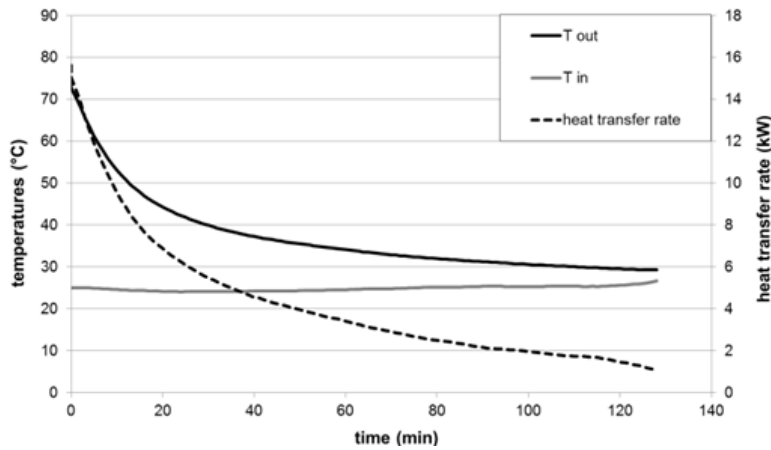
- Application temperature range: 25–90 °C

- Phase change temperature: 58 °C

- Test cycle:



- Discharge data [2]:



Top: Discharge of sensible heat ($C_{\text{short-term}}$) from liquid PCM with a HTF flow rate of 5 L/min; Bottom: Discharge of latent heat of fusion ($C_{\text{long-term}}$) during solidification from stable supercooled state (room temperature) with different flow rates.

6.3.5 SYSTEM I

Institution:

Name of your institution: Technical University of Denmark

Name of contributors from your institution: Gerald Englmaier, Simon Furbo, Mark Dannemand, Gang Wang

		Concept number in D4P1	Concept improved*
	Parameter	8 (Tank-in-tank)	Without expansion vessel (semi-open);
Capacity	Energy storage capacity of the system (ESC)	Total: 98 MJ [1] Short-term: 56 MJ [1] Long-term: 42 MJ [1]	See left column
	Energy Storage Density (ESCD)	Total: 248 MJ/m ³	Total: 272 MJ/m ³ [1]
Losses	Storage efficiency of the TES system (η)	Maximum (daily heat storage cycles, charge and discharge in the temperature range 50–90 °C): 0.8–1	
	Time of storage (from the end of the charging to the beginning of the discharging)	Minimum (long-term heat over months without utilization of sensible heat capacity): 0.43 [1]	
Reference		[1] G. Englmaier, S. Furbo, M. Dannemand, and J. Fan, "Experimental investigation	

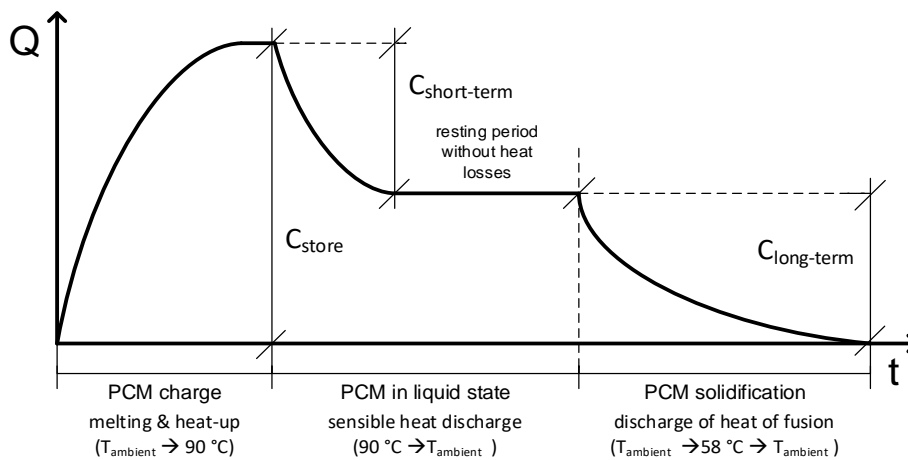
	of a tank-in-tank heat storage unit utilizing stable supercooling of sodium acetate trihydrate”, submitted to Applied Thermal Engineering.	
--	--	--

Power vs. time data

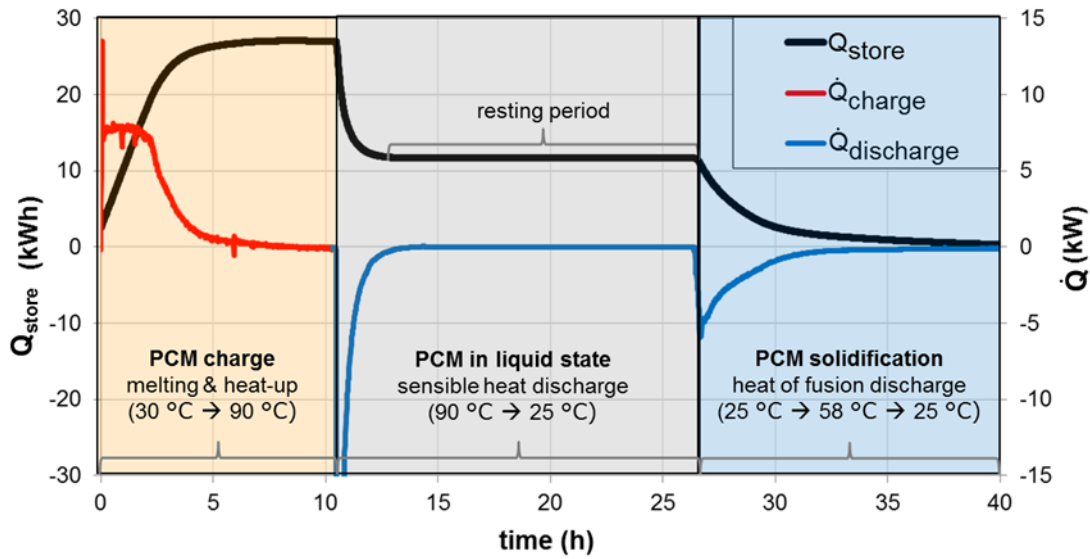
- Test conditions:

Set max. charging power:	6–9	kW;
Set max. charging temperature:	90	°C;
Mass flow charge:	~10	L/min;

Mass flow discharge: ~10 L/min with PCM in liquid state; ~4 L/min during solidification;
Constant inlet temperature during discharge: 22.5 °C
- Application temperature range: 25–90 °C
- Phase change temperature: 58 °C
- Test cycle [1]:



- Charge and discharge data [1]:



6.3.6 SYSTEM J

Institution:

Name of your institution: Technical University of Denmark

Name of contributors from your institution: Gerald Englmaier, Simon Furbo, Mark Dannemand, Gang Wang

		Concept number in D4P1	Concept improved
	Parameter	2.2 (Tank with internal H.X.), 5 cm insulation, with expansion vessel. "Thermobattery 1 st Gen."	Without expansion vessel (semi-open); optimized heat exchanger; 5 cm insulation. "Thermobattery 2 nd Gen."
Capacity	Energy storage capacity of the system (ESC)	Total: 50 MJ [1] Short-term: 26 MJ [1] Long-term: 24 MJ [1]	Total: 81 MJ Short-term: 52 MJ Long-term: 29 MJ
	Energy Storage Density (ESCD)	Total: 167 MJ/m ³	Total: 260 MJ/m ³
Losses	Storage efficiency of the TES system (η)	Maximum (daily heat storage cycles, charge and discharge in the temperature range 25–90 °C): 0.8–1	Maximum (daily heat storage cycles, charge and discharge in the temperature range 25–90 °C): 0.8–1

	Time of storage (from the end of the charging to the beginning of the discharging)	Minimum (long-term heat over months without utilization of sensible heat capacity): 0.48 [1]	Minimum (long-term heat over months without utilization of sensible heat capacity): 0.34
Reference		[1] M. Dannemand, J.B. Johansen, W. Kong, S. Furbo, Experimental investigations on cylindrical latent heat storage units with sodium acetate trihydrate composites utilizing supercooling, Appl. Energy. 177 (2016) 591–601.	G. Wang et al., publication planned in the year 2019.

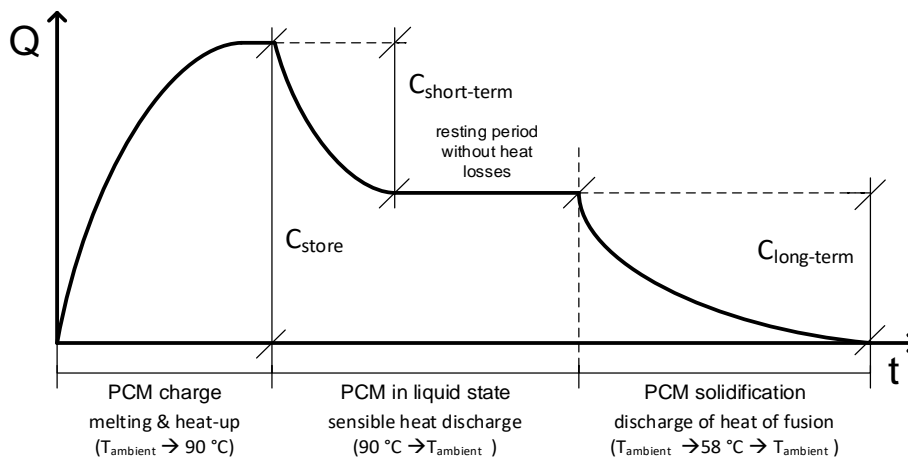
Power vs. time data

- Test conditions:

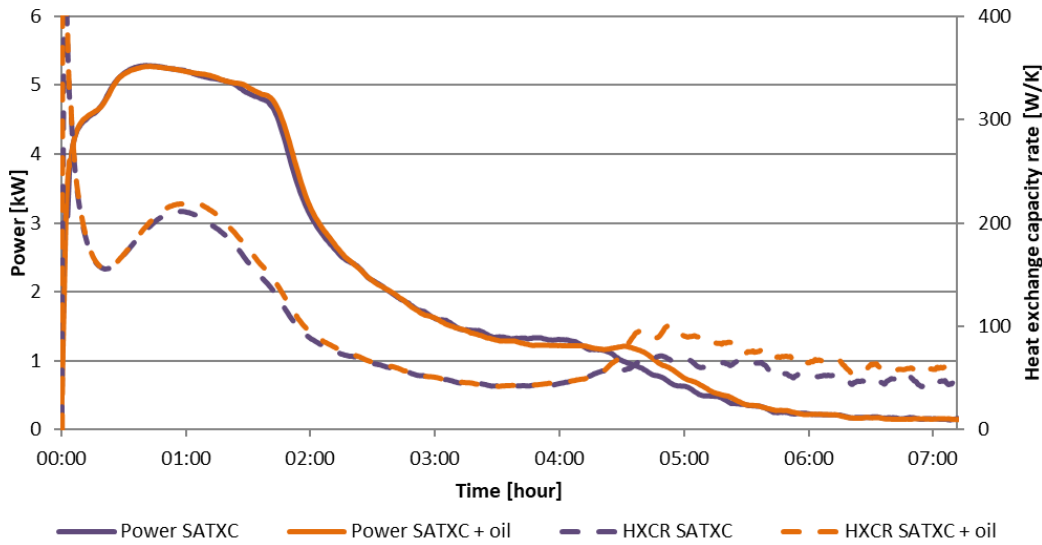
Set max. charging power: 6–9 kW;
 Set max. charging temperature: 92 °C;
 Mass flow charge: 13.7 basic concept; ~7 L/min improved concept;
 Mass flow discharge: 5.7 basic concept; ~7 L/min improved concept;
 Constant inlet temperature during discharge: 25 °C

- Application temperature range: 25–90 °C
- Phase change temperature: 58 °C

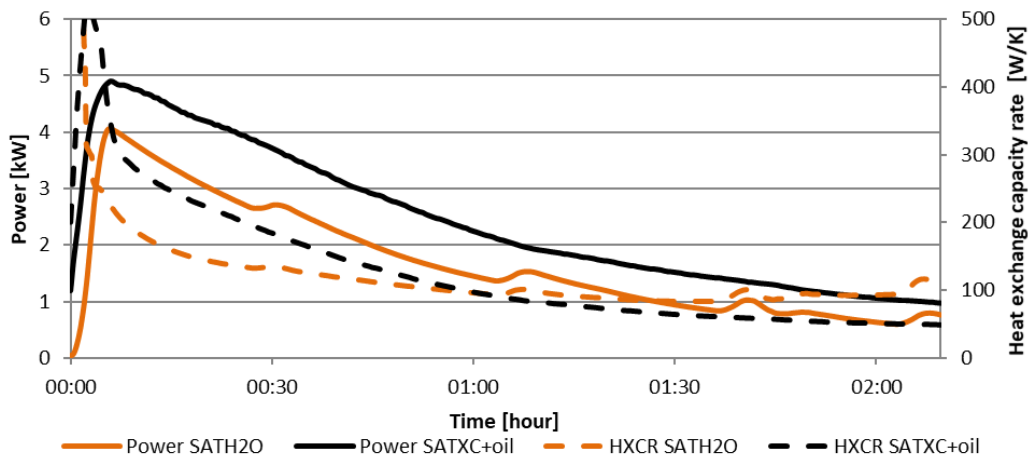
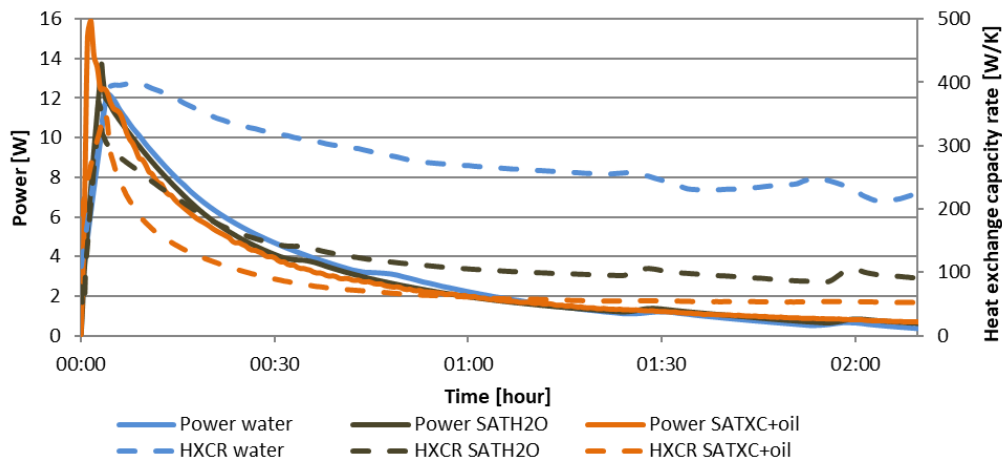
- Test cycle [1]:



- Charge basic concept with 13.7 L/min applied [1]:

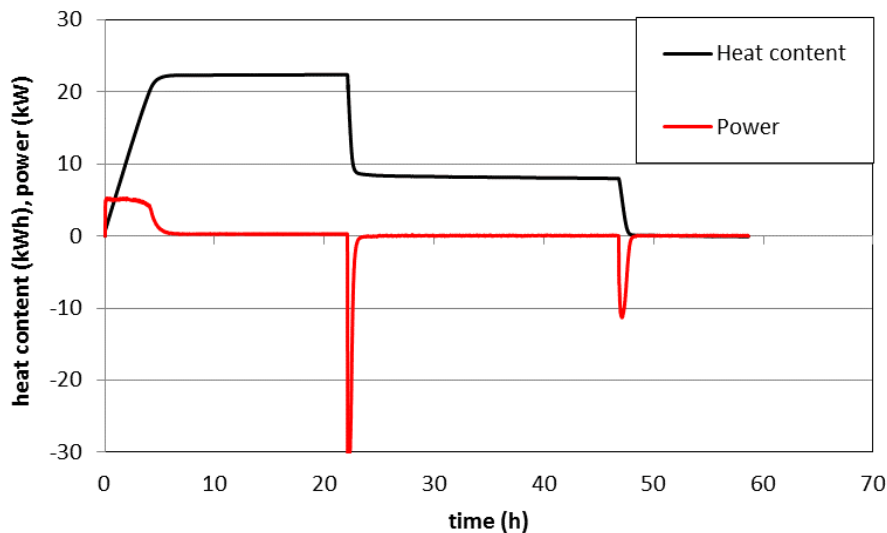


- Discharge power basic concept [1]:



Top: Discharge of sensible heat ($C_{\text{short-term}}$) from liquid PCM with a HTF flow rate of 5.7 L/min; Bottom: Discharge of latent heat of fusion ($C_{\text{long-term}}$) during solidification from stable supercooled state (room temperature) with 5.7 L/min.

- Charge and discharge power improved concept (constant flow rate of ~7 L/min):



Please note: We previously promised to deliver data for a heat storage unit where PCM is in direct contact to the heat transfer fluid (Design no. 7). However, the goals in the relevant project changed. Thus, no heat storage of the mentioned design will be investigated.

6.3.7 SYSTEM K

Institution:

Name of your institution: LAMTE – Dalhousie University

Name of contributors from your institution: Dr. Dominic Groulx

Evaluation of the existing PCM components based on the defined parameters

		Concept number in D4P1	Concept improved
	Parameter	2.1 Shell-and-tube (PCM in shell, fins on tubes)	None
Capacity	Energy storage capacity of the system (ESC)	The absolute value depends on the end point temperatures, for the results presented here 21 degC to 65 degC with 10 kg of dodecanoic acid:	

		2.8 MJ	
	Energy Storage Density (ESCD)	204 MJ/m ³ (Volume: 0.01373 m ³)	
Losses	Storage efficiency of the TES system (η) Time of storage (from the end of the charging to the beginning of the discharging)	Experimental system which is discharge the moment it is charge (so instantaneous cycle). With the very minor heat losses, and within the overall experimental uncertainty, the efficient could be considered to be 1 (although not calculated).	
Reference		HERBINGER, F., PATIL, A., GROULX, D. (2019) <i>Characterization of Different Geometrical Variations of a Vertical Finned Tube-and-Shell Heat Exchanger</i> , Eurotherm Seminar #112 Advances in Thermal Energy Storage, Lleida, Spain, 10 p.	

*Provide a description of the improvement (for example fins at PCM side, stirrer...)

Power vs time data

Please provide the power vs time data of you component, two columns as additional file (txt, xls or opj files).

In this file provide the following information:

- Describe the basic principles of your power estimation. (Example: Mass flow and inlet/outlet temperature measurements of the heat transfer fluid by using....)

The classic $\dot{m}C_p(T_{inlet} - T_{outlet})$ was used.



- Phase Change temperature range:
Dodecanoic acid melts at 43 degC.
- Operating conditions: constant mass flow, constant inlet temperature or others.
Constant flow rate (9 Lpm) and constant inlet temperature.
- Any additional information you consider relevant for the comparison.

Data is provided for both the charging and discharging experiments from the same flow rate and the same temperature range; data provided for the systems